

# Anti-atherogenic actions of (+)-catechin



Yee Hung Chan BSc (Hons), MRes

A dissertation presented for the degree of  
Doctor of Philosophy (Biosciences)

July 2021

Cardiff School of Biosciences  
The Sir Martin Evans Building  
Cardiff University  
Museum Avenue  
Cardiff  
CF10 3AX

# Table of Contents

Table of Contents .....	I
Table of Figures .....	X
Table of Tables .....	XV
Abstract .....	XVI
Acknowledgements .....	XVIII
Publications .....	XIX
List of Abbreviations .....	XXI
1 General Introduction.....	1
1.1 Cardiovascular disease: an on-going burden.....	1
1.2 An overview of lipid metabolism.....	2
1.3 Pathophysiology of atherosclerosis.....	6
1.3.1 Endothelial dysfunction.....	7
1.3.2 Inflammation: the key driver of atherosclerosis pathogenesis .....	10
1.3.3 Macrophage heterogeneity in atherosclerosis .....	13
1.3.4 Foam cell formation .....	14
1.3.5 Necrotic core formation.....	18
1.3.6 Plaque rupture .....	20
1.4 Current therapies for atherosclerosis .....	22
1.4.1 Statins and other strategies targeted to hyperlipidaemia .....	22
1.4.2 Strategies targeting inflammation .....	24
1.5 Nutraceutical agents: a promising alternative avenue.....	26
1.5.1 Catechins: important dietary flavanols.....	28
1.5.2 (+)-Catechin: a promising flavanol requiring investigation .....	32
1.6 Project aims .....	35
2 Materials and Methods.....	43
2.1 Materials .....	43
2.2 Cell culture and maintenance.....	45
2.2.1 General cell maintenance .....	45
2.2.2 Endothelial and vascular smooth muscle cells .....	46

2.2.3	THP-1 monocytic cell line .....	46
2.2.4	Freezing down and thawing frozen cells.....	47
2.2.5	Extraction of human monocyte-derived macrophages.....	47
2.2.6	Cell counting.....	49
2.3	Cell treatment and stimulation.....	49
2.3.1	Cell treatment .....	49
2.3.2	Stimulation of endothelial cells .....	50
2.3.3	Coating transwell inserts with Matrigel .....	51
2.4	Cell-based assays.....	51
2.4.1	Cell viability.....	51
2.4.2	Cell proliferation.....	52
2.4.3	Cell proliferation over 7 days .....	52
2.4.4	Cellular ROS production.....	53
2.4.5	Cellular ROS production in the presence of other mediators.....	53
2.4.5.1	oxLDL .....	54
2.4.5.2	TNF- $\alpha$ .....	54
2.4.6	ELISA for the measurement of MCP-1 release.....	54
2.4.7	Matrix metalloproteinase activity measurement.....	56
2.4.8	Mitochondrial ROS production.....	56
2.4.9	Cellular bioenergetics profiling.....	57
2.4.9.1	Mitochondrial respiration.....	57
2.4.9.2	Glycolysis .....	58
2.4.10	Mitochondrial membrane potential .....	59
2.4.11	Monocyte-endothelial adhesion (static adhesion assay) .....	59
2.4.12	Apoptosis .....	60
2.4.13	Endothelial permeability .....	61
2.4.14	Smooth muscle cell migration (invasion).....	62
2.4.15	Monocyte migration .....	63
2.5	<i>In vivo</i> techniques .....	63
2.5.1	Animal maintenance and feeding .....	63
2.5.2	Progression study .....	64

2.5.3	Regression study .....	64
2.5.4	Extraction of blood from the tail .....	65
2.5.5	Collection of blood and tissues at the endpoint .....	66
2.5.6	Measurement of plasma triglyceride .....	66
2.5.7	Plasma lipoprotein quantification and profiling.....	67
2.5.8	Plasma oxidative stress parameters .....	68
2.5.8.1	Plasma ROS/RNS .....	68
2.5.8.2	Plasma malondialdehyde.....	68
2.5.9	Plasma cytokine levels .....	69
2.5.10	Immunophenotyping of peripheral blood cell populations.....	69
2.5.11	Immunophenotyping of bone marrow cell populations .....	73
2.5.12	Sectioning .....	79
2.5.13	Histological/immunohistochemical techniques .....	79
2.5.13.1	Oil Red O staining .....	79
2.5.13.2	Haematoxylin and eosin staining .....	80
2.5.13.3	Collagen staining .....	80
2.5.13.4	Immunofluorescence staining .....	81
2.5.14	Image analysis .....	82
2.5.15	Calculation of plaque necrosis and stability.....	84
2.6	Statistical analysis.....	85
3	Effect of (+)-catechin on endothelial and VSMC dysfunction .....	86
3.1	Introduction .....	86
3.1.1	Experimental aims .....	88
3.1.2	Cell viability.....	89
3.1.3	Endothelial dysfunction.....	89
3.1.3.1	Role of oxLDL and TNF- $\alpha$ .....	89
3.1.3.2	Adhesion of monocytes to activated ECs .....	90
3.1.3.3	MCP-1 and its role in mediating monocyte migration .....	91
3.1.4	ROS production .....	92
3.1.5	Apoptosis.....	92
3.1.6	Macrophage proliferation.....	93

3.1.7	VSMC migration and proliferation.....	94
3.1.8	MMP activity.....	95
3.2	Summary of experimental strategies.....	96
3.3	Results.....	97
3.3.1	(+)-Catechin has no detrimental effects on cell viability.....	97
3.3.2	OxLDL up to 100 µg/ml and TNF-α up to 50 ng/ml has no detrimental effects on EC viability.....	98
3.3.3	(+)-Catechin has no significant effects on endothelial and VSMC proliferation.....	100
3.3.4	Proliferation of ECs is affected by oxLDL and TNF-α stimulation.....	101
3.3.5	(+)-Catechin attenuates ROS production by multiple cell types.....	102
3.3.6	(+)-Catechin attenuates EC ROS production in the presence of TNF-α after pre-treatment.....	104
3.3.7	OxLDL does not induce MCP-1 release by ECs or affect endothelial permeability and apoptosis.....	104
3.3.8	(+)-Catechin has no effect on monocyte-endothelial adhesion.....	108
3.3.9	(+)-Catechin attenuates PDGF-stimulated invasion of VSMCs with no effect on proliferation over 7 days.....	108
3.3.10	(+)-Catechin reduces macrophage MMP activity after 24 hours.....	110
3.3.11	(+)-Catechin elicits comparable effects on monocyte migration and ROS production to its isomers.....	111
3.4	Discussion.....	112
3.4.1	Use of oxLDL and TNF-α to stimulate ECs.....	113
3.4.2	(+)-Catechin attenuates ROS production in various cell types.....	114
3.4.3	(+)-Catechin has no effect on monocyte-endothelial adhesion.....	115
3.4.4	(+)-Catechin attenuates macrophage proliferation.....	116
3.4.5	(+)-Catechin attenuates PDGF-stimulated migration of SMCs with no effect on proliferation.....	117
3.4.6	(+)-Catechin dampens macrophage MMP activity.....	118
3.4.7	(+)-Catechin demonstrates comparable effects to its isomers <i>in vitro</i> .....	118
3.4.8	Future directions.....	119
3.4.9	Conclusion.....	120

4	Effect of (+)-catechin on bioenergetics and mitochondrial function .....	122
4.1	Introduction .....	122
4.1.1	The mitochondria.....	122
4.1.2	Effects of catechin on mitochondrial function and experimental aim ..	123
4.1.3	Mitochondrial respiration.....	124
4.1.4	Mitochondrial dysfunction in atherosclerosis .....	125
4.1.5	Glycolysis .....	130
4.1.6	MitoROS production .....	133
4.1.7	Mitochondrial membrane potential.....	134
4.2	Experimental strategy .....	135
4.3	Results .....	136
4.3.1	(+)-Catechin increases spare respiratory capacity and non-mitochondrial respiration in macrophages.....	136
4.3.2	(+)-Catechin has no effect on glycolysis in macrophages.....	138
4.3.3	(+)-Catechin reduces basal respiration, ATP-linked respiration and proton leak in M1 polarised macrophages.....	140
4.3.4	(+)-Catechin has no effect on glycolysis in M1 macrophages.....	142
4.3.5	(+)-Catechin reduces macrophage mitoROS production .....	144
4.3.6	(+)-Catechin has restorative effects on oxLDL-induced mitochondrial membrane hyperpolarisation in ECs .....	145
4.3.7	(+)-Catechin increases spare respiratory capacity in ECs.....	145
4.3.8	(+)-Catechin raises non-mitochondrial respiration in stimulated ECs .	147
4.4	Discussion.....	149
4.4.1	Beneficial effects of (+)-catechin in macrophages .....	150
4.4.2	Beneficial effects of (+)-catechin in ECs .....	151
4.4.3	MitoROS production .....	152
4.4.4	Limitations .....	153
4.4.5	Future directions.....	154
4.4.6	Conclusion.....	154
5	Effect of (+)-catechin on atherosclerosis development and progression.....	155
5.1	Introduction .....	155

5.1.1	Experimental aims .....	156
5.1.2	Adiposity and weight gain .....	156
5.1.3	Stem, progenitor and immune cell profiling.....	158
5.1.4	Plasma parameters .....	160
5.1.4.1	Lipid profiling .....	160
5.1.4.2	Oxidative stress markers .....	161
5.1.4.3	Quantification of key cytokines .....	162
5.1.5	Detailed plaque morphometric analyses.....	164
5.1.5.1	Burden and lipid content.....	164
5.1.5.2	Immune cell infiltration.....	164
5.1.5.3	Necrosis and stability parameters.....	165
5.1.6	Hepatic cellularity and steatosis .....	166
5.1.7	Experimental strategy .....	168
5.2	Results .....	169
5.2.1	Adiposity and key organs.....	169
5.2.2	Bone marrow stem, progenitor and immune cell population analysis .	173
5.2.2.1	(+)-Catechin reduces the proportion of HPC II cells .....	174
5.2.2.2	(+)-Catechin reduces the proportion of CMP cells.....	176
5.2.2.3	(+)-Catechin reduces the proportion of T cells.....	178
5.2.3	Peripheral blood immune cell population analysis.....	180
5.2.3.1	(+)-Catechin has no significant effect on lymphoid cell populations.	181
5.2.3.2	(+)-Catechin increases the proportion of Ly6C <sup>high</sup> monocytes .....	183
5.2.4	Plasma parameters .....	185
5.2.4.1	Lipid profile .....	185
5.2.4.2	Lipid ratios .....	186
5.2.4.3	Cytokine profile.....	187
5.2.4.4	Oxidative stress markers .....	189
5.2.5	Detailed plaque morphometric analyses.....	189
5.2.5.1	Burden and lipid content.....	189
5.2.5.2	Immune cell infiltration.....	191

5.2.5.3	Necrosis and stability parameters.....	193
5.2.6	Liver cellularity and steatosis.....	195
5.2.7	Summary.....	197
5.3	Discussion.....	197
5.3.1	Effects on adiposity and plasma lipids.....	198
5.3.2	Effects on progenitor and immune cells in the bone marrow.....	199
5.3.3	Effects on peripheral blood immune cells and plasma cytokines.....	201
5.3.4	Lack of effect on plasma oxidative stress markers.....	203
5.3.5	Effects on plaque burden and inflammation.....	204
5.3.6	Effects on plaque stability parameters.....	206
5.3.7	Future directions.....	206
5.3.8	Conclusion.....	207
6	Effect of (+)-catechin on atherosclerosis regression.....	209
6.1	Introduction.....	209
6.1.1	Experimental aims.....	210
6.1.2	Experimental strategy.....	210
6.2	Results.....	211
6.2.1	Adiposity and key organs.....	211
6.2.1.1	(+)-Catechin reduces the accumulation of inguinal, gonadal and renal fat compared to baseline.....	213
6.2.1.2	(+)-Catechin increases the ratio of brown to white fat compared to baseline.....	214
6.2.1.3	(+)-Catechin increases certain organ weights compared to baseline.....	216
6.2.2	Bone marrow stem, progenitor and immune cell population analysis.....	218
6.2.2.1	(+)-Catechin reduces the proportion of HPC II and MPP cells compared to baseline.....	219
6.2.2.2	(+)-Catechin increases the proportion of progenitor cells compared to baseline.....	220
6.2.2.3	(+)-Catechin has no significant effects on lineage <sup>+</sup> cell populations.....	223
6.2.3	Peripheral blood immune cell population analysis.....	225

6.2.3.1 (+)-Catechin reduces the number of NK cells compared to baseline	226
6.2.3.2 (+)-Catechin increases the number of monocytes .....	228
6.2.4 Plasma parameters .....	230
6.2.4.1 Lipid profile .....	230
6.2.4.2 Lipid ratios .....	233
6.2.4.3 Cytokine profile.....	235
6.2.5 Detailed plaque morphometric analyses.....	237
6.2.5.1 Burden and lipid content.....	237
6.2.5.2 Immune cell infiltration.....	239
6.2.5.3 Stability parameters.....	245
6.2.5.4 Necrosis and stability.....	247
6.2.6 Liver cellularity and steatosis.....	248
6.2.7 Summary .....	249
6.3 Discussion.....	251
6.3.1 Changes in weight gain and adipose tissue accumulation .....	252
6.3.2 Changes in plasma lipid profile.....	254
6.3.3 Changes in the liver.....	255
6.3.4 Changes in other organs .....	257
6.3.5 Changes in immune profile .....	258
6.3.6 Effects on atherosclerotic plaque regression .....	262
6.3.7 Future directions.....	264
6.3.8 Conclusion.....	266
7 General Discussion .....	268
7.1 Introduction .....	268
7.2 Summary of key findings.....	270
7.2.1 <i>In vitro</i> .....	270
7.2.2 <i>In vivo</i> .....	272
7.3 Potential mechanisms of action.....	277
7.3.1 Atherosclerosis development and progression.....	277
7.3.2 Plaque progression and stability.....	282
7.3.3 Atherosclerosis regression .....	284

7.4	Strengths and limitations .....	285
7.4.1	Use of mouse models .....	285
7.4.2	The dose and administration of (+)-catechin .....	288
7.4.3	Use of <i>in vitro</i> assays.....	289
7.5	Further work and future perspectives.....	290
7.6	Conclusion .....	293
	References.....	295

## Table of Figures

Figure 1.1 Simplified overview of lipid metabolism.....	5
Figure 1.2 Overview of the progression of atherosclerosis.....	7
Figure 1.3 Biological functions of the endothelium .....	8
Figure 1.4 Lipoprotein and immune cell infiltration. ....	10
Figure 1.5 Comparison of the characteristics of M1 and M2 macrophages.....	14
Figure 1.6 Summary of key processes that drive atherosclerosis. ....	17
Figure 1.7 Diagrammatic representation of the key processes in atherosclerosis pathogenesis.....	20
Figure 1.8 Processes that contribute to plaque stability and rupture.....	22
Figure 1.9 Molecular structure of (+)-catechin and major green tea catechins.....	29
Figure 1.10 Summary of significant changes observed in previous <i>in vitro</i> and <i>in vivo</i> studies.....	34
Figure 1.11 Summary of experiments conducted as part of the first objective. ....	37
Figure 1.12 Molecular structures of (+)-catechin and (+)-catechin hydrate. ....	38
Figure 1.13 Strategy for the progression study. ....	39
Figure 1.14 Tissue processing strategy used at the end point of the feeding procedure. ....	40
Figure 1.15 Strategy for the regression study. ....	41
Figure 1.16 Summary of contents of thesis chapters. ....	42
Figure 2.1 Gradient separation of the components in buffy coat. ....	48
Figure 2.2 Diagrammatic representation of the static adhesion assay set up. ....	60
Figure 2.3 Diagrammatic representation of the invasion assay set up. ....	62
Figure 2.4 Gating strategy for analysis of lymphoid and myeloid cells within the peripheral blood. ....	72
Figure 2.5 Protocol used for the extraction and analysis of bone marrow cells.....	77
Figure 2.6 Gating strategy for analysis of stem/progenitor and immune cells within the bone marrow. ....	78
Figure 2.7 Image analysis using the conventional threshold adjustment method.....	83
Figure 2.8 Image analysis using the colour deconvolution method. ....	84
Figure 3.1 Experiments using monocytes and macrophages.....	96
Figure 3.2 Experiments using HUVECs. ....	96
Figure 3.3 Experiments using HASMCs. ....	97

Figure 3.4 (+)-Catechin has no detrimental effects on cell viability after 24 hours. . .	98
Figure 3.5 OxLDL (up to 100 µg/ml) and TNF-α (up to 50 ng/ml) has no effects on EC viability after 24 hours. ....	99
Figure 3.6 (+)-Catechin reduces HMDM proliferation after 24 hours. ....	100
Figure 3.7 Proliferation of ECs is affected by oxLDL and TNF-α stimulation after 24 hours. ....	102
Figure 3.8 (+)-Catechin attenuates ROS production in multiple cell types. ....	103
Figure 3.9 (+)-Catechin attenuates ROS production by ECs in the presence of TNF-α after pre-treatment for 24 hours. ....	104
Figure 3.10 TNF-α induces MCP-1 release by ECs. ....	105
Figure 3.11 OxLDL has no significant effects on the permeability or apoptosis of ECs. ....	107
Figure 3.12 (+)-Catechin has no significant effect on monocyte-endothelial adhesion. ....	108
Figure 3.13 (+)-Catechin attenuates PDGF-stimulated VSMC migration without affecting basal proliferation over 7 days. ....	109
Figure 3.14 (+)-Catechin reduces macrophage MMP activity after 24 hours. ....	110
Figure 3.15 (+)-Catechin has no effect on VSMC MMP activity. ....	110
Figure 3.16 (+)-Catechin, (-)-catechin and (-)-epicatechin attenuates monocyte migration and ROS production after 3 hours. ....	112
Figure 4.1 Principle of the Mito Stress Test assay. ....	127
Figure 4.2 Parameters measured in the Mito Stress Test Assay. ....	128
Figure 4.3 Principle of the Glycolytic Rate Assay. ....	131
Figure 4.4 Parameters measured in the Glycolytic Rate Assay ....	132
Figure 4.5 Experiments using THP-1 macrophages. ....	135
Figure 4.6 Experiments using HUVECs and HASMCs. ....	136
Figure 4.7 Effect of (+)-catechin on mitochondrial respiration in THP-1 macrophages. ....	138
Figure 4.8 Effect of (+)-catechin on glycolysis in THP-1 macrophages. ....	139
Figure 4.9 Effect of (+)-catechin on mitochondrial respiration in stimulated THP-1 macrophages. ....	142
Figure 4.10 Effect of (+)-catechin on glycolysis in stimulated THP-1 macrophages. ....	143
Figure 4.11 Effect of (+)-catechin on mitoROS production. ....	144

Figure 4.12 Effect of (+)-catechin on EC mitochondrial membrane potential. ....	145
Figure 4.13 Effect of (+)-catechin on mitochondrial respiration in ECs.....	146
Figure 4.14 Effect of (+)-catechin on mitochondrial respiration in stimulated ECs. ....	149
Figure 5.1 Simplified summary of haematopoiesis.....	158
Figure 5.2 Experimental strategy for the progression study. ....	168
Figure 5.3 Changes in mouse weights over time. ....	169
Figure 5.4 White adipose tissue deposits.....	170
Figure 5.5 White and brown adipose tissue analysis. ....	171
Figure 5.6 Organ weights. ....	172
Figure 5.7 Cardiac hypertrophy index. ....	173
Figure 5.8 Total cell count and number of white blood cells in the bone marrow. ...	174
Figure 5.9 Effect of (+)-catechin on stem cell populations in the bone marrow. ....	175
Figure 5.10 Effect of (+)-catechin on progenitor cell populations in the bone marrow. .....	178
Figure 5.11 Effect of (+)-catechin on lineage <sup>+</sup> cell populations in the bone marrow. .....	180
Figure 5.12 Effect of (+)-catechin on the number of white blood cells in the peripheral blood. ....	181
Figure 5.13 Effect of (+)-catechin on lymphoid cell populations in the peripheral blood. .....	183
Figure 5.14 Effect of (+)-catechin on myeloid cell populations in the peripheral blood. .....	185
Figure 5.15 Plasma lipids. ....	186
Figure 5.16 Plasma lipid ratios. ....	187
Figure 5.17 Plasma cytokines. ....	188
Figure 5.18 Plasma oxidative stress markers.....	189
Figure 5.19. Plaque burden and lipid content.....	190
Figure 5.20 Plaque immune cell infiltration.....	192
Figure 5.21 Plaque necrosis and stability parameters.....	194
Figure 5.22 Liver cellularity and steatosis. ....	196
Figure 5.23 Summary of changes in the bone marrow cell populations. ....	201
Figure 5.24 Summary of changes in the bone marrow and peripheral blood cell populations.....	203
Figure 6.1 Summary of experimental strategy.....	211

Figure 6.2 Changes in mouse weights over time. ....	212
Figure 6.3 White adipose tissue deposits. ....	214
Figure 6.4 White and brown adipose tissue analysis. ....	216
Figure 6.5 Organ weights. ....	217
Figure 6.6 Cardiac hypertrophy index. ....	218
Figure 6.7 Total cell count and number of white blood cells in the bone marrow. ...	219
Figure 6.8 Effect of (+)-catechin on stem cell populations in the bone marrow. ....	220
Figure 6.9 Effect of (+)-catechin on progenitor cell populations in the bone marrow. .....	222
Figure 6.10 Effect of (+)-catechin on lineage <sup>+</sup> cell populations in the bone marrow. .....	224
Figure 6.11 Effect of (+)-catechin on the number of white blood cells in the peripheral blood. ....	225
Figure 6.12 Effect of (+)-catechin on lymphoid cell populations in the peripheral blood. .....	228
Figure 6.13 Effect of (+)-catechin on myeloid cell populations in the peripheral blood. .....	230
Figure 6.14 Plasma lipids. ....	232
Figure 6.15 Plasma lipid ratios. ....	234
Figure 6.16 Plasma cytokines. ....	236
Figure 6.17 Plaque burden and lipid content. ....	238
Figure 6.18 Plaque MOMA-2 <sup>+</sup> macrophage content. ....	240
Figure 6.19 Plaque iNOS <sup>+</sup> M1 macrophage content. ....	242
Figure 6.20 Plaque CD3 <sup>+</sup> T cell content. ....	244
Figure 6.21 Plaque stability parameters. ....	246
Figure 6.22 Plaque necrosis and stability. ....	247
Figure 6.23 Liver cellularity and steatosis. ....	249
Figure 6.24 Summary of changes in the bone marrow cell populations. ....	259
Figure 6.25 Summary of changes in the bone marrow and peripheral blood cell populations. ....	261
Figure 6.26 Further investigations into the effects of (+)-catechin on atherosclerosis regression. ....	266
Figure 7.1 Summary of key aims and objectives with outlines of experimental approach. ....	270

Figure 7.2 Summary of key findings <i>in vitro</i> . .....	272
Figure 7.3 Summary of key findings <i>in vivo</i> relating to atherosclerosis development and progression. ....	274
Figure 7.4 Summary of key findings <i>in vivo</i> relating to atherosclerosis regression.	276
Figure 7.5 Sources of reactive oxygen species in the vascular wall.....	280
Figure 7.6 Summary of possible future directions. ....	293

## Table of Tables

Table 1.1 Effects of key cytokines in atherosclerosis. ....	11
Table 1.2 Summary of key therapies for atherosclerosis and CVD. ....	26
Table 1.3 Summary of key types of nutraceutical agents.....	27
Table 1.4 Key observations in humans following intake of catechins.....	32
Table 2.1 Details of all materials used.....	43
Table 2.2 Markers used to identify immune cell populations within the peripheral blood. .....	70
Table 2.3 Details of antibodies used for immunophenotyping of peripheral blood cell populations.....	71
Table 2.4 Markers used to identify bone marrow stem/progenitor and immune cell populations.....	74
Table 2.5 Antibodies and reagents used for immunophenotyping of bone marrow cells. .....	76
Table 2.6 Details of antibodies used for immunofluorescence staining.....	82
Table 4.1 Parameters measured by the Mito Stress Test. ....	129
Table 4.2 Parameters measured by the Glycolytic Rate Assay.....	133
Table 4.3 Summary of changes in mitochondrial respiration induced by (+)-catechin. .....	149
Table 6.1 Summary of changes induced by chow intervention on atherosclerosis regression. ....	250
Table 6.2 Summary of key changes in the chow + group in comparison to the chow - group.....	251

## Abstract

*Introduction:* Cardiovascular disease arising from atherosclerosis persists as a major cause of global morbidity and mortality. Pharmacological therapies targeted to lipid management, such as statins, can be effective but have various limitations hence alternative avenues are required. Previous studies conducted in the host laboratory found (+)-catechin (an understudied flavanol) to exert various anti-inflammatory and anti-atherogenic effects on human monocytes/macrophages, and modulated several atherosclerosis risk factors in wild-type mice fed a high-fat diet (HFD) for 3 weeks. The aims of this study were hence to determine whether (+)-catechin can attenuate parameters associated with endothelial and smooth muscle cell (SMC) dysfunction, and to elucidate its effects on atherosclerosis development and progression, and, regression, in a mouse model.

*Methods:* Various *in vitro* assays were used to recapitulate endothelial and SMC dysfunction using human umbilical vein endothelial cells (HUVECs) and human aortic smooth muscle cells (HASMCs). Assays enabling the study of cellular bioenergetics and mitochondrial function were also used. *In vivo*, 8-week-old male *low-density lipoprotein receptor*-deficient (*Ldlr*<sup>-/-</sup>) mice were fed HFD alone or supplemented with (+)-catechin hydrate for 12 weeks to investigate atherosclerosis development and progression. For atherosclerosis regression, the same mice were fed HFD for 12 weeks to induce the formation of established lesions and then switched to chow alone or combined with (+)-catechin hydrate. Both protocols were followed up by detailed analyses of associated atherosclerosis risk factors and resulting atherosclerotic plaques in the aortic root.

*Results:* As part of the key findings, (+)-catechin consistently attenuated reactive oxygen species production in all investigated cell types, stimulated HASMC migration, and demonstrated protective effects on mitochondrial function. As part of the progression study, *Ldlr*<sup>-/-</sup> mice that had received (+)-catechin supplemented HFD for 12 weeks had attenuated plaque burden and inflammation, and enhanced plaque stability. As part of the regression study, intervention with (+)-catechin combined with chow reversed adiposity and hepatic injury, whilst plaque stability was enhanced (to a greater extent than chow intervention alone).

*Conclusions:* These data support the anti-atherogenic actions of (+)-catechin and its potential as an alternative preventative nutraceutical agent for atherosclerosis. Further studies are required to ascertain the mechanisms responsible for these beneficial observations in atherosclerosis development and progression. Future studies characterising the effect of (+)-catechin on atherosclerosis regression are also needed.

## **Acknowledgements**

First and foremost, I would like to thank my long-time supervisor, Professor Dipak Ramji, for the opportunity to complete my PhD in his lab. His continuous support, encouragement, as well as exemplary hard work and dedication to science, has greatly contributed to this project being as rewarding as it was productive. I am eternally grateful for everything I have learnt and achieved under your guidance.

I would also like to express my deepest thanks to Drs, Timothy Hughes, Joe Moss, Jessica Williams, Victoria O'Morain and Wijdan Alahmadi for taking the time to teach me various practical skills and techniques, as well as for your kindness and friendship. I also thank my fellow lab colleagues, both past and present, whom have all contributed to making this project such an enjoyable experience.

Lastly, I would like to thank my family and friends for their support and encouragement throughout my studies. Most of all, I thank my partner, Laurence, for his unwavering love, patience, support and encouragement throughout my university studies and especially during the final stages of this PhD.

## Publications

[1] Hayley Gallagher, Jessica O. Williams, Nele Ferekidis, Alaa Ismail, **Yee-Hung Chan**, Daryn R. Michael, Irina A. Guschina, Victoria Tyrrell, Valerie B. O'Donnell, John L. Harwood, Inna Khozin-Goldberg, Sammy Boussiba and Dipak P. Ramji. (2019). Dihomo- $\gamma$ -linolenic acid inhibits several key cellular processes associated with atherosclerosis. *Biochimica et Biophysica Acta - Molecular Basis of Disease* **1865**(9):2538-2550.

[2] Melanie L. Buckley, Jessica O. Williams, **Yee-Hung Chan**, Lucia Laubertová, Hayley Gallagher, Joe W. E. Moss and Dipak P. Ramji. (2019). The interleukin-33-mediated inhibition of expression of two key genes implicated in atherosclerosis in human macrophages requires MAP kinase, phosphoinositide 3-kinase and nuclear factor- $\kappa$ B signaling pathways. *Scientific Reports* **9**(1):11317.

[3] **Yee-Hung Chan** and Dipak P. Ramji. (2020). A perspective on targeting inflammation and cytokine actions in atherosclerosis. *Future Medicinal Chemistry* **12**(7):613-626.

[4] Joe W.E. Moss, Jessica O. Williams, Wijdan Al-Ahmadi, Victoria O'Morain, **Yee-Hung Chan**, Timothy R. Hughes, Juan B. Menendez-Gonzalez, Alhomidi Almotiri, Sue F. Plummer, Neil P. Rodrigues, Daryn R. Michael and Dipak P. Ramji. (2021). Protective effects of a unique combination of nutritionally active ingredients on risk factors and gene expression associated with atherosclerosis in C57BL/6J mice fed a high fat diet. *Food & Function* **12**(8):3657-3671.

[In Press] Victoria O'Morain, **Yee-Hung Chan**, Jessica O. Williams, Reem Alotibi, Alaa Alahmadi, Neil P. Rodrigues, Sue F. Plummer, Timothy R. Hughes, Daryn R. Michael and Dipak P. Ramji. The Lab4P consortium of probiotics attenuates atherosclerosis in LDL receptor deficient mice fed a high fat diet and causes plaque stabilization by inhibiting inflammation and several pro-atherogenic processes. *Molecular Nutrition & Food Research*. DOI: 10.1002/mnfr.202100214

[*Under Review*] Wijdan Al-Ahmadi, Thomas S. Webberley, Alex Joseph, Ffion Harris, **Yee-Hung Chan**, Reem Alotibi, Jessica O. Williams, Alaa Alahmadi, Thomas Decker, Timothy R. Hughes and Dipak P. Ramji. Pro-atherogenic actions of signal transducer and activator of transcription 1 serine 727 phosphorylation in LDL receptor deficient mice via modulation of plaque inflammation. *The FASEB Journal*.

[*In Production*] Review and methods-based chapters for *Methods in Molecular Biology on Atherosclerosis*:

- **Yee-Hung Chan** and Dipak P. Ramji. Atherosclerosis: pathogenesis and key cellular processes, current and emerging therapies, key challenges, and future research directions.
- **Yee-Hung Chan** and Dipak P. Ramji. Key roles of inflammation in atherosclerosis: mediators involved in orchestrating the inflammatory response and its resolution in the disease along with therapeutic avenues targeting inflammation.
- Dipak P. Ramji, **Yee-Hung Chan**, Alaa Alahmadi, Reem Alotibi and Nouf Alshehri. Survey of approaches for investigation of atherosclerosis *in vivo*.
- **Yee-Hung Chan**, Alaa Alahmadi, Reem Alotibi and Dipak P. Ramji. Evaluation of plaque burden and lipid content in atherosclerotic plaques.
- **Yee-Hung Chan**, Alaa Alahmadi, Reem Alotibi and Dipak P. Ramji. Monitoring cellularity and expression of key markers in atherosclerotic plaques.
- **Yee-Hung Chan** and Dipak P. Ramji. Investigation of mitochondrial bioenergetic profile and dysfunction in atherosclerosis.
- **Yee-Hung Chan** and Dipak P. Ramji. Probing inflammasome activation in atherosclerosis.

## List of Abbreviations

2-DG	2-Deoxyglucose
ABC	ATP binding cassette
ACAT	Acyl-coenzyme A acyltransferase
ACL	Adenosine triphosphate-citrate lyase
AF488	AlexaFluor 488
AHT	Anti-hypertensive treatment
Akt/PKB	Protein kinase B
AMPK	AMP-activated protein kinase
ANOVA	One way analysis of variance
AP-1	Activator protein-1
APC	Allophycocyanin
ApoB100	Apolipoprotein B100
ApoE	Apolipoprotein E
aSMA	Alpha smooth muscle actin
BCECF-AM	2', 7'-Bis(2-carboxyethyl)-5(6)-carboxyfluorescein tetrakis (acetoxymethyl) ester
BHF	British Heart Foundation
BrdU	5-Bromo-2'-deoxyuridine
BSA	Bovine serum albumin
CANTOS	Canakinumab Anti-Inflammatory Thrombosis Outcomes Study
CCL2	C-C motif chemokine ligand 2
CCR2	C-C chemokine receptor type 2
CD	Cluster of differentiation
CD40L	Cluster of differentiation 40 ligand
CE	Cholesteryl ester
CETP	Cholesterol ester transfer protein
CLP	Common lymphoid progenitor
CM	Chylomicron
CMP	Common myeloid progenitor
CMR	Chylomicron remnant
CRP	C-reactive protein

## List of Abbreviations

CSFE	Carboxyfluorescein diacetate succinimidyl ester
CV	Crystal violet
CVD	Cardiovascular disease
CXCL	C-X-C motif chemokine ligand
Cy7	Cyanine 7
DAMP	Damage-associated molecular pattern
DAPI	4', 6'-Diamidino-2-phenylindole
DCFDA	Dichlorofluorescein diacetate
DCFH	Dichlorodihydrofluorescein
DMEM	Dulbecco's Modified Eagle Medium
DMSO	Dimethyl sulfoxide
EC	Endothelial cell
ECAR	Extracellular acidification rate
ECG	(-)-Epicatechin-3-gallate
ECGM	Endothelial cell growth medium
ECM	Extracellular matrix
ECSCRI	European Cancer Stem Cell Research Institute
EDTA	Ethylenediaminetetraacetic acid
EFSA	European Food Safety Authority
EGC	(-)-Epigallocatechin
EGCG	(-)-Epigallocatechin-3-gallate
EGCM	Endothelial cell growth culture medium
eNOS	Endothelial nitric oxide synthase
EPA	Eicosapentaenoic acid
ER	Endoplasmic reticulum
ERK	Extracellular signal-related kinase
ETC	Electron transport chain
EV	Extracellular vesicle
FA	Fatty acid
FCCP	Carbonyl cyanide-4 (trifluoromethoxy) phenylhydrazone
FITC	Fluorescein isothiocyanate
GCG	(+)-Gallocatechin gallate
glycoPER	Glycolytic proton efflux rate
GM-CSF	Granulocyte-macrophage colony stimulating factor

## List of Abbreviations

GMP	Granulocyte-macrophage progenitor
HAOEC	Human aortic endothelial cell
HASMC	Human aortic smooth muscle cell
HBSS	Hanks Balanced Salt Solution
HDL	High-density lipoprotein
HDL-C	High-density lipoprotein cholesterol
HFD	High-fat diet
HI-FBS	Heat-inactivated foetal bovine serum
HL	Hepatic lipase
HMDM	Human monocyte-derived macrophage
HMG-CoA	3-Hydroxy-3-methyl-glutaryl-coenzyme-A
HPC	Haematopoietic progenitor cell
HRP	Horseradish peroxidase
HSC	Haematopoietic stem cells
HSPC	Haematopoietic stem and progenitor cell
HUVEC	Human umbilical vein endothelial cell
ICAM-1	Intercellular adhesion molecule-1
IDL	Intermediate density lipoprotein
IFN	Interferon
IL	Interleukin
IL-1Ra	Interleukin-1 receptor antagonist
JC-1	Tetraethylbenzimidazolylcarbocyanine iodide
JELIS	The Japan EPA Lipid Intervention Study
JNK	c-Jun N-terminal kinase
KLF	Kruppel-like factor
KO	Knock-out
LAL	Lysosomal acid lipases
LCAT	Lecithin-cholesterol acyltransferase
LDH	Lactase dehydrogenase
LDL	Low-density lipoprotein
LDL-C	Low-density lipoprotein cholesterol
LDLR	Low-density lipoprotein receptor
LFA1	Lymphocyte associated antigen 1
LMPP	Lymphoid-primed multipotent progenitor

## List of Abbreviations

LOX-1	Lectin-like oxidised low-density lipoprotein receptor
LPL	Lipoprotein lipase
LPS	Lipopolysaccharide
LXR	Liver X receptor
MACE	Major adverse cardiovascular events
MAPK	Mitogen-activated protein kinase
MCP-1	Monocyte chemoattractant/chemotactic protein-1
M-CSF	Macrophage-colony stimulating factor
MDA	Malondialdehyde
MDSC	Myeloid-derived suppressor cells
MEP	Megakaryocyte-erythroid progenitor
MI	Myocardial infarction
mitoROS	Mitochondrial reactive oxygen species
mmLDL	Minimally-modified low-density lipoprotein
MMP	Matrix metalloproteinase
MPP	Multipotent progenitors
mtDNA	Mitochondrial DNA
MYH	Myosin heavy chain
NAD	Nicotinamide adenine dinucleotide
NADPH	Nicotinamide adenine dinucleotide phosphate
NAFLD	Non-alcoholic fatty liver disease
NASH	Non-alcoholic steatohepatitis
NCD	Normal chow diet
NCEH	Neutral cholesterol ester hydrolase
NF- $\kappa$ B	Nuclear factor kappa-B
NK	Natural killer
NLR	Nucleotide-binding oligomerisation domain-like receptors
NLRP3	Nucleotide-binding oligomerisation domain leucine-rich repeat and pyrin domain containing protein 3
NO	Nitric oxide
NOD	Nucleotide-binding oligomerisation domain
NOX	Nicotinamide adenine dinucleotide phosphate oxidase
NPC1L1	Neimann-Pick C1-like 1
OCR	Oxygen consumption rate

## List of Abbreviations

OCT	Optimum cutting temperature
ORO	Oil Red O
oxLDL	Oxidised low-density lipoprotein
PAMP	Pathogen-associated molecular pattern
PBMC	Peripheral blood mononuclear cell
PBS	Phosphate buffered saline
PCSK9	Proprotein convertase subtilisin/kexin 9
PDGF	Platelet-derived growth factor
PDGFR	Platelet-derived growth factor receptor
PE	Phycoerythrin
PECAM-1	Platelet endothelial cell adhesion molecule-1
PER	Proton efflux rate
PerCP	Peridinin-chlorophyll-protein
PFA	Paraformaldehyde
PI3K	Phosphatidylinositol 3-kinase
PL	Phospholipid
PMA	Phorbol 12-myristate 13-acetate
PREDIMED	Prevencion con Dieta Mediterranea
PRR	Pattern recognition receptor
PSGL	P-selectin glycoprotein ligand
PUFA	Polyunsaturated fatty acid
RCT	Reverse cholesterol transport
REDUCE-IT	Reduction of Cardiovascular Events with Icosapent Ethyl-Intervention Trial
RNA-seq	RNA-sequencing
RNS	Reactive nitrogen species
ROS	Reactive oxygen species
Rot/AA	Rotenone/antimycin A
RPMI	Rosewell Park Memorial Institute
RT-qPCR	Real-time quantitative PCR
Sca	Stem cell antigen
scRNA-seq	Single-cell RNA-sequencing
SDS	Sodium dodecyl sulphate
SEM	Standard error of the mean

## List of Abbreviations

SHR	Spontaneously hypertensive rats
SLAM	Signalling lymphocyte activation molecule
SMC	Smooth muscle cell
SMCM	Smooth muscle cell medium
SR	Scavenger receptor
SR-B1	Scavenger receptor class B, type 1
SREBP	Sterol regulatory element-binding protein
STAT	Signal transducer and activator of transcription
TBA	Thiobarbituric Acid
TBARS	Thiobarbituric Acid Reactive Substances
TBHP	Tert-butyl hydrogen peroxide
TCA	Tricarboxylic acid
TG	Triglyceride
TGF	Transforming growth factor
T <sub>h</sub>	Helper T cell
TIMP	Tissue inhibitor of matrix metalloproteinase
TLR	Toll-like receptor
TNF	Tumour necrosis factor
T <sub>reg</sub>	Regulatory T cell
TRL	Triglyceride-rich lipoproteins
VCAM-1	Vascular cell adhesion molecule-1
VEGF	Vascular endothelial growth factor
VLA4	Very late antigen 4
VLDL	Very low-density lipoprotein
VSMC	Vascular smooth muscle cell
WHO	World Health Organisation
WT	Wild-type

# 1 General Introduction

## 1.1 Cardiovascular disease: an on-going burden

Cardiovascular disease (CVD) remains the leading cause of global mortality and morbidity in modern civilisation, being responsible for approximately 7.9 million deaths each year according to the World Health Organisation (WHO). CVD is an umbrella term used to describe the collective pathologies affecting the heart and circulatory system. In the UK alone, 27% of all deaths are attributed to CVD, with around 7.4 million people affected according to British Heart Foundation (BHF) statistics, 2021. Unfortunately, the prevalence of CVD is only expected to rise owing to an increase in risk factors, such as diabetes and obesity, attributed to widespread adaptation of the 'westernised' lifestyle. Atherosclerosis, a chronic inflammatory disorder of the vasculature, is the key underlying cause of CVD, and characterised by the formation of fibrous plaques within the arterial wall (Frostedgard 2013). The formation of atherosclerotic lesions arises from intimal lipid accumulation which instigates the recruitment of monocytes and lymphocytes, resulting in the formation of lipid-laden foam cells derived from macrophages and vascular smooth muscle cells (SMCs; VSMCs). Foam cell death resulting from excess intracellular cholesterol retention-mediated dysfunction and subsequent stress responses, leads to the formation of a necrotic core. As the plaque progresses, the continued migration and proliferation of VSMCs and their synthesis of extracellular matrix proteins (ECM) results in the formation of a fibrous cap that encapsulates and stabilises the plaque. Progression and evolution of the atherosclerotic plaque occurs over decades, and atherosclerosis is usually asymptomatic until the late stages, where the plaque reaches a sizeable volume (detrimentally reducing the space available for blood flow through the arterial lumen), and eventually ruptures, causing acute thrombosis. Clinically, this manifests most commonly as myocardial infarction (MI; heart attack) or cerebrovascular accident (stroke), with other, consequences including coronary (ischaemic) heart disease and peripheral vascular disease (Virani et al. 2021). Improvements in healthcare and medical developments have meant prolonged life expectancies of the general population; however, this coincides with increasing occurrence of chronic diseases in the increasingly ageing population (Libby 2021). Although statins have had substantial impact on reducing mortality rates, the prevailing risk of primary and secondary major

cardiovascular events (MACE) occurring post therapy, combined with issues such as adverse side effects, have encouraged the exploration of alternative therapies. The high prevalence of CVD and the substantial burden it poses on healthcare systems has hence fuelled much of past and continuing research into alternative preventative/therapeutic avenues for atherosclerosis. (McLaren et al. 2011; Ramji and Davies 2015; Chan and Ramji 2020)

### 1.2 An overview of lipid metabolism

Amongst the various risk factors for atherogenesis, hyperlipidaemia is particularly important and relevant in today's population, arising from elevated levels of cholesterol, especially low-density lipoprotein (LDL) cholesterol (LDL-C), and triglyceride (TG; triacylglycerol), including triglyceride-rich lipoproteins (TRLs). Dyslipidaemia, whether associated with dietary intake or genetic predisposition (e.g., familial hypercholesterolaemia), is hence a key risk factor for atherosclerosis initiation, and many developed therapies are aimed at restoring a 'normal' lipid profile to combat cardiovascular risk. Lipid metabolism is regulated by the sterol regulatory element-binding protein (SREBP) family of transcription factors, which activates the expression of specific genes involved in the synthesis and uptake of cholesterol, fatty acids (FAs), TG and phospholipids (PL), regulating lipid biosynthesis and adipogenesis (Horton et al. 2002; Buckley and Ramji 2015). The majority of endogenous cholesterol, ~75-80%, is obtained via *de novo* synthesis (which occurs mainly in the liver but also in peripheral tissues), whereas ~20-25% is of dietary origin (Phan et al. 2012). A high intake of saturated fats (i.e., excessive calories) can result in increased circulating cholesterol levels (i.e., hypercholesterolaemia) (Smart et al. 2011).

Cholesterol is transported in the bloodstream via specific and specialised lipoproteins and TG, which act as transport mediums for lipids due to their insolubility in the plasma (Buckley and Ramji 2015). Lipoprotein particles are comprised of a core region (which stores TGs and cholesteryl esters (CEs)), and a surrounding polar region (which consists of PLs, apolipoproteins and free cholesterol) (Buckley and Ramji 2015). Lipoproteins exist in various forms that are involved in select processes within lipid trafficking, which is facilitated by the exchange of various apolipoproteins (Buckley and Ramji 2015). Chylomicrons for example, facilitate the delivery of dietary TGs from the

intestine to cells of the periphery. Lipoprotein lipase (LPL) is responsible for the digestion of TGs within chylomicrons, resulting in the production of non-esterified FAs and 2-monoacyl glycerol, which may be utilised for energy in skeletal muscle or stored as TG in adipose tissue, for example (McLaren et al. 2011). Specific receptors then enable the chylomicron remnants to be procured by the liver to be metabolised (Tomkin and Owens 2012). Very low-density lipoproteins (VLDLs) are implicated in the transportation of TGs synthesised by the liver (McLaren et al. 2011). LPL and hepatic lipase mediate the hydrolysis of TG in VLDL, forming intermediate density lipoprotein (IDL) (McLaren et al. 2011). Hepatic lipase carries out additional processing and hydrolysis of TGs in IDL, resulting in the formation of LDL (McLaren et al. 2011). LDL is responsible for the transportation of cholesterol from the liver to cells of the peripheral tissues, where it is taken up by receptor-mediated endocytosis via its cognate receptor, the low-density lipoprotein receptor (LDLR; mediated by apolipoprotein B100 (apoB100) contained within the LDL), into the cell (Buckley and Ramji 2015). Cholesterol is susceptible to different types of enzymatic modification, including hydroxylation and esterification within the endoplasmic reticulum (ER), which results in the production of oxysterols and sterol esters, respectively (Michael et al. 2012b; Ono 2012; Phillips 2014). Esterification decreases its solubility and encourages the storage of cholesterol molecules within cytoplasmic lipid droplets (Michael et al. 2012b; Ono 2012; Phillips 2014).

Cells possess homeostatic mechanisms to protect against lipid overload, which act to incite cholesterol efflux and modulate the inflammatory response. This is necessary as excess intracellular cholesterol is cytotoxic and promotes ER stress, and so must be removed from the cell. This is predominantly via two routes; conversion to a more soluble, transportable form, or reverse cholesterol transport (RCT). The latter is the predominant pathway that mediates the removal of excess cholesterol for excretion from the liver via the bile system. The generation of oxysterols and desmosterol from excess cholesterol can activate liver-X receptors (LXRs), resulting in the expression of lipid efflux transporters and subsequently excretion via RCT (Michael et al. 2012a; Spann et al. 2012). Additionally, cholesterol loading within macrophages stimulates autophagy, which involves the sequestering of intracellular contents by double-membrane vacuoles; fusion with secondary lysosomes targets them for degradation and ultimately, RCT. High-density lipoprotein (HDL) clears the cholesterol effluxed

## Chapter 1: General Introduction

from cells in the periphery by mediating its transport to the liver for excretion via RCT. Cholesterol is effluxed from cells via action of lipid transporters, including ATP-binding cassette (ABC)-A1 (ABCA1) and -G1 (ABCG1), leading to its release from the plasma membrane (McLaren et al. 2011; Michael et al. 2013; Phillips 2014). The lipid transporters facilitate movement of cholesterol from peripheral cells to designated extracellular acceptors, including HDL and associated apolipoproteins, which transport the cholesterol to the liver, where it is converted to bile salts for excretion (Michael et al. 2012b; Ono 2012; Phillips 2014). For example, produced in the liver and by macrophages, apolipoprotein E (apoE) is a key component of lipoprotein particles, acting as a ligand for lipoprotein receptors and contributing to cholesterol efflux (Lusis 2000; Greenow et al. 2005; Mahley 2016). Additional HDL lipidation and maturation in the plasma is followed by eventual hepatic uptake, as scavenger receptor (SR) class B type 1 (SR-B1) binds the mature HDL, and subsequent cholesterol removal via catabolism and excretion (Trigatti et al. 2000a; Trigatti et al. 2000b). The LDL is endocytosed via the LDLR into hepatocytes, resulting in its clearance from the plasma, as summarised in Figure 1.1. Therefore, both LDLR and apoE are vital for the clearance of circulating LDL-C and maintaining cholesterol homeostasis. (McLaren et al. 2011)

## Chapter 1: General Introduction

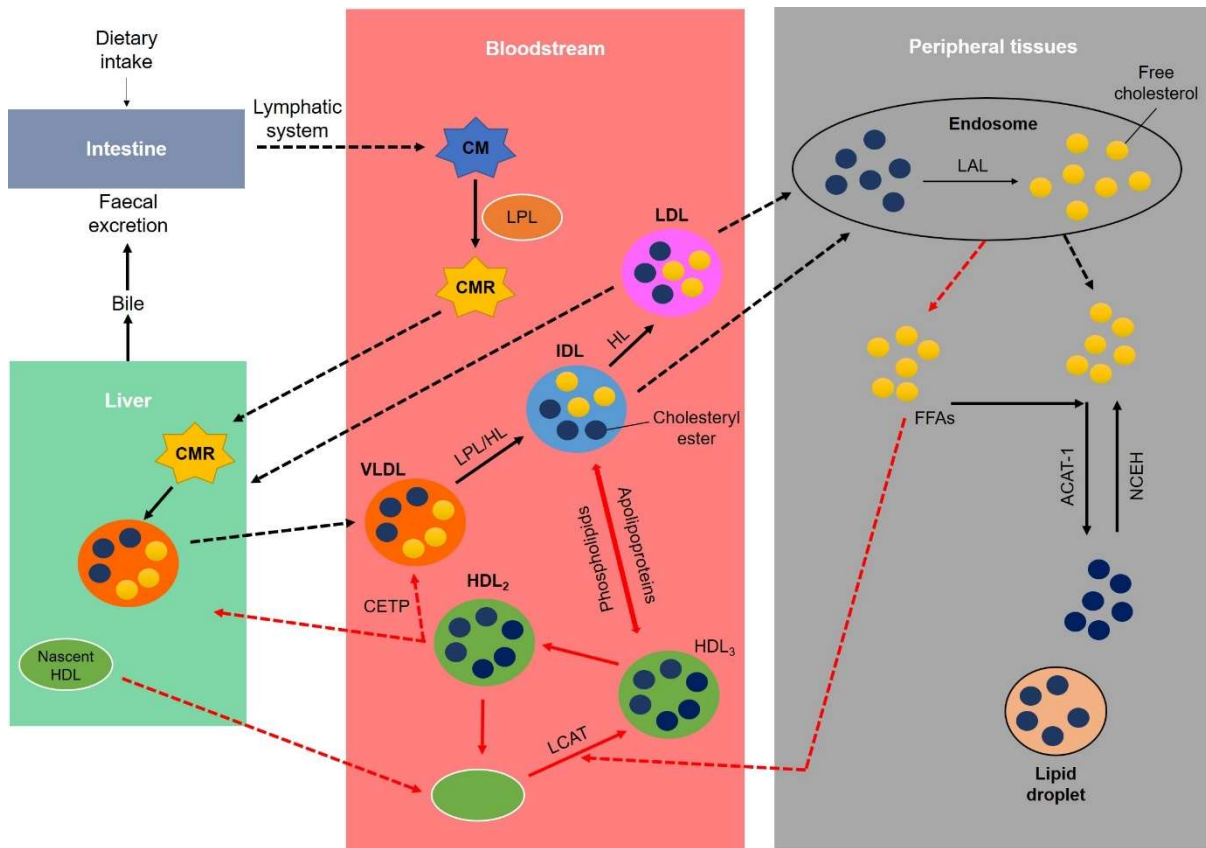


**Figure 1.1 Simplified overview of lipid metabolism.**

Dietary lipids are absorbed in the intestine and are transported by CMs to peripheral tissues. Lipolysis by lipases precedes delivery of the dietary lipids to the liver by CMRs. VLDLs derived from the liver facilitate the transport of endogenously synthesised lipids. CMs are transported in the lymphatic system to the circulation where LPL (present on the surface of endothelial cells) hydrolyses the TG component to FFAs and 2-monoacyl glycerol for utilisation by peripheral tissues. The resulting CMRs are taken up by the liver via their receptors and packaged with apoB100, cholesterol and CEs, forming VLDL (which contains apolipoproteins B and E3), which is then transferred to the blood. Here, the VLDL acquires various apolipoproteins from circulating HDL, and is hydrolysed into IDL via the actions of LPL and HL in a process that involves the hydrolyses of TG and transfer of PLs and apolipoproteins back to HDL. Further HL-mediated hydrolysis of TG and loss of more apolipoproteins enables the conversion of HDL into LDL. Both IDL and LDL are then transported to peripheral tissues or the liver where they are endocytosed via LDL receptors. RCT is the main route for the return of cholesterol from peripheral tissues to the liver (highlighted with red arrows). This process begins with the synthesis of HDL within the liver and its secretion into the bloodstream as a complex with ApoA-I. Nascent HDL then sequesters free cholesterol effluxed from cells via cell surface efflux transporters. Esterification of accumulated free cholesterol by LCAT facilitates the conversion of the HDL into HDL<sub>3</sub> particles which transfer part of its CE content to CMs and VLDL, simultaneously acquiring apolipoproteins. This results in their transformation into mature HDL<sub>2</sub> particles. Cholesterol is returned to the liver mainly via LDLR-mediated uptake of HDL<sub>2</sub> particles; selective trafficking of HDL CEs via SR-B1 or CETP-mediated transfer of CEs to LDL particles, which are subject to LDLR-mediated endocytosis. The CEs are hydrolysed to cholesterol in the liver, enabling excretion as bile acids and as neutral steroids in bile. Abbreviations: CMR, chylomicron remnants; HDL, high-density lipoprotein; CM, chylomicron; LDL, low-density lipoprotein; IDL, intermediate-density lipoprotein; HL, hepatic lipase; LPL, lipoprotein lipase; CETP, cholesterol ester transfer protein; LCAT, lecithin-cholesterol acyltransferase; HDL, high-density lipoprotein; LAL, lysosomal acid lipases; ACAT, acyl-coenzyme A acyltransferase; FFA, free fatty acid; NCEH, neutral cholesterol ester hydrolase; apo, apolipoprotein.

*LDLR* and *APOE* knock-out (KO)/deficient mice have been widely used as animal models of atherosclerosis. This genetic manipulation is necessary since mice are naturally resistant to atherosclerosis, as cholesterol is transported via HDL particles (Getz and Reardon 2005,2012; Emini Veseli et al. 2017). *Apo<sup>e</sup><sup>-/-</sup>* mice can develop atherosclerosis spontaneously on a standard chow diet, though this can be accelerated by feeding with a high-fat diet (HFD), whereas *Ldlr<sup>-/-</sup>* mice develop little or no atherosclerosis and require feeding with such an atherogenic diet to induce the formation of established lesions (Getz and Reardon 2012; Emini Veseli et al. 2017; Oppi et al. 2019). This results in hypercholesterolaemia associated with elevated circulating levels of VLDL in *Apo<sup>e</sup><sup>-/-</sup>* mice, and LDL in *Ldlr<sup>-/-</sup>* mice (Getz and Reardon 2012; Emini Veseli et al. 2017). Various studies conducted in these mouse models of atherosclerosis have provided important mechanistic insights to the pathogenesis of the disease, as well as therapeutic avenues.

### 1.3 Pathophysiology of atherosclerosis

Atherosclerosis initiates predominantly at the sites of bifurcations and inner curvatures which are prone to disturbed laminar flow (Vanderlaan et al. 2003), as well as being associated with persistent low-grade inflammation (Jongstra-Bilen et al. 2006). Atherosclerosis is a chronic inflammatory disorder of the medium and large arteries that develops over a prolonged period, although this process may not be linear or continuous (Libby 2021). Generally, however, growth of the atherosclerotic plaque results in progressive occlusion of the lumen, and hence disrupted arterial blood flow (Figure 1.2). Plaque rupture results in acute thrombosis, where the anatomical location of the thrombus within the vascular bed dictates the clinical manifestation. For example, coronary syndromes (including MI or angina pectoris) if affecting the circulatory system of the heart itself, whilst disruption of peripheral arteries can result in gangrene (Libby et al. 2019a). In general, the aetiology and progression of atherosclerosis is complex and yet to be fully understood. The high prevalence of atherosclerosis-associated morbidity and mortality has fuelled continued research devoted to uncovering its underlying mechanisms and in the identification of novel preventative/therapeutic avenues.

## Chapter 1: General Introduction

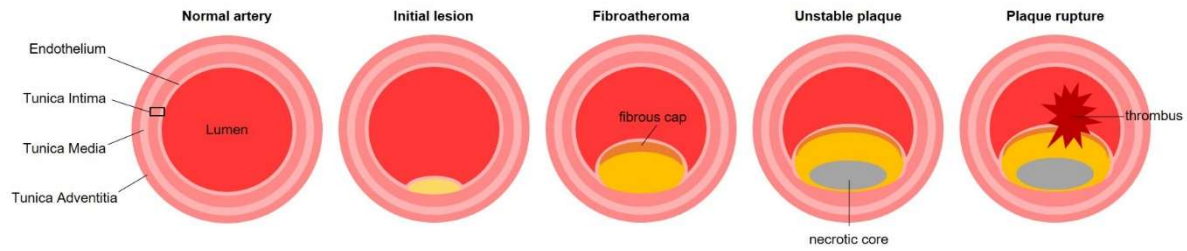


**Figure 1.2 Overview of the progression of atherosclerosis.**

A normal artery consists of 4 major layers that constitute the arterial wall; the endothelium (a monolayer of endothelial cells), the tunica intima (consists of the endothelium and internal elastic membrane), the tunica media (consists mostly of vascular smooth muscle cells), and the outermost tunica adventitia layer (consists of collagen and elastic fibres). Growth of the atherosclerotic plaque and the necrotic core within (due to increasing cell death) leads to progressive occlusion, as the narrowing lumen increasingly disrupts blood flow. Degradation and continued inflammation of the fibrous cap that encapsulates the atherosclerotic plaque leads to plaque rupture and acute thrombosis, commonly resulting in heart attack or stroke.

### 1.3.1 Endothelial dysfunction

Atherogenesis begins with the endothelium, a continuous, single layer of endothelial cells (ECs) that form the barrier between circulating blood and the arterial wall. Normal endothelial function is vital in maintaining cardiovascular homeostasis and the endothelium has various functions, as described in Figure 1.3 For example, ECs regulate vascular tone as well as various anti-inflammatory, anti-oxidative and homeostatic responses. The regulation of vascular tone is mediated via the production of various factors, such as nitric oxide (NO; also known as 'endothelium-dependent relaxing factor'), a vasodilator of VSMCs (Sandoo et al. 2010), and endothelium-dependent contracting factor. Endothelial NO synthesis is mediated by enzymatic activity of endothelial NO synthase (eNOS) from its precursor, L-arginine (Palmer et al. 1988). The caveolin-1 protein binds to calmodulin, inhibiting eNOS activity; binding of calcium to calmodulin causes displacement of caveolin-1, resulting in eNOS activation and subsequently, NO production (Kuchan and Frangos 1994). This process also involves the cofactors, nicotinamide adenine dinucleotide phosphate (NADPH) and tetrahydrobiopterin (Forstermann and Sessa 2012). Basal NO production by ECs hence facilitates the regulation of vasomotor tone, along with the preservation of non-thrombogenic behaviour (Davignon and Ganz 2004; Gimbrone Jr and Garcia-Cardena 2016). ECs are continually exposed to various types of shear stress induced by the flow of circulating blood; this is sensed by mechanosensing complexes (present on EC membranes), which transduce the mechanosignal to the ECs (Fang et al. 2019).

In normal homeostatic conditions, the endothelium does not recruit circulating leukocytes in the bloodstream (Libby 2021). However, exposure of ECs to atherogenesis-provoking stimuli associated with cardiovascular risk factors (e.g., changes in blood flow patterns leading to altered mechanotransduction), causes their activation, resulting in the gathering of blood leukocytes (Libby 2021). Key risk factors for atherosclerosis, such as elevated LDL-C, hypertension, inflammation and oxidative stress, can all disrupt endothelial homeostasis and encourage endothelial activation/dysfunction (Ramji and Davies 2015).

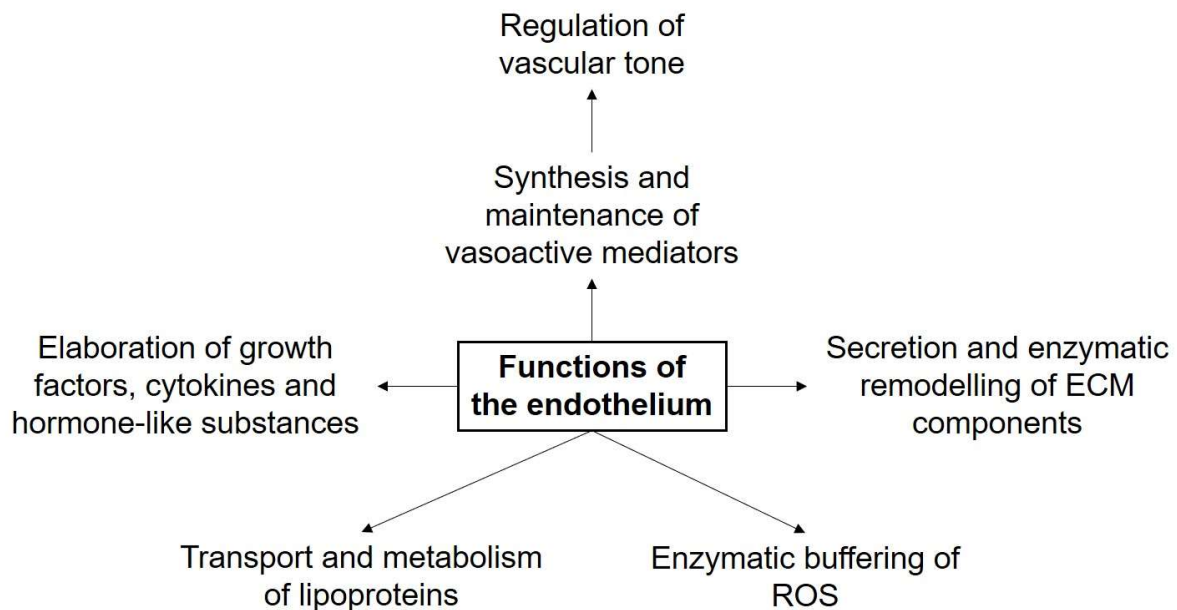


**Figure 1.3 Biological functions of the endothelium**

Abbreviations: ECM, extracellular matrix; ROS, reactive oxygen species.

Endothelial damage disrupts the balance between vasoconstriction and vasodilation, and stimulates processes that promote atherogenesis and atherosclerosis progression, such as enhanced endothelial permeability, platelet aggregation, leukocyte adhesion and cytokine generation (Ross 1999). Endothelial injury can be induced by various noxious substances, for example oxidised cholesterol, toxins in cigarette smoke, hyperglycaemia and altered haemodynamic forces (such as hypertension-induced disturbances/alterations in normal blood flow). Hence metabolic syndrome, which describes the combination of Type II diabetes mellitus, hypertension and obesity, non-alcoholic fatty liver disease (NAFLD) and atherosclerosis (and other conditions that may arise as a consequence of hyperlipidaemia) are closely associated

and tend to occur as co-morbidities (Lonardo et al. 2018). Increased levels of LDL-C in the plasma increases the risk of its infiltration to the arterial wall; recent evidence supports the role of SR-B1 in the delivery of LDL particles to the intima via EC LDL transcytosis (Huang et al. 2019), although these particles may also infiltrate the arterial wall via passive diffusion (McLaren et al. 2011). Increased endothelial permeability that occurs in association with endothelial dysfunction also aids the infiltration of circulating lipoproteins and immune cells into the sub-endothelial layer. The apoB within LDL encourages its aggregation and retention within the subendothelial space, promoting further endothelial dysfunction and a subsequent immune response (McLaren et al. 2011). The key initiating step of atherogenesis, endothelial dysfunction, is characterised by various changes, such as reduced NO synthesis (and endothelium-dependent vasodilation), enhanced reactive oxygen species (ROS) production, hyperpermeability, and increased expression of pro-inflammatory mediators (e.g., cytokines and chemokines) and adhesion molecules by ECs (Davignon and Ganz 2004; Sitia et al. 2010; Gimbrone Jr and Garcia-Cardena 2016). These include vascular cell adhesion molecule (VCAM)-1 (which binds monocytes and T cells) and intercellular adhesion molecule (ICAM)-1 (which binds other leukocytes) (Sitia et al. 2010; Gimbrone Jr and Garcia-Cardena 2016). Together, these changes promote the recruitment and infiltration of circulating leukocytes (e.g., monocytes, T cells, neutrophils and B cells), which adhere and 'roll' on the endothelium, as per the leukocyte adhesion cascade, to the site of LDL retention (Koenen and Weber 2010; Weber and Noels 2011; Moore et al. 2013; Zerneck and Weber 2014) (Figure 1.4). Monocyte chemoattractant/chemotactic protein (MCP)-1, also known as 'C-C motif chemokine ligand 2' (CCL2) whose action is mediated via its receptor, C-C chemokine receptor type 2 (CCR2), is the key chemokine responsible for the recruitment of circulating monocytes to the site of intimal LDL accumulation, and is generated by monocytes/macrophages, ECs and VSMCs (Deshmane et al. 2009). Dyslipidaemia and inflammation are hence interlinked, as the retention and accumulation of LDL within the arterial wall instigates and perpetuates chronic inflammation.

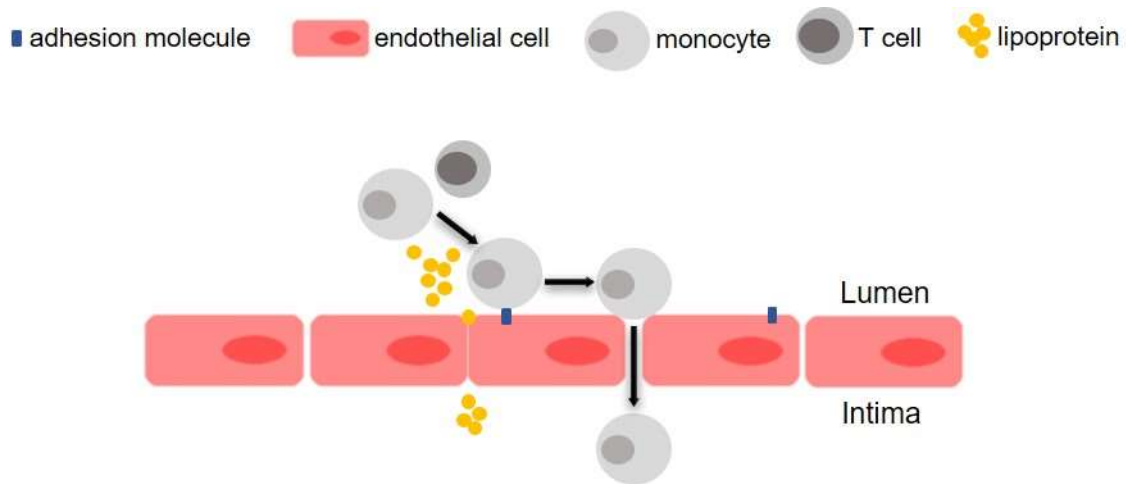


**Figure 1.4 Lipoprotein and immune cell infiltration.**

The aggregation and retention of lipoprotein in the intima instigates endothelial dysfunction; increased permeability and expression of adhesion molecules and pro-inflammatory mediators by activated endothelial cells (and other resident vascular cells) facilitates the recruitment and *trans*-endothelial diapedesis of circulating blood leukocytes (e.g., monocytes and T cells). Scavenger receptor class B type 1 facilitates delivery of LDL to the arterial intima where apolipoprotein B encourages its aggregation and retention, stimulating an immune response.

### 1.3.2 Inflammation: the key driver of atherosclerosis pathogenesis

Although mechanisms underlying chronic, unresolving vascular inflammation in atherosclerosis are not completely understood, it is generally accepted that the accumulated mediators within the arterial wall perpetuates chronic low-grade inflammation to further pathogenesis. The immune system (both innate and adaptive responses) is regulated by cytokines, a large group of proteins subdivided into various classes, including interleukins (IL), chemokines, tumour necrosis factors (TNF) and interferons (IFN) (Ait-Oufella et al. 2011; Ramji and Davies 2015). The balance of anti- and pro-inflammatory cytokines is vital for the maintenance of cardiovascular health and homeostasis. In atherosclerosis, this balance is tipped in favour of pro-inflammatory cytokines resulting in incessant and amplified inflammation, which, unsurprisingly, has been positively associated with plaque rupture risk (Libby et al. 2009; Lichtman et al. 2013; Hansson et al. 2015; Nus and Mallat 2016). The actions of key anti- and pro-inflammatory mediators in atherosclerosis are summarised in Table 1.1.

**Table 1.1 Effects of key cytokines in atherosclerosis.**

<b>Cytokine</b>	<b>Key actions</b>
<i>Pro-inflammatory/atherogenic</i>	
IL-1 $\beta$	Produced by various cells Inducer of M1 macrophage polarisation Stimulator of cell proliferation and differentiation, and release of matrix degrading enzymes
IL-2	Produced by T <sub>h1</sub> cells Further activates T <sub>h</sub> cells and affects expansion of T <sub>regs</sub>
IL-4	Produced by ECs, and T <sub>h2</sub> and B cells Induces inflammation via upregulation of various pro-inflammatory mediators, including cytokines, chemokines and adhesion molecules by ECs May also have anti-inflammatory actions
IL-6	Produced by macrophages, ECs and others Induced by IL-1 signalling, stimulates production of CRP in the liver
IL-12	Regulates differentiation of T <sub>h1</sub> cells Inducer of IFN- $\gamma$ production with IL-18
IL-18	Produced by NLRP3 inflammasome along with IL-1 $\beta$ Upregulates IFN- $\gamma$ production
TNF- $\alpha$	Produced by T <sub>h1</sub> and myeloid cells e.g., monocytes and macrophages Pleiotropic cytokine Promotes ROS production, upregulates expression of adhesion molecules (e.g., ICAM-1, VCAM-1) and MCP-1, encouraging endothelial dysfunction
IFN- $\gamma$	Produced by monocytes/macrophages, T <sub>h1</sub> , NK and CD8 <sup>+</sup> T cells Promotes SR-A expression and foam cell formation by reducing expression of efflux transporters, promoting foam cell apoptosis Activates macrophages, CD8 <sup>+</sup> T cells, B cells etc. Inducer of M1 macrophage polarisation
MCP-1	Mobilisation of monocytes from the bone marrow and recruitment of neutrophils Major chemokine that mediates monocyte recruitment during atherogenesis
CXCL1	Also known as growth related oncogene $\alpha$ (GRO- $\alpha$ ) Chemoattractant for monocytes, T cells and neutrophils involved in recruitment of leukocytes to the vessel wall Facilitates atherosclerosis progression in response to lysophosphatidic acid
<i>Anti-inflammatory/atherogenic</i>	
IL-5	Produced by T <sub>h2</sub> cells and mast cells Stimulates production of anti-oxLDL antibodies (IgM) by B cells
IL-10	Produced by M2 macrophages and T <sub>regs</sub> Suppresses activation of T <sub>h1</sub> cells and macrophages Regulates TNF- $\alpha$ production and endothelial ICAM-1 expression
IL-33	Attenuates foam cell formation Reduces expression of adhesion molecules e.g., ICAM-1 and MCP-1
IL-35	Produced by T <sub>regs</sub> and B cells Regulates expression of anti-inflammatory molecules Induces T <sub>regs</sub>
TGF- $\beta$	Produced by M2 macrophages and T <sub>regs</sub> Inhibits proliferation, activation and differentiation of T <sub>h</sub> cells

Key actions of various mediators in atherosclerosis and their key sources are described (Tedgui and Mallat 2006; Ait-Oufella et al. 2011; Ramji and Davies 2015; Fatkhullina et al. 2017). Abbreviations: IL, interleukin; TNF, tumour necrosis factor; IFN, interferon; ICAM-1, intercellular adhesion molecule-1; VCAM-1, vascular cell adhesion molecule-1; MCP, monocyte chemotactic/chemoattractant protein;

## Chapter 1: General Introduction

CXCL1, C-X-C motif chemokine ligand 1; TGF, transforming growth factor; EC, endothelial cell; NK, natural killer; T<sub>h</sub>, helper T; T<sub>reg</sub>; regulatory T cell; SR, scavenger receptor; oxLDL, oxidised low-density lipoprotein; Apoe; apolipoprotein E; ROS, reactive oxygen species; CRP, C-reactive protein; NLRP3; nucleotide-binding oligomerisation domain leucine-rich repeat and pyrin domain containing protein 3.

All cell types present within atherosclerotic lesions are capable of producing cytokines whilst also being susceptible to their effects, contributing to the inflammatory burden through a range of mechanisms. For example, macrophages, lymphocytes, natural killer (NK) cells and VSMCs are all capable of secreting potent pro-inflammatory cytokines, TNF- $\alpha$ , IL-1 and IL-6 (Tedgui and Mallat 2006). Both TNF- $\alpha$  and IL-1 signalling can augment the expression of other cytokines and adhesion molecules, encouraging interactions between circulating immune cells in the blood to the activated endothelium, along with the migration and mitogenesis of both VSMCs and ECs (Tousoulis et al. 2016). Both IFN- $\gamma$  and TNF- $\alpha$  can promote foam cell formation as well as endothelial permeability by stimulating reorganisation of actin and tubulin cytoskeletons of ECs, to widen the gap between adjacent cells (Pober and Sessa 2007). Therefore, TNF- $\alpha$  is implicated in numerous key pro-atherogenic processes and its elevation enhances endothelial dysfunction to promotes atherogenesis, which has been supported by abundant *in vivo* evidence (Zhang et al. 2009). Indeed, deficiency in potent pro-inflammatory cytokines, such as IL-1 $\beta$  and TNF- $\alpha$ , in various mouse models of atherosclerosis has been shown to retard atherosclerosis development and enhancement of the expression of these has demonstrated the reverse (Ramji and Davies 2015; Moss and Ramji 2016a). However, the comprehensive actions and effects of all cytokines implicated in atherosclerosis still requires elucidation, with some cytokines not being strictly pro- or anti-atherogenic (such as in the case of IL-4).

Activated ECs secrete various pro-inflammatory mediators that facilitate the recruitment of blood leukocytes, including MCP-1, IL-1 and IL-8, and their enhanced expression of adhesion molecules, such as ICAM-1 and VCAM-1, facilitate the binding of these immune cells to the endothelium (Li and Glass 2002). Specifically, monocyte-endothelial adhesion involves the binding of the adhesion molecules expressed by ECs to the integrins on the monocytes; VCAM-1 binds to very late antigen 4 (VLA4), and ICAM-1 binds to lymphocyte function-associated antigen 1 (LFA1) (Ley et al. 2007; Moore et al. 2013; Soehnlein et al. 2013). Platelet EC adhesion molecule-1

(PECAM-1), VCAM-1 and chemokines produced by other cell types residing in the lesion (e.g., SMCs and emigrated leukocytes) collectively facilitate the transmigration of monocytes across the endothelium and into the intima layer (Ley et al. 2007; Moore et al. 2013; Soehnlein et al. 2013). Here, the monocytes are stimulated to differentiate into macrophages by granulocyte-macrophage colony stimulating factor (GM-CSF) and macrophage-colony stimulating factor (M-CSF) (Li and Glass 2002; Mantovani et al. 2009).

### 1.3.3 Macrophage heterogeneity in atherosclerosis

Macrophages are heterogeneous, highly plastic cells that are sensitive to the local signals and stimuli present in their microenvironment (Koelwyn et al. 2019). As such, macrophages can be triggered to polarise into different subsets now understood to go far beyond the basic M1 (classically activated, pro-inflammatory) and M2 (alternatively activated, anti-inflammatory) classes (Shirai et al. 2015). M-CSF-induced monocyte differentiation, along with exposure of macrophages to IFN- $\gamma$ , IL-1 $\beta$  and lipopolysaccharide (LPS), promotes polarisation and activation of the M1 phenotype (Khallou-Laschet et al. 2010; Moss and Ramji 2016a). IFN- $\gamma$  also promotes M1 polarisation via the signal transducer and activator of transcription (STAT)-1 signalling (Shirai et al. 2015). Macrophages express pattern recognition receptors (PRRs) that include SRs, Toll-like receptors (TLRs) and nucleotide-binding oligomerisation domain (NOD)-like receptors (NLRs) that are involved in foam cell formation and/or the stimulation of an inflammatory response against foreign particles or endogenously generated danger signals (McLaren et al. 2011; Moore et al. 2013). A characteristic of M1 macrophages include the production of pro-inflammatory cytokines, such as IL-6, IL-12 and TNF- $\alpha$ , which stimulates ROS production that promotes oxidative stress, furthering endothelial dysfunction (Zhang et al. 2009; Ramji and Davies 2015). M1 macrophages also contribute to T helper-1 (T<sub>H1</sub>) responses (Mantovani et al. 2009). On the contrary, M2 macrophages have athero-protective functions, including production of anti-inflammatory cytokines IL-10 and transforming growth factor (TGF)- $\beta$ . However, in atherosclerotic plaques, M1 macrophages predominate over M2 macrophages, and so pro-inflammatory processes overwhelm anti-inflammatory

actions, favouring inflammation over its resolution. A summary of M1 and M2 macrophage characteristics is illustrated in Figure 1.5.

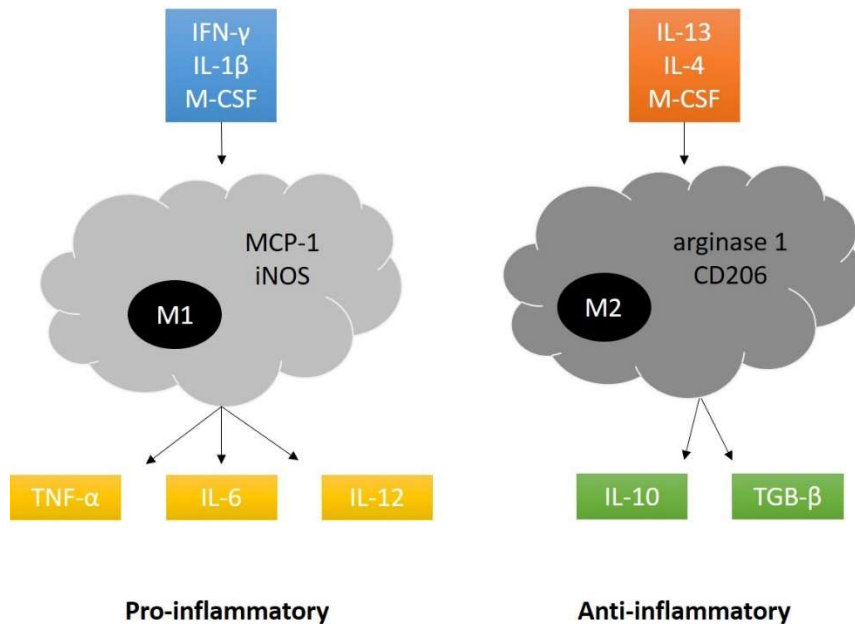


**Figure 1.5 Comparison of the characteristics of M1 and M2 macrophages.**

Different mediators can induce the differential polarisation of macrophages into the pro-inflammatory (M1) or anti-inflammatory (M2) phenotypes which produce pro- and anti-inflammatory cytokines respectively. Markers of M1 macrophages include MCP-1 and iNOS whilst those of M2 macrophages include arginase 1 and mannose receptor, CD206. Abbreviations: IFN, interferon; IL, interleukin; M-CSF, macrophage-colony stimulating factor; TNF, tumour necrosis factor; TGF, transforming growth factor; CD, cluster of differentiation; MCP, monocyte chemoattractant/chemotactic protein; iNOS, inducible nitric oxide synthase.

#### 1.3.4 Foam cell formation

LDL is subject to a range of enzymatic and non-enzymatic modifications, particularly ROS-induced oxidation. The LDL accumulated within the intima may hence be oxidised by ROS generated by various cells, including ECs, SMCs and macrophages (Yoshida and Kisugi 2010). LDL modification by ROS is a progressive process that ultimately results in the formation of oxidised LDL (oxLDL). Minimally modified LDL (mmLDL) is not recognised, and hence taken up, by SRs but mediates inflammation and instigates the production of pro-inflammatory cytokines in a TLR4-dependent manner (whilst extensively oxLDL is taken up by SRs) (Bae et al. 2009). OxLDL is immunogenic, as lipid peroxidation generates ROS that can stimulate inflammatory processes to encourage activation of ECs, platelets and macrophages (Frostedgard

2013; Libby et al. 2013; Wraith et al. 2013). The presence and accumulation of oxLDL in the intima provokes surrounding cells, promoting the mitogenesis of VSMCs, as well as activation of necroptosis, a non-apoptotic, programmed cell death pathway, along with inflammation in the surrounding tissues (Ruan et al. 2019). Additionally, oxLDL may bind to its lectin-like oxLDL receptor (LOX-1) in ECs (Sawamura et al. 1997; Mehta et al. 2007) and activate cluster of differentiation (CD)40/CD40 ligand (CD40L) signalling (Li et al. 2003). This signalling pathway triggers the synthesis of chemokines (Mach et al. 1997; Li and Mehta 2000) and cell adhesion molecules (Gebuhrer et al. 1995; Amberger et al. 1997) by ECs, which further encourages the recruitment, adherence and infiltration of immune cells. Whilst T cells in the lesion do not contribute to foam cell formation, they participate in the inflammatory response, whereby different subsets produce different cytokines and may contribute to pro- or anti-atherogenic processes. For example,  $T_{H1}$  cells secrete cytokines such as IFN- $\gamma$ , TNF- $\alpha$  and IL-2 which propagate inflammation, whilst  $T_{regs}$  produce anti-inflammatory cytokines, such as TGF- $\beta$  and IL-10 (Ait-Oufella et al. 2014; Witztum and Lichtman 2014).

Contrary to LDLR-mediated endocytosis of LDL into the cell, SR-mediated uptake is not regulated by intracellular cholesterol levels via negative feedback, leading to excess intracellular lipid accumulation (McLaren et al. 2011; Michael et al. 2012b). Besides receptor-mediated endocytosis, lipoproteins can also be internalised into the cell via other mechanisms, including phagocytosis and macropinocytosis (Michael et al. 2012b; Michael et al. 2013). Any cell capable of engulfing lipids in an unregulated and excessive manner has the potential to transform into foam cells (these cells are full of lipid droplets that appear 'foamy' under the microscope). Macrophages engulf the oxLDL via SRs, including SR-A1 and -B1, and CD36 and 68, which induces the release of IL-1 $\beta$ , TNF- $\alpha$  and other pro-inflammatory cytokines (Stewart et al. 2010). Platelet-derived growth factor (PDGF) stimulates local VSMCs to migrate from the tunica media, through the basement membrane and into the intima, where they proliferate and internalise lipids (De Donatis et al. 2008). Whilst macrophages were previously thought to contribute to the majority of foam cells within atherosclerotic plaques, lineage-tracing studies have highlighted the heterogeneity and plasticity of VSMCs, which contribute a larger proportion of plaque cells than previously thought (Basatemur et al. 2019). VSMCs can adopt various phenotypes akin not only to that of macrophages and foam cells, but also of mesenchymal stem cells and

osteochondrogenic cells, and so may, in fact, be the predominant source of cells within the atherosclerotic lesion, influencing disease progression and contributing to pathogenesis via different mechanisms (Basatemur et al. 2019; Grootaert and Bennett 2021).

Both macrophages and VSMCs (or VSMC-derived macrophage-like cells) can internalise native and modified lipoproteins to transform into the characteristic lipid-laden foam cells. For example, rapid and unregulated internalisation of oxLDL via SRs by M2 macrophages triggers the release of various pro-inflammatory cytokines, including IL-1 $\beta$  and TNF- $\alpha$  (Stewart et al. 2010), as their functional phenotype is shifted towards a pro-inflammatory profile. This is attributed to a simultaneous reduction in their expression of Kruppel-like factor (KLF)2, a nuclear transcription factor that suppresses inflammation in ECs and monocytes (Shirai et al. 2015). OxLDL within macrophages (and other stimuli abundant within atherosclerotic lesions) may also promote inflammasome activation, whereby activation of the NOD leucine-rich repeat and pyrin domain containing protein 3 (NLRP3) inflammasome results in the cleavage and secretion of the mature forms of IL-1 $\beta$  and IL-18, which is mediated by lysosomal destabilisation, ROS release and action of the caspase-1 protease (Tschopp and Schroder 2010; Latz et al. 2013; Patel et al. 2017). This inflammasome is hence implicated in driving pro-inflammatory signalling and pathogenesis in atherosclerosis and other immune-related pathologies (Swanson et al. 2019). Stimulation of macrophages, VSMCs and various other cells by IL-1 $\beta$  can induce their production of IL-6, a stimulator of the acute phase response that enhances hepatic C-reactive protein (CRP) production and expression of atherothrombosis mediators (Castell et al. 1990; Libby 2017). This pathway of inflammation is hence implicated in the pathogenesis and progression of atherosclerosis. Therefore, oxLDL can exert both direct and indirect effects on ECs to promote their activation. Chronic inflammation ultimately drives atherosclerosis propagation and plaque formation and growth as summarised in Figure 1.6.

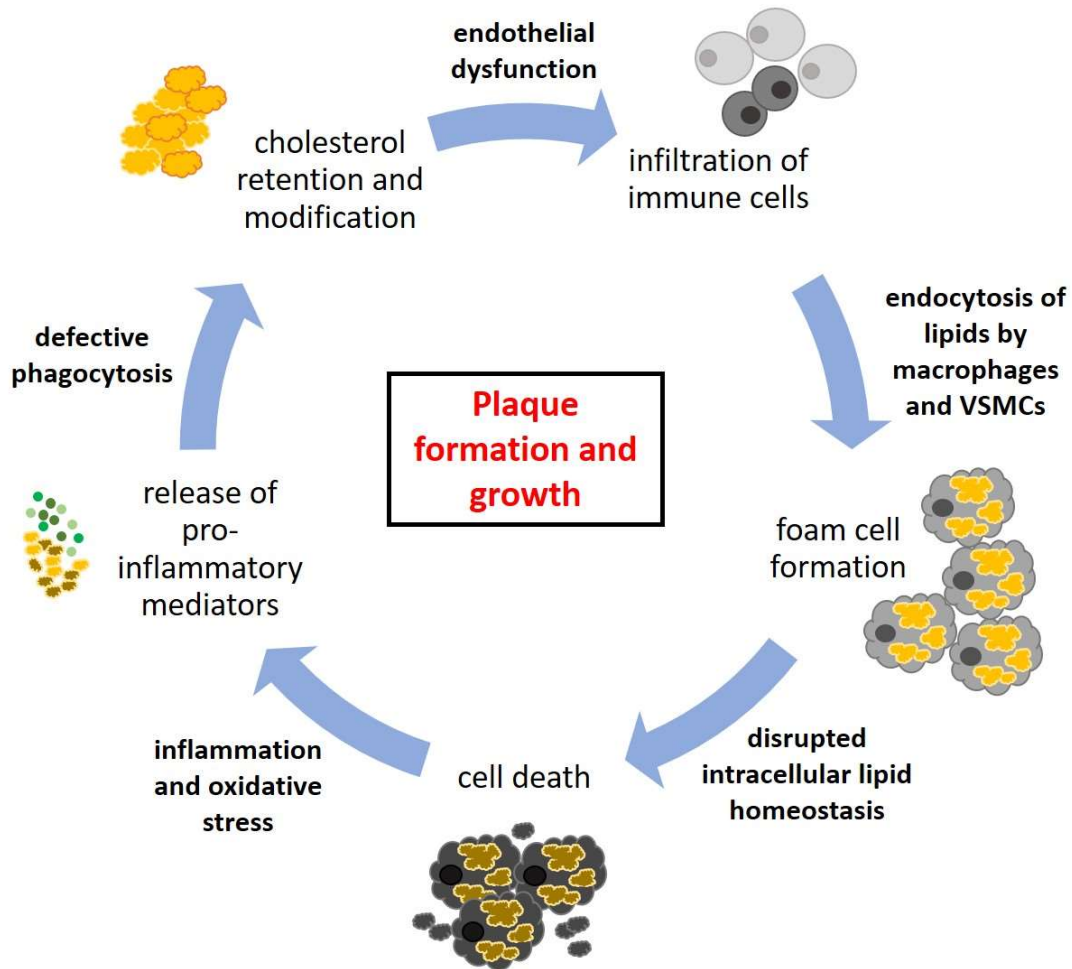


**Figure 1.6 Summary of key processes that drive atherosclerosis.**

Cholesterol accumulation within the arterial wall can instigate endothelial dysfunction which promotes the infiltration of immune cells, including monocytes and T cells. The monocytes differentiate into macrophages, and along with VSMCs that invade from the tunica media layer, endocytose the lipids to become lipid-laden foam cells. Excess intracellular cholesterol accumulation leads to cell death, which results in the release of various pro-inflammatory mediators. Defective efferocytosis (phagocytic clearance) results in the retention of these dead cells, cellular debris and lipid etc., within the intima and the formation of a necrotic core within the atherosclerotic plaque. Pro-inflammatory mediators, including cytokines, ROS and oxLDL, drives inflammation and dysfunction. Abbreviations: VSMCs, vascular smooth muscle cells; ROS, reactive oxygen species; oxLDL, oxidised low-density lipoprotein.

Besides its role in the oxidation modification of lipoproteins, excess ROS can lead to oxidative stress and induce damage to cellular components (e.g., via lipid peroxidation), as well as impact on apoptosis and autophagy to instigate an inflammatory response (Prasanth et al. 2019). For example, mitochondrial DNA (mtDNA) is particularly susceptible to damage by ROS due to its close proximity to the site of ROS production within the mitochondria, combined with the absence of protective histones (Trifunovic et al. 2004). Damage to mtDNA can alter mitochondrial

function and cellular metabolism; in atherosclerosis, reduced mitochondrial respiration associated with endogenous mtDNA damage can promote plaque instability (such as VSMC apoptosis) and other processes that favour pathogenesis and dysfunction (Yu et al. 2017). Therefore, maintenance of mitochondrial function and output is vital for energy-consuming processes and in protecting against cellular dysfunction.

### 1.3.5 Necrotic core formation

Death of the foam cells leads to the formation of a necrotic core (if not promptly and sufficiently cleared away), consisting of dead cells, cellular debris, and lipids etc. within the centre of the atherosclerotic plaque. Such materials are retained and amass within the intima layer, as the phagocytic capabilities of appropriate cells targeted to the clearance of these materials (efferocytosis) are overwhelmed by the production of such materials. Defective and insufficient efferocytosis encourages the accumulation of these pro-inflammatory mediators, which form a necrotic environment that promotes cellular dysfunction and further proinflammatory signalling (Shirai et al. 2015). This forms a detrimental cycle, as activated immune cells and pro-inflammatory signalling can impair cholesterol efflux from cells (Tall and Yven-Charvet 2015), encouraging the generation and accumulation of foam cells, and their subsequent death exacerbates inflammation and promotes pro-atherogenic processes. For example, IFN- $\gamma$  (whose production is driven by  $T_{H1}$ -driven responses) can exert inhibitory effects on LXR signalling (which stimulates the expression of cholesterol efflux transporters), attenuating cholesterol efflux from the cell and enhancing cholesterol retention. Apoptotic cells also release further inflammatory material, including damage-associated molecular patterns (DAMPs), as they undergo secondary necrosis (Back et al. 2019). Increased apoptosis is hence correlated to disease exacerbation as the necrotic core within the atherosclerotic plaque grows (Clarke et al. 2010). These macrophage/VSMC-derived foam cells undergo cell death via apoptosis, necrosis and other mechanisms, contributing to plaque burden and the increasingly necrotic phenotype, as lysis of the cells results in the release of various pro-inflammatory mediators within the arterial wall. The accumulation of dead macrophages and VSMCs, cellular debris and cholesterol within the arterial intima aggravates inflammation and facilitates progression to fibroatheromas (a necrotic core covered by

## Chapter 1: General Introduction

a fibrous cap) (Clarke et al. 2010; Otsuka et al. 2016). VSMCs also undergo a phenotypic shift from quiescent to synthetic state, contributing to plaque stability by producing and secreting ECM proteins (e.g., collagen and elastin), generating the fibrous cap that encapsulates and stabilises the plaque (Bennett et al. 2017; Basatemur et al. 2019). In the early stages, this cap is abundant with VSMC-derived  $\alpha$ -smooth muscle actin ( $\alpha$ SMA)<sup>+</sup> cells with increased presence of type I and III collagens (Bentzon et al. 2006; Yu et al. 2011a; Jacobsen et al. 2017). VSMCs may therefore have both positive and negative effects on plaque progression and remodelling, facilitated by their phenotypic plasticity. A summary of the key processes that drive atherosclerosis is illustrated in Figure 1.7.

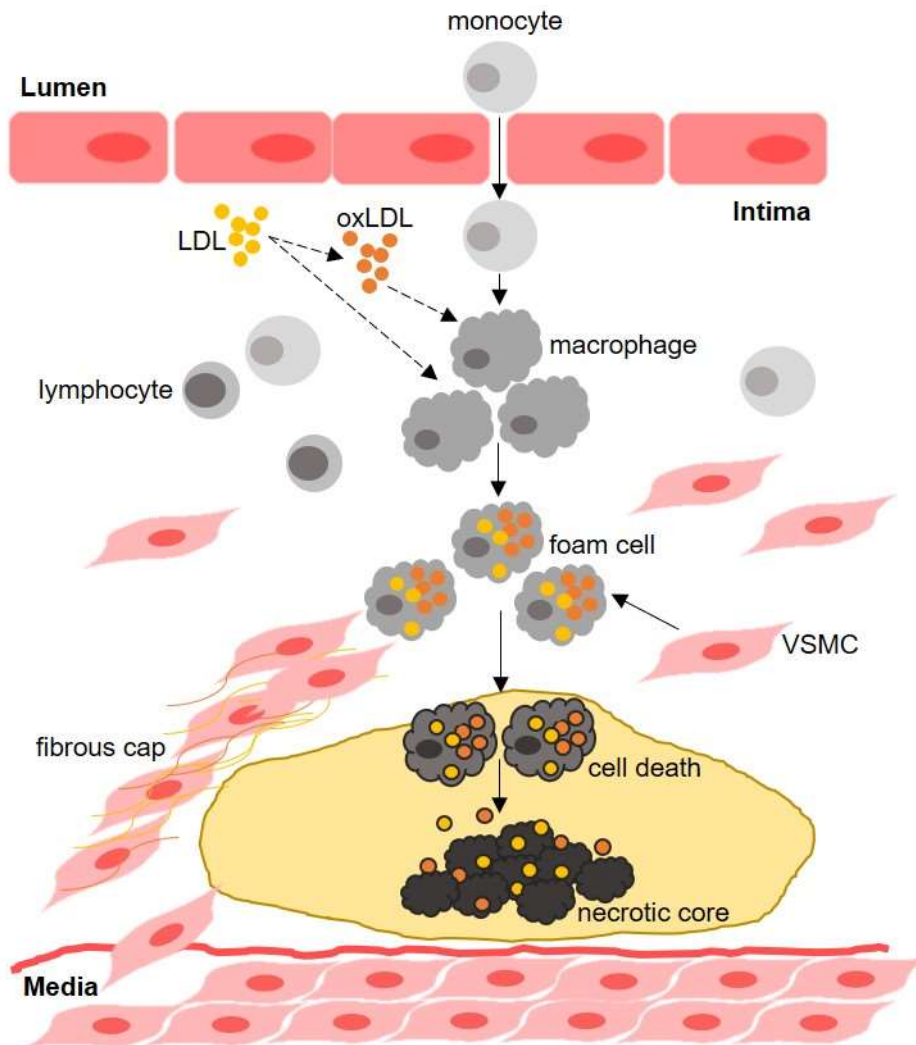


**Figure 1.7 Diagrammatic representation of the key processes in atherosclerosis pathogenesis.** Circulating immune cells, including monocytes and T lymphocytes are recruited from the bloodstream into the arterial intima where lipoprotein is accumulated, facilitated by chemokines (expressed by various vascular cells) and adhesion molecules expressed by endothelial cells. The lipoprotein is subject to modification by reactive oxygen species into oxLDL; both native and modified LDL is taken up by macrophages (differentiated from monocytes induced by M-CSF and GM-CSF) and VSMCs forming foam cells. Foam cell death and defective clearance of the materials leads to the formation of a necrotic core. VSMCs contribute to plaque foam cells and production of ECM proteins to form a fibrous cap after switching from a contractile to a synthetic phenotype. Abbreviations: LDL, low-density lipoprotein; oxLDL, oxidised LDL; M-CSF, macrophage-colony stimulating factor; GM-CSF, granulocyte-macrophage colony stimulating factor; VSMC, vascular smooth muscle cell.

### 1.3.6 Plaque rupture

In the advanced lesion, ROS can also stimulate macrophages to produce matrix metalloproteinases (MMPs), which digest and breakdown the ECM protein components of the fibrous cap (Dollery and Libby 2006). Vulnerable plaques tend to consist of a large lipid-rich necrotic core with a thin and inflamed fibrous cap, along

## Chapter 1: General Introduction

with monocytes, macrophages and T cells (Bergheanu et al. 2017). Furthermore, senescence (a state of irreversible growth arrest) of the VSMCs can also contribute to plaque instability (Bennett et al. 2017; Basatemur et al. 2019). Beyond replicative exhaustion of the cellular lifespan, senescence can also be provoked by external, stress-inducing stimuli, such as DNA-damaging agents or oxidative stress (Coppe et al. 2010). These factors, along with reduced expression of tissue inhibitor of MMP (TIMP) and limited viable VSMCs due to increasing cell death and senescence, promotes the weakening and degradation of the fibrous cap, leading to plaque instability (Bergheanu et al. 2017), rupture and subsequent thrombosis. Key processes that contribute to plaque stability and rupture are summarised in Figure 1.8. Inflammation also promotes VSMC apoptosis via the actions of cytokines, such as IFN- $\gamma$ . Rupture of the fibrous cap exposes the coagulation proteins present in blood to thrombogenic substances, such as tissue factor, within the atherosclerotic plaque, instigating acute thrombosis (Libby 2013). Another mechanism of plaque disruption and clot formation is superficial erosion, which does not involve rupture of the fibrous cap but a discontinuity in the intimal endothelial lining (Crea and Libby 2017; Franck et al. 2019; Libby et al. 2019b). Granulocytes within the plaque or attached to the basement membrane of the intima layer may form neutrophil extracellular traps which can perpetuate both inflammation and thrombosis (Franck et al. 2019; Libby 2019; Molinaro et al. 2021).

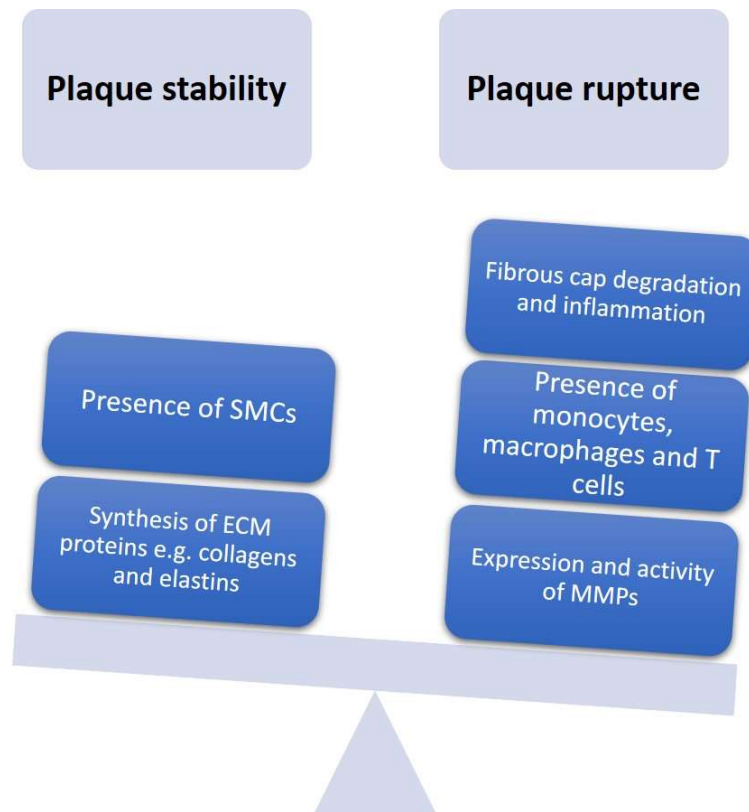


**Figure 1.8 Processes that contribute to plaque stability and rupture.**

Abbreviations: SMC, smooth muscle cells; ECM, extracellular matrix; MMP, matrix metalloproteinase.

## 1.4 Current therapies for atherosclerosis

### 1.4.1 Statins and other strategies targeted to hyperlipidaemia

For decades, LDL-C has been used as a major biomarker in the assessment of cardiovascular risk, due to its implication in plaque formation and growth arising from its accumulation within the arterial wall. The removal of LDL via LDLR-mediated endocytosis is critical in its clearance from the plasma and preventing atherosclerosis development. Current interventions have hence been targeted to lowering circulating levels of LDL-C and thus cardiovascular risk. Statins (3-hydroxy-3-methyl-glutaryl-coenzyme-A (HMG-CoA) reductase inhibitors) function by inhibiting the rate-limiting step of endogenous cholesterol synthesis (Haslinger-Loffler 2008) and enhancing hepatocyte LDLR expression (Bergheanu et al. 2017) whilst exerting other anti-inflammatory and pleiotropic effects (Antonopoulos et al. 2012), such as improvement of endothelial dysfunction (Davignon and Ganz 2004). Statins are the current, predominant therapeutic strategy widely used in cardiovascular medicine and are an

effective strategy for combating hyperlipidaemia whilst being of relatively low cost. However, the significant residual cardiovascular risk that persists post therapy (Campbell et al. 2007; Libby et al. 2011; Sampson et al. 2012), along with various issues (relating to adverse side effects and tolerability etc.) (Calderon et al. 2010), has driven the exploration of alternative approaches. This has also been encouraged by a shift in the classical risk factors used to determine cardiovascular risk, such as the use of CRP as a marker of IL-1-driven inflammation.

Proprotein convertase subtilisin/kexin 9 (PCSK9) mediates the degradation of LDLR (Scherer et al. 2017), and so monoclonal antibodies (evolocumab and alirocumab) and small interfering RNA (inclisiran) have been used to inhibit PCSK9 and promote LDL absorption by the liver to encourage LDL-C clearance. Inclisiran is currently under investigation in a large-scale clinical trial as part of the continuing 'ORION' program, to elucidate its effect on cardiovascular outcomes (Stoekenbroek et al. 2018). However, although efficient at controlling LDL-C levels and subsequent cardiovascular risk (Hadjiphilippou and Ray 2017; Bohula et al. 2018), evolocumab and alirocumab (along with inclisiran) require regular subcutaneous injection, and their substantial cost continues to restrict their medical application. Ezetimibe can also attenuate LDL-C levels by inhibiting cholesterol absorption at the intestinal brush border (Jia et al. 2011). Ezetimibe targets the Neimann-Pick C1-like 1 (NPC1L1) protein (which facilitates the internalisation of cholesterol) via selective inhibition in the jejunal brush enterocyte border to reduce cholesterol absorption (Phan et al. 2012). These strategies have demonstrated efficacy in reducing plasma cholesterol and hence controlling cardiovascular risk in various clinical trials, either alone or in combination with statins (Cannon et al. 2015; Tsujita et al. 2015; Bohula et al. 2018). Bempedoic acid, an inhibitor of adenosine triphosphate-citrate lyase (ACL), has also been combined with ezetimibe to successfully lower LDL-C and CRP (Ballantyne et al. 2020). ACL is critically involved in the endogenous cholesterol synthesis pathway upstream of HMG-CoA reductase (Pinkosky et al. 2013). Bempedoic acid may be a favourable alternative to statins as it is selectively activated in the liver rather than skeletal muscle (Pinkosky et al. 2016), and has, so far, not been associated with adverse side effects even in patients that are statin-intolerant (Ballantyne et al. 2018; Laufs et al. 2019). However, further clinical trials are required to delineate whether this fixed dose combination therapy can lower cardiovascular risk.

### 1.4.2 Strategies targeting inflammation

Although strategies that target LDL-C levels can be effective, MACE can also occur in normolipidemic patients (Ridker et al. 2018), and elevated CRP levels have been identified in statin-treated patients (Ridker et al. 2005; Puri et al. 2013), indicating the presence of persistent inflammation post intervention and its role in driving atherosclerosis and the occurrence of clinical complications. Therefore, the realisation that in addition to hyperlipidaemia, inflammation must also be controlled in order to combat cardiovascular risk, has led to more attention focusing on anti-inflammatory therapies. To dampen inflammation and pro-inflammatory signalling, cytokines must hence be targeted. Advances in bespoke pharmaceutical design have provided the possibility of generating highly specific antibodies against mediators with vital roles in the propagation of inflammation (Tousoulis et al. 2016). Cytokines have long been recognised as potential therapeutic targets for atherosclerosis, given the plethora of preclinical studies demonstrating that attenuation of disease progression can be achieved by decreasing levels of various pro-inflammatory cytokines via the generation of KO models, or use of recombinant antibodies and receptor antagonists (Ramji and Davies 2015; Moss and Ramji 2016a). However, it was not until the Canakinumab Anti-Inflammatory Thrombosis Outcomes Study (CANTOS) in 2017, that the success of directly neutralising IL-1 $\beta$  using a monoclonal antibody (canakinumab) proved the ability to lower risk of secondary MACE in survivors of MI with  $\geq 2$  mg/dl CRP, despite having no effects on plasma LDL-C (Ridker et al. 2017). However, aside from the issues surrounding increasing infection risk with any therapy that directly suppresses the immune system, the major dilemma is with its particularly high cost, especially as regular subcutaneous injection is required, and hence resulting in low cost effectiveness (Sehested et al. 2019).

In contrast to this, low-dose methotrexate (a broad-spectrum anti-inflammatory) had no effect on circulating levels of IL-1 $\beta$ , IL-6 or CRP, and hence did not confer any reduction of cardiovascular risk in CVD patients with type 2 diabetes/metabolic syndrome (Ridker et al. 2019). This is despite the association of this agent with reduced occurrence of cardiovascular events in arthritis patients in previous observational studies (Choi et al. 2002; Westlake et al. 2010; Micha et al. 2011). Colchicine is currently the only broad-spectrum anti-inflammatory agent that has

demonstrated efficacy in lowering cardiovascular risk in several clinical trials involving coronary disease patients and patients suffering from MI within 30 days (Nidorf et al. 2013; Tardif et al. 2019; Nidorf et al. 2020). Colchicine may confer cardiovascular protection via inhibition of the NLRP3 inflammasome (Nidorf et al. 2014) and hence generation of mature IL-1 $\beta$  (Martinez et al. 2018). Results from other smaller clinical trials focusing on anakinra, an antagonist of the IL-1 receptor (IL-1Ra), have also demonstrated promise (Abbate et al. 2010; Abbate et al. 2015; Morton et al. 2015; Abbate et al. 2020), although progression onto the next phase of clinical trials is required to determine the long-term safety and efficacy of anakinra administration in CVD patients.

The promise of targeting IL-1 has also been supported by data obtained from previous animal studies, whereby administration of IL-1Ra attenuated neointima formation after vessel wall injury in a porcine coronary artery model (Morton et al. 2005) and inhibited fatty streak formation in *Apoe*<sup>-/-</sup> mice (Elhage et al. 1998). IL-1Ra overexpression and transplantation of IL-1-deficient bone marrow also dampened diet-induced atherogenesis in *Ldlr*<sup>-/-</sup> mice (Devlin et al. 2002; Duewell et al. 2010). This was also true for *Apoe*<sup>-/-</sup> mice treated with the monoclonal antibody for IL-1 $\beta$  (Bhaskar et al. 2011). Fittingly, IL-1Ra deficiency promoted spontaneous atherosclerosis development in *Apoe*<sup>-/-</sup> mice (Isoda et al. 2004) and led to lethal aneurysms (arising from transmural arterial inflammation) (Nicklin et al. 2000). Deficiency in the IL-1 receptor also decreased lesion size in *Apoe*<sup>-/-</sup> mice, although impaired outward vessel remodelling and signs of plaque instability were also observed (Alexander et al. 2012), suggesting that IL-1 promotes lesion stability in late atherosclerosis due to its profibrotic and proliferative effects on VSMCs. Therefore, both preclinical studies and data from human trials support that targeting IL-1 signalling is an efficacious strategy in combating residual inflammation and cardiovascular risk in advanced disease. However, until cost effective anti-inflammatory agents are identified and their long-term safety and efficacy is verified in large scale clinical trials, alternative anti-inflammatory and anti-atherogenic agents are still required, especially given the high prevalence of atherosclerotic CVD. A summary of current promising pharmacological therapies being used or under investigation is included in Table 1.2.

**Table 1.2 Summary of key therapies for atherosclerosis and CVD.**

<b>Lipid management</b>	<b>Ant-inflammatory</b>
Endogenous cholesterol synthesis inhibition via statins and bempedoic acid	Canakinumab - IL-1 $\beta$ monoclonal antibody
PCSK9 inhibition via monoclonal antibodies (evolocumab and alirocumab) or small interfering RNA (inclisiran) to enhance LDLR-mediated plasma lipoprotein clearance	Anakinra - IL-1Ra
Inhibition of intestinal cholesterol absorption via ezetimibe	Colchicine - broad spectrum anti-inflammatory

Abbreviations: IL-1 $\beta$ , interleukin-1 $\beta$  PCSK9, proprotein convertase subtilisin/kexin 9; IL-1Ra, interleukin-1 receptor antagonist.

### **1.5 Nutraceutical agents: a promising alternative avenue**

Nutraceuticals are food constituents with additional health benefits beyond nutritional value and represent promising preventative/therapeutic avenues for atherosclerosis that can be combined with pharmacological therapies (Moss and Ramji 2016; Moss *et al.* 2018). This is due to their various cardiovascular health benefits that may be attributed to their anti-inflammatory and antioxidative activities, for example. The benefits of nutraceuticals include their availability, low cost and good safety profiles (and hence minimal side effects, if any). Promising nutraceutical agents that have received notable attention include omega-3 and -6 polyunsaturated fatty acids (PUFAs), green tea catechins, and olive oil polyphenols. The potential of combining nutraceutical agents with statins to attenuate atherosclerosis has been demonstrated in recent clinical trials, whereby 4 g daily intake of a purified ethyl ester of eicosapentaenoic acid (EPA; an omega-3 PUFA) (icosapent ethyl) by CVD patients on statins significantly reduced the incidence of ischemic events in the Reduction of Cardiovascular Events with Icosapent Ethyl-Intervention Trial (REDUCE-IT) (Bhatt *et al.* 2019), and attenuated plaque burden (Budoff *et al.* 2020). Therefore, nutraceuticals could be exploited as part of dual strategies in combination with pharmaceutical agents to attenuate atherosclerosis progression and confer protection against MACE.

**Table 1.3 Summary of key types of nutraceutical agents**

<b>Nutraceutical</b>	<b>Major effects</b>
Omega-3 PUFAs	Attenuates atherosclerosis development and inflammation <i>in vivo</i> Regulation of blood pressure and thrombosis, involved in formation of eicosanoids, modulates cholesterol metabolism (e.g., reduces uptake and promotes efflux) Attenuates cardiovascular risk in combination with statins (JELIS trial, REDUCE-IT)
Flavanols e.g., catechins	Attenuates atherosclerotic lesion formation and downregulates genes involved in cell migration and inflammation <i>in vivo</i> Improves flow-mediated vasodilation and NO production/activity and blood pressure with antioxidative effects
Polyphenols e.g., hydroxytyrosol	Increases serum HDL levels, reduces oxLDL levels and TG levels, and as well as oxidative stress markers (EUROLIVE study and others)
Phytosterols (steroid compounds found in plants)	Attenuates atherosclerotic lesion formation and inflammation, and modulates genes associated with sterol metabolism <i>in vivo</i> Reduces plasma LDL-C levels

Key actions of investigated nutraceutical agents are summarised (Moss and Ramji 2016b; Moss et al. 2018). Abbreviations: PUFA, polyunsaturated fatty acid; EPA, eicosapentaenoic acid; JELIS, The Japan EPA Lipid Intervention Study; REDUCE-IT, Reduction of Cardiovascular Events with Icosapent Ethyl-Intervention Trial; NO, nitric oxide; HDL, high-density lipoprotein; oxLDL, oxidised low-density lipoprotein; TG, triglyceride, LDL-C, low-density lipoprotein cholesterol.

A diet rich in fruits and vegetables, green tea, and controlled, moderate intake of red wine, has been long associated with cardiovascular health and protection against CVD. This has been shown by various epidemiological studies that correlate a Mediterranean diet with reduced incidence of CVD. However, antioxidant supplement trials have completely failed to demonstrate any cardiovascular benefits even though a diet high in fruit and vegetables etc. has. Furthermore, there is limited literature that defines exactly how the individual micro/macro-nutrients found within these foods reduce CVD and mortality incidence (Mangels and Mohler (III) 2017); as such, underlying mechanisms are generally not well understood (Moss and Ramji 2016b). Additionally, the presence of different nutrients within the foods which may mediate their beneficial effects via different mechanisms adds to the complexity and difficulty in data interpretation. Therefore, more studies investigating specific and individual components of diets associated with cardiovascular protection are still required.

Comprehensive characterisation of the actions and underlying mechanisms of individual nutraceuticals are hence needed.

### 1.5.1 Catechins: important dietary flavanols

Catechins are secondary plant metabolites, belonging to the flavanol class of flavonoids and sharing a general flavan-3-ol structure (Niemeyer and Brodbelt 2008). Sources of catechins include green tea, cocoa, certain fruits (e.g., grapes and apples) and legumes (e.g., broad beans), and red wine (Ritchey and Waterhouse 1999; Arts et al. 2000; Bell et al. 2000). According to the European Food Safety Authority (EFSA), 126 mg of catechins is present per 100 ml of green tea. Various fruits such as blue and blackberries, black plums and apple skin contain between 24-54 mg of catechins, according to the USDA Database for the Flavonoid Content of Selected Foods (Release 3.2). The major catechins include (+)-catechin, (-)-epicatechin, (-)-epigallocatechin (EGC), (-)-epicatechin-3-gallate (ECG), (-)-epigallocatechin-3-gallate (EGCG) and (+)-gallocatechin gallate (GCG) (Chu and Juneja 1997; Li *et al.* 2018), where they exist as four pairs of stereoisomers (catechin and epicatechin; EGC and (-)-gallocatechin; (-)-catechin gallate and ECG; EGCG and GCG) (Niemeyer and Brodbelt 2008). Of these, EGCG, ECG and EGC constitute the majority of the total catechins in green tea, with the majority of previous research focusing on EGCG (Eng et al. 2018; Grzesik et al. 2018). However, different catechins are more abundantly present than others in different sources; for example, whilst EGCG is one of the most abundant catechins found in green tea, (+)-catechin is one of the most abundant flavonoids in red wine (Ritchey and Waterhouse 1999), and (-)-epicatechin and (+)-catechin are the major flavonoids in cocoa (Flores 2019). Catechins enter the digestive system via the diet, and are subject to metabolism and biotransformation by digestive enzymes and microbes within the gastrointestinal tract, which generally involves methylation, glucuronidation, sulfation and ring fission (Sang et al. 2011). The bioavailability and bioefficacy of catechins differ depending on their molecular structure, which directly influences their absorption, metabolism and excretion/elimination (Demeule et al. 2002). For example, EGCG is preferentially excreted in bile whilst non-gallated catechins are readily eliminated in urine. Therefore, different catechins may exert different effects *in vivo*. However, further studies are

required to elucidate the concentrations of catechins and their metabolites, especially for (+)-catechin, in human plasma after consumption. The molecular structures of major catechins are included in Figure 1.9.

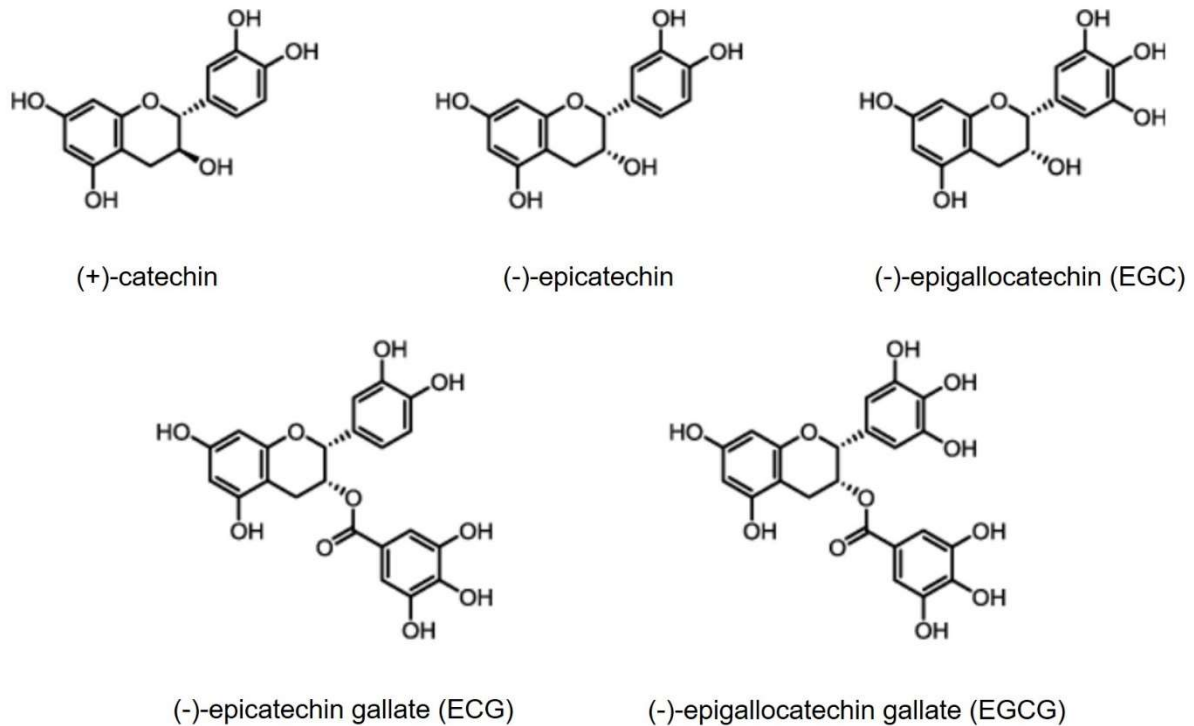


**Figure 1.9 Molecular structure of (+)-catechin and major green tea catechins.**

Modified from Miyoshi et al. (2015).

In general, a plethora of evidence suggests that catechins may help lower incidences of MACE and related mortality via inhibitory effects on endothelial dysfunction, decreasing biomarkers of inflammation, combined with their antioxidant, antiplatelet and anti-proliferative actions (Islam 2012), but questions remain regarding their underlying mechanisms. In humans, investigation of the cardio-protective activities of catechins has mainly been done using foods containing a mixture of flavanols, such as green tea/green tea extracts (Islam 2012) or flavanol-enriched cocoa (Bhardwaj and Khanna 2013; Moss and Ramji 2016b). However, regardless of the source, catechins in general have been associated with a reduction in ischaemic heart disease mortality risk (Arts et al. 2001a). Flavanol supplementation, mainly through cocoa and green tea, resulted in multiple positive effects on cardiovascular health in a range of populations. In healthy individuals, consumption of 500 mg of catechins extracted from

green tea leaves for 4 weeks led to decreased plasma oxLDL concentrations (Inami et al. 2007), and LDL oxidisability was significantly reduced an hour after intake of 1 g of total catechin (consisting of mostly gallated catechins) (Suzuki-Sugihara et al. 2016). Healthy women receiving green tea extract also had reduced oxLDL concentration and serum oxidisability (Tinahones et al. 2008). Moreover, healthy men receiving 714 mg green tea polyphenols daily for 3 weeks had reduced ratio of total cholesterol to HDL cholesterol (Frank et al. 2008). In healthy, low-risk individuals, daily intake of cocoa flavanols (450 mg) for 1 month also increased flow mediated vasodilation, decreased blood pressure (systolic and diastolic), decreased LDL-C and increased HDL-C (Sansone et al. 2015). These individuals also had a lower predicted 10-year risk for coronary heart disease. In another study, cocoa flavanol intake (450 mg) for 14 days by elderly individuals without CVD decreased peripheral resistance and systolic blood pressure (Heiss et al. 2015). Furthermore, elderly individuals consuming 993 mg of flavanols for 8 weeks also demonstrated improved insulin resistance, blood pressure and lipid peroxidation (Mastroiacovo et al. 2015). Observations from the Prevencion con Dieta Mediterranea (PREDIMED) study population also suggested that flavanol consumption is associated with reduced CVD risk (Tresserra-Rimbau et al. 2014). In otherwise healthy, (pre)hypertensive subjects, daily intake of 100 mg epicatechin improved endothelial function (Dower et al. 2015); intake of flavonoid-rich cocoa also induced vasodilation via activation of the NO system in healthy individuals (Fisher et al. 2003). Therefore, intake of flavanols from different sources appears to elicit different benefits in healthy subjects, emphasising that different flavanols are responsible for different cardiovascular health benefits.

In patients with systemic arterial hypertension, daily infusion of green tea, dehydrated apple and dark chocolate (dietary flavonoids) to obtain a dose of approximately 425 mg of epicatechin equivalents decreased blood pressure, and plasma CRP and TG levels when combined with pharmacological anti-hypertensive treatment (AHT) compared to AHT alone (Romero-Prado et al. 2015). In otherwise healthy male smokers, intake of green tea beverages containing 580 mg total catechins for 2 weeks increased levels of NO and decreased oxidative stress markers, CRP and MCP-1 in the plasma (Oyama et al. 2010). In high-risk males, intake of phenolic compounds in red wine downregulated serum CD40 (both the antigen and ligand), IL-16, MCP-1 and VCAM-1 levels (Chiva-Blanch et al. 2011). In obese/near-obese children, ingestion of

green tea containing 576 mg catechins daily for 24 weeks reduced waist circumference, systolic blood pressure and was not associated with any adverse effects (Matsuyama et al. 2008). Furthermore, in Type 2 diabetes patients with hypertension, consumption of 25 g dark chocolate for 8 weeks decreased systolic and diastolic blood pressure (Rostami et al. 2015). In hypercholesterolemic postmenopausal women, flavanol-rich cocoa (containing 446 mg of flavanols) improved endothelial function (as determined by brachial artery-reactive hyperaemia) and decreased plasma levels of soluble VCAM-1 (Wang-Polagruto et al. 2006). Administration of flavanol-rich chocolate to congestive heart failure patients improved flow-mediated vasodilation and reduced platelet adhesion, improving vascular function (Flammer et al. 2011). In haemodialysis patients, cocoa flavanol-rich supplements (900 mg of cocoa flavanols) improved flow-mediated dilation; after 30 days, baseline flow-mediated vasodilation was increased whilst diastolic blood pressure was reduced, suggesting alleviation of haemodialysis-induced vascular dysfunction (Rassaf et al. 2016). In another study, green tea extracts also reduced haemodialysis-induced atherosclerosis-associated risk factors, including ROS production and inflammation after 3 months (Hsu et al. 2007). Therefore, consumption of flavanols in cocoa (i.e., (+)-catechin and (-)-epicatechin) seems to have beneficial effects on parameters associated with endothelial dysfunction, in particular leukocyte adhesion, whereas green tea flavanols (i.e., EGCG) may attenuate plasma parameters associated with atherosclerosis, specifically by modulating lipoprotein profile by lowering LDL and oxLDL. A summary of observations resulting from the intake of catechins by humans is included in Table 1.4.

**Table 1.4 Key observations in humans following intake of catechins.**

<b>Observation</b>	<b>Reference(s)</b>
Beneficial effects on lipoprotein profile	(Frank et al. 2008; Romero-Prado et al. 2015; Sansone et al. 2015)
↓ plasma oxidative stress markers or oxLDL/LDL oxidisability	(Hsu et al. 2007; Inami et al. 2007; Tinahones et al. 2008; Oyama et al. 2010; Mastroiacovo et al. 2015; Suzuki-Sugihara et al. 2016)
↑ flow mediated vasodilation or endothelial/vascular function	(Fisher et al. 2003; Faridi et al. 2008; Flammer et al. 2011; Sansone et al. 2015; Rassaf et al. 2016)
↓ blood pressure	(Matsuyama et al. 2008; Heiss et al. 2015; Mastroiacovo et al. 2015; Romero-Prado et al. 2015; Sansone et al. 2015)
↓ inflammatory markers	(Hsu et al. 2007; Oyama et al. 2010; Chiva-Blanch et al. 2011; Romero-Prado et al. 2015)
Improvement of adiposity-associated parameters	(Matsuyama et al. 2008; Nirengi et al. 2016; Yoneshiro et al. 2017)

Abbreviations: oxLDL, oxidised low-density lipoprotein; LDL, low-density lipoprotein.

### 1.5.2 (+)-Catechin: a promising flavanol requiring investigation

Whilst various studies in humans have shown the cardio-protective effects of catechins, these studies mostly use catechin-containing products rather than individual catechins. Hence associating specific observations to specific compounds is difficult, given that different mechanisms of actions may also be involved. Despite a large prospective study demonstrating a strong inverse association between (+)-catechin and (-)-epicatechin intake and coronary heart disease after controlling for many confounding risk factors (Arts et al. 2001b), mouse studies conducted since have mainly focused on other catechins, such as (-)-epicatechin and other galloylated catechins (e.g. EGCG), with little done on (+)-catechin itself. Mouse studies have been particularly used to explore the efficacy of specific compounds on atherosclerosis development and progression *in vivo*, allowing the exploration of mechanistic insights not always possible with human studies. A transcriptomic study found (+)-catechin supplementation to reduce atherosclerotic lesion area in *ApoE*<sup>-/-</sup> mice, and altered the expression of 450 genes in the aorta, including those involved in leukocyte endothelial adhesion and lipid metabolism, despite no significant changes in plasma cholesterol and TG levels (Auclair et al. 2009). Although this suggests that (+)-catechin attenuates

atherosclerosis development by dampening the adhesion and hence infiltration of immune cells to the lesion, insight as to how (+)-catechin affects atherosclerosis development (e.g., presence of macrophages and T cells in the lesion) was limited.

Previous work conducted in host laboratory found (+)-catechin (1.5 µg/ml) to have inhibitory effects on multiple key pro-atherogenic processes associated with monocytes and macrophages *in vitro* (Moss 2018). These included MCP-1 driven monocyte migration, monocyte and macrophage proliferation and ROS production, macrophage MMP activity and expression of genes involved in a range of pro-atherogenic processes by macrophages. The expression of several genes implicated in atherosclerosis was also modulated; (+)-catechin-treated THP-1 macrophages has significantly reduced expression of *SELL* (L-selectin; adhesion molecule), *LDLR* and *IFN-γ*. Together, these data suggest that the anti-inflammatory and anti-oxidative effects of (+)-catechin help mitigate monocyte recruitment, local macrophage proliferation and ROS-stimulated macrophage MMP production. Additionally, in a pilot study involving male wild-type (WT) C57BL/6J mice fed high-fat diet (HFD) for 3 weeks, daily gavage of 200 mg/kg (+)-catechin (in the form of (+)-catechin hydrate) modulated several risk factors of the disease, including plasma TG levels and circulating levels of pro-atherogenic/pro-inflammatory mediators as summarised in Figure 1.5 (Moss 2018). Analysis of liver gene expression also found several genes to be significantly modulated by (+)-catechin supplementation, including upregulation of *NR1H3* (an anti-inflammatory regulator of gene transcription) and down regulation of *ITGA2* (a cell adhesion molecule). Therefore, (+)-catechin might offer protection against HFD-induced inflammation and elevation of TG in WT mice.

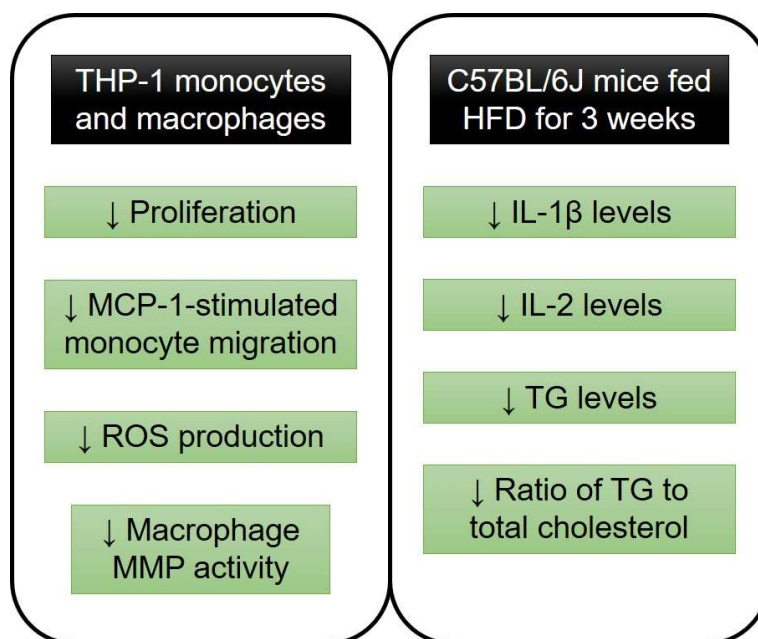


**Figure 1.10 Summary of significant changes observed in previous *in vitro* and *in vivo* studies.**

(+)-Catechin treated THP-1 monocytes and macrophages demonstrated significantly reduced proliferation and ROS production. Migration of THP-1 monocytes towards monocyte chemotactic protein (MCP)-1 was also attenuated, along with THP-1 macrophage MMP activity. Wild-type mice fed high-fat diet (HFD) for 3 weeks with daily gavage of (+)-catechin hydrate had significantly reduced plasma levels of IL-1 $\beta$  and IL-2, along with decreased triglyceride (TG) levels and ratio of TG to total cholesterol.

The dose of (+)-catechin used in this short term study was based upon a previously published study of equal duration, whereby spontaneously hypertensive rats (SHR) were gavaged daily with 200 mg/kg EGCG for 3 weeks, resulting in reduced systolic blood pressure, significantly lowered infarct size and improved cardiac function (Potenza et al. 2007). Male golden Syrian hamsters fed a hypercholesterolemia diet for 16 weeks receiving 200 mg/kg/day catechin hydrate combined with vitamin E attenuated fatty streak formation, similarly to vitamin E at a higher dose alone (Xu et al. 1998). Male Wistar rats with high fructose consumption receiving 20 mg/kg (+)-catechin improved insulin resistance, plasma adiponectin, adiposity, and adipose tissue inflammation, and hence attenuated adipose proinflammatory signalling and regulated molecules involved in insulin sensitivity (Vazquez Prieto et al. 2015). In another study also using male Wistar rats, oral supplementation of 10 mg/kg/day (-)-catechin significantly reduced levels of malondialdehyde, along with expression of pro-inflammatory cytokines, offering protection against induced cardiotoxicity (El-Aziz et al. 2011). Furthermore, Apoe\*3-Leiden mice on a HFD supplemented with 0.1% (w/v) (-)-epicatechin for 20 weeks had smaller atherosclerotic lesions (but no changes in

plasma lipids) and microarray analysis showed changes in the expression of a number of genes involved in cell migration (Morrison et al. 2014). Therefore, (+)-catechin (and its isomers) demonstrates various beneficial effects on multiple parameters associated with atherosclerosis and metabolic syndrome *in vivo*. However, detailed characterisation of its effects in the context of atherosclerosis is still required, and so it would hence be of interest to explore the effect of (+)-catechin supplementation on atherosclerosis development in *Ldlr*<sup>-/-</sup> mice, which bears more similarity to human atherosclerosis compared to the more aggressive *Apoe*<sup>-/-</sup> model (Emini Veseli *et al.*, 2017). This is since *Apoe*<sup>-/-</sup> mice develop atherosclerosis spontaneously on a normal chow diet without the need for dietary manipulation, and lesion development is more rapid in comparison to *Ldlr*<sup>-/-</sup> mice fed a pro-atherogenic diet (e.g., HFD) (Getz and Reardon 2016). Additionally, further *in vitro* experiments are required to elucidate the effect of (+)-catechin on other key processes that drive atherogenesis. Therefore, more focus should be placed on defining how the individual food components, such as (+)-catechin, confer cardiovascular protection, given the potential of nutraceutical agents to be used as part of preventative and therapeutic strategies for atherosclerosis.

### 1.6 Project aims

Atherosclerotic CVD remains the top contributor of global morbidity and mortality. Current therapeutic strategies targeting hyperlipidaemia (e.g., statins) which have been widely used in cardiovascular medicine have limited effectiveness in combating the cardiovascular risk with other issues including adverse side effects. The realisation that MACE can also occur in normolipidemic individuals post statin therapy has highlighted the role of residual inflammation in driving clinical complications. The success of targeting IL-1 $\beta$  using canakinumab as shown by the CANTOS trial has offered new hope in the use of anti-inflammatory therapies. However, with any therapy that directly targets cytokines and hence the immune system naturally raises issues associated with increased risk of infections and suitability for patients already immunocompromised. Until drug delivery strategies enabling the direct targeting of these anti-inflammatory agents to the specific site of atherosclerosis to minimise undesirable, systemic effects are developed, alternative avenues that are affordable/cost-effective and widely available, with good safety profiles are required.

## Chapter 1: General Introduction

Recent successes with omega-3 PUFAs used in combination with statins in human clinical trials have demonstrated the promise of utilising nutraceutical agents as part of a dual strategy with statins to attenuate plaque progression. Due to the anti-inflammatory and anti-atherogenic actions of (+)-catechin observed in human monocytes and macrophages, it is hypothesised that the athero-protective properties will also extend to other key cell types implicated in the disease (i.e., ECs and VSMCs), with the ability to attenuate disease development and progression, and even, regression in the *Ldlr*<sup>-/-</sup> model. This is as a previous pilot study conducted in host laboratory also found daily gavage of 200 mg/kg (+)-catechin WT mice fed HFD for 3 weeks modulated several atherosclerosis-associated risk factors, combined with its anti-atherogenic effects on human monocytes and macrophages. Whilst catechin has demonstrated anti-inflammatory and anti-oxidative effects *in vitro* and *in vivo*, little is known about (+)-catechin, especially in the context of atherosclerosis. Several important questions hence require answering;

- Do the protective actions of (+)-catechin extend to key processes involving other important cell types (i.e., ECs and VSMCs)?
- What is the effect of (+)-catechin on plaque development, progression and stability *in vivo*?
- Can (+)-catechin induce plaque regression?

Firstly, to delineate whether (+)-catechin can inhibit parameters associated with endothelial and VSMC dysfunction, key processes were recapitulated *in vitro* using a range of assays. These assays enabled the study of (+)-catechin treatment on migration and invasion, proliferation, apoptosis, permeability, ROS production, MMP production and monocyte-endothelial adhesion. This was done to assess the anti-inflammatory, anti-oxidative and anti-atherogenic actions of (+)-catechin on stimulated ECs (to model endothelial dysfunction) and VSMCs. ECs were stimulated with either 100 µg/ml oxLDL or 50 ng/ml TNF-α (concentrations based upon published literature and subsequent optimisation/experience in the host laboratory) to induce their activation. This was based on the fact that oxLDL is a key mediator of EC activation and dysfunction mediated via both direct and indirect effects (e.g., upregulation of TNF-α). Key results obtained in THP-1 cells from previous work conducted in the host

laboratory were also confirmed using primary macrophages (human monocyte-derived macrophages), to verify that observations were not specific to the cell line (Figure 1.11).

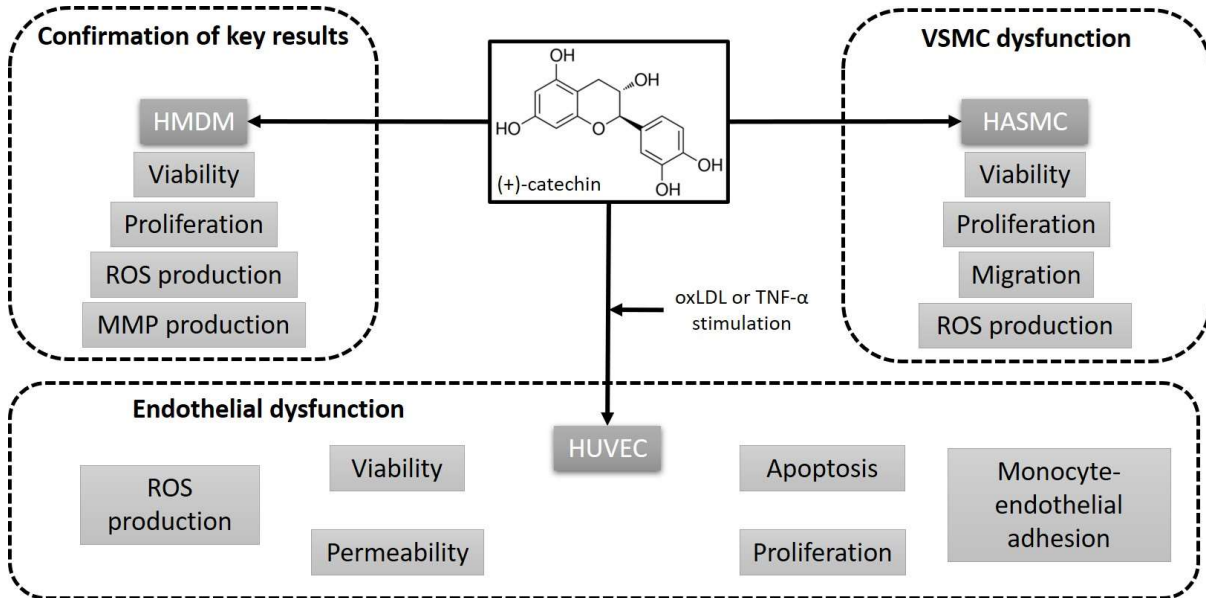


**Figure 1.11 Summary of experiments conducted as part of the first objective.**

Studies parameters for each cell type are indicated. In all *in vitro* experiments, cells were treated with 1.5 µg/ml (+)-catechin, the previously optimised concentration from studies conducted in host laboratory. Abbreviations: HMDM, human monocyte-derived macrophages; VSMC, vascular smooth muscle cell; HASMC, human aortic smooth muscle cell; ROS, reactive oxygen species; MMP, matrix metalloproteinase; oxLDL, oxidised low-density lipoprotein; TNF-α, tumour necrosis factor-α; HUVEC; human umbilical vein endothelial cell.

Secondly, to elucidate the effect of (+)-catechin treatment on mitochondrial bioenergetics, glycolysis and dysfunction, various mitochondrial-based assays were used to assess mitochondrial ROS production, respiration, membrane depolarisation, and cellular glycolysis in THP-1 macrophages and ECs (in basal and stimulated conditions). THP-1 macrophages were stimulated with 100 ng/ml LPS and 250 U/ml IFN-γ (to induce polarisation into pro-inflammatory M1 macrophages) and ECs were stimulated with 100 µg/ml oxLDL (to induce activation). This provided mechanistic insights to how (+)-catechin mediates its beneficial effects in these cell types, given that the mitochondria are a major source of ROS as well as the provider of energy (ATP) required for various processes (e.g., the maintenance of ionic homeostasis and repair pathways), and (+)-catechin possesses potent anti-oxidative activity.

Thirdly, to determine whether (+)-catechin supplementation can attenuate atherogenesis, atherosclerosis progression and encourage plaque stabilisation *in vivo*, *Ldlr*<sup>-/-</sup> mice were fed HFD for 12 weeks to induce atherosclerosis with or without 200 mg/kg/day (+)-catechin supplementation (in the form of (+)-catechin hydrate) (Figure 1.15). The use of (+)-catechin hydrate mitigated the high cost of using (+)-catechin, as well as the use of toxic dimethyl sulfoxide (DMSO) (since (+)-catechin is only soluble in this solvent and not in water) in animals. The molecular structure of (+)-catechin hydrate is identical to that of (+)-catechin except with the addition of a water molecule, making it soluble in non-toxic solvents (Figure 1.12).

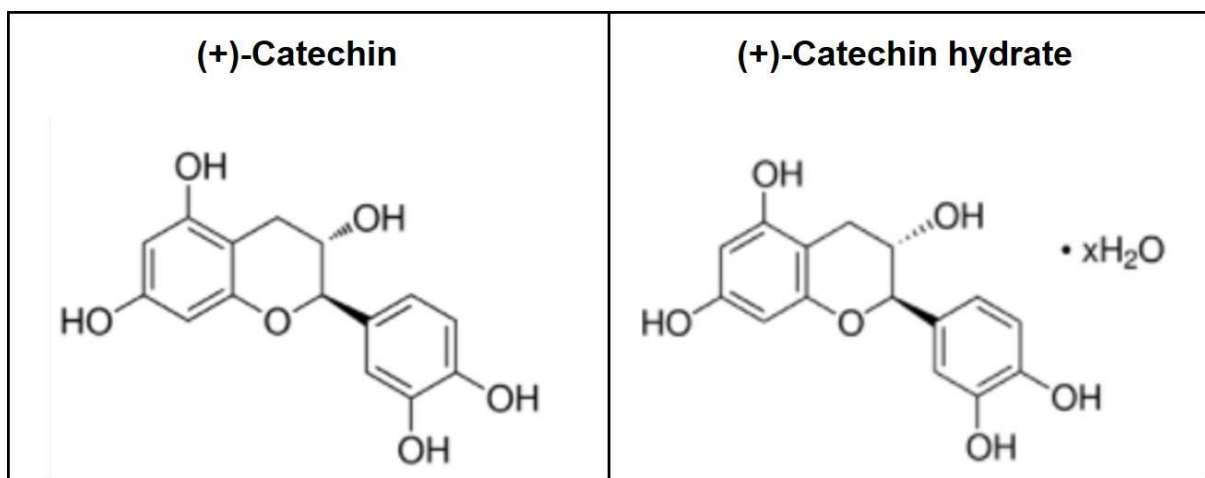


**Figure 1.12** Molecular structures of (+)-catechin and (+)-catechin hydrate.

The (+)-catechin hydrate was dissolved in 1X phosphate-buffered saline (PBS; to enable ease of mixing into the HFD) as per previous pilot study conducted in the host laboratory using WT mice. Various parameters were analysed at the end point of the feeding procedure to assess adiposity, inflammation profile, atherosclerotic plaque burden, inflammation and stability, and hepatic steatosis. This enabled assessment of the preventative potential of (+)-catechin via its efficacy to attenuate diet-induced atherogenesis, along with associated risk factors. Group sizes of 15-20 were used based on power calculations and previous experience of the host laboratory, combined with that of their collaborators within the same field (Figure 1.13). A summary of the analyses conducted following the feeding protocol is shown in Figure 1.14.

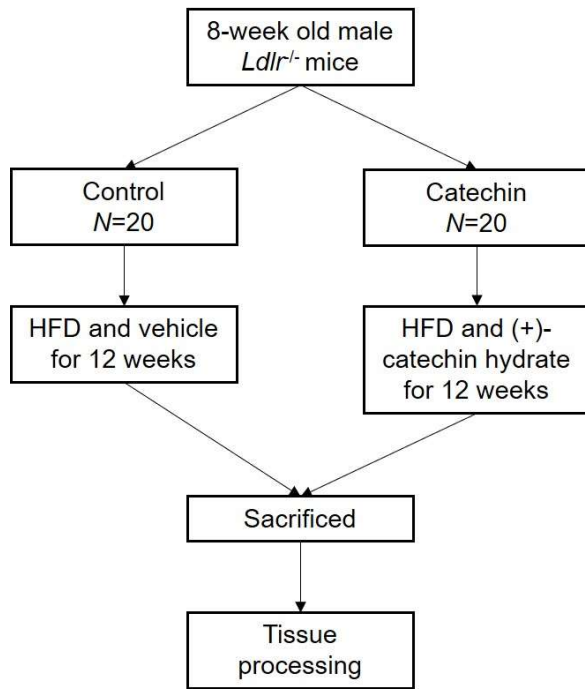


**Figure 1.13 Strategy for the progression study.**

Eight-week-old male *Ldlr*<sup>-/-</sup> mice were randomly assigned to two different groups; 'Control' or 'Catechin', and received the indicated dietary interventions before being sacrificed. Abbreviations: *Ldlr*<sup>-/-</sup>; low-density lipoprotein deficient mice; HFD, high-fat diet.

## Chapter 1: General Introduction

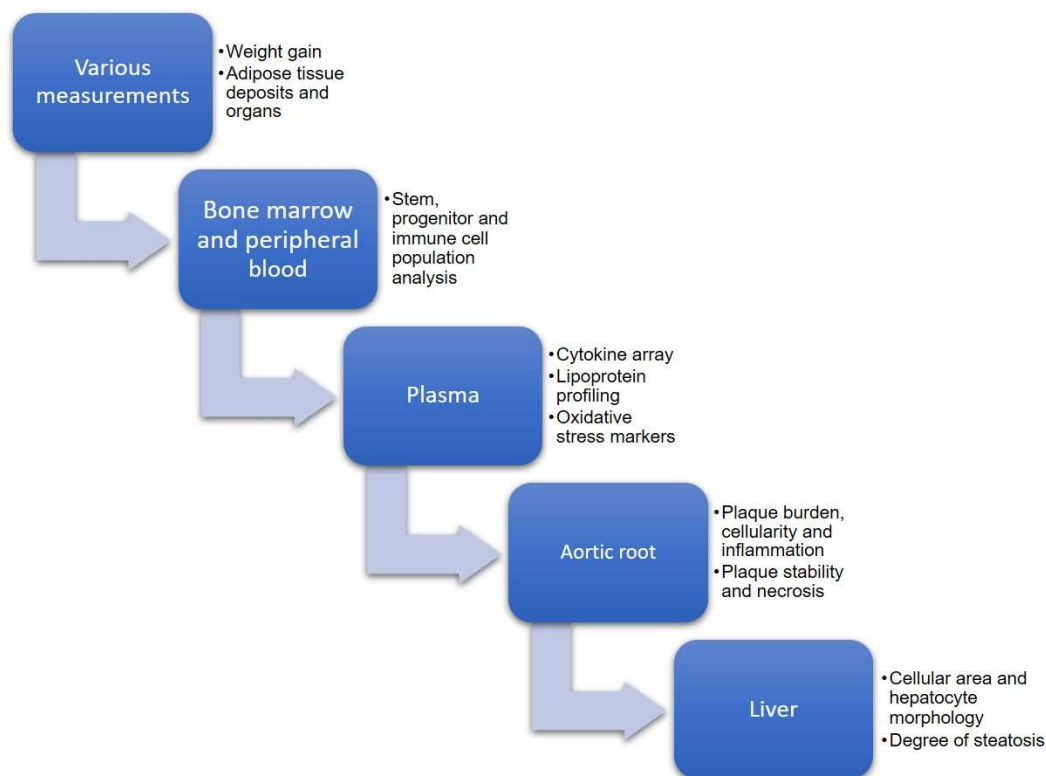


**Figure 1.14 Tissue processing strategy used at the end point of the feeding procedure.**

Weight gain and consumption were measured throughout the feeding procedure at regular intervals from start to finish. Stem, progenitor, and immune cells within the bone marrow, along with immune cells within peripheral blood were analysed using flow cytometry. Plasma parameters were analysed using a range of colorimetric assays for example. The aortic root within the heart was sectioned at the three valve cusps for detailed plaque morphometric analyses after different immunohistochemical stains and similarly, the liver tissue was sectioned and stained to analyse morphology and steatosis.

Lastly, to study whether (+)-catechin supplementation can stimulate the regression of established atherosclerotic plaques (after promising data were obtained in the previous progression study), *Ldlr*<sup>-/-</sup> mice were fed HFD for 12 weeks to induce atherogenesis and then switched to a normal chow diet (NCD) for 8 weeks with or without (+)-catechin supplementation (in the form of (+)-catechin hydrate) (Figure 1.15). This was done to assess the therapeutic potential of (+)-catechin, to determine whether (+)-catechin can be used to treat established atherosclerosis via assessment of the parameters as mentioned above and shown in Figure 1.14. During this study, the opportunity was also taken to increase the number of mice for the treatment group of the progression study (i.e., mice fed HFD alone or supplemented with (+)-catechin for 12 weeks), since the mice were available. This was done to make up for samples lost during the sectioning process (e.g., via unsuccessful sectioning of the aortic root, the site assessed for atherosclerotic plaque content) and variation of the histological

analyses which led to various trends that were close to significance. This also provided the opportunity to include immunophenotyping of peripheral blood cell populations via flow cytometry analysis, which was a new technique introduced to the host laboratory.

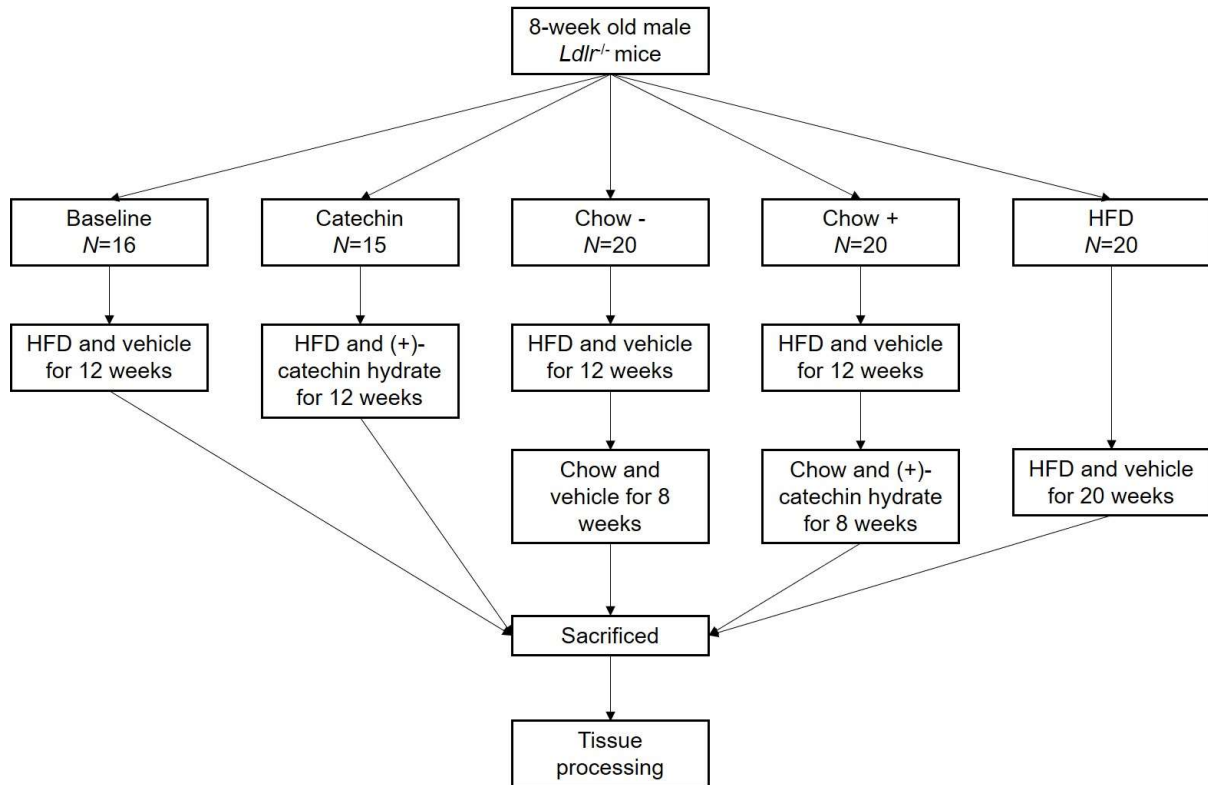


**Figure 1.15 Strategy for the regression study.**

Eight-week-old male *Ldlr*<sup>-/-</sup> mice were randomly assigned to five different groups; ‘Baseline’, ‘Catechin’, ‘Chow -’, ‘Chow +’ and ‘HFD’ and received the indicated dietary interventions before being sacrificed. Abbreviations: *Ldlr*<sup>-/-</sup>; low-density lipoprotein deficient mice; HFD, high-fat diet.

Therefore, Chapter 5 details the combined data for the ‘Control’ and ‘Baseline’ groups (i.e., all mice receiving HFD and vehicle for 12 weeks), and both ‘Catechin’ groups (i.e., all mice receiving HFD and (+)-catechin hydrate for 12 weeks) from the progression and regression studies (unless otherwise stated). Subsequently, the data constituting the ‘Baseline’ group used of the regression study as detailed in Chapter 6 are also the combined data for the ‘Control’ and ‘Baseline’ groups (i.e., all mice receiving HFD and vehicle for 12 weeks) from the progression and the regression study. The contents of the subsequent chapters with respect to these aims and objectives are summarised in Figure 1.16.

## Chapter 1: General Introduction

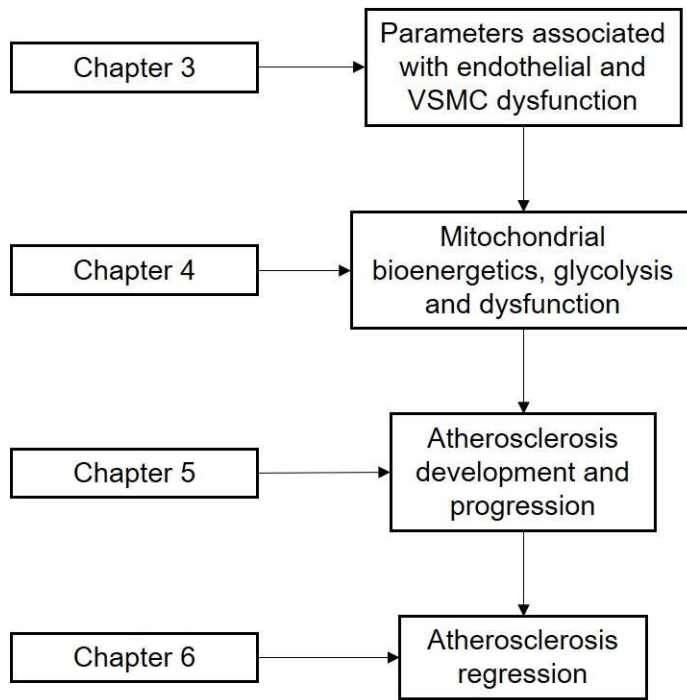


**Figure 1.16 Summary of contents of thesis chapters.**

## 2 Materials and Methods

### 2.1 Materials

All materials used in this project, along with their suppliers are outlined in Table 2.1 below.

**Table 2.1 Details of all materials used.**

<b>Supplier</b>	<b>Material</b>
Abcam, UK	Annexin V-FITC Apoptosis Detection Kit; antibodies for immunofluorescence staining (see Section 2.5.13.4 for details); DCFDA Cellular ROS Detection Assay Kit; HDL and LDL/VLDL Cholesterol Assay Kit; JC-1 Mitochondrial Membrane Potential Assay Kit; MMP Activity Assay Kit (Fluorometric - Green); Triglyceride Quantification Assay Kit; Van Geison's solution
Agilent Seahorse Technologies, UK	Seahorse XFe96 FluxPak mini cell culture microplates; Seahorse XF Base Medium and supplements; Seahorse XF Cell Mito Stress Test Kit; Seahorse XF Glycolytic Rate Assay Kit
Alfa Aesar, UK	Human oxLDL (99%, BT-910); heparin sodium salt (250 mg)
BD Bioscience, UK	FITC-conjugated anti-mouse CD34 (553733)
Biolegend, USA	APC anti-mouse c-Kit (105811); PE anti-mouse Sca-1 (108107); FITC anti-mouse CD48 (103403); PE/Cy7 anti-mouse CD150 (115913); APC/Cy7 anti-mouse Sca-1 (108125); PE/Cy7 anti-mouse CD16/32 (101317); PE anti-mouse CD127 (121111); PE/Cy7 anti-mouse NK-1.1 (108714); PE anti-mouse CD115 (135505); PE/Cy7 anti-mouse Ly-6C (128018); FITC anti-mouse Ly-6G (127605); FITC anti-mouse/human CD45R/B220 (103206); PE anti-mouse CD3 (100206); APC anti-mouse/human CD11b (101212); PerCP anti-mouse CD4 (100537); APC/Cy7 anti-mouse CD8a (100714)
Cell Biolabs, UK	OxiSelect <i>In Vitro</i> ROS/RNS Assay Kit (green fluorescence); OxiSelect TBARS Assay Kit (MDA Quantification)

## Chapter 2: Materials and Methods

Helena Biosciences, UK	12- and 96-well tissue culture plates (for seeding PBMCs)
Labtech, UK	Foetal bovine serum (South American origin)
Life Technologies, UK	1X PBS (pH 7.4, sterile filtered)
MediSupplies, UK	25 G needles; 10 ml syringes
Peprtech, UK	Recombinant human MCP-1; M-CSF; PDGF-BB; VEGF; TNF- $\alpha$ ; IFN- $\gamma$
R&D Systems, USA	Human MCP-1 DuoSet ELISA; DuoSet ELISA Ancillary Reagent Kit
Sigma-Aldrich, UK	(+)-catechin; (+)-catechin hydrate; (-)-catechin; (-)-epicatechin; 1, 2-propanediol (propylene glycol); BCECF-AM; 2-propanol (isopropanol), 12- and 96-well tissue culture plates; 15 and 50-ml Falcon tubes; acetone; Accuspin tubes; Aquamount (aqueous mounting medium); bovine serum albumin (Fraction V); crystal violet; DAPI (for nucleic acid staining); dimethyl sulfoxide; DMEM; Dulbecco's PBS; lipopolysaccharide; DPX mounting medium for histology; Pasteur pipettes (plastic); Endothelial Cell Growth Culture Medium; eosin solution; FITC-dextran (MW: 40,000); Fluoroshield with DAPI; Hanks Balanced Salt Solution; Harris Modified Haematoxylin Solution; Human Aortic Smooth Muscle Cells (adult); Human Umbilical Vein Endothelial Cells; Nalgene Mr. Frosty™ freezing container; Oil Red O solution (0.5% (w/v) in propylene glycol); Pap pen for immunostaining; paraformaldehyde; penicillin-streptomycin; phorbol 12-myristate 13-acetate; RPMI-1640 medium (with L-glutamine and sodium bicarbonate, sterile-filtered); serum (goat and donkey); Smooth Muscle Cell Growth Medium; THP-1 cell line; xylene
Special Diets Services, UK	High-fat diet (21% (w/w) pork lard and 0.15% (w/w) cholesterol)
Starlabs, UK	25 and 75 cm <sup>2</sup> tissue culture flasks; 250 mm CytoOne cell scraper (with 10 mm pivoting blade); reagent reservoirs
Stemcell Technologies, UK	Ammonium chloride solution; Lymphoprep™
ThermoFisher Scientific, UK	Shandon base cryomolds; Falcon™ round-bottom polystyrene tubes; Fisherbrand™ borosilicate glass square coverslip; Fisherbrand™ sterile cell strainers (40 and 70 $\mu$ m mesh size); Invitrogen™ eBioscience™

## Chapter 2: Materials and Methods

streptavidin eFluor™ 450; MitoSOX™ Red Mitochondrial Superoxide Indicator; nuclease-free water; Nunc™ Biobanking and cell culture cryogenic tubes; OCT embedding matrix; Pierce™ LDH Cytotoxicity Assay Kit; *RNAlater*™ stabilisation solution; trypsin-EDTA (0.05%); Sarstedt Microvette CB300 EDTA (EDTA microtubes); Tailveiner Restrainer

---

VWR Jencons, UK

Ethanol absolute; feather microtome blades type S22; Falcon® 8 and 0.4 µm inserts with 12- and 24-well companion plates respectively; rectangular glass coverslips; Superfrost® microscope slides

Abbreviations: FITC, fluorescein isothiocyanate; DCFDA, dichlorofluorescein diacetate; ROS, reactive oxygen species; HDL, high-density lipoprotein; LDL/VLDL, low density lipoprotein/very-low density lipoprotein; JC-1, tetraethylbenzimidazolylcarbocyanine iodide; MMP, matrix metalloproteinase; oxLDL, oxidised LDL; APC, allophycocyanin; PE, phycoerythrin; Cy7, cyanine-7; PerCP, peridinin-chlorophyll-protein; RNS, reactive nitrogen species; TBARS, OxiSelect thiobarbituric acid reactive substances; MDA, malondialdehyde; PBS, phosphate-buffered saline; M-CSF, macrophage colony-stimulating factor; PDGF-BB, platelet derived growth factor (homodimeric form); VEGF, vascular endothelial growth factor; TNF-α, tumour necrosis factor-α; IFN-γ, interferon-γ; ELISA, enzyme-linked immunosorbent assay; BCECF-AM, 2', 7'-Bis(2-carboxyethyl)-5(6)-carboxyfluorescein tetrakis (acetoxymethyl) ester; DAPI, 4', 6'-diamidino-2-phenylindole; DMEM, Dulbecco's Modified Eagle Medium; MW, molecular weight; RPMI, Rosewell Park Memorial Institute; OCT, optimum cutting temperature; LDH, lactate dehydrogenase; EDTA, ethylenediaminetetraacetic acid.

## 2.2 Cell culture and maintenance

### 2.2.1 General cell maintenance

All cells were cultured in a humidified, 37°C incubator containing 5% (v/v) CO<sub>2</sub> and maintained within T25 or T75 cm<sup>2</sup> tissue culture flasks. The culture medium was completely changed a minimum of once per week and cells were periodically monitored by checking morphology under the microscope. Cells were sub-cultured when approximately 80% confluency was reached and passages 4-10 were used for experiments. Prior to use for experiments, cell morphology was also checked under the microscope to ensure cells were healthy and without abnormalities.

## Chapter 2: Materials and Methods

### 2.2.2 Endothelial and vascular smooth muscle cells

Human umbilical vein endothelial cells (HUVECs) were used as a model of ECs to study parameters associated with endothelial dysfunction, whilst human aortic smooth muscle cells (HASMCs) were used as a model of VSMCs. HUVECs and HASMCs were maintained in Endothelial Cell Growth Culture Medium (EGCM) or Smooth Muscle Cell Growth Medium (SMCM) respectively, in accordance with the supplier's guidance (Sigma-Aldrich). To remove the cells from flasks (e.g., for experimental use or sub-culturing), HUVECs or HASMCs were washed with 1X phosphate-buffered saline (PBS) or Hanks Balanced Salt Solution (HBSS) respectively, then trypsinised using 0.05% (w/v) trypsin-EDTA and gently scraped off the flask surface using a cell scraper. To inhibit further trypsin activity, an equal volume of fresh culture medium was added, and the flask contents were transferred to a new Falcon tube for centrifugation at 220 x *g* for 5 minutes (room temperature). The resulting cell pellet was then resuspended in a small volume of fresh culture medium. Cells were then counted as defined in Section 2.2.6 and plated at the required density for experiments. Cells were seeded into tissue culture plates in their respective culture mediums, placed back into the humidified 37°C incubator with 5% (v/v) CO<sub>2</sub> and left undisturbed for a minimum of 1 hour and a maximum of 24 hours to allow adherence before proceeding with experimental protocols.

### 2.2.3 THP-1 monocytic cell line

THP-1 cells were cultured and maintained in RPMI-1640 medium (containing L-glutamine and sodium bicarbonate), supplemented with 10% (v/v) heat-inactivated foetal bovine serum (HI-FBS; heated at 56°C for 30 minutes), 100 U/ml penicillin and 100 µg/ml streptomycin (referred to as 'complete medium' from hereon). The THP-1 cell line is an established monocytic cell line commonly used as an *in vitro* model of human inflammation; the monocytes are suspension cells but upon differentiation into macrophages, become adherent. To obtain cells from the flask, the contents of the flask were transferred to a 50 ml Falcon tube and centrifuged at 110 x *g* for 5 minutes (room temperature). The supernatant was poured off and the cell pellet was resuspended in a small volume of fresh complete medium. For sub-culturing, the cell suspension was aliquoted between 2-3 flasks (depending on the size of the pellet),

## Chapter 2: Materials and Methods

which were then topped up with sufficient volumes of complete medium. For experimental use, cells were counted as described in Section 2.2.6 and the desired number of cells seeded into tissue culture plates. Cells were then treated with 0.16  $\mu\text{M}$  phorbol 12-myristate 13-acetate (PMA) solution (made with complete medium) before being placed back into the humidified 37°C incubator with 5% (v/v) CO<sub>2</sub> for 24 hours to allow differentiation. After this, the PMA solution was removed, and cells were washed with 1X PBS before commencing experimental protocols.

### 2.2.4 Freezing down and thawing frozen cells

Cells first obtained from the supplier were cultured and expanded; cells no older than passage 4 were frozen down and stored at -80°C or in liquid nitrogen until use. To do this, cells were obtained from culture flasks (once a minimum confluency of 80% was reached) as described previously (in Sections 2.2.2 and 2.2.3) and resuspended in 10% (v/v) DMSO in HI-FBS within cryovials. Vials were then frozen by placing in a Mr. Frosty™ freezing container filled with isopropanol before being transferred to -80°C for uniform and consistent cell freezing. Once completely frozen, vials were either transferred to liquid nitrogen for long-term storage or kept at -80°C for short-term storage until use. For use, vials were defrosted by thawing for 1-2 minutes in a 37°C water bath with constant movement of the vial. Cells were then pipetted up and down multiple times in the vial to homogenise the cell suspension before being transferred to a culture flask containing fresh culture medium pre-warmed to 37°C to dilute the DMSO. The flask was placed into the humidified 37°C incubator containing 5% (v/v) CO<sub>2</sub> and left undisturbed for 24 hours before the culture medium was changed to remove all traces of DMSO.

### 2.2.5 Extraction of human monocyte-derived macrophages

Primary human monocyte-derived macrophages (HMDMs) were obtained from buffy coats supplied by the Welsh Blood Service. Ethical approval and informed consent for each donor was granted to the Welsh Blood Service for use of human blood samples for research purposes. To obtain the peripheral blood mononuclear cells (PBMCs), 15 ml of Lymphoprep™ was placed at the bottom of 50 ml Accuspin tubes,

and 25 ml of buffy coat (diluted with equal parts with Dulbecco's PBS) was slowly layered on top using a plastic Pasteur pipette. The tubes were then centrifuged at  $250 \times g$  for 30 minutes at room temperature with no brake to enable gradient separation as illustrated in Figure 2.1.

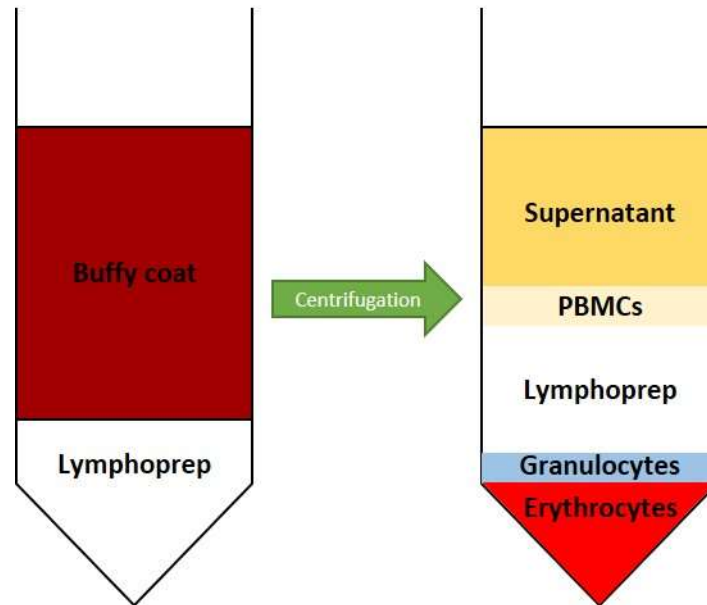


**Figure 2.1 Gradient separation of the components in buffy coat.**

Centrifugation of buffy coat (diluted with equal parts with Dulbecco's PBS) without brake in the presence of Lymphoprep™ enables the separation of PBMCs, granulocytes and erythrocytes. Abbreviations: PBMCs, peripheral blood mononuclear cells; PBS; phosphate-buffered saline.

The supernatant (uppermost layer) was then removed and the PBMC layer (which appears as a white, cloudy layer) was carefully aspirated using a pipette and transferred to a new 50 ml Falcon tube containing a small volume (~1.5 ml) of ice-cold ammonium chloride solution (0.8%  $\text{NH}_4\text{Cl}$  in 0.1 mM EDTA in water buffered with  $\text{KHCO}_3$  to achieve a final pH of 7.2-7.6). The tube was then incubated at room temperature for 2-3 minutes to lyse any contaminating erythrocytes. To remove the ammonium chloride (and any contaminating erythrocytes), cells were centrifuged at  $250 \times g$  for 7 minutes at  $4^\circ\text{C}$ , and the resulting cell pellet was washed 4-6x in ice-cold Dulbecco's PBS via centrifugation using the same settings. After the last wash, the remaining cells were resuspended in complete medium pre-warmed to  $37^\circ\text{C}$  and counted as described in Section 2.2.6, before the desired numbers were seeded into Helena Bioscience 12- or 96-well tissue culture plates, ready for experimentation after differentiation. To induce monocyte differentiation into macrophages, cells were

## Chapter 2: Materials and Methods

treated with 20 ng/ml M-CSF and incubated for 4-6 days within a humidified 37°C incubator containing 5% (v/v) CO<sub>2</sub>. The cells were then washed thoroughly multiple times using 100-200 µl of fresh complete RPMI medium (via pipetting and aspiration) prewarmed to 37°C to remove any contaminating platelets and any non-adherent leukocytes, leaving the adherent HMDMs within the wells.

### 2.2.6 Cell counting

To seed the desired number of cells for experiments, the number of cells present in a suspension was determined using a haemocytometer, which contains a 5 x 5 grid, under a microscope. Cells were pelleted and resuspended in a small volume of fresh culture medium (volume dependent on the cells e.g., pellet size); 7.5 µl of cell suspension was loaded onto the haemocytometer and covered with a glass cover slip to ensure even distribution of cells on the grid. All cells within the four corner squares along with the centre square of the 5 x 5 grid were counted, and the total number of cells within this grid was calculated via multiplication by 5. This number was then used to calculate the volume (µl) of cell suspension required to obtain the desired number of cells using the following formula: (number of cells required / cell count)/10. Alternatively, the concentration of the cell suspension was calculated by multiplying the cell count by 10<sup>4</sup> to obtain cells/ml.

## 2.3 Cell treatment and stimulation

### 2.3.1 Cell treatment

(+)-Catechin was dissolved in DMSO, which hence forms the vehicle control for all experiments; stock solutions were aliquoted and stored at -20°C until use. The final concentration of (+)-catechin used to treat the cells was 1.5 µg/ml (in 0.1% (v/v) DMSO), made up in the appropriate cell culture medium, for all *in vitro* experiments. This concentration was previously optimised via various dose response experiments using THP-1 cells conducted in the host laboratory, which was found to be the lowest effective concentration *in vitro* (Moss 2018). Treatment time varied from a minimum of 3 hours (short-term effect) to a maximum of 7 days (long-term effect) depending on the experiment. All treatment incubations were carried out in a humidified 37°C

## Chapter 2: Materials and Methods

incubator containing 5% (v/v) CO<sub>2</sub>. Where prolonged treatment times were involved, cells were provided with fresh treatment solution made up in the appropriate culture medium every 24 hours, due to the ability of (+)-catechin to be oxidised over time at room temperature and above.

For comparison of the effect of (+)-catechin with its isomers on THP-1 monocyte migration and ROS production, the same concentrations (1.5 µg/ml) of (-)-catechin and (-)-epicatechin were also used to treat the cells. According to information from the manufacturer (Sigma-Aldrich), (-)-catechin is soluble in water, whereas (-)-epicatechin and (+)-catechin are not and so were dissolved in DMSO, hence different vehicle controls for the isomers were used. This comparison was only done on these two key assays in order to gain insights into the efficacy of (+)-catechin compared to its isomers *in vitro*.

### 2.3.2 Stimulation of endothelial cells

OxLDL is a key inducer of endothelial dysfunction (Buckley and Ramji 2015; Gimbrone Jr and Garcia-Cardena 2016) and so was used in initial experiments to stimulate HUVECs, in order to study the effect of (+)-catechin on various associated parameters. However, during the project, the commercial supply of oxLDL was drastically reduced and the cost increased substantially. Furthermore, the efficacy of using oxLDL to stimulate the ECs was brought into question after expected changes (e.g., in ROS production, permeability and MCP-1 release), were not seen in various assays. This may be due to the unknown degree of LDL oxidation (information not provided by the supplier), as well as other factors relating to the assay itself, and so stimulation using TNF-α was also pursued. This is since one of the ways in which oxLDL acts is via the proinflammatory cytokine, TNF-α, as oxLDL induces its production by various cells and has been used by other published studies to activate ECs *in vitro* (Jovinge et al. 1996; Zhang et al. 2009; Rastogi et al. 2011; Chen and Khismatulin 2015). The final concentrations of oxLDL and TNF-α used were based upon initial dose response experiments, to identify the maximal concentration that had no detrimental effects on HUVEC viability after 24 hours. To explore the effect of (+)-catechin on parameters associated with endothelial dysfunction, cells were stimulated via incubation with

either 100 µg/ml oxLDL or 50 ng/ml TNF-α (diluted in ECGM) for a maximum of 48 hours (unless otherwise defined). All incubations as part of cell stimulations were carried out in a humidified 37°C incubator with 5 (v/v) CO<sub>2</sub>.

### 2.3.3 Coating transwell inserts with Matrigel

Coating of surfaces with Matrigel (ECM gel from Engelbreth-Holm-Swarm murine sarcoma) for experiments which required adherent cells to grow on porous transwell inserts was done according to manufacturer's instructions (Sigma-Aldrich). Matrigel was stored at 20°C until use and thawed at 4°C prior to use; during use, the Matrigel was kept on ice to prevent solidification. The Matrigel was diluted at a ratio of 2:1 with ice-cold DMEM for use (as recommended by the manufacturer). Transwell inserts were examined beforehand to check for the presence of any wrinkles or tears. Using pipette tips that had been pre-cooled to 4°C and working quickly, 100-200 µl (depending on the size of the inserts used) of the diluted Matrigel solution was deposited onto the upper surface of the insert, ensuring complete and consistent coverage by a thin layer. Excess gel solution was rapidly removed via manual aspiration using a pipette, and the inserts were placed into their appropriate companion plate wells and left undisturbed for 30 minutes at 37°C to allow for solidification.

## 2.4 Cell-based assays

### 2.4.1 Cell viability

To verify that (+)-catechin has no cytotoxic effects, the Pierce™ Lactate Dehydrogenase (LDH) Cytotoxicity Assay Kit was used according to manufacturer's instructions (ThermoFisher Scientific) to determine cell viability, and to confirm that any observations were not a result of cell death. LDH is a cytosolic enzyme released into cell culture medium when the plasma membrane is damaged; its quantification is hence a suitable method for measuring cell cytotoxicity (Kumar et al. 2018). HMDMs (10<sup>5</sup> cells/well), HUVECs (10<sup>4</sup> cells/well) or HASMCs (10<sup>4</sup> cells/well) were seeded into a 96-well plate and treated with vehicle or (+)-catechin for 24 hours (as described in Section 2.2.7). HUVECs were also stimulated with oxLDL or TNF-α (at the defined

## Chapter 2: Materials and Methods

concentrations) with or without vehicle/(+)-catechin for 24 hours. Lysis buffer (provided in the kit) was added to the positive control wells (whilst the same volume of H<sub>2</sub>O was added to all other wells), and cells were incubated at 37°C for 45 minutes to induce lysis (forming the positive control). Samples of cell supernatants were then transferred to a new 96-well plate and assayed for LDH. The released LDH catalyses a reaction involving nicotinamide adenine dinucleotide (NAD), where NAD<sup>+</sup> is reduced to NADH. Diaphorase uses this NADH to reduce tetrazolium salt to formazan (a red product) that can be measured at 570 nm. The cellular LDH concentration is hence directly proportional to the quantity of red product formed. The absorbance at 570 nm was then measured after adding stop solution (provided in the kit) in a microplate reader. Increasing absorbance values correlates to increasing LDH concentration, suggesting reduced cell viability. Where the lysis buffer failed to induce a sufficient increase in LDH, data for those experiments were discarded.

### 2.4.2 Cell proliferation

The remaining cells from the viability assay were stained with 0.2% (w/v) crystal violet (CV) solution (in 10% (v/v) ethanol) via incubation for 5 minutes at room temperature. The CV binds to intracellular proteins and nucleic acids (Feoktistova et al. 2016) whereby the intensity of purple colour is indicative of the number of viable cells. Cells were then washed thrice with 1X PBS and intracellular CV was solubilised using 0.1 M NaH<sub>2</sub>PO<sub>4</sub> (in 50% (v/v) ethanol) before measuring absorbance at 570 nm in a microplate reader. Increasing absorbance corresponds to the increased viable cell numbers, suggesting increased proliferation, and hence is an indirect measure of cell proliferation. Both viability (as measured by the LDH assay) and proliferation (as measured by CV staining) were expressed as percentage of vehicle control, which was arbitrarily assigned as 100%.

### 2.4.3 Cell proliferation over 7 days

To assess the effect of (+)-catechin on HASMC proliferation over a prolonged period of time, CV staining as described in Section 2.4.2 was carried after various time points up to day 7. Cells were seeded into six separate 96-well plates at a density of 10<sup>4</sup>

## Chapter 2: Materials and Methods

cells/well and treated with vehicle or (+)-catechin for the required duration before staining with CV on days 0 (done one hour after seeding i.e., after cells had adhered), 1, 2, 3, 4 and 7. Proliferation was calculated relative to the vehicle control, which was set arbitrarily as fold change 1 for each time point.

### 2.4.4 Cellular ROS production

The Dichlorofluorescein Diacetate (DCFDA) Cellular ROS Detection Assay Kit was used to measure ROS production according to manufacturer's instructions (Abcam). DCFDA is a fluorogenic dye internalised by the cells; tert-butyl hydrogen peroxide (TBHP) stimulates intracellular ROS production, oxidising DCFDA to fluorescent dichlorofluorescein. THP-1 monocytes ( $1.5 \times 10^5$  cells/well), HMDMs ( $3 \times 10^5$  cells/well), HUVECs ( $2.5 \times 10^4$  cells/well) or HASMCs ( $1.5 \times 10^4$  cells/well) were seeded into a 96-well plate. The cell densities used were based upon previous optimisation experiments to account for differences in cell size, and where maximal changes in ROS production induced by TBHP were seen. Cells were stained with 20 (for THP-1 cells), 25 (for HUVECs or HASMCs) or 40 (for HMDMs)  $\mu\text{M}$  DCFDA solution via incubation in a humidified incubator at  $37^\circ\text{C}$  with 5% (v/v)  $\text{CO}_2$  for 45 minutes in darkness. The stain was then removed and cells were washed with 1X dilution buffer (provided in kit) and treated (as described in Section 2.2.7) with vehicle alone, or vehicle/(+)-catechin in the presence of 50  $\mu\text{M}$  TBHP (75  $\mu\text{M}$  was used for HMDMs) for 3 hours in a humidified incubator at  $37^\circ\text{C}$  with 5% (v/v)  $\text{CO}_2$  in darkness. For THP-1 monocytes, cells were also treated with (-)-catechin and (-)-epicatechin in order to compare (+)-catechin with its isomers. Fluorescence was then measured at  $\text{Ex}_{485}/\text{Em}_{535}$  nm in a microplate reader, and readings were standardised to the TBHP-positive vehicle control, set arbitrarily as fold change 1.

### 2.4.5 Cellular ROS production in the presence of other mediators

TBHP-stimulated ROS production was also measured in the presence of oxLDL and TNF- $\alpha$  in HUVECs for comparison, as part of initial optimisation experiments to identify the effects of these pro-inflammatory mediators.

### 2.4.5.1 oxLDL

The DCFDA Cellular ROS Detection Assay Kit was used to measure the effect of oxLDL on TBHP-stimulated ROS production in HUVECs. HUVECs were seeded into a 96-well plate and assayed, with or without prior stimulation using 100 µg/ml oxLDL before conducting the assay as described in Section 2.4.4. The same concentration of oxLDL was also included in the 3-hour TBHP incubation step, to measure the effect of oxLDL on TBHP-induced HUVEC ROS production after a maximum of 48 hours.

### 2.4.5.2 TNF- $\alpha$

The DCFDA Cellular ROS Detection Assay Kit was also used to measure the effect of TNF- $\alpha$  on TBHP-stimulated ROS production in HUVECs. HUVECs were seeded into a 96-well plate, stimulated with vehicle or 50 ng/ml TNF- $\alpha$  for 24 hours. Alternatively, HUVECs were treated with vehicle or (+)-catechin for 24 hours beforehand. This was to compare the effect of pre-treatment vs short-term treatment combined with stimulation and pre-stimulation on ROS production. The assay was then conducted as described in Section 2.2.4. The same concentration of TNF- $\alpha$  was also included in the 3-hour TBHP incubation step to measure the effect of TNF- $\alpha$  on TBHP-induced HUVEC ROS production.

### 2.4.6 ELISA for the measurement of MCP-1 release

HUVECs were stimulated with 100 µg/ml oxLDL or different concentrations of TNF- $\alpha$  (200 and 400 ng/ml) for 24 hours before the cell supernatants were used to measure MCP-1 released by the cells. The TNF- $\alpha$  concentration used here was higher than usual, as supernatants were taken from cells seeded for the optimisation of other assays for efficiency, as this was purely to compare the effects of oxLDL and TNF- $\alpha$  (to identify the optimal method of EC stimulation/activation *in vitro*). Activated ECs are known to have increased secretion of various pro-inflammatory mediators (e.g., chemokines, which include MCP-1; a critical mediator of monocyte recruitment). A DuoSet MCP-1 enzyme-linked immunosorbent assay (ELISA) Kit (a 'sandwich' format ELISA) (with the accompanying Ancillary Kit that contains the associated buffers, reagents and materials required for the assay) was used according to manufacturer's

## Chapter 2: Materials and Methods

instructions (R&D Systems). The assay utilises a specific antibody-to-antigen interaction; the capture antibody is raised against the antigen of interest, which is immobilised on the microplate surface. The antigen is then complexed with an enzyme-conjugated (e.g., horseradish peroxidase (HRP)) detection antibody, which catalyses a colorimetric reaction involving a substrate, enabling indirect antigen quantification.

All incubation steps described below were carried out at room temperature; all volumes of antibodies, samples/standards etc. added to the wells were 100  $\mu$ l unless otherwise stated. On the day prior to the assay, the microplate was coated in capture antibody (provided in the kit) via incubation overnight. The next day, the wells were washed 3x with 400  $\mu$ l of wash buffer (provided in the Ancillary kit); after the last wash, the plate was blotted dry on paper towels to ensure removal of all residual solution in the wells. The plate was then incubated with blocking buffer (provided in the Ancillary kit) for 1 hour, followed by washing as previously described. Samples (diluted as appropriate to ensure that the detection limit was not exceeded) and standards (an antigen at known, increasing concentrations (from 15.6 to 1000 pg/ml), prepared according to manufacturer's instructions via 2-fold dilution) were then plated before incubation for 2 hours. The wells were then washed again as previously described; detection antibody (provided in the kit) was added, and the plate incubated for another 2 hours. The wells were then washed again as described above, HRP-conjugated streptavidin (provided in the kit) was then added, and the plate incubated for 20 minutes in darkness. After the wells were washed again as above, substrate solution (provided in the Ancillary kit) was added, and the plate incubated for another 20 minutes in darkness, followed by the addition of 50  $\mu$ l of stop solution (provided in the Ancillary kit). Finally, absorbance was measured at 490 nm in a microplate reader (with correction at 590 nm to increase the accuracy of the readings). The concentration of MCP-1 in the samples were then calculated via comparison with the standard curve after background subtraction, taking into account the original dilution factor used.

### 2.4.7 Matrix metalloproteinase activity measurement

Activities of proteases, such as MMPs (produced by a variety of sources), promotes plaque vulnerability by degrading key components of the plaque-stabilising fibrous cap (Visse and Nagase 2003; Heo et al. 2011; Olejarz et al. 2020). Assessment of (+)-catechin on cellular MMP production was done using the MMP Activity Assay Kit according to manufacturer's instructions (Abcam). HMDMs ( $10^5$  cells/well) or HASMCs ( $1.5 \times 10^4$  cells/well) were seeded into a 96-well plate. The cells were then treated with vehicle or (+)-catechin for 3 and 24 hours, to assess the short and long-term effects of (+)-catechin respectively. Following this, 50  $\mu$ l of the cell supernatant was transferred to a new microplate, and an equal volume of MMP green substrate solution (provided in the kit) was added to the wells. The plate was then returned to the 37°C incubator for an additional 30 minutes. The substrate solution contains a fluorescent resonance energy transfer peptide which consists of an emitter and a quencher subunit. The peptide is designed to be broken down by MMP enzymes; when this happens, the emitter and quencher subunits separate, recovering the fluorescent signal of the emitter (which was previously blocked by the quencher). Therefore, increasing fluorescence correlates to increasing MMP activity. Following the incubation period, fluorescence was measured in a microplate reader at Ex<sub>485</sub>/Em<sub>535</sub> nm, and data were expressed as a percentage relative to the vehicle control, which was set arbitrarily as 100%.

### 2.4.8 Mitochondrial ROS production

The mitochondria are a major source of ROS within the cell; excess mitochondrial ROS (mitoROS) production can lead to mitochondrial DNA damage and subsequently, compromised mitochondrial function. THP-1 monocytes ( $8 \times 10^4$  cells/well), HUVECs (cells/well) or HASMCs ( $6 \times 10^4$  cells/well for both) were seeded into a 96-well plate and treated with vehicle or (+)-catechin for 24 hours, or with simultaneous stimulation using 50 ng/ml TNF- $\alpha$  (for HUVECs only). The cells were then washed with 1X PBS, and mitoROS production was measured by staining cells with 5  $\mu$ M MitoSOX™ Red solution (diluted in HBSS) via incubation in a humidified 37°C incubator containing 5% (v/v) CO<sub>2</sub> in darkness for 30 minutes. MitoSOX™ Red is a fluorogenic dye that selectively targets the mitochondria after permeating live cells and is readily oxidised

## Chapter 2: Materials and Methods

by superoxide to produce red fluorescence. Cells were then washed with fresh HBSS and 100  $\mu$ l of HBSS was added to the wells before fluorescence measurement at Ex<sub>510</sub>/Em<sub>580</sub> nm in a microplate reader, as per the manufacturer's instructions (ThermoFisher Scientific). Readings were standardised to vehicle-treated cells stained with MitoSOX™ Red (with or without stimulation), which was set arbitrarily as fold change 1.

### 2.4.9 Cellular bioenergetics profiling

#### 2.4.9.1 Mitochondrial respiration

To determine the effect of (+)-catechin treatment (with and without stimulation) on mitochondrial bioenergetic profile, key parameters associated with mitochondrial function were investigated as a way of monitoring cellular metabolic shifts (which may indicate dysfunction). Agilent Seahorse Technology uses specific drug compounds to inhibit mitochondrial respiration and glycolysis in a controlled manner, whilst oxygen consumption rate (OCR) and proton efflux rate (PER) are monitored using an XF96 Analyzer machine. This enables calculation of different parameters associated with mitochondrial function, including basal respiration/glycolysis, proton leak, spare respiratory capacity and compensatory glycolysis.

The Mito Stress Test Assay Kit was used to determine the effect of (+)-catechin on mitochondrial respiration using the Agilent Seahorse XFe96 Analyser according to manufacturer's instructions (Agilent Seahorse Technologies). THP-1 macrophages ( $2 \times 10^5$  cells/well; differentiated from monocytes as described in Section 2.2.3) or HUVECs ( $10^5$  cells/well) were seeded into an XF 96-well tissue culture microplate and stimulated with 250 U/ml IFN- $\gamma$  and 100 ng/ml LPS (to induce M1 polarisation) or 100  $\mu$ g/ml oxLDL respectively, in the presence of vehicle or (+)-catechin for 24 hours. Where stimulation was not used, cells were treated with vehicle or (+)-catechin only, for 24 hours. On the day prior to the assay, the XF96 sensor cartridge was hydrated with XF calibrant solution (pre-warmed to 37°C) and placed in a non-CO<sub>2</sub> incubator set to 37°C overnight, for a minimum of 12 hours. The XF96 Analyzer machine was also turned on (and the Wave software opened) to enable start-up and temperature equilibration, ready for the assay the next day.

## Chapter 2: Materials and Methods

On the day of the assay, the cells were washed with assay medium (prepared according to manufacturer's recommendation (Agilent Seahorse Technologies) and pre-warmed to 37°C) and fresh assay medium was left in the wells. The microplate containing the treated cells was then incubated for 1 hour in a non-CO<sub>2</sub> incubator set to 37°C immediately prior to running the assay. During this incubation time, the mitochondrial inhibitor drug compounds (supplied in the kit) were prepared. The following concentrations were used for HUVECs: 1 µM oligomycin; 2 µM carbonyl cyanide-4 (trifluoromethoxy) phenylhydrazone (FCCP); 0.1 µM mixture of rotenone and antimycin A (rotenone (rot)/antimycin A (AA)). Oligomycin inhibits ATP synthase of complex V, FCCP uncouples oxygen consumption from ATP production, and rotenone and antimycin A inhibit complex I and complex III respectively, ceasing mitochondrial respiration entirely. The same concentrations of inhibitor drugs were also used for THP-1 macrophages, except for rot/AA, where 0.15 µM was used. The prepared solutions of oligomycin, FCCP and rot/AA were then loaded into ports A, B and C respectively of the XF96 sensor cartridge (25 µl each). These concentrations of drug inhibitor compounds and cell seeding densities had been previously optimised in the host laboratory. The loaded cartridge was then incubated in a non-CO<sub>2</sub> incubator set to 37°C for a minimum of 15 minutes prior to running the assay. The assay was then run according to on-screen instructions; the sensor cartridge and utility plate (provided with the sensor cartridge) was first loaded into the Analyzer. After calibration was completed, the utility plate was replaced with the cell culture microplate containing the treated cells and the assay was initiated according to the on-screen prompts.

### 2.4.9.2 Glycolysis

Similarly, the Glycolytic Rate Assay Kit was used to determine the effect of (+)-catechin on glycolysis (with or without stimulation) according to manufacturer's instructions (Agilent Seahorse Technologies). The protocol for this assay is similar to that of the Mito Stress Test assay as described previously, except that inhibitor drugs, 0.5 µM rot/AA and 50 µM 2-deoxy-D-glucose (2-DG), were used instead (injected into port A and port B respectively of the sensor cartridge). Inhibition of glycolysis was achieved with 2-DG which stops glycolytic acidification (and confirms pathway specificity).

### 2.4.10 Mitochondrial membrane potential

Changes in mitochondrial membrane potential were monitored using tetraethylbenzimidazolylcarbocyanine iodide (JC-1), a cationic dye that accumulates in energised mitochondria, using the JC-1 Mitochondrial Membrane Potential Assay Kit according to manufacturer's instructions (Abcam). HUVECs ( $1.5 \times 10^4$  cells/well) were seeded in a 96-well plate. After washing with 1X dilution buffer (provided in the kit), cells were stained with 20  $\mu$ M JC-1 solution (prepared according to manufacturer's instructions) via incubation for 10 minutes at 37°C with 5% (v/v) CO<sub>2</sub>. Cells were then washed twice with 1X dilution buffer and treated with vehicle or (+)-catechin in the presence of 100  $\mu$ g/ml oxLDL for 4 and 24 hours. Cells were also treated with 100  $\mu$ M FCCP to induce mitochondrial membrane depolarisation, which hence forms the positive control. After incubation, fluorescence was measured at EX<sub>485</sub>/EM<sub>535+590</sub> nm in a microplate reader, to detect the monomer and aggregate forms of JC-1 respectively. At a low mitochondrial membrane potential, JC-1 is predominantly a monomer that yields green fluorescence with emission of 530 nm, whereas a high mitochondrial membrane potential, JC-1 aggregates, yielding red-orange emission of 590 nm. Mitochondrial membrane potential was expressed as JC-1 ratio (aggregate to monomer); a decrease in aggregate fluorescent count is indicative of membrane depolarisation whereas an increase indicates hyperpolarisation.

### 2.4.11 Monocyte-endothelial adhesion (static adhesion assay)

The adhesion of recruited monocytes to activated ECs enables their infiltration into the intima layer via *trans*-endothelial diapedesis, and so the effect of (+)-catechin on monocyte-endothelial adhesion was studied using a static adhesion assay. HUVECs were seeded into a 96-well plate and allowed to grow for 2-3 days in a humidified incubator at 37°C with 5% (v/v) CO<sub>2</sub> until the formation of a continuous monolayer. Cells were then treated with vehicle or (+)-catechin for 24 hours, then stimulated with 50 ng/ml TNF- $\alpha$  for 3 hours in the presence of vehicle or (+)-catechin. Near the end of this incubation period, THP-1 monocytes were fluorescently labelled with 10  $\mu$ M 2', 7'-Bis(2-carboxyethyl)-5(6)-carboxyfluorescein tetrakis (acetoxymethyl) ester (BCECF-AM) diluted in 1X PBS via incubation at 37°C for 10 minutes. BCECF readily permeates the cell membrane; once permeated, non-specific cellular esterases cleave

the lipophilic blocking groups, resulting in a fluorescent form of the molecule. The stained monocytes were then washed with PBS via centrifugation at  $110 \times g$  for 5 minutes at room temperature and resuspended in ECGM, before being added to the activated HUVECs for 30 minutes at  $37^{\circ}\text{C}$  to allow their interaction (see Figure 2.2 below). Following this, any unattached cells were gently washed away using 1X PBS, before a small volume of fresh 1X PBS was added to the wells for fluorescence measurement at  $\text{Ex}_{485}/\text{Em}_{535}$  nm using a microplate reader (protocol adapted from (Wang et al. 2011)). Adhesion was calculated as fold change relative to TNF- $\alpha$ -stimulated HUVECs treated with vehicle control, which was set arbitrarily as fold change 1.

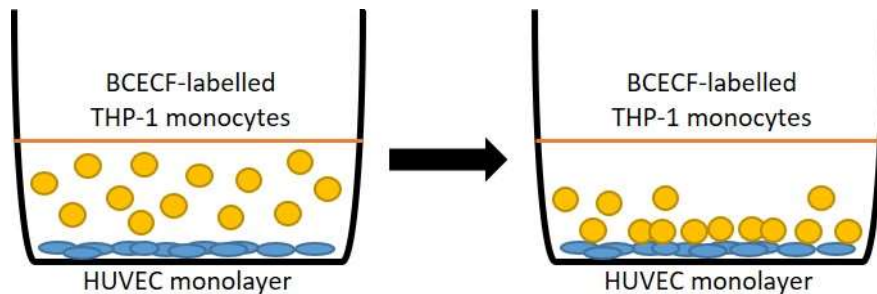


**Figure 2.2 Diagrammatic representation of the static adhesion assay set up.**

Human umbilical vein endothelial cells (HUVECs) were allowed to grow into a monolayer on the microplate surface. Monocytes were fluorescently labelled via incubation with  $10 \mu\text{M}$  2', 7'-Bis(2-carboxyethyl)-5(6)-carboxyfluorescein tetrakis (acetoxymethyl) ester (BCECF-AM) solution for 10 minutes, before being allowed to interact with the monolayer of endothelial cells for 30 minutes at  $37^{\circ}\text{C}$ . Any unattached monocytes were washed away before fluorescence measurement, with increased fluorescence corresponding to increased monocyte-endothelial adhesion.

#### 2.4.12 Apoptosis

Apoptosis of cells within the atherosclerotic plaque contribute to the formation and growth of the necrotic core within the atherosclerotic plaque. To investigate the effect of (+)-catechin on EC apoptosis, the Annexin V-FITC Apoptosis Detection Assay Kit was used according to manufacturer's instructions (Abcam). HUVECs ( $2 \times 10^4$  cells/well) were seeded into 12-well culture plates and stimulated with  $100 \mu\text{g}/\text{ml}$  of oxLDL in the presence of vehicle or (+)-catechin for 24 hours. To induce apoptosis, cells were treated with  $400 \text{ ng}/\text{ml}$  TNF- $\alpha$  in serum-free DMEM (i.e., serum-starved) and incubated for 24 hours at  $37^{\circ}\text{C}$  in 5% (v/v)  $\text{CO}_2$ , which hence forms the positive control. Cells were then removed from the plate surface via trypsinisation and scraping

## Chapter 2: Materials and Methods

(as described in Section 2.2.2) and gently washed with 1X PBS, before 100  $\mu$ l of annexin V-FITC solution (prepared according to manufacturer's instructions using the reagents provided in the kit) was added. The cells were then incubated at room temperature in darkness for 5 minutes to enable binding of the annexin V to markers of apoptosis. Fluorescence at Ex<sub>485</sub>/Em<sub>535</sub> nm was then measured in a microplate reader, and data were presented as fold change relative to the positive control, which was set arbitrarily as 1.

### 2.4.13 Endothelial permeability

Hyperpermeability of the endothelium facilitates the infiltration of circulating immune cells and LDL particles to the arterial wall, encouraging lesion formation and progression. The permeability assay was carried out to determine the effect of (+)-catechin on the permeability of ECs in the presence of oxLDL. Microporous transwell inserts containing 0.4  $\mu$ m pores were coated with Matrigel (as described in Section 2.3.3). HUVECs ( $8 \times 10^4$ ) were then seeded into the inserts and allowed to grow into a continuous monolayer for 3 days in a humidified 37°C incubator containing 5% (v/v) CO<sub>2</sub>. Cells in the insert were then stimulated with 100  $\mu$ g/ml oxLDL in the presence vehicle or (+)-catechin (whilst EGCM was added to the well) and incubated for up to 24 hours in a humidified 37°C incubator containing 5% (v/v) CO<sub>2</sub>. Cells were also treated with 100 ng/ml vascular endothelial growth factor (VEGF), a known permeability inducer, as a positive control, and inserts without cells were also included as a no cells control. FITC-conjugated dextran was also added to the insert at a final concentration of 1 mg/ml, and its presence in the transwell (i.e., its movement from the insert through the cell monolayer) was measured periodically to monitor changes in permeability over 6 hours. This was done by transferring 10  $\mu$ l aliquots of the transwell contents at the defined times into a 96-well plate (diluted with 90  $\mu$ l of H<sub>2</sub>O) for fluorescence measurement at Ex<sub>485</sub>/Em<sub>535</sub> nm in a microplate reader. Data were presented as fluorescence over time.

2.4.14 Smooth muscle cell migration (invasion)

To monitor the migration of HASMCs, a modified Boyden chamber with an 8  $\mu\text{m}$  porous insert coated with Matrigel (as described in Section 2.3.3) was used. The inserts (upper chamber) contained cells incubated for 48 hours with serum-free DMEM to induce quiescence. Cells were then treated with serum-free DMEM containing vehicle or (+)-catechin, whilst PDGF-BB (homodimeric form of PDGF; 20 ng/ml) solution made up in SMCM was added to the transwell. Following incubation in a humidified incubator with 5% (v/v)  $\text{CO}_2$  for 4 hours at 37°C, membrane of the inserts was carefully removed using a scalpel and the cells on the underside of the membrane mounted onto microscope slides using Fluoroshield™ with DAPI (4', 6'-diamidino-2-phenylindole). The membranes were then visualised via fluorescence microscopy (using an Olympus BX61 microscope) under x20 magnification, and the total number of cells in five different high-power fields were counted (protocol adapted from (Liu et al. 2013; Alahmadi 2019). Fold change was then calculated relative to the PDGF-positive control, which was set arbitrarily as fold change 1.

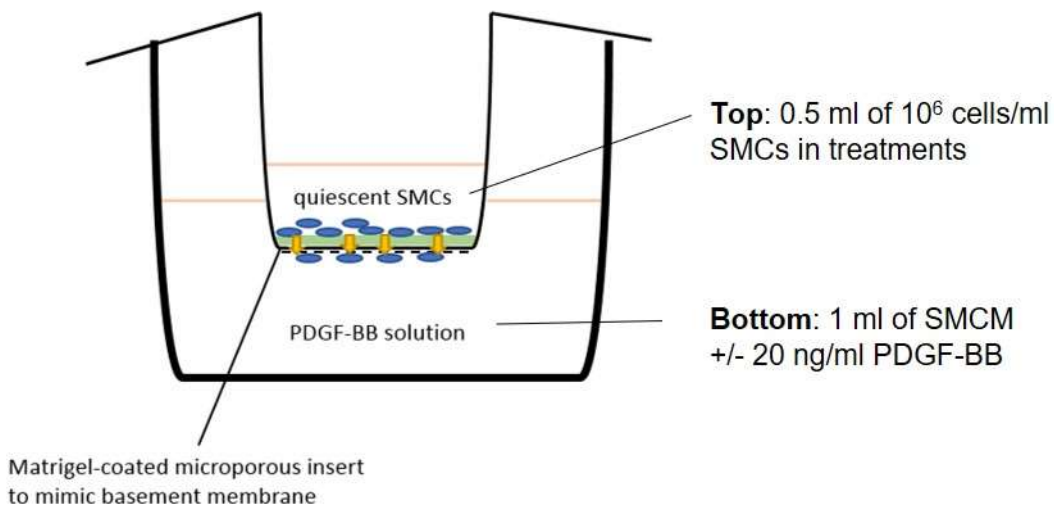


**Figure 2.3 Diagrammatic representation of the invasion assay set up.**

Smooth muscle cells (SMCs) were seeded into 8  $\mu\text{m}$  porous inserts pre-coated with Matrigel. Quiescence was induced via incubation of the SMCs with serum-free medium for 48 hours. After this, cells were treated whilst platelet-derived growth factor (PDGF) solution was added to the transwell, to induce the migration of SMCs from the top of the insert to the underside of the insert, towards the PDGF.

### 2.4.15 Monocyte migration

Migration of THP-1 monocytes was assessed using the modified Boyden chamber method; microporous transwell inserts containing 8 µm pores were used to mimic the arterial endothelial layer. The chemokine, MCP-1, a key inducer of monocyte recruitment *in vivo*, at a concentration of 25 ng/ml was used to induce the migration of monocytes ( $5 \times 10^5$ ) seeded in the insert, through the microporous membrane and into the transwell. To compare the effect of (+)-catechin with that of its isomers, cells were incubated with treatments ((+)-catechin, (-)-catechin, (-)-epicatechin or their respective vehicle controls made up in complete medium) for 3 hours in a humidified incubator at 37°C containing 5% (v/v) CO<sub>2</sub>, while MCP-1 solution made up in complete medium (containing vehicle) was present in the transwell. The underside of the inserts was then washed with 0.5 ml of 1X PBS (into the transwell) before discarding. The remaining contents of the transwell were transferred into a 15 ml tube and centrifuged at 110 x *g* for 5 minutes (room temperature). The pelleted cells were then resuspended in 1 ml of fresh 1X PBS for counting as described in Section 2.2.6. Migration was calculated as fold change relative to the MCP-1-positive vehicle control, which was arbitrary set as fold change 1.

## 2.5 *In vivo* techniques

### 2.5.1 Animal maintenance and feeding

Eight-week-old male *Ldlr*<sup>-/-</sup> (C57BL/6J background) were obtained using *Ldlr*<sup>-/-</sup> mice homozygous for the *LDLRtm1Her* mutation and backcrossed to the C57BL/6J strain (originally obtained from the Jackson Laboratory) and expanded locally (in-house) in a pathogen-free environment. Mice were randomly assigned to different groups as required and used for all *in vivo* studies, to delineate the effect of (+)-catechin on atherosclerosis development and progression, and even, regression. Mice were housed in a light and temperature-controlled facility (lights on 7am-7pm, 22°C) within conventional open top cages. Based on previous studies conducted on *Ldlr*<sup>-/-</sup> mice in the host laboratory, 15-20 mice were used per group; weight and food consumption (and water intake where necessary) were measured and recorded twice weekly. All studies and protocols had received approval by the Cardiff University Institutional

## Chapter 2: Materials and Methods

Ethics Review Committee and the United Kingdom Home Office. Experiments were carried out in accordance with the Guide for the Care and Use of Laboratory Animals (NIH Publication No. 85-23, revised in 1996; Experimental Licence 30/3365).

### 2.5.2 Progression study

Mice were fed HFD (21% (w/w) pork lard and 0.15% (w/w) cholesterol) *ad libitum*, to induce atherogenesis. The HFD was supplemented with 200 mg/kg/day (+)-catechin, in the form of (+)-catechin hydrate (this molecule is identical to (+)-catechin but with an additional H<sub>2</sub>O group) for 12 weeks. The (+)-catechin hydrate was dissolved in 1X PBS (which hence forms the vehicle control), enabling it to be easily mixed into the HFD. This HFD feeding duration was based upon previous studies conducted in the host laboratory, which found the 12-week duration to be an optimal time point for the formation of established lesions. Previous verification that (+)-catechin hydrate elicits similar anti-atherogenic effects in comparison to (+)-catechin in a number of *in vitro* experiments, allowed (+)-catechin hydrate to be used for *in vivo* studies, drastically reducing the implicated cost (since pure (+)-catechin is substantially more expensive) and avoids the use of toxic DMSO in animals. The dose is based on a previous pilot study conducted in the host laboratory using wild-type C57BL/6J male mice fed HFD with daily gavage of (+)-catechin hydrate for 3 weeks, which successfully modulated several atherosclerosis-associated risk factors (Moss 2018). The dose used in this short-term study was based upon a previously published study of the same duration in rats but using the catechin, EGCG (Potenza et al. 2007).

### 2.5.3 Regression study

To study the ability of (+)-catechin to stimulate the regression of established plaques after promising effects on atherosclerosis development and progression was seen, mice were fed HFD for 12 weeks to induce atherogenesis then switched back to the NCD for 8 weeks to stimulate atherosclerosis regression. This duration was selected based upon a previous study conducted in the host laboratory which saw a lack of changes in plaque burden after 4 weeks of NCD feeding (which was based upon studies previously published in the literature (Gijbels et al. 1999; Rayner et al. 2011;

Zimmer et al. 2016)). Therefore, a pilot study (trial) involving 3-4 mice per group was used to compare the effects of 8 vs 12 weeks of NCD (with and without (+)-catechin hydrate supplementation) feeding after 12 weeks of HFD on plaque burden (prior to starting the regression study). Results of this trial suggested that there were changes in the atherosclerotic plaque after 8 weeks (which was similar to those observed after 12 weeks), and so the 8-week duration was proceeded with. During NCD feeding and for the relevant group, mice were also given 200 mg/kg/day (+)-catechin hydrate, which was dissolved in the drinking water (which was changed 2-3 times weekly). This avoided the need to laboriously soften chow pellets by soaking in water overnight before being able to combine with the (+)-catechin hydrate solution. The volume of water intake was monitored regularly to ensure that there were no issues relating to palatability. An additional group were maintained on HFD for the duration of the 12 + 8 weeks (i.e., a total 20 weeks), to enable comparison of switching to NCD vs continued HFD feeding on atherosclerosis progression.

#### 2.5.4 Extraction of blood from the tail

On the day prior to the designated end point of the feeding procedure, blood was extracted from the tails of the mice in order to analyse circulating myeloid and lymphoid cell populations within the peripheral blood. Circulating immune cells can be stimulated to infiltrate the atherosclerotic plaque by various chemokines and cytokines, influencing plaque burden and inflammation. To isolate blood from the tail, the mouse was restrained in a Tailveiner Restrainer, which restrains the mouse while allowing full access to the entire tail. The tip of the tail was sprayed with ethyl chloride (a topical anaesthetic) and approximately 1 mm of tail was cut off using a smooth scalpel, and flowing blood was collected into EDTA microvette tubes (to prevent clotting) one drop at a time. Blood flow was encouraged by gently massaging the tail with the thumb and forefinger from the start of the tail towards the tip. This was done until approximately 50 µl of blood was obtained. Pressure was then applied to the tip of the tail with some tissue, and the mouse was closely monitored to ensure that the bleeding had stopped before being placed back into their original cage.

## Chapter 2: Materials and Methods

### 2.5.5 Collection of blood and tissues at the endpoint

At the end point of the feeding procedure, mice were sacrificed via exposure to increasing levels of CO<sub>2</sub> in a chamber, and death was confirmed by exsanguination via cardiac puncture. The blood obtained from cardiac puncture was transferred to a tube containing 50 U/ml of heparin (to prevent clotting) and kept at room temperature until isolation of the plasma. To isolate the plasma, the blood was centrifuged at 12,000 x g for 10 minutes at room temperature. The plasma (upper, straw-coloured layer) was then taken using a pipette and transferred to a new Eppendorf tube for storage at -80°C until use. After the mouse was pinned to a dissection board and the skin, peritoneal cavity and thoracic cavity was cut open to expose the internal organs, the heart was gently flushed with ~5 ml of PBS after slitting the left ventricle to gradually perfuse the organs. Five different adipose tissue deposits were also taken (subcutaneous, inguinal, gonadal, renal and brown), along with three sections of the intestine at consistent intervals, samples of urine (where possible) and faeces, the spleen, thymus and liver. The heart, brachiocephalic artery and a small proportion of the liver were mounted onto Shandon base cryomolds in optimum cutting temperature (OCT) embedding matrix and snap frozen, ready for sectioning. Extracted adipose tissue deposits and organs of interest were weighed at the time of harvest using an electronic scale and all measurements subsequently standardised to body weight. The descending aorta (thoracic and abdominal) was also isolated from the aortic arch to the subclavian arteries and stored in *RNALater*<sup>TM</sup> Stabilisation Solution for future RNA extraction. Tissue samples were snap frozen in dry ice before storage at -80°C. The two rear legs were also taken and stored in 1X PBS supplemented with 2% (v/v) HI-FBS (referred to as '2% PBS' hereon) at 4°C until bone marrow extraction.

### 2.5.6 Measurement of plasma triglyceride

TG levels in the isolated plasma were determined using a Triglyceride Quantification Assay Kit according to manufacturer's instructions (Abcam). In the assay, plasma TGs are metabolised into free fatty acids and glycerol. The glycerol is oxidised into a product capable of interacting with the target probe to induce a colour change; a greater colour change indicates a higher level of TG. Samples were incubated with lipase for 20 minutes at room temperature to convert TGs into glycerol and fatty acids.

## Chapter 2: Materials and Methods

Assay buffer, probe and enzyme mix (all provided in the kit) were then added and incubated for 1 hour at room temperature (in darkness). The colour changes (i.e., absorbance at 570 nm) was measured in a microplate reader and TG levels were determined by comparison to a standard curve, prepared according to manufacturer's instruction. Where necessary, samples were diluted (using the buffer provided in the kit) as appropriate before assaying to ensure that values did not exceed the maximum limit of detection (10 nmol).

### 2.5.7 Plasma lipoprotein quantification and profiling

Hypercholesterolemia, specifically, elevated levels of circulating LDL-C, is a key risk factor for atherosclerosis as well as being associated with metabolic syndrome (Lonardo et al. 2018). Cholesterol levels in the isolated plasma were determined using the HDL and LDL/VLDL Cholesterol Assay Kit according to manufacturer's instructions (Abcam). Whilst total and free cholesterol determination did not require any additional preparations of the plasma beyond dilution, precipitation steps were required to separate the HDL and LDL/VLDL fractions. Samples of plasma were mixed with precipitation buffer (provided in the kit) and the mixture was incubated at room temperature for 10 minutes, before centrifugation at 2,000 x g for 10 minutes. The HDL fraction was then present in the supernatant, whilst the LDL/VLDL fraction was pelleted in the tube. The HDL fraction (supernatant) was transferred to a clean microfuge tube and the remaining LDL/VLDL fraction was centrifuged again (same conditions) to remove any residual HDL by aspirating any resulting supernatant. The pellet was then resuspended in fresh 1X PBS (this was the LDL/VLDL fraction). Samples were then assayed to determine levels of total, free, HDL and LDL/VLDL (using colorimetric detection) by comparing to a standard curve prepared according to manufacturer's instructions, after the absorbance at 570 nm was measured in a microplate reader. Samples were diluted using the provided buffer as appropriate prior to assaying, to ensure that the detection limit (1 µg) was not exceeded.

## Chapter 2: Materials and Methods

### 2.5.8 Plasma oxidative stress parameters

#### 2.5.8.1 Plasma ROS/RNS

The levels of reactive oxygen/nitrogen species (ROS/RNS) were assessed in the mouse plasma samples, using an OxiSelect *In Vitro* ROS/RNS Assay Kit (green fluorescence) according to manufacturer's instructions (Cell Biolabs). The assay uses a dichlorodihydrofluorescein (DCFH) probe which is readily oxidised by ROS into a highly fluorescent form that produces a fluorescent signal. Increasing fluorescence is hence correlated to increasing presence of ROS in the plasma sample. No additional sample preparation was required for the assay; 50 µl of samples and H<sub>2</sub>O<sub>2</sub> standard (prepared according to manufacturer's instructions) were transferred to a 96-well plate. An equal volume of catalyst solution (provided in the kit) was added to each well and the plate was incubated for 5 minutes at room temperature in darkness. The samples were then mixed with DCFH solution (provided in the kit), a probe which is broken down in the presence of H<sub>2</sub>O<sub>2</sub> into its fluorescent form and incubated for 30 minutes in darkness at room temperature. Fluorescence was then measured in a microplate reader at Ex<sub>485</sub>/Em<sub>535</sub> nm and samples were compared to the H<sub>2</sub>O<sub>2</sub> standard curve to calculate ROS/RNS concentration (sensitivity of the assay is up to 10 pM).

#### 2.5.8.2 Plasma malondialdehyde

Malondialdehyde (MDA) is a product of lipid peroxidation, an indicator of oxidative stress (Gawel et al. 2004; Ayala et al. 2014), and so plasma MDA levels were quantified using an OxiSelect Thiobarbituric Acid (TBA) Reactive Substances (TBARS) Assay Kit according to manufacturer's instructions (Cell Biolabs). The TBA reacts with MDA to produce a fluorescent molecule and so is used as an indicator of the degree of lipid peroxidation in the samples. To prevent further oxidation of the samples, 0.05% (v/v) butylated hydroxytoluene solution was added to the plasma. An equal volume of sodium dodecyl sulphate (SDS) lysis solution (provided in the kit) was added to the samples, which were then incubated at room temperature for 5 minutes. TBA was added to the mixture and the samples were subsequently heated at 95°C for 30 minutes before being cooled on ice. Samples were then centrifuged at 500 x g for 15 minutes and the supernatant was transferred to a new 96-well plate. Fluorescence

## Chapter 2: Materials and Methods

was measured in a microplate reader at Ex<sub>535</sub>/Em<sub>590</sub> nm. The levels of MDA in the samples were then calculated by comparing to the standard curve, prepared according to manufacturer's instructions. Samples were diluted if necessary, to ensure that they did not exceed the detection limit (125 µmol).

### 2.5.9 Plasma cytokine levels

Plasma cytokine levels were determined by the Central Biotechnology Services facility based in the School of Medicine, Cardiff University using a V-PLEX Plus Pro-inflammatory Panel1 Mouse Kit (Meso Scale Diagnostics, USA) according to manufacturer's instructions and 25 µl of plasma from each mouse (assayed in duplicate). Any samples that fell beyond the pre-defined detection range for each cytokine were removed prior to statistical analysis.

### 2.5.10 Immunophenotyping of peripheral blood cell populations

Analysis of immune cell populations within the peripheral blood via flow cytometry was done in collaboration with Dr Neil Rodrigues' laboratory at the European Cancer Stem Cell Research Institute (ECSCRI). Peripheral blood was extracted from the tail (as described in Section 2.5.4) and processed within 4 hours of extraction (to maintain >80% cell viability). Ice-cold ammonium chloride solution (600 µl; 0.8% NH<sub>4</sub>Cl in 0.1 mM EDTA in water buffered with KHCO<sub>3</sub> to achieve a final pH of 7.2-7.6) was added to microfuge tubes and 12 µl of blood was added to the ammonium chloride. This was done twice for each sample; one for the analysis of myeloid cells and the other for that of lymphoid cells. The tubes were inverted 6x and incubated at room temperature for 6 minutes (this was done twice). The tubes were then centrifuged for 10 minutes at 500 x g, 4°C. The supernatant was aspirated and removed, and the cell pellet was resuspended in 50 µl of antibody mix (diluted in 2% PBS) containing antibodies used to label specific populations of lymphoid and myeloid cells, according to the markers stated in Table 2.2.

**Table 2.2 Markers used to identify immune cell populations within the peripheral blood.**

<b>Class</b>	<b>Cell type</b>	<b>Marker</b>
<b>Lymphoid</b>	B cells	B220 <sup>+</sup>
	Natural killer cells	NK-1.1 <sup>+</sup>
	T cells	CD3 <sup>+</sup>
	T helper cells	CD4 <sup>+</sup>
	Cytotoxic T cells	CD8a <sup>+</sup>
<b>Myeloid</b>	Macrophages	CD11b <sup>+</sup>
	Monocytes	CD115 <sup>+</sup>
	Ly6C monocytes	CD11b <sup>+</sup> Ly6C <sup>low/middle/high</sup>
	Neutrophils	CD11b <sup>+</sup> Ly6G <sup>+</sup>

The following antibodies were used to analyse the lymphoid cells: FITC-conjugated anti-mouse B220; phycoerythrin (PE)/cyanine-7 (Cy7)-conjugated anti-mouse NK-1.1; PE-conjugated CD3; peridinin-chlorophyll-protein (PerCP)-conjugated anti-mouse CD4; and allophycocyanin (APC)/Cy7-conjugated anti-mouse CD8a. The following antibodies were used to analyse the myeloid cells: APC-conjugated anti-mouse CD11b; PE-conjugated anti-mouse CD115; PE/Cy7-conjugated anti-mouse Ly-6C; and FITC-conjugated anti-mouse Ly-6G. Details of the antibodies used are included in Table 2.3.

## Chapter 2: Materials and Methods

**Table 2.3 Details of antibodies used for immunophenotyping of peripheral blood cell populations.**

Reagent	Fluorochrome where applicable	Clone	Catalogue number
<b><u>Myeloid</u></b>			
CD11b	APC	M1/70	101212
CD115 (CSF-1R)	PE	AFS98	135505
Ly-6C	PE/Cy7	HK1.4	128018
Ly-6G	FITC	1A8	127605
2% PBS			
<b><u>Lymphoid</u></b>			
CD45R/B220	FITC	RA3-6B2	103206
NK-1.1	PE/Cy7	PK136	108714
CD3	PE	17A2	100206
CD8a	APC/Cy7	53-6.7	100714
CD4	PerCP	RM4-5	100537
2% PBS			

All reagents were purchased from Biolegend. Antibodies were diluted 1:1000 in 2% PBS. Abbreviations: FITC, fluorescein isothiocyanate; APC, allophycocyanin; PE, phycoerythrin; Cy7, cyanine-7; PerCP, peridinin-chlorophyll-protein; 2% PBS, 1X phosphate-buffered saline containing 2% (v/v) heat inactivated foetal bovine serum.

Cells were incubated with the antibodies for 30 minutes at 4°C, before being washed with 1 ml of 2% PBS via centrifugation for 5 minutes at 500 x g (4°C). The supernatant was aspirated, and cells were resuspended in a small volume (~400 µl) of fresh 2% PBS in round-bottom polystyrene tubes and kept on ice until flow cytometry analysis. Immediately prior to running samples on a BD Fortessa flow cytometer, 0.5 µg/ml DAPI (which stains dead cells) was added to all samples (excluding the unstained control sample (used as a negative control) and all other single stain controls, which were used for sample compensation (i.e., population adjustment to minimise spill-over between channels)) and mixed by vortexing (to minimise clustering of cells within the sample). Samples were analysed for 2x10<sup>4</sup> events whilst 10<sup>4</sup> events were recorded for the single stain controls. The gating strategy used to detect the different immune cell populations is shown in Figure 2.4 below. The final gated populations were overlay with the preceding parent populations (backgating) to ensure gating accuracy. Data analysis and creation of dot plots were performed using FlowJo™ 10.

## Chapter 2: Materials and Methods

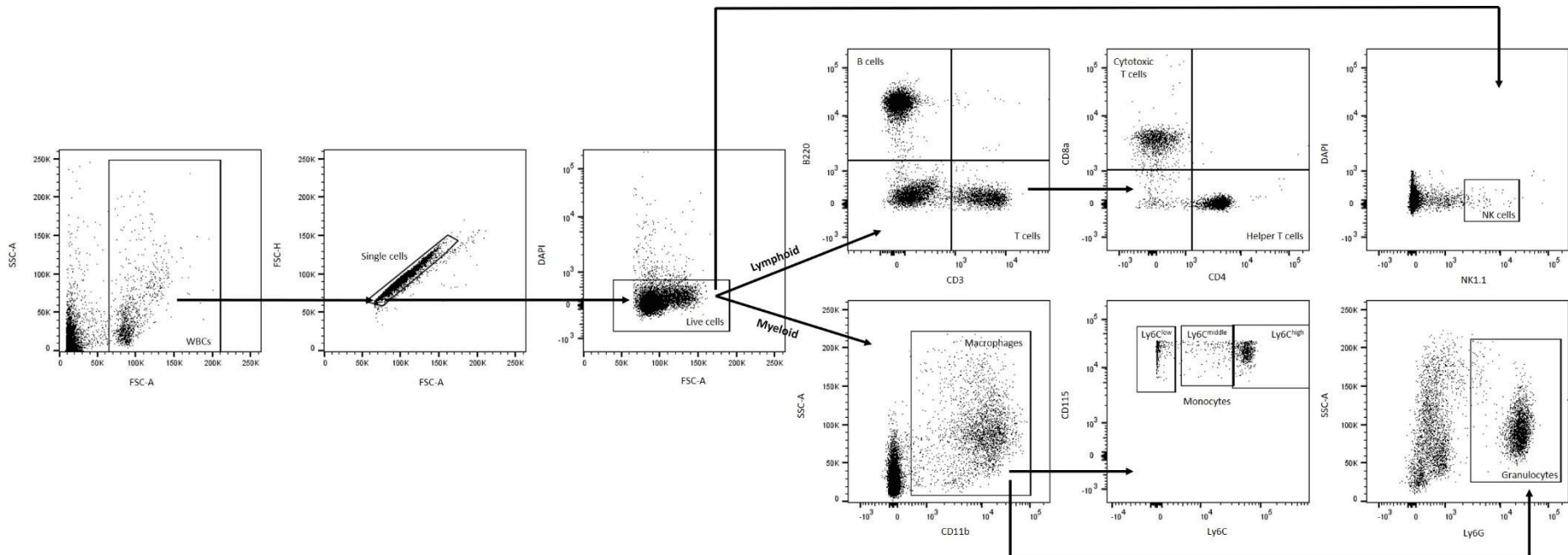


**Figure 2.4 Gating strategy for analysis of lymphoid and myeloid cells within the peripheral blood.**

Lymphoid cells detected: B220<sup>+</sup> B cells; CD3<sup>+</sup> CD4<sup>+</sup> helper T cells; CD8<sup>+</sup> cytotoxic T cells; NK-1.1<sup>+</sup> NK cells. Myeloid cells detected: CD11b<sup>+</sup> macrophages; Ly6G<sup>+</sup> granulocytes; CD115<sup>+</sup> monocytes; CD115<sup>+</sup> Ly6C<sup>+</sup> monocytes. Abbreviations: SSC, side scatter; FSC, forward scatter; DAPI, 4', 6'-diamidino-2-phenylindole; NK, natural killer.

### 2.5.11 Immunophenotyping of bone marrow cell populations

Immunophenotyping of bone marrow cells via flow cytometry analysis was carried out using a previously employed method in the host laboratory (Moss 2018; Alahmadi 2019; O'Morain 2019) and in collaboration with Dr Neil Rodrigues' laboratory at ECSCRI. HFD consumption is known to induce changes in the proportion of haematopoietic stem/progenitor cell (HSPC) populations within the bone marrow (Adler et al. 2014; van den Berg et al. 2016; Xiao et al. 2020). All markers used for identifying different stem/progenitor and immune cell populations within the bone marrow are described in Table 2.3 below.

To extract bone marrow cells from the rear legs, as much soft tissue was removed from the leg bones (femur and tibia) as possible before crushing using a pestle and mortar in a small volume (~3 ml) of ice-cold 2% PBS on the day of harvest. Samples were crushed until completely homogenised and filtered through 70 µm cell strainers into a 50 ml Falcon tube. This step was repeated another two times, and the final volume in the tube was made up to 30 ml with fresh ice-cold 2% PBS. Cell suspensions were stored at 4°C and flow cytometry analysis was completed the next day. For cell counting, 1 ml of the cell suspension was taken and incubated with 200 µl of ammonium chloride solution (0.8% NH<sub>4</sub>Cl in 0.1 mM EDTA in water buffered with KHCO<sub>3</sub> to achieve a final pH of 7.2-7.6) to lyse contaminating erythrocytes before counting as described in Section 2.2.6

## Chapter 2: Materials and Methods

**Table 2.4 Markers used to identify bone marrow stem/progenitor and immune cell populations.**

CLASS	CELL TYPE	MARKER
SLAM	Lineage -	
	LSK	Lin <sup>-</sup> Sca-1 <sup>+</sup> c-Kit <sup>+</sup>
	HSC	CD150 <sup>+</sup> CD48 <sup>-</sup>
	MPP	CD150 <sup>-</sup> CD48 <sup>-</sup>
	HPC I	CD150 <sup>-</sup> CD48 <sup>+</sup>
	HPC II	CD150 <sup>+</sup> CD48 <sup>+</sup>
Progenitor	Lineage -	
	LK	Lin <sup>-</sup> Sca-1 <sup>-</sup> c-Kit <sup>+</sup>
	CMP	CD34 <sup>+</sup> CD16/32 <sup>-</sup>
	MEP	CD34 <sup>-</sup> CD16/32 <sup>-</sup>
	GMP	CD34 <sup>+</sup> CD16/32 <sup>+</sup>
	CLP	CD127 <sup>+</sup>
Lineage +	Lineage +	
	Granulocytes	Gr1 <sup>+</sup> Mac1 <sup>-</sup>
	Macrophages	Gr1 <sup>-</sup> Mac1 <sup>+</sup>
	MDSCs	Gr1 <sup>+</sup> Mac1 <sup>+</sup>
	B cells	B220 <sup>+</sup>
	T cells	CD3 <sup>+</sup>
	Erythrocytes	Ter119 <sup>+</sup>

Abbreviations: SLAM, signalling lymphocyte activation molecule; HSC, haematopoietic stem cells; MPP, multipotent progenitors; HPC, haematopoietic progenitor cell; CMP, common myeloid progenitor; MEP, megakaryocyte-erythroid progenitor; GMP, granulocyte-macrophage progenitor; CLP, common lymphoid progenitor; MDSCs, myeloid-derived suppressor cells.

To analyse the signalling lymphocyte activation molecule (SLAM) and progenitor cell populations,  $1 \times 10^7$  and  $8 \times 10^6$  cells respectively were transferred to new tubes. These high cell numbers were necessary to ensure that a sufficient number of target cells are detected, since these populations only constitute a small percentage of the total cells. Cells were then pelleted via centrifugation at  $500 \times g$  for 5 minutes at  $4^\circ\text{C}$ . These centrifugation settings were applied to all subsequent centrifugation steps unless otherwise stated. Cells were then resuspended with a mixture of biotinylated lineage marker antibodies present within the SLAM and progenitor cell populations (described

## Chapter 2: Materials and Methods

in Figure 2.5 below) and incubated for 30 minutes at 4°C. The following antibodies were used to analyse the SLAM class of cells: PE/Cy7-conjugated anti-mouse CD150; FITC-conjugated anti-mouse CD48; APC-conjugated anti-mouse c-Kit; and PE-conjugated anti-mouse Sca-1. The following antibodies were used to analyse the progenitor class of cells: PE-conjugated anti-mouse CD127; PE/Cy7-conjugated anti-mouse CD16/32; FITC-conjugated anti-mouse CD34; APC-conjugated anti-mouse c-Kit; and APC/Cy7-conjugated anti-mouse Sca-1. Cells were then washed with 2% PBS by centrifugation, resuspended in PerCP-Cy5.5-conjugated streptavidin (2% (v/v)) and incubated for an additional 15 minutes at 4°C. Cells were then washed again with 2% PBS by centrifugation and resuspended in fresh 2% PBS, ready for flow cytometry analysis.

For lineage cell population analysis, 1 ml of cell suspension was taken. Cells were pelleted, resuspended in lineage marker fluorochrome-conjugated antibodies (APC-conjugated anti-mouse B220; FITC-conjugated anti-mouse CD3; PE/Cy7-conjugated anti-mouse Gr1; PE-conjugated anti-mouse Mac1; and APC/Cy7-conjugated anti-mouse Ter119) and incubated for 20 minutes at 4°C. Cells were then washed in 2% PBS by centrifugation and resuspended in 200 µl of 2% PBS. Additional samples incubated with the lineage antibodies separately were also prepared to represent individual fluorochromes (including DAPI, which stains dead cells, and unstained cells as controls). This was done to enable sample compensation as per Section 2.5.10. Details of all antibodies and reagents used are described in Table 2.5.

## Chapter 2: Materials and Methods

**Table 2.5 Antibodies and reagents used for immunophenotyping of bone marrow cells.**

<b>Reagent</b>	<b>Fluorochrome where applicable</b>	<b>Clone</b>	<b>Catalogue number</b>
<b><u>SLAM</u></b>			
Ly-6A/E (Sca-1)	PE	D7	108107
CD48	FITC	HM48-1	103403
CD150	PE/Cy7	TC15-12F12.2	115913
CD117 (c-Kit)	APC	2B8	105811
Lineage cocktail 2% PBS			
<b><u>Progenitor</u></b>			
Ly-6A/E (Sca-1)	APC/Cy7	D7	108125
CD127 (IL-7R $\alpha$ )	PE	SB/199	121111
CD117 (c-Kit)	APC	2B8	105811
Lineage cocktail 2% PBS			
<b><u>Lineage</u></b>			
Ly-6G/Ly-6C (Gr-1)	PE/Cy7	RB6-8C5	108415
CD11b (Mac-1)	PE	M1/70	101207
CD45R/B220	APC	RA3-6B2	103212
CD3	FITC	17A2	100203
TER-119	APC/Cy7	TER-119	116223
2% PBS			
<b><u>Lineage cocktail</u></b>			
Biotin CD3		17A2	100244
Biotin CD4		GK1.5	100404
Biotin CD8a		53-6.7	100703
Biotin Ly-6G/Ly-6C (Gr-1)		RB6-8C5	108404
Biotin CD11b		M1/70	101204
Biotin CD45R/B220		RA3-6B2	103204
Biotin TER-119		TER-119	116204

All reagents were purchased from Biolegend. Abbreviations: SLAM, signalling lymphocyte activation molecule; FITC, fluorescein isothiocyanate; APC, allophycocyanin; PE, phycoerythrin; Cy7, cyanine-7; PerCP, peridinin-chlorophyll-protein; 2% PBS, 1X phosphate-buffered saline containing 2% (v/v) heat inactivated foetal bovine serum.

## Chapter 2: Materials and Methods

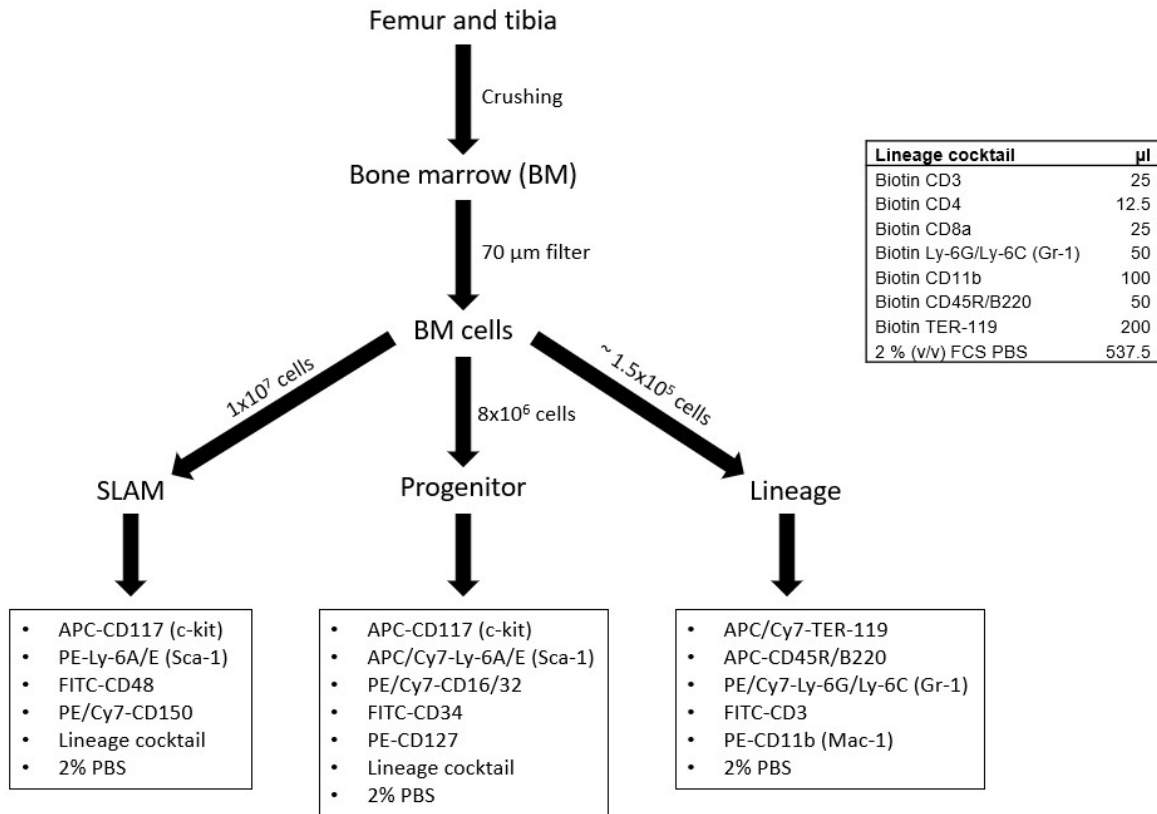


**Figure 2.5 Protocol used for the extraction and analysis of bone marrow cells.**

The femur and tibia were extracted from mice and homogenised via crushing. The bone marrow cells were filtered and passed through a filter, before the required number of cells were taken to analyse cells belonging to the SLAM, progenitor and lineage classes by staining using the defined antibodies (all staining preparations were done simultaneously). Abbreviations: SLAM, signalling lymphocyte activation molecule; APC, allophycocyanin; PE, phycoerythrin; Sca, stem cell antigen; Cy7, cyanine-7; 2% PBS, 1X phosphate-buffered saline containing 2% (v/v) heat inactivated foetal bovine serum; FITC, fluorescein isothiocyanate.

Following these preparations, all samples were filtered through sterile 40 µm cell strainers into round-bottom polystyrene tubes and kept on ice. Immediately prior to running samples on a BD LSR Fortessa 4 lasers flow cytometer, 0.5 µg/ml DAPI was added to all samples (excluding the unstained control sample and all other single lineage stain controls) and mixed by vortexing. SLAM and progenitor samples were analysed for 5 minutes or until no sample remained, lineage samples were analysed for 1 minute and single stain samples were run until  $10^4$  events were recorded. Compensation was done using the single lineage stains, and cell populations were gated according to the cell specific markers, with the gating strategy illustrated in Figure 2.6. The final gated populations were overlay with the preceding parent populations (backgating) to ensure gating accuracy. Data analysis and creation of dot plots were performed using FlowJo™ 10.

## Chapter 2: Materials and Methods

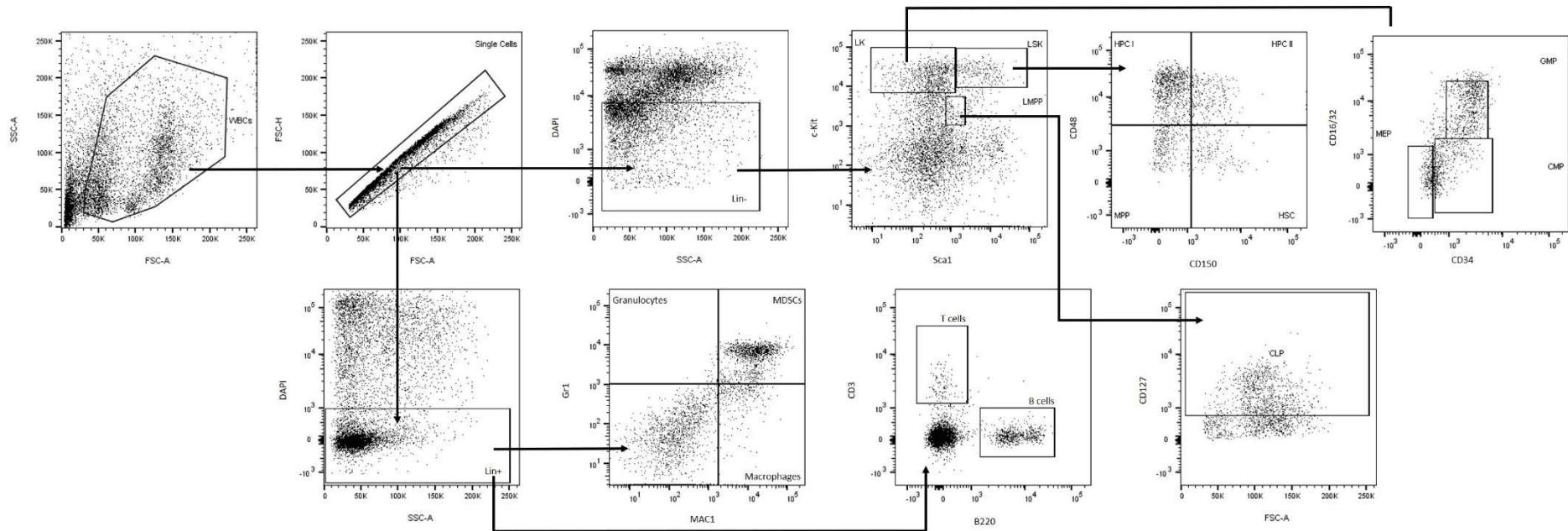


**Figure 2.6 Gating strategy for analysis of stem/progenitor and immune cells within the bone marrow.**

SLAM class of cells detected: Lin<sup>-</sup> Sca-1<sup>+</sup> c-Kit<sup>+</sup> (LSK) cells; CD150<sup>+</sup> CD48<sup>-</sup> HSCs; CD150<sup>-</sup> CD48<sup>-</sup> MPPs; CD150<sup>-</sup> CD48<sup>+</sup> HPC I; CD150<sup>+</sup> CD48<sup>+</sup> HPC II. Progenitor class of cells detected: Lin<sup>-</sup> Sca-1<sup>-</sup> c-Kit<sup>+</sup> (LK) cells; CD34<sup>+</sup> CD16/32<sup>-</sup> CMPs; CD34<sup>-</sup> CD16/32<sup>-</sup> MEPs; CD34<sup>+</sup> CD16/32<sup>+</sup> GMPs; CD127<sup>+</sup> CLPs. Lineage class of cells detected: Gr1<sup>+</sup> Mac1<sup>-</sup> granulocytes; Gr1<sup>-</sup> Mac1<sup>+</sup> macrophages; Gr1<sup>+</sup> Mac1<sup>+</sup> MDSCs; CD3<sup>+</sup> T cells; B220<sup>+</sup> B cells. Abbreviations: SSC, side scatter; FSC, forward scatter; DAPI, 4', 6'-diamidino-2-phenylindole; SLAM, signalling lymphocyte activation molecule; HSC, haematopoietic stem cells; MPP, multipotent progenitors; HPC, haematopoietic progenitor cell; CMP, common myeloid progenitor; MEP, megakaryocyte-erythroid progenitor; GMP, granulocyte-macrophage progenitor; LMPP, lymphoid-primed multipotent progenitor; CLP, common lymphoid progenitor; MDSCs, myeloid-derived suppressor cells.

## Chapter 2: Materials and Methods

### 2.5.12 Sectioning

For detailed plaque morphometric analyses, the heart was sectioned to visualize atherosclerotic plaques in the aortic root at the three valve cusps. In addition, the liver was sectioned to analyse hepatocyte morphology (e.g., cell number/cellularity) and degree of steatosis (i.e., lipid accumulation). Microtome-cryostat sectioning of frozen, OCT-mounted heart and liver samples was done at  $-15^{\circ}\text{C}$  with  $8\ \mu\text{m}$  sections cut using microtome blades and collected onto Superfrost® microscope slides. For the heart, three sections were collected per slide from the origin of the three valve cusps for a minimum of ten slides or until the valves started to disappear (whichever was sooner). For the liver, two or three sections were collected per slide when the tissue section was large enough for adequate immunohistochemical staining. All slides were air-dried at room temperature for 1 hour before storage at  $-80^{\circ}\text{C}$  until use.

### 2.5.13 Histological/immunohistochemical techniques

#### 2.5.13.1 Oil Red O staining

Analysis of atherosclerotic plaque size and lipid content was done via histological staining of sections using Oil Red O (ORO) solution, which stains lipid droplets red (only neutral lipids). Frozen sections were thawed for 5 minutes before fixation using 4% (w/v) paraformaldehyde (PFA) for 5 minutes. Sections were then washed thrice in distilled water ( $\text{dH}_2\text{O}$ ) for 5 minutes each before staining in Harris Modified Haematoxylin solution for 3 minutes. Slides were then rinsed in tap water via indirect exposure to the water stream to flush away excess residual haematoxylin (this was done until the colour of the water became clear). Sections were placed in absolute propylene glycol for 5 minutes before incubating in ORO solution (0.5% (w/v) in propylene glycol, Sigma-Aldrich) for 30 minutes at  $65^{\circ}\text{C}$ , followed by 85% (v/v) propylene glycol for 5 minutes. Finally, sections were rinsed in  $\text{dH}_2\text{O}$  twice for 5 minutes before mounting with Aquamount, (aqueous mounting medium) and sealed with a coverslip. After allowing the slides to dry at room temperature for a minimum of 2-3 hours, images of the sections were captured using a Leica DMRB microscope under x5 magnification for analysis.

## Chapter 2: Materials and Methods

For ORO staining of the liver, frozen sections were thawed for 5 minutes and marked with a Pap pen to create a hydrophobic barrier around individual sections. ORO solution was then added directly to the sections and incubated at room temperature for 18-20 minutes. The ORO solution was then removed, and slides were incubated in Harris Modified Haematoxylin solution for 2 minutes. This was followed by rinsing in running tap water to remove excess haematoxylin as previously described. Finally, slides were mounted using Aquamount as described above, and images of the sections were captured using a Leica DMRB microscope under x20 magnification for analysis.

### 2.5.13.2 Haematoxylin and eosin staining

To analyse hepatocyte morphology, haematoxylin and eosin staining was used. Frozen slides containing liver sections were thawed for 5 minutes before rinsing 2-3 times in tap water. Slides were then incubated in Harris Modified Haematoxylin (ready-to-use solution from Sigma-Aldrich) solution for 5 minutes and rinsed in running tap water to remove excess haematoxylin (as described Section 2.5.13.1). Slides were then stained in eosin solution for 10 minutes before being dehydrated in 95% (v/v) ethanol twice, 100% (v/v) ethanol twice and 100% xylene thrice, all for 5 minutes each. Slides were then mounted using DPX mounting medium and sealed with a coverslip. Images of the sections were captured using a Leica DMRB microscope under x20 magnification for analysis.

### 2.5.13.3 Collagen staining

To analyse collagen content present within atherosclerotic plaques, Van Geison's solution for collagen staining was used to stain aortic root sections. Frozen slides were thawed for 10 minutes before fixing with ice-cold 4% (w/v) PFA solution for 5 minutes. Slides were then washed with dH<sub>2</sub>O for 5 minutes before staining with Harris Modified Haematoxylin solution for 3 minutes. Slides were then rinsed in running tap water to remove excess haematoxylin (as described in Section 2.5.13). Slides were stained with Van Gieson's solution (ready-to-use solution from Abcam) for 5 minutes and dehydrated using 100% ethanol for 5 minutes before clearing in 100% xylene for 15

minutes. Finally, slides were mounted using DPX mounting medium and sealed with a coverslip. Images of the sections were captured using a Leica DMRB microscope under x5 magnification for analysis.

### 2.5.13.4 Immunofluorescence staining

Analysis of plaque cellularity and inflammation was carried out by staining for CD3, anti-monocyte and macrophage antibody (MOMA-2), inducible nitric oxide synthase (iNOS) and  $\alpha$ SMA to detect T cells, macrophages, M1 macrophages and VSMCs respectively. Details of the antibodies used are detailed in Table 2.6. All secondary antibodies used were conjugated with Alexa Fluor 488 (AF488), which can be visualised under a fluorescence microscope using the FITC filter. Sections were thawed for 10 minutes, fixed in ice-cold acetone for 10 minutes, washed with 1X PBS twice (for 5 minutes each) and marked with a Pap pen to create a hydrophobic barrier around individual sections. Sections were treated with blocking buffer (1X PBS supplemented with 5% (v/v) serum (species dependent on that of the secondary antibody species) and 5% (w/v) bovine serum albumin (BSA)) for 30 minutes at room temperature before incubation with the primary antibody or isotype control overnight at 4°C. Sections were then washed twice with 1X PBS (5 minutes each) and incubated with secondary antibody for 1 hour at room temperature. All antibodies (and isotype controls) were diluted in 1X PBS containing 1% (v/v) BSA to give the final concentrations stated in Table 2.6. Following this, sections were incubated with 0.3% (w/v) Sudan Black in 70% (v/v) ethanol for 20 minutes (to prevent auto-fluorescence) at room temperature, before mounting using DAPI with Fluoroshield and sealed with a coverslip. Images were captured using an Olympus BX61 microscope under x4 magnification using the DAPI (blue) and FITC (green) filters. Composite and overlay images (single and dual filters) were created using the AnalySIS software.

**Table 2.6 Details of antibodies used for immunofluorescence staining.**

<b>Serum</b>	<b>Antibody</b>	<b>Type</b>	<b>Dilution</b>	<b>Final concentration (mg/ml)</b>
Donkey	Rabbit anti-mouse $\alpha$ SMA (ab5694)	Primary	1:100	0.002
	Rabbit anti-mouse CD3 (ab5690)	Primary	1:100	0.002
	Rabbit IgG (ab171870)	Isotype	1:500	0.002
	Donkey anti-rabbit IgG AF488 (ab150073)	Secondary	1:500	0.004
Goat	Rat anti-mouse MOMA-2 (ab33451)	Primary	1:100	0.005
	Rat IgG2b (ab18541)	Isotype	1:100	0.005
	Goat anti-rat IgG AF488 (ab150157)	Secondary	1:500	0.004
	Rabbit anti-mouse iNOS (ab15323)	Primary	1:100	0.005
	Rabbit IgG (ab171870)	Isotype	1:100	0.005
	Goat anti-rabbit IgG AF488 (ab150077)	Secondary	1:500	0.004

The type of serum used for blocking is defined in the first column (this is dependent on the species that the secondary antibody is raised in). Both antibodies for  $\alpha$ SMA and CD3 share the same isotype control and secondary antibody. The final concentrations used were in accordance with previous optimisation experiments conducted in host laboratory. Abbreviations:  $\alpha$ SMA,  $\alpha$ -smooth muscle actin; AF488, Alexa Fluor 488; MOMA-2, anti-monocyte and macrophage antibody; iNOS, inducible nitric oxide synthase.

#### 2.5.14 Image analysis

All image analysis was conducted in ImageJ (Fiji) and where possible, in a blinded manner. All data presented as percentage of plaque where appropriate and unless otherwise stated. For images of aortic root sections stained with ORO, the vessel, lumen and plaque areas were outlined as accurately as possible using the selection brush tool (as shown in Figures 2.7 and 2.8) and saved as templates, whereas for collagen and immunofluorescence images, only drawings of the plaque areas were required. To quantify positively stained areas of interest, the threshold was adjusted after converting the image to 8-bit format (as shown in Figure 2.7) and the same

threshold was applied to all images. This method was used for Van Geison's- and immunofluorescence-stained aortic root sections, as well as haematoxylin and eosin-stained liver sections.

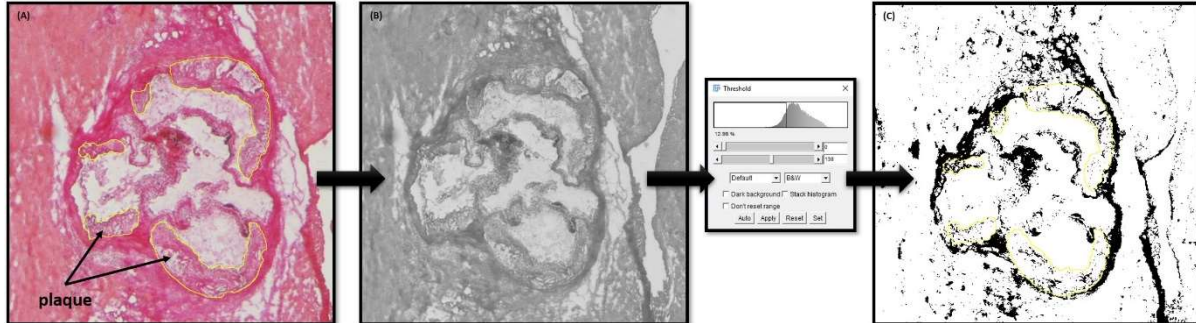


**Figure 2.7 Image analysis using the conventional threshold adjustment method.**

An example of image analysis using manual threshold adjustment on an aortic root section stained for collagen. The plaque area is outlined; the image is converted to 8-bit format and the threshold is adjusted so that areas of positive staining are selected. After an appropriate threshold was identified, this threshold was applied to all images.

For images of ORO-stained aortic root sections, the 'colour deconvolution' function was used to separate the red (ORO) from the purple (haematoxylin) staining (due to the presence of different colours). After trial and error, it was found that the 'FastRed FastBlue' vector detected the red staining the best and so this vector was used for analysis of all ORO images. The software then produces three different versions of the original image and version that captured the ORO staining the best was used. The pinkish 'Colour\_3' image (as shown in Figure 2.8B) was hence used for threshold adjustment. As an alternative to manual threshold adjustment, the threshold generated automatically by the software was applied, as this was found to consistently detect positive stained areas effectively whilst removing subjectivity. Therefore, this image analysis method was used where possible to provide a more systematic and less subjective way of quantifying lipid staining (which produced consistent results even between different researchers). Data were presented as plaque, lumen and vessel size ( $\text{mm}^2$ ), occlusion (plaque area / lumen area x 100), plaque content (plaque area / vessel area x 100) and lipid content ( $\text{ORO}^+$  area / plaque area x 100). Conversion of pixels into  $\text{mm}^2$  for the measurements was achieved using the relevant scale bar.

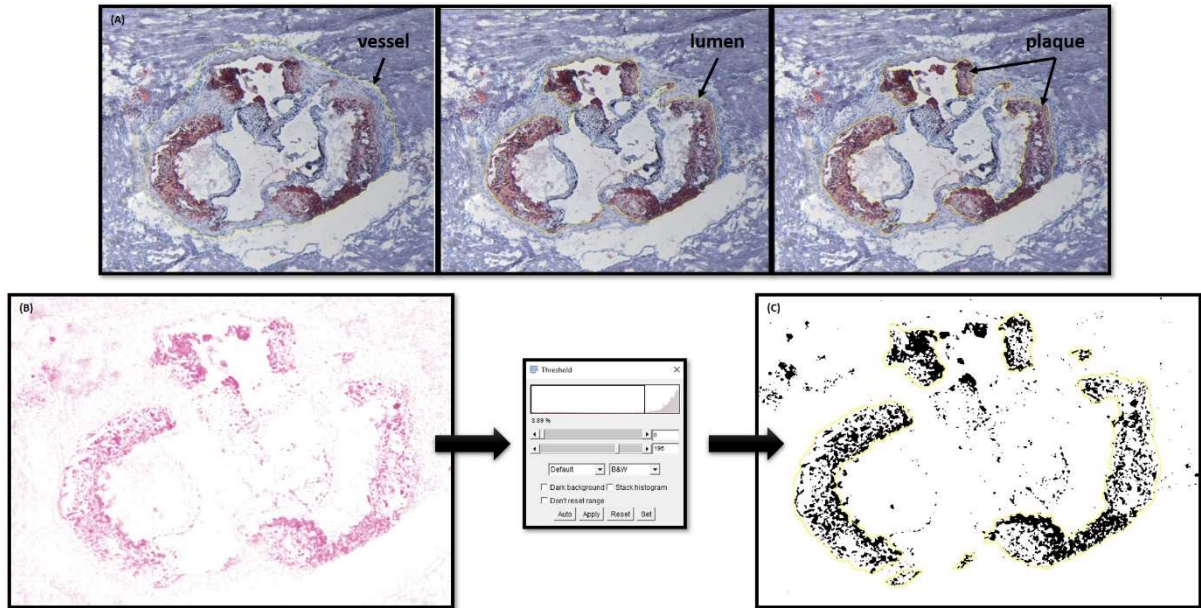


**Figure 2.8 Image analysis using the colour deconvolution method.**

Areas of interest (plaque, vessel and lumen) are outlined using a selection tool and saved as individual templates. The colour deconvolution then produces three different versions of the image; (B) is the version that detects the ORO staining the best and so is proceeded with for threshold adjustment. The threshold that is automatically applied results in (C), which consistently detects the red staining without the need for manual adjustment thus removing bias and subjectivity whilst enabling systematic analysis.

To analyse ORO-stained liver sections, images were analysed for the intensity of the red staining; this is as the contrast between the purple haematoxylin and red ORO is far less prominent in these images, compared to that of the aortic root. Therefore, the colour deconvolution method could not be relied upon to accurately detect neutral lipids present within the hepatocytes. As intensity analysis involves splitting the image into the three different colour channels (red, blue and green) followed by intensity measurement in the software, subjectivity and bias is minimal, as no areas of interest require outlining, nor is threshold adjustment involved.

#### 2.5.15 Calculation of plaque necrosis and stability

Necrosis was quantified as the total acellular area within the atherosclerotic plaque (as a percentage), as described by (Solanki et al. 2016). This was done using images of ORO-stained aortic root sections. To calculate plaque stability index, the following formula was used:  $(VSMC \text{ area} + \text{collagen area}) / (\text{macrophage area} + \text{lipid area})$ , as described by (Liu et al. 2019). All values used in the formula were percentage positive staining of plaque. Detailed plaque morphometric analyses, by evaluating parameters

associated with plaque burden, inflammation, necrosis and stability, provides valuable insights to disease severity and risk of rupture (although plaque rupture is rare in mouse models).

### **2.6 Statistical analysis**

All data are presented as mean +/- standard error of the mean (SEM); outliers +/- two standard deviations from the mean were removed prior to statistical analysis. Normality of data were assessed using histograms, QQ-plots and the Shapiro-Wilk normality test (where  $p \geq 0.05$  was considered normal distribution). Where there were two data groups, a two-sample, unpaired t-test (for normally distributed data) with (for unequal variances) or without Welch's correction (for equal variances) or Mann-Whitney U test (for abnormally distributed data) was used. Where there were three or more groups, a one-way analysis of variance (ANOVA) was used followed by either a Tukey's (for equal variances) or Games-Howell/Dunnett's T3 (for unequal variances) post-hoc test, where  $0.05 > p < 0.1$  was considered a trend, \*,  $p < 0.05$ ; \*\*,  $p < 0.01$  and \*\*\*,  $p < 0.001$ . For time course data, linear or curved regression analysis was used depending on which gave the best fit of data, as assessed by the proximity of the adjusted R-squared value to 1. Statistical analyses were carried out in RStudio version 1.1.383 (R Core Team 2017) and graphs were created using GraphPad Prism 8.

### **3 Effect of (+)-catechin on endothelial and VSMC dysfunction**

#### **3.1 Introduction**

Catechins have long been associated with various cardiovascular health benefits, as various strands of evidence link the consumption of catechin-rich foods with lowered risk of CVD-associated mortality. These include green tea, cocoa, red wine and various fruits and vegetables, which are key components of a Mediterranean diet. Catechins possess potent antioxidant activities which may be mediated via direct effects on ROS and/or antioxidant enzymes. The antioxidant activities of catechins are well known; for example, catechins can directly scavenge ROS (due to their phenolic hydroxyl groups which can stabilise free radicals) and chelate metal ions involved in the generation of free radicals, as well as induce the activities of antioxidant enzymes, inhibit those of pro-oxidant enzymes, and even suppress oxidative stress-related, pro-inflammatory signalling pathways (Fan et al. 2017). Catechins can modulate the activities of nuclear factor kappa-B (NF- $\kappa$ B) and activator protein-1 (AP-1), which are redox-sensitive transcription factors critically involved in the response to pathological oxidative stress (Braicu et al. 2013). NF- $\kappa$ B regulates the expression of numerous genes involved in inflammation, oxidative stress and endothelial dysfunction (Kumar et al. 2004; dela Paz et al. 2007). Catechins have also been known to inhibit NADPH oxidase (NOX), a major source of ROS in the vascular system that, along with other pro-hypertensive factors (e.g., angiotensin II) augments blood pressure and can be activated by TNF- $\alpha$  (Yousefian et al. 2019). In human cardiomyocytes, NOX is involved in the regulation of TNF- $\alpha$ -induced NF- $\kappa$ B activation and upregulation of IL-1 $\beta$  and VCAM-1 expression (Moe et al. 2014). Therefore, catechins may inhibit NOX assembly/expression and associated ROS generating activity whilst enhancing NO availability to protect against oxidative stress-induced endothelial dysfunction (Yousefian et al. 2019). The antioxidant and anti-inflammatory properties of catechins make them promising candidates that can be combined with current lipid-lowering pharmacological therapies to lower risk of MACE associated with atherosclerosis. However, further research is required on individual catechins, especially (+)-catechin, since focus has largely been placed on other catechins (e.g., EGCG), despite both (+)-catechin (along with (-)-epicatechin) intake being inversely associated with

### Chapter 3: Effect of (+)-catechin on endothelial and VSMC dysfunction

coronary heart disease in a large prospective study (Arts et al. 2001b). This is vital for the characterisation and understanding of the activities and underlying mechanisms of individual catechins, and how they contribute to the observed anti-atherogenic, cardioprotective effects. The difficulty in associating specific observations with specific biological effects is at least in part, attributed to previous studies using a combination of catechins or polyphenols, rather than individual constituents (Islam 2012; Bhardwaj et al. 2013; Moss and Ramji 2016b).

Previous epidemiological and observational studies have associated the intake of catechins with reduced risk of ischaemic/coronary heart disease (Arts et al. 2001b; Sansone et al. 2015) or CVD (Tresserra-Rimbau et al. 2014). Administration of catechins in the form of green tea or cocoa induces various beneficial effects associated with cardiovascular health in a range of human populations. For example, improvements in endothelial function associated with increased NO activity/bioavailability or flow-mediated dilation have been reported (Fisher et al. 2003; Wang-Polagruto et al. 2006; Oyama et al. 2010; Flammer et al. 2011; Dower et al. 2015; Sansone et al. 2015; Rassaf et al. 2016). Reductions in plasma oxLDL concentration (Inami et al. 2007; Tinahones et al. 2008), LDL oxidation (Tinahones et al. 2008; Suzuki-Sugihara et al. 2016), lipid peroxidation (Mastroiacovo et al. 2015) and other oxidative stress markers (Hsu et al. 2007; Oyama et al. 2010) have also been reported. This is combined with improvements in blood pressure (Matsuyama et al. 2008; Heiss et al. 2015; Mastroiacovo et al. 2015; Rostami et al. 2015; Sansone et al. 2015; Rassaf et al. 2016) and inflammation (Wang-Polagruto et al. 2006; Hsu et al. 2007; Oyama et al. 2010; Chiva-Blanch et al. 2011; Romero-Prado et al. 2015). Therefore, evidence supports a positive role of catechins in the maintenance of cardiovascular health.

In animal studies, hypercholesterolemic Syrian hamsters receiving catechin hydrate combined with vitamin E had reduced fatty streak formation (Xu et al. 1998), and (+)-catechin supplementation in *Apoe*<sup>-/-</sup> mice attenuated atherosclerotic lesion size and modulated the expression of various genes, including those involved in leukocyte endothelial adhesion, without affecting plasma levels of cholesterol and TG (Auclair et al. 2009). Likewise in a murine model of hyperhomocysteinemia, intake of catechin attenuated endothelial dysfunction-associated pro-inflammatory cytokine expression

## Chapter 3: Effect of (+)-catechin on endothelial and VSMC dysfunction

(Noll et al. 2013). In a previous pilot study conducted in the host laboratory, WT mice fed HFD for 3 weeks receiving daily (+)-catechin hydrate via oral gavage resulted in reduced levels of IL-1 $\beta$ , IL-2 and TG (along with ratio of TG to total cholesterol) in the plasma compared to controls (Moss 2018). Furthermore, in *in vitro* studies, (+)-catechin attenuated monocytic migration, ROS production, proliferation, and macrophage MMP activity in THP-1 monocytes/macrophages. Taken together, these data suggest that (+)-catechin contributes to protection against endothelial dysfunction via its anti-inflammatory effects to prevent atherogenesis and may inhibit macrophage-associated processes to inhibit atherosclerosis progression. However, further investigation of (+)-catechin *in vitro* in the context of other key cellular processes implicated in atherosclerosis focusing on parameters associated with endothelial and VSMC dysfunction are still required.

### 3.1.1 Experimental aims

The overall aim of studies in this chapter was to investigate the effect of (+)-catechin on parameters associated with endothelial and VSMC dysfunction, in order to ascertain whether the previously observed anti-inflammatory and anti-atherogenic effects in monocytes and macrophages also extend to other key cell types critically involved in atherosclerosis. HUVECs and HASMCs were hence used as *in vitro* models of ECs and VSMCs respectively, and primary HMDMs were used to confirm several key results obtained previously in THP-1 macrophages. This was for the purpose of verifying that those previous observations were not specific to the cell line, and so the effect of (+)-catechin on HMDM proliferation, ROS production and MMP activity was studied, given that these parameters were found to be significantly modulated. THP-1 monocytes were also used to study the effect of (+)-catechin and its isomers, (-)-catechin and (-)-epicatechin, on monocyte migration and ROS production, to gain insights to the *in vitro* efficacy of these catechins in a comparative setting. Monocyte migration and ROS production are also implicated in the early stages of atherosclerosis. OxLDL-mediated endothelial dysfunction is the key initiating step of atherogenesis and one of the ways in which oxLDL acts, is via enhancing the elaboration of potent pro-inflammatory cytokine, TNF- $\alpha$ , by monocytes and macrophages (Chen and Khismatulin 2015). To investigate the effect of (+)-catechin

## Chapter 3: Effect of (+)-catechin on endothelial and VSMC dysfunction

on parameters associated with endothelial dysfunction, HUVECs were stimulated with oxLDL or TNF- $\alpha$  to induce their activation before the following parameters were measured; proliferation, ROS production, MCP-1 release, permeability, apoptosis and monocyte adhesion. The effect of (+)-catechin on HASMC ROS production, migration, proliferation and MMP activity was also studied, given the key involvement of VSMCs in all stages of atherosclerosis.

### 3.1.2 Cell viability

Prior to conducting experiments, the effect of (+)-catechin on the viability of all investigated cell types (HMDMs, HUVECs and HASMCs) was measured, to verify that no significant cytotoxic effects were induced by (+)-catechin treatment after 24 hours. This was the most commonly used, maximum time point for the majority of experiments based on previous optimisation conducted in the host laboratory. Initial investigation of cell viability was important to verify that any subsequent observations were not attributed to cell death. In HUVECs, viability was also assessed after 24 hours stimulation with oxLDL and TNF- $\alpha$ , firstly to identify the optimal concentrations of these stimuli to use for subsequent experiments, and secondly to verify that no detrimental effects on viability was induced in combination with (+)-catechin. Cell viability was measured by assaying for LDH contents in the cell supernatants, since this cytoplasmic enzyme is released by cells when their plasma membrane is damaged, and hence is indicative of non-specific cell death (Kumar et al. 2018).

### 3.1.3 Endothelial dysfunction

#### 3.1.3.1 Role of oxLDL and TNF- $\alpha$

The functional phenotype of ECs can be modified in response to certain stimuli, including modified lipoproteins such as oxLDL and cytokines such as IL-1, IFN- $\gamma$  and TNF- $\alpha$ , as well as pathogen-associated molecular patterns (PAMPs) and DAMPs (Poher and Cotran 1990). Activated ECs secrete various pro-inflammatory mediators including MCP-1, IL-1 and IL-8, and along with their enhanced expression of adhesion molecules, promote the binding of the recruited immune cells to enable their subsequent *trans*-endothelial diapedesis. The progressive oxidation modification of

LDL by ROS ultimately leads to the formation of immunogenic oxLDL. Its retention and accumulation in the intima instigates an immune response in ECs, which involves the elaboration of TNF- $\alpha$  by various vascular cells. TNF- $\alpha$  can induce activation of NF- $\kappa$ B, which controls the expression of various effector molecules, including VCAM-1 and MCP-1. Therefore, oxLDL can exert both direct and indirect effects on ECs to promote their activation and instigate processes associated with endothelial dysfunction. TNF- $\alpha$  signalling can augment the expression of other cytokines and adhesion molecules, encouraging interactions between circulating leukocytes in the blood and the activated endothelium (Tousoulis et al. 2016), and may restructure intracellular junctions of ECs to increase permeability hence facilitating leukocyte transmigration. Increased permeability can also promote the influx of circulating lipoproteins, thus further enhancing leukocyte recruitment. *TNF- $\alpha$*  and *APOE* double KO mice and *Apoe*<sup>-/-</sup> mice treated with a recombinant soluble decoy receptor to inhibit TNF- $\alpha$  attenuated atherogenesis, endothelial adhesion and the presence of inflammatory markers (Canault et al. 2004; Ohta et al. 2005). Moreover, *Apoe*<sup>-/-</sup> mice lacking TNF- $\alpha$  also had decreased lesion size which was attributed to reduced accumulation of lipids along with expression of multiple proinflammatory mediators after 6 weeks (Xiao et al. 2009). These included IFN- $\gamma$ , ICAM-1, VCAM-1 and MCP-1/CCL2, which were also shown to be reduced in *LDLR* and TNF receptor (p55) double KO mice fed a HFD which also had smaller atherosclerotic lesions (Xanthoulea et al. 2011). In humans, TNF- $\alpha$  mediates the interaction between circulating blood leukocytes and the endothelium via upregulation of the expression of adhesion molecules (Mackesy and Goalstone 2014). Therefore, oxLDL and TNF- $\alpha$  are critical mediators of EC activation and hence were used to stimulate HUVECs to recapitulate endothelial dysfunction *in vitro* in this study.

#### 3.1.3.2 Adhesion of monocytes to activated ECs

The recruitment of circulating monocytes is a strictly regulated, multi-step process facilitated by a combination of cell surface adhesion molecules. Leukocytes recruited to the activated endothelium undergo binding with the ECs via their cognate ligands. Activated ECs express P-selectin, which binds to P-selectin glycoprotein ligand-1 (PSGL-1) and other glycosylated ligands present on monocytes, to facilitate their tethering and rolling. Integrins (heterodimeric cell surface receptors) assist both the

rolling and adhesion of leukocytes. As mentioned, monocyte-endothelial adhesion also involves the binding of the adhesion molecules (e.g., VCAM-1 and ICAM-1) expressed by ECs to the integrins present on the surface of the monocytes; VCAM-1 VLA4 and ICAM-1 binds to LFA1 (Ley et al. 2007; Moore et al. 2013; Soehnlein et al. 2013). PECAM-1, VCAM-1 and chemokines produced by other cell types residing in the lesion (e.g., SMCs and emigrated leukocytes) collectively facilitate the transmigration of monocytes across the endothelium and into the intima layer (Ley et al. 2007; Moore et al. 2013; Soehnlein et al. 2013). In *Apoe*<sup>-/-</sup> mice, reduction of monocytic adhesion to the endothelium using a glucagon-like peptide-1 receptor agonist dampened atherogenesis (Arakawa et al. 2010), and *Apoe*<sup>-/-</sup> mice deficient in P-selectin or ICAM-1 had substantially attenuated atherosclerotic lesions (Collins et al. 2000). Therefore, dampening monocyte-endothelial adhesion can attenuate atherosclerosis development. Given that catechins can modulate the expression of various adhesion molecules and chemokines involved in leukocyte adhesion, (+)-catechin was investigated in this regard in a static adhesion assay set up to study the adhesion of fluorescently labelled monocytes to TNF- $\alpha$ -stimulated HUVECs.

#### 3.1.3.3 MCP-1 and its role in mediating monocyte migration

MCP-1 is highly expressed in atherosclerotic lesions and a critical chemokine involved in the initiation and amplification of monocyte recruitment to the arterial wall (Gerszten et al. 1999; Colonnello et al. 2003). MCP-1 is produced by monocytes/macrophages, ECs and VSMCs (Shirai et al. 2015) and its activity is mediated through its receptor, CCR2 (Deshmane et al. 2009). The CCL2/CCR2 axis hence controls monocyte recruitment to atherosclerotic lesions; hyperlipidaemic mice susceptible to atherosclerosis deficient for either *CCL2* (Gu et al. 1998) or *CCR2* (Boring et al. 1998; Dawson et al. 1999) demonstrated substantially fewer and smaller atherosclerotic lesions with decreased intimal lipid deposition and macrophage accumulation. Therefore, the secretion of MCP-1 by activated ECs is a potent factor that mediates the infiltration of recruited monocytes to the intimal layer and a key hallmark of endothelial dysfunction. The release of MCP-1 by HUVECs stimulated with oxLDL and TNF- $\alpha$  was hence quantified and compared using a sandwich format ELISA, to compare and ascertain the efficacy of using oxLDL and TNF- $\alpha$  to stimulate the cells.

## Chapter 3: Effect of (+)-catechin on endothelial and VSMC dysfunction

Furthermore, MCP-1-stimulated migration of THP-1 monocytes was studied using a modified Boyden chamber method to compare the action of (+)-catechin with its isomers, as well as confirm previously obtained data in the host laboratory (which found (+)-catechin to significantly attenuate this parameter).

### 3.1.4 ROS production

The maintenance of cellular redox status is necessary for homeostasis of the vascular system. ROS are produced by various sources in the vascular wall; sustained elevations in ROS levels can lead to oxidative stress. Although excessive oxidative stress can be detrimental, moderate basal levels are required for proper cell signalling. Oxidative stress, defined as the imbalance of anti- and pro-oxidant activities in favour of the latter, has been shown to contribute to endothelial dysfunction and atherosclerosis via a range of mechanisms. ROS generated by local vascular cells can contribute to LDL oxidation, and hence endothelial dysfunction and foam cell formation, oxidative stress, and even MMP activity. H<sub>2</sub>O<sub>2</sub> is a major type of ROS synthesised by activated leukocytes, local injured cells and other sources (Huang et al. 2003; Chien et al. 2004). H<sub>2</sub>O<sub>2</sub> can transform LDL into oxLDL via oxidation modification, as well as stimulate endothelial injury. H<sub>2</sub>O<sub>2</sub> can also act as secondary messenger to activate the expression of pro-inflammatory genes regulated by NF-κB, including ICAM-1, MCP-1 and TNF-α, to promote vascular dysfunction (Chien et al. 2014). Therefore, H<sub>2</sub>O<sub>2</sub> is implicated in multiple pro-atherogenic processes that may encourage foam cell formation and promote oxidative stress-associated cellular dysfunction. The ability of (+)-catechin to attenuate H<sub>2</sub>O<sub>2</sub>-induced ROS activity was measured in all three investigated cell types; in the case of HUVECs this was also done in the presence of TNF-α, which is known to stimulate ROS production by activated ECs.

### 3.1.5 Apoptosis

Apoptosis is a type of programmed cell death implicated in the pathogenesis of atherosclerosis, as apoptosis of macrophages, SMCs and ECs occurs during atherosclerosis development. Defective phagocytic clearance (efferocytosis) of the

dead cells, cellular debris etc. results in their accumulation within the arterial wall and the formation of a necrotic core. The deposition and accumulation of pro-inflammatory mediators can hence propagate inflammatory responses and provide further apoptotic signals for lesional cells, including ECs, SMCs and leukocytes. Macrophage and SMC-derived foam cells can undergo apoptosis as a result of ER stress associated with excess intracellular cholesterol loading, and apoptosis of VSMCs present within fibrous cap is a prerequisite for plaque rupture. Apoptosis of ECs can be induced as a response to atherosclerosis-associated risk factors, such as elevated plasma LDL concentrations and glucose levels, shear stress and ROS. As well as encouraging local lipid deposition in the arterial wall, endothelial cell injury and apoptosis can also mediate plaque instability and erosion (Sun et al. 2011; Peng et al. 2014), arising from a discontinuity in the endothelium. Furthermore, senescence (a condition of cell proliferation/replicative arrest associated with cellular ageing) of ECs can also increase the susceptibility of ECs to apoptotic cell death, which has previously been attributed to insufficient NO generation. Therefore, the effect of (+)-catechin on oxLDL-induced HUVEC apoptosis was measured using an annexin-V FITC assay kit.

#### 3.1.6 Macrophage proliferation

Macrophages are a key cell type of atherosclerotic plaques, contributing to foam cell formation and subsequently, to plaque burden, and produce pro-inflammatory mediators to contribute to plaque inflammation. Macrophages are highly heterogeneous and plastic cells that are sensitive to the signals present in their local microenvironment. Macrophage proliferation has been shown to occur in both inflammatory (Jenkins et al. 2011) and normal tissues (Hashimoto et al. 2013; Yona et al. 2013) to sustain its accumulation. In atherosclerosis, monocytes permeate the endothelium and accumulate within the arterial intima, where they are stimulated to differentiate into macrophages. In murine atherosclerotic lesions, macrophage turnover occurs every 4 weeks, and lesional macrophage maintenance relies predominantly on local proliferation rather than monocyte infiltration (Robbins et al. 2013). Therefore, although circulating monocytes may give rise to lesional macrophages initially at least, macrophages have self-renewal capacities and proliferate locally, replenishing and increasing their numbers independently of the

recruited monocytes. The proliferation of HMDMs was hence measured (indirectly) after 24 hours treatment with (+)-catechin using crystal violet staining, which binds to protein and DNA (Feoktistova et al. 2016) enabling qualitative measurement of viable, intact cells. This was done to ascertain whether the anti-proliferative effects of (+)-catechin observed in THP-1 monocytes and macrophages in previous experiments conducted in the host laboratory also translate to primary macrophages.

### 3.1.7 VSMC migration and proliferation

Unlike macrophages, the role of VSMCs in atherogenesis is much more ambiguous, since they may contribute to both plaque cellularity and inflammation, as well as plaque stability (Schwartz et al. 2000). The recently recognised plasticity and heterogeneity of VSMCs thanks to lineage-tracing studies has shifted the view of their role in atherogenesis, and now recognised to be a major source of plaque cells and ECM in all stages of the disease (Basatemur et al. 2019). PDGF, produced by macrophages and activated ECs, stimulates VSMC migration (from the tunica media layer to the intima), proliferation and their switch to a synthetic phenotype (Basatemur et al. 2019). Along with macrophages, VSMCs can become foam cells via the internalisation of lipids; however, VSMCs also contribute to the formation of a plaque-stabilising fibrous cap via synthesis of ECM proteins, such as collagen and elastin. In *Apoe*<sup>-/-</sup> mice, blockade of the PDGF receptor (PDGFR), PDGFR- $\beta$ , using monoclonal antibodies significantly decreased atherosclerosis (Sano et al. 2001). Moreover, enhanced PDGFR- $\beta$  signalling has been shown to enhance inflammation and accelerate atherosclerosis progression in the thoracic aorta and coronary arteries of *Apoe*<sup>-/-</sup> and *Ldlr*<sup>-/-</sup> mice (He et al. 2015). In another study, blockade of all three dimers of PDGFR in *Apoe*<sup>-/-</sup> mice was found only to delay the accumulation of SMCs and fibrous cap generation within advanced plaques, but not prevent these altogether (Kozaki et al. 2002). Therefore, PDGF/PDGFR signalling may have ambiguous, less clear-cut roles in the pathogenesis of atherosclerosis, and its inhibition as a therapeutic target requires further investigation in this context. Nevertheless, the ability of (+)-catechin to attenuate PDGF-stimulated migration of HASMCs was measured using a modified Boyden chamber method (similar to that used to measure monocytic migration).

### 3.1.8 MMP activity

In atherosclerosis, the formation and maintenance of a fibrous cap abundant in VSMCs and ECM proteins, such as collagens and elastins, is associated with beneficial vessel remodelling and plaque stability. Degradation of this plaque-stabilising fibrous cap is thought to lead to plaque rupture and acute thrombosis, which disrupts arterial blood flow and causes the onset of clinical complications. MMPs are a family of endopeptidases and are specialised enzymes produced by various inflammatory and vascular cells, known for their capability of proteolytic degradation of ECM components. A form of MMP activity regulation is via the interaction of MMPs with TIMPs (Brew et al. 2000). *In vitro*, ECs and SMCs constitutively generate MMP-2, TIMP-1 and TIMP-2 (Hanemaaijer et al. 1993; Galis et al. 1994a) with no detectable *in situ* enzymatic activity in normal human arteries and experimental animal arteries (Galis et al. 1994b; Galis et al. 1995b). However, the expression and activity of several MMPs are focally increased in pathological human arteries (Galis and Khatri 2002). In accordance with this, *Apoe*<sup>-/-</sup> mice lacking MMP-2 had reduced atherogenesis (Kuzuya et al. 2006) and in the same mice, inactivation of MMP-8 substantially attenuated atherosclerotic lesion development (Laxton et al. 2009). Furthermore, both MMP-2 and MMP-9 have been associated with plaque instability in carotid atherosclerotic disease (Heo et al. 2011). Pro-inflammatory mediators such as lipoprotein, cytokines and ROS can also induce and upregulate MMP gene expression in vascular cells (Galis et al. 1994a). For example, in human atheroma (Shah et al. 1995) and a rabbit model of plaque rupture (Rekhter et al. 2000), MMPs generated by macrophage foam cells were responsible for the focal degeneration of fibrous cap collagen. Moreover, accumulated intercellular lipids and *in vitro* incubation with oxidised lipoproteins has been found to increase MMP expression in macrophages (Galis et al. 1995a; Xu et al. 1999). Therefore, given the influence of MMP activity in unfavourable vessel remodelling (i.e., fibrous cap degradation and plaque instability), MMP activity was measured after short- (3 hours) and long- (24 hours) term treatment with (+)-catechin in HMDMs and HASMCs. This was also to confirm previous results obtained in the host laboratory, whereby (+)-catechin was found to attenuate THP-1 macrophage MMP activity after both time points.

### 3.2 Summary of experimental strategies

A summary of the experimental strategies for HMDMs, HUVECs and HASMCs in this study are shown in Figures 3.1-3.3.

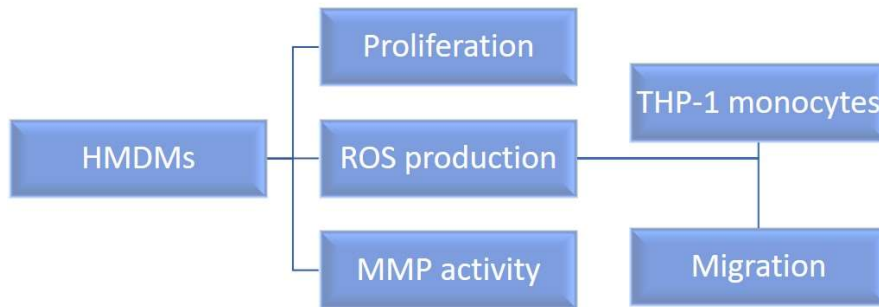


**Figure 3.1 Experiments using monocytes and macrophages.**

Abbreviations: HMDMs, human monocyte-derived macrophages; ROS, reactive oxygen species; MMP, matrix metalloproteinase.

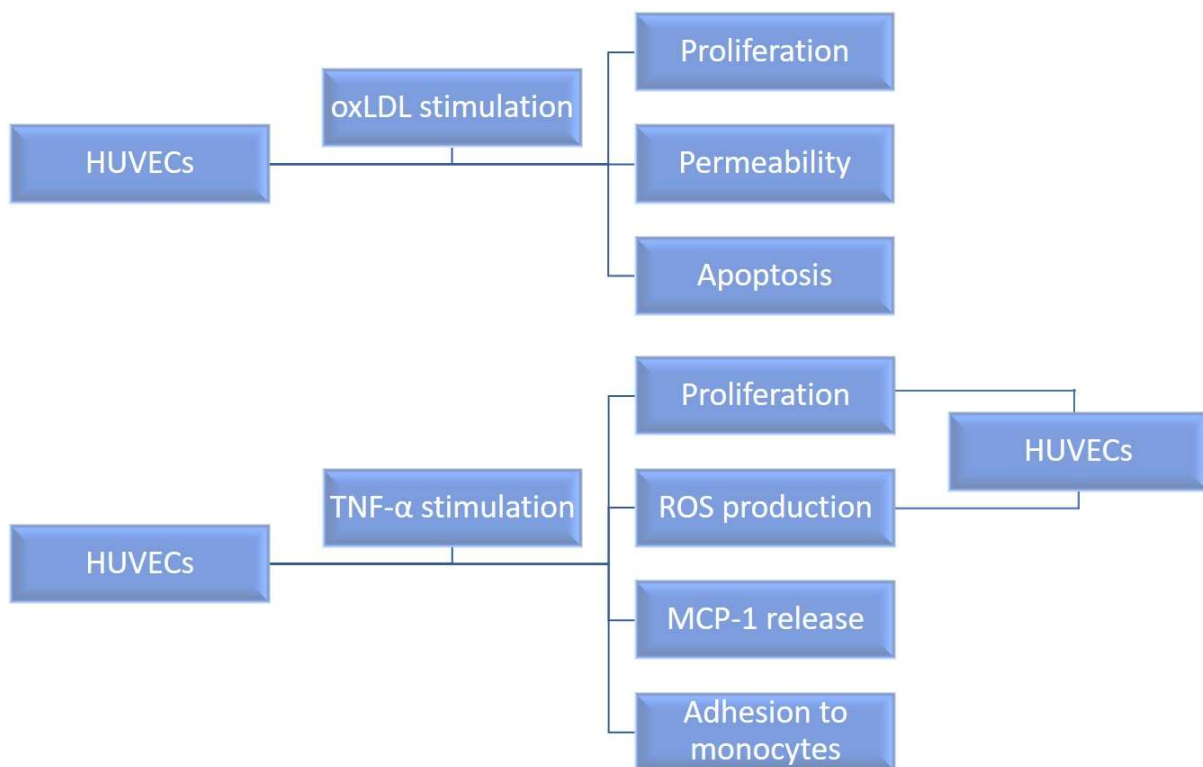


**Figure 3.2 Experiments using HUVECs.**

Abbreviations: HUVEC, human umbilical vein endothelial cell; oxLDL, oxidised low- density lipoprotein; TNF- $\alpha$ , tumour necrosis factor- $\alpha$ ; ROS, reactive oxygen species; MCP-1, monocyte chemotactic protein-1.

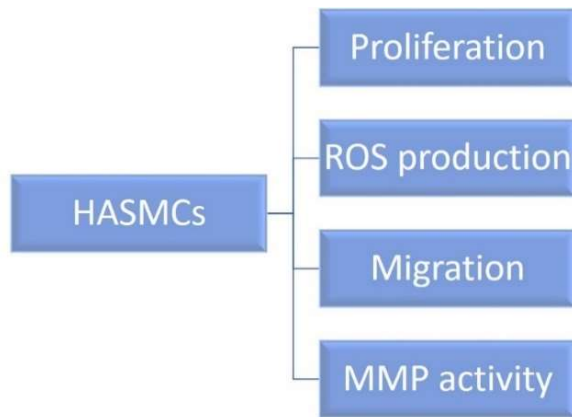


**Figure 3.3 Experiments using HASMCs.**

Abbreviations: HASMCs, human aortic smooth muscle cells; ROS, reactive oxygen species; MMP, matrix metalloproteinase.

### 3.3 Results

#### 3.3.1 (+)-Catechin has no detrimental effects on cell viability

To confirm that (+)-catechin treatment has no cytotoxic effects on the cell types being used for investigation, cells were assayed for LDH after treatment with vehicle (0.01% DMSO) or (+)-catechin (1.5 µg/ml) for 24 hours. This concentration of (+)-catechin was found to be optimal after a series of experiments conducted in the host laboratory using THP-1 cells, and hence this was used for all *in vitro* experiments described in this project. After 24 hours, (+)-catechin had no significant effects on cell viability compared to the respective vehicle control (which was set arbitrarily as 100%), except in the case of HASMCs, where a 4.56% reduction ( $p=0.011$ ) in viability was seen (Figure 3.4).

### Chapter 3: Effect of (+)-catechin on endothelial and VSMC dysfunction

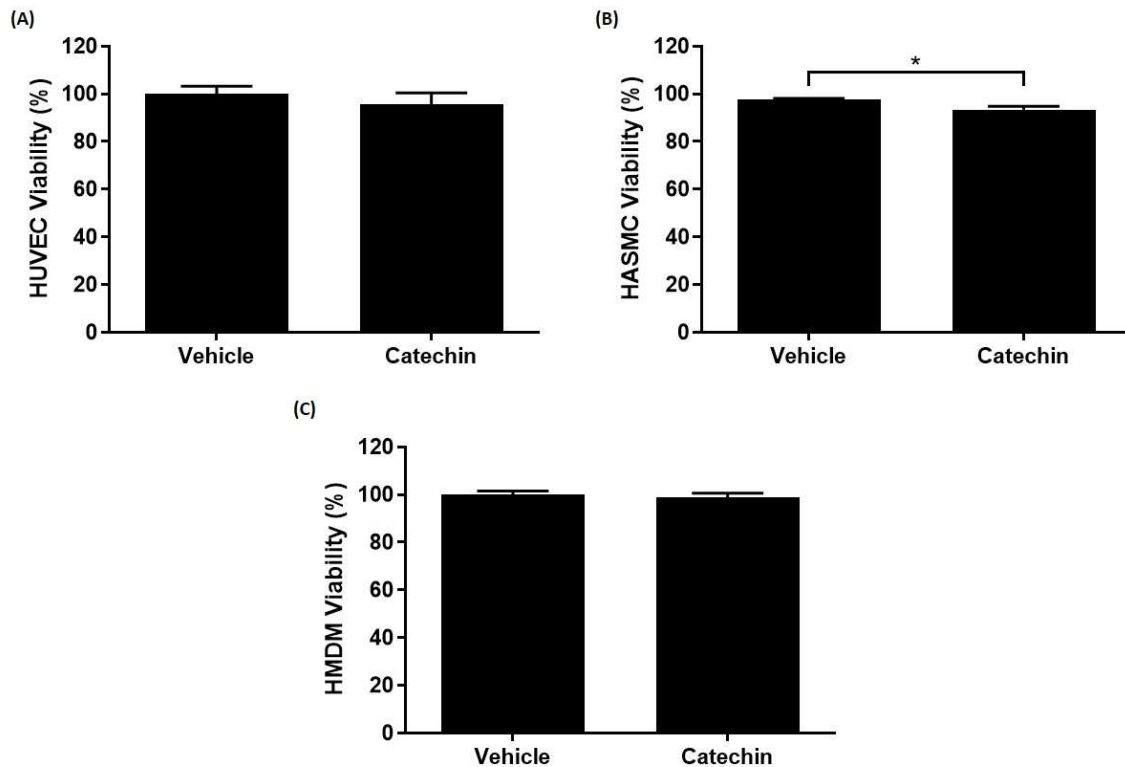


**Figure 3.4 (+)-Catechin has no detrimental effects on cell viability after 24 hours.**

Data presented as mean  $\pm$  SEM from three (A; C) or five (B) independent experiments. Statistical analysis was via unpaired t-test where \*,  $p \leq 0.05$  compared to vehicle control, which was set arbitrarily as 100% viability. Viability was assessed by assaying for lactate dehydrogenase released after 24 hours treatment with vehicle or (+)-catechin. The only significant change observed was in HASMCs, where (+)-catechin treatment reduced cell viability by 4.56%. Abbreviations: HUVEC, human umbilical vein endothelial cells; HASMC, human aortic smooth muscle cells; HMDM, human monocyte-derived macrophages.

#### 3.3.2 OxLDL up to 100 $\mu\text{g/ml}$ and TNF- $\alpha$ up to 50 $\text{ng/ml}$ has no detrimental effects on EC viability

To mimic endothelial dysfunction *in vitro*, HUVECs were stimulated with oxLDL or TNF- $\alpha$  and subject to a range of assays used to recapitulate key processes associated with endothelial dysfunction. To ascertain the effect of oxLDL and TNF- $\alpha$  stimulation on HUVEC viability, and to confirm that any experimental observations were not attributed to cell death, cells were stimulated with the indicated concentrations of oxLDL or TNF- $\alpha$  in the absence or presence of vehicle or (+)-catechin for 24 hours. Cells were then assayed for LDH (released into the cell supernatant by dying/dead cells), with the negative vehicle control or control set arbitrarily as 100%. HUVECs stimulated with 50 (Figure 3.5A) and 100 (Figure 3.5B)  $\mu\text{g/ml}$  oxLDL in the presence

or vehicle or (+)-catechin had no significant effect on viability compared to the vehicle control. Furthermore, a dose response experiment was conducted to find the maximal concentration of TNF- $\alpha$  (from 10 to 100 ng/ml) that does not affect cell viability (Figure 3.5C). Up to 50 ng/ml, TNF- $\alpha$  had no significant effects on HUVEC viability; however, 100 ng/ml significantly reduced viability ( $p=0.046$ ) compared to control by 20.54%. Therefore, 50 ng/ml TNF- $\alpha$  was used to stimulate HUVECs in subsequent *in vitro* experiments unless otherwise stated. This concentration was also used in previous work conducted in host laboratory to stimulate THP-1 macrophages. Therefore, the effect of 50 ng/ml TNF- $\alpha$  stimulation in the presence of vehicle or (+)-catechin on HUVEC viability was also investigated after 24 hours, which found no changes compared to vehicle control (Figure 3.5D).

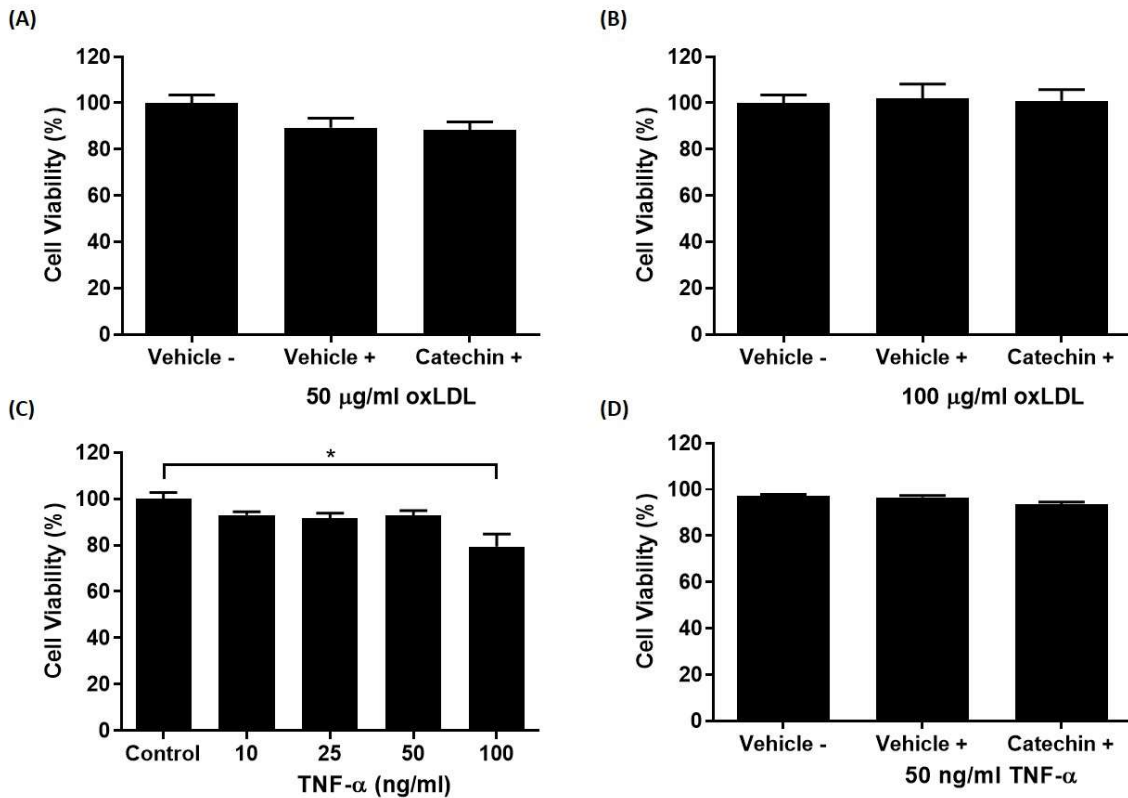


**Figure 3.5 OxLDL (up to 100 µg/ml) and TNF- $\alpha$  (up to 50 ng/ml) has no effects on EC viability after 24 hours.**

Data presented as mean  $\pm$  SEM from three (A; B; C (10 and 25 ng/ml); D) or six (C (50 and 100 ng/ml)) independent experiments. Statistical analysis via one-way ANOVA with Games Howell (C) or Tukey's (A; B; D) post-hoc test where \*,  $p \leq 0.05$  compared to vehicle control or control, which was set arbitrarily as 100%. Cell viability was measured by assaying HUVECs for lactate dehydrogenase after 24 hours treatment as indicated. Abbreviations: oxLDL, oxidised low-density lipoprotein; TNF- $\alpha$ , tumour necrosis factor- $\alpha$ ; HUVECs, human umbilical vein endothelial cells.

3.3.3 (+)-Catechin has no significant effects on endothelial and VSMC proliferation

At the same time that cell supernatants were assayed for LDH content, remaining viable cells were stained with crystal violet as an indirect measure of cell proliferation. No significant effects on HUVEC (Figure 3.6A) or HASMC (Figure 3.6B) proliferation were found after 24 hours treatment with vehicle or (+)-catechin. HMDMs treated with (+)-catechin for 24 hours had decreased proliferation by 11.43% ( $p=0.010$ ) compared to the vehicle control (Figure 3.6C). This coincides with previous data obtained in the host laboratory, where (+)-catechin was found to attenuate both THP-1 monocyte and macrophage proliferation.

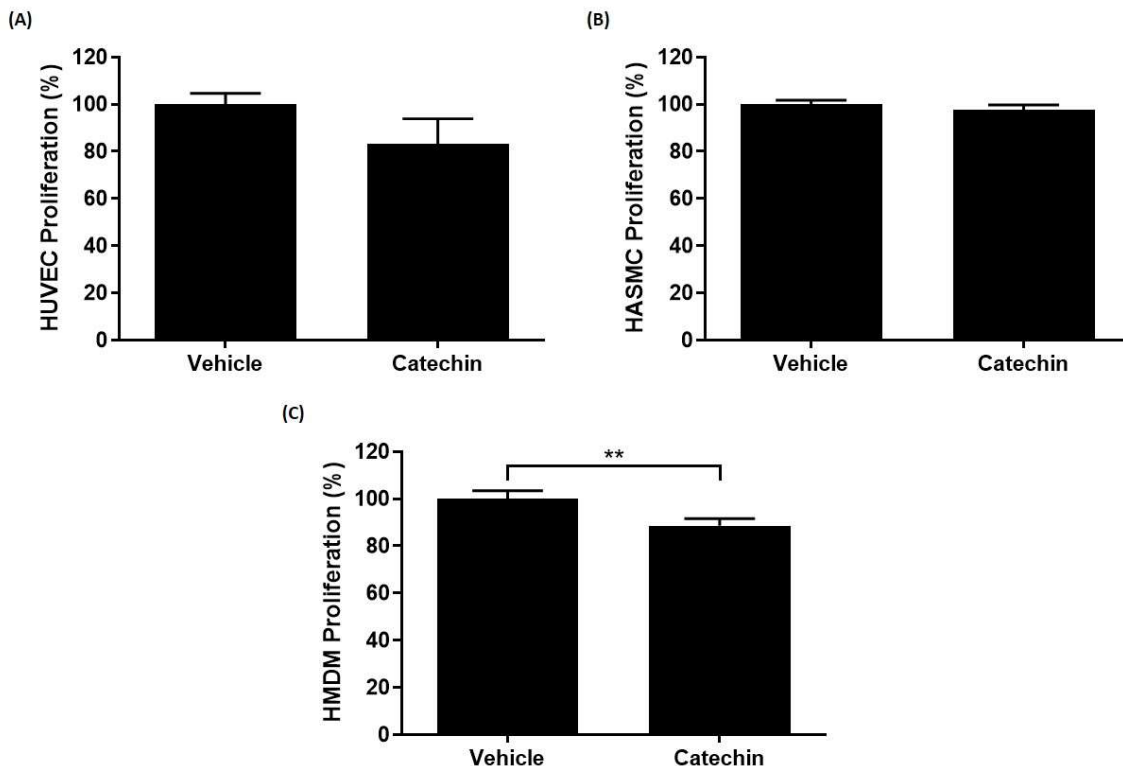


**Figure 3.6 (+)-Catechin reduces HMDM proliferation after 24 hours.**

Data presented as mean  $\pm$  SEM from three (A) or five (B; C) independent experiments. Proliferation was indirectly measured by staining viable cells with crystal violet after 24 hours treatment with vehicle or (+)-catechin. Statistical analysis via unpaired t-test compared to vehicle control, which was set arbitrarily as 100%. Abbreviations: HUVEC, human umbilical vein endothelial cell; HASMC, human aortic smooth muscle cell; HMDM, human monocyte-derived macrophage.

#### 3.3.4 Proliferation of ECs is affected by oxLDL and TNF- $\alpha$ stimulation

HUVECs stimulated with 50  $\mu\text{g/ml}$  oxLDL in the presence of vehicle or (+)-catechin for 24 hours had no significant changes in proliferation compared to control (Figure 3.7A). However, HUVECs stimulated with the higher concentration of 100  $\mu\text{g/ml}$  oxLDL in the presence of vehicle had significantly reduced proliferation by 11.59% ( $p=0.024$ ) compared to vehicle control (Figure 3.7B). In the presence of (+)-catechin, proliferation was not significantly affected by 100  $\mu\text{g/ml}$  oxLDL compared to the oxLDL-negative or -positive vehicle controls (Figure 3.7B). In the TNF- $\alpha$  dose response experiment, the 10 and 25 ng/ml concentrations had no significant effects on HUVEC proliferation compared to control after 24 hours. However, the 50 and 100 ng/ml concentrations resulted in a 12.75% ( $p=0.034$ ) and 15.66% ( $p=0.012$ ) decrease in proliferation respectively compared to the control after 24 hours (Figure 3.7C). For simplicity, only significances compared to the control are described for data obtained from the dose response experiment. In contrary to this, HUVECs stimulated with 50 ng/ml TNF- $\alpha$  in the presence of vehicle or (+)-catechin for 24 hours had no significant changes in proliferation compared to the vehicle control (Figure 7D). Therefore, both 100  $\mu\text{g/ml}$  oxLDL and 50 ng/ml TNF- $\alpha$  (although the latter was not consistent) affects the proliferation of HUVECs after 24 hours without significantly affecting viability.

### Chapter 3: Effect of (+)-catechin on endothelial and VSMC dysfunction

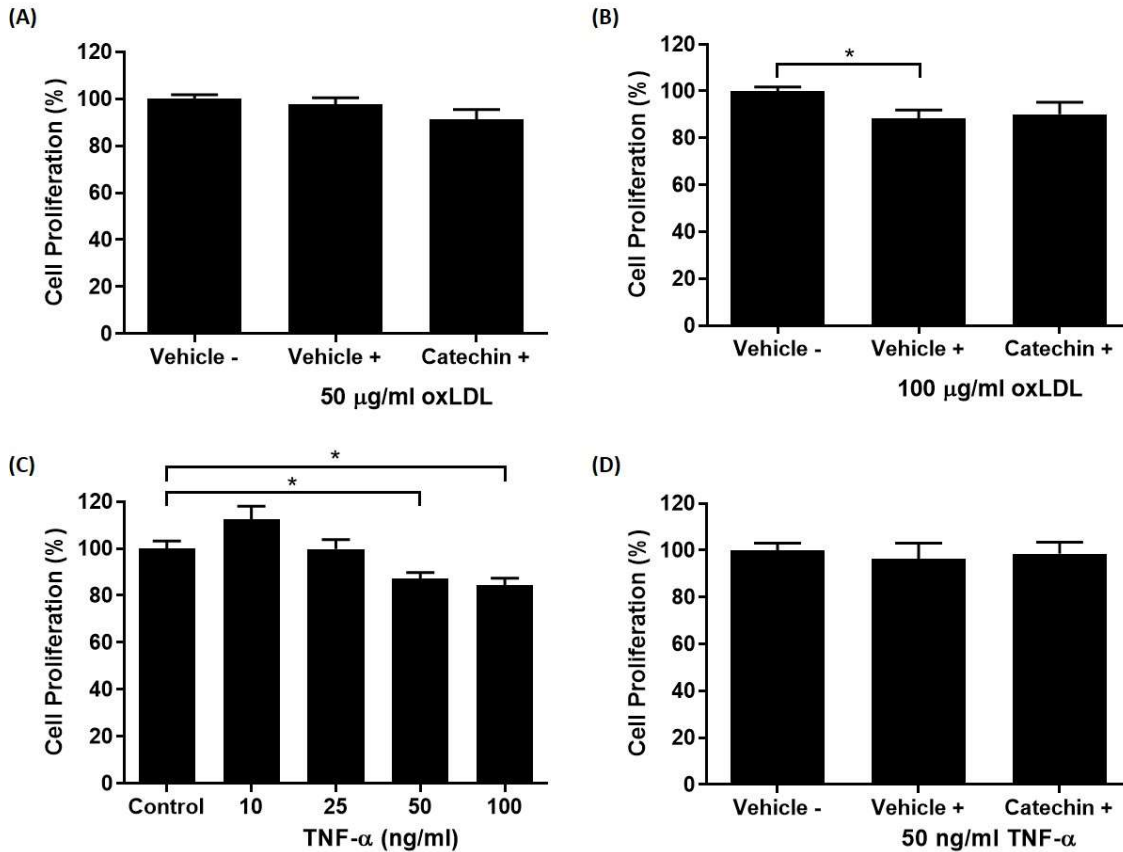


**Figure 3.7 Proliferation of ECs is affected by oxLDL and TNF- $\alpha$  stimulation after 24 hours.**

Data presented as mean  $\pm$  SEM from three (A; B; C (10 and 25 ng/ml); D) or six (C (50 and 100 ng/ml)) independent experiments. Statistical analysis via one-way ANOVA with Games Howell (C) or Tukey's (A; B; D) post-hoc test where \*,  $p \leq 0.05$  compared to vehicle control or control, which was set arbitrarily as 100%. Proliferation of HUVECs was indirectly assessed after 24 hours treatment as indicated using crystal violet staining. Abbreviations: oxLDL, oxidised low-density lipoprotein; TNF- $\alpha$ , tumour necrosis factor- $\alpha$ ; HUVECs, human umbilical vein endothelial cells.

#### 3.3.5 (+)-Catechin attenuates ROS production by multiple cell types

In the initial stages of atherogenesis, LDL accumulated within the arterial intima are subject to oxidation modification by ROS produced by local vascular cells, including macrophages, ECs and VSMCs. The resulting oxLDL is internalised via SRs by lesional macrophages and VSMCs in an unregulated manner, inducing their transformation into foam cells. Furthermore, excess ROS production and dampened antioxidant activities can result in oxidative stress, which can encourage pro-inflammatory signalling, endothelial dysfunction and other pathological processes. Previous work conducted in host laboratory found (+)-catechin to significantly attenuate THP-1 monocyte and macrophage ROS production (Moss 2018). This was

### Chapter 3: Effect of (+)-catechin on endothelial and VSMC dysfunction

also confirmed in HMDMs, where (+)-catechin treatment significantly dampened TBHP-induced ROS production after 3 hours by 24.30% ( $p < 0.001$ ) compared to the TBHP-positive vehicle control, which was set arbitrarily as fold change 1 (Figure 3.8A). The anti-oxidative activity of (+)-catechin was also consistent in the other cell types, where (+)-catechin significantly attenuated TBHP-induced ROS production after 3 hours in HUVECs by 38.73% ( $p < 0.001$ ) (Figure 3.8B), and in HASMCs after both 3 and 24 hours (Figure 3.8C) by 23.77% ( $p = 0.009$ ) and 19.41% ( $p < 0.001$ ) respectively, compared to their TBHP-positive vehicle controls.

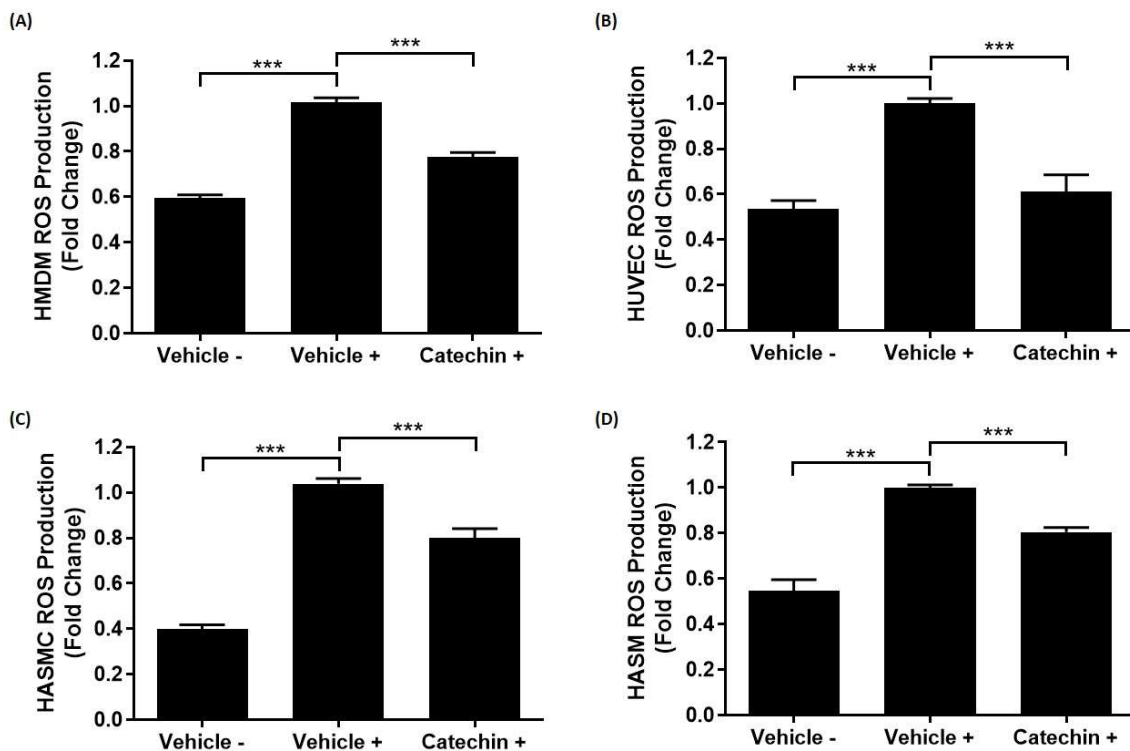


**Figure 3.8 (+)-Catechin attenuates ROS production in multiple cell types.**

Data presented as mean  $\pm$  SEM from three (A); or four (B; C) independent experiments. TBHP-stimulated ROS production by vehicle or (+)-catechin treated cells was measured after 3 (A; B; C) and 24 hours (D). Statistical analysis via one-way ANOVA with Tukey's (A; C) or Games-Howell (B; D) post-hoc test where \*\*\*,  $p < 0.001$  compared to the TBHP-positive vehicle control, which was set arbitrarily as fold change 1. Abbreviations: HMDM, human monocyte-derived macrophage; HUVEC, human umbilical vein endothelial cell; HASMC, human aortic smooth muscle cell; TBHP, tert-butyl hydroperoxide; ROS, reactive oxygen species.

### 3.3.6 (+)-Catechin attenuates EC ROS production in the presence of TNF- $\alpha$ after pre-treatment

TBHP-stimulated ROS production was also measured in HUVECs in the presence of TNF- $\alpha$  and (+)-catechin. After 3 hours, (+)-catechin had no effect on ROS production (Figure 3.9A) compared the TBHP and TNF- $\alpha$ -positive vehicle control (i.e., double positive vehicle control), which was set arbitrarily as fold change 1. It was only after HUVECs were pre-treated with (+)-catechin for 24 hours, before measurement of TBHP-induced ROS production in the presence of TNF- $\alpha$  after 3 hours, that there was a significant reduction of 15.18% ( $p < 0.001$ ) compared to the double positive vehicle control (Figure 9B).

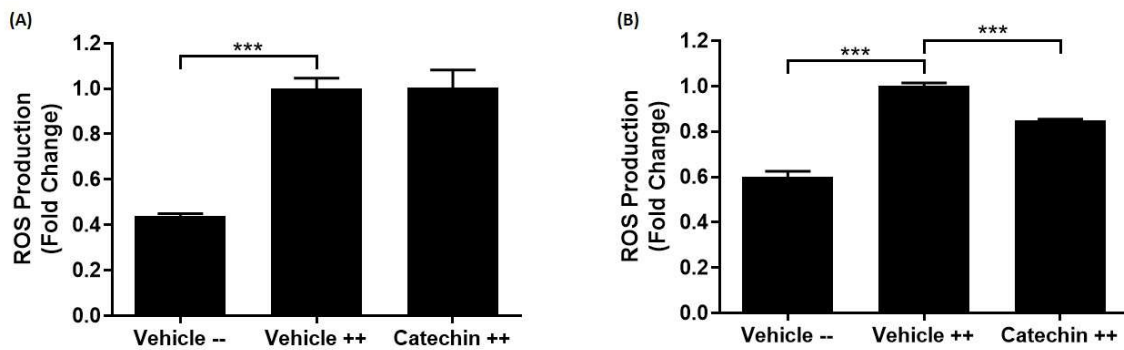


**Figure 3.9 (+)-Catechin attenuates ROS production by ECs in the presence of TNF- $\alpha$  after pre-treatment for 24 hours.**

Data presented as mean  $\pm$  SEM from three independent experiments. Statistical analysis via one-way ANOVA with Tukey's post-hoc test where \*\*\*,  $p < 0.001$  compared to TNF- $\alpha$  and TBHP-stimulated HUVECs in the presence of vehicle for 3 hours (A) or TNF- $\alpha$  and TBHP-stimulated HUVECs in the presence of vehicle for 3 hours after pre-treatment with vehicle for 24 hours (B), which was set arbitrarily as fold change 1. Abbreviations: ROS, reactive oxygen species; ECs, endothelial cells; TNF- $\alpha$ , tumour necrosis factor- $\alpha$ ; TBHP, tert-butyl hydroperoxide; HUVECs, human umbilical vein endothelial cells.

### 3.3.7 OxLDL does not induce MCP-1 release by ECs or affect endothelial permeability and apoptosis

The supernatants of HUVECs stimulated with 100  $\mu$ g/ml oxLDL and TNF- $\alpha$  (200 and 400 ng/ml) were taken for measurement of MCP-1 content after 24 hours using ELISA. The concentrations of TNF- $\alpha$  used here were much higher than 50 ng/ml as supernatants were taken from HUVECs being used to optimise the apoptosis assay; specifically, to find an appropriate stimulus that would induce a detectable and

significant increase in apoptosis for use as a positive control. Data from two independent experiments suggest that 100 µg/ml oxLDL does not induce MCP-1 release by HUVECs, producing similar results to unstimulated, control cells. However, after HUVECs were stimulated with 200 and 400 ng/ml of TNF-α, 44.80 ng/ml and 53.13 ng/ml of MCP-1 respectively was detected in the cell supernatants (Figure 3.10).

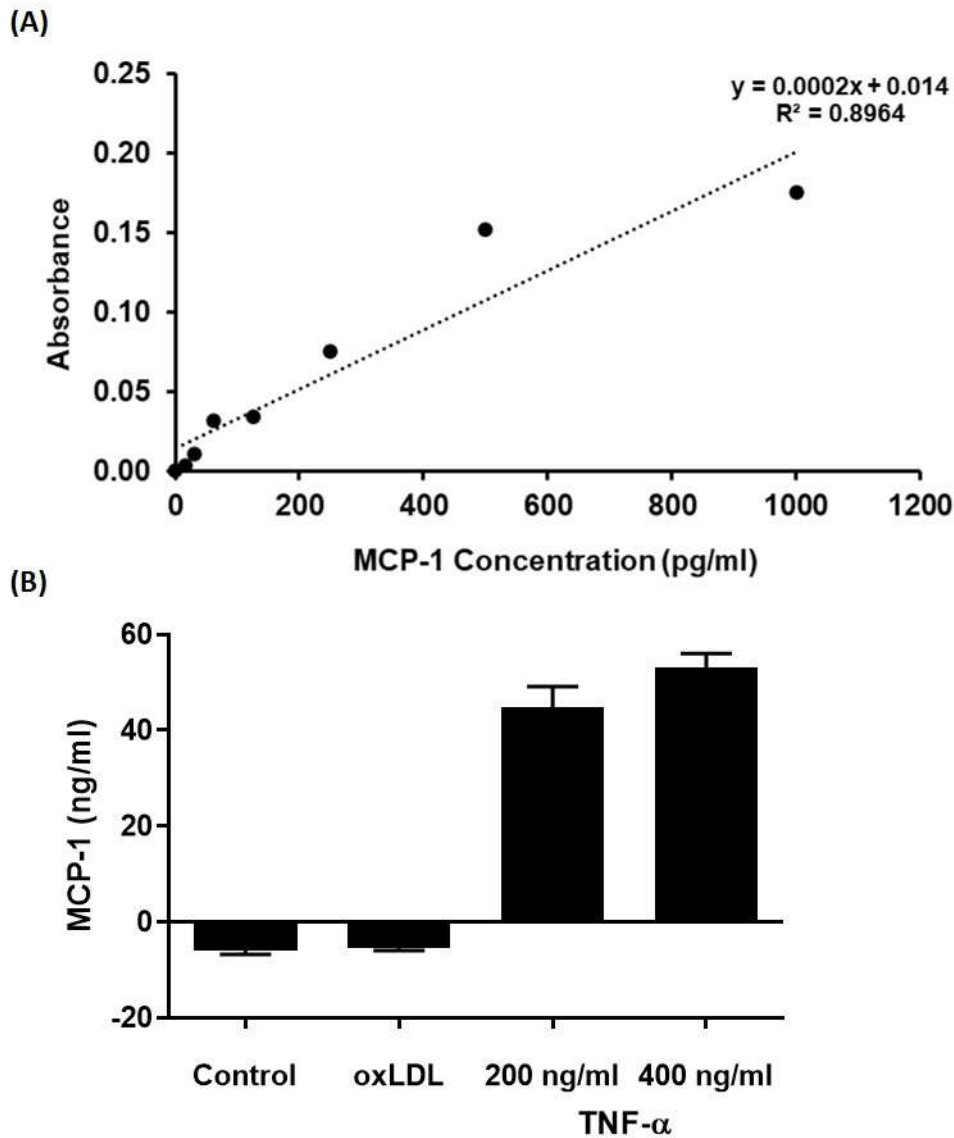


**Figure 3.10 TNF-α induces MCP-1 release by ECs.**

Data presented as mean  $\pm$  SEM from two independent experiments. Samples of supernatants from HUVECs were assayed for MCP-1 content using a sandwich format ELISA after 24 hours treatment with 100 µg/ml oxLDL or the indicated concentrations of TNF-α. A representative standard curve for the MCP-1 ELISA used to calculate MCP-1 concentration of the samples is shown in (A). Abbreviations: MCP-1, monocyte chemotactic protein-1; oxLDL, oxidised low-density lipoprotein; TNF-α, tumour necrosis factor-α; HUVECs; human umbilical vein endothelial cells.

### Chapter 3: Effect of (+)-catechin on endothelial and VSMC dysfunction

Permeability was studied by monitoring the influx of FITC-dextran at 1-hour intervals through a monolayer of HUVECs stimulated with oxLDL over a course of 6 hours. VEGF, a known permeability inducer and at a concentration of 100 ng/ml, was used as the positive control for the assay. Whilst there was an increase in permeability (as shown by the increase in fluorescence) over the course of the 6 hours compared to the oxLDL-negative vehicle control, this was not statistically significant ( $p=0.169$ ). Therefore, further optimisation of the duration may be required (e.g., extending to 8 or 10 hours) to allow VEGF to induce a significant effect. The permeability of HUVECs was also not affected by oxLDL over the 6 hours compared to the oxLDL-negative vehicle control after three independent experiments.

Apoptosis was investigated in HUVECs stimulated with oxLDL and TNF- $\alpha$  for 24 hours, whereby cells treated with 400 ng/ml TNF- $\alpha$  was used as the positive control for the assay (set arbitrarily as fold change 1). Whilst there may be possible differences in apoptosis between the TNF- $\alpha$ -treated or oxLDL-stimulated cells compared to the vehicle control, none of these were statistically significant. Similarly, in the presence of (+)-catechin, oxLDL-induced apoptosis may be lower compared to the oxLDL-positive vehicle control, although this was also not significant (Figure 3.11B). Therefore, since oxLDL did not induce any significant changes to the permeability or apoptosis of HUVECs (or affect TBHP-stimulated ROS production after 48 hours (preliminary  $n=1$  (data not shown))), this avenue of research could not be continued and hence the effect of (+)-catechin on these parameters cannot be reliably inferred.

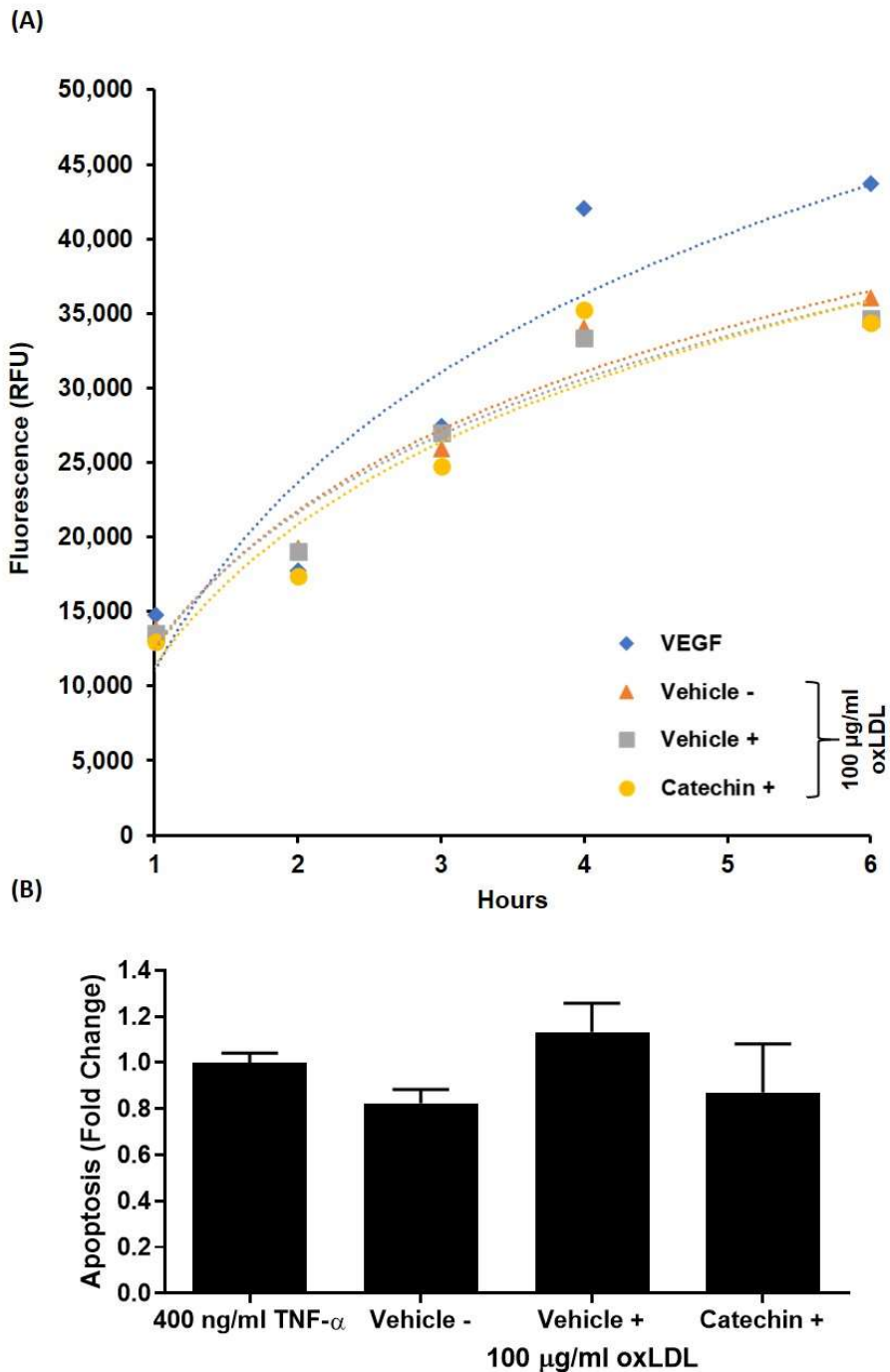


**Figure 3.11 OxLDL has no significant effects on the permeability or apoptosis of ECs.**

Data presented as mean  $\pm$  SEM from three independent experiments. Permeability of HUVECs was measured by monitoring the flux of fluorescent FITC-dextran through the cell monolayer at 1-hour intervals up to 6 hours (A). Apoptosis was analysed via annexin-V FITC labelling of HUVECs with fluorescent measurement after 24 hours (B). Statistical analysis via curved regression (A) or one-way ANOVA with Tukey's post-hoc test (B), where the positive control (400 ng/ml TNF- $\alpha$ ) was set arbitrarily as fold change 1. Abbreviations: VEGF, vascular endothelial growth factor; oxLDL, oxidised low-density lipoprotein; TNF- $\alpha$ , tumour necrosis factor- $\alpha$ ; HUVECs, human umbilical vein endothelial cells.

### 3.3.8 (+)-Catechin has no effect on monocyte-endothelial adhesion

Due to the lack of expected changes in apoptosis and permeability seen with oxLDL stimulation, further experiments were carried out using TNF- $\alpha$ . HUVECs were stimulated with TNF- $\alpha$  for 3 hours before being allowed to interact with THP-1 monocytes in a static adhesion assay set up. HUVECs stimulated with TNF- $\alpha$  in the presence of (+)-catechin for 3 hours did not demonstrate significantly altered adhesion to THP-1 monocytes compared to the TNF- $\alpha$ -positive vehicle control, which was set arbitrarily as fold change 1 (Figure 3.12A).

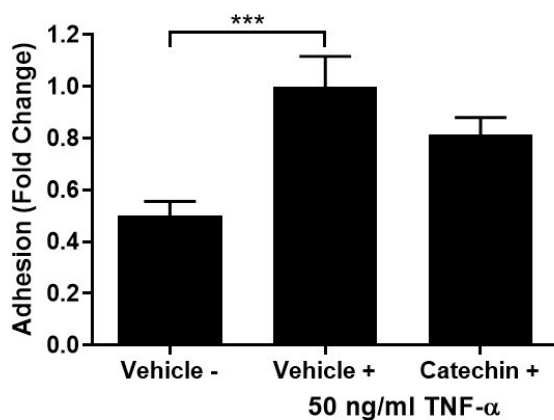


**Figure 3.12 (+)-Catechin has no significant effect on monocyte-endothelial adhesion.**

Data presented as mean  $\pm$  SEM from four independent experiments. Statistical analysis was via one-way ANOVA with Tukey's post-hoc test, with TNF- $\alpha$  positive vehicle control set arbitrarily as fold change 1 where  $***, p < 0.001$ . Adhesion was measured using a static adhesion assay to measure adherence of fluorescently labelled THP-1 monocytes to HUVECs in the presence of TNF- $\alpha$  after 3 hours interaction. Abbreviations: TNF- $\alpha$ ; tumour necrosis factor- $\alpha$ .

### 3.3.9 (+)-Catechin attenuates PDGF-stimulated invasion of VSMCs with no effect on proliferation over 7 days

Migration of quiescent HASMCs through a microporous membrane towards PDGF was hence measured using a modified Boyden chamber after 4 hours treatment with vehicle or (+)-catechin. This treatment duration was based upon previous experiments conducted in the host laboratory (and methods of other published studies), which was found to be sufficient to observe an effect. (+)-Catechin significantly attenuated PDGF-induced migration of HASMCs by 35.39% ( $p = 0.006$ ) compared to the PDGF-positive vehicle control, which was arbitrarily set as fold change 1 (Figure 3.13A). However,

(+)-catechin had no significant effect on the proliferation of HASMCs over 7 days compared to vehicle control, which was set arbitrarily as fold change 1 for each time point (Figure 3.13B).

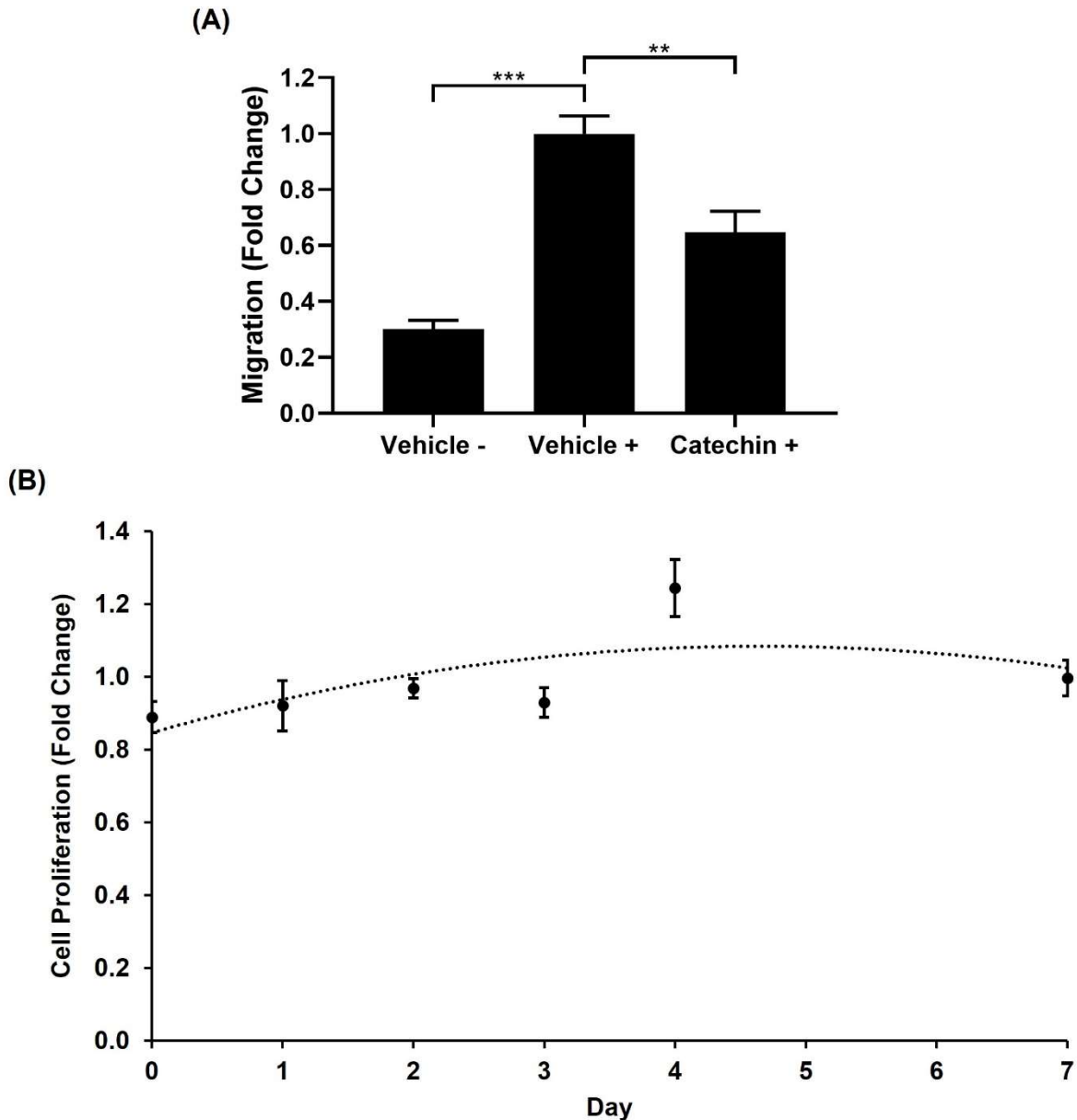


**Figure 3.13 (+)-Catechin attenuates PDGF-stimulated VSMC migration without affecting basal proliferation over 7 days.**

Data presented as mean  $\pm$  SEM from four (A) and three (B) independent experiments. Statistical analysis via one-way ANOVA with Tukey's post-hoc test where \*\*,  $p < 0.01$ ; \*\*\*,  $p < 0.001$  and (B) curved regression. A modified Boyden chamber was used to quantify the migration of HASMCs through a porous membrane towards PDGF after 4 hours. Cell proliferation was indirectly measured using crystal violet staining after the specified time point and the vehicle control was arbitrarily set as fold change 1 for each time point. Abbreviations: PDGF, platelet-derived growth factor; VSMC; vascular smooth muscle cell; HASMCs, human aortic smooth muscle cells.

3.3.10 (+)-Catechin reduces macrophage MMP activity after 24 hours

In HMDMs, MMP activity was only significantly reduced after 24 hours treatment, and this was by 8.38% ( $p=0.005$ ) compared to the vehicle control, which was set arbitrarily as fold change 1 (Figure 3.14).

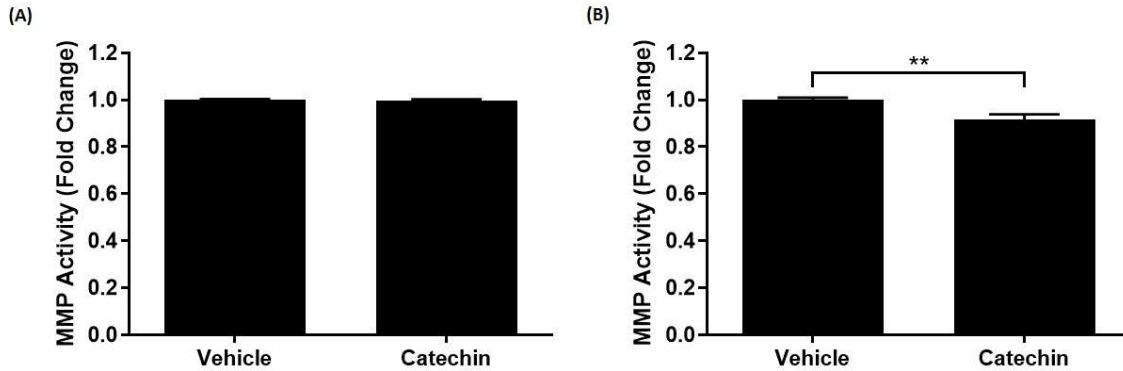


**Figure 3.14 (+)-Catechin reduces macrophage MMP activity after 24 hours.**

Data presented as mean fold change  $\pm$  SEM from four (A) and five (B) independent experiments. HMDMs were assayed for MMP after 3 (A) and 24 hours (B) treatment with vehicle or (+)-catechin. Statistical analysis via unpaired t-test where \*\*,  $p<0.01$  compared to vehicle control, which was set arbitrarily as fold change 1. Abbreviations: MMP, matrix metalloproteinase; HMDMs, human monocyte-derived macrophages.

MMP activity was also measured in HASMCs treated with vehicle or (+)-catechin for 3 and 24 hours; however, no changes were observed after either time point after two independent experiments and hence were discontinued (Figure 3.15).

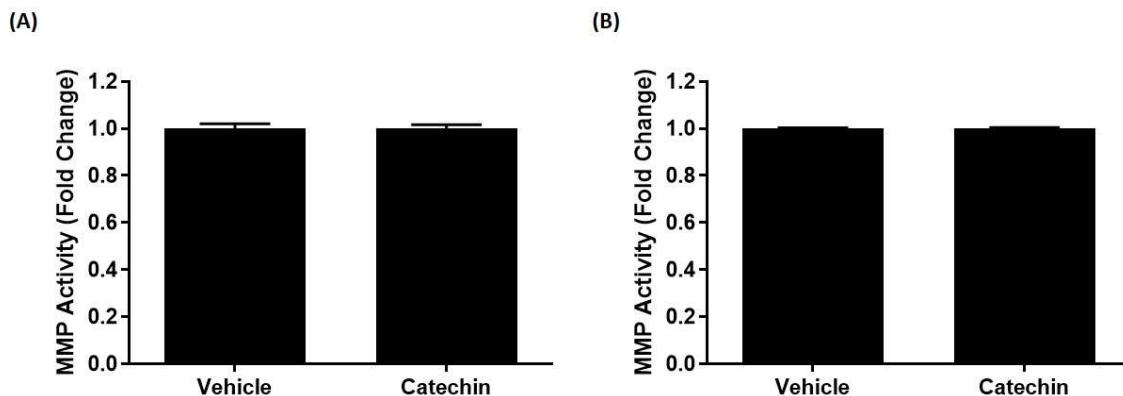


**Figure 3.15 (+)-Catechin has no effect on VSMC MMP activity.**

Data presented as mean fold change  $\pm$  SEM from two independent experiments. HASMCs were assayed for MMP after 3 (A) and 24 hours (B) treatment with vehicle (set arbitrarily as fold change 1) or (+)-catechin. Abbreviations: MMP, matrix metalloproteinase; HASMC, human aortic smooth muscle cell.

3.3.11 (+)-Catechin elicits comparable effects on monocyte migration and ROS production to its isomers

To compare the efficacy of (+)-catechin with (-)-catechin and (-)-epicatechin, two key assays were selected; MCP-1-stimulated migration of THP-1 monocytes and TBHP-stimulated THP-1 monocyte ROS production. In accordance with previously obtained data in the host laboratory, (+)-catechin significantly attenuated monocyte migration by 57.84% ( $p < 0.001$ ) and THP-1 monocyte ROS production by 24.19% ( $p < 0.001$ ) compared to their respective MCP-1 or TBHP-positive vehicle (DMSO or water) controls (Figure 3.16). (-)-Catechin is soluble in water, which forms the vehicle controls, whereas (+)-catechin and (-)-epicatechin are not, and hence were dissolved in DMSO. Similarly, (-)-epicatechin and (-)-catechin also significantly attenuated monocyte migration (55.02% ( $p = 0.002$ ); 48.89% ( $p = 0.006$ ) respectively) and ROS production (39.11% ( $p < 0.001$ ); 32.35% ( $p < 0.001$ ) respectively) compared to their respective positive vehicle controls. When the individual isomers were compared to each other, (-)-epicatechin was better at attenuating monocyte ROS production compared to (+)-catechin by 14.92% (trend;  $p = 0.052$ ). Therefore, (+)-catechin and its isomers generally demonstrate comparable effects on both monocytic migration and ROS production.

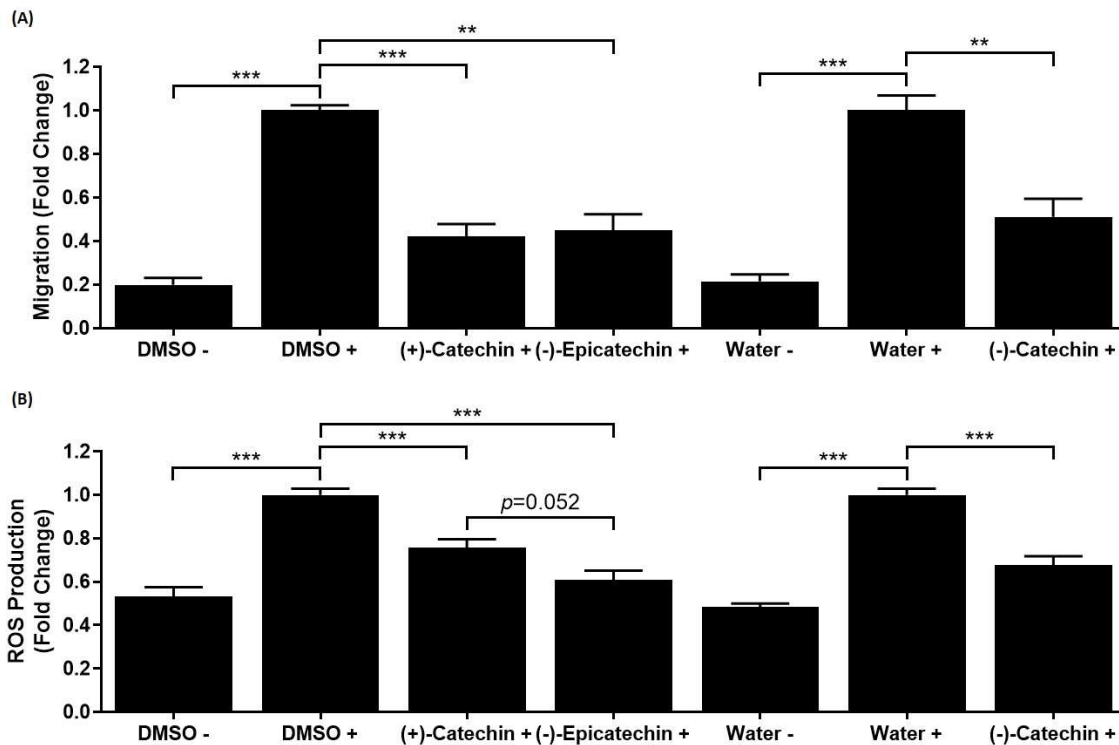


**Figure 3.16 (+)-Catechin, (-)-catechin and (-)-epicatechin attenuates monocyte migration and ROS production after 3 hours.**

Data presented as mean  $\pm$  SEM from three independent experiments. Statistical analysis via one-way ANOVA with Games-Howell (A; square-root transformed data) or Tukey's (B) post-hoc test where \*\*,  $p < 0.01$ ; \*\*\*,  $p < 0.001$ . Migration of THP-1 monocytes towards MCP-1 was measured after 3 hours treatment with vehicle or the specified catechin using a modified Boyden chamber method. ROS production was measured in THP-1 monocytes stimulated with TBHP (stimulates ROS production) in the presence of vehicle or the defined catechin. The respective positive vehicle controls were set arbitrarily as fold change 1; (+)-catechin and (-)-catechin are soluble in DMSO whilst (-)-catechin is soluble in water. Abbreviations: DMSO, dimethyl sulfoxide; ROS, reactive oxygen species; MCP-1, monocyte chemoattractant protein-1; TBHP, tert-butyl hydroperoxide.

### 3.4 Discussion

Catechins in green tea, cocoa, red wine and other sources have long been recognised as major contributors to the health benefits associated with their long-term consumption. A diet rich in fruits and vegetables with moderate intake of red wine (i.e., the Mediterranean diet) has long been associated with CVD protection in various epidemiological studies. However, the properties, actions and underlying mechanisms of individual constituents within these foods are less well researched, mainly due to the use of a combination of these in human and animal studies, for example in the form of green tea extracts and flavanol-enriched cocoa. Although there has been an increase in studies investigating individual catechins, such as EGCG and (-)-

### Chapter 3: Effect of (+)-catechin on endothelial and VSMC dysfunction

epicatechin, both *in vitro* and *in vivo*, little has been done on (+)-catechin itself, despite demonstrating promising anti-atherogenic activities. Studies conducted in this chapter aimed to investigate the *in vitro* activities of (+)-catechin further, using other key cell types implicated in atherosclerosis beyond monocytes and macrophages. Results described in this chapter show that (+)-catechin dampens ROS production in all investigated cell types (macrophages, ECs and VSMCs); reduces macrophage proliferation; attenuates invasion of VSMCs towards PDGF; lessens macrophage MMP activity; and attenuates monocyte migration; and ROS production comparable to its isomers, (-)-catechin and (-)-epicatechin. However, (+)-catechin had no significant effects on VSMC proliferation and MMP activity, TNF- $\alpha$ -stimulated monocyte-endothelial adhesion and proliferation of ECs. Furthermore, its effect on oxLDL/TNF- $\alpha$ -stimulated MCP-1 release and apoptosis could not be inferred from the data. Therefore, (+)-catechin demonstrates some anti-proliferative, anti-inflammatory, anti-oxidative and anti-atherogenic activities *in vitro*.

#### 3.4.1 Use of oxLDL and TNF- $\alpha$ to stimulate ECs

OxLDL-mediated endothelial dysfunction is a key step in atherogenesis; various studies have demonstrated that oxLDL has cytotoxic effects on vascular ECs, impedes NO bioavailability, and hence activates the endothelium. One of the ways in which oxLDL acts is via stimulating the release of potent pro-inflammatory cytokine, TNF- $\alpha$ , by surrounding cells. With respect to oxLDL, concentrations of 10 to 100  $\mu\text{g/ml}$  (for durations of up to 24 hours) have been used in a range of previously published studies (Dandapat et al. 2007; Sugimoto et al. 2009; Ryoo et al. 2011). With respect to TNF- $\alpha$ , 50 ng/ml has been previously used in various experiments conducted in the host laboratory; for example, a significant increase in MCP-1 and ICAM-1 expression was induced in THP-1 macrophages after 24 hours (Gallagher 2016). Stimulation of HUVECs with 100  $\mu\text{g/ml}$  oxLDL and 50 ng/ml TNF- $\alpha$  significantly reduced proliferation after 24 hours without detrimental effects on viability, and so these concentrations were used for subsequent experiments. The oxLDL data appears to concur with published literature, which show that low concentrations of oxLDL up to 20  $\mu\text{g/ml}$  enhance proliferation, while higher concentrations reduce it (Chen et al. 2000; Heinloth et al. 2000; Seibold et al. 2004; Yu et al. 2011b). In this study, oxLDL stimulation did

not induce the expected changes in HUVECs in several assays (i.e., MCP-1 secretion and increased permeability), hence TNF- $\alpha$  stimulation was pursued. Since oxLDL-stimulated ECs did not have significantly increased apoptosis due to the variation of the data, further repeats are required before firm conclusions can be drawn. The lack of significant changes induced by oxLDL, which was obtained commercially, may be attributed to the degree of oxidation (i.e., minimally, moderately and strongly) or even mode of oxidation, which has been known to have substantially different pro-inflammatory effects (Zhang et al. 2017a).

Additionally, slight reoptimisation of certain protocols may also be required. In the permeability assay, VEGF failed to induce a significant increase in permeability over time and in the apoptosis assay, the high concentration of TNF- $\alpha$  failed to induce a significant increase in apoptosis compared to their respective controls. Given that TNF- $\alpha$  is known to increase endothelial permeability by stimulating reorganisation of the actin and tubulin cytoskeletons of ECs to enhance the gap between adjacent cells (Poerber and Sessa 2007), it would be of interest to see how TNF- $\alpha$  performs in place of oxLDL in the assay. Therefore, the effect of (+)-catechin on endothelial permeability cannot be inferred from results of this assay as oxLDL had no effect. Although (+)-catechin might possibly dampen oxLDL-induced apoptosis of HUVECs, this assay requires further repeats before definitive conclusions can be drawn due to the variability the data. This may attributed to the use of cell passages 4-10 for experiments, whereas perhaps a tighter range of passages 2-4 should have been considered, especially when studying cell cytotoxicity parameters.

#### 3.4.2 (+)-Catechin attenuates ROS production in various cell types

ROS are involved in the maintenance of cardiovascular homeostasis and are potent signalling molecules in numerous processes, including cell migration and adhesion, proliferation and hypertrophy, and apoptosis and senescence. Excess ROS production and associated oxidative stress can lead to pathophysiological changes that contribute to CVD. Results of this study found that (+)-catechin significantly attenuated TBHP (H<sub>2</sub>O<sub>2</sub>)-induced ROS production in HUVECs, HASMCs and HMDMs in accordance with data obtained from previously conducted experiments in the host

laboratory, whereby (+)-catechin significantly attenuated TBHP-induced ROS production in THP-1 monocytes and macrophages (Moss 2018), which were also confirmed in this study. Although the viability of HASMCs was significantly reduced by (+)-catechin after 24 hours by 4.56%, this was minor compared to the 23.77% and 19.41% decreases in ROS production observed after 3 and 24 hours respectively. As mentioned previously, TNF- $\alpha$  is capable of inducing ROS production by ECs as part of processes that encourage oxidative stress-mediated endothelial dysfunction. In the presence of TNF- $\alpha$ , pre-treatment of HUVECs with (+)-catechin was required to attenuate TBHP-induced ROS production in the presence of TNF- $\alpha$ , suggesting that a preventative approach is necessary. This suggests that the antioxidative activities of (+)-catechin are insufficient to buffer the acute ROS production induced by multiple stimuli in the form of TNF- $\alpha$  and H<sub>2</sub>O<sub>2</sub>, and pre-treatment is required for the antioxidative effects of (+)-catechin to manifest in these conditions. Overall, (+)-catechin might prevent ROS-mediated LDL oxidation and subsequent foam cell formation (attributed to excessive oxLDL internalisation via SRs), dampening oxLDL-mediated endothelial dysfunction and associated pro-inflammatory signalling. Further exploration of the antioxidative activities of (+)-catechin are required to ascertain whether other types of ROS (e.g., superoxide anion and hydroxyl ion) are also attenuated, and if other parameters associated with protection against oxidative stress are also attenuated beyond its free radical scavenging ability.

#### 3.4.3 (+)-Catechin has no effect on monocyte-endothelial adhesion

(+)-Catechin had no significant effect on the adhesion of monocytes to HUVECs stimulated with TNF- $\alpha$  for 3 hours under static conditions; however, due to the variation within the data, further repeats should be conducted before firm conclusions can be drawn. Moreover, retrospective power calculations could be employed to determine the number of additional independent experiments that would be required to detect a significant effect, especially since this may be subtle (as is common with nutraceutical agents such as (+)-catechin). Furthermore, confirmation of the results would be required by repeating the adhesion assay under flow conditions (via the use of flow chambers), which is a closer and more accurate representation of the arterial conditions *in vivo*. This is important especially as select adhesive interactions only

occur under flow conditions and hence cannot be investigated in a static environment (Finger et al. 1996; Lawrence et al. 1997). Additionally, since adhesion of leukocytes to the activated endothelium is tightly controlled by various adhesion molecules and chemokines (e.g., ICAM-1 and MCP-1), the expression of these by ECs could be quantified using real-time quantitative PCR (RT-qPCR) as a secondary confirmation of the assay results. Given that catechins can modulate the interaction of ligands with their receptors, including those of TNF- $\alpha$  (Fan et al. 2017), (+)-catechin might dampen the adhesion of monocytes to ECs by inhibiting the activation of TNF- $\alpha$ -induced NF- $\kappa$ B associated expression of adhesion molecules and chemokines to mediate its anti-inflammatory effects.

#### 3.4.4 (+)-Catechin attenuates macrophage proliferation

In primary HMDMs treated with (+)-catechin for 24 hours, proliferation was significantly reduced, in accordance with data previously obtained in the host laboratory. The anti-proliferative properties of catechins are well known, and one of the reasons responsible for their recognition as a potential avenue for the treatment of cancers (Bernatoniene and Kopustinskiene 2018). In this study, proliferation was indirectly assessed using crystal violet staining which binds to protein and DNA (Feoktistova et al. 2016), giving an indication of the number of viable cells present. Although this is a fast, convenient and simple method that allows the detection of changes in cell numbers via comparative analysis and hence changes in cell proliferation compared to a control, significant changes should be confirmed using secondary method, such as 5-bromo-2'-deoxyuridine (BrdU) ELISA. BrdU (uridine with a bromine substituted at the fifth carbon atom) is incorporated into RNA within cells. Changes in RNA levels as measured by ELISA are hence indicative of changes in cell number, giving a quantitative measurement of cell number in comparison to crystal violet staining. Alternatively, flow cytometry analysis could be used to monitor cell proliferation over time using carboxyfluorescein diacetate succinimidyl ester (CFSE) which readily incorporates into the cell. Monitoring the loss of CFSE fluorescence over time using flow cytometry to trace cell generations can hence provide insight into the number of cell divisions that occur and allow monitoring of cell proliferation. Use of a tritiated thymidine incorporation assay is another alternative method. Overall, although these

data need to be confirmed using a direct method of measurement, results obtained in this study, along with the previous study conducted in the host laboratory support the anti-proliferative actions of (+)-catechin in macrophages.

#### 3.4.5 (+)-Catechin attenuates PDGF-stimulated migration of SMCs with no effect on proliferation

VSMCs are stimulated, for example, by PDGF to invade from the tunica media (where they normally reside as contractile cells) to the intima layer, where they switch to the synthetic phenotype and contribute to both plaque burden and inflammation, as well as stability via different mechanisms. Along with macrophages, VSMCs can become foam cells via the internalisation of lipids; however, VSMCs also contribute to the formation of a plaque-stabilising fibrous cap via synthesis of ECM components. The expression of PDGF and its receptors are markedly upregulated and activated in human atherosclerotic plaques (Tanizawa et al. 1996; Abe et al. 1998; Ross 1999). This study found (+)-catechin treatment to significantly attenuate the migration of quiescent HASMCs towards PDGF after 4 hours, with no effect on basal proliferation over 7 days. Given that (+)-catechin consistently attenuated MCP-1-induced monocytic migration in separately conducted experiments in the host laboratory, and that (+)-catechin has demonstrated anti-migratory effects in various cancer cell lines (Silva et al. 2019), this was unsurprising. Furthermore, in rat and human VSMCs, red wine containing (+)-catechin abrogated PDGFR signalling (Sparwel et al. 2009). Therefore, (+)-catechin demonstrates anti-migratory effects on both THP-1 monocytes and HASMCs towards MCP-1 and PDGF-BB respectively. However, confirmation of the results should be done using an *in vitro* scratch assay along with analysis of PDGFR expression and activity in VSMCs to ascertain how (+)-catechin mediates its anti-migratory effects. Taken together, (+)-catechin might attenuate mitogen-stimulated VSMC invasion/migration in pathological conditions with no effect on their proliferation under normal conditions, leaving normal vascular maintenance uninhibited.

### 3.4.6 (+)-Catechin dampens macrophage MMP activity

MMPs are produced by various cells in the atherosclerotic lesion; MMP-mediated degradation of the ECM protein constituents of the fibrous cap contributes to cap degradation and subsequent plaque instability. Thinning of the cap precedes plaque rupture, hence the activity of MMPs produced by macrophages (which can be stimulated by ROS) is considered detrimental in advanced atherosclerosis. This study found that (+)-catechin significantly attenuated MMP activity in HMDMs after 24 hours but no effect was seen after 3 hours. In previous studies conducted in host laboratory, (+)-catechin treatment significantly dampened MMP activity in THP-1 macrophages after both 3 and 24 hours (i.e., short and long term). However, the use of individual inhibitors is required to investigate the activity of specific MMPs with confirmation using zymography for example, to decipher how these are modulated by (+)-catechin. Other studies have reported the ability of green tea catechins to attenuate the activities/expression of MMP-2, -9 and -12 (Demeule et al. 2000; Bedoui et al. 2005; Kim-Park et al. 2015). Taken together, (+)-catechin might attenuate ROS-induced macrophage MMP activity, since both these parameters were found to be reduced *in vitro*. Indeed, ROS scavenging (as well as lowering lipid (Aikawa et al. 1998)) has been found to reduce MMP expression in experimental atheroma (Galis et al. 1998), and ROS-dependent MMP activation has also been reported to occur in the shoulder region of atherosclerotic plaques in association with mast cell degranulation (Johnson et al. 1998).

### 3.4.7 (+)-Catechin demonstrates comparable effects to its isomers *in vitro*

(+)-Catechin is present in various food sources in combination with its isomers, including (-)-catechin and (-)-epicatechin (e.g., in cocoa, green tea and red wine) along with other catechins/flavanols. Whilst there have been various studies investigating (-)-epicatechin and EGCG, relatively little has been done on (-)- and (+)-catechin itself, despite a previous prospective study identifying a strong inverse correlation between (+)-catechin and (-)-epicatechin intake and coronary heart disease (Arts et al. 2001b). (+)-Catechin, (-)-catechin and (-)-epicatechin all significantly attenuated THP-1 monocyte migration towards MCP-1 and ROS production after 3 hours, supporting the anti-inflammatory and anti-oxidative actions of these catechins *in vitro*. Overall, all

investigated catechins exhibited similar effects on monocytic migration and ROS production suggesting similarities in their actions *in vitro*, although further experiments are required to substantiate this assumption. The results reported here based on these experiments suggest that the anti-atherogenic activities of (+)-catechin may be as potent as its isomers, and possibly even other catechins. Therefore, the cardiovascular health benefits associated with consumption of catechin-containing foods may also be attributed to (+)-catechin pending further investigation. Taken together, (+)-catechin demonstrates anti-inflammatory effects on monocytes; by attenuating their recruitment and migration in response to MCP-1 and their infiltration to the subendothelial layer. This, combined with their anti-proliferative and antioxidative activities in macrophages, suggests that (+)-catechin might reduce monocyte/macrophage presence within the atherosclerotic plaque, and delay its progression by dampening MMP activity to preserve the ECM components of the fibrous cap. Therefore, to begin to answer the original question of whether the protective actions of (+)-catechin extend to key processes involving ECs and VSMCs, results obtained thus far suggest that (+)-catechin may exert more anti-atherogenic effects on monocytes/macrophages in comparison to ECs and VSMCs. However, further experiments focusing on ECs and especially, VSMCs are first required in order to delve deeper into parameters associated with endothelial/SMC dysfunction and substantiate this conclusion.

#### 3.4.8 Future directions

To investigate the actions of (+)-catechin further, other parameters associated with endothelial dysfunction yet to be studied include NO production (and eNOS expression), cell senescence and release of extracellular vesicles (EVs), which are processes associated with and affected by oxidative stress. Both apoptosis and senescence are closely related and consequences of oxidative stress in several cardiovascular cells, such as ECs (Maejima et al. 2008), VSMCs (Mistry et al. 2013) and cardiomyocytes (Maejima et al. 2008). High ROS levels can induce the activation of cell cycle arrest proteins via inactivation of growth factor signalling mediators. EVs have gained significant attention in recent years, especially in the context of inflammation and atherosclerosis, due to the involvement of their cargo in intercellular communication and other processes (Paone et al. 2018). Forms of EVs include

### Chapter 3: Effect of (+)-catechin on endothelial and VSMC dysfunction

exosomes, microvesicles/microparticles and apoptotic bodies, which are released by ECs during cellular activation and apoptosis (Kalra et al. 2016). Apoptotic bodies for example, are a major subset of EVs released during EC apoptosis that may influence atherosclerosis progression (Paone et al. 2018). The alpha isoform of potent pro-inflammatory cytokine, IL-1 (IL-1 $\alpha$ ), has been identified in endothelial apoptotic bodies which were found to stimulate monocyte chemokine secretion *in vitro* and neutrophil-mediated inflammation *in vivo* (Berda-Haddad et al. 2011). Therefore, further investigation of the anti-inflammatory actions of (+)-catechins in this regard may provide insights into how it elicits its beneficial effects on ECs.

Additionally, further studies focused on the effect of (+)-catechin on VSMCs is also important, given the heterogeneity and plasticity of VSMCs and their various roles in the pathogenesis of atherosclerosis. Previous studies conducted in the host laboratory have largely focused on parameters of macrophage foam cell formation; investigation of the effect of (+)-catechin treatment on VSMC foam cell formation is hence still required and could be measured using immunocytochemistry via ORO staining. The effect of (+)-catechin treatment on VSMC gene expression in the context of phenotypic markers is also of interest and could be investigated using single cell RNA-sequencing (RNA-seq; scRNA-seq) to study how the overall cellular transcriptome is modulated by (+)-catechin. Together, these studies will provide valuable insights into the actions of (+)-catechin and help develop understanding of its underlying mechanisms in the context of atherosclerosis.

#### 3.4.9 Conclusion

(+)-Catechin demonstrates various anti-atherogenic effects *in vitro* in various key cell types implicated in all stages of atherosclerosis. In particular, (+)-catechin demonstrates potent and consistent antioxidant activities in all investigated cell types, and attenuates several parameters associated with endothelial and VSMC dysfunction *in vitro*. Given that ROS are potent signalling molecules involved in various processes, it is likely that (+)-catechin mediates its beneficial effects via its antioxidative activities to suppress oxidative stress-mediated pathological signalling and inflammation. Further investigations are required to delineate its actions on other parameters and

### Chapter 3: Effect of (+)-catechin on endothelial and VSMC dysfunction

gain insights to the underlying mechanisms responsible for these actions. Therefore, the effect of (+)-catechin on cellular bioenergetics and mitochondrial function is explored in the next chapter, especially given the potent antioxidative properties of (+)-catechin and the mitochondria is a key source of ROS.

## **4 Effect of (+)-catechin on bioenergetics and mitochondrial function**

### **4.1 Introduction**

(+)-Catechin has demonstrated various anti-atherogenic activities in macrophages, ECs and VSMCs. Importantly, the results of this study combined with that obtained from previous work conducted in the host laboratory (Moss 2018), demonstrate that (+)-catechin consistently attenuates ROS production in key cell types implicated in all stages of atherosclerosis (ECs, monocytes/macrophages and VSMCs). The mitochondria are key sources of ROS and abnormal metabolic shifts are indicative of cellular dysfunction. Furthermore, mitochondrial dysfunction has been implicated in atherosclerosis by compromising respiration and increasing oxidative stress. Therefore, the effect of (+)-catechin on cellular bioenergetics and mitochondrial function was investigated with focus on macrophages and ECs, the two most investigated cell types in the host laboratory thus far.

#### **4.1.1 The mitochondria**

The mitochondrion is a highly dynamic organelle of particular interest given its involvement in the regulation of cell function and phenotypic modulation. The mitochondria are critical mediators of cellular homeostasis due to their involvement in ATP generation, ion transport, ROS production, proliferation, inflammation and apoptotic signalling (Nunnari and Suomalainen 2012). Their communication with the rest of the cell is mediated via various mechanisms, including cytochrome c release to stimulate cell death; AMP-activated protein kinase (AMPK) activation to control mitochondrial fission and fusion; ROS generation to activate transcription factors; mtDNA release to instigate immune responses; and release of tricarboxylic acid (TCA) metabolites to regulate cell fate and function (Martinez-Reyes and Chandel, 2020). The release of mitochondrial components, such as mitoROS and mtDNA, induce activation of the NLRP3 inflammasome, which leads to the formation and release of mature IL-1 $\beta$  and IL-18 (Shimada et al. 2012). Furthermore, mitochondrial function is essential for the energy-consuming cellular repair pathways activated in response to

enhanced deposition of proteins damaged by ROS/RNS (Nunnari and Suomalainen 2012). Therefore, their critical involvement in the regulation of cell death, inflammation, metabolism and ROS production renders the mitochondria of particular interest in the context of atherosclerosis. Although the exact mechanisms by which mitochondrial dysfunction mediate pathogenesis still require elucidation, studies have supported a role for mitochondrial dysfunction in contributing to atherosclerosis development and progression (Madamanchi and Runge 2007). This is unsurprising, given that mitochondrial dysfunction can directly alter cellular metabolism, and encourage cell death, inflammation and oxidative stress (Yu and Bennett 2014).

### 4.1.2 Effects of catechin on mitochondrial function and experimental aim

Mitochondrial dysfunction is implicated in the pathogenesis of atherosclerosis; restoring mitochondrial function has demonstrated promise as a potential therapeutic target. Catechin has been shown to protect against induced mitochondrial dysfunction in a range of cell types. These include HepG2 hepatocytes exposed to oleic acid (a steatosis model) (Rafiei et al. 2019), PC12 cells (neuron cell model) (Chen et al. 2003), the kidney (Wongmekiat et al. 2018), MRC-5 (lung fibroblast) cells (Santos et al. 2016) and EA-hy926 cells (an EC line obtained by the fusion of HUVECs with lung carcinoma cells) (Zhang et al. 2017b). Furthermore, Swiss albino mice that had received pre-treatment of catechin (40 mg/kg) significantly attenuated mitochondrial oxidative stress parameters induced by tamoxifen (Tabassum et al. 2007), and in myocardial ischaemia/reperfusion rats, catechin was shown to improve mitochondrial function and alleviate apoptosis (Cong et al. 2020). Together, these studies demonstrate that catechin may have protective effects on mitochondrial function in pathological conditions. However, investigations of its effects on endothelial and macrophage metabolism and mitochondrial function in the context of atherosclerosis has been lacking. Therefore, in this study, the effect of (+)-catechin on cellular bioenergetics and metabolism, along with parameters associated with mitochondrial function was investigated, to explore how (+)-catechin might mediate its anti-atherogenic activities in ECs and macrophages.

### 4.1.3 Mitochondrial respiration

Within the cell, ATP is produced predominantly via two pathways; oxidative phosphorylation in the mitochondria and glycolysis in the cytosol. Most cells possess the ability to switch between these two pathways, thus adapting to alterations in their environment and energy requirements. Glycolysis, although yielding much less ATP molecules compared to oxidative phosphorylation, is much more rapid, and hence a more suitable metabolic pathway to support proliferation, since metabolic intermediates can be taken for biosynthesis (Koelwyn et al. 2019). On the other hand, the TCA cycle and oxidative phosphorylation are typically linked to non-proliferating or quiescent cells (Koelwyn et al. 2019). In the mitochondria, ATP production occurs in the inner membrane and is mediated by the proton motive force generated by the electron transport chain (ETC) (Scheffler 2001). The ETC is comprised of transmembrane protein complexes, I-IV, along with the freely mobile electron transporters, ubiquinone and cytochrome c (located in the cristae of the mitochondria) (Zhao et al. 2019). The two electron transport pathways within the electron transport chain are complex I/III/IV, with nicotine adenine dinucleotide (NADH) as the substrate, and complex II/III/IV, with succinic acid as the substrate (Zhao et al. 2019). ATP production is mediated by ATP synthase of complex V which utilises the energy accumulated from the coupling of electron flow and proton gradient across the membrane (Zhao et al. 2019). A proportion of the electrons are also transferred directly to O<sub>2</sub> to produce ROS. Under normal physiological conditions, over 98% of the electron transport is used by the respiratory chain for ATP synthesis, while only up to 2% of electrons are used to generate superoxide (Chistiakov et al. 2018; Siasos et al. 2018), which is quickly converted to H<sub>2</sub>O<sub>2</sub> by superoxide dismutase enzymes (Li et al. 2013). Impaired functioning of the mitochondrial ETC results in excessive ROS generation, leading to lipid and protein oxidation, and widespread cellular damage (Peng et al. 2019). This is due to the 'ROS-induced ROS' process, whereby adjacent mitochondria are also stimulated to release large amounts of ROS and have substantially reduced membrane potential (Peng et al. 2019). Therefore, amplification of the ROS signal promotes further mitochondrial and cellular dysfunction (Peng et al. 2019).

### 4.1.4 Mitochondrial dysfunction in atherosclerosis

Mitochondrial dysfunction is characterised by compromised respiratory output and decreased oxidative phosphorylation, along with excessive ROS production, which correlate with reduced respiration and mitochondrial membrane potential. Mitochondrial dysfunction is involved in the activation of apoptosis; opening of the mitochondrial permeability transition pore mediates membrane depolarisation and loss of oxidative phosphorylation (Richardson and Schadt 2014; Peng et al. 2019). Sustained opening of the mitochondrial permeability transition pore causes expansion of the mitochondrial matrix and fissuring of the outer membrane, resulting in the release of pro-apoptotic factors and ultimately apoptosis (Madamanchi and Runge 2007). In atherosclerosis, apoptosis of lesional vascular cells contributes to growth of the necrotic core as well as plaque instability and rupture. For example, death of macrophage and VSMC foam cells propagates inflammation and loss of VSMCs and their synthesis of ECM components within the fibrous cap promotes its thinning and rupture.

OxLDL-mediated endothelial dysfunction is a key initiating process that drives atherogenesis, due to its immunogenic status and cytotoxic effects on ECs. EC apoptosis and disruption of the continuous endothelial barrier promotes the infiltration of lipoproteins and immune cells to the vascular wall to promote atherogenesis. Exposure of the cells to oxidised lipids, such as those in oxLDL, stimulate the production of ROS (Zmijewski et al. 2005). OxLDL has been shown to disrupt mitochondrial function and promote apoptosis in HUVECs, as shown by loss of mitochondrial membrane potential, ROS generation and cytochrome c release (Yu et al. 2019). Moreover, in porcine aortic ECs, modified lipoproteins in the form of oxidised or glycated LDL reduced the activity of various enzymes of mitochondrial ETC complexes, leading to insufficient oxygen consumption, disrupted mitochondrial membrane potential and ROS production (Chowdhury et al. 2009; Sangle et al. 2010; Xie et al. 2010). Indeed, decreased mitochondrial respiration has been observed in human atherosclerotic plaque cells, particularly in the fibrous cap and core regions (Reinhold et al. 2017; Yu et al. 2017). Furthermore, lesion-derived VSMCs also demonstrated impaired mitochondrial respiration and enhanced mitophagy, which was stimulated by oxLDL (Reinhold et al. 2017; Yu et al. 2017). Accordingly, a subset of

VSMCs in the fibrous cap of human atherosclerotic lesions exhibited reduced oxidative phosphorylation, and plaque cells demonstrate increased glycolytic activity to account for the loss of mitochondrial function (Docherty et al. 2018). In HFD-fed *ApoE*<sup>-/-</sup> mice or *ApoE*<sup>-/-</sup> mice lacking the essential autophagy gene, *Atg7*, the presence or accumulation of damaged mitochondria and compromised mitochondrial respiratory function is associated with enhanced mitoROS production/oxidative stress and plaque instability (Yu et al. 2017; Nahapetyan et al. 2019). Furthermore, overexpression of mitochondrial helicase, Twinkle (an important regulator of mtDNA copy number), in *ApoE*<sup>-/-</sup> mice has been found to enhance mtDNA integrity and copy number, mitochondrial abundance of respiratory complexes and respiration, as well as promote plaque stability (Yu et al. 2017). Therefore, targeting mitochondrial damage in atherosclerosis to restore mitochondrial respiration may be a promising therapeutic target and agents that can confer mitochondrial protection may attenuate disease progression.

Given that (+)-catechin has demonstrated various anti-atherogenic effects on macrophages and ECs *in vitro*, Agilent Seahorse Technologies were used to investigate mitochondrial respiration and glycolysis and hence determine how (+)-catechin modulates cellular metabolism. The Mito Stress Test assay kit manufactured by Agilent Seahorse Technologies uses inhibitor drugs that target specific complexes of the electron transport chain. Controlled and sequential injection of the inhibitor drugs combined with continuous measurement of oxygen consumption rate (OCR) of the cells by the XF Analyzer machine enables calculation of various parameters. Oligomycin inhibits ATP synthase of complex V and injected first; FCCP then uncouples oxygen consumption from ATP production, as the proton gradient is collapsed and mitochondrial membrane potential is disrupted; and lastly, rotenone and antimycin A inhibit complex I and complex III respectively (Figure 4.1).

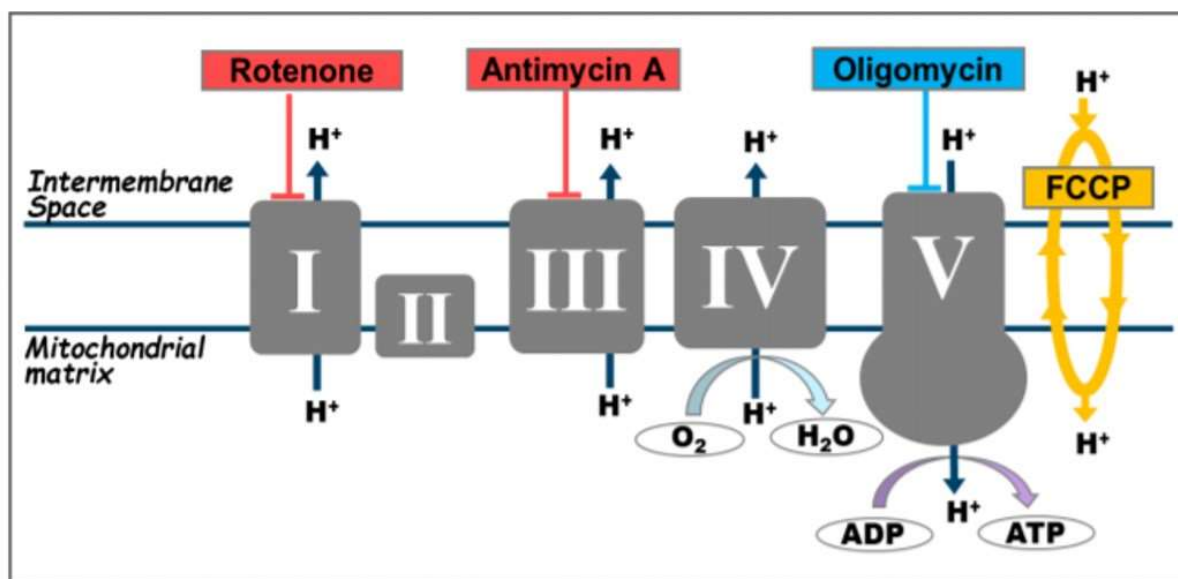


**Figure 4.1 Principle of the Mito Stress Test assay.**

Oligomycin inhibits ATP synthase of complex V, carbonyl cyanide 4-(trifluoromethoxy)phenylhydrazone (FCCP) uncouples oxygen consumption from ATP production, and rotenone and antimycin A inhibits complex I and complex III respectively. FCCP stimulation imitates a physiological rise in energy demand by collapsing the proton gradient and disturbing mitochondrial membrane potential, resulting in uninhibited electron flow through the electron transport chain and maximal oxygen consumption (i.e., maximal respiration) by complex IV. Abbreviations: ADP, adenosine diphosphate; ATP, adenosine triphosphate.

The effect of these mitochondrial inhibitor drugs on OCR is illustrated in Figure 4.2. The changes induced to OCR measured from the live cells enables the calculation of various parameters associated with mitochondrial respiration.

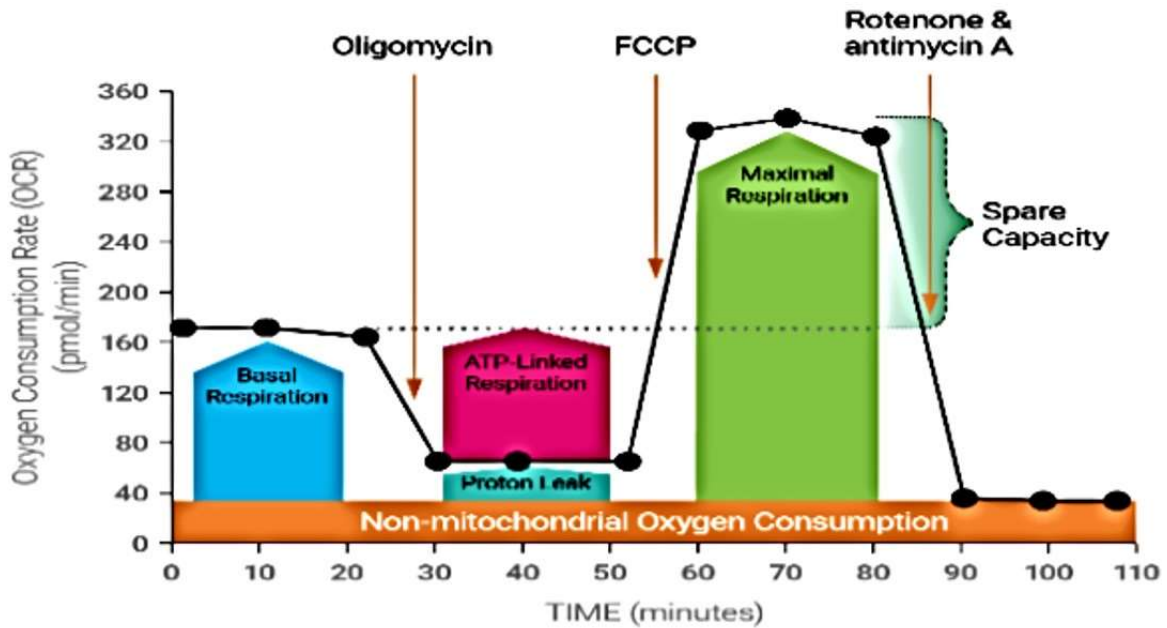


**Figure 4.2 Parameters measured in the Mito Stress Test Assay.**

Sequential stimulations with select mitochondrial inhibitor drugs induce changes in oxygen consumption rate (OCR), allowing measurement of multiple parameters associated with respiration. Oligomycin, carbonyl cyanide 4-(trifluoromethoxy)phenylhydrazone (FCCP) and rotenone/antimycin A induce different changes to OCR (which is constantly monitored) enabling calculation of the indicated parameters.

An explanation and summary of parameters calculated from these induced changes in OCR are described in Table 4.1.

**Table 4.1 Parameters measured by the Mito Stress Test.**

<b>Parameter</b>	<b>Explanation</b>
Basal respiration	The oxygen consumption used to meet the normal cellular ATP demand that results from proton leak.
ATP-linked respiration	The proportion of basal respiration used to fuel ATP production calculated from the decrease in OCR induced by oligomycin.
Proton leak	Basal respiration not coupled to ATP production. May be used as a regulatory mechanism for ATP production and can be an indicator of mitochondrial damage.
Coupling efficiency	The proportion of oxygen used to drive ATP-linked respiration compared to that of proton leak.
Maximal respiration	The maximal operation point of the respiratory chain that causes rapid oxidation of substrates to meet the metabolic demand/challenge.
Spare respiratory capacity	Represents the ability of the cell to respond to an increased energy demand i.e., an indicator of cell fitness/flexibility.
Non-mitochondrial respiration	Respiration that occurs independently of the mitochondria.

Abbreviations: OCR, oxygen consumption rate; ATP, adenosine triphosphate.

Defective mitochondrial function as shown by reduced respiration and lower ATP output can promote pathogenesis via a range of mechanisms. Therefore, parameters measured as part of the Mito Stress Test assay were used to investigate how mitochondrial respiration in THP-1 macrophages and HUVECs is affected by (+)-catechin in both unstimulated (normal) and stimulated (pro-inflammatory) conditions. THP-1 macrophages were stimulated with 100 ng/ml LPS and 250 U/ml IFN- $\gamma$  to induce their polarisation to the proinflammatory, M1 phenotype. HUVECs were stimulated with 100  $\mu$ g/ml oxLDL to induce their activation (to mimic endothelial dysfunction).

### 4.1.5 Glycolysis

During glycolysis, glucose is converted into lactate, and the energy released during this process is used to form ATP. In ECs, the preferred route of ATP generation is via glycolysis rather than mitochondrial oxidative phosphorylation (regardless of the oxygen concentration) (Quintero et al. 2006; Zhou et al. 2018; Wang et al. 2020). In normal physiological conditions, the mitochondria of ECs are highly coupled and function at sub-maximal capacity, suggesting substantial bioenergetic reserve capacity, which is important in protecting against oxidative and nitrosative stress (Dranka et al. 2010; Sansbury et al. 2011; Hill et al. 2012). In C57BL/6J mice, reduced glycolysis of ECs impaired endothelial maintenance and accelerated atherogenesis, a phenotype that was rescued by increasing EC glycolysis (Yang et al. 2018). In another study, partial inhibition of glycolysis in *ApoE*<sup>-/-</sup> mice restricted intraplaque angiogenesis and reduced plaque formation (without affecting composition), and downregulated the expression of endothelial adhesion molecules (Perrotta et al. 2020). Therefore, glycolysis is vital for EC turnover and maintenance of the endothelial barrier to inhibit pathogenesis arising from endothelial dysfunction.

Increased glycolysis has been observed in activated inflammatory cells (Kelly and O'Neill 2015). Classical activation of macrophages relies on anabolic metabolism to balance the increased energy demand with high glycolytic rates, along with the requirements for macromolecular substances (e.g., lipids and proteins) with an active (although partially defective) mitochondrial TCA cycle (O'Neill et al. 2016). Enhanced glycolysis in inflammatory macrophages is associated with inhibition of select steps of the TCA cycle which assist inflammatory processes, hence aerobic glycolysis is critical for inflammatory cell activation (Van den Bossche et al. 2017; Zhang et al. 2019a). On the other hand, alternatively activated macrophages channel degraded nutrients through oxidative phosphorylation for effective ATP generation (Huang et al. 2014; O'Neill et al. 2016). Therefore, investigation of cellular glycolysis may provide additional insights to cellular homeostasis and metabolism beyond mitochondrial respiration.

The effect of (+)-catechin on the glycolysis of THP-1 macrophages was hence investigated using the Glycolytic Rate Assay (Agilent Seahorse Technologies). The

outflow of protons during the breakdown of glucose to lactate in glycolysis is detected by the XF Analyzer machine as extracellular acidification rate (ECAR). Mitochondrial TCA activity generates CO<sub>2</sub>, which hydrates and acidifies the cell medium. Therefore, the cellular ECAR and OCR measurements are indicators of the two major energy-producing pathways, glycolysis and oxidative phosphorylation respectively. In the assay, both parameters are monitored to determine glycolytic PER (glycoPER) of the cells. By inhibiting respiration, measured by OCR, using rotenone (complex I inhibitor) and antimycin A (complex III inhibitor), the separation and calculation of PER from respiration leaves only glycoPER. The glycolysis inhibitor, 2-DG, is then injected to terminate glycolytic acidification to confirm pathway specificity (Figure 4.3).

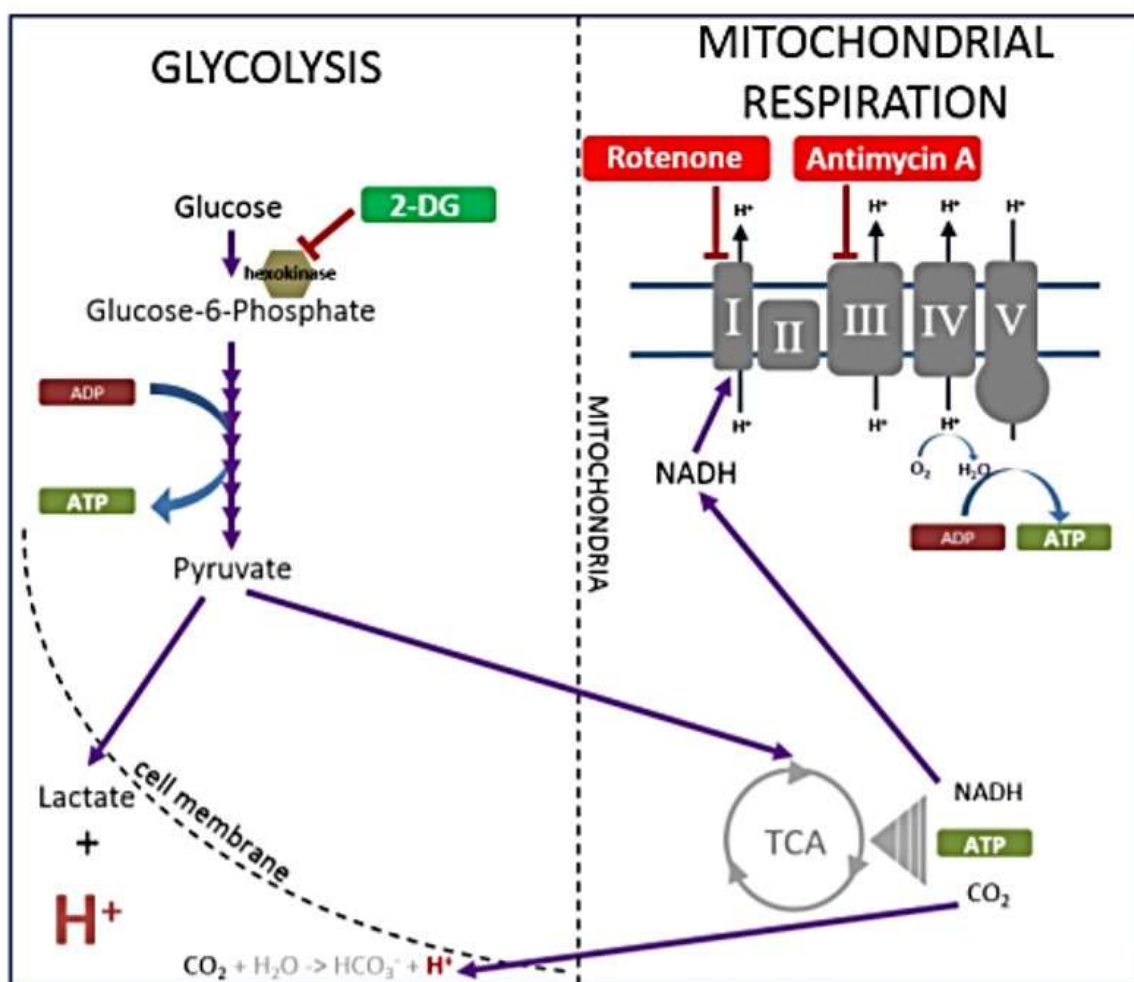


**Figure 4.3 Principle of the Glycolytic Rate Assay.**

Rotenone and antimycin A inhibit complexes I and III respectively of the electron transport chain, and 2-DG is a glucose analogue which inhibits glycolysis through competitive binding of glucose hexokinase (first enzyme in the glycolytic pathway), causing a rapid reduction in PER (also confirms that the PER produced before injection is predominantly due to glycolysis i.e., pathway specificity).

The effect of these inhibitor drugs on PER is illustrated in Figure 4.4. The changes induced to PER measured from the live cells enables the calculation of various parameters associated with glycolysis.

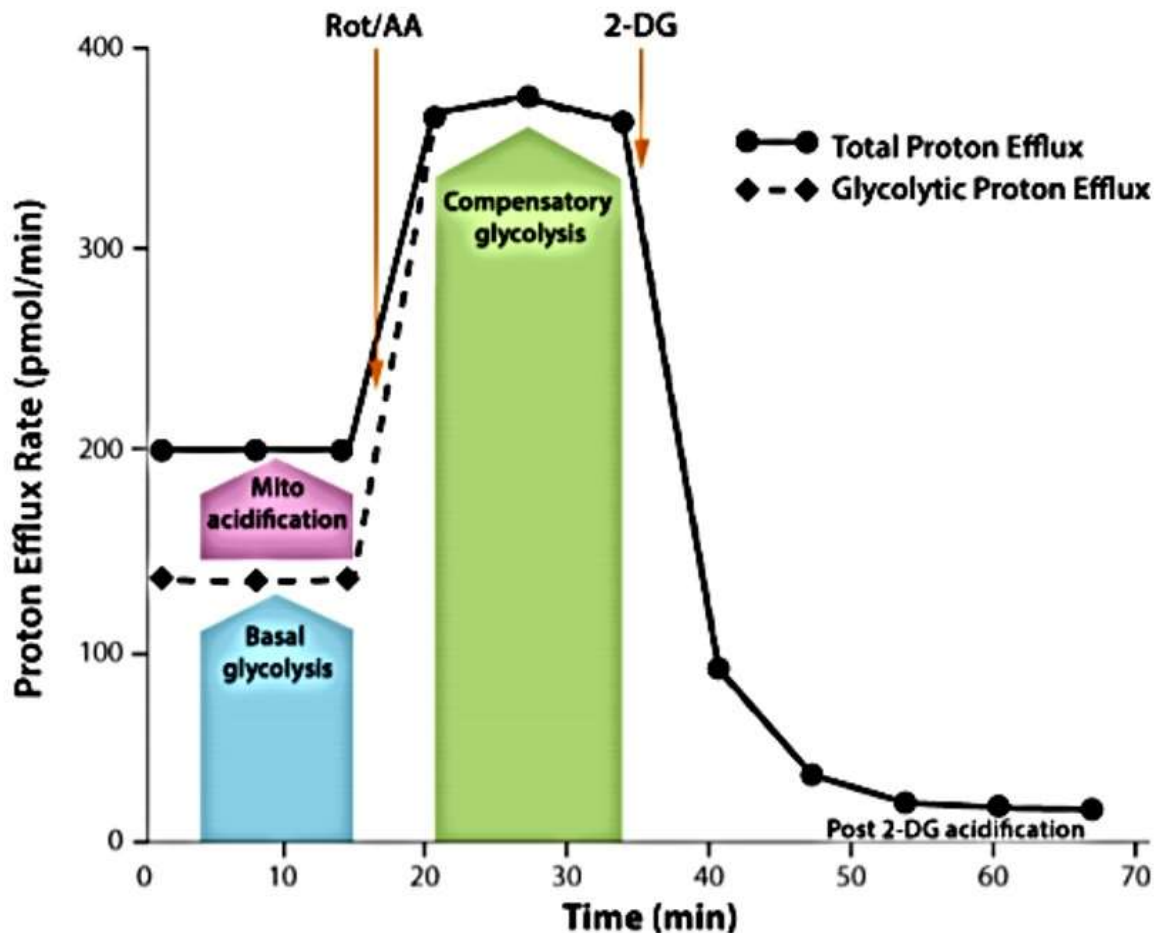


**Figure 4.4 Parameters measured in the Glycolytic Rate Assay**

Proton efflux comprises of both glycolytic and mitochondrial-derived acidification. Inhibition of mitochondrial function by Rotenone and Antimycin A (Rot/AA) allows calculation of mitochondrial-linked acidification. Glycolytic proton efflux rate is calculated by subtraction of mitochondrial acidification to total proton efflux rate.

An explanation and summary of parameters calculated from these induced changes in PER are described in Table 4.2.

**Table 4.2 Parameters measured by the Glycolytic Rate Assay.**

<b>Parameter</b>	<b>Explanation</b>
Basal glycolysis	The process of converting glucose to lactate.
Basal PER	The number of protons effluxed by the cells into the assay medium over time, expressed as pmol/min.
Compensatory glycolysis	The rate of glycolysis following inhibition of mitochondrial oxidative phosphorylation which drives compensatory changes in the cell to use glycolysis to produce ATP and meet the cells' energy demands.
GlycoPER	PER derived from glycolysis (discounting the effect of CO <sub>2</sub> -dependent acidification). This measurement is highly correlated with the extracellular lactate production rate.
Post 2-DG acidification	Value indicates other sources of extracellular acidification that are not attributed to glycolysis or mitochondrial TCA activity (i.e., residual glycolysis not inhibited by 2-DG).

Abbreviations: PER, proton efflux rate; glycoPER, glycolytic PER; 2-DG, 2-deoxyglucose; TCA, tricarboxylic acid.

Given that changes in the mode of cellular ATP production via shifts between oxidative phosphorylation and glycolysis can indicate cellular dysfunction, the effect of (+)-catechin on the glycolysis of THP-1 macrophages was studied.

#### 4.1.6 MitoROS production

Within the cell, mitochondria are major producers of superoxide and H<sub>2</sub>O<sub>2</sub> (Zmijewski et al. 2005); the latter being an important signal transduction molecule involved in the regulation of cell proliferation, hypoxia adaptation and establishing cell fate (Li et al. 2013). Elevations in mitoROS production combined with reduced antioxidant activities results in mitochondrial oxidative stress. Excessive ROS generation and mitochondrial oxidative stress can lead to impaired mitochondrial dynamics and ATP production, all of which can contribute to pathological changes. MtDNA encodes 37 genes, including the 13 proteins that constitute the subunits of respiratory complexes that mediate

oxidative phosphorylation (Peng et al. 2019). MtDNA are particularly susceptible to damage by ROS due to their close proximity to the site of ROS production in the ETC, lack of introns and protective histones, combined with limited repair capacity (Yakes and Van Houten 1997; Ballinger et al. 1999; Trifunovic et al. 2004). Moreover, mitochondrial DNA polymerase is error-prone; synthesis of mtDNA is continuous in the entire cycle, during which, the mtDNA is unstable and vulnerable to external interference (Peng et al. 2019). Therefore, mtDNA damage can result in defective oxidative phosphorylation and respiratory output. Indeed, mitoROS have been demonstrated to promote oxidative damage of mtDNA (Mikhed et al. 2015), with significant roles in atherosclerotic lesion development (Wang et al. 2014; Wang et al. 2017). However, mtDNA damage has also been found to enhance atherosclerosis independently of mitoROS, and preceded lesion formation in *ApoE*<sup>-/-</sup> mice (Yu et al. 2013). Therefore, oxidative stress-mediated damage to mtDNA can lead to mitochondrial dysfunction and hence promote pathogenesis. Given that the mitochondria are major ROS sources within the cell, and previous studies found (+)-catechin to attenuate intracellular ROS production in all investigated cell types, the effect of (+)-catechin on mitochondrial superoxide production in THP-1 macrophages, HASMCs and HUVECs was investigated using MitoSOX<sup>TM</sup> Red staining. MitoSOX<sup>TM</sup> Red permeates live cells and selectively targets the mitochondria, where it is rapidly oxidised by superoxide.

### 4.1.7 Mitochondrial membrane potential

The mitochondria use oxidisable substrates to create a membrane potential (in the form of a proton gradient) across the inner membrane. Oxidative phosphorylation is sustained via generation of a membrane potential gradient by the ETC to fuel ATP synthesis (Mitchell and Moyle 1965). Changes in the mitochondrial membrane potential can signify alterations in cellular homeostasis; for example, a reduction in the transmembrane potential occurs during apoptosis, which leads to condensing of the matrix (Gottlieb et al. 2003). Alterations in mitochondrial membrane potential at the onset of apoptosis govern matrix remodelling prior to cytochrome c release. The supply of oxidative substrates is governed by the abundance of external growth factors (O'Neill et al. 2016). In healthy cells, condensing of the matrix can be stimulated via

the removal of oxidisable substrates or glucose supply, or via exposure to protonophores which dissipate the transmembrane potential. Apoptosis is then triggered by mitochondrial cytochrome c release if the glucose or growth factor deficit continues (Huang et al. 2014; O'Neill et al. 2016). The release of cytochrome c stimulates assembly of the apoptosome, which is necessary for the activation of downstream caspases and subsequent cell death (Liu et al. 2016; Stienstra et al. 2017). Additionally, irrevocable mitochondrial damage causes the release of pro-apoptotic proteins into the cytoplasm, triggering the mitochondria-mediated death pathway. Therefore, the loss of mitochondrial membrane potential may be a consequence of the apoptotic signalling pathway (although cytochrome c release is not dependent on this loss). A decline in mitochondrial membrane potential and elevated ROS generation are hence associated with mitochondrial dysfunction or damage and apoptosis. Several studies have demonstrated that 50-100 µg/ml oxLDL stimulation induces a substantial reduction in the mitochondrial membrane potential of both macrophages and ECs (Asmis and Begley 2002; Hort et al. 2014; Zheng and Lu 2020). The effect of (+)-catechin on oxLDL-stimulated mitochondrial membrane depolarisation of HUVECs was hence measured using a JC-1 mitochondrial membrane potential assay kit.

## 4.2 Experimental strategy

Summaries of the experimental strategies are illustrated in Figures 4.5 and 4.6.

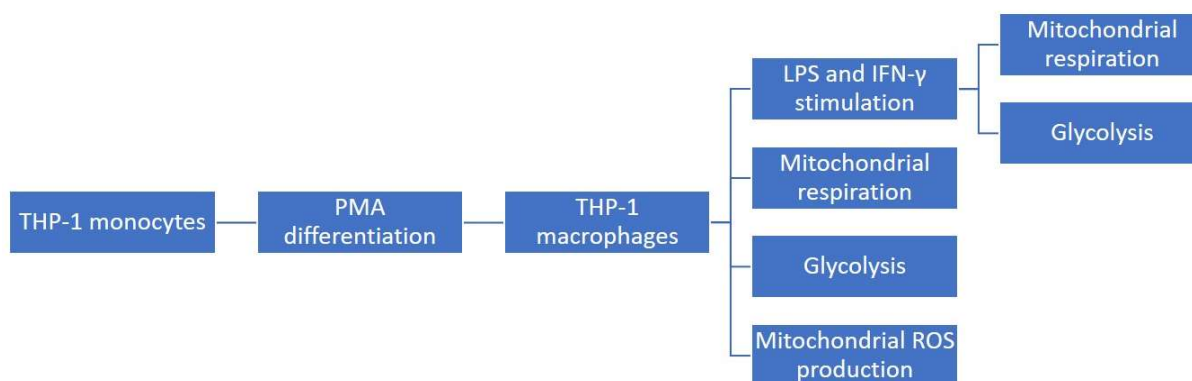


**Figure 4.5 Experiments using THP-1 macrophages.**

Abbreviations: PMA, phorbol 12-myristate 13-acetate; LPS, lipopolysaccharide; IFN, interferon; ROS, reactive oxygen species.

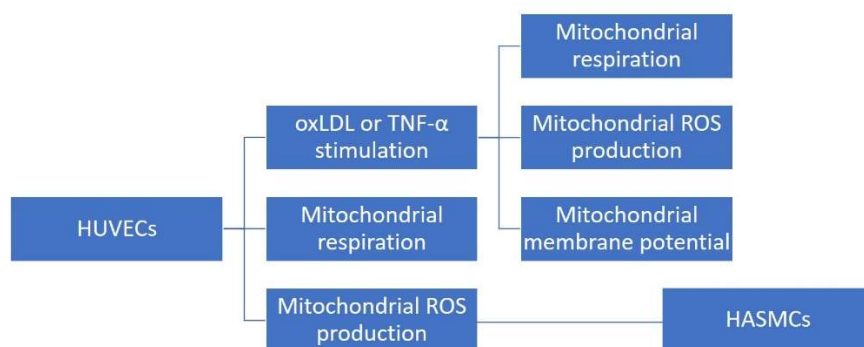


**Figure 4.6 Experiments using HUVECs and HASMCs.**

Abbreviations: HUVECs, human umbilical vein endothelial cells; HASMCs, human aortic smooth muscle cells; oxLDL, oxidised low-density lipoprotein; TNF, tumour necrosis factor; ROS, reactive oxygen species.

### 4.3 Results

#### 4.3.1 (+)-Catechin increases spare respiratory capacity and non-mitochondrial respiration in macrophages

Due to a lack of standardisation of all Seahorse data to protein concentration or cell number in error, only limited interpretation of these results is possible without conducting further repeats to ascertain that any detected changes were not attributed to disparities in cell density. Moreover, any parameters producing negative OCR values (caused by starting OCR values being too low) were omitted due to the possibility of further unreliable data interpretation.

In PMA-differentiated THP-1 macrophages, (+)-catechin significantly increased percentage spare respiratory capacity ( $p=0.032$ ; Figure 4.7F) and non-mitochondrial respiration ( $p=0.050$ ; Figure 4.7H) compared to the vehicle control. No significant changes in other parameters were observed.

## Chapter 4: Effects of (+)-catechin on bioenergetics and mitochondrial function

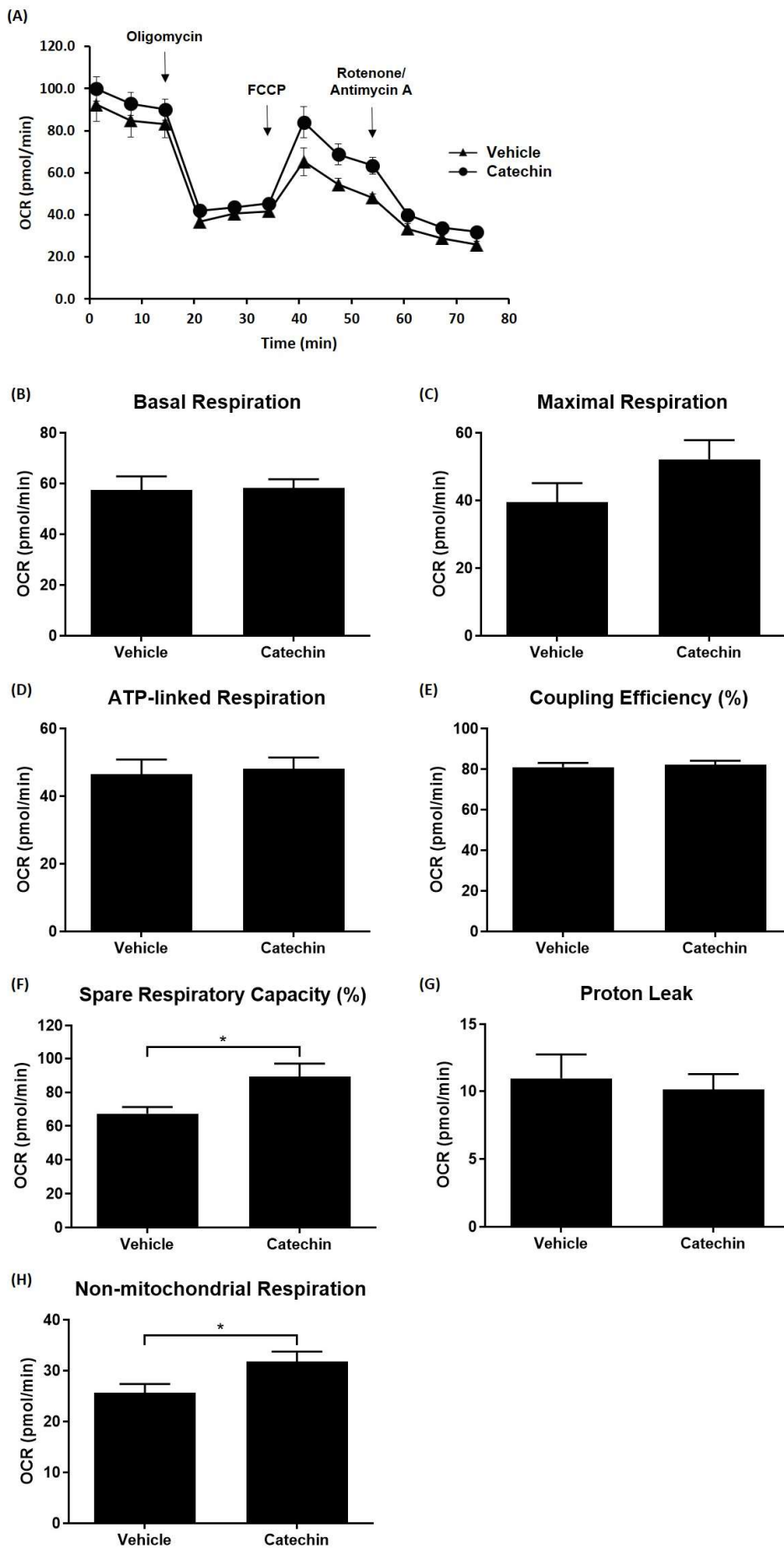


### **Figure 4.7 Effect of (+)-catechin on mitochondrial respiration in THP-1 macrophages.**

Data presented as mean  $\pm$  SEM from three independent experiments. Assessment of mitochondrial respiration was done using Agilent Seahorse Technologies (Mito Stress Test Assay) in PMA-differentiated THP-1 macrophages treated with vehicle or (+)-catechin for 24 hours. Parameters producing negative OCR values were omitted. Statistical analysis via unpaired t-test where \*,  $p \leq 0.05$ . Abbreviations: OCR, oxygen consumption rate; FCCP, carbonyl cyanide 4-(trifluoromethoxy)phenylhydrazone.

### 4.3.2 (+)-Catechin has no effect on glycolysis in macrophages

No significant changes in glycolytic function of PMA-differentiated THP-1 macrophages were produced by (+)-catechin treatment after 24 hours compared to the vehicle control (Figure 4.8).

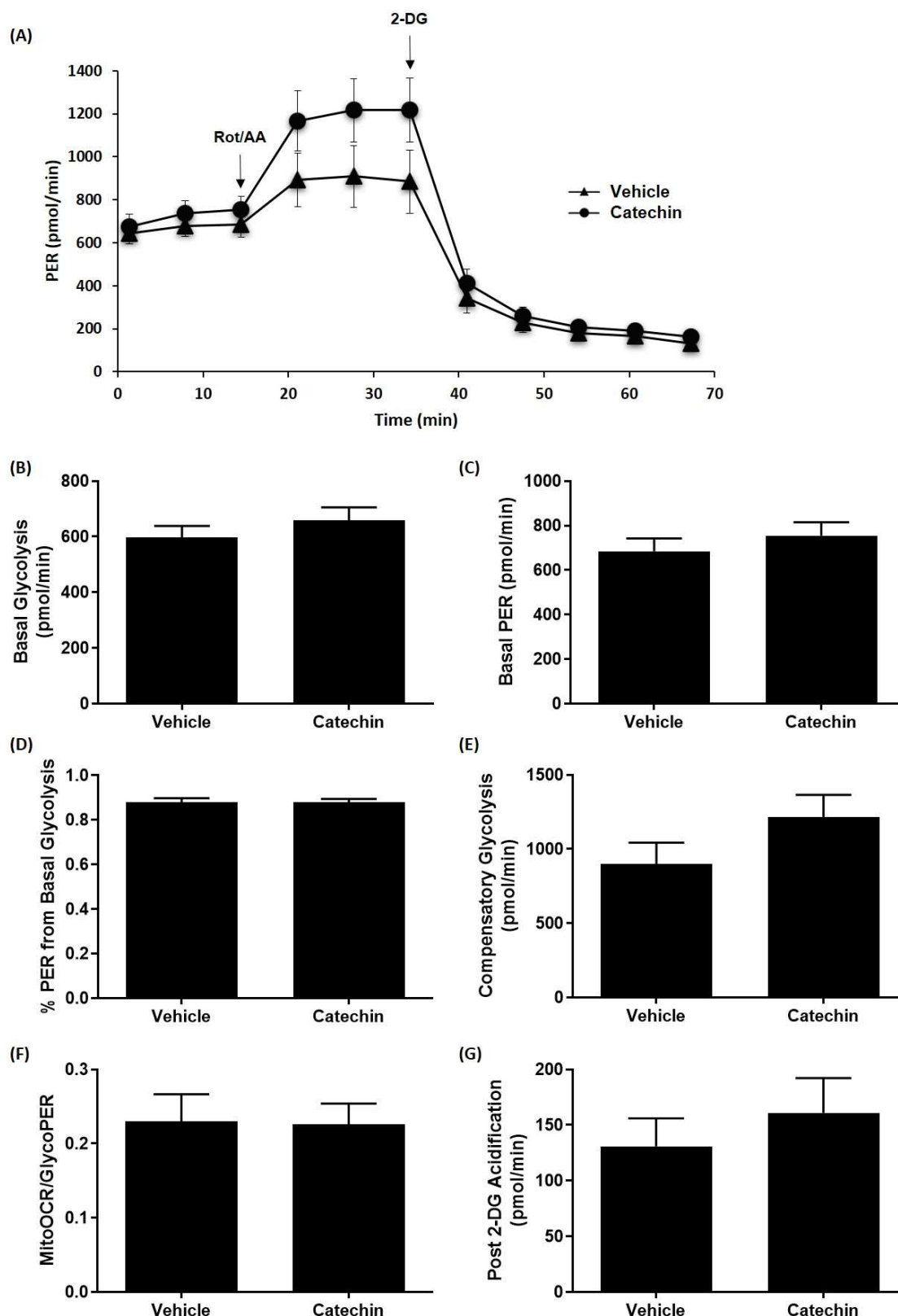


**Figure 4.8 Effect of (+)-catechin on glycolysis in THP-1 macrophages.**

Data presented as mean  $\pm$  SEM from three independent experiments. Assessment of mitochondrial respiration was done using Agilent Seahorse Technologies (Glycolytic Rate Assay) in PMA-differentiated THP-1 macrophages treated with vehicle or (+)-catechin for 24 hours. Statistical analysis via unpaired t-test. Abbreviations: PER, proton efflux rate; MitoOCR; mitochondrial oxygen consumption rate; GlycoPER; glycolytic proton efflux rate; Rot/AA, rotenone/antimycin A; 2-DG, 2-deoxyglucose.

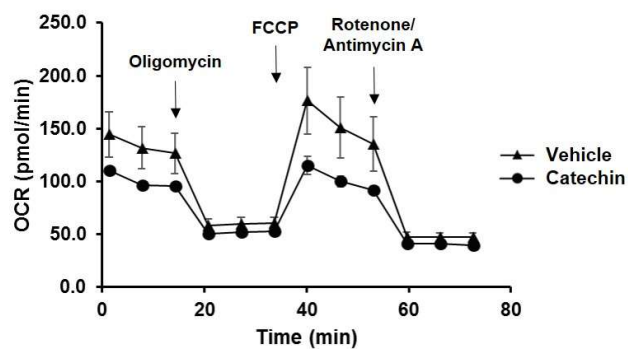
## Chapter 4: Effects of (+)-catechin on bioenergetics and mitochondrial function

### 4.3.3 (+)-Catechin reduces basal respiration, ATP-linked respiration and proton leak in M1 polarised macrophages

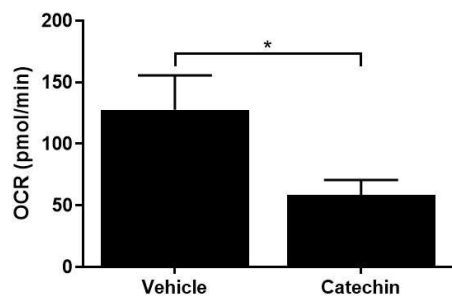
In PMA-differentiated THP-1 macrophages stimulated with 100 ng/ml LPS and 250 U/ml IFN- $\gamma$  for 24 hours to induce M1 polarisation, (+)-catechin significantly reduced basal respiration ( $p=0.044$ ) (Figure 4.9B), ATP-linked respiration ( $p=0.047$ ) (Figure 4.9D) and proton leak ( $p=0.029$ ) (Figure 4.9H) compared to the vehicle control. There was also a trend in reduction of coupling efficiency ( $p=0.056$ ) (Figure 4.9E). No significant changes in other parameters were observed.

# Chapter 4: Effects of (+)-catechin on bioenergetics and mitochondrial function

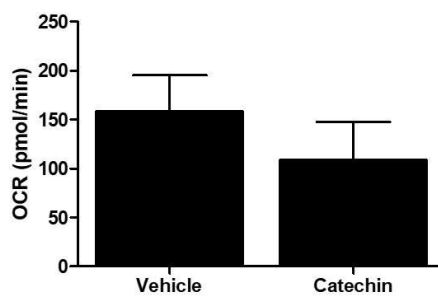
(A)



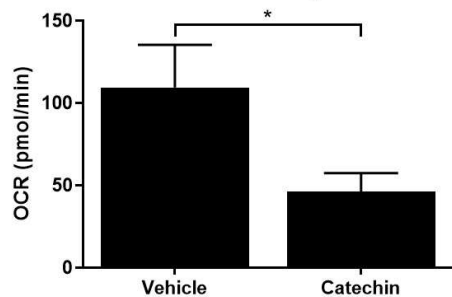
(B) Basal Respiration



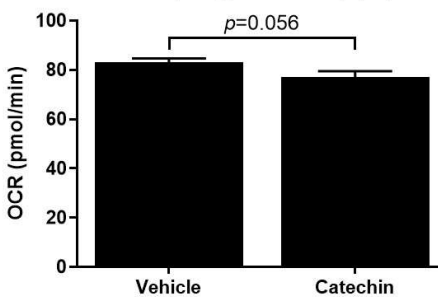
(C) Maximal Respiration



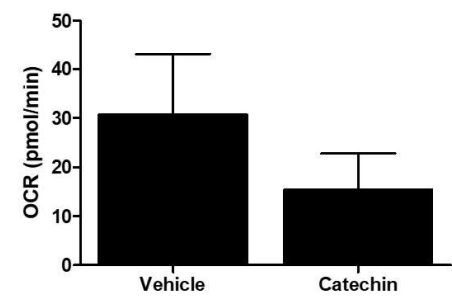
(D) ATP-linked Respiration



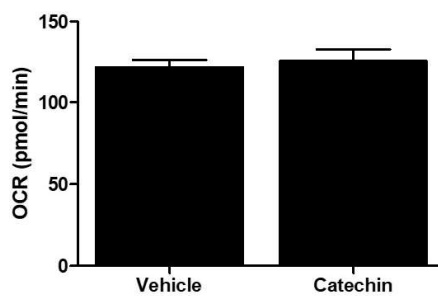
(E) Coupling Efficiency (%)



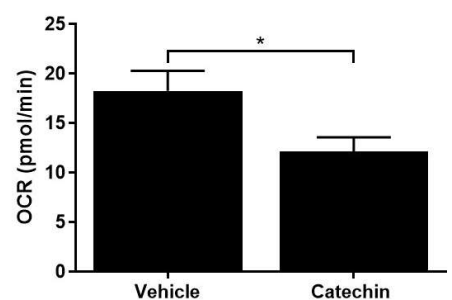
(F) Spare Respiratory Capacity



(G) Spare Respiratory Capacity (%)



(H) Proton Leak



(I) Non-mitochondrial Respiration

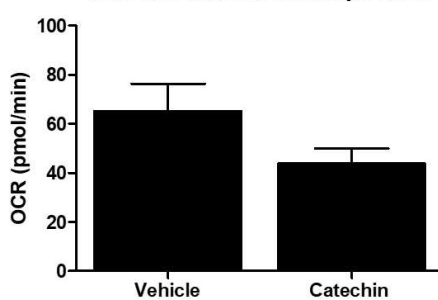


**Figure 4.9 Effect of (+)-catechin on mitochondrial respiration in stimulated THP-1 macrophages.** Data presented as mean  $\pm$  SEM from three independent experiments. Assessment of mitochondrial respiration was done using Agilent Seahorse Technologies (Mito Stress Test Assay) in PMA-differentiated THP-1 macrophages stimulated with LPS and IFN- $\gamma$  in the presence of vehicle or (+)-catechin for 24 hours. Statistical analysis via unpaired t-test where \*,  $p \leq 0.05$ . Abbreviations: OCR, oxygen consumption rate; FCCP, carbonyl cyanide 4-(trifluoromethoxy)phenylhydrazone.

### 4.3.4 (+)-Catechin has no effect on glycolysis in M1 macrophages

In M1 polarised THP-1 macrophages, (+)-catechin had no significant effects on glycolytic function compared to the vehicle control (Figure 4.10). Additionally, M1 polarised macrophages were less susceptible to rotenone/antimycin A-induced increase in PER compared to unstimulated macrophages (Figure 4.10A vs Figure 4.8A).

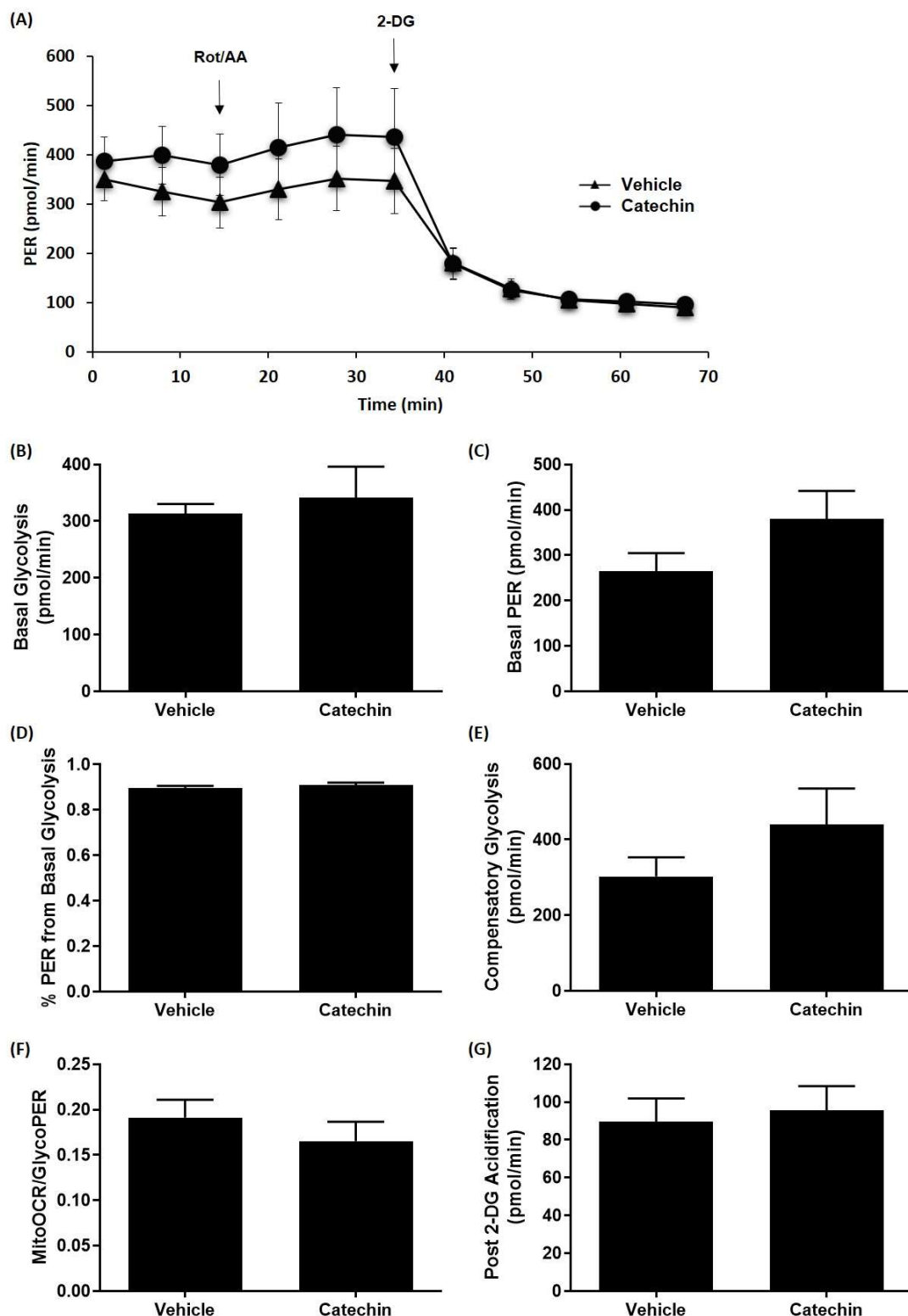


**Figure 4.10 Effect of (+)-catechin on glycolysis in stimulated THP-1 macrophages.**

Data presented as mean  $\pm$  SEM from three independent experiments. Assessment of mitochondrial glycolysis was done using Agilent Seahorse Technologies (Glycolytic Rate Assay) in THP-1 macrophages stimulated with 100 ng/ml LPS and 250 U/ml IFN- $\gamma$  for 24 hours (to induce M1 polarisation) in the presence of vehicle or (+)-catechin. Parameters producing negative OCR values were omitted. Statistical analysis via unpaired t-test where \*,  $p \leq 0.05$ . Abbreviations: PER, proton efflux rate; MitoOCR, mitochondrial oxygen consumption rate; GlycoPER, glycolytic proton efflux rate; Rot/AA, Rotenone/Antimycin A; 2-DG, 2-deoxyglucose.

## 4.3.5 (+)-Catechin reduces macrophage mitoROS production

(+)-Catechin significantly attenuated mitochondrial superoxide production by 12.70% in PMA-differentiated THP-1 macrophages after 24 hours treatment compared to the vehicle control ( $p < 0.001$ ), which was arbitrarily set as fold change 1 (Figure 4.11A). However, no changes were seen in HASMCs (Figure 4.11B) or HUVECs (Figure 4.11C). Furthermore, HUVECs stimulated with 50 ng/ml TNF- $\alpha$  for 24 hours (to induce their activation) did not show any changes in mitochondrial superoxide production compared to the vehicle control, and the presence of (+)-catechin also had no effect compared to the unstimulated or stimulated vehicle controls (Figure 4.11D).

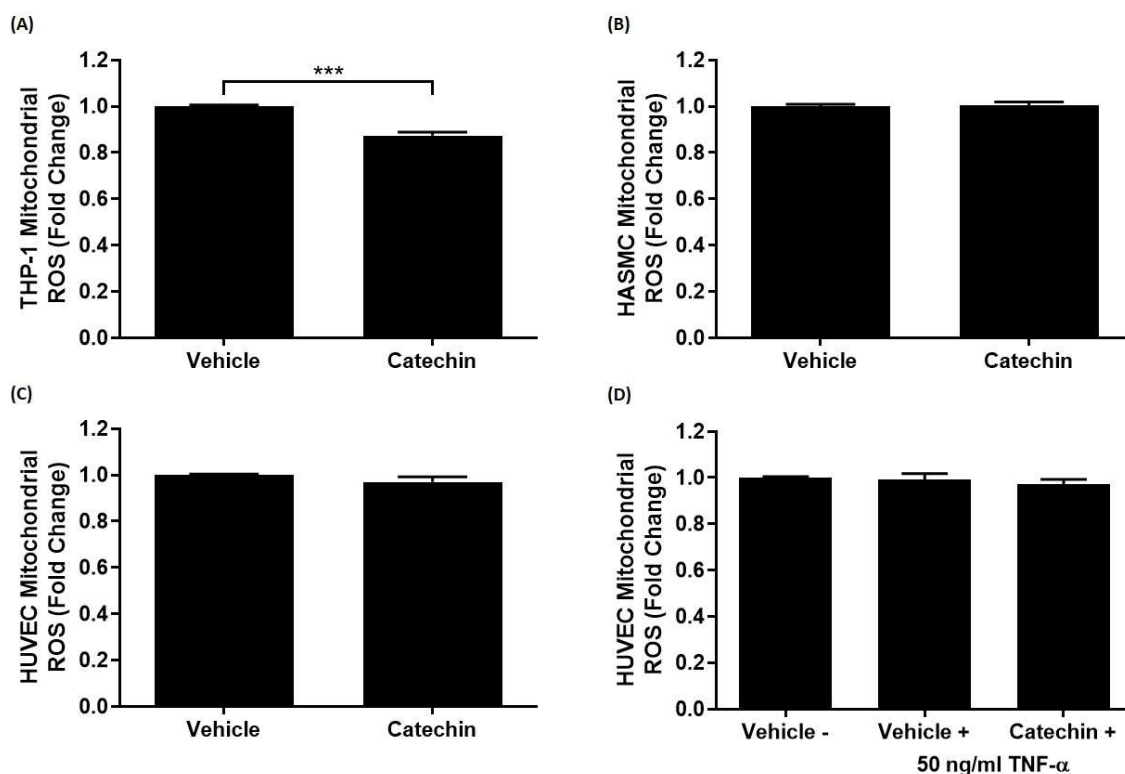


**Figure 4.11 Effect of (+)-catechin on mitoROS production.**

Data presented as mean  $\pm$  SEM from three (B) or four (A; C; D) independent experiments. Mitochondrial superoxide production was measured after 24 hours treatment using MitoSOX<sup>TM</sup> Red staining whereby the vehicle control was set arbitrarily as fold change 1. (+)-Catechin significantly reduces mitochondrial superoxide production in THP-1 macrophages but has no effect in human umbilical vein endothelial cells (HUVECs) or human aortic smooth muscle cells (HASMCs). Statistical analysis via unpaired t-test (A-C) or one-way ANOVA with Tukey's post-hoc test (D) where  $***$ ,  $p < 0.001$ .

#### 4.3.6 (+)-Catechin has restorative effects on oxLDL-induced mitochondrial membrane hyperpolarisation in ECs

In HUVECs, stimulation with 100  $\mu\text{g/ml}$  oxLDL induced a significant decrease in mitochondrial membrane potential (as shown by the reduction in JC-1 aggregate to monomer ratio) after both 4 and 24 hours compared to the vehicle control ( $p < 0.001$ ). This was similar to the reduction in mitochondrial membrane potential induced by the ionophore uncoupler of oxidative phosphorylation, FCCP (100  $\mu\text{M}$ ), at both time points. At both time points, (+)-catechin increased mitochondrial membrane potential compared to the oxLDL-stimulated vehicle control; however, this was only significant after 24 hours ( $p < 0.001$ ) (Figure 4.12).

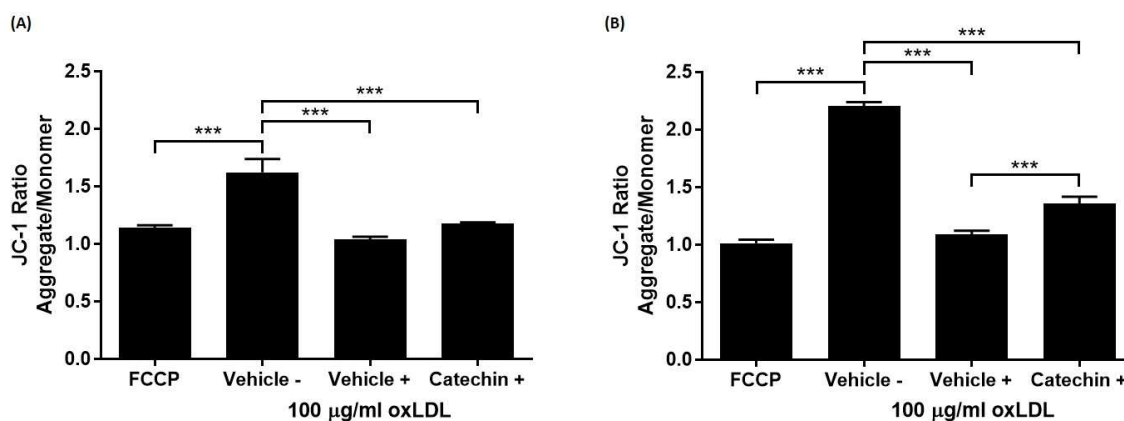


**Figure 4.12 Effect of (+)-catechin on EC mitochondrial membrane potential.**

Data presented as mean  $\pm$  SEM from three independent experiments. Mitochondrial membrane potential was measured using a tetraethylbenzimidazolylcarbocyanine iodide (JC-1)-based kit after 4 (A) and 24 (B) hours. Increasing JC-1 aggregate to monomer ratio corresponds to increasing mitochondrial membrane potential. Statistical analysis via one-way ANOVA with Tukey's post-hoc test using square-root transformed (A) or untransformed (B) data where \*\*\*,  $p < 0.001$ .

#### 4.3.7 (+)-Catechin increases spare respiratory capacity in ECs

HUVECs treated with (+)-catechin for 24 hours had significantly increased spare respiratory capacity compared to the vehicle control ( $p = 0.014$ ) (Figure 4.13F). There was also a trend of reduction in basal respiration ( $p = 0.084$ ) (Figure 4.13B). No other significant changes in other parameters were observed.

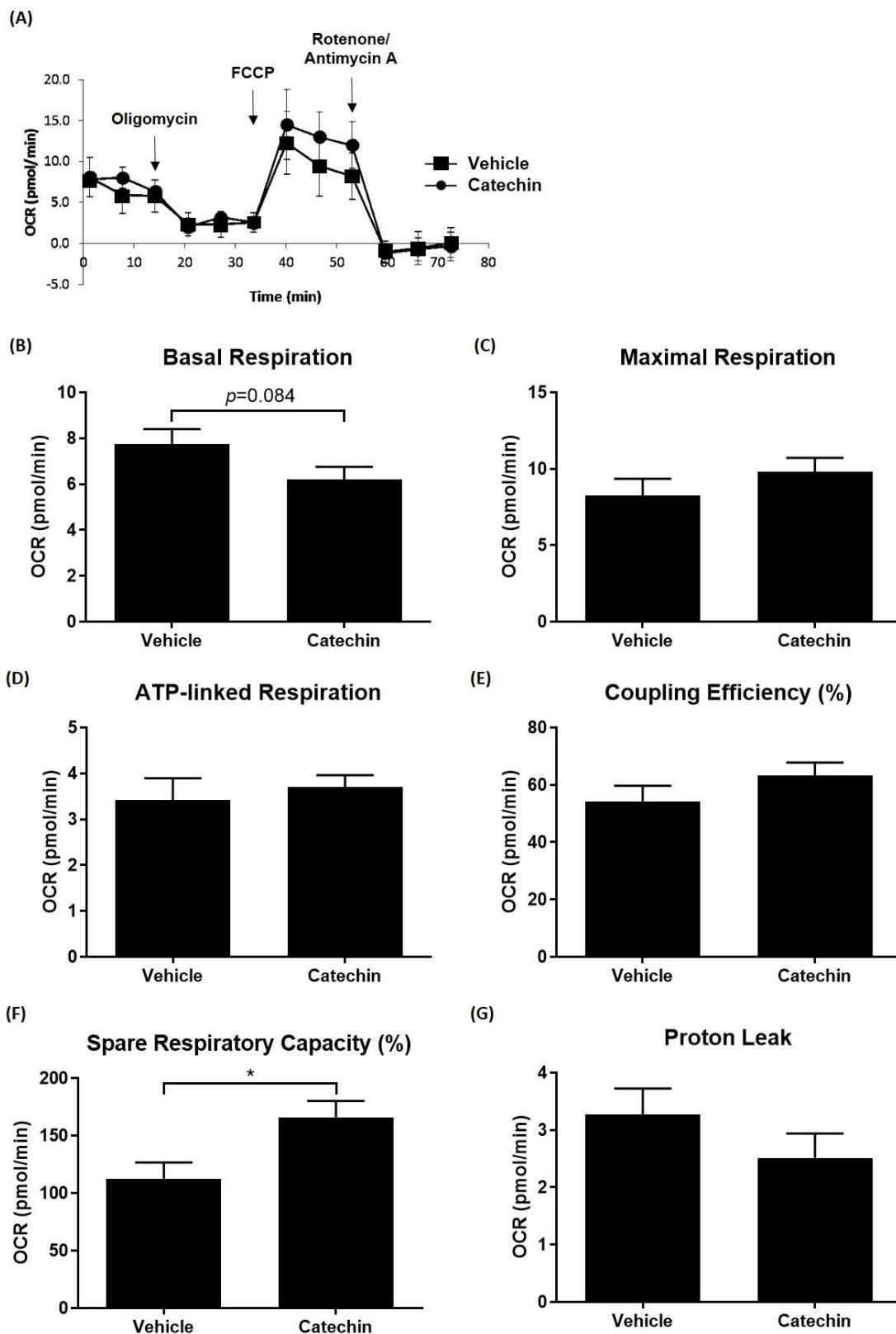


**Figure 4.13 Effect of (+)-catechin on mitochondrial respiration in ECs.**

Data presented as mean  $\pm$  SEM from three independent experiments. Assessment of human umbilical vein endothelial cells mitochondrial respiration was done using Agilent Seahorse Technologies (Mito Stress Test Assay) after 24 hours treatment with vehicle or (+)-catechin. Parameters producing negative OCR values were omitted. Statistical analysis via unpaired t-test where  $*$ ,  $p \leq 0.05$ . Abbreviations: OCR, oxygen consumption rate; FCCP, carbonyl cyanide 4-(trifluoromethoxy)phenylhydrazone.

4.3.8 (+)-Catechin raises non-mitochondrial respiration in stimulated ECs

Although results described in Chapter 3 demonstrated no significant effects on multiple parameters associated with endothelial dysfunction (e.g., ROS production and permeability), the effect of oxLDL on mitochondrial function was investigated since cell proliferation was reduced (Figure 3.7B), suggesting a possible change in cellular metabolism. In HUVECs stimulated with 100 µg/ml oxLDL in the presence of vehicle or (+)-catechin for 24 hours, (+)-catechin significantly increased non-mitochondrial respiration compared to the vehicle control ( $p=0.003$ ) (Figure 4.14F). No significant changes in other parameters were observed.

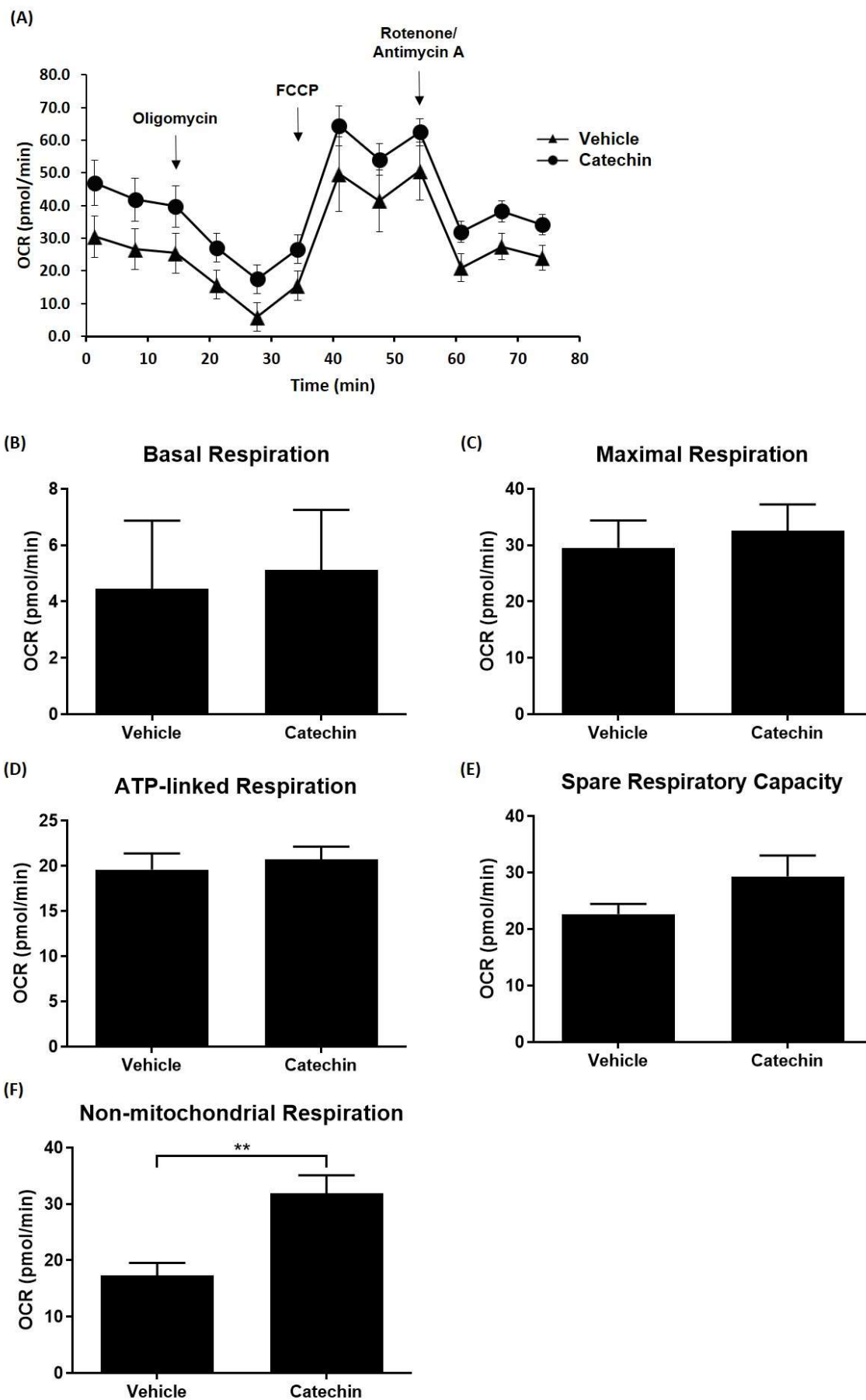


**Figure 4.14 Effect of (+)-catechin on mitochondrial respiration in stimulated ECs.**

Data presented as mean +/- SEM from three independent experiments. Assessment of mitochondrial respiration in human umbilical vein endothelial cells was done using Agilent Seahorse Technologies (Mito Stress Test assay) following 100 µg/ml oxLDL stimulation in the presence of vehicle or (+)-catechin for 24 hours. Parameters yielding negative OCR values were omitted. Statistical analysis via unpaired t-test where \*,  $p \leq 0.05$ . Abbreviations: OCR, oxygen consumption rate; FCCP, carbonyl cyanide 4-(trifluoromethoxy)phenylhydrazone.

A summary of the significant changes in mitochondrial respiration induced by (+)-catechin are outlined in Table 4.3.

**Table 4.3 Summary of changes in mitochondrial respiration induced by (+)-catechin.**

	THP-1 macrophages		HUVECs	
	Unstimulated	Stimulated	Unstimulated	Stimulated
Basal respiration	=	↓ (*)	↓? (trend)	=
ATP-linked respiration	=	↓ (*)	=	=
% Spare respiratory capacity	↑ (*)	=	↑ (*)	=
Proton leak	=	↓ (*)	=	=
Non-mitochondrial respiration	↑ (*)	=	=	↑ (**)

Summary of changes in mitochondrial respiration induced by (+)-catechin in THP-1 macrophages and human umbilical vein endothelial cells (HUVECs). Statistical analysis via unpaired t-test where \*,  $p < 0.05$ ; \*\*,  $p < 0.01$ .

**4.4 Discussion**

(+)-Catechin has demonstrated various anti-inflammatory, anti-oxidative and anti-atherogenic effects in macrophages and ECs. Mitochondrial dysfunction has been implicated in the progression of atherosclerosis and plaque rupture, especially due to its role in the regulation of apoptosis, as well as involvement in inflammation and oxidative stress. Apoptosis of ECs compromises the endothelial monolayer, facilitating the infiltration of lipoproteins and activated immune cells to the vascular wall. Apoptosis of macrophages contributes to the growth of the necrotic core and plaque progression, and apoptosis of VSMCs precedes thinning of the fibrous cap and subsequent plaque instability. Catechin has demonstrated protective effects on mitochondrial function in various cell types implicated in other pathologies; however, exploration of its effect on cellular metabolism and mitochondrial function in the context of atherosclerosis is still required. Therefore, the aim of studies in this chapter was to investigate the effect of (+)-catechin on cellular bioenergetics and mitochondrial

function with specific focus on macrophages and ECs. Whilst beneficial effects were seen in a small number of parameters, interpretation of the bioenergetics data is limited due to the lack of standardisation warranting the need to repeat these experiments. Therefore, a major limitation of this chapter is that the Seahorse data cannot be interpreted fully and provide limited insight.

### 4.4.1 Beneficial effects of (+)-catechin in macrophages

In unstimulated THP-1 macrophages, (+)-catechin significantly increased spare respiratory capacity and non-mitochondrial respiration, while mitochondrial superoxide generation was decreased (as shown by reduction in MitoSOX<sup>TM</sup> staining). However, no significant changes in other bioenergetics parameters were observed, including a lack of effect on glycolysis. Therefore, (+)-catechin appears to have mild effects on the cellular bioenergetics of PMA-differentiated THP-1 macrophages, but may improve cell fitness/flexibility and protect against oxidative stress-induced/associated mitochondrial dysfunction in these cells. Taken together, these data suggest that (+)-catechin might improve the ability of the cell to deal with acute increases in energy demand by enhancing spare respiratory capacity, whilst protecting against mitochondrial oxidative stress by reducing ROS production.

In M1-activated THP-1 macrophages, (+)-catechin significantly reduced ATP-linked respiration, and proton leak, with a trend towards reduction in coupling efficiency. However, there was also a significant reduction in basal respiration with no effect on glycolysis. Therefore, in proinflammatory macrophages, (+)-catechin appears to reduce mitochondrial function. However, glycolytic function may be more relevant and important in proinflammatory macrophages, as activated immune cells undergo a metabolic shift. Glycolysis is the major energy source for M1 macrophages while mitochondrial oxidative phosphorylation predominates in M2 macrophages (Vats et al. 2006). Mitochondrial function and oxygen consumption is inhibited by M1 activation, suggesting mitochondrial dysfunction in M1 macrophages. Interestingly, mitochondrial function is also necessary to induce and maintain the M2 phenotype (Van den Bossche et al. 2016). Therefore, it would be interesting to expand on this and compare the effect of (+)-catechin on the bioenergetics of M2-activated macrophages (which

could be achieved via stimulation with IL-4 and IL-13 (Van Dyken and Locksley 2013)), to determine any differential effects between pro- and anti-inflammatory macrophages.

### 4.4.2 Beneficial effects of (+)-catechin in ECs

In unstimulated ECs, (+)-catechin significantly enhanced spare respiratory capacity despite a trend towards reduction in basal respiration, suggesting an improvement in the ability of the cell to deal with acute rises in energy demand. In oxLDL-activated HUVECs, (+)-catechin significantly increased non-mitochondrial respiration and had restorative effects on mitochondrial membrane depolarisation. Indeed, stimulation of ECs or macrophages with oxLDL has been shown to decrease mitochondrial membrane potential (Asmis and Begley 2002; Yu et al. 2019; Zheng and Lu 2020), concurring with the JC-1 assay results of this study. Various other studies have also demonstrated the ability of catechin to increase mitochondrial membrane potential in other cell types induced by various membrane hyperpolarisation-inducing stimuli and hence improve mitochondrial function (Chen et al. 2003; Zhang et al. 2017b; Wongmekiat et al. 2018; Rafiei et al. 2019; Cong et al. 2020). In other studies, catechin also improved mitochondrial function by other means including, restoring complex I and ATP biosynthesis, along with the balance of pro- and anti-oxidant enzyme activities in the mitochondria (Tabassum et al. 2007; Santos et al. 2016). Taken together, (+)-catechin might protect against oxLDL-induced endothelial dysfunction by maintaining mitochondrial function and improving the metabolic fitness of the cells, while protecting against oxidative stress-induced cellular damage and inflammation. Indeed, preliminary results suggest (+)-catechin might possibly induce a reduction in oxLDL-stimulated apoptosis of ECs as described in Chapter 3 (Figure 3.11), although further optimisation of the assay is required before the effect of (+)-catechin can be reliably inferred. Therefore, (+)-catechin might improve oxLDL-induced cytotoxicity of ECs by protecting against oxLDL-induced mitochondrial dysfunction, although further repeats and experiments are required to verify this.

### 4.4.3 MitoROS production

Although (+)-catechin had no effect on basal mitoROS production in HUVECs or HASMCs, results of studies described in Chapter 3 found intracellular ROS production to be significantly attenuated by (+)-catechin in these cells. Whilst the mitochondria are responsible for the majority of ATP and ROS generation in living cells, these organelles are equipped with a mechanism that inhibits mitoROS production. Mild depolarisation of the inner membrane reduces the transmembrane potential to a level adequate to generate ATP, but inadequate to produce mitoROS (Vyssokikh et al. 2020). Fittingly, inactivation of this mechanism can be a consequence of aging, and leads to chronic mitoROS-derived oxidative stress (Vyssokikh et al. 2020). Therefore, unstimulated HUVECs and HASMCs may not produce significant or detectable levels of basal mitoROS, at least using this method. Investigation of mitoROS production in oxLDL-stimulated HUVECs and HASMCs should hence be carried out, since stimulation of HUVECs with TNF- $\alpha$  did not induce an increase in mitochondrial superoxide generation. This was surprising since TNF- $\alpha$  (at much lower concentrations than that used in this study) has been reported to induce mitoROS production in HUVECs (Corda et al. 2000). Moreover, TNF- $\alpha$  mediates its cytotoxic effects by altering mitochondrial function (Chen et al. 2010) (e.g., damaging complex III of the ETC and inducing radical production at the ubiquinone site) (Schulze-Osthoff et al. 1992). In this study, the lack of effect seen in HASMCs and HUVECs, in contrast to the significant reduction observed in THP-1 macrophages, after (+)-catechin treatment may be attributed to PMA. PMA differentiation may induce polarisation of the differentiated macrophages to an M1-like phenotype. Therefore, these cells may have increased mitoROS production arising from their switching to the glycolysis pathway for ATP production, and reduced efficiency of oxidative phosphorylation associated with pro-inflammatory activation. Confirmation of this theory would hence require MitoSOX<sup>TM</sup> staining of definitive M1-polarised macrophages (as induced by LPS and IFN- $\gamma$  stimulation) for comparison. The ability of (+)-catechin to attenuate mitoROS production in macrophages also requires confirmation using primary cultures (e.g., HMDMs).

### 4.4.4 Limitations

As all bioenergetic data obtained via Agilent Seahorse analysis have not been standardised to protein concentration or cell number in error, only limited, qualitative interpretation is possible, although the number of cells between all wells were equal at the start of each assay. This is to account for any changes in cell proliferation or death (that may have occurred during the assay) and hence is used to verify that any observed changes are not attributed to reduced cell numbers. Although preliminary data from one experiment suggested there were no considerable differences in protein concentration after the assay (data not shown), further repeats are required to verify this. The high cost of the Seahorse Agilent consumables was a limiting factor in this study, amplified by the need for empirical optimisation of cell seeding densities and inhibitor drug concentrations for each cell type prior to experimentation. Furthermore, additional independent experiments (to increase  $n$  numbers) are also required to verify these results, especially in the case of HUVECs, whereby a high level of variation within the data was present for certain parameters. Moreover, experiments could be repeated in HUVECs stimulated with TNF- $\alpha$ , which would also enable comparison with the effects induced by oxLDL stimulation. However, due to the high cost and much slower growth rate of HUVECs, it was not possible to carry out additional experiments. Although previous optimisation experiments were carried out in the host laboratory, further optimisations may be required as some starting OCR values in the Mito Stress Test assay were lower than the recommended range (Figures 4.13B and 4.14B), resulting in negative values for certain measured parameters (which were omitted). Furthermore, on occasions, certain inhibitor drugs did not appear to induce the expected changes in OCR/PER by a maximal extent (Figures 4.10A and 4.14A), suggesting suboptimal concentrations in select conditions. Therefore, results obtained from Agilent Seahorse analyses should be interpreted with caution and results obtained using cell lines should be confirmed in primary cells. Nonetheless, these data, although preliminary, provide insights to how (+)-catechin might affect cellular bioenergetics and metabolism, and support the beneficial role of this nutraceutical agent in both macrophages and ECs.

### 4.4.5 Future directions

To correlate the changes seen in respiration with the activities of specific mitochondrial ETC complexes, it would be interesting to investigate the effect of (+)-catechin on the expression of these complexes using Western blot for example, to gain an insight to how (+)-catechin mediates its protective effects on mitochondrial function. Indeed aortic VSMCs cultured from atherosclerotic plaques exhibit significantly reduced expression of complex I and complex II with impaired mitochondrial respiration and enhanced autophagy compared to normal aortic VSMCs (Yu et al. 2017). Additionally, the effect of (+)-catechin on the activities of mitochondrial antioxidant enzymes in THP-1 macrophages could be investigated to explore its anti-oxidative actions further, given that mitoROS production was significantly attenuated in these cells. Beyond this, investigation of the effect of (+)-catechin on cellular bioenergetics could also be carried out on oxLDL-stimulated HASMCs, given their critical involvement in fibrous cap maintenance and plaque stability. Agents able to maintain VSMC function and viability by protecting mitochondrial function and enhancing respiration may hence delay plaque rupture and the onset of clinical complications. Taken together, results obtained from studies conducted thus far suggest that (+)-catechin might attenuate atherogenesis via protection against oxLDL-mediated mitochondrial dysfunction, and delay disease progression by various athero-protective actions on macrophages through anti-inflammatory and anti-oxidative effects.

### 4.4.6 Conclusion

(+)-Catechin may exert multiple protective effects on parameters associated with mitochondrial function in macrophages and, to a lesser extent, in ECs. However, without repeated and further experiments, only limited interpretation of the bioenergetics data is possible. Nevertheless, the results obtained to date support the potential of (+)-catechin as a nutraceutical candidate used in strategies for the prevention and/or treatment of atherosclerosis, given its various anti-atherogenic activities in all key cell types involved. Therefore, investigation of the effect of (+)-catechin on atherosclerosis development and progression in the *Ldlr*<sup>-/-</sup> mouse model of atherosclerosis is described in the next chapter, to determine whether (+)-catechin can attenuate atherogenesis *in vivo* and to verify these *in vitro* observations.

## 5 Effect of (+)-catechin on atherosclerosis development and progression

### 5.1 Introduction

Results of this project so far support the potential of (+)-catechin as a preventative/therapeutic agent for atherosclerosis, given the various athero-protective actions observed *in vitro*. It is hence hypothesised that (+)-catechin can attenuate atherogenesis and disease progression *in vivo*. This is also supported by results of a previous pilot study conducted in the host laboratory, whereby daily gavage of (+)-catechin (in the form of (+)-catechin hydrate) modulated several atherosclerosis-associated risk factors in WT mice fed HFD for 3 weeks (Moss 2018). These included a significant reduction in TG, IL-1 $\beta$  and IL-2 levels in the plasma, suggesting attenuation of hypertriglyceridaemia and inflammation. Furthermore, in other studies, (+)-catechin supplementation has been found to attenuate atherosclerosis in male golden Syrian hamsters fed a hypercholesterolemic diet after 12 weeks (Xu et al. 1998), *Ldlr*<sup>-/-</sup>; *hApoB*<sup>+/+</sup> pre-atherosclerotic mice after 9 months (Gendron et al. 2010) and *ApoE*<sup>-/-</sup> mice after 6 weeks (Hayek et al. 1997; Auclair et al. 2009). However, other mouse studies that include analysis of the resulting atherosclerotic plaques have utilised (+)-catechin in combination with caffeic acid and resveratrol, or in the form of red wine (Norata et al. 2007; Chassot et al. 2018), and so it is difficult to associate the observations with the specific nutraceutical agent due to possible interactions and synergistic or antagonistic effects. Meanwhile, other studies have reported protection against atherosclerosis risk factors, including endothelial dysfunction and oxidative stress, dampened expression of pro-inflammatory cytokines, and regulation of insulin sensitivity/levels in rat models of diabetes or metabolic syndrome induced by ( $\pm$ )-catechin intake (Ihm et al. 2009; Abd El-Aziz et al. 2011; Bhardwaj et al. 2013; Prieto et al. 2015). Therefore, there have been no detailed studies on (+)-catechin conducted in the *Ldlr*<sup>-/-</sup> mouse model that include detailed assessment of the atherosclerotic plaque along with associated risk factors, despite demonstrating potential in various *in vivo* studies.

### 5.1.1 Experimental aims

The aims of studies presented in this chapter were to explore the effect of (+)-catechin supplemented HFD feeding on the development and progression of atherosclerosis in male *Ldlr*<sup>-/-</sup> mice, along with associated risk factors. Unlike *Apoe*<sup>-/-</sup> mice which spontaneously develop atherosclerotic lesions, *Ldlr*<sup>-/-</sup> mice require feeding with HFD to induce atherogenesis, and are hence more similar to the diet-induced atherosclerosis situation in humans. *Ldlr*<sup>-/-</sup> mice also mirror atherosclerosis development observed in humans with familial hypercholesterolemia (Ishibashi et al. 1993). Moreover, *Apoe*<sup>-/-</sup> mice develop more severe lesions in comparison to *Ldlr*<sup>-/-</sup> mice, and so this was the model of choice for all *in vivo* studies in this project. The form of (+)-catechin used was (+)-catechin hydrate, which has identical molecular structure to (+)-catechin but with a water molecule attached, rendering it soluble in PBS (to enable ease of mixing with the HFD) and avoiding the use of DMSO in animals. This also meant that the substantially high cost of (+)-catechin was mitigated, and previous studies conducted in the host laboratory verified that (+)-catechin and (+)-catechin hydrate exert similar effects *in vitro*. The feeding duration of 12 weeks had been previously optimised based on studies conducted in the host laboratory and was hence also applied in this study. Given that in a previous pilot study conducted in the host laboratory using male WT mice fed HFD for 3 weeks, daily gavage of 200 mg/kg (+)-catechin hydrate modulated various atherosclerosis-associated risk factors (Moss 2018), the same dose was used for all *in vivo* studies in this project.

### 5.1.2 Adiposity and weight gain

Adipose tissue is a heterogeneous type of tissue that includes ECs, immune cells (e.g., monocytes and macrophages) and adipocytes (Halberg et al. 2008). Obesity, the accumulation of excess adipose tissue, is a major risk factor for atherosclerotic CVDs (such as coronary heart disease), as well as hypertension, type 2 diabetes mellitus and certain types of cancer. A characteristic feature of metabolic syndrome (Bassuk and Ridker 2004), obesity, results from a positive energy balance derived from energy expenditure being lower than energy intake (Krzysztozek et al. 2015). This is as, stimulation of extra nutrients causes hyperplasia and/or hypertrophy of adipocytes as a response of the adipose tissue (Ellulu et al. 2017). Diets rich in fat can hence induce

obesity in humans and animals (Rothwell and Stock 1984; Warwick and Sciffman 1992; Buettner et al. 2007). For example, in rodents, a positive relationship between dietary fat consumption and body weight (or fat accumulation) exists (Bourgeois et al. 1983; Boozer et al. 1995; Takahashi et al. 1999; Ghibaudi et al. 2002). Other factors may also contribute to HFD-induced obesity, such as a failure of fat oxidation adjustment to the added fat consumption (Schrauwen and Westerterp 2000), and enhanced adipose tissue LPL activity (Preiss-Landl et al. 2002). Adipose tissue is classified as white or brown (Curat et al. 2004). Unlike white adipocytes, brown adipocytes are abundant with mitochondria, with high expression of uncoupling protein 1 (Zhang et al. 2019b). Brown adipose tissue is implicated in non-shivering thermogenesis, with roles in thermoregulation and glucose homeostasis (Frontini and Cinti 2010; Kajimura et al. 2015; Zhang et al. 2019b). Brown adipose tissue is considered beneficial fat due to its ability to protect against weight gain and metabolic disorders (Bostrom et al. 2012; Stanford et al. 2013). On the contrary, white adipose tissue is involved in the regulation of both physiological and pathological processes, including immunity and inflammation (Karastergiou and Mohamed-Ali 2010). This is mediated via their secretion of anti- and pro-inflammatory mediators (termed adipokines), such as leptin, MCP-1, TNF- $\alpha$  and IL-6. IL-6 stimulates the synthesis and secretion of CRP in the liver, and 33% of all circulating IL-6 is calculated to be derived from adipose tissue (Fontana et al. 2007). Increased adipose tissue mass coincides with increased secretion of adipokines; overproduction of these pro-inflammatory mediators hence links obesity with inflammation (Hotamisligil 2006). Therefore, in this study, the weights of the mice were monitored weekly, along with food consumption. At the end point, the white (subcutaneous, inguinal, gonadal and renal) and interscapular brown adipose tissue depots (along with the heart, liver, spleen and thymus) were harvested and weighed. To account for differences in the weights of the mice, all measurements were standardised to body weight of individual mice (organ weight (mg)/body weight (mg)). This enabled elucidation of the effect of (+)-catechin supplementation on HFD-induced weight gain and accumulation of adipose tissue.

### 5.1.3 Stem, progenitor and immune cell profiling

HSPCs are responsible for the production of all blood cells (i.e., erythrocytes, platelets and leukocytes), due to their multilineage differentiation capacity (Cheng et al. 2019). Within the HSPC population, HSCs generate MPPs which subsequently generate progenitor cells, lineage-specific precursors and finally, fully differentiated blood cells (Zhang et al. 2018). A simplified summary of the haematopoietic hierarchy is illustrated in Figure 5.1.

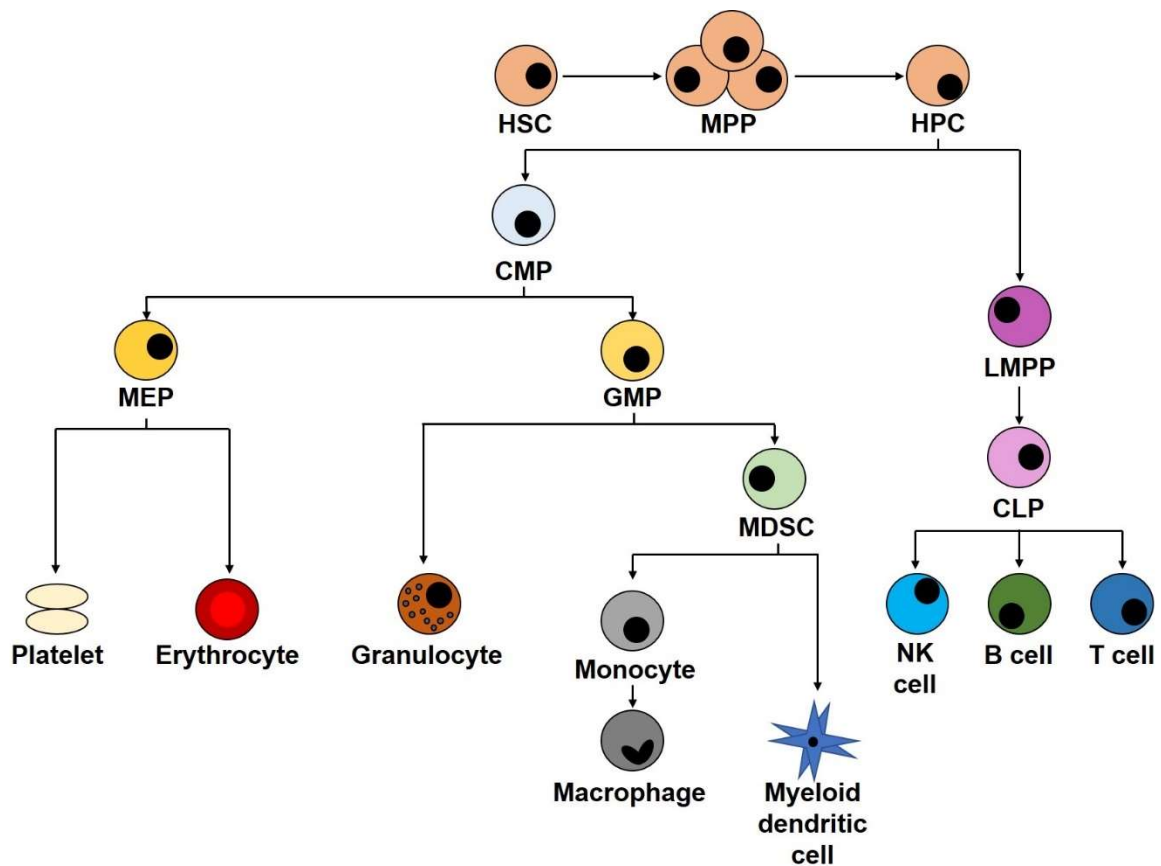


**Figure 5.1 Simplified summary of haematopoiesis.**

Abbreviations: HSC, haematopoietic stem cell; MPP, multipotent progenitor; HPC, haematopoietic progenitor cell; CMP, common myeloid progenitor; MEP, megakaryocyte-erythroid progenitor; GMP, granulocyte-macrophage progenitor; MDSC, myeloid derived suppressor cell; LMPP, lymphoid-primed multipotent progenitor; CLP, common lymphoid progenitor; NK, natural killer.

Changes in bone marrow cell populations is associated with hypercholesterolaemia and atherosclerosis progression, and HFD is well known to affect bone marrow cell populations. Diet-induced obesity alters haematopoiesis, resulting in skewing of the mature cell production towards the myeloid lineage (Vanhie et al. 2020). Consumption

of HFD enhances the proliferation of HSPCs, which is promoted by hypercholesterolaemia (Vanhie et al. 2020). Large meta-analyses have identified the presence of clonal haematopoiesis in individuals with increased risk of atherosclerotic morbidity (Jaiswal et al. 2014; Jaiswal et al. 2017; Bick et al. 2020). In atherosclerosis, persistent activation of the haematopoietic system is present in mouse models of atherosclerosis (*Ldlr<sup>-/-</sup>* and *Apoe<sup>-/-</sup>*) (Swirski et al. 2007; Tacke et al. 2007; Murphy et al. 2011), and in humans (Tacke et al. 2007; van der Valk et al. 2017), as shown by increased proportion of HSPCs or haematopoietic activity in the bone marrow respectively. Progressive monocytosis or leukocytosis is also observed in atherosclerotic animals (Feldman et al. 1991; Murphy et al. 2011) and humans (Madjid et al. 2004). HDL-C has been suggested to inhibit HSPC proliferation and differentiation whereas impaired cholesterol efflux and LDL may increase this (Feng et al. 2012). Therefore, chronic inflammation and impaired immune function associated with obesity could be attributed to changes in haematopoiesis (in part at least) (Vanhie et al. 2020).

A variety of leukocytes contribute to plaque formation and progression via their production of pro-inflammatory cytokines and other mechanisms. Monocytes, in particular Ly6C<sup>high</sup> monocytes, amass at sites of inflammation and differentiate into macrophages and dendritic cells (Geissmann et al. 2003). These monocytes preferentially adhere to activated ECs and infiltrate to the arterial intima, becoming atherosclerotic lesional macrophages. Atherosclerosis severity is hence correlated to an increasing number of circulating Ly6C<sup>high</sup> monocytes (Swirski et al. 2006; Tacke et al. 2007). On the other hand, Ly6C<sup>low</sup> monocytes are early responders to infection and monitor the integrity of the endothelium (Auffray et al. 2007; Carlin et al. 2013). Arising from circulating Ly6C<sup>high</sup> cells (Sunderkötter et al. 2004; Yona et al. 2013), Ly6C<sup>low</sup> monocytes do not directly contribute to the macrophage pool within atherosclerotic lesions (Hamers et al. 2012; Hanna et al. 2012; Hilgendorf et al. 2014), despite their ability to endocytose oxidised lipoproteins (Wu et al. 2010). Beyond monocytes and macrophages, atherosclerotic plaques also contain neutrophils, NK cells, T cells and B cells which can all contribute to the inflammatory phenotype. Neutrophils such as granulocytes can exacerbate tissue injury and inflammation in atherosclerosis (Sanda et al. 2017), for example by inducing SMC death, hence promoting plaque destabilisation (Fernandez-Ruiz 2019). Helper T cells (e.g., T<sub>H1</sub>) are deemed pro-

inflammatory due to their association with M1 macrophages and secretion of IFN- $\gamma$  (Mallat et al. 2009). In human atherosclerotic plaques, T<sub>h1</sub> cells are the predominant type of T cells, with various studies supporting a pro-atherogenic role of this T cell subset (Chistiakov et al. 2016). Moreover, cytotoxic T cells govern monopoiesis and macrophage accumulation in early atherosclerosis, being implicated in macrophage death and necrotic core development (Schafer and Zerneck 2020). NK cells are involved in the defence against infectious agents, and influence the acquired immune response via its cytotoxic activity and the secretion of various cytokines, particularly IFN- $\gamma$ , and those associated with T<sub>h2</sub> cells, such as IL-5 and IL-10 (Lodoen and Lanier 2006; Grant et al. 2008). In contrast to IFN- $\gamma$ , IL-5 and IL-10 are considered anti-atherogenic cytokines, and so the role of NK cells in atherosclerosis remains ambiguous, especially since neither NK cell deficiency or hyperactivation has been shown to affect atherosclerosis (Winkels and Ley 2018). Similarly, B cells have also been assigned both pro- and anti-atherogenic properties, and this is dependent on their subsets and functional targeting (Sage et al. 2019). Therefore, the pool of immune cells circulating in the blood provides valuable insights to inflammatory status and disease severity, since these can be recruited and infiltrate atherosclerotic plaques. Analysis of bone marrow stem, progenitor and lineage+ cell populations, along with lymphoid and myeloid cell populations in the peripheral blood was hence conducted to study how (+)-catechin supplementation affects haematopoietic activity and the presence of circulating leukocytes.

### 5.1.4 Plasma parameters

#### 5.1.4.1 Lipid profiling

Elevated circulating plasma LDL-C levels is a major risk factor of atherosclerosis, due to their susceptibility to accumulate within the arterial wall and instigate an inflammatory response. The accumulated LDL is internalised by macrophages and VSMCs, which form lipid-loaded foam cells and release various pro-inflammatory mediators. HDL mediates cholesterol clearance via RCT and has anti-oxidative properties; one of its major functions is to inhibit vascular cell activation, thereby prohibiting inflammatory cell infiltration and atherosclerosis progression (Gordon et al. 1989; Yvan-Charvet et al. 2010a; Khera et al. 2011). HDL also has a suppressive role

on HSC proliferation via ABCA1 (Yvan-Charvet et al. 2010b). In contrast, hypercholesterolaemia has been shown to promote bone marrow cell mobilisation in both humans and mice (Gomes et al. 2010; Crysandt et al. 2011). Therefore, LDL has been considered as the bad, pro-atherogenic cholesterol that promotes atherogenesis and inflammation, whereas HDL has been labelled the opposite. A 1 mmol/l reduction in LDL-C is associated with a 19% reduction in coronary heart disease mortality (Baigent et al. 2005), and an increase of HDL-C by 1 mg/dl decreases the incidence of coronary heart disease by ~3% (Gordon et al. 1989). Statins hence remain the major cornerstone therapy for CVD and are targeted for attenuating hyperlipidaemia by reducing endogenous cholesterol synthesis and promoting hepatocyte LDL uptake, while also exerting other anti-inflammatory and pleiotropic activities (Haslinger-Löffler 2008; Antonopoulos et al. 2012; Bergheanu et al. 2017). However, there is substantial residual cardiovascular risk post-successful hyperlipidaemia treatment with statins (Campbell et al. 2007; Libby et al. 2011; Sampson et al. 2012). This has emphasised the presence and influence of inflammation that persists post-statin therapy, driving atherosclerotic clinical complications in normolipidemic patients, as shown by their elevated plasma IL-1 $\beta$ , -6 and CRP levels (Ridker 2017). Other strategies targeted to lowering LDL-C (such as inhibition of PCSK9-mediated hepatic LDLR degradation (Ray et al. 2020); intestinal cholesterol absorption (Jia et al. 2011); and endogenous cholesterol synthesis upstream of HMG CoA reductase (Ballantyne et al. 2020)) also exist and are in various stages of clinical trials. This is as hyperlipidaemia (hypercholesterolaemia and hypertriglyceridaemia) is also capable of promoting other pathologies, including type 2 diabetes mellitus and NAFLD. However, strategies boosting HDL-C levels have not yielded the cardiovascular protection as previously hoped and expected (Hafiane and Genest 2013), suggesting that their anti-atherogenic actions are more important than their concentration. Therefore, as well as quantification of the levels of key plasma lipids, their ratios were also measured in this study to gain a more comprehensive view of lipid profile.

#### 5.1.4.2 Oxidative stress markers

Oxidative stress is implicated in atherosclerosis (and other chronic pathologies) and occurs when the balance of ROS/RNS (i.e., pro-oxidants) exceed that of antioxidants

(Lushchak 2014). Chronic oxidative stress can promote cellular damage and inflammation to encourage pathogenesis. Superoxide anion, hydroxyl and H<sub>2</sub>O<sub>2</sub> are key types of ROS, whereas peroxynitrite and nitrogen dioxide are major types of RNS (Meo et al. 2016). High levels of these reactive species promote oxidative modification of LDL, and it is the unregulated and excessive endocytosis of modified LDL by macrophages and VSMCs that leads to foam cell formation and death via apoptosis, necrosis and other mechanisms (Ruan et al. 2019). Lipid peroxidation (i.e., the reaction of oxygen with unsaturated lipids) generates a range of oxidation products with MDA seemingly being the most mutagenic and 4-hydroxynonenal being the most toxic (Esterbauer et al. 1990). The hydroxyl radical is the most reactive type of ROS and initiates lipid peroxidation by attacking unsaturated lipids, such as PUFA, hence measurement of lipid peroxidation markers is a useful tool for the assessment of oxidative stress (Le 2014). The aldehyde, MDA, is therefore a commonly used indicator of lipid peroxidation and oxidative stress (Meo et al. 2016), being the end product that results from enzymatic and free radical peroxidation of various PUFAs (Ito et al. 2019). PUFAs, cholesterol and other lipids are all well-known targets of peroxidative modification and damage by ROS/RNS, although lipids may also be oxidised by enzymes such as lipoxygenases and cyclooxygenases (Ayala et al. 2014). Therefore, to assess the degree of oxidative stress and lipid peroxidation, plasma ROS/RNS and MDA levels were quantified using DCFH- and TBA-based assays respectively.

#### 5.1.4.3 Quantification of key cytokines

Atherosclerosis is a chronic inflammatory disorder, driven by the imbalance of anti- and pro-inflammatory cytokines in favour of the latter, resulting in persistent and non-resolving inflammation. Various cytokines are implicated in all stages of the disease and contribute to plaque development, progression, stability, and rupture via multiple mechanisms. IL-1 $\beta$  is a particularly potent pro-inflammatory cytokine that mediates various pro-atherogenic processes, including the induction of M1 macrophage polarisation (Wolfs et al. 2011; Leitinger and Schulman 2013; Chinetti-Gbaguidi et al. 2015), and autocrine production of PDGF, a key stimulator of VSMC migration and proliferation (Libby et al. 1988; De Donatis et al. 2008). Importantly, IL-1 $\beta$  augments

its own expression and stimulates the production of IL-6 by various cells, which stimulates hepatic production of acute phase proteins namely, CRP (Schmidt-Arras and Rose-John 2016). As such, various clinical trials have explored the potential of IL-1 $\beta$  attenuation to improve cardiovascular outcomes (Abbate et al. 2010; Abbate et al. 2015; Morton et al. 2015; Ridker et al. 2017; Abbate et al. 2020). Therefore, TNF- $\alpha$  and IL-1 signalling promote atherogenesis by augmenting the expression of other cytokines and adhesion molecules, as well as the migration and mitogenesis of VSMCs and ECs (Tousoulis et al. 2016). All key atherosclerotic lesional cell types (macrophages, lymphocytes, NK cells and VSMCs) are capable of secreting various pro-inflammatory cytokines, including TNF- $\alpha$ , IL-1 and IL-6 (Tedgui and Mallat 2006). TNF- $\alpha$  and IL-1 signalling is predominantly mediated by the p38 mitogen-activated protein kinase (MAPK)/NF- $\kappa$ B pathway (Chan et al. 2000), which affects most cells implicated in atherogenesis via enhancing expression of cytokines, adhesion molecules, along with the migration and mitogenesis of VSMCs and ECs (Tedgui and Mallat 2006). Other MAPKs, such as extracellular signal-related kinase (ERK) and c-Jun N-terminal kinase (JNK), are also involved (Moens et al. 2013). T<sub>h1</sub>-driven responses produce IFN- $\gamma$ , which can also activate M1 macrophage polarisation (along with LPS) (Khallou-Laschet et al. 2010; Moss and Ramji 2016a) and promote endothelial permeability (along with TNF- $\alpha$ ) (Pober and Sessa 2007). T<sub>regs</sub> secrete anti-inflammatory cytokines such as TGF- $\beta$  and IL-10 (Ait-Oufella et al. 2011), and down regulate TNF- $\alpha$  production (Rajasingh et al. 2006) and endothelial ICAM-1 expression (Lisinski and Furie 2002). The lysophosphatidic acid component of LDL has been shown to induce endothelial CXCL1 (C-X-C motif chemokine ligand 1) release (Zhou et al. 2011); this cytokine is implicated in facilitating the mobilisation of monocytes and neutrophils to the inflammation site via its receptor, CXCR2 (Drechsler et al. 2010; Zhou et al. 2011; Soehnlein et al. 2013). Therefore, unsaturated lysophosphatidic acid encourages CXCL1-dependent monocyte-endothelial adhesion and atherogenesis (Zhou et al. 2011). IL-2 is generated by activated T<sub>h1</sub> cells, which in turn furthers activation of other T cells to potentially exacerbate atherosclerosis. Indeed, injection of this cytokine in *ApoE*<sup>-/-</sup> mice has been found to increase atherosclerosis (Upadhyaya et al. 2004). In contrast, IL-5 has demonstrated atheroprotective properties; for example, its overexpression has been found to attenuate atherosclerosis in *Ldlr*<sup>-/-</sup> mice (Zhao et al. 2015). Therefore, assessment of circulating immune cell populations combined with levels of key anti- and pro-inflammatory

cytokines in the plasma enables a more comprehensive assessment of inflammatory status.

### 5.1.5 Detailed plaque morphometric analyses

#### 5.1.5.1 Burden and lipid content

Plaque content within the vessel, plaque occlusion and plaque size are key indicators of atherosclerosis severity and progression; growth of the atherosclerotic plaque leads to progressive encroachment of the arterial lumen, reducing the volume available for blood flow. Increasing presence of lipid within the arterial wall is indicative of increasing abundance of lipid-rich foam cells; hence, greater lipid burden coincides with greater plaque burden. Plaques rich in lipid and pro-inflammatory activated macrophages with a highly inflamed and thinned fibrous cap are especially susceptible to rupture (Bergheanu et al. 2017), although plaque rupture does not occur in the most commonly-used mouse models of atherosclerosis (Emini Veseli et al. 2017). Therefore, analysis of atherosclerotic plaque burden, inflammation and stability can only be assessed. Sections of the aortic root at the three valve cusps (used as a reference point for consistency) were taken at 8  $\mu\text{m}$  intervals and stained with ORO, enabling analysis of lipid content, overall plaque size and occlusion. ORO is a red diazo dye readily solubilised in hydrophobic and natural fat (Andres-Manzano et al. 2015). Further stains were also employed to analyse plaque inflammation and stability for detailed assessment of plaque composition and cellularity.

#### 5.1.5.2 Immune cell infiltration

The infiltration of circulating immune cells, such as monocytes and T cells, into the lesion is driven by various pro-inflammatory cytokines and chemokines expressed by vascular cells in particular, activated ECs (McLaren et al. 2011). The monocytes are stimulated to differentiate into macrophages and depending on the local environmental cues, can be triggered to polarise into different subsets that go beyond the M1 (classically activated, pro-inflammatory) and M2 (alternatively activated, anti-inflammatory) classes (Shirai et al. 2015). Macrophages engulf native and modified

LDL via LDLR and SRs respectively; the latter process stimulates the release of various pro-inflammatory cytokines, such as IL-1 $\beta$  and TNF- $\alpha$  (Stewart et al. 2010). Although the phagocytic capacity of macrophages is beneficial and vital for clearing the accumulated cholesterol initially in the early lesion, their accumulation and death (triggered by intracellular cholesterol overloading and ER stress) within the vascular wall drives plaque inflammation and oxidative stress. In the lesion, macrophages are a potent source of pro-inflammatory cytokines as well as ROS. For example, activation of the NLRP3 inflammasome (e.g., triggered by aggregated/crystalline cholesterol within the cell) involves phagolysosomal rupture, ROS generation and the production of IL-1 $\beta$  and IL-18 (Grebe et al. 2018). M1 macrophages also produce other pro-atherogenic cytokines, such as IL-6, IL-12 and TNF- $\alpha$ , which stimulates ROS production, promoting oxidative stress and atherosclerosis progression (Zhang et al. 2009; Ramji and Davies 2015). Whilst T cells do not transform into foam cells, they have key roles in mediating various pro-inflammatory processes (as mentioned previously). Therefore, the abundance of macrophages and T cells contribute to the inflammatory phenotype of the atherosclerotic plaque and, along with the presence of a large lipid-rich necrotic core with a thin and inflamed fibrous cap, are characteristics of vulnerable plaques (Bergheanu et al. 2017). Therefore, sections were stained using immunofluorescence cell surface marker antibodies that target MOMA-2, iNOS and CD3 to detect the presence of macrophages, M1 macrophages and general T cells respectively.

#### 5.1.5.3 Necrosis and stability parameters

Like macrophages, VSMCs also have a high level of heterogeneity and plasticity but unlike macrophages, their role in atherogenesis is less clear-cut. Along with macrophages, VSMCs also contribute to foam cell formation via the internalisation of lipids; however, they are also vital for the formation of the plaque stabilising fibrous cap. PDGF stimulates local VSMCs to migrate from the tunica media, through the basement membrane and into the intima, where they proliferate and also internalise lipids, forming additional foam cells (De Donatis et al. 2008). Continued death of the foam cells add to plaque burden and the increasingly necrotic phenotype, which is also furthered by continued inflammation. VSMCs also contribute to plaque

development in the early stages of disease via the production of pro-inflammatory mediators (Schwartz et al. 1995; Visse and Nagase 2003). The accumulation of dead cells, cellular debris and cholesterol within the vascular wall aggravates inflammation and facilitates progression to fibroatheromas (necrotic core covered by a fibrous cap) (Clarke et al. 2010; Ait-Oufella et al. 2011). VSMCs also contribute to plaque stability by secreting ECM proteins (e.g., collagen and elastin) generating the fibrous cap that surrounds the plaque. In the early stages, this cap is rich in VSMC-derived  $\alpha$ SMA<sup>+</sup> cells (Bentzon et al. 2006; Yu et al. 2011a; Jacobsen et al. 2017) with increased type I and III collagens. VSMCs may therefore have both positive and negative effects on plaque progression and remodelling, facilitated by their recently recognised phenotypic plasticity (Basatemur et al. 2019). Therefore, plaque stability parameters were analysed by staining of the sections for VSMC (using an immunofluorescence cell surface marker antibody for  $\alpha$ SMA) and collagen content, enabling analysis of plaque stability (calculated as, (sum of plaque VSMC and collagen content) / (sum of plaque macrophage and lipid content)). Plaque necrosis was also analysed via quantification of the acellular regions of the stained sections for a more comprehensive view of atherosclerosis progression and disease severity since the size of the necrotic core increases with cell death, promoting plaque growth and progression.

#### 5.1.6 Hepatic cellularity and steatosis

Hepatic steatosis is an early indicator of NAFLD, the most common chronic liver disease associated with metabolic syndrome phenotype (Wojcik-Cichy et al. 2018). The spectrum of NAFLD ranges from steatosis to non-alcoholic steatohepatitis (NASH) with the presence of fibrosis, which can progress to liver cirrhosis (Hyogo et al. 2014). Due to the classical risk factors of atherosclerosis overlapping with that of NAFLD, such as obesity, dyslipidaemia, hypertension and oxidative stress, the two conditions are closely associated and tend to co-occur (Wojcik-Cichy et al. 2018). Therefore, sections of the liver were taken at 10  $\mu$ m intervals and stained with haematoxylin and eosin and ORO for analysis of hepatic morphology and steatosis respectively. Together, these analyses enable a comprehensive view of atherosclerosis severity in the mice, along with associated risk factors, including

## Chapter 5: Effect of (+)-catechin on atherosclerosis development and progression

inflammatory profile, lipid profile, oxidative stress, and signs of co-morbidities, such as fatty liver disease and cardiac hypertrophy.

5.1.7 Experimental strategy

The experimental strategy is illustrated in Figure 5.2.

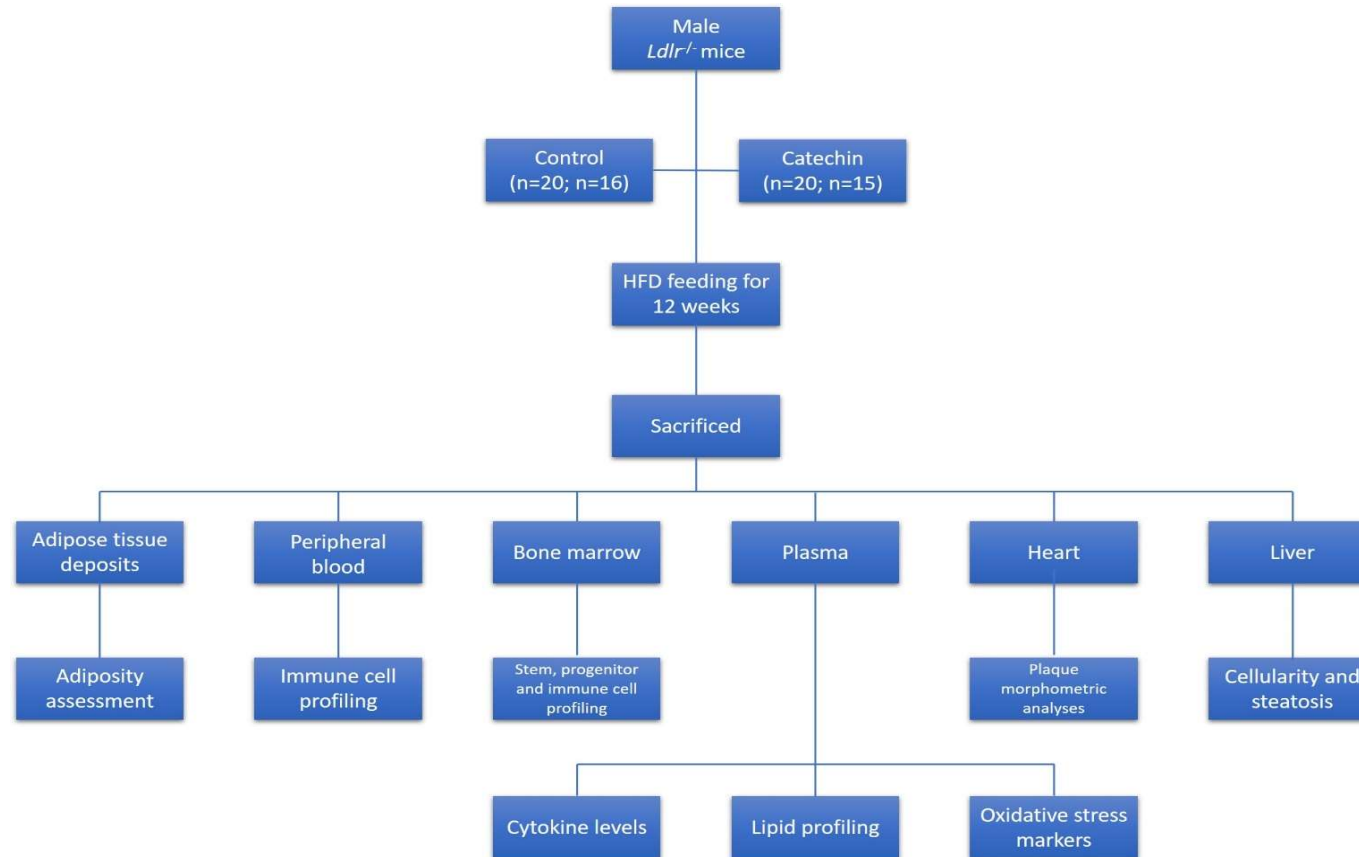


**Figure 5.2 Experimental strategy for the progression study.**

Experimental series consisted of the progression study (n=20 per group) and the subsequent regression study (n=15-16 per group). Hence the data presented in this chapter are the combined data obtained from the two studies (where available), as results were similar in both studies.

## 5.2 Results

### 5.2.1 Adiposity and key organs

During the feeding procedure, mouse weight and HFD consumption was monitored twice weekly until the end point to determine weight gain and food intake (and ensure that there were no issues relating to the palatability of the HFD). There were no significant changes in total weight gain between the control and catechin groups after the 12-week feeding period, with the mean  $\pm$  SEM being  $7.45 \pm 0.34$  g for the control group and  $7.49 \pm 0.37$  g for the catechin group (Figure 5.3A). There was also no significant difference in the weight change over time between the two groups (i.e., rate of weight gain) (Figure 5.3B). Additionally, there was no difference in estimated total HFD consumption between the two groups (data not shown).

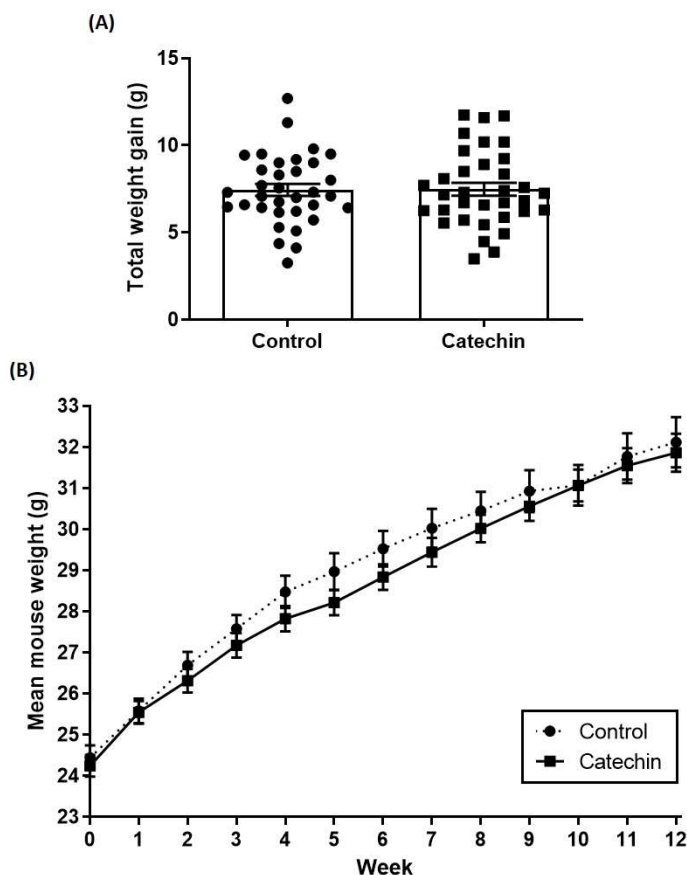


**Figure 5.3 Changes in mouse weights over time.** Male *Ldlr*<sup>-/-</sup> mice (8 weeks old) were fed high-fat diet supplemented with vehicle ('control') or (+)-catechin hydrate ('catechin') for 12 weeks. Total weight gain is shown in (A) with  $n=34$  per group. The mean mouse weight per week for both groups is shown in (B) ( $n=36$  for control;  $n=35$  for catechin). Data from two separate experiments have been combined. Statistical analysis via unpaired t-test for (A) and linear regression for (B).

To analyse adiposity, samples of the white adipose tissue deposits were harvested at the end point and weighed. All weight measurements of adipose tissue depots and organs were subsequently standardised to body weight. There were no significant differences in the individual white adipose tissue deposits (subcutaneous, inguinal, gonadal and renal) between the two groups (Figure 5.4). However, the subcutaneous and renal adipose tissue deposits were found to be reduced by 8.05% (1.59 mg) and 19.85% (1.50 mg) respectively, compared to the control group.

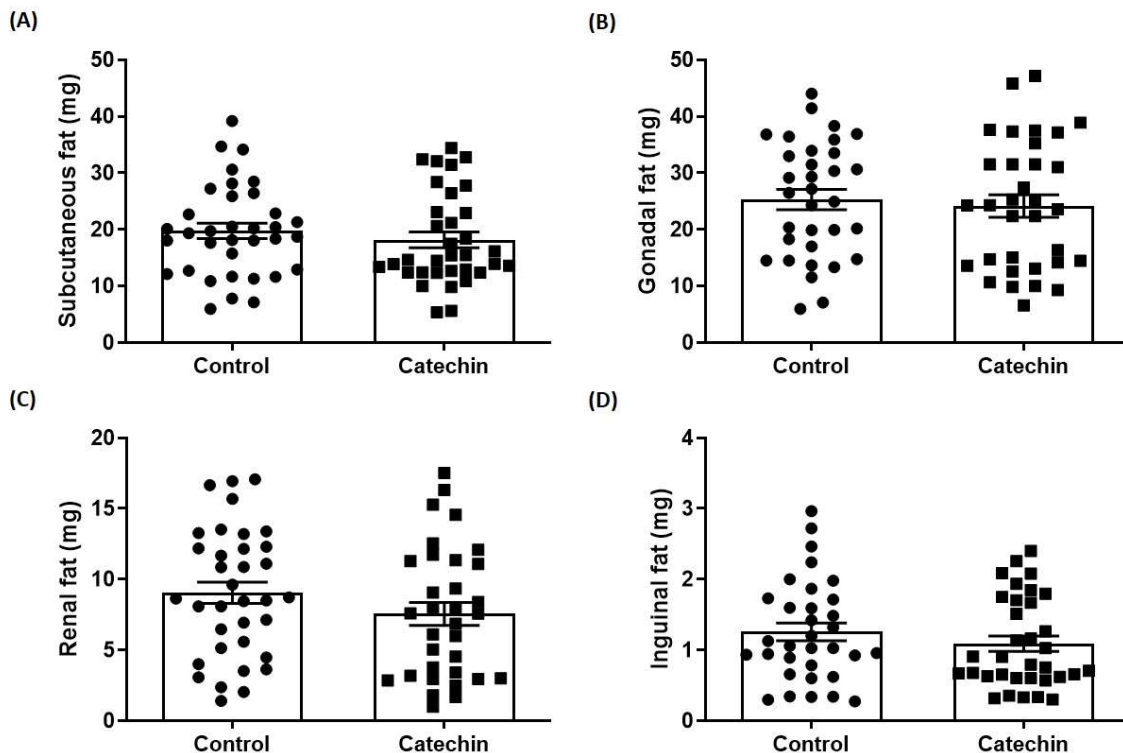


**Figure 5.4 White adipose tissue deposits.**

Male *Ldlr*<sup>-/-</sup> mice (8 weeks old) were fed high-fat diet supplemented with vehicle ('control') or (+)-catechin hydrate ('catechin') for 12 weeks. Mice were then sacrificed and samples of the subcutaneous (A), gonadal (B), renal (C) and inguinal (D) adipose tissue deposits were extracted, weighed, and standardised to body weight. Data from two separate experiments have been combined to give n=33 (B and D) or 35 (A and C) for control, and n=33 (B and D) or 34 (A and C) for catechin. Statistical analysis via unpaired t-test.

The interscapular brown adipose tissue deposit was also taken and weighed, for analysis of brown and white adipose tissue accumulation. The catechin group had significantly increased ratio of brown to white adipose tissue deposits by 25.78% (ratio of 0.02) compared to the control ( $p=0.035$ ) (Figure 5.5C). However, there were no

significant differences in total, total white or brown adipose tissue deposits between the two groups, although total white adipose tissue was reduced by 10.04% (5.65 mg).

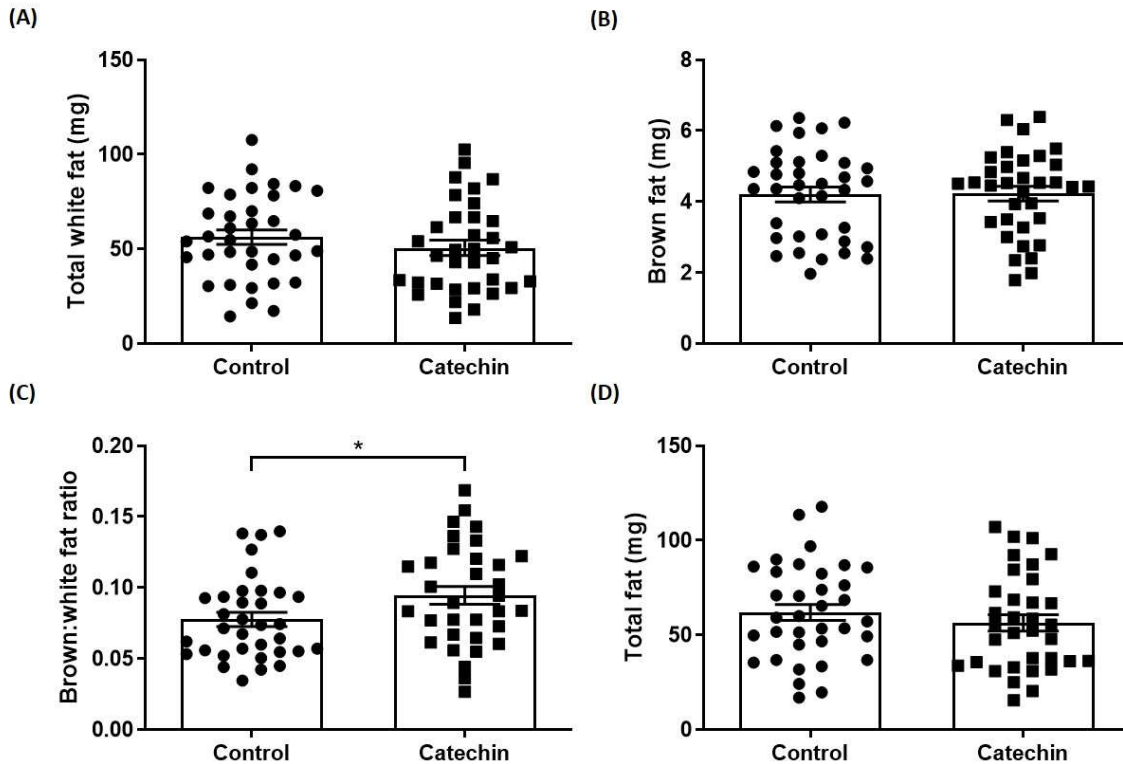


**Figure 5.5 White and brown adipose tissue analysis.**

Male *Ldlr*<sup>-/-</sup> mice (8 weeks old) were fed high-fat diet supplemented with vehicle ('control') or (+)-catechin hydrate ('catechin') for 12 weeks. The adipose tissue deposits were harvested at the end point and weighed; all measurements have been standardised to body weight. Total white fat was calculated as sum of subcutaneous, inguinal, renal and gonadal adipose tissue deposits (A). Total fat was calculated a sum of all white and brown adipose tissue deposits (D). Data from two separate experiments have been combined to give n=34 (C), 35 (A; D) or 36 (B) for control, and n=33 (C) or 34 (A; B; D) for catechin. Statistical analysis via unpaired t-test where \*,  $p \leq 0.05$ .

The weights of the key organs were also measured at the end point to check for any abnormalities, such as splenomegaly and cardiac hypertrophy, or signs of other pathologies, such as NAFLD. No significant changes were seen in the weights of the spleen, liver, heart or thymus between the two groups (standardised to body weight) (Figure 5.6).

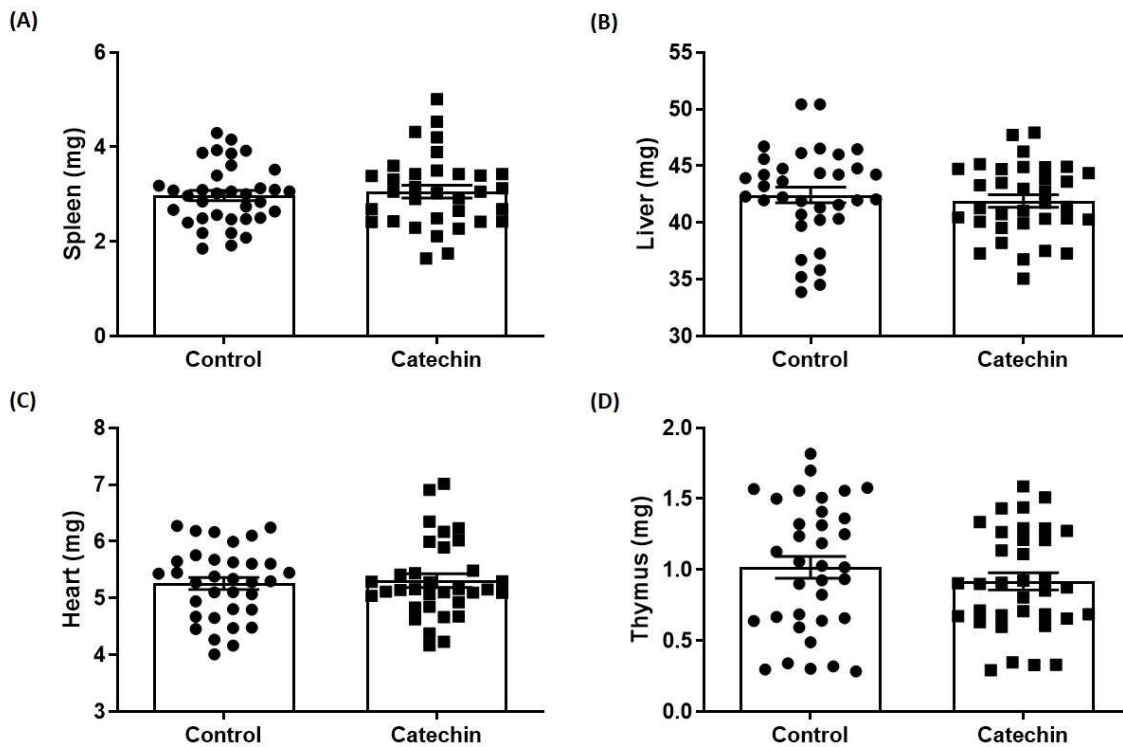


**Figure 5.6 Organ weights.**

Male *Ldlr*<sup>-/-</sup> mice (8 weeks old) were fed high-fat diet supplemented with vehicle ('control') or (+)-catechin hydrate ('catechin') for 12 weeks. The organs were harvested at the end point and weighed; all measurements have been standardised to body weight. Data from two separate experiments have been combined to give n=34 (C) or 35 (A; B; D) for control, and n=33 (A; C), 34 (B) or 35 (D) for catechin. Statistical analysis via unpaired t-test.

Cardiac hypertrophy index was also determined using the heart weight and tibia length (measured at the time of bone marrow cell extraction). There was no difference in cardiac hypertrophy index between the two groups, calculated as the ratio of heart weight to tibia length (Figure 5.7).

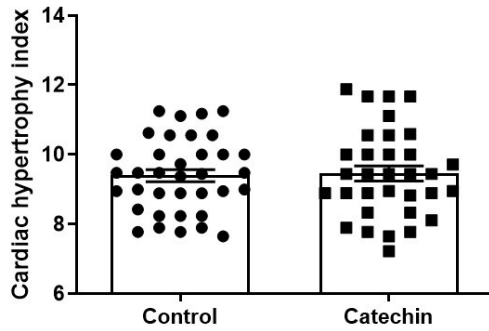


**Figure 5.7 Cardiac hypertrophy index.**

Male *Ldlr*<sup>-/-</sup> mice (8 weeks old) were fed high-fat diet supplemented with vehicle ('control') or (+)-catechin hydrate ('catechin') for 12 weeks. Cardiac hypertrophy index calculated as heart weight (mg) divided by tibia length (mm). Data from two separate experiments have been combined to give n=36 for control and n=33 for catechin. Statistical analysis via unpaired t-test.

### 5.2.2 Bone marrow stem, progenitor and immune cell population analysis

Bone marrow cells were extracted on following day of the end point for immunophenotyping of the stem, progenitor, and immune cell populations. There were no significant changes in the total number of cells extracted from the bone marrow counted immediately following extraction (Figure 5.8B), or in the total number of white blood cells (WBCs) between the two groups as determined by flow cytometry analysis (Figure 5.8C).

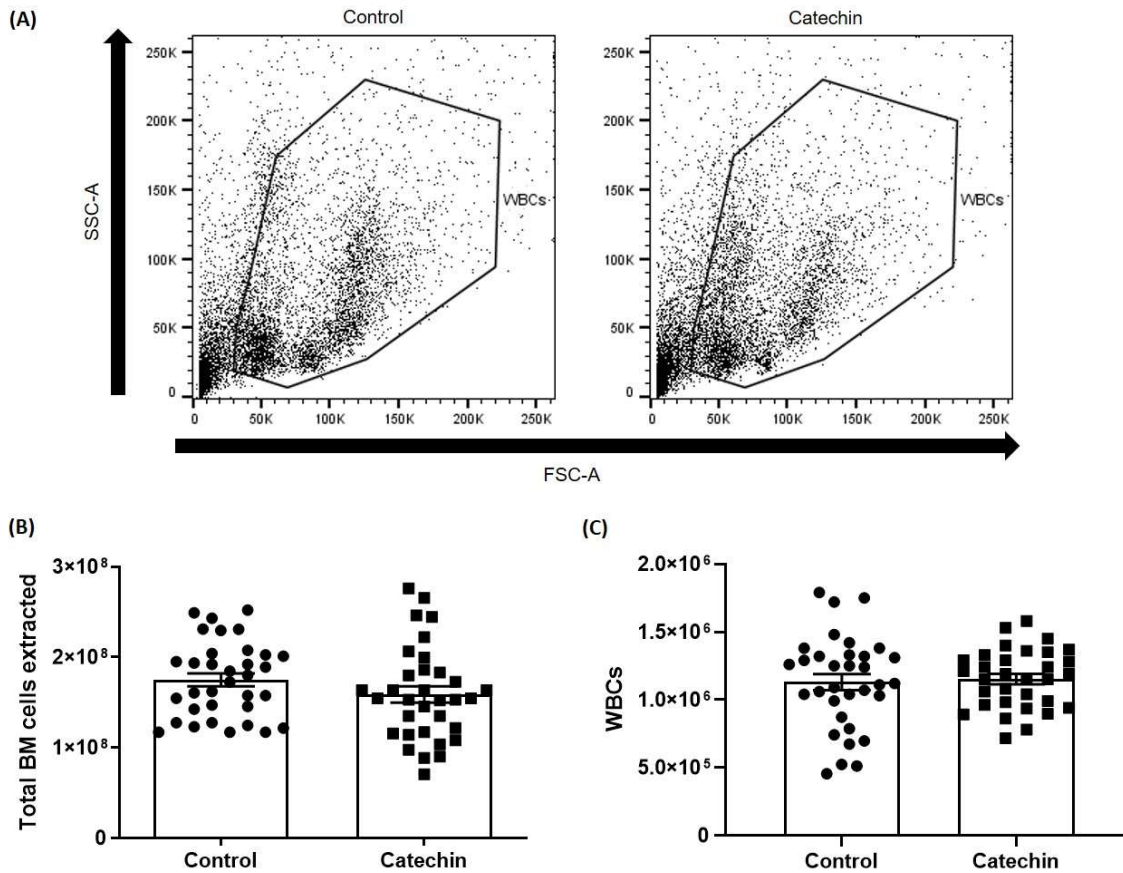


**Figure 5.8 Total cell count and number of white blood cells in the bone marrow.**

Male *Ldlr*<sup>-/-</sup> mice (8 weeks old) were fed high-fat diet supplemented with vehicle ('control') or 200 mg/kg (+)-catechin hydrate ('catechin') for 12 weeks before being sacrificed. The tibia and fibula were then taken, and BM cells were extracted for immunophenotyping using flow cytometry. Data from two separate experiments have been combined. The total number of BM cells extracted prior to analysis was manually counted using a haemocytometer under a microscope (B; n=34 for control and n=33 for catechin). The total number of WBCs was then obtained using flow cytometry (C; n=33 for control and n=32 for catechin), with representative dot plots and gating shown in (A). Statistical analysis via unpaired t-test.

### 5.2.2.1 (+)-Catechin reduces the proportion of HPC II cells

As there was no significant difference in the number of total WBCs in the bone marrow between the two groups, all subsequent data are presented as percentage of total WBCs. In the SLAM class of cells, the catechin group reduced proportion of HSCs by 10.94% ( $p=0.081$ ; trend) (Figure 5.9E) and HPC II by 6.96% ( $p=0.047$ ) (Figure 5.9C) in the bone marrow compared to the control group.

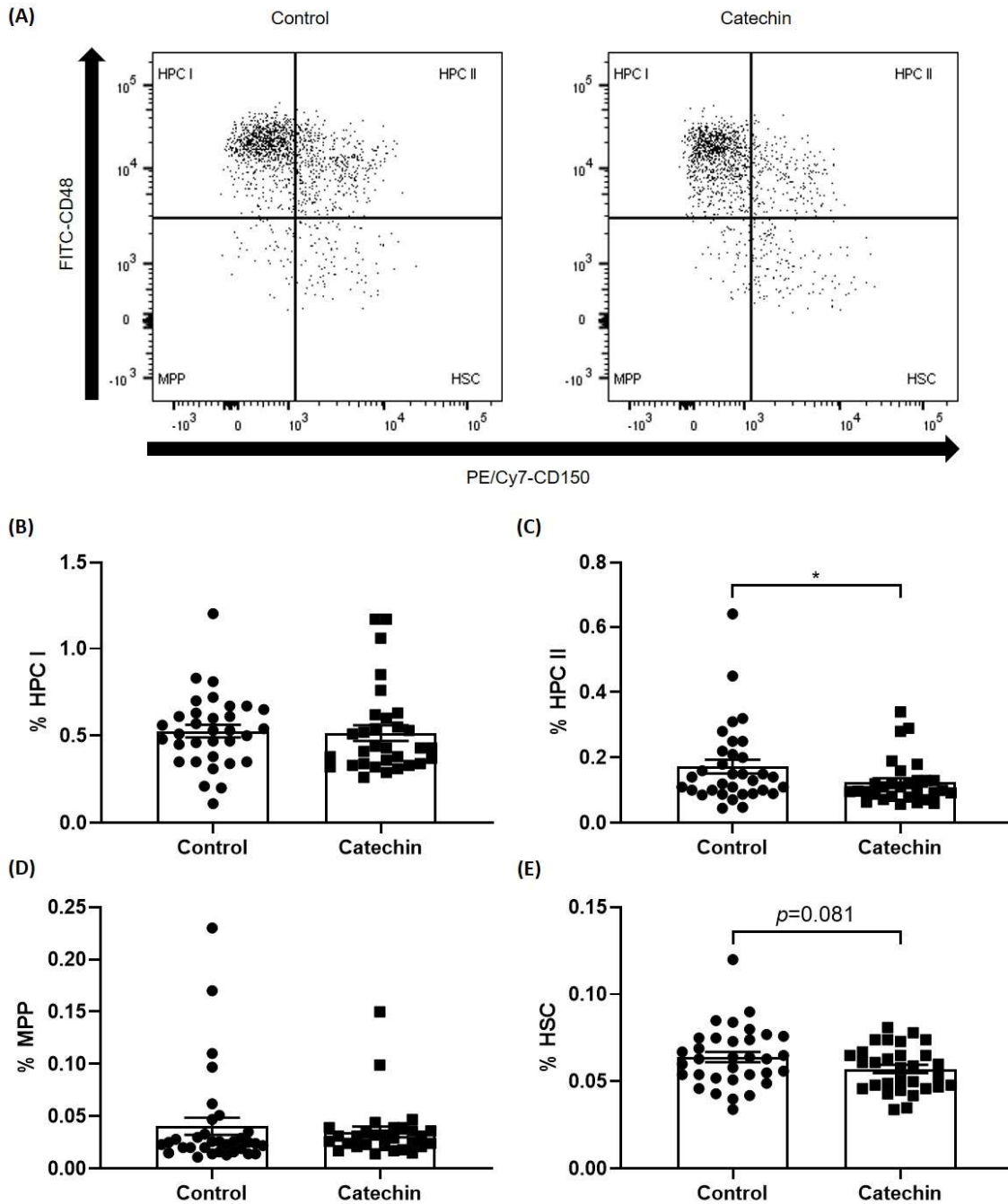


**Figure 5.9 Effect of (+)-catechin on stem cell populations in the bone marrow.**

Male *Ldlr*<sup>-/-</sup> mice (8 weeks old) were fed high-fat diet supplemented with vehicle ('control') or (+)-catechin hydrate ('catechin') for 12 weeks before being sacrificed and the bone marrow cells extracted for immunophenotyping using flow cytometry analysis. Data presented as percentage of total white blood cells. Data from two separate experiments have been combined. Representative dot plots along with the gating strategy are shown in (A), enabling analysis of the fluorescein isothiocyanate (FITC)-CD48<sup>-</sup> phycoerythrin/cyanine7 (PE/Cy7)-CD34<sup>-</sup> multipotent progenitor (MPP), FITC-CD48<sup>-</sup> PE/Cy7-CD34<sup>+</sup> haematopoietic stem cell (HSC), and haematopoietic progenitor cell (HPC) I (FITC-CD48<sup>+</sup> PE/Cy7-CD34<sup>-</sup>) and II (FITC-CD48<sup>+</sup> PE/Cy7-CD34<sup>+</sup>) populations. Data presented as percentage of total white blood cells for control (n=33) and catechin (n=29 (D), 30 (C and E) or 31(B)). Statistical analysis via unpaired t-test (E) or Mann-Whitney U test (B-D).

5.2.2.2 (+)-Catechin reduces the proportion of CMP cells

In the progenitor class of cells, the catechin group had significantly reduced proportion of CMP cells by 45.99% ( $p=0.016$ ) in the bone marrow compared to the control group (Figure 5.10E). However, no significant changes were seen in the proportion of MEP (Figure 5.10C), GMP (Figure 5.10D) or CLP (Figure 5.10F) cells between the two groups.

# Chapter 5: Effect of (+)-catechin on atherosclerosis development and progression

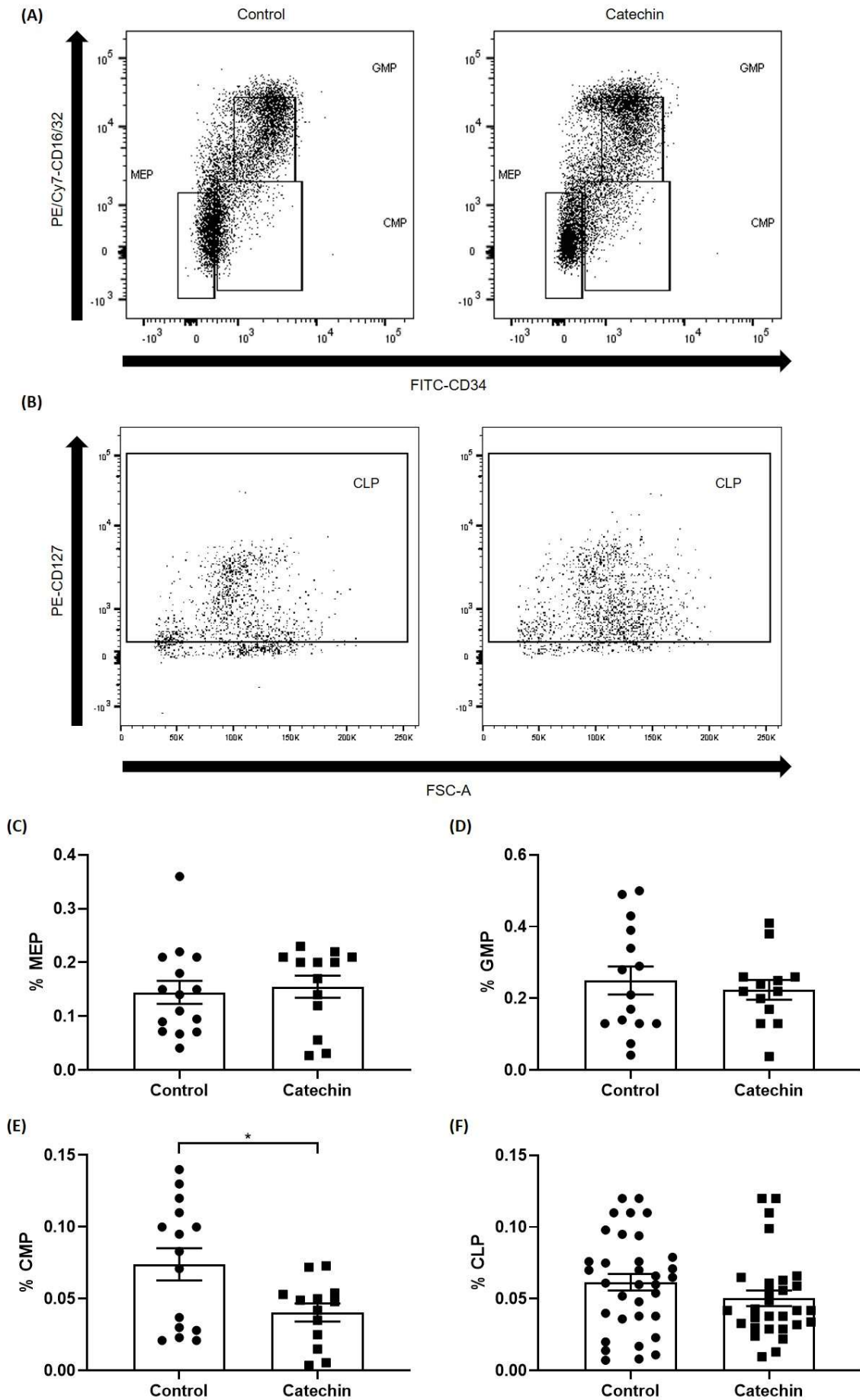


**Figure 5.10 Effect of (+)-catechin on progenitor cell populations in the bone marrow.**

Male *Ldlr*<sup>-/-</sup> mice (8 weeks old) were fed high-fat diet supplemented with vehicle ('control') or (+)-catechin hydrate ('catechin') for 12 weeks before being sacrificed and the bone marrow cells extracted for immunophenotyping using flow cytometry analysis. Data presented as percentage of total white blood cells. Data from two separate experiments have been combined (for F only as the CMP/GMP/MEP staining failed for the entirety of one experiment) to give n=14 (E), 15 (C; D) or 34 (F) for control, and n=12 (E), 13 (C; D) or 29 (F) for catechin. Representative dot plots along with the gating strategies are shown in (A) and (B), enabling analysis of the phycoerythrin/cyanine7 (PE/Cy7)-CD16/32<sup>-</sup> fluorescein isothiocyanate (FITC)-CD34<sup>-</sup> megakaryocyte-erythroid progenitor (MEP), PE/Cy7-CD16/32<sup>+</sup> FITC-CD34<sup>+</sup> granulocyte-macrophage progenitor (GMP), PE/Cy7-CD16/32<sup>-</sup> FITC-CD34<sup>+</sup> common myeloid progenitor (CMP) and PE-CD127<sup>+</sup> common lymphoid progenitor (CLP) cell populations respectively. Statistical analysis via unpaired t-test where \*,  $p \leq 0.05$ .

5.2.2.3 (+)-Catechin reduces the proportion of T cells

In the lineage<sup>+</sup> class of cells, the catechin group had significantly reduced proportion of T cells by 16.03% compared to the control group ( $p=0.044$ ) (Figure 5.11E). However, no significant changes were seen in the proportion of MDSCs (Figure 5.11C), macrophages (Figure 5.11D), or B cells (Figure 5.11F).

Chapter 5: Effect of (+)-catechin on atherosclerosis development and progression

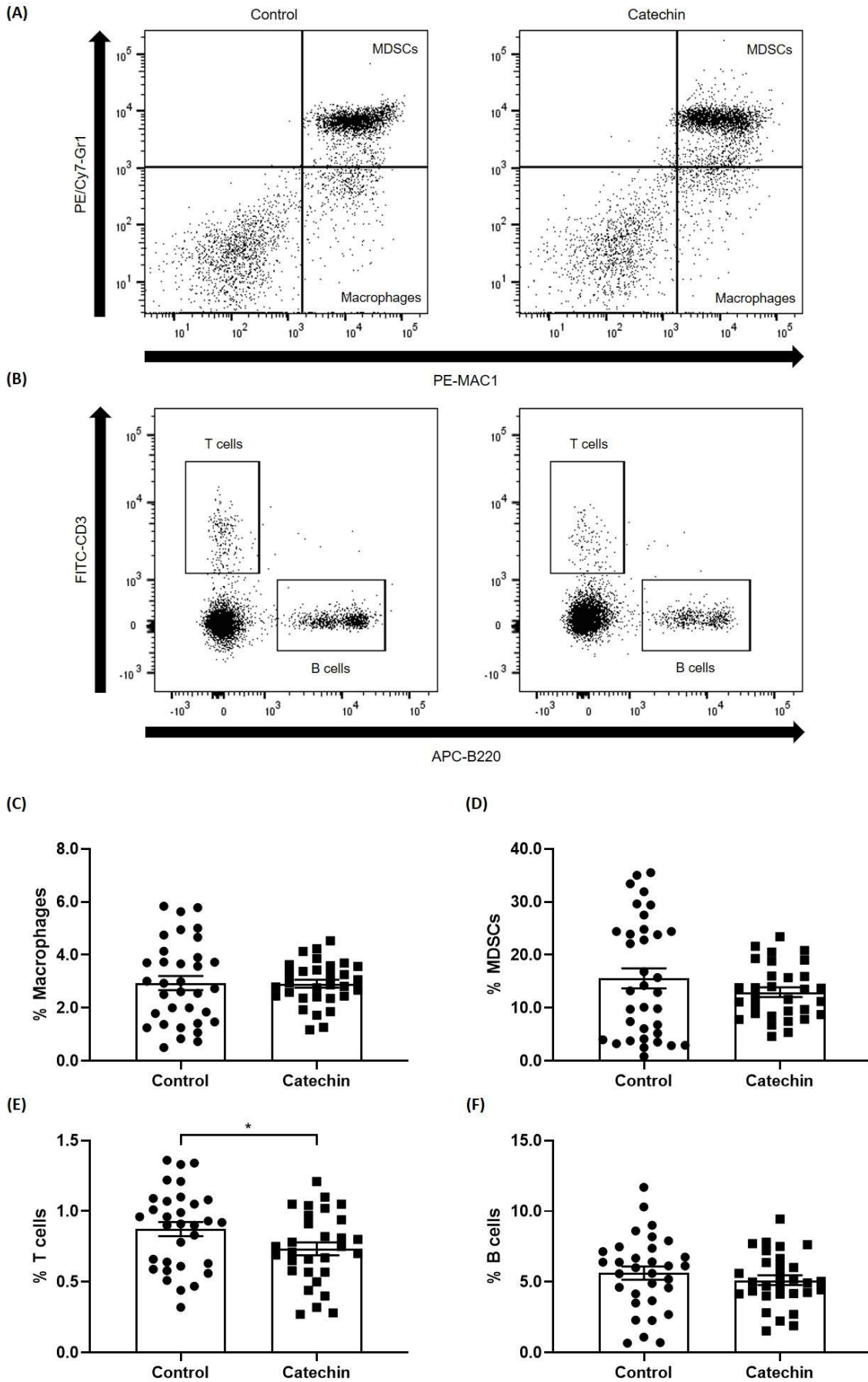


**Figure 5.11 Effect of (+)-catechin on lineage<sup>+</sup> cell populations in the bone marrow.**

Male *Ldlr*<sup>-/-</sup> mice (8 weeks old) were fed high-fat diet supplemented with vehicle ('control') or (+)-catechin hydrate ('catechin') for 12 weeks before being sacrificed and the bone marrow cells extracted for immunophenotyping using flow cytometry analysis. Data presented as percentage of total white blood cells. Representative dot plots along with the gating strategies are shown in (A) and (B), enabling analysis of the phycoerythrin/cyanine7 (PE/Cy7)-Gr1<sup>+</sup> PE-CD11b<sup>+</sup> myeloid-derived suppressor cells (MDSCs) and PE/Cy7-Gr1<sup>-</sup> PE-CD11b (MAC1)<sup>+</sup> macrophages, as well as fluorescein isothiocyanate (FITC)-CD3<sup>+</sup> T and allophycocyanin (APC)-B220<sup>+</sup> B cells respectively. Statistical analysis via unpaired t-test where \*  $p \leq 0.05$ .

### 5.2.3 Peripheral blood immune cell population analysis

On the day prior to the end point, samples of peripheral blood were extracted from the tail for immunophenotyping of circulating myeloid and lymphoid cell populations. There were no significant differences in the number of total WBCs in the peripheral blood between the control and catechin groups (Figure 5.12). Therefore, all subsequent flow cytometry data are presented as percentage of total WBCs.

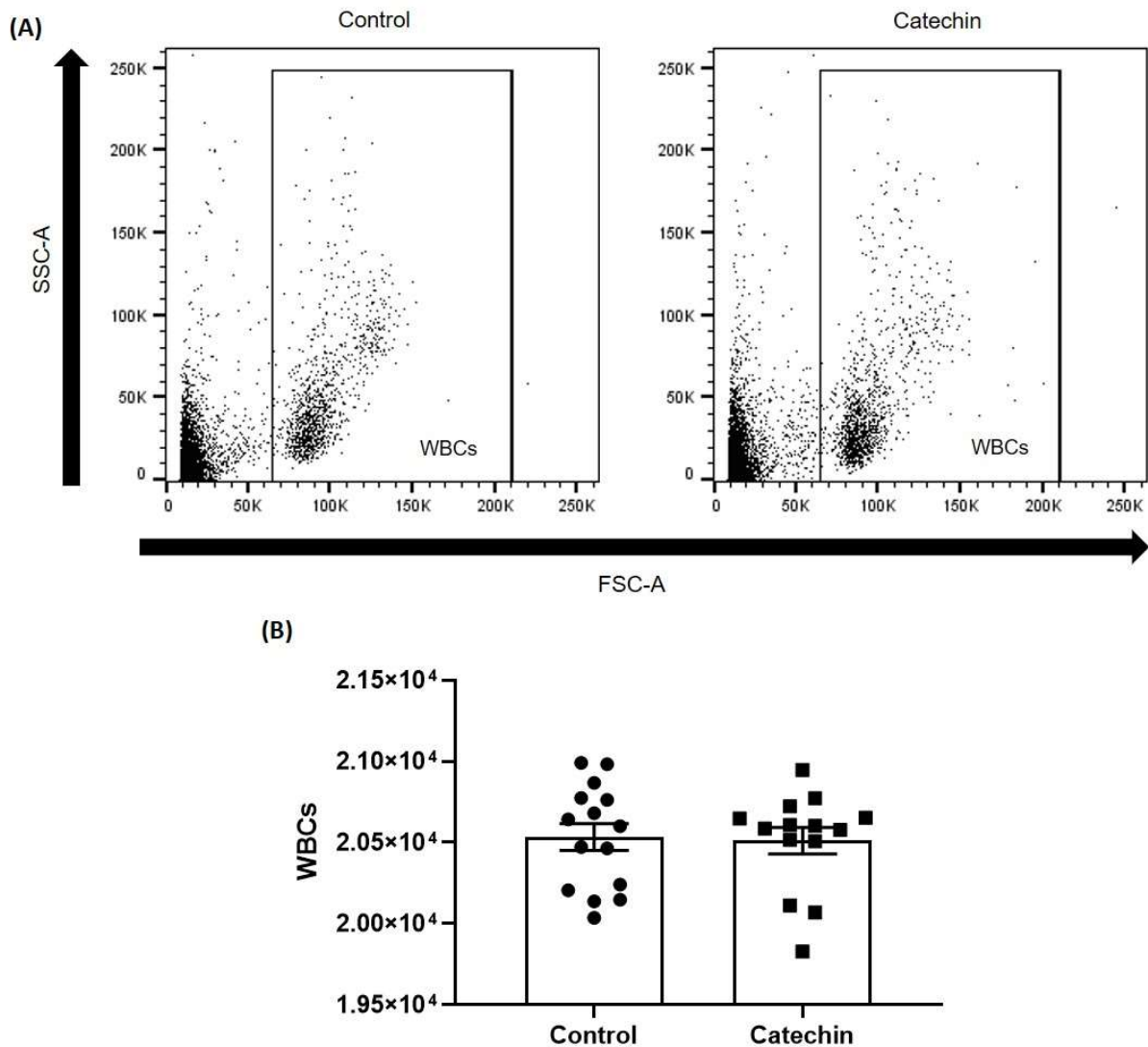


**Figure 5.12 Effect of (+)-catechin on the number of white blood cells in the peripheral blood.** Male *Ldlr*<sup>-/-</sup> mice (8 weeks old) were fed high-fat diet supplemented with vehicle ('control') or (+)-catechin hydrate ('catechin') for 12 weeks. Peripheral blood was extracted from the tail on the day before the scheduled end point for immunophenotyping using flow cytometry analysis. Representative dot plots and gating strategy are shown in (A) which enabled quantification of total white blood cells (WBCs) (B). Statistical analysis via unpaired t-test where n=15 for control and n=14 for catechin.

### 5.2.3.1 (+)-Catechin has no significant effect on lymphoid cell populations

Analysis of the lymphoid cell population found that the catechin group had a trend of reduction in the proportion of NK cells by 38.39% compared to the control group ( $p=0.058$ ) (Figure 5.13H). However, there were no significant differences in the proportion of B cells (Figure 5.13D) and CD3<sup>+</sup> T cells (Figure 5.13E), or the subsets of CD4<sup>+</sup> (Figure 5.13F) and CD8<sup>+</sup> T cells (Figure 5.13G), between the two groups.

# Chapter 5: Effect of (+)-catechin on atherosclerosis development and progression

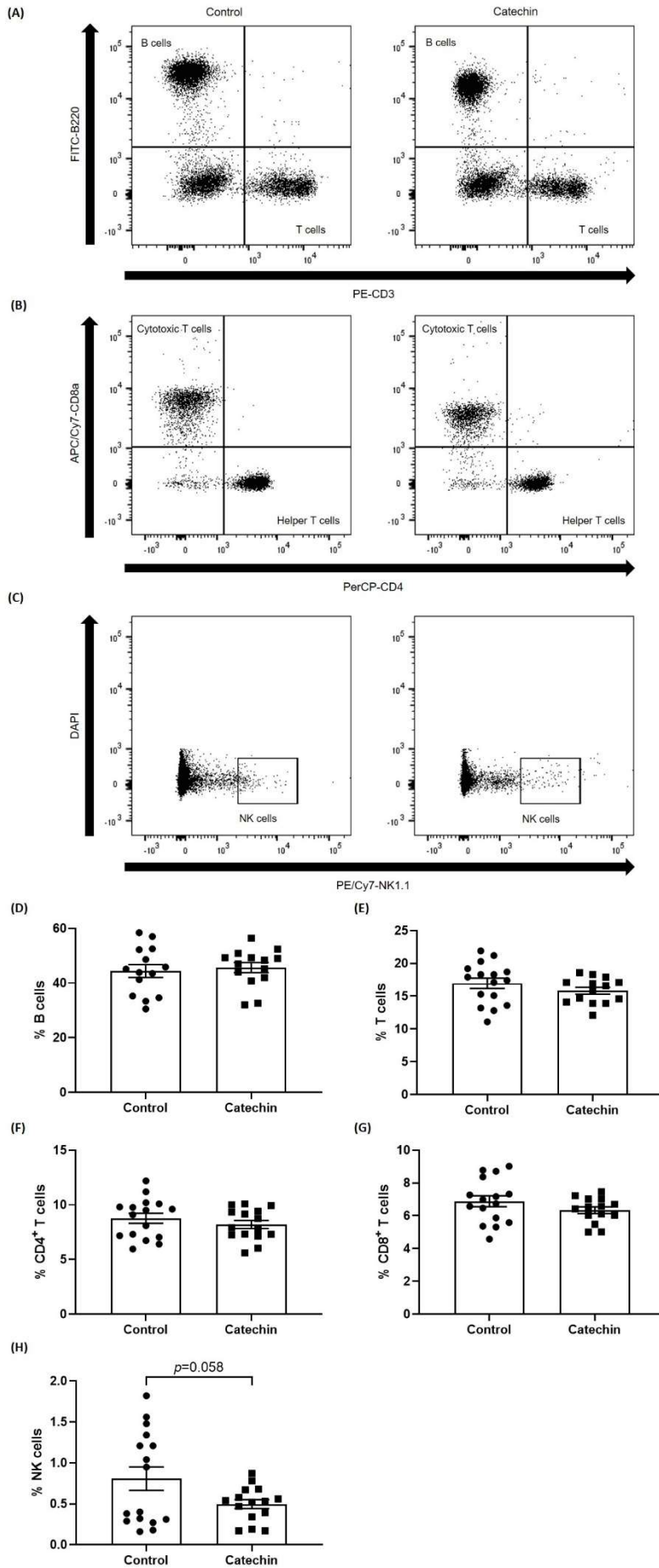


**Figure 5.13 Effect of (+)-catechin on lymphoid cell populations in the peripheral blood.**

Male *Ldlr*<sup>-/-</sup> mice (8 weeks old) were fed high-fat diet supplemented with vehicle ('control') or (+)-catechin hydrate ('catechin') for 12 weeks. Peripheral blood was extracted from the tail on the day before the end point for immunophenotyping using flow cytometry analysis. Data presented as percentage of total white blood cells. Representative dot plots and gating strategies for fluorescein isothiocyanate (FITC)-B220<sup>+</sup> B and phycoerythrin (PE)-CD3<sup>+</sup> T cells (A); peridinin-chlorophyll-protein (PerCP)-CD4<sup>+</sup> helper and allophycocyanin/cyanine7 (APC/Cy7)-CD8<sup>+</sup> cytotoxic T cells (B); and PE/Cy7-NK1.1<sup>+</sup> natural killer (NK) cells (C) are shown. Statistical analysis via unpaired t-test where n=14 (D), 15, 16 (E; F; G; H) for control and n=14 (D; E; G), 15 (F; H) for catechin.

5.2.3.2 (+)-Catechin increases the proportion of Ly6C<sup>high</sup> monocytes

Analysis of the myeloid cell population found that the catechin group had significantly increased proportion of Ly6C<sup>high</sup> monocytes by 31.81% in the peripheral blood compared to the control group ( $p=0.045$ ) (Figure 5.14G). However, there were no significant differences in Ly6C<sup>middle/low</sup> monocytes (Figure 5.14H and I), total monocytes (Figure 5.14F), macrophages (Figure 5.13D) or granulocytes (Figure 5.14E) between the two groups.

# Chapter 5: Effect of (+)-catechin on atherosclerosis development and progression

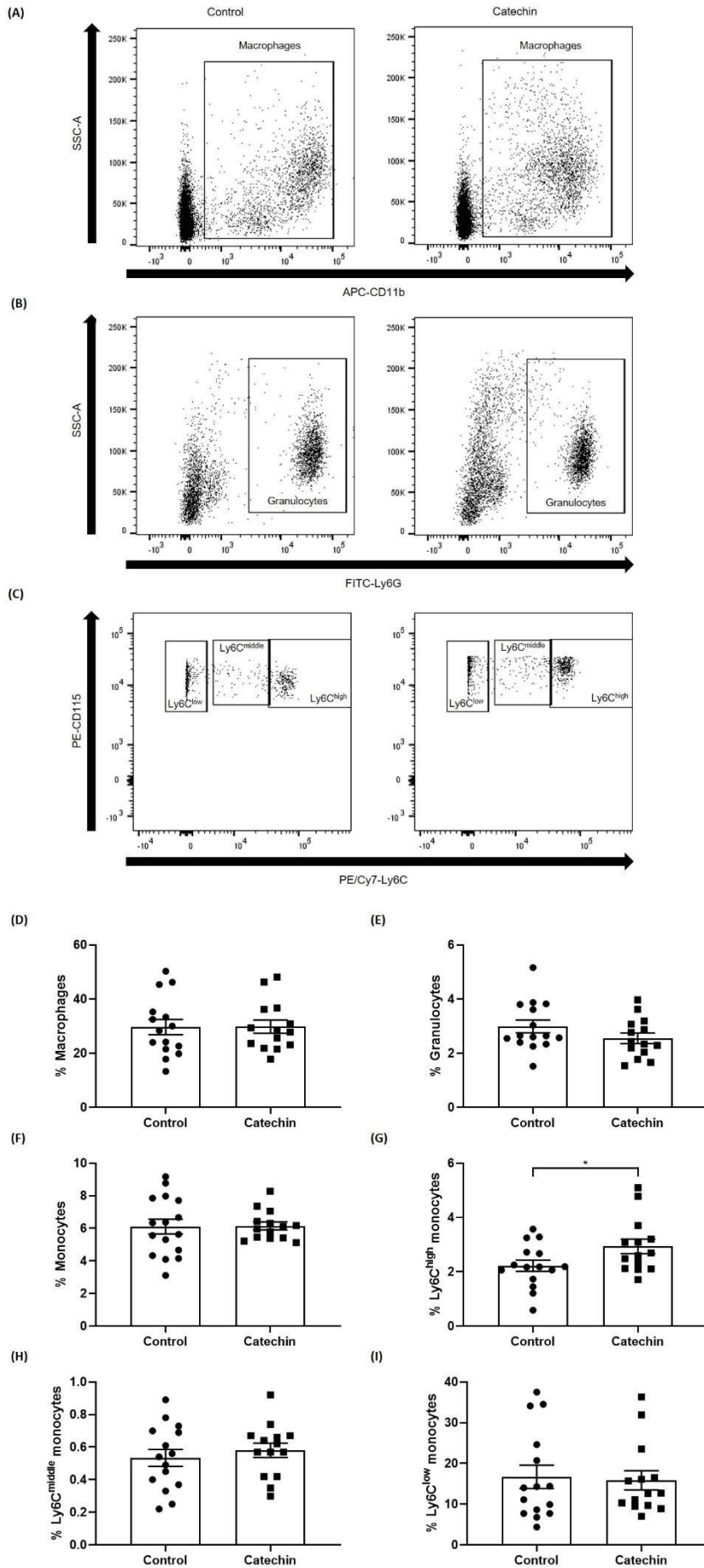


### **Figure 5.14 Effect of (+)-catechin on myeloid cell populations in the peripheral blood.**

Male *Ldlr*<sup>-/-</sup> mice (8 weeks old) were fed high-fat diet supplemented with vehicle ('control') or (+)-catechin hydrate ('catechin') for 12 weeks. Peripheral blood was extracted from the tail on the day before the end point for immunophenotyping using flow cytometry analysis. Representative dot plots and gating strategies for allophycocyanin (APC)-CD11b<sup>+</sup> macrophages (A), fluorescein isothiocyanate (FITC)-Ly6G<sup>+</sup> granulocytes (B) and phycoerythrin (PE)-CD115<sup>+</sup> phycoerythrin/cyanine7 (PE/Cy7)-Ly6C<sup>low/middle/high</sup> monocytes (C) are shown. Data presented as percentage of total white blood cells where n=15 (D-H) or 16 (I) for control and n=14 for catechin. Statistical analysis via unpaired t-test (D-H) or Mann-Whitney U test (I) where \*,  $p \leq 0.05$ .

## 5.2.4 Plasma parameters

### 5.2.4.1 Lipid profile

For comprehensive analysis of the lipid profile, the plasma was isolated from blood obtained via cardiac puncture and levels of different lipids were measured using colorimetric assays. The catechin group had a trend towards increase in total cholesterol by 10.99% (110.00 mg/dl) compared to the control group ( $p=0.072$ ) (Figure 5.15A). However, there were no significant changes in any of the specific lipoprotein concentrations (Figure 5.15B-D). Furthermore, there was no significant difference in TG levels between the two groups (Figure 5.15E).

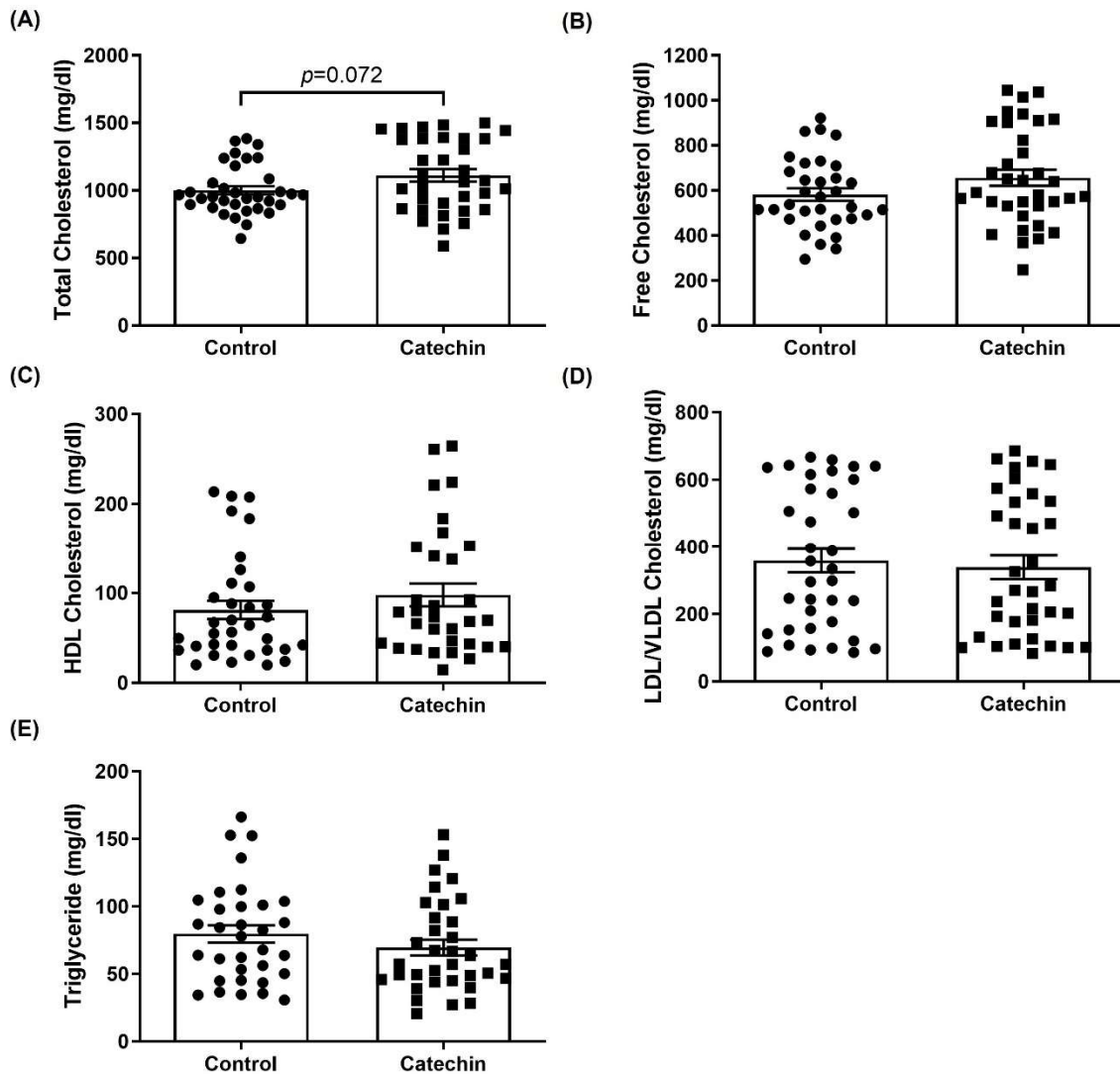


**Figure 5.15 Plasma lipids.**

Male *Ldlr*<sup>-/-</sup> mice (8 weeks old) were fed high-fat diet supplemented with vehicle ('control') or (+)-catechin hydrate ('catechin') for 12 weeks. The plasma was analysed for total, free, high-density lipoprotein (HDL) and low-density lipoprotein/very low-density lipoprotein (LDL/VLDL) cholesterol and triglyceride levels using colorimetric assay kits. Data from two separate studies have been combined to give n=33 (B; E), 34 (A; C) or 36 (D) for control and n=32 (C), 34 (A; E) or 35 (B; D) for catechin. Statistical analysis via unpaired t-test where \*,  $p \leq 0.05$ .

#### 5.2.4.2 Lipid ratios

For a more comprehensive assessment of lipid profile, clinically relevant lipid ratios were also calculated. The catechin group had a trend towards reduction in the ratio of TG to HDL-C by 33.18% (ratio of 0.42) compared to the control group ( $p=0.065$ ) (Figure 5.16F), with no differences in any other ratios.

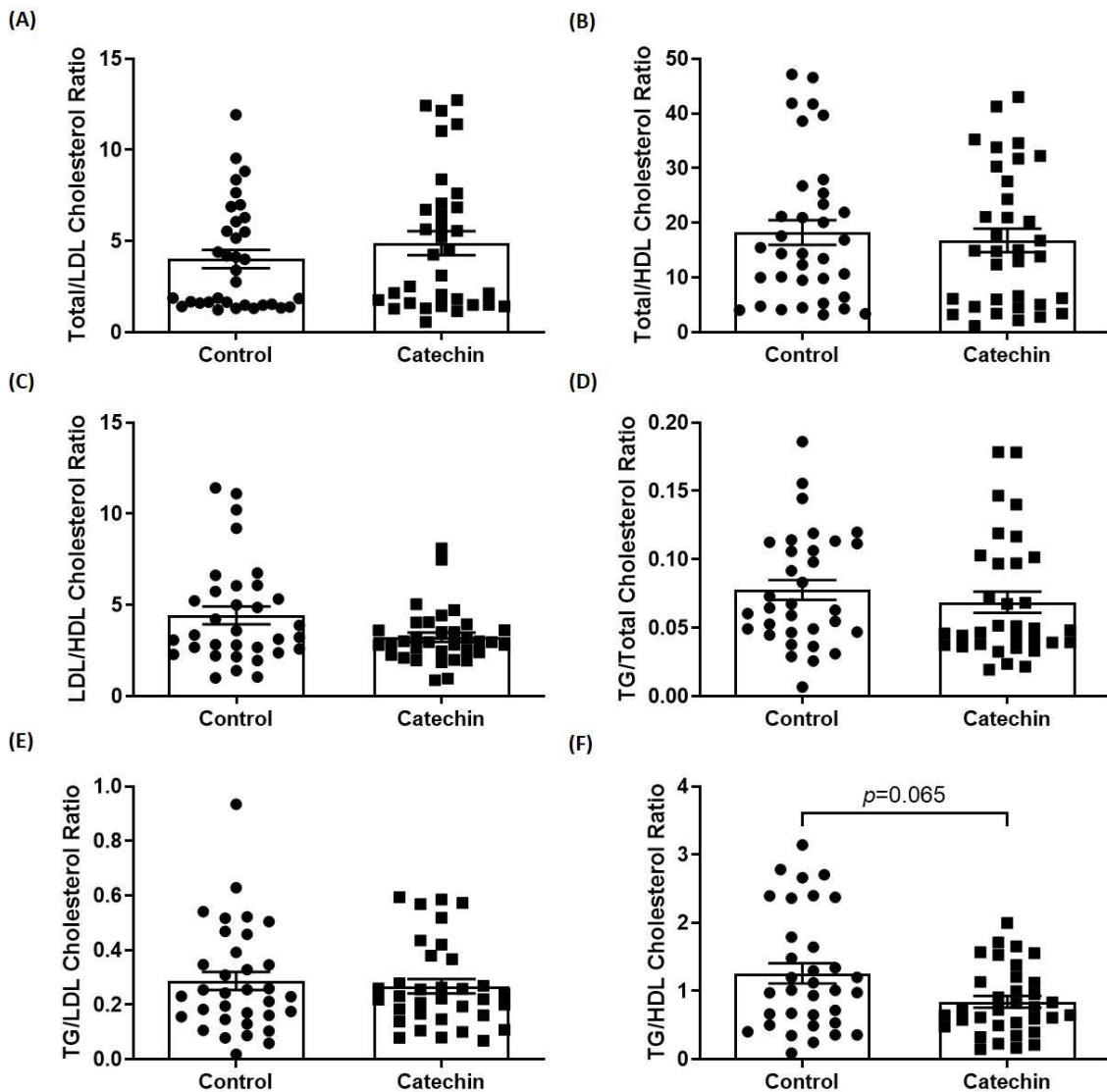


**Figure 5.16 Plasma lipid ratios.**

Male *Ldlr*<sup>-/-</sup> mice (8 weeks old) were fed high-fat diet supplemented with vehicle ('control') or (+)-catechin hydrate ('catechin') for 12 weeks before being sacrificed. Blood was obtained via cardiac puncture and collected into tubes containing heparin, and plasma obtained via centrifugation. Ratios were calculated using data presented in Figure 5.14. For simplicity, LDL/VLDL cholesterol is referred to as 'LDL cholesterol'. Data from two separate studies have been combined to give n=33 (C; D), 34 (A; E; F) or 35 (B) for control and n=33 (A; D) or 34 (B; C; E; F) for catechin. Statistical analysis via Mann-Whitney U test where \*,  $p \leq 0.05$ .

#### 5.2.4.3 Cytokine profile

To assess inflammatory profile further, the levels of key pro- and anti-inflammatory cytokines in the plasma was quantified. The catechin group had significantly reduced levels of IL-5 by 19.98% (0.68 pg/ml) in the plasma compared to the control group

( $p=0.026$ ) (Figure 5.17F). There were no significant differences in the levels of any other measured cytokines between the two groups.

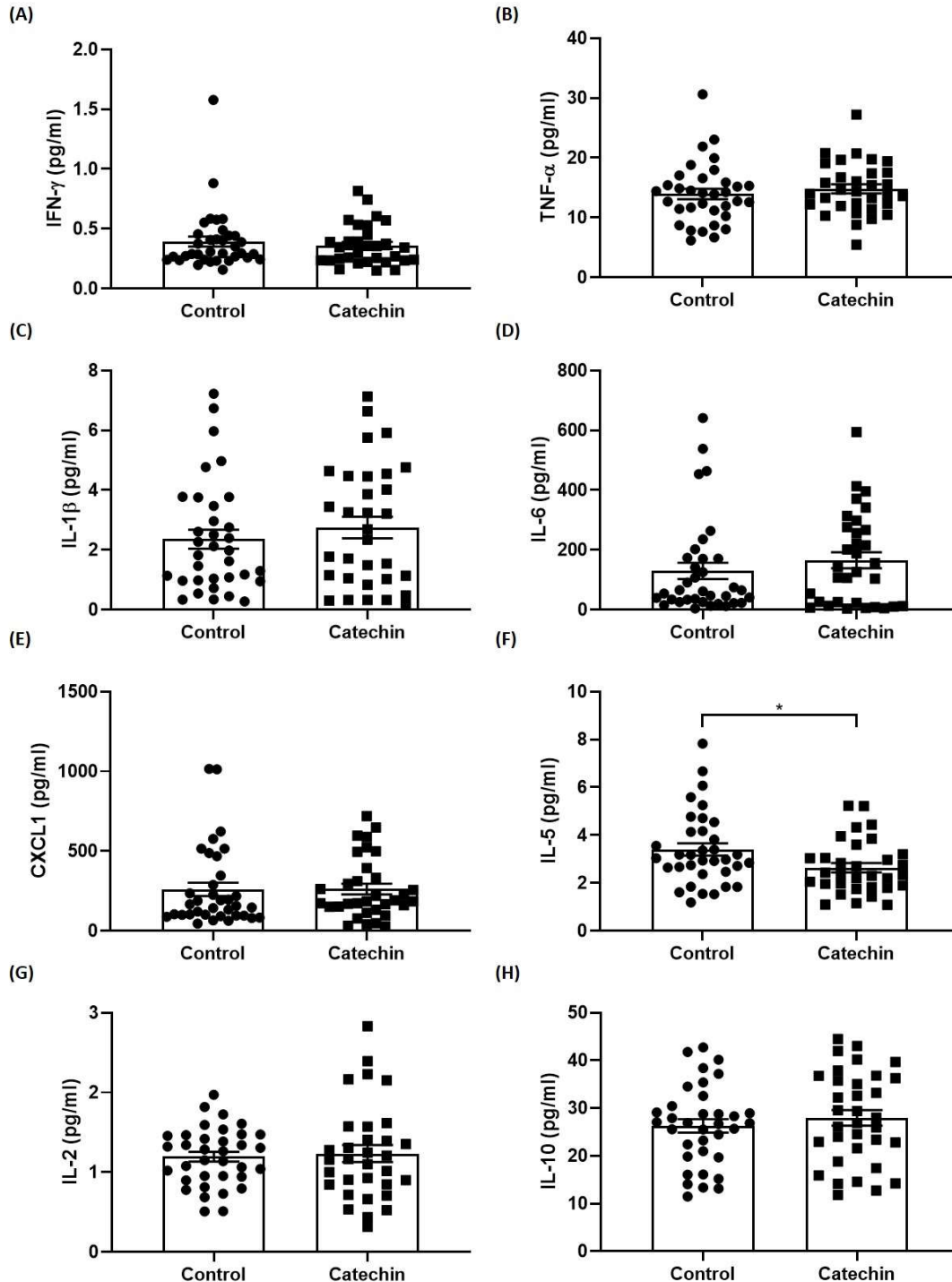


**Figure 5.17 Plasma cytokines.**

Male *Ldlr*<sup>-/-</sup> mice (8 weeks old) were fed high-fat diet supplemented with vehicle ('control') or (+)-catechin hydrate ('catechin') for 12 weeks. Levels of cytokines in the plasma were quantified using an MSD Cytokine Array. Data from two separate studies have been combined to give n=35 (A; D; E-H) or 34 (B; C; H) for control, and n=33 (E; F), 32 (B-D; G), or 31 (A), for catechin. Statistical analysis via unpaired t-test (A; H) or Mann-Whitney U test (B-G) where \*,  $p < 0.05$ .

#### 5.2.4.4 Oxidative stress markers

For assessment of oxidative stress, levels of ROS/RNS and MDA in the plasma were also quantified. The catechin group had a trend towards increase in plasma ROS/RNS levels by 14.83% (6.71  $\mu\text{M}$ ) compared to the control group ( $p=0.093$ ) (Figure 5.18A). However, there was no significant difference in plasma MDA levels between the two groups (Figure 5.18B).

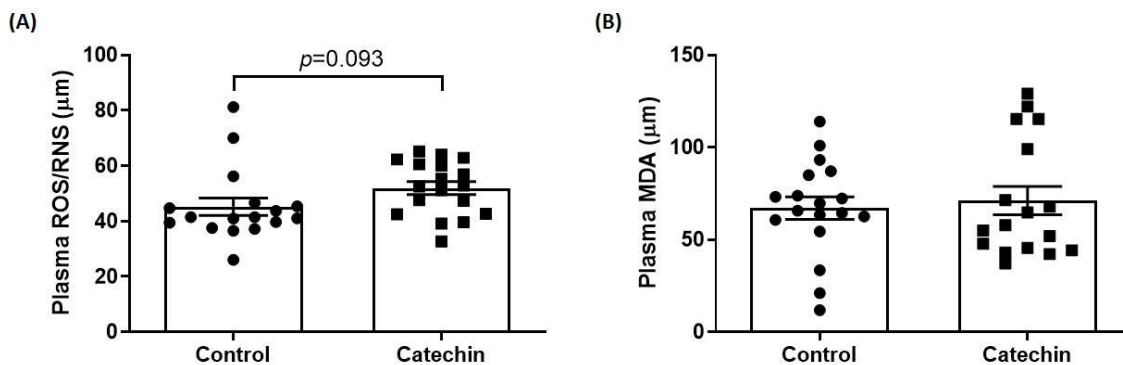


**Figure 5.18 Plasma oxidative stress markers.**

Male *Ldlr*<sup>-/-</sup> mice (8 weeks old) were fed high-fat diet supplemented with vehicle ('control') or (+)-catechin hydrate ('catechin') for 12 weeks. Plasma reactive oxygen species/reactive nitrogen species (ROS/RNS) and malondialdehyde (MDA) levels were quantified using *in vitro* assays. Due to the high cost of the assay kits, quantification was only done for one set of samples for each group to give n=17 for control and n=18 for catechin (A); n=18 for control and n=20 for catechin (B). Statistical analysis via unpaired t-test where \*,  $p \leq 0.05$ .

#### 5.2.5 Detailed plaque morphometric analyses

##### 5.2.5.1 Burden and lipid content

For assessment of atherosclerotic plaque development and burden, sections of the aortic root were taken at 8  $\mu\text{m}$  intervals and stained with ORO. The catechin group had significantly reduced plaque content ( $p=0.048$ ) (Figure 5.19C) and occlusion ( $p=0.049$ ) by 18.51% and 12.31% respectively (Figure 5.19D) compared to the control group. Furthermore, the catechin group also had a trend of reduction in total plaque area by 17.27% compared to the control group ( $p=0.067$ ) (Figure 5.19E). However, there were no significant differences in plaque lipid content or vessel area between the two groups.

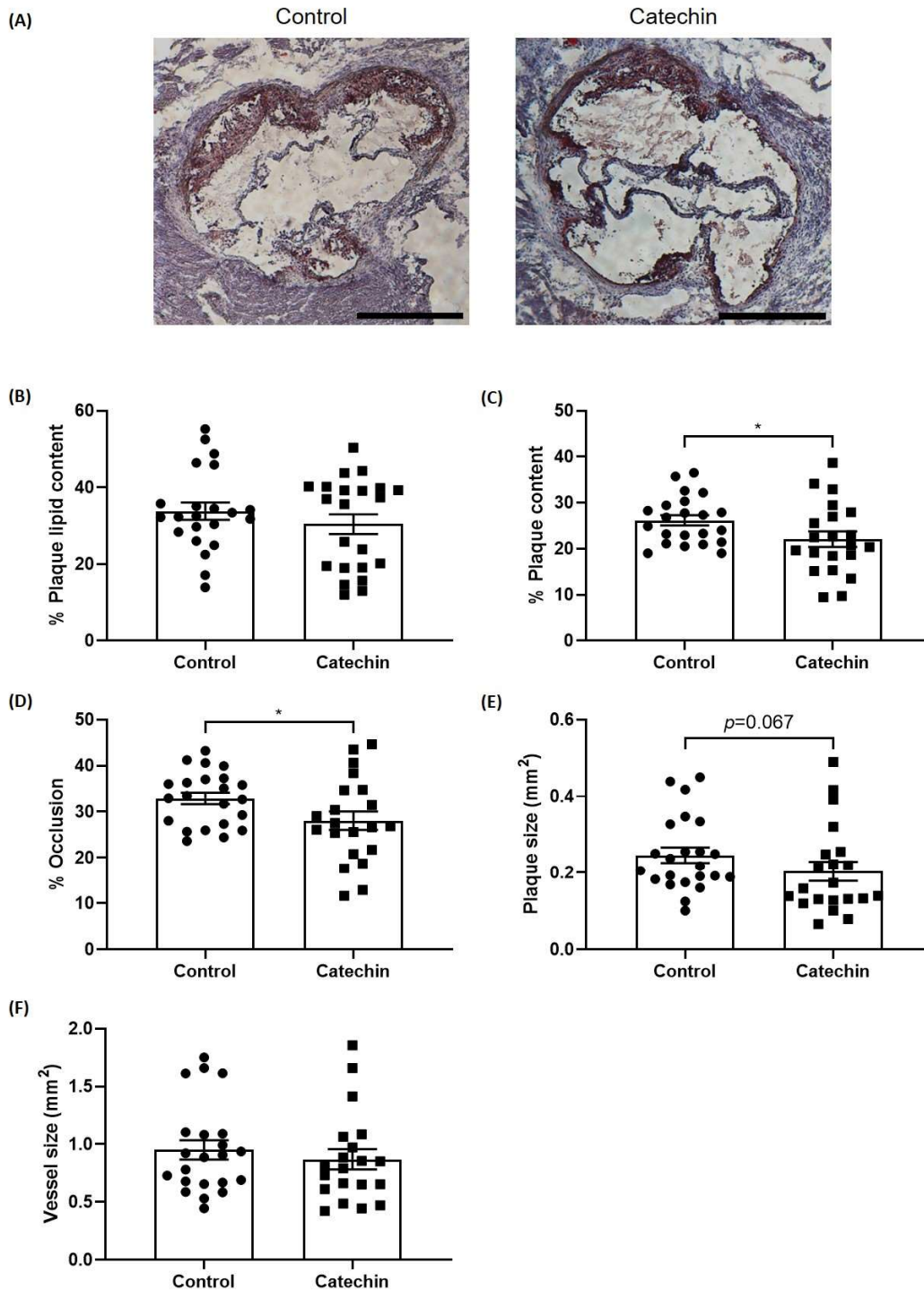


**Figure 5.19. Plaque burden and lipid content.**

Male *Ldlr*<sup>-/-</sup> mice (8 weeks old) were fed high-fat diet supplemented with vehicle ('control') or (+)-catechin hydrate ('catechin') for 12 weeks before being sacrificed. Sections of the aortic root at the three valve cusps were taken using a cryostat and stained with Oil Red O (ORO). Images were captured using a Leica DMRB microscope under x5 magnification and representative images with scale bars indicating 400  $\mu\text{m}$  are shown in (A). Image analysis was conducted using ImageJ software in a blinded manner where possible. Lipid content was calculated as percentage ORO+ staining (B; n=22 for control and catechin); plaque content was calculated as percentage plaque area of vessel area (C; n=22 for control and n=21 for catechin) and occlusion (D; n=22 for control and n=21 for catechin) was calculated as percentage plaque area of lumen area. Total plaque area (E; n=23 for control and n=21 for catechin) and vessel area (F; n=22 for control and n=20 for catechin) are also shown. Statistical analysis via unpaired t-test where \*,  $p \leq 0.05$ .

#### 5.2.5.2 Immune cell infiltration

Plaque inflammation was also studied using immunofluorescence staining to detect the presence of the major cell types, macrophages and T cells, in the lesion. The catechin group had significantly reduced proportion of MOMA-2<sup>+</sup> macrophages ( $p < 0.001$ ) (Figure 5.20B) and iNOS<sup>+</sup> M1 macrophages ( $p = 0.038$ ) (Figure 5.20C) by 45.49% and 48.54% respectively in the plaque compared to the control group. There was no significant difference in the proportion of CD3<sup>+</sup> T cells in the plaques of the two groups (Figure 5.20D).

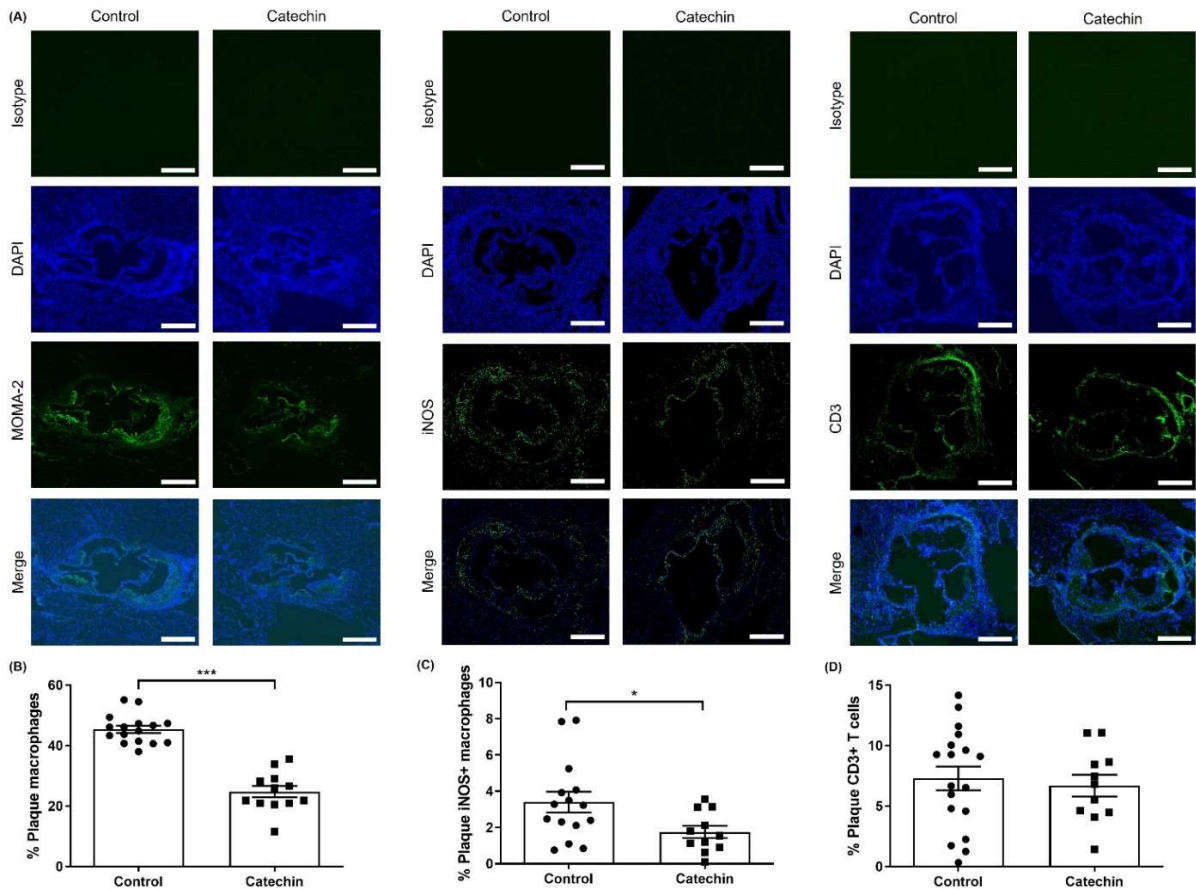


**Figure 5.20 Plaque immune cell infiltration.**

Male *Ldlr*<sup>-/-</sup> mice (8 weeks old) were fed high-fat diet supplemented with vehicle ('control') or (+)-catechin hydrate ('catechin') for 12 weeks before being sacrificed. Sections of the aortic root at the three valve cusps were taken using a cryostat and immunofluorescence staining was used to detect MOMA-2+ macrophages (B; n=16 for control and n=12 for catechin), inducible nitric oxide synthase (iNOS)<sup>+</sup> M1 macrophages (C; n=15 for control and n=11 for catechin) and CD3<sup>+</sup> T cells (D; n=18 for control and n=11 for catechin). Images were captured using an Olympus BX61 microscope under x4 magnification and representative images with scale bars indicating 400  $\mu$ m are shown in (A). Image analysis was conducted using ImageJ software in a blinded manner where possible. Statistical analysis via unpaired t-test where \*,  $p \leq 0.05$ ; \*\*\*,  $p < 0.001$ .

### 5.2.5.3 Necrosis and stability parameters

The catechin group had significantly increased collagen content ( $p=0.033$ ) (Figure 5.21C) and  $\alpha$ SMA<sup>+</sup> VSMCs ( $p=0.038$ ) (Figure 5.21D) by 47.86% and 60.08% respectively in the plaque compared to the control group. There was hence a significant increase in plaque stability index by 58.87% ( $p=0.026$ ) (Figure 5.21F), although no significant differences in plaque necrosis was found between the two groups.

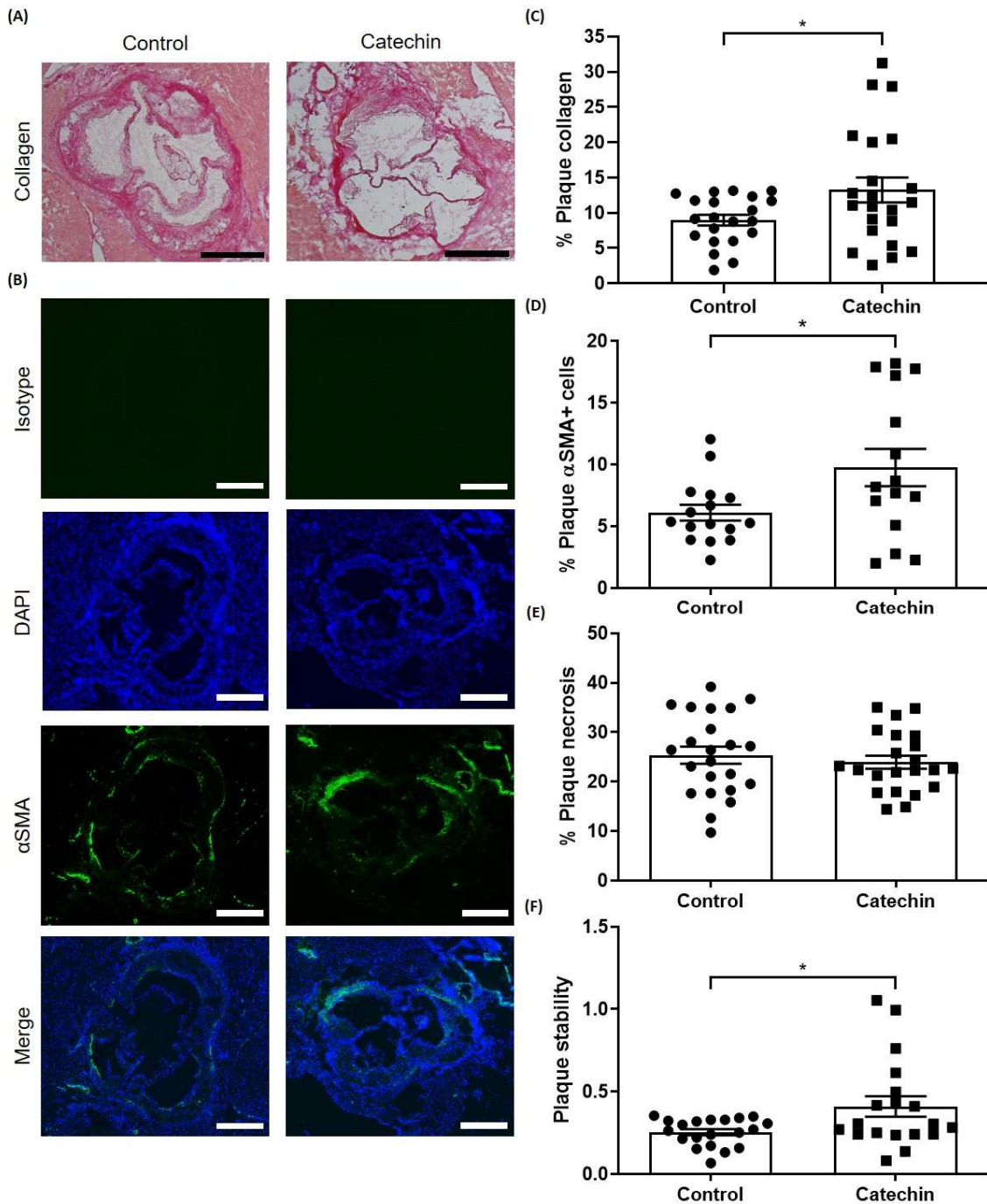


**Figure 5.21 Plaque necrosis and stability parameters.**

Male *Ldlr*<sup>-/-</sup> mice (8 weeks old) were fed high-fat diet supplemented with vehicle ('control') or (+)-catechin hydrate ('catechin') for 12 weeks before being sacrificed. Sections of the aortic root at the three valve cusps were taken using a cryostat. Sections were stained with Van Geison's solution and captured using a Leica DMRB microscope at x5 magnification (A; C; n=21 for control and n=22 for catechin). Immunofluorescence staining of the sections was also used to detect α-smooth muscle actin (SMA)+ smooth muscle cells in the plaque (B; D; n=16 for control and n=15 for catechin). Necrosis was calculated as the acellular regions within the plaque (E; n=23 for control and n=22 for catechin) and plaque stability was calculated as (collagen + smooth muscle cells) / (lipid + macrophages) (F; n=20 for control and n=19 for catechin). Statistical analysis via unpaired t-test where \*,  $p \leq 0.05$ . Image analysis was conducted using ImageJ software in a blinded manner where possible.

### 5.2.6 Liver cellularity and steatosis

Sections of the liver were taken at 10  $\mu\text{m}$  intervals and stained with haematoxylin and eosin, and ORO to enable analysis of cellularity/morphological changes and steatosis respectively. There were no significant differences in liver cellular area, cell count or average cell size between the two groups. There was also no significant difference in liver steatosis (ORO content) between the two groups (Figure 5.22).

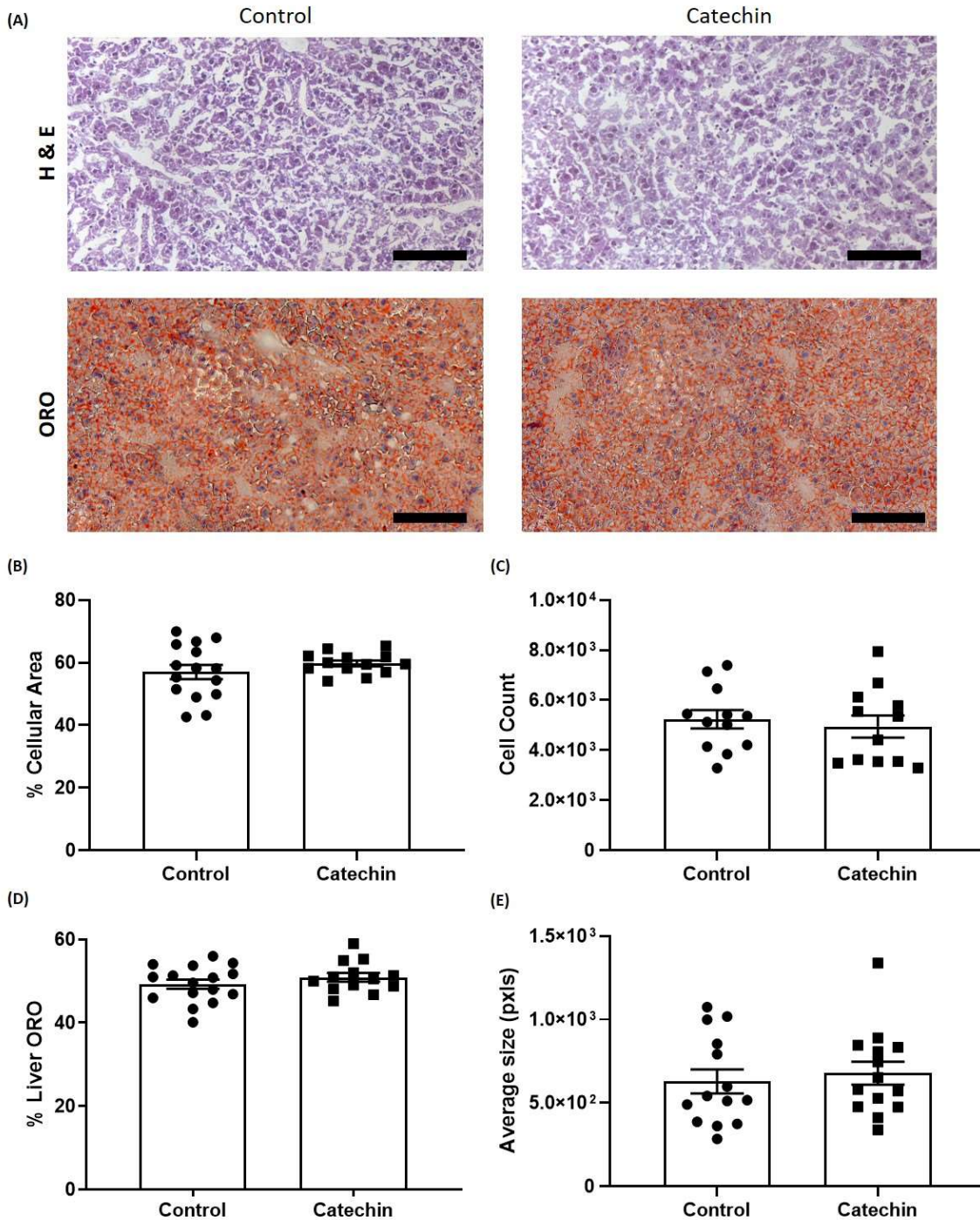


**Figure 5.22 Liver cellularity and steatosis.**

Male *Ldlr*<sup>-/-</sup> mice (8 weeks old) were fed high-fat diet supplemented with vehicle ('control') or (+)-catechin hydrate ('catechin') for 12 weeks before being sacrificed. Sections of the liver were taken using a cryostat and stained with haematoxylin and eosin (H & E) to analyse hepatic morphology, and Oil Red O (ORO) to measure steatosis. Images of the stained sections were captured using a Leica DMRB microscope at x20 magnification with scale bars indicating 200  $\mu$ m (A). Image analysis was conducted using ImageJ software. Statistical analysis via unpaired t-test where n=12 (C), 14 (E), 15 (B) or 16 (D) for control and n= 12 (C), 13 (B; D) or 14 (E) for catechin.

### 5.2.7 Summary

In summary, 8-week-old male *Ldlr*<sup>-/-</sup> mice receiving HFD supplemented with 200 mg/kg/day (+)-catechin hydrate for 12 weeks exhibited the following significant changes.

- Increased ratio of brown to white adipose tissue deposits (\*) (Figure 5.5)
- Reduced proportion of HPC II (\*), CMP (\*) and T cells (\*) in the bone marrow (Figures 5.9-11)
- Increased Ly6C<sup>high</sup> monocytes (\*) in the peripheral blood (Figure 5.14)
- Reduced plasma IL-5 levels (\*) (Figure 5.17)
- Decreased plaque content in the vessel (\*) and occlusion (\*) (Figure 5.19)
- Reduced plaque macrophages (\*\*\*) and M1 macrophages (\*) (Figure 5.20)
- Increased plaque collagen content (\*) and presence of VSMCs (\*) (Figure 5.21)
- Increased plaque stability index (\*) (Figure 5.21)

### 5.3 Discussion

(+)-Catechin has been found to modulate several risk factors associated with atherosclerosis in various animal studies, and even attenuate atherogenesis in *ApoE*<sup>-/-</sup> mice (Auclair et al. 2009). However, detailed characterisation of its actions on plaque development and atherosclerosis-associated risk factors in *Ldlr*<sup>-/-</sup> mice, combined with key pro-atherogenic processes *in vitro* has been lacking. *In vitro*, (+)-catechin has demonstrated various anti-atherogenic actions in key cell types implicated in all stages of atherosclerosis (Chapters 3 and 4), and hence the potential of (+)-catechin to prevent atherogenesis and disease progression was explored in *Ldlr*<sup>-/-</sup> mice fed HFD for 12 weeks. Mice receiving (+)-catechin hydrate demonstrated multiple beneficial changes associated with the atherosclerotic plaque itself, along with various atherosclerosis-associated risk factors. The ratio of brown to white adipose tissue deposits was significantly increased without differences in total weight gain. In the bone marrow, reductions in SLAM (HPC II), progenitor (CMP) and lineage<sup>+</sup> (T lymphocytes) classes of cells were seen. In the aortic root, (+)-catechin hydrate supplementation favourably modified the atherosclerotic plaque by attenuating its development (reduced plaque content and occlusion without affecting lipid content)

and the infiltration of pro-inflammatory immune cells (macrophages and in particular, M1 macrophages), as well as promoting parameters associated with stability (collagen and VSMC content). Therefore, (+)-catechin hydrate supplementation induces various anti-atherogenic effects and positive changes to the atherosclerotic plaque in *Ldlr*<sup>-/-</sup> mice. However, there were also some less favourable changes; increased presence of Ly6C<sup>high</sup> monocytes in the peripheral blood, and in the plasma, failed to attenuate markers of oxidative stress, along with reduced levels of anti-inflammatory cytokine, IL-5. Nevertheless, results of studies conducted thus far support the potential of (+)-catechin as a promising nutraceutical candidate capable of inhibiting atherogenesis and delaying disease progression.

### 5.3.1 Effects on adiposity and plasma lipids

Results of this study found that (+)-catechin hydrate supplementation positively modulated adipogenesis without affecting body weight or total weight gain. The ratio of brown to white adipose tissue was significantly increased. This appeared to be predominantly attributed to a reduction in the total white adipose tissue depots (not statistically significant but attributed to the combined changes in different white adipose tissue depots), rather than an increase in brown fat. Indeed, male WT (C57BL/6J) mice fed HFD supplemented with catechin-rich grape seed extracts exhibited protection against HFD-induced obesity, as shown by the suppressed increase in body weight and fat pads (Ohyama et al. 2011). Contrary to this, in the previous study conducted in the host laboratory, the same WT mice fed HFD for 3 weeks receiving daily gavage of (+)-catechin hydrate had increased accumulation of subcutaneous, gonadal and renal adipose tissue (Moss 2018). In other studies, supplementation of catechins (mainly EGCG) has been found to reduce white adipose tissue deposits and adiposity (Wolfram et al. 2005; Lee et al. 2009; Ferreira et al. 2020). In the previous short-term study conducted in the host laboratory using WT mice fed HFD for 3 weeks with daily gavage of (+)-catechin hydrate, plasma TG levels were significantly reduced, although there was no effect on other plasma lipids (Moss 2018). Indeed, various other studies have also reported the ability of green tea catechins to decrease plasma TG levels in humans (with no effect on plasma cholesterol) (Inami et al. 2007; Tinahones et al. 2008; Eichenberger et al. 2009;

Chatree et al. 2020) and in mice (Lee et al. 2009; Suzuki et al. 2013; Li et al. 2018). However, in *ApoE*<sup>-/-</sup> mice, tea catechin or (+)-catechin supplementation also had no effect on plasma total cholesterol or TG levels, although atherosclerotic lesion size was reduced (Miura et al. 2001; Auclair et al. 2009). Furthermore, several human studies have reported a lack of effect on total cholesterol and LDL-C in the plasma after intake of catechins (Trautwein et al. 2009; Miyazaki et al. 2012). Although this study found a trend of increased plasma cholesterol levels and ratio of TG to HDL-C in the catechin group, there were no statistically significant changes in any of the plasma lipid levels or ratios. Therefore, supplementation of (+)-catechin, seems to have mild effects on plasma lipids at best, in comparison to other green tea catechins, and where effects are seen, these appear to be mainly targeted to/associated with TG. This suggests that (+)-catechin might moderately dampen hypertriglyceridemia, and attenuate atherosclerosis via other mechanisms independent of hypercholesterolaemia, such as anti-inflammatory and anti-oxidative activities. Other catechins, such as the galloylated types, may have more potent modulatory effects on plasma lipid profile. Moreover, the lack of effect of (+)-catechin hydrate supplementation on liver cellularity and steatosis was expected due to its mild effects on plasma lipids (combined with the lack of change in liver weight), although it has been reported that other catechins, such as EGCG, can attenuate hepatic steatosis in HFD-fed mice (Bose et al. 2008).

### 5.3.2 Effects on progenitor and immune cells in the bone marrow

In this study, (+)-catechin hydrate supplemented HFD induced several changes in the bone marrow cell populations; significant changes are summarised in Figure 5.23. The reduction in HPSCs suggests attenuation of the HFD-induced increase in haematopoiesis with (+)-catechin hydrate supplementation, as well as dampened T cell-driven inflammation. Although a significant reduction in CD3<sup>+</sup> T cells was seen in the catechin group, further analyses are required to determine the exact subset(s) of T cells (e.g., CD4<sup>+</sup> and CD8<sup>+</sup>) that are affected, since different subsets of T cells may have anti- or pro-atherogenic activities. Furthermore, since chow-fed *Ldlr*<sup>-/-</sup> mice do not develop atherosclerosis, a chow control group as such was not included, although it would have been useful to verify that HFD-feeding indeed induces changes in the

bone marrow cell populations as an additional control. Nevertheless, these findings contradict those of the previous pilot study conducted in the host laboratory, whereby HFD-fed WT mice receiving daily gavage of (+)-catechin hydrate for 3 weeks had increased populations of MPP, CMPs and B cells, and decreased MDSCs in the bone marrow (although these changes were based upon small n numbers per group and in WT mice) (Moss 2018). Indeed, intraperitoneal injection of (+)-catechin has been found to increase the population of leukocytes (monocytes, granulocytes, T and B cells) in the bone marrow of chow-receiving mice (Takano et al. 2004). This suggests differential effects of (+)-catechin supplementation based on the type of mouse used and duration of HFD feeding. However, in the context of atherosclerosis, (+)-catechin hydrate supplementation appears to elicit protective effects on HFD-induced enhanced proliferation of haematopoietic progenitor cells and hence the generation of pro-inflammatory immune cells.

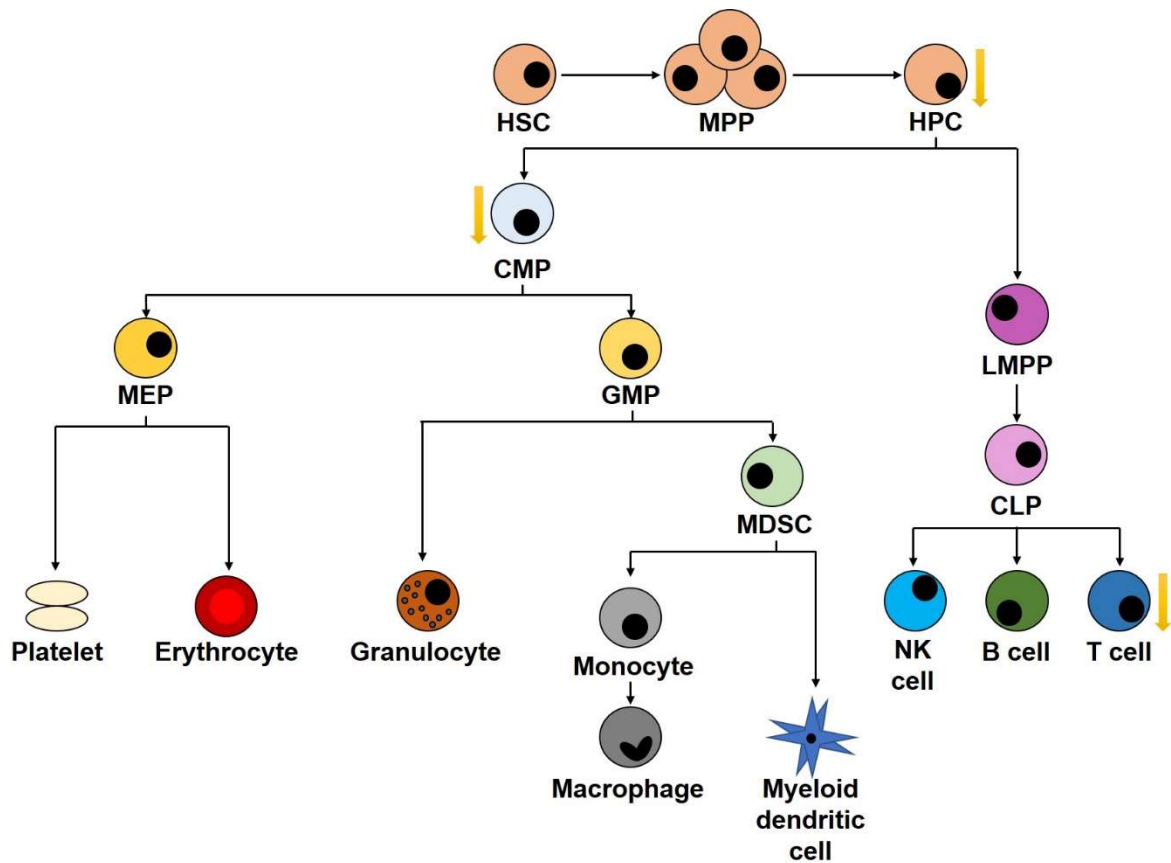


**Figure 5.23 Summary of changes in the bone marrow cell populations.**

Male *Ldlr*<sup>-/-</sup> mice fed high-fat diet supplemented with 200 mg/kg/day (+)-catechin hydrate for 12 weeks exhibited changes in the bone marrow stem, progenitor and lineage<sup>+</sup> cell populations compared to the vehicle control. Changes of significance or trend of significance are shown by yellow arrows. Abbreviations: HSC, haematopoietic stem cell; MPP, multipotent progenitor; HPC, haematopoietic progenitor cell; CMP, common myeloid progenitor; MEP, megakaryocyte-erythroid progenitor; GMP, granulocyte-macrophage progenitor; MDSC, myeloid derived suppressor cell; LMPP, lymphoid-primed multipotent progenitor; CLP, common lymphoid progenitor; NK, natural killer.

### 5.3.3 Effects on peripheral blood immune cells and plasma cytokines

Apart from a significant increase in Ly6C<sup>high</sup> monocytes (by 31.81%) in the peripheral blood, no changes in any other lymphoid or myeloid cells were seen, although there was a trend of reduction in NK cells. All significant changes in bone marrow and peripheral blood cell populations are summarised in Figure 5.24. The possible reduction in NK cells in the peripheral blood may coincide with the reduction in plasma IL-5 levels, although there was no significant change in plasma IFN- $\gamma$  levels. In the context of atherosclerosis, IL-5 is considered an anti-atherogenic cytokine due to its ability to stimulate the generation of IgM antibodies which mediate the clearance of apoptotic cells and oxLDL (Knutsson et al. 2019). Indeed, in *ApoE*<sup>-/-</sup> mice, deficiency

of IL-5 was correlated with enhanced plaque formation at sites of oscillatory shear stress and in humans, individuals with high concentrations of IL-5 were less likely to have a carotid plaque, although evidence supporting an association with reduced risk of MACE is weak (Silveira et al. 2015; Knutsson et al. 2019). Beyond atherosclerosis, IL-5 is implicated in allergic disease, in particular, in driving asthmatic and allergic responses and a potential target for the treatment of allergies (Silveira et al. 2015). Indeed, other studies have reported a reduction in serum IL-5 levels induced by catechin in mice with allergic rhinitis (Pan et al. 2018) and EGCG administration significantly reduced asthmatic reaction associated with IL-5 (Kim et al. 2006). Taken together, these studies support a role of catechins in modulating the allergic response, possibly via the reduction of NK cell production in the bone marrow. Besides the peripheral blood, NK cells also reside in the lung and spleen. As the spleen regulates systemic immune response, immune cell populations could also be analysed in splenocytes. In mice, administration of EGCG fraction of green tea extract for 6 weeks resulted in increased NK cell cytotoxicity and splenic secretion of IFN- $\gamma$  (Kuo et al. 2014) and oral administration of (+)-catechin augmented splenic NK cell activity (Ikeda et al. 1984). As the distribution of NK (and other) cells in different tissues can affect their role in immune responses (Michel et al. 2012), immunophenotyping of immune cell populations could also be expanded to other sites beyond the bone marrow and peripheral blood.

Although a significant increase in Ly6C<sup>high</sup> monocytes was detected in the peripheral blood, this did not correlate to worsened atherosclerosis severity in the aortic root (discussed later in more detail). This was surprising since an abundance of evidence strongly links Ly6C<sup>high</sup> monocytosis with atherosclerosis in humans and mice, especially as these monocytes give rise to the pro-inflammatory macrophages that drive disease progression (Olivares et al. 1993; Swirski et al. 2007; Murphy and Tall 2016). To gain a more dynamic view of how these immune cell populations fluctuate within the peripheral blood during atherosclerosis development, immunophenotyping could be conducted throughout the feeding period at regular intervals. Additionally, baseline measurements could also be taken for comparison between chow and HFD feeding. The intention was to include chow controls (i.e., *Ldlr*<sup>-/-</sup> mice maintained on chow for 12 weeks) with the 'second' progression study (as part of the regression

study); however, immunophenotyping could not be carried out due to school closures (in response to the pandemic).

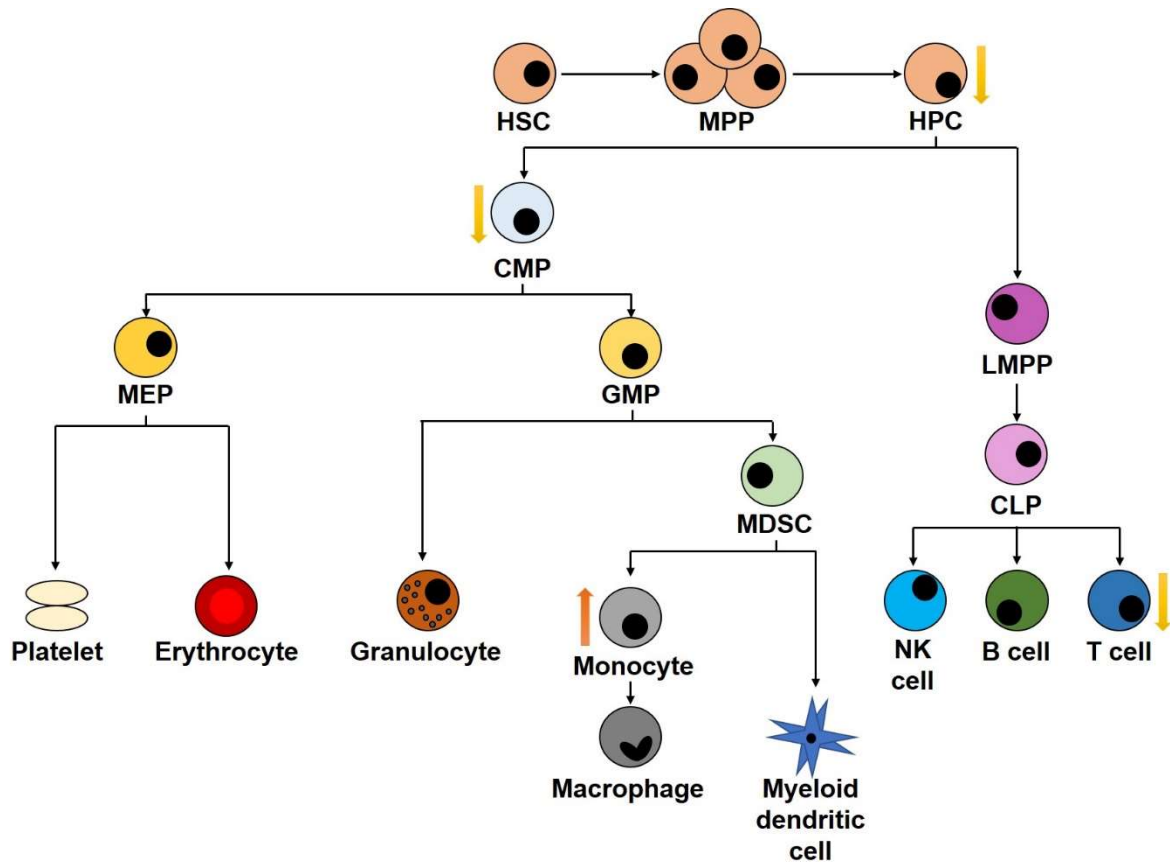


**Figure 5.24 Summary of changes in the bone marrow and peripheral blood cell populations.** Male *Ldlr*<sup>-/-</sup> mice fed high-fat diet supplemented with 200 mg/kg/day (+)-catechin hydrate for 12 weeks exhibited changes in the bone marrow stem, progenitor and lineage<sup>+</sup> cell populations compared to the vehicle control. Changes of significance or trend of significance in the bone marrow are shown by yellow arrows, whereas those of the peripheral blood are shown by orange arrows. Abbreviations: HSC, haematopoietic stem cell; MPP, multipotent progenitor; HPC, haematopoietic progenitor cell; CMP, common myeloid progenitor; MEP, megakaryocyte-erythroid progenitor; GMP, granulocyte-macrophage progenitor; MDSC, myeloid derived suppressor cell; LMPP, lymphoid-primed multipotent progenitor; CLP, common lymphoid progenitor; NK, natural killer.

#### 5.3.4 Lack of effect on plasma oxidative stress markers

The possible increase in plasma ROS/RNA (trend) was surprising (although there was no significant change in plasma MDA), given the potent antioxidant activities of (+)-catechin reported *in vitro* and *in vivo*. This suggests a possible increase in oxidative stress and potentially increased oxLDL levels, unless antioxidant enzyme activities were also elevated. In the previous pilot study conducted in the host laboratory, WT

mice fed HFD for 3 weeks with daily gavage of the same dose of (+)-catechin hydrate also failed to attenuate plasma ROS/RNS and MDA levels (as although reductions were seen, these were not statistically significant) (Moss 2018). On the contrary, in male Wistar rats, daily supplementation of (-)-catechin (10 mg/kg/day) significantly decreased plasma MDA concentration and enhanced the activities of catalase, glutathione peroxidase and superoxide dismutase (Abd El-Aziz et al. 2011). Additionally, in diabetic rats, catechin hydrate (50 mg/kg/day) attenuated vascular oxidative stress (Bhardwaj et al. 2013), and in a rat model of type 2 diabetes, catechin (30 mg/kg/day) intake reduced aortic ROS production and dampened the expression of NOX subunits (Ihm et al. 2009). Additionally, *Apoe*<sup>-/-</sup> mice receiving catechin (50 µg/day) were less susceptible to LDL oxidation (Hayek et al. 1997). Therefore, further investigation of the effect of (+)-catechin on the levels or activities of antioxidant enzymes, as well as analysis of plasma oxLDL concentrations, are needed to gain further insights on the effect of (+)-catechin supplementation on oxidative stress and LDL oxidisability *in vivo*.

### 5.3.5 Effects on plaque burden and inflammation

Results of the progression study found (+)-catechin hydrate supplementation to attenuate atherosclerotic lesion development and progression in the aortic root, as shown by the significant reductions in plaque content (in the vessel) and plaque occlusion, as well as trend of reduction in plaque size (despite no effect on lipid content). Indeed, other studies have reported the ability of (+)-catechin supplementation to attenuate atherosclerotic plaque burden in *Apoe*<sup>-/-</sup> mice alone (Hayek et al. 1997; Auclair et al. 2009) or in combination with other nutraceutical agents (Norata et al. 2007). Furthermore, analyses of plaque immune cell infiltration found a marked reduction in plaque macrophages and specifically, a decrease in iNOS<sup>+</sup> M1 proinflammatory macrophages (although there was no significant difference in plaque CD3<sup>+</sup> T cells). Although the reductions in parameters associated with plaque burden were mild (less than 20%), the most drastic changes were the decrease (over 40%) in plaque macrophages and increases in plaque collagen (just less than 50%) and SMC (60%) content. These observations coincide with *in vitro* data described in Chapter 3, whereby (+)-catechin significantly attenuated MCP-1-stimulated migration

## Chapter 5: Effect of (+)-catechin on atherosclerosis development and progression

of monocytes and proliferation of HMDMs, suggesting a reduction in monocyte recruitment and infiltration to the plaque, reduced presence of macrophages and dampened local macrophage proliferation. This may explain why elevated levels of Ly6C<sup>high</sup> monocytes was detected in the peripheral blood, since their infiltration to the arterial wall was prevented. Additionally, (+)-catechin might also attenuate endothelial dysfunction via possible protective effects on mitochondrial function in ECs (described in Chapter 4), to inhibit early pro-atherogenic processes. Together, these data suggest that (+)-catechin attenuates atherosclerotic lesion development and plaque progression by modulating monocyte/macrophage-driven inflammatory processes, as shown by the reduced plaque burden and inflammation.

The lack of effect on plaque lipid content also coincides with the mild changes in plasma lipids, suggesting (+)-catechin mediates its beneficial effects via its anti-inflammatory effects rather than lipid-modulating activities. Although the proportion of CD3<sup>+</sup> T cells in the bone marrow was significantly reduced, no significant changes in T cells were seen in the peripheral blood or in the plaque itself, emphasizing that changes seen in the bone marrow lineage<sup>+</sup> cells aren't necessarily reflected in the peripheral blood or the atherosclerotic plaque. For further analysis of the atherosclerotic plaque, other stains could be used to measure adhesion molecules such as ICAM-1 and VCAM-1, and MMP expression, for example. Additionally, markers for other macrophage phenotypes, such as arginase I and the mannose receptor, CD206, for M2 macrophages (Jablonski et al. 2015; Tsuchiya et al. 2019) could be used. However, the availability of slides is a limiting factor, and so any staining pursued must be meaningful and insightful to avoid wastage of precious sections. Given that (+)-catechin has also been shown to attenuate macrophage MMP production *in vitro* (Chapter 3), these further stains would be logical. Furthermore, as atherosclerotic plaques possess a high level of heterogeneity even within the same individual depending on the anatomical location, detailed plaque morphometric analyses should also be done in the brachiocephalic artery to confirm changes seen in the aortic root with that of another vascular bed.

### 5.3.6 Effects on plaque stability parameters

(+)-Catechin hydrate supplemented HFD feeding for 12 weeks resulted in beneficial modifications to the aortic root atherosclerotic plaque; the presence of VSMCs was significantly increased, along with collagen content. This, combined with the marked reduction in plaque macrophages resulted in a significantly increased plaque stability index (by almost 60%), although there was no significant difference in plaque lipid content. There was also a lack of significant difference in plaque necrosis between the two groups. Indeed, *in vitro*, (+)-catechin allowed the normal proliferation of VSMCs in culture but attenuated PDGF-stimulated migration (Chapter 3), suggesting that (+)-catechin might delay plaque progression but enable the proliferation of VSMCs to encourage fibrous cap formation and maintenance. This is also supported by the ability of (+)-catechin to dampen macrophage ROS production and MMP activity, suggesting MMP-mediated degradation of the fibrous cap ECM components is inhibited. Indeed, intraperitoneal injection of EGCG has been found to enhance brachiocephalic atherosclerotic plaque stability in HFD-fed *Apoe*<sup>-/-</sup> mice, as shown by increased fibrous cap thickness, reduced macrophage content, and increased SMC and collagen in the plaque (Wang et al. 2018). The study also found expression levels of MMP-2 and -9 to be significantly reduced, along with circulating TNF- $\alpha$ , IL-6, MCP-1 and IFN- $\gamma$  levels. In another study, ECG-treated VSMCs exhibited reduced inflammatory response, expression of MMP-2 and ICAM-1, and foam cell formation induced by oxLDL stimulation (Li et al. 2021). Therefore, this study along with others support the ability of catechins to attenuate plaque progression and promote plaque stability. However, confirmation of VSMC staining should be done using different markers, such as myosin heavy chain 11 (MYH11), myocardin or smoothelin (Bennett et al. 2017), and specific types of collagens present within the plaque could also be investigated.

### 5.3.7 Future directions

This study has identified various beneficial effects of (+)-catechin hydrate supplementation on the development and progression of atherosclerotic lesions in the aortic root. Although *en face* preparations of the descending aorta can provide a more global insight to the distribution of atherosclerotic plaques and disease severity, this was not pursued in this study. *En face* also has various limitations (Ko et al. 2017),

and so the aortas were preserved (stored) for alternative analyses. To gain insight to the underlying mechanisms of action and to aid the generation of future mechanistic hypotheses, RNA-seq could be carried out on the descending thoracic aorta, to investigate genome-wide, whole transcriptome-level changes in gene expression induced by (+)-catechin hydrate supplementation. To aid in this, preparation of aortic RNA samples was completed and sent to Novogene at the end of this project. Pending results would provide valuable insights to how (+)-catechin induces its positive effects on the atherosclerotic plaque in the aortic root and modulates atherosclerosis-associated risk factors. Indeed, there has been an increase in studies opting for this approach, whether at the tissue or single cell level, to gain deeper mechanistic insights (Bao et al. 2016; Rippe et al. 2017; Baron et al. 2018; Kalluri et al. 2019). Beyond this, the ability of (+)-catechin to attenuate atherosclerosis development and progression should also be investigated in female *Ldlr*<sup>-/-</sup> mice, due to sex differences influencing atherosclerosis development and severity. Due to the increased susceptibility of male mice to diet-induced metabolic syndrome phenotype compared to females, males were used in all *in vivo* studies in this project. Moreover, other studies on inflammation and complement also showed major changes in male mice (Pettersson et al. 2012; Marek et al. 2017; Szpak et al. 2018). Indeed, differences in atherosclerotic plaques have been observed between male and female *Ldlr*<sup>-/-</sup> mice in another study conducted in the host laboratory investigating another nutraceutical agent, and in various other studies (Man et al. 2020). For example, female *Ldlr*<sup>-/-</sup> mice exhibit more severe, larger atherosclerotic lesions compared to their male counter parts after 12 weeks HFD feeding. Other studies also report sex differences in both *Ldlr*<sup>-/-</sup> (Zhang et al. 2006; Engelbertsen et al. 2012; Chen et al. 2020) and *ApoE*<sup>-/-</sup> (An et al. 2009; Matsumoto et al. 2016; Douglas et al. 2018) mice.

### 5.3.8 Conclusion

(+)-Catechin demonstrates anti-atherogenic activities in different cell types implicated in atherosclerosis and has protective effects on mitochondrial function. In male *Ldlr*<sup>-/-</sup> mice fed HFD, (+)-catechin hydrate supplementation modulates several atherosclerosis risk factors and attenuates plaque development and progression by attenuating macrophage infiltration. Furthermore, plaque stability was also increased

## Chapter 5: Effect of (+)-catechin on atherosclerosis development and progression

owing to fibrous cap formation and maintenance coinciding with increased VSMC and collagen content. These data are in keeping with the *in vitro* observations described in the previous chapters. Therefore, (+)-catechin demonstrates potential as a preventative agent for atherosclerosis that could be combined with current pharmacological therapies. These promising results provided the rationale for the progression onto an additional study in the same mouse model, to investigate whether (+)-catechin hydrate can induce the regression of established plaques and be used to treat clinically diagnosed atherosclerosis. This 'regression' study is hence described in the next chapter.

## 6 Effect of (+)-catechin on atherosclerosis regression

### 6.1 Introduction

(+)-Catechin demonstrates promise as a nutraceutical candidate for the prevention of atherosclerosis. This has been demonstrated by its ability to attenuate multiple early pro-atherogenic processes associated with various key cell types implicated in the disease (Chapter 3), combined with its protective effects on mitochondrial function in macrophages and ECs (Chapter 4). These positive results obtained *in vitro* prompted progression onto *in vivo* studies using the *Ldlr*<sup>-/-</sup> model. The ability of (+)-catechin to attenuate atherosclerosis development and progression was investigated in male *Ldlr*<sup>-/-</sup> mice fed HFD for 12 weeks (Chapter 5). Mice fed (+)-catechin hydrate supplemented HFD exhibited decreased plaque burden (without affecting lipid content) and inflammation, combined with increased plaque stability. Additionally, various risk factors were modulated, including reduced T cells in the bone marrow and plasma TG to HDL-C ratio, with increased brown to white adipose tissue ratio. Therefore, (+)-catechin attenuates multiple key cellular processes implicated in early atherogenesis, protecting against parameters associated with endothelial dysfunction and stimulated VSMC migration to suppress atherosclerotic plaque development *in vivo*. However, the ability of (+)-catechin to induce atherosclerosis regression is yet to be investigated. Given the promising results obtained thus far, the therapeutic potential of (+)-catechin was investigated in the same mouse model, to determine whether this agent could potentially be used to treat clinically diagnosed atherosclerosis by stimulating the regression of established plaques. Plaque development was induced with HFD feeding first, followed by dietary intervention with a NCD combined with (+)-catechin hydrate to evaluate whether plaque regression i.e., disease reversal, can be stimulated. Comparisons were then made with mice fed HFD for 12 weeks ('baseline' group), intervention with chow combined with vehicle ('chow -' group) and mice fed HFD for the full duration of the 20 weeks ('HFD' group). The data for the baseline group are the combined data obtained from the progression and regression studies (unless otherwise stated), after verification that results were the same with or without data combination (as small changes can arise if experiments are conducted at different times).

## Chapter 6: Effect of (+)-catechin on atherosclerosis regression

### 6.1.1 Experimental aims

The aims of the studies presented in this chapter were to investigate the effect of (+)-catechin on atherosclerosis regression in *Ldlr*<sup>-/-</sup> mice along with associated risk factors, to ascertain whether the regression of established plaques could be induced. Mice were fed HFD for 12 weeks to induce atherosclerosis as per studies in Chapter 5. The 'baseline' group was then sacrificed after this time whereas the chow groups were switched to NCD with vehicle ('chow -') or 200 mg/kg/day (+)-catechin hydrate ('chow +') supplemented drinking water for 8 weeks, to stimulate plaque regression. Unlike HFD, liquids cannot easily be mixed with chow pellets, which would have required softening with water overnight due to their dry and hard texture, and so the (+)-catechin hydrate solution was dissolved into the drinking water (which was changed regularly). The amount of this modified drinking water drunk by the mice was also monitored regularly, to ensure that there were no issues relating to palatability affecting the volume of water intake. This time point was selected based upon a previous study conducted in the host laboratory whereby atherosclerotic plaque regression was not observed after 4 weeks of NCD compared to baseline (although plaque inflammation was attenuated). Prior to starting the regression study, and based upon the published literature, a trial involving 3-4 mice per group was conducted to compare intervention of 8 vs 12 weeks NCD (with and without agent) on the regression of established plaques induced by 12 weeks of HFD feeding. As changes were seen after 8 weeks of NCD feeding (data not shown), and other published studies having used 6-8 weeks (Gijbels et al. 1999; Peled et al. 2017; Chassot et al. 2018; Guo et al. 2018), the 8-week duration was selected for the regression study. An additional control group maintained on HFD for the entirety of the 20 weeks was also included, to compare the effects of chow with continued HFD-induced atherosclerosis progression.

### 6.1.2 Experimental strategy

A summary of the experimental strategy is illustrated in Figure 6.1.

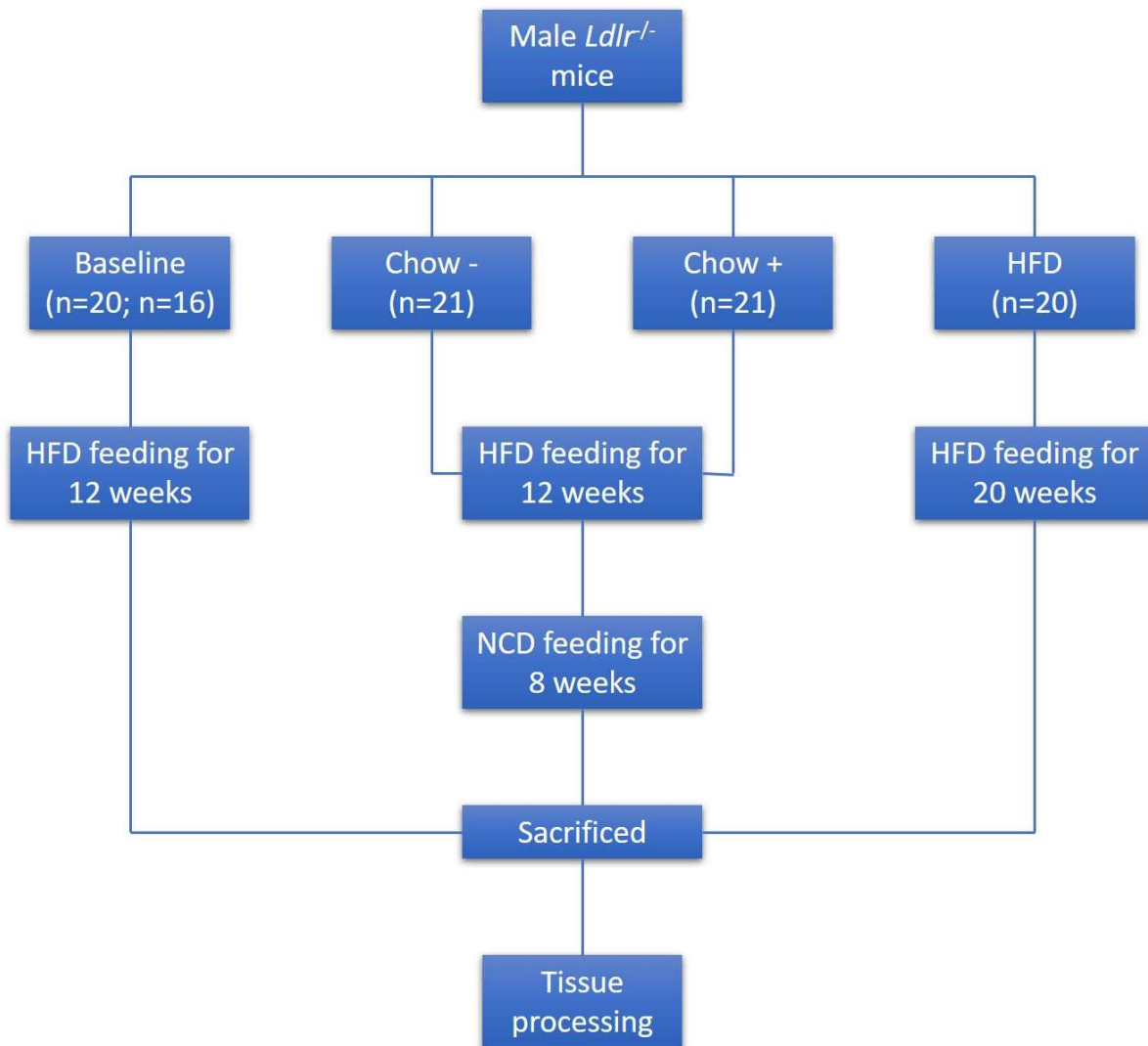


**Figure 6.1 Summary of experimental strategy.**

*Ldlr*<sup>-/-</sup> mice were randomly assigned to four groups. All mice received HFD for 12 weeks; the baseline group were sacrificed after this time whereas the chow groups were switched to NCD for 8 weeks before being sacrificed. The HFD group was continued on HFD for these 8 weeks before being sacrificed. Processing of the relevant tissue samples was then done as described in Chapter 5. The baseline group consists of the combined data for both *in vivo* studies as part of the experimental series conducted in this project. Abbreviations: *Ldlr*, low-density lipoprotein; HFD, high-fat diet; NCD, normal chow diet.

## 6.2 Results

### 6.2.1 Adiposity and key organs

There were no significant differences in total weight gain between the chow - ( $7.59 \pm 0.37$  g) or the chow + ( $7.11 \pm 0.31$  g) groups, or when these were compared to the baseline group ( $7.45 \pm 0.34$  g). However, the HFD group ( $11.67 \pm 0.82$  g) gained significantly more weight compared to all other groups ( $p < 0.001$ ) (Figure 6.2A).

Furthermore, from the point of switching to NCD after 12 weeks of HFD feeding, both the chow - ( $-0.73 \pm 0.32$  g) and chow + ( $0.30 \pm 0.31$  g) groups gained substantially less weight compared to the HFD group ( $3.38 \pm 0.46$  g) ( $p < 0.001$ ). However, there was no significant difference in weight gain between the two chow groups, despite the chow + group having a higher average weight gain of 1.035 g compared to the chow - group (Figure 6.2B). The mean mouse weights for the chow and HFD groups for the entire 20 weeks are shown in Figure 6.2C. The mean mouse weights of both chow groups were significantly lower than that of the HFD group ( $p < 0.001$ ) from weeks 12 to 20, and mice of the chow + group maintained significantly lower body weights compared to those of the chow - group ( $p < 0.001$ ) during these 8 weeks (Figure 6.2D).

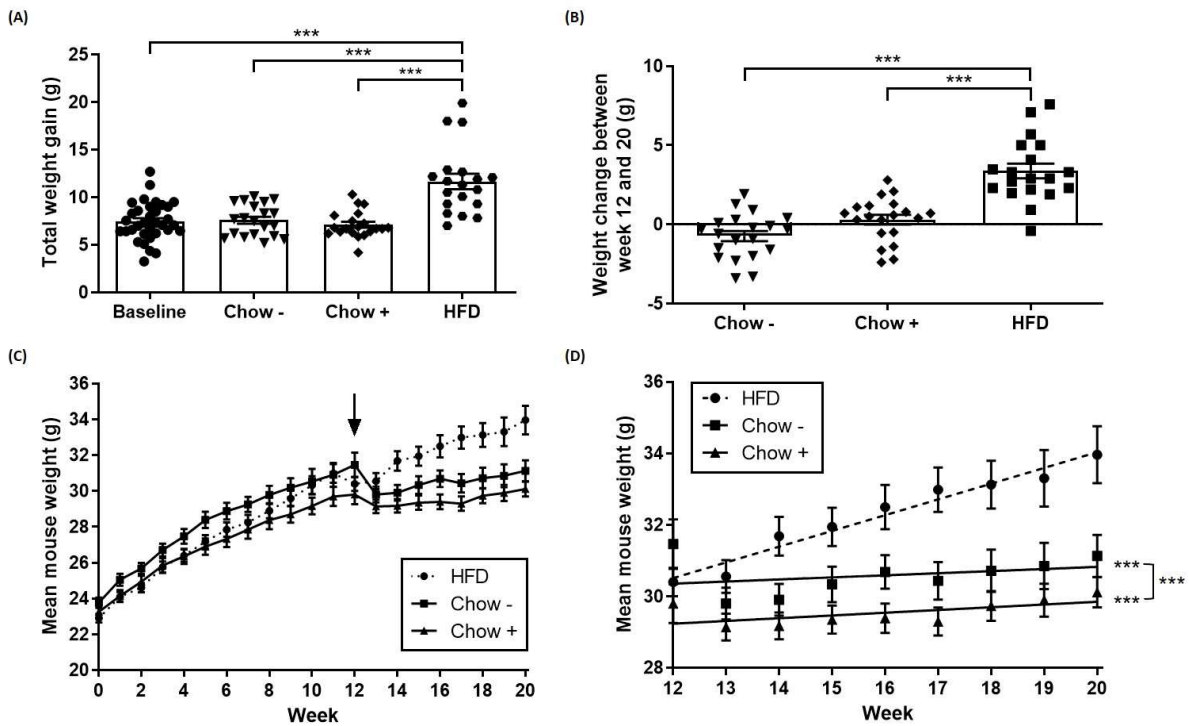


**Figure 6.2** Changes in mouse weights over time.

Male *Ldlr*<sup>-/-</sup> mice (8-week-old) were fed high-fat diet (HFD) supplemented with vehicle for 12 weeks. The 'baseline' group were then sacrificed, whereas the chow groups were switched to normal chow diet (NCD) with vehicle ('chow -') or 200 mg/kg/day (+)-catechin hydrate ('chow +') given in the drinking water for 8 weeks before being sacrificed. The 'HFD' group was maintained on vehicle supplemented HFD for a further 8 weeks before being sacrificed. The total weight gain for all groups is shown in (A; n=34, 20, 20 and 19 respectively). The baseline group consists of the combined data obtained from both *in vivo* studies as part of the experimental series conducted in this project. The weight change from week 12 to week 20 for the relevant groups are shown in (B; n=20, 20 and 19 respectively), along with the mean mouse weights for the duration of the study, with the arrow indicating the point of switching to NCD (C), and linear regression analysis of the mean mouse weights from week 12 to week 20 (D). Statistical analysis via one-way ANOVA with Tukey's post-hoc test (A and B) where \*\*\*,  $p < 0.001$  compared to HFD unless otherwise indicated.

6.2.1.1 (+)-Catechin reduces the accumulation of inguinal, gonadal and renal fat compared to baseline

All subsequent adipose tissue and organ weights have been standardised to individual body weights. The baseline, chow - and chow + groups had significantly less subcutaneous adipose tissue compared to the HFD group by 43.92% (15.47 mg;  $p=0.001$ ), 51.28% (18.06 mg;  $p<0.001$ ) and 54.09% (19.05 mg;  $p<0.001$ ) respectively (Figure 6.3A). Only the chow + group had significantly reduced inguinal adipose tissue compared to both the baseline and HFD groups by 45.93% (0.65 mg;  $p=0.014$ ) and 41.58% (0.54 mg;  $p=0.004$ ) respectively (Figure 6.3B). Furthermore, the chow + group had significantly decreased gonadal adipose tissue compared to both the baseline and HFD groups by 30.25% (7.66 mg;  $p=0.021$ ) and 56.82% (23.24 mg;  $p<0.001$ ) respectively (Figure 6.3C). The baseline and chow - groups also had significantly reduced gonadal fat compared to the HFD group by 38.09% (15.58 mg;  $p=0.005$ ) and 45.50% (18.61 mg;  $p=0.001$ ) respectively. Moreover, the chow + group had reduced renal adipose tissue compared to the baseline and HFD groups by 32.07% (2.90 mg;  $p=0.092$ ; trend) and 61.22% (9.71 mg;  $p<0.001$ ) respectively (Figure 6.3D). The baseline and chow - groups also had significantly decreased renal fat by 42.91% (6.81 mg;  $p=0.006$ ) and 53.70% (8.52 mg;  $p=0.009$ ) respectively. When the chow groups were compared in isolation using an unpaired t-test, the chow + group had significantly reduced inguinal adipose tissue compared to the chow - group by 22.83% (0.23 mg;  $p=0.037$ ) (data not shown).

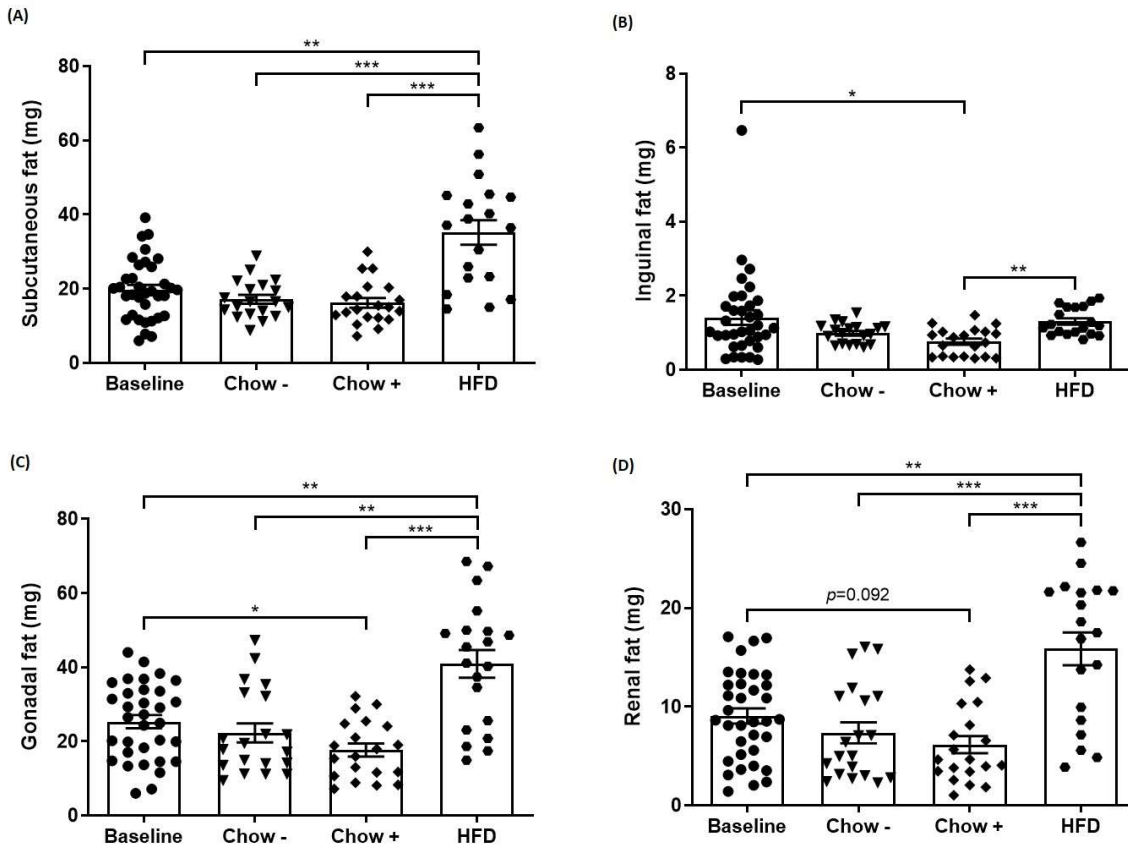


**Figure 6.3 White adipose tissue deposits.**

Male *Ldlr*<sup>-/-</sup> mice (8-week-old) were fed high-fat diet (HFD) supplemented with vehicle for 12 weeks. The 'baseline' group were then sacrificed, whereas the chow groups were switched to normal chow diet with vehicle ('chow -') or 200 mg/kg/day (+)-catechin hydrate ('chow +') given in the drinking water for 8 weeks before being sacrificed, and the 'HFD' group were maintained on vehicle-supplemented HFD for 8 weeks (a total of 20 weeks) before being sacrificed. The subcutaneous (A; n=35, 19, 20 and 19 respectively), inguinal (B; n=34, 19, 20 and 19 respectively), gonadal (C; n=33, 20, 20 and 20 respectively) and renal (D; n=35, 20, 20 and 19 respectively) adipose tissue deposits were then taken and weighed (and standardised to body weight). The baseline group consists of the combined data obtained from both *in vivo* studies as part of the experimental series conducted in this project. All measurements standardised to the individual mouse weights. Statistical analysis via one-way ANOVA with Games-Howell post-hoc test (A, C, D) or Kruskal-Wallis test (B) where \*,  $p \leq 0.05$ ; \*\*,  $p < 0.01$ ; \*\*\*,  $p < 0.001$ .

### 6.2.1.2 (+)-Catechin increases the ratio of brown to white fat compared to baseline

The baseline, chow - and chow + groups had less interscapular brown adipose tissue compared to the HFD group by 21.31% (1.14 mg;  $p=0.004$ ), 20.94% (1.12 mg;  $p=0.016$ ) and 16.83% (0.90 mg;  $p=0.077$ , trend) respectively (Figure 6.4A). The chow + group also had significantly reduced total white adipose tissue (calculated as the sum of the subcutaneous, inguinal, gonadal and renal fat) compared to the baseline and HFD groups by 27.59% (15.52 mg;  $p=0.038$ ) and 55.67% (51.17 mg;  $p < 0.001$ )

respectively (Figure 6.4B). The baseline and chow - groups also had significantly reduced total white adipose tissue compared to the HFD group by 38.79% (35.65 mg;  $p=0.005$ ) and 49.97% (45.93 mg;  $p<0.001$ ) respectively. Furthermore, only the chow + group had significantly increased ratio of brown to white adipose tissue compared to both the baseline and HFD groups by 51.55% (ratio of 0.04) and 92.89% (ratio of 0.06) respectively ( $p<0.001$ ) (Figure 6.4C). The chow - group also had a significantly higher ratio of brown to white adipose tissue compared to the HFD group by 55.41% (ratio of 0.03;  $p=0.003$ ). The baseline, chow - and chow + groups had significantly reduced total fat (calculated as the sum of all five adipose tissue deposits) compared to the HFD group by 36.23% (35.20 mg;  $p=0.007$ ), 48.32% (46.94 mg;  $p<0.001$ ) and 53.47% (51.95 mg;  $p<0.001$ ) respectively; however, only the chow + group had significantly decreased total fat compared to the baseline group by 27.04% (16.75 mg;  $p=0.038$ ) (Figure 6.4D). Although the chow + group had increased ratio of brown to white adipose tissue compared to the chow - group by 24.71% (ratio of 0.02), this was only found to be significant when the two groups were analysed in isolation using an unpaired t-test ( $p=0.030$ ) (data not shown).

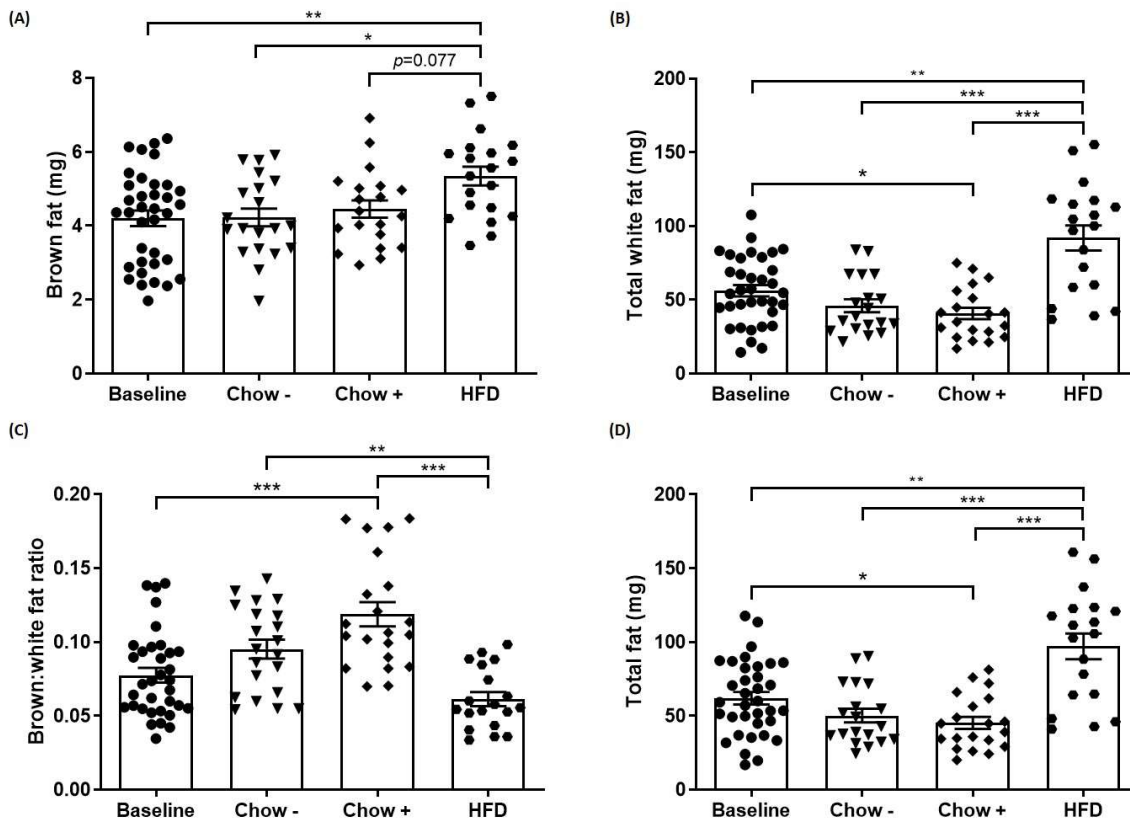


**Figure 6.4 White and brown adipose tissue analysis.**

Male *Ldlr*<sup>-/-</sup> mice (8-week-old) were fed high-fat diet (HFD) supplemented with vehicle for 12 weeks. The 'baseline' group were then sacrificed, whereas the chow groups were switched to normal chow diet with vehicle ('chow -') or 200 mg/kg/day (+)-catechin hydrate ('chow +') given in the drinking water for 8 weeks before being sacrificed. The 'HFD' group was maintained on vehicle supplemented HFD for a further 8 weeks before being sacrificed. The baseline group consists of the combined data obtained from both *in vivo* studies as part of the experimental series conducted in this project. All measurements standardised to the individual mouse weights. The weights of the interscapular brown fat (A; n=36, 20, 20 and 20 respectively), total white fat (B; n=35, 19, 20 and 19 respectively), ratio of brown to white fat (C; n=34, 21, 21 and 19 respectively) and total fat (D; n=35, 19, 20 and 19 respectively) are shown. Total white fat calculated as the sum of the subcutaneous, inguinal, gonadal and renal adipose tissue weights. Total fat calculated as the sum of these plus the brown adipose tissue weight. Statistical analysis via one-way ANOVA with Tukey's (A, B) or Games-Howell (D) post-hoc test, or Kruskal Wallis test (C) where \*,  $p \leq 0.05$ ; \*\*,  $p < 0.01$ ; \*\*\*,  $p < 0.001$ .

### 6.2.1.3 (+)-Catechin increases certain organ weights compared to baseline

There were no significant differences in the spleen weights between all groups (Figure 6.5A). However, both the chow - and chow + groups had significantly increased liver weights compared to the baseline group by 8.44% (3.58 mg;  $p=0.006$ ) and 10.01% (4.25 mg;  $p < 0.001$ ) respectively, as well as compared to the HFD group by 9.18% (3.87 mg;  $p=0.010$ ) and 10.77% (4.54 mg;  $p=0.002$ ) respectively (Figure 6.5B). Moreover, the chow - group had significantly greater heart weight compared to the

HFD group by 13.37% (0.68 mg;  $p=0.040$ ) (Figure 6.5C). Additionally, the chow -, chow + and HFD groups all had increased thymus weights compared to the baseline group by 36.38% (0.37 mg;  $p=0.009$ ), 29.11% (0.30 mg;  $p=0.054$ ; trend) and 27.93% (0.28 mg;  $p=0.077$ , trend) respectively (Figure 6.5D).

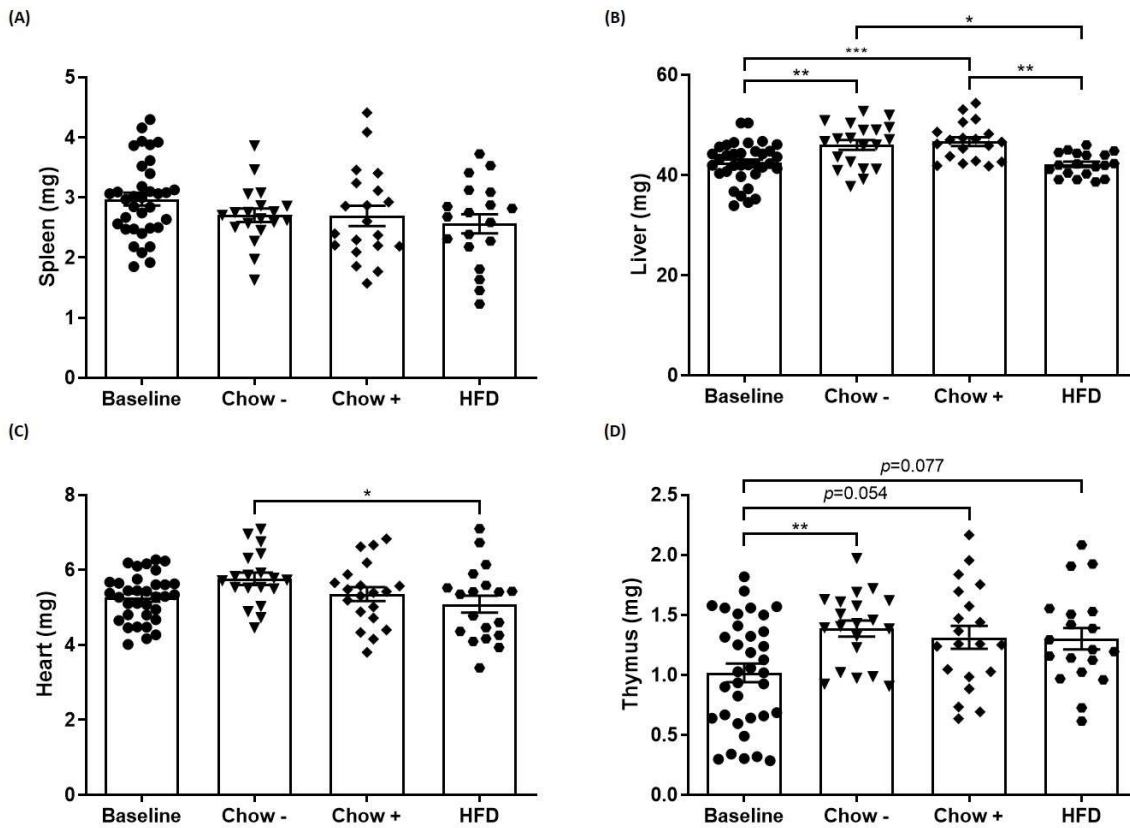


**Figure 6.5 Organ weights.**

Male *Ldlr*<sup>-/-</sup> mice (8-week-old) were fed high-fat diet (HFD) supplemented with vehicle for 12 weeks. The 'baseline' group were then culled, whereas the chow groups were switched to normal chow diet with vehicle ('chow -') or 200 mg/kg/day (+)-catechin hydrate ('chow +') given in the drinking water for 8 weeks before being sacrificed, whereas the 'HFD' group were maintained on vehicle-supplemented HFD for a further 8 weeks before being sacrificed. The baseline group consists of the combined data obtained from both *in vivo* studies as part of the experimental series conducted in this project. All measurements standardised to the individual mouse weights. The weights of the spleen (A; n=35, 19, 20 and 19 respectively), liver (B; n=35, 20, 19 and 19 respectively), heart (C; n=34, 19, 20 and 19 respectively) and thymus (D; n=35, 20, 20 and 19 respectively) are shown. Statistical analysis via one-way ANOVA with Tukey's post-hoc test where \*,  $p \leq 0.05$ ; \*\*,  $p < 0.01$ ; \*\*\*,  $p < 0.001$ .

There were no statistically significant differences in cardiac hypertrophy index (calculated as the ratio of heart weight to tibia length) between all groups (Figure 6.6). However, when the chow groups were compared in isolation using an unpaired t-test, the chow + group had a trend of reduced cardiac hypertrophy compared to the chow - group by 7.73% ( $p=0.059$ ) (data not shown).

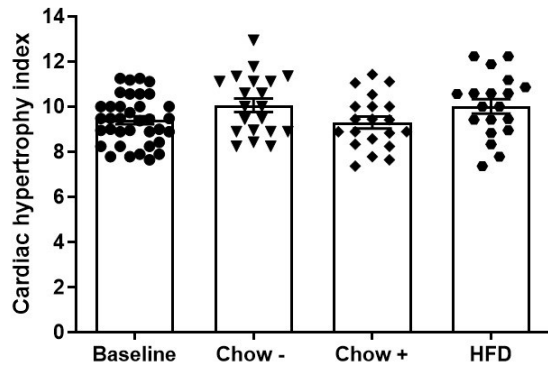


**Figure 6.6 Cardiac hypertrophy index.**

Male *Ldlr*<sup>-/-</sup> mice (8-week-old) were fed high-fat diet (HFD) supplemented with vehicle for 12 weeks. The 'baseline' group were then culled, whereas the chow groups were switched to normal chow diet with vehicle ('chow -') or 200 mg/kg/day (+)-catechin hydrate ('chow +') given in the drinking water for 8 weeks before being sacrificed, whereas the 'HFD' group were maintained on vehicle-supplemented HFD for a further 8 weeks before being sacrificed. The baseline group consists of the combined data obtained from both *in vivo* studies as part of the experimental series conducted in this project. Cardiac hypertrophy index calculated as heart weight (mg) divided by tibia length (mm). Statistical analysis via one-way ANOVA with Tukey's post-hoc test.

### 6.2.2 Bone marrow stem, progenitor and immune cell population analysis

Due to school closures and a cease in research activity during the pandemic, flow cytometry analysis could not be conducted on all samples and so the subsequent data presented are that obtained from the affected study only (i.e., the regression study). No bone marrow or peripheral blood cell population analysis data are available for mice fed HFD for 20 weeks. The total number of bone marrow cells extracted in the chow + groups was significantly greater than that of the baseline ( $p=0.046$ ) and chow - ( $p<0.001$ ) groups (Figure 6.7B). However, there were no significant differences in total WBCs between the groups as measured by flow cytometry analysis (Figure 6.7C). Therefore, all subsequent bone marrow cell population analysis data are presented as percentage of total WBCs.

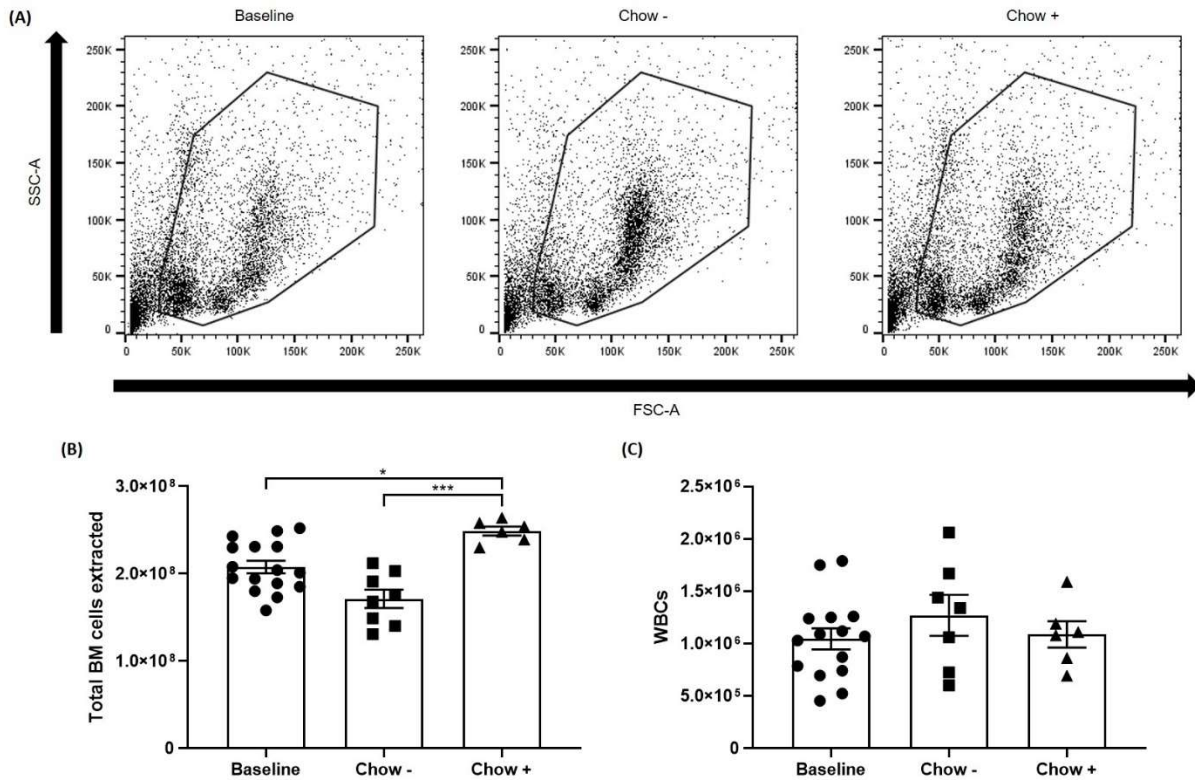


**Figure 6.7 Total cell count and number of white blood cells in the bone marrow.**

Male *Ldlr*<sup>-/-</sup> mice (8-week-old) were fed high-fat diet supplemented with vehicle for 12 weeks. The 'baseline' group were then culled, whereas the chow groups were switched to normal chow diet with vehicle ('chow -') or 200 mg/kg/day (+)-catechin hydrate ('chow +') given in the drinking water for 8 weeks before being sacrificed. The tibia and fibula were then taken, and BM cells were extracted for immunophenotyping using flow cytometry. The total number of bone marrow cells extracted prior to analysis was manually counted using a haemocytometer under a microscope (B; n=16, 8 and 6 respectively). The total number of WBCs was then obtained using flow cytometry (C; n=15, 7 and 6 respectively), with representative dot plots and gating shown in (A). Statistical analysis via one-way ANOVA with Tukey's post-hoc test (C) or Kruskal Wallis test (B) where \*,  $p \leq 0.05$ ; \*\*\*,  $p < 0.001$ .

### 6.2.2.1 (+)-Catechin reduces the proportion of HPC II and MPP cells compared to baseline

In the SLAM class of cells, the chow - group had significantly reduced proportion of HPC I and II compared to the baseline group (Figure 6.8B and C) by 41.29% ( $p=0.003$ ) and 64.45% ( $p=0.002$ ) respectively. The chow + group also had significantly decreased proportion of HPC II compared to the baseline group by 67.33% ( $p=0.001$ ) (Figure 6.8C). However, the chow + group had significantly increased proportion of MPP cells compared to the baseline group by 37.55% ( $p=0.006$ ) (Figure 6.8D). There were no significant differences in the proportion of HSCs between the three groups.

## Chapter 6: Effect of (+)-catechin on atherosclerosis regression

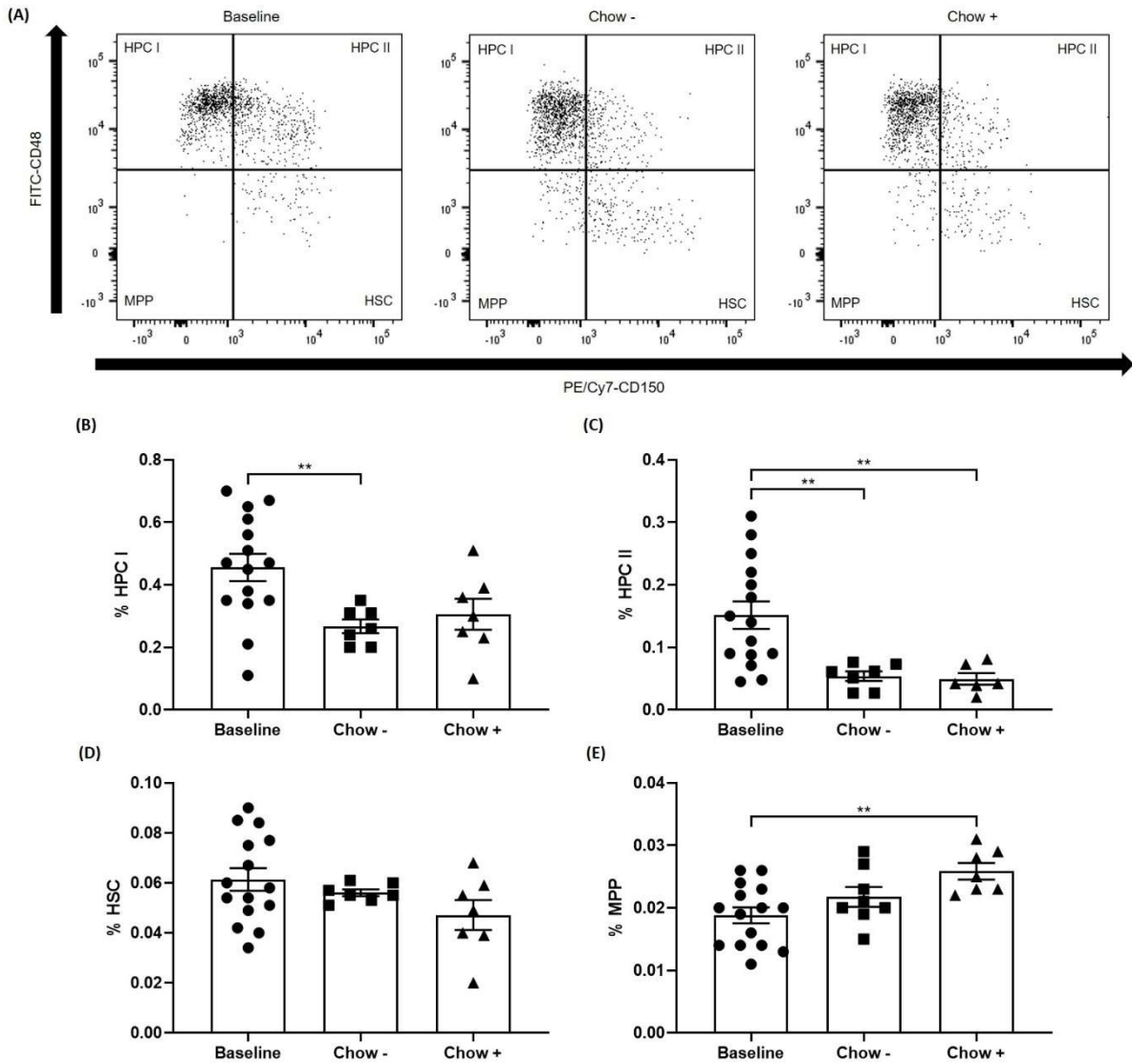


**Figure 6.8 Effect of (+)-catechin on stem cell populations in the bone marrow.**

Male *Ldlr*<sup>-/-</sup> mice (8-week-old) were fed high-fat diet supplemented with vehicle for 12 weeks. The 'baseline' group were then culled, whereas the chow groups were switched to normal chow diet with vehicle ('chow -') or 200 mg/kg/day (+)-catechin hydrate ('chow +') given in the drinking water for 8 weeks before being sacrificed. The tibia and fibula were then taken, and BM cells were extracted for immunophenotyping using flow cytometry. Data presented as percentage of total white blood cells. Representative dot plots along with the gating strategy are shown in (A), enabling analysis of the fluorescein isothiocyanate (FITC)-CD48<sup>-</sup> phycoerythrin/cyanine7 (PE/Cy7)-CD34<sup>-</sup> multipotent progenitor (MPP), FITC-CD48<sup>-</sup> PE/Cy7-CD34<sup>+</sup> haematopoietic stem cell (HSC), and haematopoietic progenitor cell (HPC) I (FITC-CD48<sup>+</sup> PE/Cy7-CD34<sup>-</sup>) and II (FITC-CD48<sup>+</sup> PE/Cy7-CD34<sup>+</sup>) populations. Statistical analysis via one-way ANOVA with Tukey's (E) or Games-Howell (B-D) post-hoc test where \*\*,  $p < 0.01$ .

### 6.2.2.2 (+)-Catechin increases the proportion of progenitor cells compared to baseline

In the progenitor class of cells, the chow + group had an increase in the proportion of CMP and MEP cells compared to the baseline group by 58.16% ( $p = 0.065$ ; trend)

## Chapter 6: Effect of (+)-catechin on atherosclerosis regression

(Figure 6.9C) and 61.63% ( $p=0.042$ ) (Figure 6.9E) respectively. However, no significant changes were found in the GMP or CLP cells compared to the baseline group, or in all types of progenitor cells between the chow - and chow + groups themselves.

## Chapter 6: Effect of (+)-catechin on atherosclerosis regression

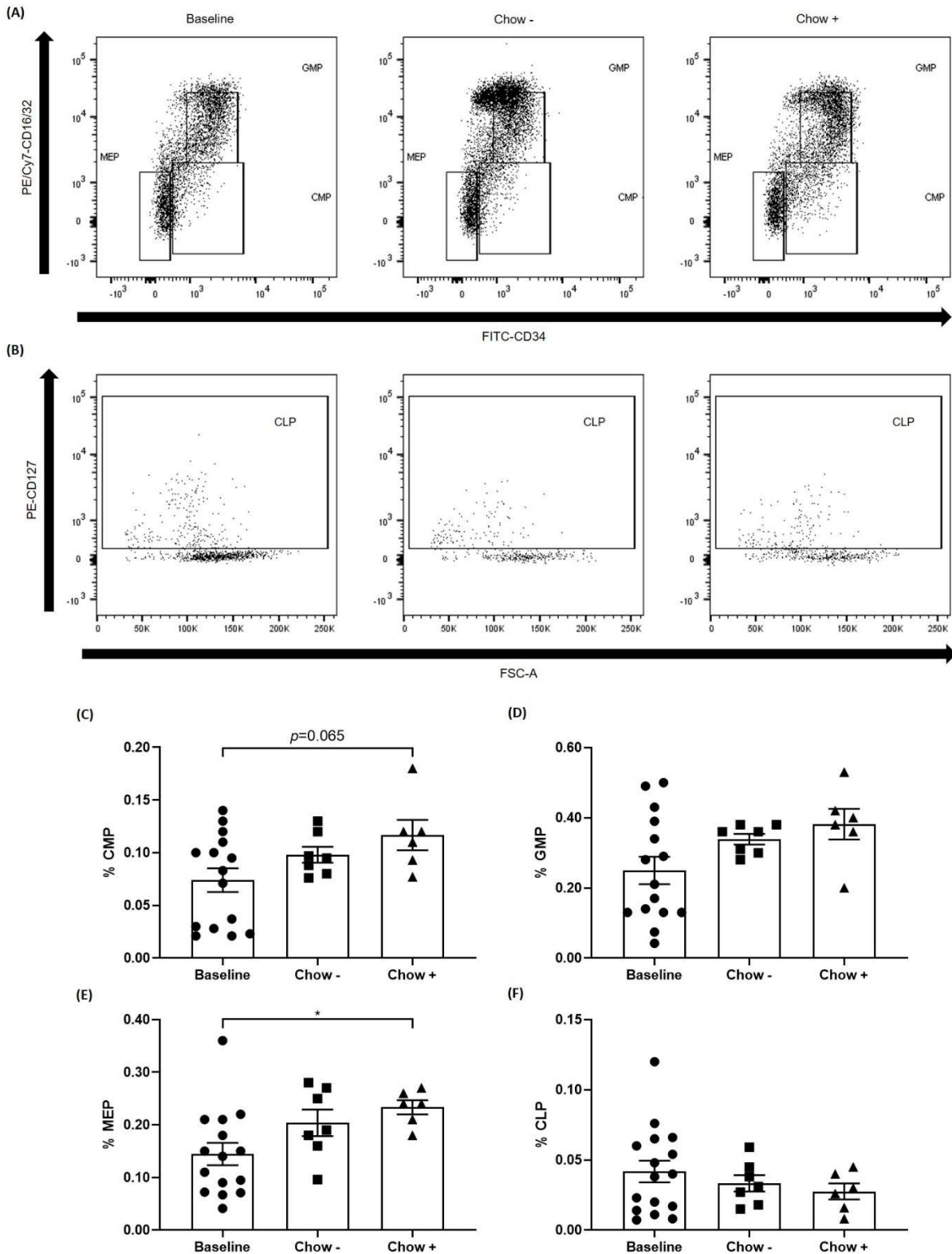


**Figure 6.9** Effect of (+)-catechin on progenitor cell populations in the bone marrow.

Male *Ldlr*<sup>-/-</sup> mice (8-week-old) were fed high-fat diet supplemented with vehicle for 12 weeks. The 'baseline' group were then culled, whereas the chow groups were switched to normal chow diet with vehicle ('chow -') or 200 mg/kg/day (+)-catechin hydrate ('chow +') given in the drinking water for 8 weeks before being sacrificed. The tibia and fibula were then taken, and BM cells were extracted for immunophenotyping using flow cytometry. Data presented as percentage of total white blood cells. Representative dot plots along with the gating strategies are shown in (A) and (B), enabling analysis of

## Chapter 6: Effect of (+)-catechin on atherosclerosis regression

the phycoerythrin/cyanine7 (PE/Cy7)-CD16/32<sup>-</sup> fluorescein isothiocyanate (FITC)-CD34<sup>-</sup> megakaryocyte-erythroid progenitor (MEP) (E; n=15, 7 and 6 respectively), PE/Cy7-CD16/32<sup>+</sup> FITC-CD34<sup>+</sup> granulocyte-macrophage progenitor (GMP) (D; n=15, 7 and 6 respectively) and PE/Cy7-CD16/32<sup>-</sup> FITC-CD34<sup>+</sup> common myeloid progenitor (CMP) (C; n=15, 7 and 6 respectively), and PE-CD127<sup>+</sup> common lymphoid progenitor (CLP) (F; n=16, 7 and 6 respectively) cell populations respectively. Statistical analysis via one-way ANOVA with Tukey's (C, E, F) or Games-Howell (D) post-hoc test where \*,  $p \leq 0.05$ .

### 6.2.2.3 (+)-Catechin has no significant effects on lineage<sup>+</sup> cell populations

The chow + group had a trend of increased proportion of T cells compared to the baseline group by 42.56% ( $p=0.085$ ; trend) (Figure 6.10E). However, no significant changes in the proportion of MDSCs (Figure 6.10C), macrophages (Figure 6.10D) or B cells (Figure 6.10F) were found between all three groups.

## Chapter 6: Effect of (+)-catechin on atherosclerosis regression

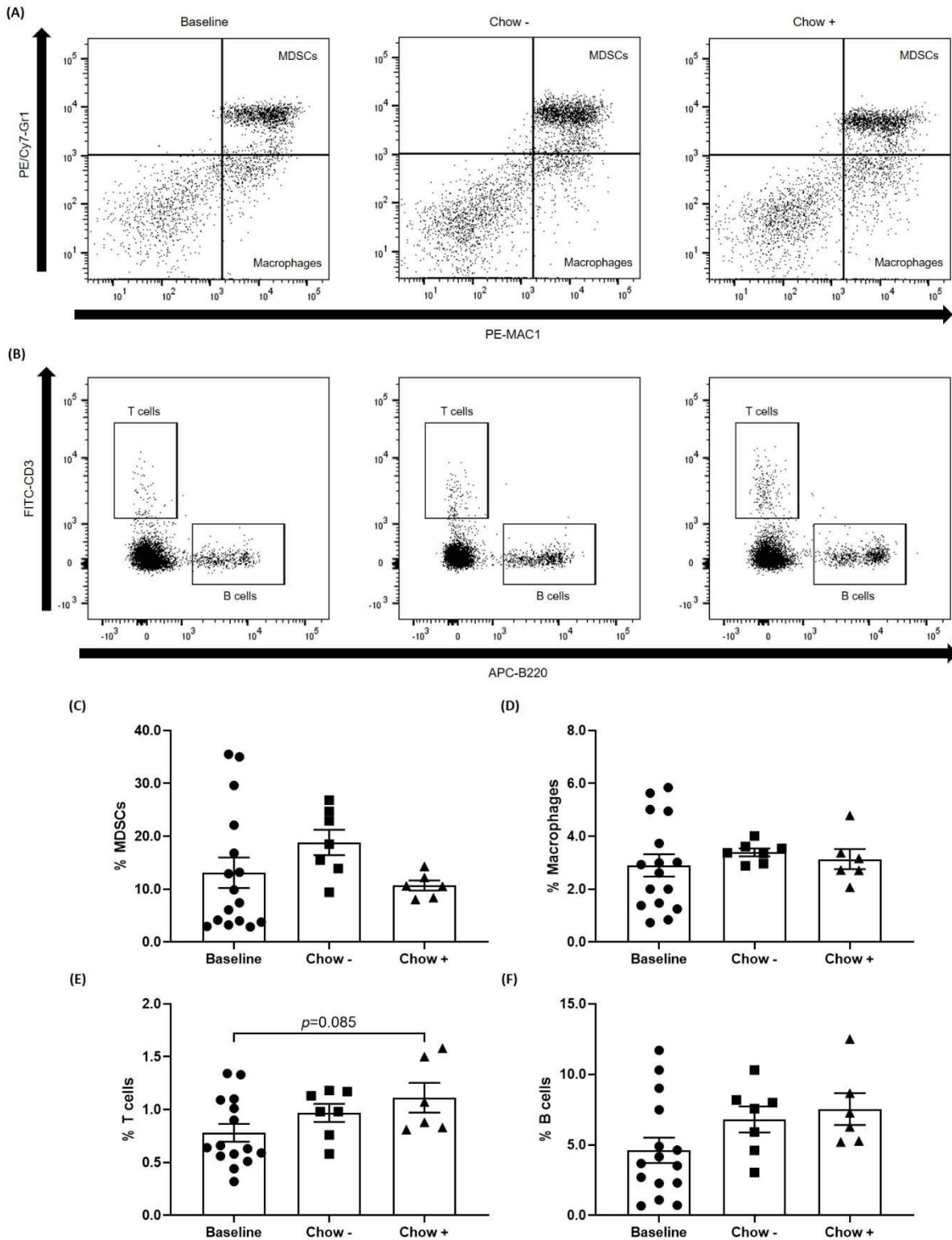


**Figure 6.10 Effect of (+)-catechin on lineage<sup>+</sup> cell populations in the bone marrow.**

Male *Ldlr*<sup>-/-</sup> mice (8-week-old) were fed high-fat diet supplemented with vehicle for 12 weeks. The 'baseline' group were then culled, whereas the chow groups were switched to normal chow diet with vehicle ('chow -') or 200 mg/kg/day (+)-catechin hydrate ('chow +') given in the drinking water for 8 weeks before being sacrificed. The tibia and fibula were then taken, and BM cells were extracted for immunophenotyping using flow cytometry. Data presented as percentage of total white blood cells. Representative dot plots along with the gating strategies are shown in (A) and (B), enabling analysis of the phycoerythrin/cyanine7 (PE/Cy7)-Gr1<sup>+</sup> PE-CD11b<sup>+</sup> myeloid-derived suppressor cells (MDSCs) (C;

## Chapter 6: Effect of (+)-catechin on atherosclerosis regression

n=16, 7 and 6 respectively) and PE/Cy7-Gr1<sup>-</sup> PE-CD11b (MAC1)<sup>+</sup> macrophages (D; n=16, 7 and 6 respectively), and fluorescein isothiocyanate (FITC)-CD3<sup>+</sup> T (E; n=15, 7 and 6 respectively) and allophycocyanin (APC)-B220<sup>+</sup> B (F; n=15, 7 and 6 respectively) cells respectively. Statistical analysis via one-way ANOVA with Tukey's (E and F) or Games-Howell (D) post-hoc test, or Kruskal-Wallis test (C) where  $p \leq 0.05$  was considered significant.

### 6.2.3 Peripheral blood immune cell population analysis

The chow - group had a trend of increased number of total WBCs in the peripheral blood compared to baseline ( $p=0.093$ ), but not compared to the chow + group (Figure 6.11B). Therefore, due to possible differences in the total WBC counts as determined by flow cytometry analysis, all subsequent data are presented as cell counts, rather than percentage of total WBCs.

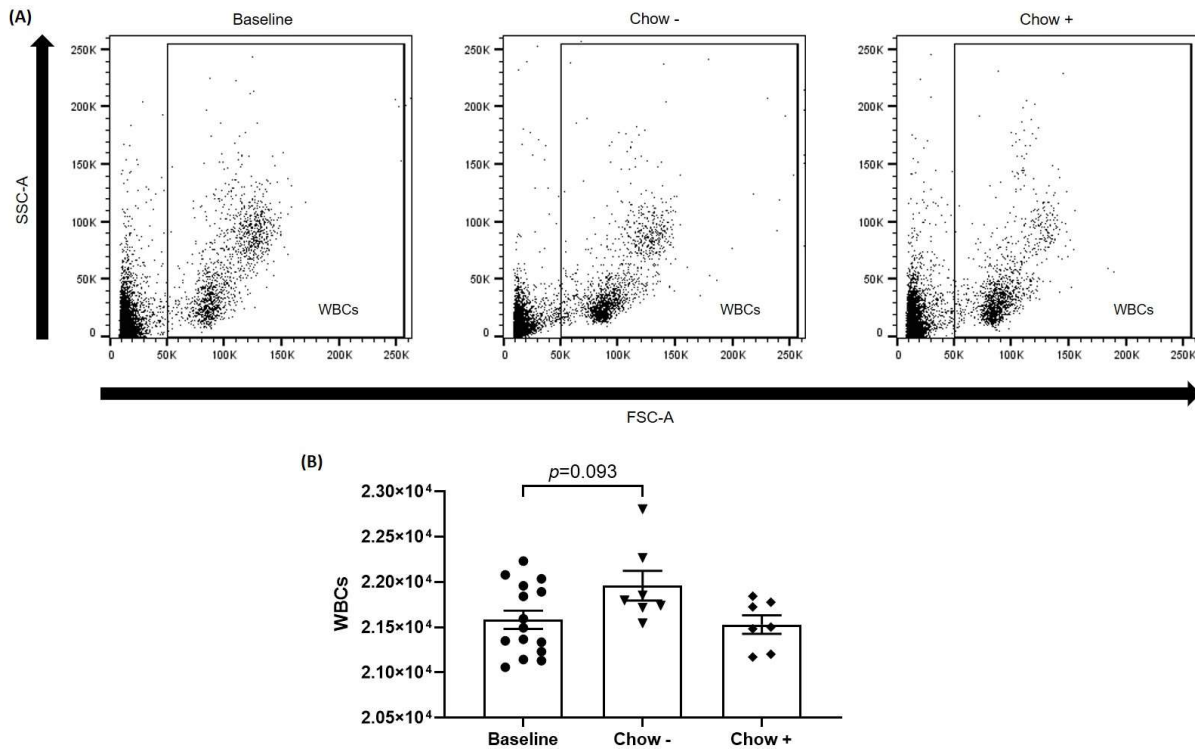


**Figure 6.11 Effect of (+)-catechin on the number of white blood cells in the peripheral blood.** Male *Ldlr*<sup>-/-</sup> mice (8-week-old) were fed high-fat diet supplemented with vehicle for 12 weeks. The 'baseline' group were then culled, whereas the chow groups were switched to normal chow diet with vehicle ('chow -') or 200 mg/kg/day (+)-catechin hydrate ('chow +') given in the drinking water for 8 weeks before being sacrificed. Peripheral blood was extracted from the tail on the day before the scheduled end point for immunophenotyping using flow cytometry analysis. Representative dot plots and gating strategy are shown in (A) which enabled quantification of total white blood cells (WBCs) (B; n=15, 7 and 7 respectively). Statistical analysis via one-way ANOVA with Tukey's post-hoc test where  $p \leq 0.05$  was considered significant.

6.2.3.1 (+)-Catechin reduces the number of NK cells compared to baseline

The (+)-catechin group had significantly decreased the number of NK cells in the peripheral blood compared to the baseline group (Figure 6.12H). However, no significant changes in the number of B cells (Figure 6.12D), T cells (Figure 6.12E), or analysed subsets of T cells (Figures 6.12F and G) were found between all groups.

# Chapter 6: Effect of (+)-catechin on atherosclerosis regression

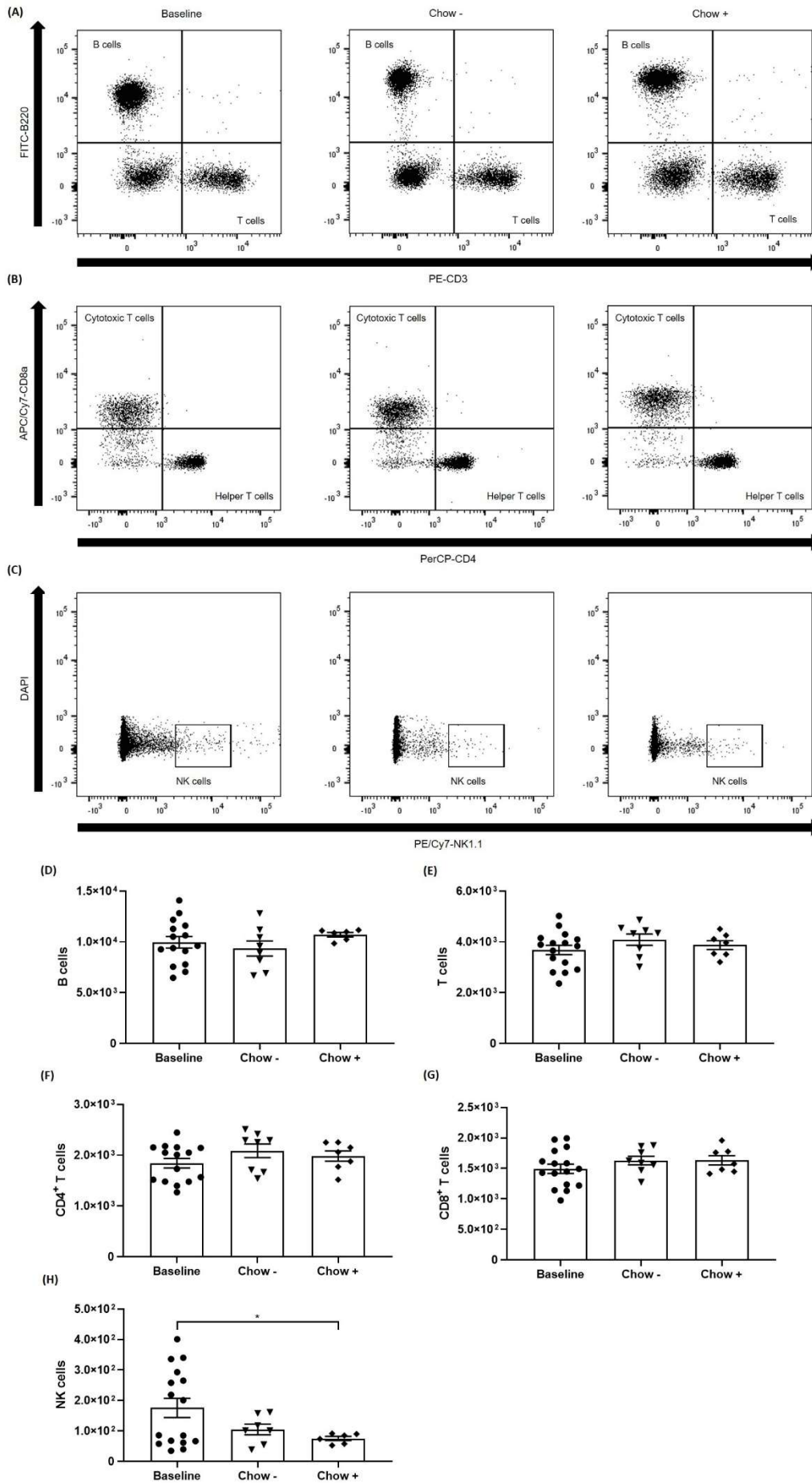


**Figure 6.12 Effect of (+)-catechin on lymphoid cell populations in the peripheral blood.**

Male *Ldlr*<sup>-/-</sup> mice (8-week-old) were fed high-fat diet supplemented with vehicle for 12 weeks. The 'baseline' group were then culled, whereas the chow groups were switched to normal chow diet with vehicle ('chow -') or 200 mg/kg/day (+)-catechin hydrate ('chow +') given in the drinking water for 8 weeks before being sacrificed. Peripheral blood was extracted from the tail on the day before the end point for immunophenotyping using flow cytometry analysis. Representative dot plots and gating strategies for fluorescein isothiocyanate (FITC)-B220<sup>+</sup> B and phycoerythrin (PE)-CD3<sup>+</sup> T cells (A), peridinin-chlorophyll-protein (PerCP)-CD4<sup>+</sup> helper and allophycocyanin/cyanine7 (APC/Cy7)-CD8<sup>+</sup> cytotoxic T cells (B), and PE/Cy7-NK1.1<sup>+</sup> natural killer (NK) cells (C) are shown. This enabled quantification of B (D; n=15, 8 and 6 respectively), general T (E; n=16, 8 and 7 respectively), CD4<sup>+</sup> T (F; n=15, 8 and 7 respectively), CD8<sup>+</sup> T (G; n=16, 8 and 7 respectively) and NK (H; n=16, 7 and 6 respectively) cells. Statistical analysis via one-way ANOVA with post-hoc Tukey's (E, G) or Games-Howell (D, H) post-test, or Kruskal Wallis (F) test where \*,  $p \leq 0.05$ .

6.2.3.2 (+)-Catechin increases the number of monocytes

No significant differences were found in the number of macrophages (Figure 6.13D), granulocytes (Figure 6.13E), or Ly6C<sup>low/high</sup> monocytes (Figure 6.13G and I) between the three groups. However, the chow + group had significantly increased number of monocytes compared to the chow - group ( $p=0.030$ ) (Figure 6.13F). Specifically, the chow + group had increased number of Ly6C<sup>middle</sup> monocytes compared to the baseline ( $p=0.011$ ) and chow - ( $p=0.092$ ; trend) groups (Figure 6.13H).

# Chapter 6: Effect of (+)-catechin on atherosclerosis regression

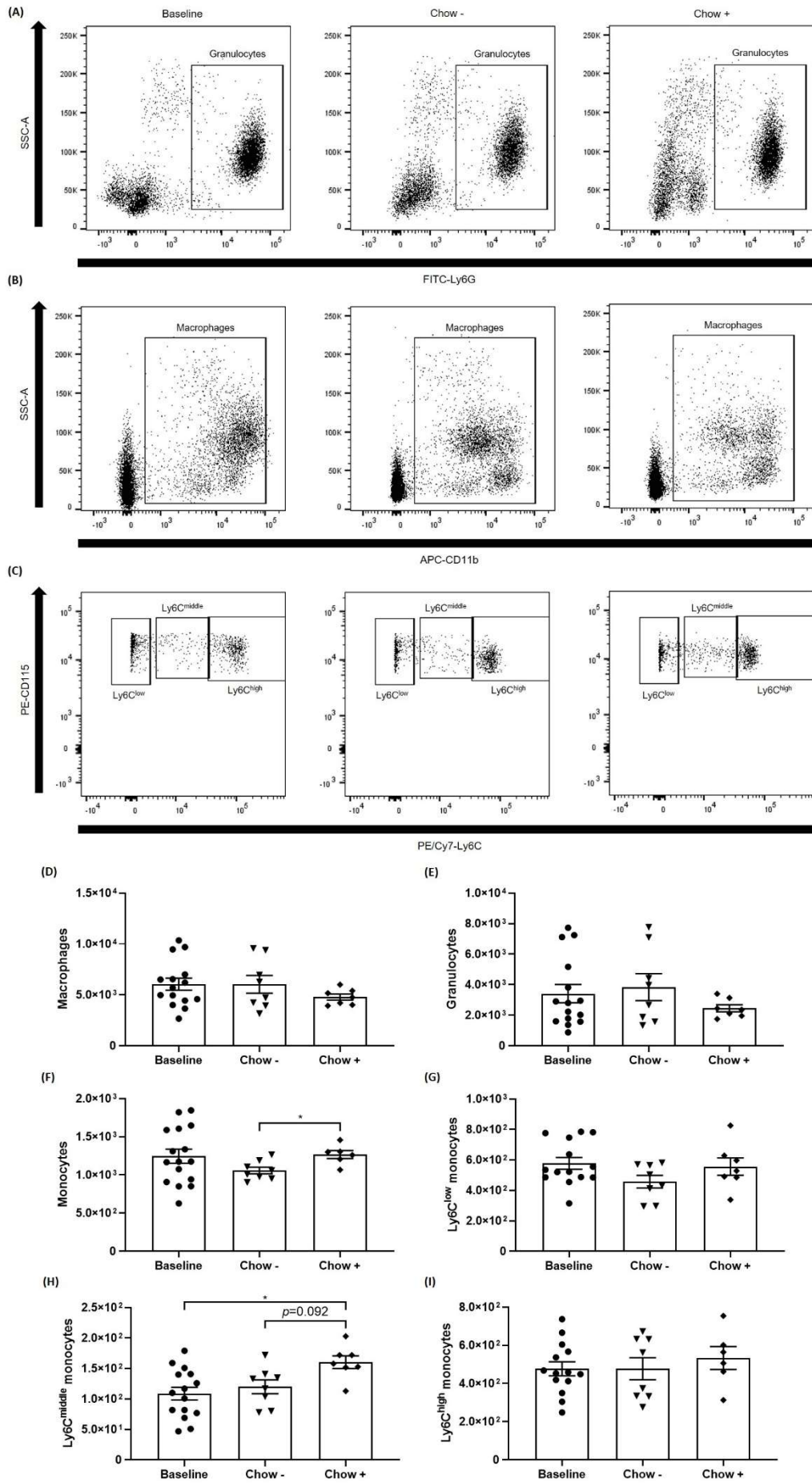


### Figure 6.13 Effect of (+)-catechin on myeloid cell populations in the peripheral blood.

Male *Ldlr*<sup>-/-</sup> mice (8-week-old) were fed high-fat diet supplemented with vehicle for 12 weeks. The 'baseline' group were then culled, whereas the chow groups were switched to normal chow diet with vehicle ('chow -') or 200 mg/kg/day (+)-catechin hydrate ('chow +') given in the drinking water for 8 weeks before being sacrificed. Peripheral blood was extracted from the tail on the day before the end point for immunophenotyping using flow cytometry analysis. Representative dot plots and gating strategies for allophycocyanin (APC)-CD11b<sup>+</sup> macrophages (A), fluorescein isothiocyanate (FITC)-Ly6G<sup>+</sup> granulocytes (B), and phycoerythrin (PE)-CD115<sup>+</sup> phycoerythrin/cyanine7 (PE/Cy7)-Ly6C<sup>low/middle/high</sup> monocytes (C) are shown. This enabled quantification of macrophages (D; n=15, 8 and 7 respectively), granulocytes (E; n=15, 8 and 7 respectively), and monocytes (F; n=16, 8 and 6 respectively), namely Ly6C<sup>low</sup> (G; n=14, 8 and 6 respectively), Ly6C<sup>middle</sup> (H; n=15, 8 and 7 respectively) and Ly6C<sup>high</sup> (I; n=14, 8 and 6 respectively) monocytes. Statistical analysis via one-way ANOVA with Tukey's (G-I) or Games-Howell (D and F) post-hoc test, or Kruskal Wallis test (E) where \*,  $p \leq 0.05$ .

### 6.2.4 Plasma parameters

#### 6.2.4.1 Lipid profile

The chow - and chow + groups had significantly lower levels of total cholesterol levels compared to the baseline group by 46.96% (470.10 mg/dl) and 46.55% (466.00 mg/dl) respectively, as well as compared to the HFD group by 43.30% (405.40 mg/dl) and 42.86% (401.30 mg/dl) respectively ( $p < 0.001$  for all) (Figure 6.14A). The mean total cholesterol levels for the baseline (1001.00±31.33 mg/dl) and HFD (936.30±19.26 mg/dl) groups were similar and not statistically different. This was also true for the chow - (530.90±28.99 mg/dl) and chow + (535.00±31.92 mg/dl) groups.

Similarly, the chow - and chow + groups had significantly reduced levels of free cholesterol levels compared to the baseline group by 75.56% (decrease of 439.70 mg/dl) and 78.33% (decrease of 455.80 mg/dl) respectively, as well as compared to the HFD group by 77.29% (decrease of 484.00 mg/dl) and 79.86% (decrease of 500.10 mg/dl) respectively ( $p < 0.001$  for all) (Figure 6.14B). The mean free cholesterol levels for the baseline (581.90±27.70 mg/dl) and HFD (626.20±35.77 mg/dl) groups were also similar and not significantly different. This was also true for the chow - (142.20±8.22 mg/dl) and chow + (126.10±9.88 mg/dl) groups.

Moreover, the chow -, chow + and HFD groups had significantly greater levels of HDL-C compared to the baseline group (81.00±10.14 mg/dl) by 220.45% (increase of 178.40 mg/dl;  $p < 0.001$ ), 146.67% (118.80 mg/dl;  $p < 0.001$ ) and 115.68% (increase of 93.70 mg/dl;  $p = 0.003$ ) respectively (Figure 6.14C). However, no significant differences

were found in HDL-C levels between the chow - ( $259.40 \pm 24.04$  mg/dl) and chow + ( $199.80 \pm 21.06$  mg/dl) groups.

Furthermore, the chow - and chow + groups had significantly reduced levels of LDL/VLDL cholesterol compared to the baseline group by 68.10% ( $244.60$  mg/dl;  $p < 0.001$ ) and 47.97% ( $172.30$  mg/dl;  $p = 0.005$ ) respectively, as well as compared to the HFD group by 87.92% ( $834.00$  mg/dl) and 80.30% ( $761.70$  mg/dl) respectively ( $p < 0.001$  for both) (Figure 6.14D). Additionally, the HFD group ( $948.60 \pm 90.21$  mg/dl) had significantly greater levels of LDL/VLDL cholesterol compared to the baseline group ( $359.20 \pm 35.26$  mg/dl) by 164.09% ( $589.40$  mg/dl;  $p < 0.001$ ). However, no significant differences were found in the LDL/VLDL cholesterol levels between the chow - ( $114.60 \pm 21.06$  mg/dl) and chow + ( $186.90 \pm 32.81$  mg/dl) groups, despite a difference of  $72.30$  mg/dl.

Lastly, the baseline, chow - and chow + groups had significantly decreased levels of TG compared to the HFD group ( $142.90 \pm 13.83$  mg/dl) by 44.24% ( $63.22$  mg/dl;  $p = 0.002$ ), 49.15% ( $70.23$  mg/dl;  $p < 0.001$ ) and 50.45% ( $72.10$  mg/dl;  $p = 0.002$ ) respectively (Figure 6.14E). However, no significant differences were found in TG levels between the chow - ( $72.67 \pm 5.65$  mg/dl) and chow + ( $70.80 \pm 10.83$  mg/dl) groups.

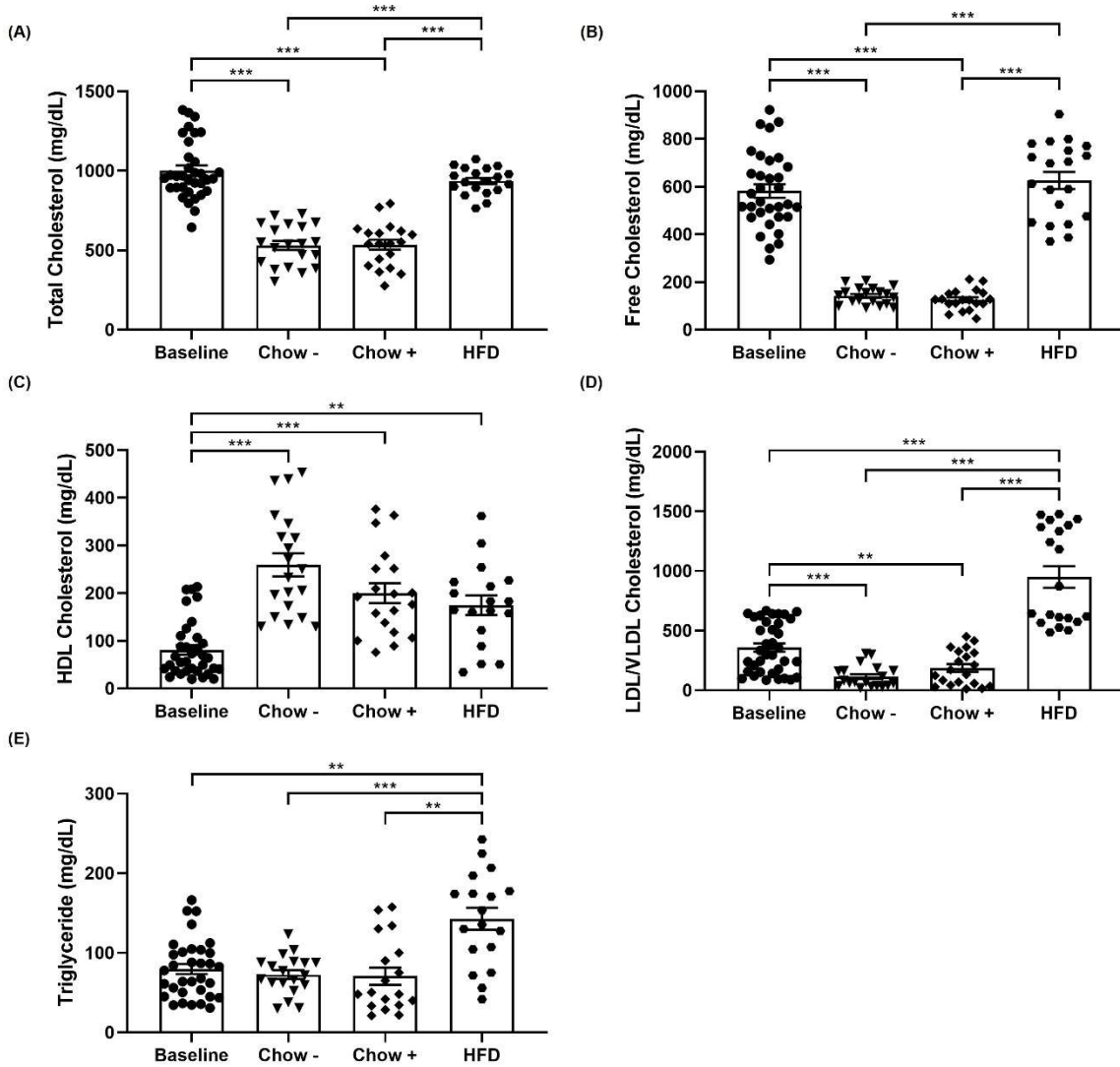


**Figure 6.14 Plasma lipids.**

Male *Ldlr*<sup>-/-</sup> mice (8-week-old) were fed high-fat diet (HFD) supplemented with vehicle for 12 weeks. The 'baseline' group were then culled, whereas the chow groups were switched to normal chow diet with vehicle ('chow -') or 200 mg/kg/day (+)-catechin hydrate ('chow +') given in the drinking water for 8 weeks before being sacrificed, whereas the 'HFD' group were maintained on vehicle-supplemented HFD for a further 8 weeks before being sacrificed. Blood was obtained via cardiac puncture and collected into tubes containing heparin, and plasma obtained via centrifugation. The plasma was analysed for total, free, high-density lipoprotein (HDL) and low-density lipoprotein/very low-density lipoprotein (LDL/VLDL) cholesterol and triglyceride levels using colorimetric assay kits. The baseline group consists of the combined data obtained from both *in vivo* studies as part of the experimental series conducted in this project. The plasma was analysed for total (A; n=34, 20, 19 and 19 respectively), free (B; n=33, 19, 19 and 20 respectively), high-density lipoprotein (HDL) (C; n=34, 20, 19 and 18 respectively) and low-density lipoprotein/very low-density lipoprotein (LDL/VLDL) (D; n=36, 19, 20 and 20 respectively) cholesterol and triglyceride (E; n=33, 19, 18 and 18 respectively) levels using colorimetric assay kits. Statistical analysis via one-way ANOVA with Games-Howell (A, B, D, E) post-hoc test, or Kruskal-Wallis test (C) where \*,  $p < 0.05$ ; \*\*,  $p < 0.01$ ; \*\*\*,  $p < 0.001$ .

#### 6.2.4.2 Lipid ratios

The baseline, chow - and chow + groups had significantly increased ratio of total to LDL/VLDL cholesterol compared to the HFD group by 70.49% ( $p < 0.001$ ), 160.90% ( $p < 0.001$ ) and 100.37% ( $p = 0.001$ ) respectively (Figure 6.15A). The chow - and chow + groups also had a lower ratio of total to HDL-C compared to the baseline group by 87.23% and 84.54% ( $p < 0.001$  for both) respectively, as well as compared to the HFD group by 62.58% ( $p = 0.007$ ) and 54.70% ( $p = 0.057$ ; trend) respectively (Figure 6.15B). The HFD group also had significantly reduced ratio of total to HDL-C compared to the baseline group by 65.90% ( $p = 0.022$ ). Furthermore, the chow - and chow + groups had significantly decreased ratio of LDL/VLDL cholesterol to HDL-C compared to the baseline group by 87.53% and 77.37% respectively, and compared to the HFD group by 92.14% and 85.71% respectively ( $p < 0.001$  for all) (Figure 6.15C). Moreover, the baseline group had significantly reduced ratio of TG to total cholesterol compared to the chow - and HFD groups by 38.14% and 61.02% respectively ( $p < 0.001$  for both) (Figure 6.15D). Additionally, the chow - group had significantly increased ratio of TG to LDL/VLDL cholesterol compared to the baseline and HFD groups by 282.33% ( $p = 0.002$ ) and 464.64% ( $p < 0.001$ ) respectively (Figure 6.15E). This ratio was also significantly increased in the chow + group compared to the HFD group by 150.96% ( $p = 0.027$ ), but not when compared to the baseline group. Finally, the chow - and chow + groups had significantly reduced ratio of TG to HDL cholesterol compared to the baseline group by 76.13% and 71.37% respectively ( $p < 0.001$  for both) and compared to the HFD group by 76.02% ( $p = 0.005$ ) and 71.50% ( $p = 0.022$ ) respectively (Figure 6.15F). However, no significant differences in any of these ratios were found between the chow - and chow + groups themselves.

## Chapter 6: Effect of (+)-catechin on atherosclerosis regression

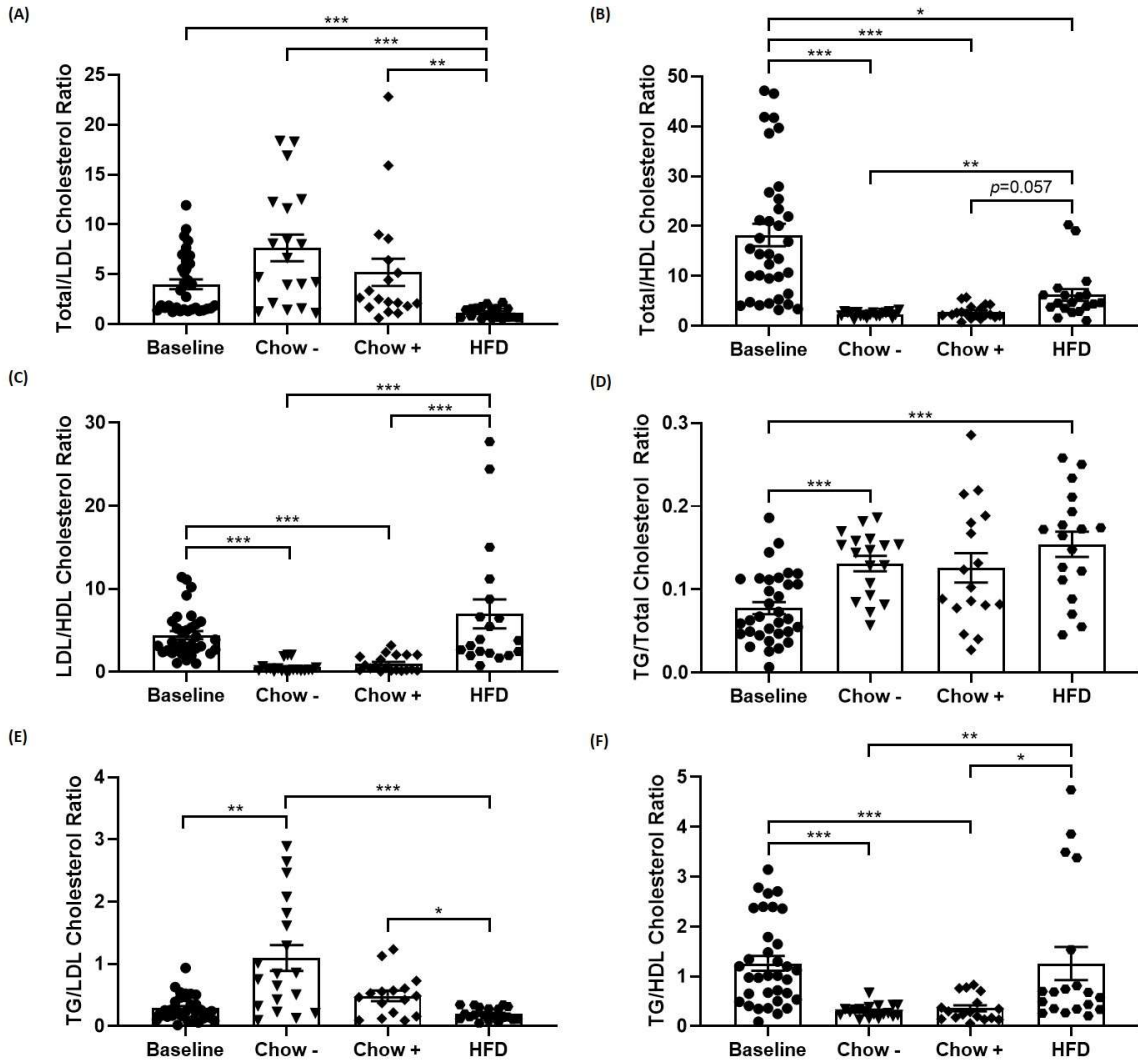


**Figure 6.15 Plasma lipid ratios.**

Male *Ldlr*<sup>-/-</sup> mice (8-week-old) were fed high-fat diet (HFD) supplemented with vehicle for 12 weeks. The 'baseline' group were then culled, whereas the chow groups were switched to normal chow diet with vehicle ('chow -') or 200 mg/kg/day (+)-catechin hydrate ('chow +') given in the drinking water for 8 weeks before being sacrificed, whereas the 'HFD' group were maintained on vehicle-supplemented HFD for a further 8 weeks before being sacrificed. Ratios were calculated using data presented in Figure 6.14. The baseline group consists of the combined data obtained from both *in vivo* studies as part of the experimental series conducted in this project. The ratios of total to low-density lipoprotein (LDL)/very LDL (VLDL) cholesterol (A; n=34, 19, 18 and 20 respectively), total to high-density lipoprotein (HDL) cholesterol (B; n=35, 19, 19 and 19 respectively), LDL/VLDL to HDL cholesterol (C; n=33, 19, 19 and 19 respectively), triglyceride (TG) to total cholesterol (D; n=33, 18, 17 and 18 respectively) TG to LDL cholesterol (E; n=34, 19, 16 and 20 respectively) and TG to HDL cholesterol (F; n=34, 19, 17 and 19 respectively) are shown. For simplicity, LDL/VLDL is referred to as 'LDL'. Statistical analysis via one-way ANOVA with Games-Howell post-hoc test (D), or Kruskal-Wallis test (A-F excluding D) where \*,  $p \leq 0.05$ ; \*\*,  $p < 0.01$ ; \*\*\*,  $p < 0.001$ .

#### 6.2.4.3 Cytokine profile

A trial of n=5 samples per group for the chow groups were assayed to determine levels of key cytokines in the plasma as these could provide future directions for more focused analysis. However, due to the high cost of the assay, only a small number of samples were analysed. No statistically significant differences were found between the chow - and chow + groups for any of the measured cytokines, although there were reductions in the levels of IL-6 and CXCL1 by 83.61% (67.31 pg/ml) and 54.38% (144.60 and pg/ml) respectively (Figure 6.16).

Chapter 6: Effect of (+)-catechin on atherosclerosis regression

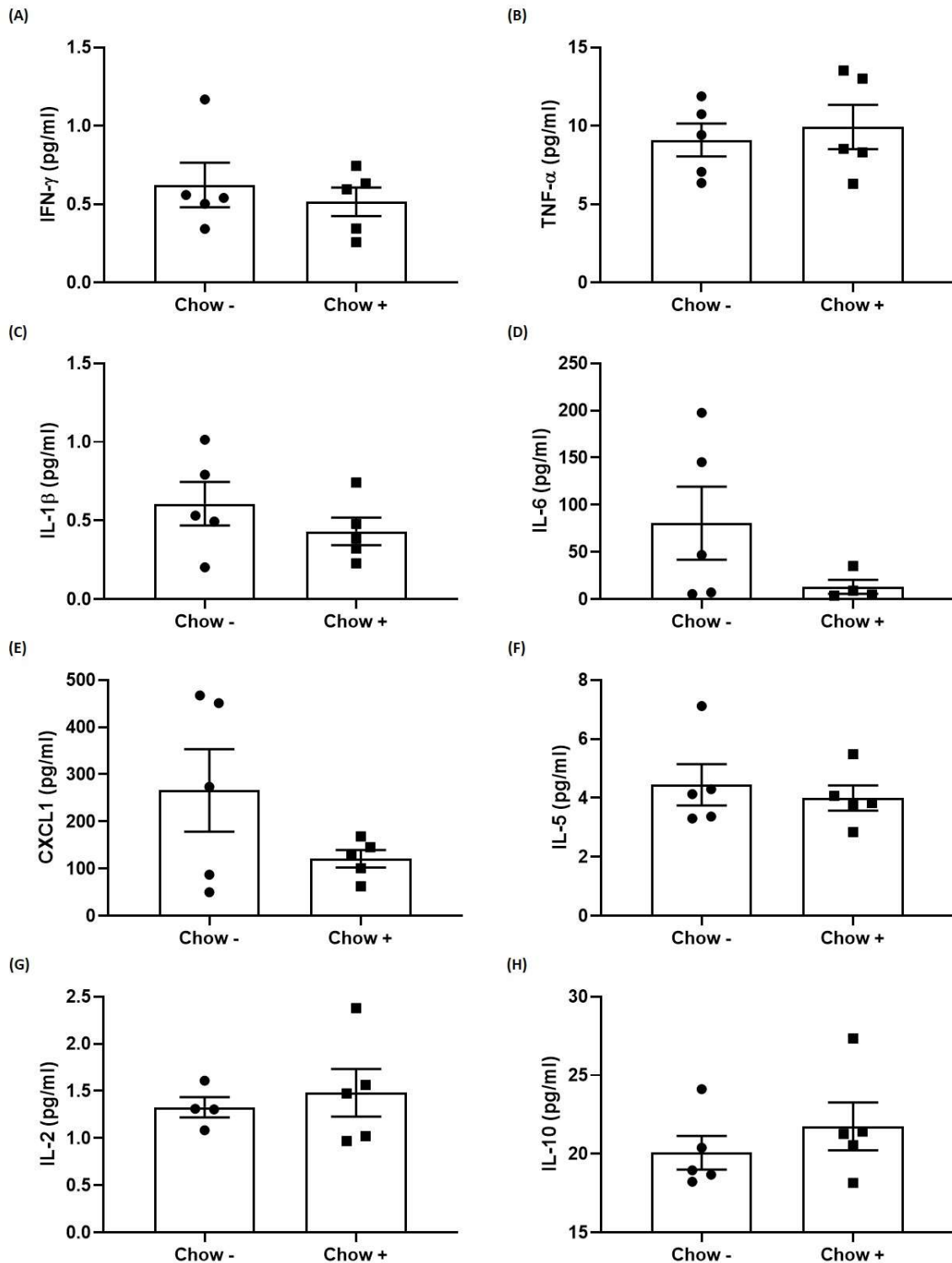


**Figure 6.16 Plasma cytokines.**

Male *Ldlr*<sup>-/-</sup> mice (8-week-old) were fed high-fat diet supplemented with vehicle for 12 weeks. The mice were then switched to normal chow diet with vehicle ('chow -') or 200 mg/kg/day (+)-catechin hydrate ('chow +') given in the drinking water for 8 weeks before being sacrificed. Blood was obtained via cardiac puncture and collected into tubes containing heparin, and plasma obtained via centrifugation. Levels of cytokines in the plasma were quantified using an MSD Cytokine Array. Statistical analysis via unpaired t-test (A-H excluding F) or Mann Whitney U test (F).

## 6.2.5 Detailed plaque morphometric analyses

### 6.2.5.1 Burden and lipid content

In the aortic root, the HFD group had reduced lipid content in the atherosclerotic plaques compared to the baseline and chow + groups by 23.34% ( $p=0.065$ ; trend) and 22.42% ( $p=0.009$ ) respectively (Figure 6.17B). The HFD group also had significantly increased plaque content compared to the baseline, chow - and chow + groups by 23.48% ( $p=0.006$ ), 35.84% ( $p<0.001$ ) and 44.54% ( $p<0.001$ ) respectively (Figure 6.17C). Although the chow + had reduced plaque content, occlusion and plaque size compared to the baseline by 14.57%, 15.14% and 16.22% respectively, none of these were statistically significant. There were also no significant changes in these parameters for the chow - group. Additionally, the HFD group had significantly increased plaque occlusion compared to the baseline, chow - and chow + groups by 28.02%, 36.58% and 50.86% respectively ( $p<0.001$  for all) (Figure 6.17D). Moreover, the HFD group also had significantly increased plaque size compared to the baseline, chow - and chow + groups by 56.29%, 69.85% and 82.14% respectively ( $p<0.001$  for all) (Figure 6.17E). Furthermore, the HFD group exhibited signs of outward vessel remodelling as shown by the significant increase in lumen and vessel size compared to the baseline group by 15.10% (increase of 0.12 mm<sup>2</sup>;  $p=0.050$ ) (Figure 6.17F) and 25.25% (increase of 0.24 mm<sup>2</sup>;  $p=0.072$ ; trend) (Figure 6.17G) respectively. The HFD group also had increased vessel size by 20.13% and 20.17% compared to the chow - ( $p=0.003$ ) and chow + groups ( $p=0.053$ ; trend) (Figure 6.17G) respectively. However, there were no significant differences in any of these parameters between the chow - and chow + groups.

## Chapter 6: Effect of (+)-catechin on atherosclerosis regression

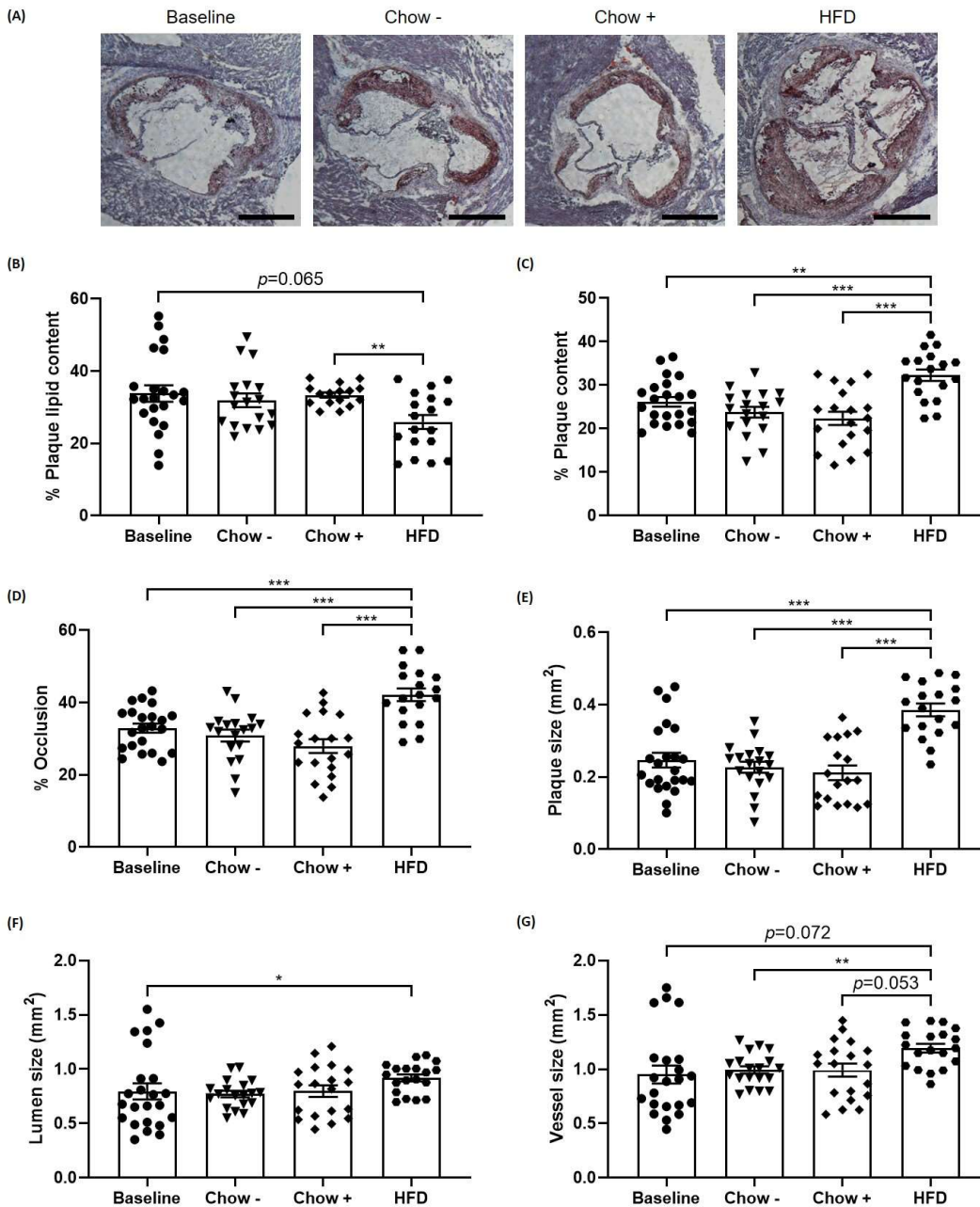


**Figure 6.17 Plaque burden and lipid content.**

Male *Ldlr*<sup>-/-</sup> mice (8-week-old) were fed high-fat diet supplemented with vehicle for 12 weeks. The 'baseline' group were then sacrificed, whereas the chow groups were switched to normal chow diet with vehicle ('chow -') or 200 mg/kg/day (+)-catechin hydrate ('chow +') given in the drinking water for 8 weeks before being sacrificed, whereas the 'HFD' group were maintained on vehicle-supplemented high-fat diet for the 8 weeks (a total of 20 weeks) before being sacrificed. Sections of the aortic root at the three valve cusps were taken using a cryostat and stained with Oil Red O (ORO). Images were captured using a Leica DMRB microscope under x5 magnification and representative images with scale bars indicating 400  $\mu$ m are shown in (A). Image analysis was conducted using ImageJ software in a blinded manner where possible. Lipid content was calculated as percentage ORO+ staining of plaque (B; n=22, 18, 16 and 18 respectively); plaque content was calculated as percentage plaque area of vessel area (C; n=22, 18, 19 and 18 respectively) and occlusion was calculated as percentage plaque area of lumen area (D; n=22, 18, 19 and 18 respectively). The total plaque (E; n=23, 19, 18 and 18 respectively), lumen (F; n=23, 19, 19 and 19 respectively) and vessel (G; n=22, 19, 19 and 19 respectively) sizes are also included. Statistical analysis via one-way ANOVA with Tukey's (C-E) or Games-Howell (B and G) post-hoc test or Kruskal-Wallis test (F) where \*,  $p < 0.05$ ; \*\*,  $p < 0.01$ ; \*\*\*,  $p < 0.001$ .

#### 6.2.5.2 Immune cell infiltration

The chow - and chow + groups had reduced the proportion of MOMA-2<sup>+</sup> macrophages in the plaque compared to the baseline group by 19.40% ( $p=0.045$ ) and 18.05% ( $p=0.071$ ; trend) respectively (Figure 6.18B). However, there were no significant differences in plaque macrophage content compared to the HFD group, or between the chow - and chow + groups themselves.

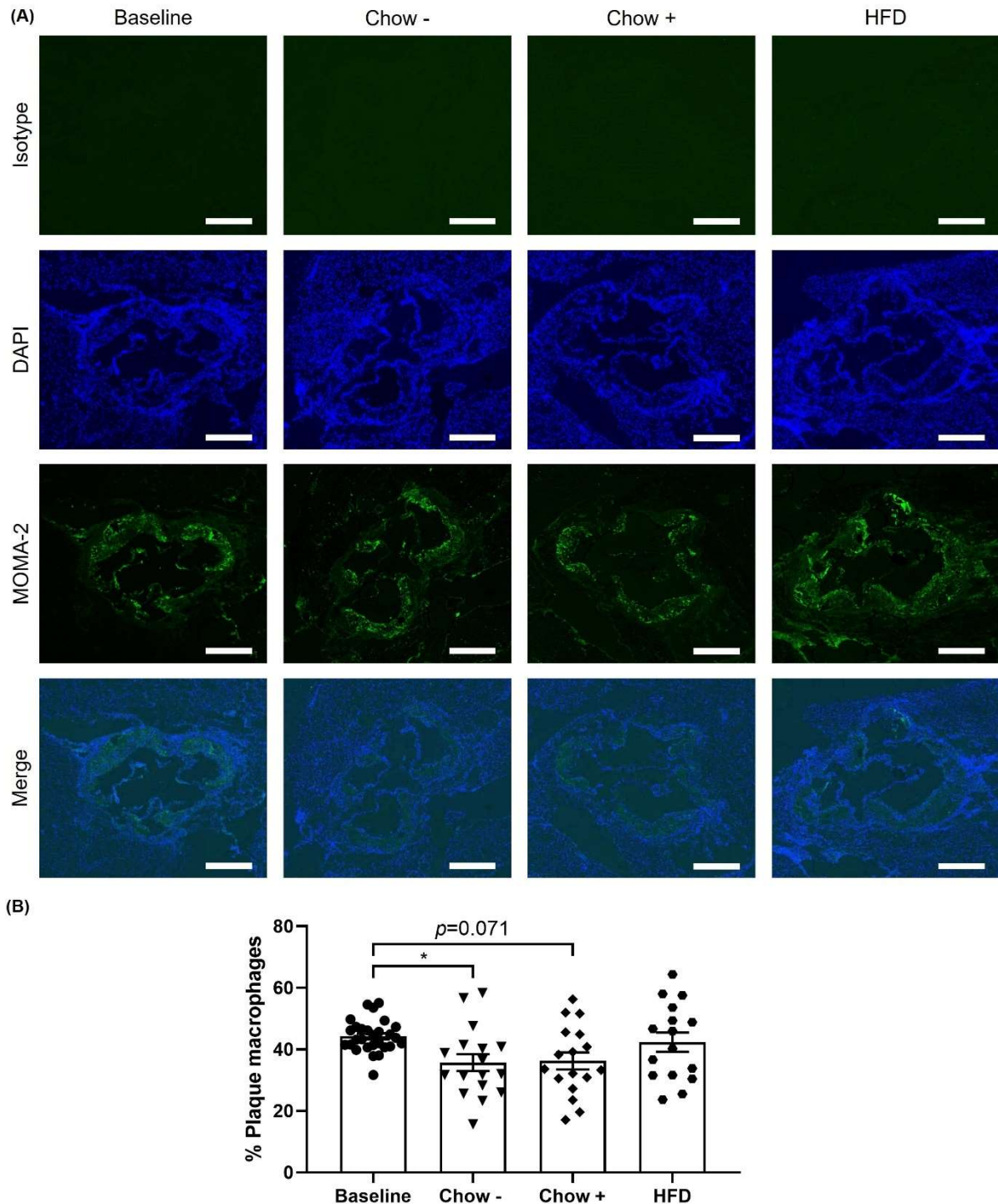


**Figure 6.18 Plaque MOMA-2<sup>+</sup> macrophage content.**

Male *Ldlr*<sup>-/-</sup> mice (8-week-old) were fed high-fat diet supplemented with vehicle for 12 weeks. The 'baseline' group were then sacrificed, whereas the chow groups were switched to normal chow diet with vehicle ('chow -') or 200 mg/kg/day (+)-catechin hydrate ('chow +') given in the drinking water for 8 weeks before being sacrificed, whereas the 'HFD' group were maintained on vehicle-supplemented high-fat diet for the 8 weeks (a total of 20 weeks) before being sacrificed. Sections of the aortic root at the three valve cusps were taken using a cryostat and immunofluorescence staining was used to detect MOMA-2<sup>+</sup> macrophages (B; n=28, 17, 17 and 18 respectively). Images were captured using an Olympus BX61 microscope under x4 magnification and representative images with scale bars indicating 400 μm are shown in (A). Image analysis was conducted using ImageJ software in a blinded manner where possible. Statistical analysis via one-way ANOVA with Games-Howell post-hoc test where \*,  $p \leq 0.05$ .

## Chapter 6: Effect of (+)-catechin on atherosclerosis regression

The HFD group had increased percentage of iNOS<sup>+</sup> M1 macrophages in the plaque compared to the baseline and chow + groups by 42.69% ( $p=0.004$ ) and 34.81% ( $p=0.081$ ; trend) respectively (Figure 6.19B).

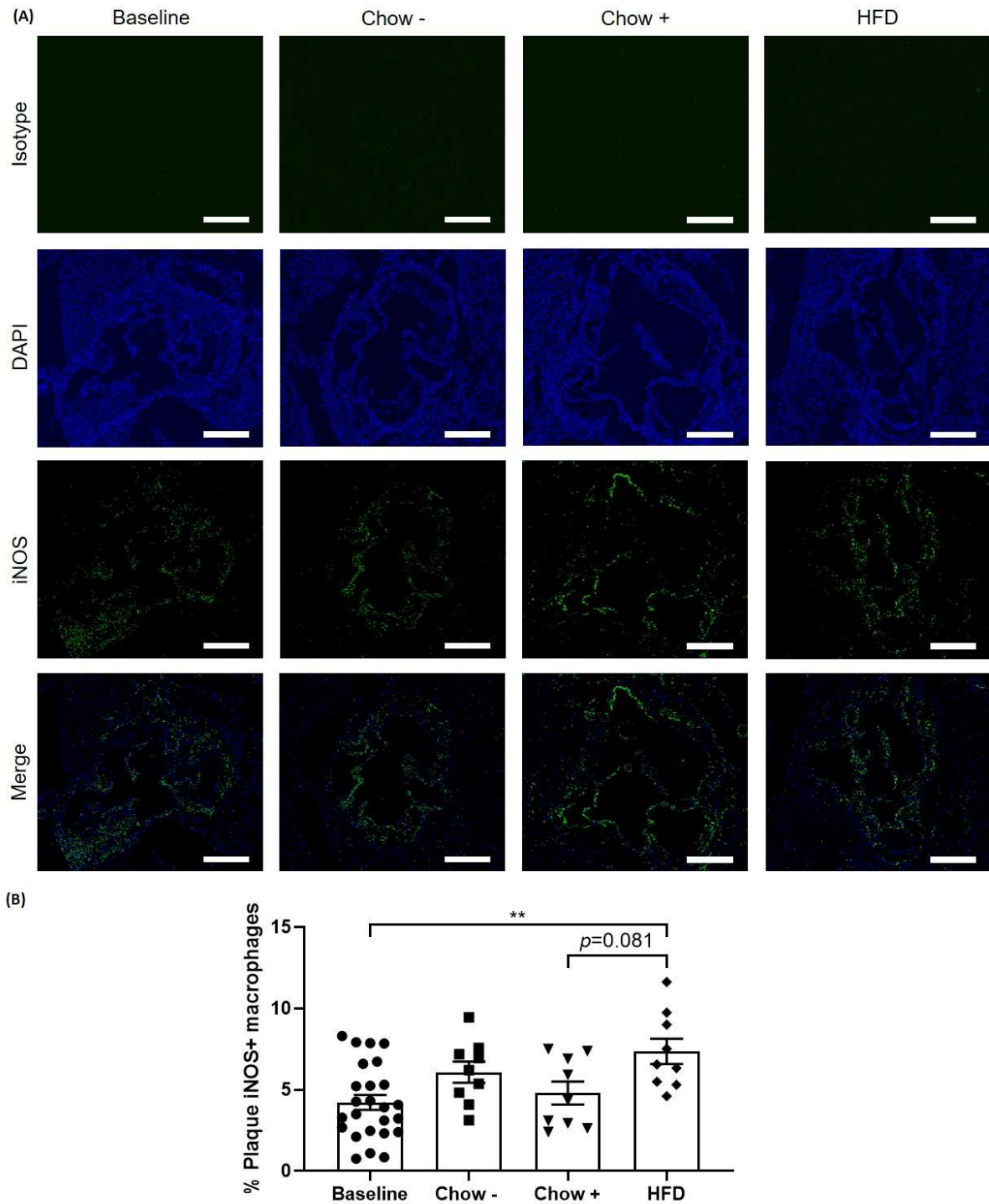


**Figure 6.19 Plaque iNOS<sup>+</sup> M1 macrophage content.**

Male *Ldlr*<sup>-/-</sup> mice (8-week-old) were fed high-fat diet supplemented with vehicle for 12 weeks. The 'baseline' group were then sacrificed, whereas the chow groups were switched to normal chow diet with vehicle ('chow -') or 200 mg/kg/day (+)-catechin hydrate ('chow +') given in the drinking water for 8 weeks before being sacrificed, whereas the 'HFD' group were maintained on vehicle-supplemented high-fat diet for the 8 weeks (a total of 20 weeks) before being sacrificed. Sections of the aortic root at the three valve cusps were taken using a cryostat and immunofluorescence staining was used to detect inducible nitric oxide synthase (iNOS)<sup>+</sup> M1 macrophages (B; n=25, 9, 9 and 9 respectively). Images were captured using an Olympus BX61 microscope under x4 magnification and representative images with scale bars indicating 400  $\mu$ m are shown in (A). Image analysis was conducted using ImageJ software in a blinded manner where possible. Statistical analysis via one-way ANOVA with Tukey's post-hoc test where \*\*,  $p < 0.01$ .

## Chapter 6: Effect of (+)-catechin on atherosclerosis regression

The chow - and chow + groups had significantly reduced proportion of CD3<sup>+</sup> T cells in the plaque compared to the baseline group by 44.99% ( $p=0.002$ ) and 47.13% ( $p=0.003$ ) respectively, and compared to the HFD group by 36.11% ( $p=0.005$ ) and 38.61% ( $p=0.010$ ) respectively (Figure 6.20B). However, there was no significant difference in the proportion of T cells in the plaque between the chow - and chow + groups.

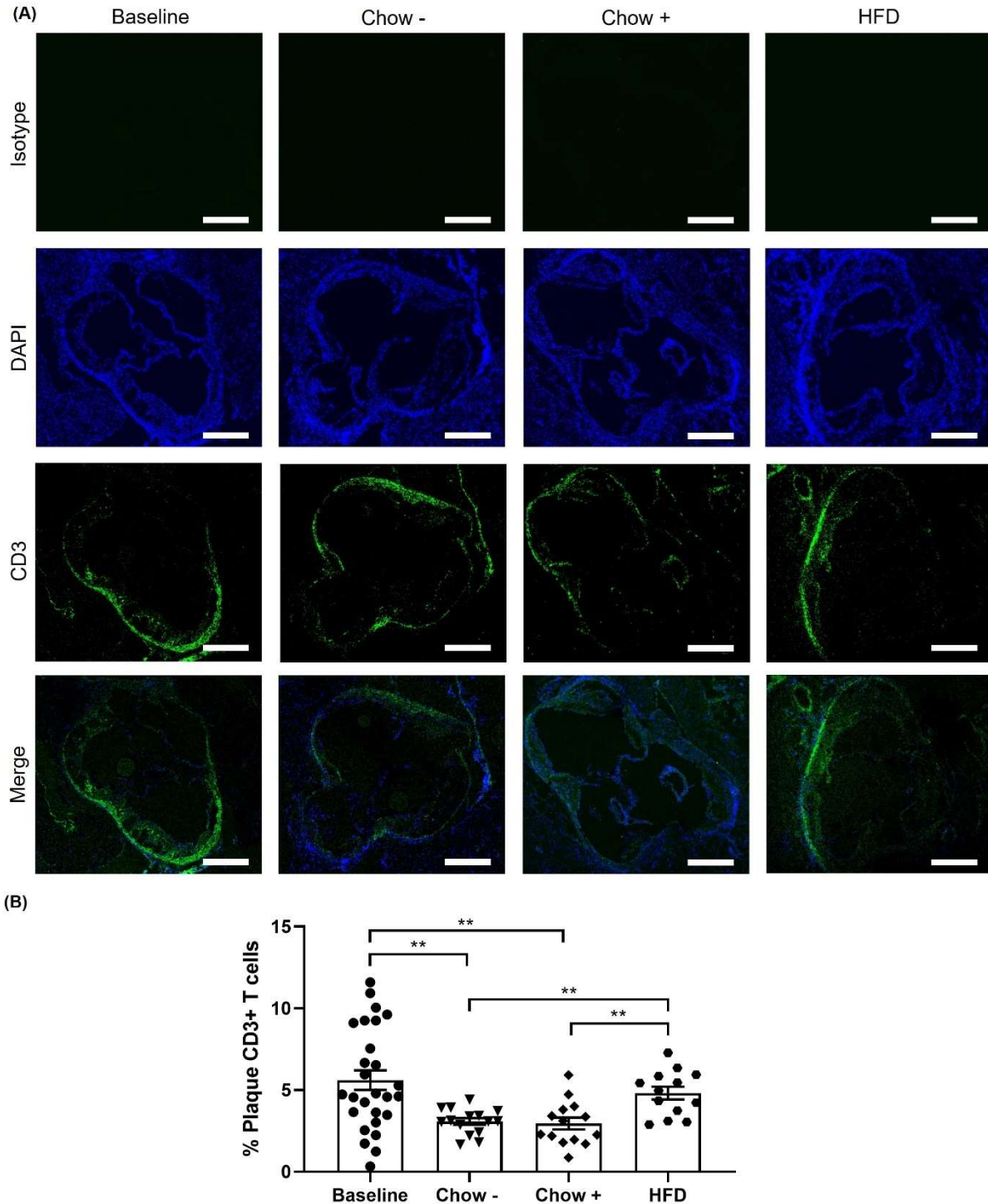


**Figure 6.20 Plaque CD3<sup>+</sup> T cell content.**

Male *Ldlr*<sup>-/-</sup> mice (8-week-old) were fed high-fat diet supplemented with vehicle for 12 weeks. The 'baseline' group were then sacrificed, whereas the chow groups were switched to normal chow diet with vehicle ('chow -') or 200 mg/kg/day (+)-catechin hydrate ('chow +') given in the drinking water for 8 weeks before being sacrificed, whereas the 'HFD' group were maintained on vehicle-supplemented high-fat diet for the 8 weeks (a total of 20 weeks) before being sacrificed. Sections of the aortic root at the three valve cusps were taken using a cryostat and immunofluorescence staining was used to detect CD3<sup>+</sup> T cells (B; n=27,15, 14 and 13 respectively). Images were captured using an Olympus BX61 microscope under x4 magnification and representative images with scale bars indicating 400  $\mu$ m are shown in (A). Image analysis was conducted using ImageJ software in a blinded manner where possible. Statistical analysis via one-way ANOVA with Games-Howell post-hoc test where \*\*,  $p < 0.01$ .

### 6.2.5.3 Stability parameters

The chow + group had significantly increased percentage of  $\alpha$ SMA<sup>+</sup> VSMCs in the plaque compared to the baseline and HFD groups by 37.35% ( $p=0.007$ ) and 42.44% ( $p=0.009$ ) respectively (Figure 6.21B). The chow + group also had increased proportion of VSMCs compared to the chow - group by 18.93%; however, this was not statistically significant unless the two groups were analysed in isolation using an unpaired t-test ( $p=0.029$ ) (data not shown).

Furthermore, the chow + group had significantly increased plaque collagen content compared to the baseline and HFD groups by 63.25% ( $p<0.001$ ) and 28.67% ( $p=0.042$ ) respectively (Figure 6.21C). The chow - group also had significantly increased plaque collagen content compared to the baseline and HFD groups by 63.14% ( $p<0.001$ ) and 28.58% ( $p=0.032$ ) respectively. However, there was no significant difference in plaque collagen content between the chow - and chow + groups.

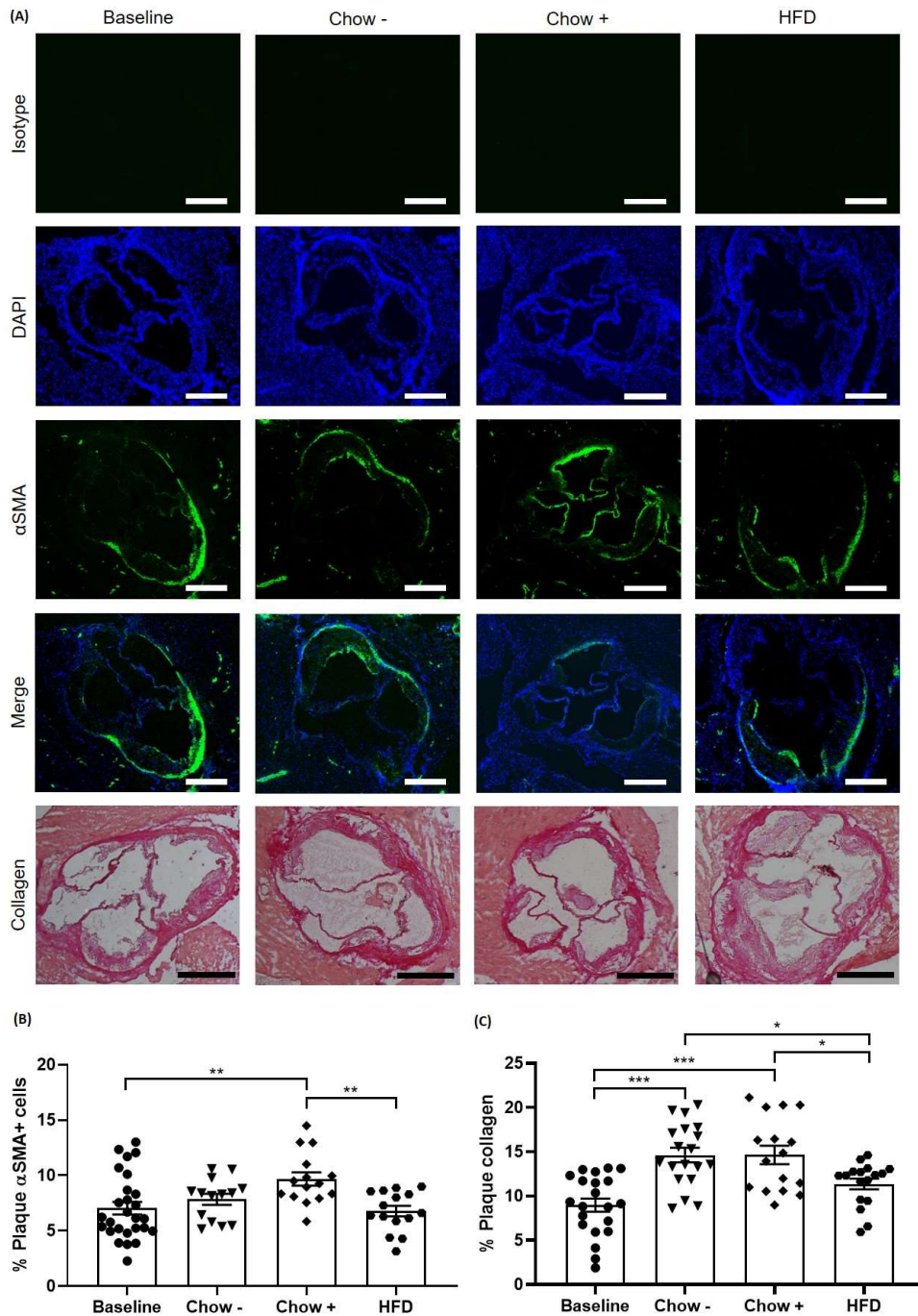


**Figure 6.21 Plaque stability parameters.**

Male *Ldlr*<sup>-/-</sup> mice (8-week-old) were fed high-fat diet supplemented with vehicle for 12 weeks. The 'baseline' group were then sacrificed, whereas the chow groups were switched to normal chow diet with vehicle ('chow -') or 200 mg/kg/day (+)-catechin hydrate ('chow +') given in the drinking water for 8 weeks before being sacrificed, whereas the 'HFD' group were maintained on vehicle-supplemented high-fat diet for the 8 weeks (a total of 20 weeks) before being sacrificed. Sections of the aortic root at the three valve cusps were taken using a cryostat. Immunofluorescence staining of the sections was used to detect α-smooth muscle actin (SMA)<sup>+</sup> smooth muscle cells (B; n=27, 14, 15 and 15 respectively). Sections were also stained with Van Geison's solution to measure collagen content (C; n=21, 19, 16 and 17 respectively). Images of αSMA-stained sections were captured using an Olympus BX61 microscope at x4 magnification and those of collagen-stained sections captured using a Leica DMRB microscope at x5 magnification with scale bars indicating 400 μm (A). Image analysis was conducted using ImageJ software in a blinded manner where possible. Statistical analysis via one-way ANOVA with Tukey's post-hoc test where \*,  $p \leq 0.05$ ; \*\*,  $p < 0.01$ ; \*\*\*,  $p < 0.001$ .

## 6.2.5.4 Necrosis and stability

There were no significant differences in percentage necrosis of plaque between all groups (Figure 6.22A); however, the HFD group had significantly greater necrotic area within the plaque compared to the baseline, chow - and chow + groups by 64.45% (increase of 0.04 mm<sup>2</sup>), 63.48% (increase of 0.04 mm<sup>2</sup>) and 71.38% (increase of 0.05 mm<sup>2</sup>) respectively ( $p < 0.001$  for all) (Figure 6.22B). Only the chow + group had increased plaque stability index compared to the baseline and HFD groups by 43.17% ( $p = 0.016$ ) and 37.84% ( $p = 0.080$ ; trend) respectively (Figure 6.22C).

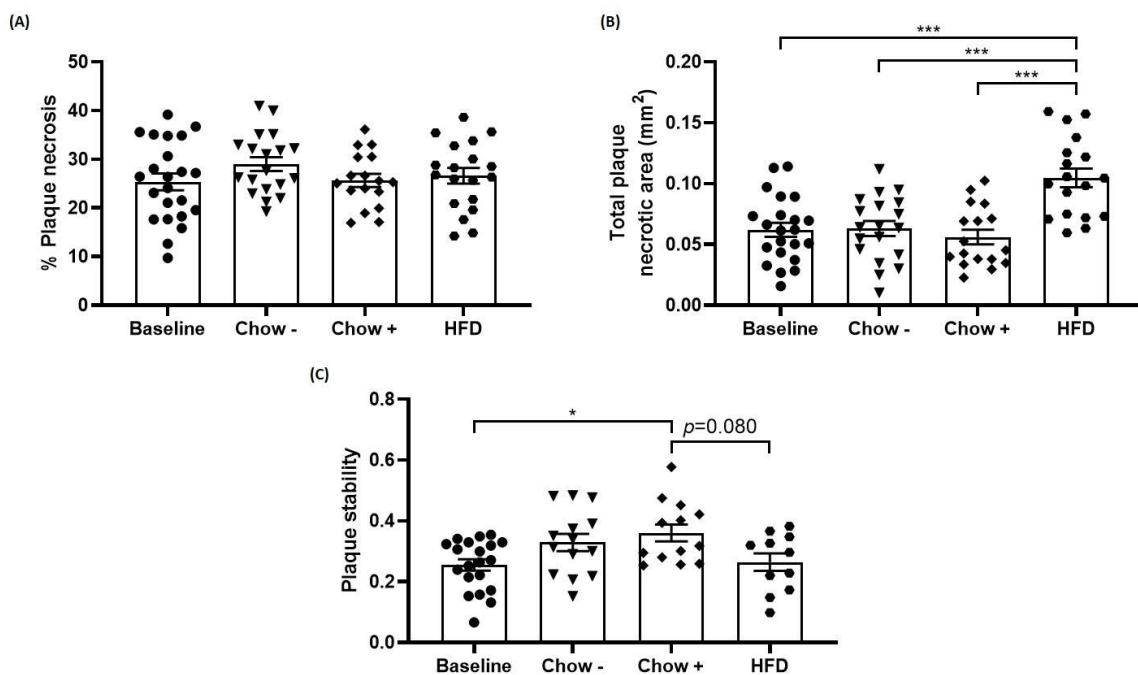


**Figure 6.22 Plaque necrosis and stability.**

Male *Ldlr*<sup>-/-</sup> mice (8-week-old) were fed high-fat diet supplemented with vehicle for 12 weeks. The 'baseline' group were then sacrificed, whereas the chow groups were switched to normal chow diet with vehicle ('chow -') or 200 mg/kg/day (+)-catechin hydrate ('chow +') given in the drinking water for 8 weeks before being sacrificed, whereas the 'HFD' group were maintained on vehicle-supplemented high-fat diet for the 8 weeks (a total of 20 weeks) before being sacrificed. Necrosis was calculated as the acellular regions within the plaque expressed as both a percentage (A; 23, 19, 17 and 19 respectively) and total area (B; n=22, 19, 17 and 18 respectively), due to differences in total plaque area between the groups. Plaque stability was calculated as (collagen + smooth muscle cells) / (lipid + macrophages) (C; n=20, 14, 13 and 11 respectively). Image analysis was conducted using ImageJ software in a blinded manner where possible. Statistical analysis via one-way ANOVA with Tukey's post-hoc test where \*,  $p \leq 0.05$ ; \*\*\*,  $p < 0.001$ .

### 6.2.6 Liver cellularity and steatosis

The HFD group had significantly reduced liver cellular area compared to the baseline and chow + groups by 26.76% ( $p < 0.001$ ) and 27.51% ( $p = 0.002$ ) respectively (Figure 6.23B). The HFD group also had reduced number of hepatocytes ( $p = 0.075$ ; trend) (Figure 6.23C) and a 13.82% increase in percentage liver steatosis (ORO content) ( $p = 0.066$ ) (Figure 6.23E) compared to the baseline group. The chow + group had increased liver cellularity and average cell size compared to the chow - group; however, these were not statistically significant unless the two groups were analysed in isolation using an unpaired t-test. This found that the chow + group had significantly increased liver cellular area by 12.10% ( $p = 0.043$ ) and average cell size ( $p = 0.049$ ) compared to the chow - group (data not shown).

## Chapter 6: Effect of (+)-catechin on atherosclerosis regression

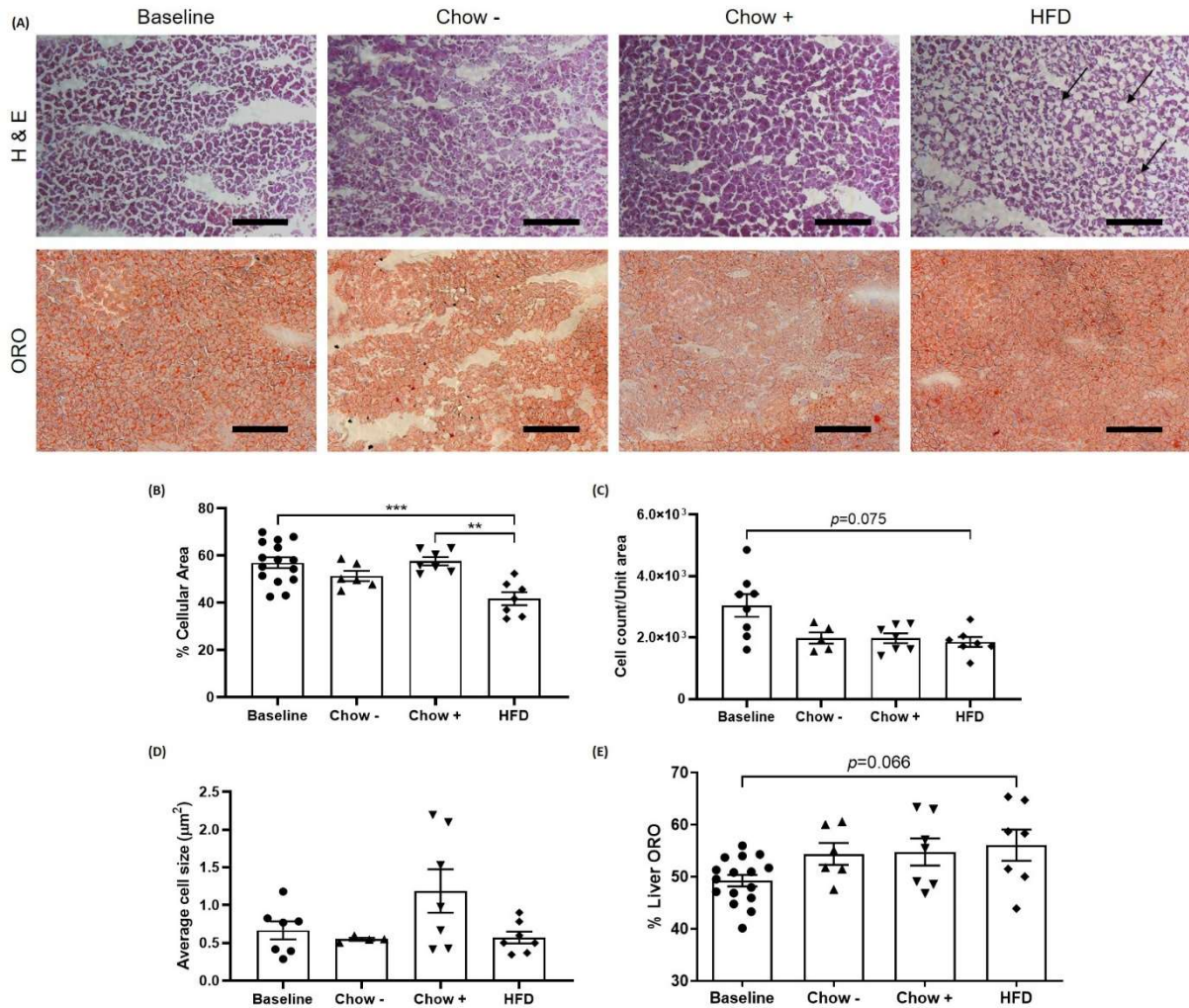


**Figure 6.23 Liver cellularity and steatosis.**

Male *Ldlr*<sup>-/-</sup> mice (8-week-old) were fed high-fat diet (HFD) supplemented with vehicle for 12 weeks. The 'baseline' group were then culled, whereas the chow groups were switched to normal chow diet with vehicle ('chow -') or 200 mg/kg/day (+)-catechin hydrate ('chow +') given in the drinking water for 8 weeks before being sacrificed, whereas the 'HFD' group were maintained on vehicle-supplemented high-fat diet for the 8 weeks (a total of 20 weeks) before being sacrificed. Sections of the liver were taken using a cryostat and stained with haematoxylin and eosin (H & E) to analyse hepatic morphology, and Oil Red O (ORO) to measure steatosis. Images of the stained sections were captured using a Leica DMRB microscope at x20 magnification with scale bars indicating 200 µm (A). Image analysis was conducted using ImageJ software. Arrows indicate ballooning degeneration of hepatocytes seen in the livers of the HFD group mice. Statistical analysis via one-way ANOVA with Tukey's (B and E) or Games-Howell (C and D) post-hoc test where \*\*\*,  $p < 0.001$ .

### 6.2.7 Summary

A summary of the significant changes or changes with a trend towards significance observed in the chow groups compared to the baseline group are listed in Table 6.1.

Chapter 6: Effect of (+)-catechin on atherosclerosis regression

Table 6.1 Summary of changes induced by chow intervention on atherosclerosis regression.

Comparison to baseline				
Parameter	Chow -		Chow +	
	Change	Significance	Change	Significance
<i>Adipose tissue weights</i>				
Inguinal fat	=	NS	↓	*
Gonadal fat	=	NS	↓	*
Total white fat	=	NS	↓	*
Brown:white fat	=	NS	↑	***
Total fat	=	NS	↓	*
<i>Organ weights</i>				
Liver weight	↑	**	↑	***
Thymus weight	↑	**	↑?	trend
<i>Bone marrow cell populations</i>				
HPC I	↓	**	=	NS
HPC II	↓	**	↓	**
MPP	=	NS	↑	**
MEP	=	NS	↑	*
<i>Peripheral blood cell populations</i>				
NK cells	=	NS	↓	*
Ly6C <sup>middle</sup> monocytes	=	NS	↑	*
<i>Plasma lipid profile</i>				
Total cholesterol	↓	***	↓	***
Free cholesterol	↓	***	↓	***
HDL cholesterol	↑	***	↑	***
LDL/VLDL cholesterol	↓	***	↓	**
Total:HDL cholesterol	↓	***	↓	***
LDL/VLDL:HDL cholesterol	↓	***	↓	***
TG:Total cholesterol	↑	***	=	NS
TG:LDL/VLDL cholesterol	↑	**	=	NS
TG:HDL cholesterol	↓	***	↓	***
<i>Aortic root plaque analyses</i>				
Plaque macrophages	↓	*	↓?	trend
Plaque T cells	↓	**	↓	**
Plaque VSMCs	=	NS	↑	**
Plaque collagen	↑	***	↑	***
Plaque stability index	=	NS	↑	*

Significance was defined as  $p \leq 0.05$  whilst trend of significance was defined as  $0.1 < p < 0.05$ . Abbreviations: NS, not significant; HPC, haematopoietic progenitor cell; MPP, multipotent progenitors; CMP, common myeloid progenitor; MEP, megakaryocyte-erythroid progenitor; WBCs, white blood cells; NK, natural killer; HDL, high-density lipoprotein; LDL, low-density lipoprotein; TG, triglyceride; VSMCs, vascular smooth muscle cells.

A summary of changes seen in the chow + group compared to the chow - group are indicated in Table 6.2. Where obvious changes were seen between the two groups but these were not found to be statistically significant when compared using a one-way ANOVA (to include all groups), statistical analysis was also conducted using an unpaired t-test to compare the chow groups in isolation.

**Table 6.2 Summary of key changes in the chow + group in comparison to the chow - group.**

Parameter	Change	Significance
Body weight after switching to chow	↓	***
Inguinal adipose tissue	↓	NS but * when t-test used
Brown to white fat ratio	↑	NS but * when t-test used
Plaque $\alpha$ SMA <sup>+</sup> cells	↑	NS but * when t-test used
Liver cellular area	↑	NS but * when t-test used
Average hepatocyte size	↑	NS but * when t-test used

In addition to the one-way ANOVA used to compare all groups simultaneously, t-tests were used to compare the chow - and chow + groups in isolation (since a greater number of comparisons can result in reduced sensitivity of the statistical test). Significance was defined as  $p \leq 0.05$  where \*,  $p < 0.05$ ; \*\*\*,  $p < 0.001$ . Abbreviations: NS, not significant;  $\alpha$ SMA, alpha-smooth muscle actin.

### 6.3 Discussion

Atherosclerosis is a chronic inflammatory disorder of the vasculature that develops over decades and is largely asymptomatic until the late stages of the disease, whereby lumen-occlusive plaques disrupt normal arterial blood flow. Although statins have had substantial impact on reducing mortality rates over the years of its application, significant residual cardiovascular risk remains post therapy, and so the exploration of alternative preventative and therapeutic avenues has been pursued. This study firstly investigated the ability of (+)-catechin to attenuate parameters associated with endothelial and VSMC dysfunction, after promising results were obtained from previous experiments conducted in the host laboratory on human monocytes and macrophages. Following promising results obtained from all key cell types implicated in the disease, the ability of (+)-catechin to attenuate atherosclerosis development and progression in the *Ldlr*<sup>-/-</sup> model was investigated. *Ldlr*<sup>-/-</sup> mice receiving (+)-catechin hydrate supplemented HFD for 12 weeks had attenuated atherosclerotic plaque burden and inflammation, and improved plaque stability (Chapter 5). This corresponded to *in vitro* results whereby (+)-catechin demonstrated various anti-atherogenic effects in multiple key cell types implicated in the disease and attenuated

multiple processes that occur in early atherosclerosis (Chapters 3 and 4). However, exploration of the ability of natural agents to stimulate atherosclerosis regression has been lacking, since the majority of regression studies conducted thus far employ genetic manipulation (Burke and Huff 2018). In particular, the ability of (+)-catechin to induce atherosclerosis regression is yet to be explored, hence this chapter set out to investigate whether chow combined with (+)-catechin hydrate could stimulate the regression of established plaques in *Ldlr*<sup>-/-</sup> mice. Mice were fed HFD for 12 weeks to induce the formation of established atherosclerotic lesions, then switched to NCD supplemented with (+)-catechin hydrate to induce atherosclerosis regression. Key findings demonstrate that intervention with chow combined with (+)-catechin modulated certain atherosclerosis risk factors (i.e., reversed adiposity and hepatic injury) and promoted plaque stability to a greater extent than chow intervention alone.

### 6.3.1 Changes in weight gain and adipose tissue accumulation

As expected, mice receiving HFD for 20 weeks had significantly increased subcutaneous and renal fat compared to the baseline group, corresponding to increased total white and total (white and brown) fat (trend for all). The HFD group also gained significantly more weight in total compared to all three groups. The weights of the HFD mice continued to increase linearly, whilst those of the mice switched to NCD declined significantly. Moreover, mice switched to NCD had significantly less white adipose tissue depots (subcutaneous, gonadal and renal) compared to the HFD group, resulting in reduced total white and total (white and brown) adipose tissue, as well as increased ratio of brown to white fat. Furthermore, the chow + group exhibited reduced inguinal (significant), gonadal (significant) and renal (trend) adipose tissue compared to baseline mice. As such, these mice had significantly reduced total white and total (white and brown) adipose tissue accumulation compared to the baseline group, along with increased ratio of brown to white adipose tissue.

Notably, mice receiving (+)-catechin hydrate supplemented chow maintained a significantly lower mean body weight for the 8-week duration than that of the chow control group, and this was consistent with reductions in adipose tissue depots. Although these changes were not statistically significant when compared to the chow

- group using a one-way ANOVA, the chow + group had significantly greater ratio of brown to white adipose tissue compared to the chow - group when these two groups were compared in isolation using an unpaired t-test. This suggests that intervention with chow combined with (+)-catechin reversed HFD-induced adiposity and promoted apoptosis of white adipose tissue deposits, improving the ratio of brown to white fat to a greater extent than chow intervention alone. These results are similar to previous observations in *Ldlr<sup>-/-</sup>* mice fed (+)-catechin hydrate supplemented HFD for 12 weeks (Chapter 5), whereby the ratio of brown to white fat was also significantly increased, owing to reduced accumulation of certain types of white fat (rather than an increase in beneficial brown fat). Taken together, these results suggest that the anti-obesity effects of (+)-catechin may be augmented when combined with a chow diet. Furthermore, when the chow groups were compared in isolation using an unpaired t-test, the chow + group had a trend of reduced cardiac hypertrophy index compared to the chow - group, suggesting possible reversal of diet-induced pressure overload by (+)-catechin intervention. However, the mechanisms responsible for this change still requires elucidation, although this may be associated with its anti-adiposity effects reducing the workload on the heart.

Indeed, the anti-obesity effects of other catechins have been well reported (Yan et al. 2013; Akhlaghi and Kohanmoo 2018; Carrasco-Pozo et al. 2019; Cremonini et al. 2020). The regulation of adipocyte differentiation and intracellular lipolysis are key for the maintenance of metabolic homeostasis and treatment of obesity (Jou et al. 2010). Agents that can achieve this could hence be utilised to combat adiposity, in combination with dietary modification. In a study using 3T3-L1 preadipocytes, (+)-catechin inhibited their differentiation and the deposition of lipids by mature adipocytes, with potential effects on signalling pathways that regulate adipogenesis and lipolysis (Jiang et al. 2019). Further analyses of the individual white adipose tissue deposits would hence be of interest to identify morphological changes (i.e., the number and size of the constituent adipocytes). This could be determined via sectioning of the adipose tissue depots (which have all been stored) and staining with ORO, for example. Analysis of adipokine expression could also be conducted to determine whether these reductions in adipose tissue mass correspond to dampened expression of pro-inflammatory adipokines, such as IL-6 and TNF- $\alpha$ . Analysis of the architecture of the adipose tissue would provide valuable insights to how (+)-catechin attenuates

adiposity and affects adipocyte-associated inflammation. *In vitro* models of adipocyte differentiation could also be employed to ascertain how (+)-catechin might affect this process and hence reverse adipocyte accumulation *in vivo*. It would also have been interesting to employ 3-D whole body imaging techniques to monitor the distribution and redistribution of adipose tissue (Bidar et al. 2012) during the course of the chow intervention to obtain a more dynamic view of adiposity-associated changes.

### 6.3.2 Changes in plasma lipid profile

Mice fed HFD for 12 (baseline) and 20 (HFD) weeks had similar levels of plasma total cholesterol and free cholesterol levels. However, the HFD group had significantly increased plasma concentrations of HDL-C and LDL/VLDL cholesterol, along with TG levels, compared to the baseline group, suggesting altered plasma lipid profile. The HFD group had significantly increased ratios of total to LDL/VLDL cholesterol and TG to total cholesterol, and decreased ratio of total to HDL-C compared to the baseline group. Therefore, the duration of HFD feeding appears to be correlated with severity of LDL/VLDL cholesterol and TG-derived hyperlipidaemia, as well as adiposity, which concurs with other published studies (Calligaris et al. 2013; Ramalho et al. 2017; He et al. 2020). Both chow groups had significantly reduced plasma levels of total cholesterol, free cholesterol and LDL/VLDL cholesterol compared to the baseline and the HFD groups. Moreover, both chow groups had significantly increased HDL-C compared to the baseline group, and reduced TG levels compared to the HFD group.

However, no significant differences in the levels of plasma lipids were found between the chow - and chow + groups themselves. This suggests that intervention with NCD alone produces comparable effects to chow combined with (+)-catechin on the reversal of hyperlipidaemia induced by HFD and restoring levels of HDL-C. This resulted in both chow groups having a much-improved plasma lipid profile compared to mice receiving HFD. The chow groups had significantly increased ratios of total and TG to LDL/VLDL cholesterol compared to the HFD group, suggesting reversal of elevated LDL/VLDL cholesterol induced by HFD feeding. Furthermore, both groups had significantly decreased ratios of total to HDL-C, LDL/VLDL cholesterol to HDL-C and TG to HDL-C compared to both the baseline and the HFD groups. However, the

chow - group also had significantly increased ratios of TG to total and LDL/VLDL cholesterol compared to the baseline group which was not seen with the chow + group. This suggests that chow intervention may reverse LDL/VLDL cholesterol-derived hypercholesterolaemia better than intervention with chow combined with (+)-catechin. Indeed, the mean plasma LDL/VLDL cholesterol concentration for the chow - group was  $114.60 \pm 21.06$  mg/dl whilst that of the chow + group was  $186.9 \pm 32.81$  mg/dl. However, despite having higher concentrations of LDL/VLDL cholesterol in the plasma, mice receiving chow combined with (+)-catechin intervention demonstrated significant reversal of HFD-induced accumulation of white adipose tissue depots which was not seen with the chow - group. Overall, intervention with chow alone reverses the detrimental changes in plasma lipid profile induced by HFD feeding to a greater extent than chow combined with (+)-catechin. On the other hand, intervention with the latter appears more efficacious at reversing HFD-induced adiposity (as shown by the significantly reduced mass of white adipose tissue depots compared to the baseline group), suggesting the involvement of other mechanisms beyond attenuation of hypercholesterolaemia (as per results of Chapter 5).

### 6.3.3 Changes in the liver

Both chow groups had significantly increased liver weights compared to those of the baseline and the HFD groups, although there were no differences between the chow groups themselves. Moreover, analysis of hepatic morphology and lipid content via immunohistochemical staining of the liver sections found the HFD group to have significantly reduced liver cellular area and hepatocyte count, along with increased hepatic steatosis, compared to the baseline group. Therefore, prolonged HFD feeding appears to enhance hepatocyte injury and steatosis, which are well characterised changes that occur in the progression to non-alcoholic steatohepatitis. This corresponds to the ballooning degeneration of hepatocytes visible in the sections of the HFD mice that were not seen in the other groups. Indeed, both short-term and chronic HFD feeding has been reported to induce liver steatosis, hepatocyte injury, inflammation and fibrosis in C57BL/6J mice (Echeverria et al. 2019; Sheng et al. 2019; Velazquez et al. 2019). Only the chow + group had significantly increased liver cellular area compared to the HFD group.

Importantly, when the chow groups were analysed in isolation using an unpaired t-test, the chow + group had significantly greater liver cellular area and average hepatocyte size compared to the chow - group. This suggests that (+)-catechin combined with chow intervention halted hepatic injury induced by HFD without affecting steatosis, which was not seen in the chow - group. This may be associated with the greater reversal of adiposity induced by chow combined with (+)-catechin intervention compared to intervention with chow alone. Although no significant difference in liver steatosis was seen as per Chapter 5 in atherosclerosis progression, improved cellularity induced by (+)-catechin combined with chow intervention (which was not seen with chow intervention alone), suggests termination of HFD-induced hepatocyte degeneration. Indeed, EGCG has been shown to improve hepatic steatosis and hepatic inflammation associated with hepatic macrophage M1-to-M2 polarisation in HFD-fed mice (Du et al. 2021).

However, the mechanisms underlying the positive changes in liver cellularity induced by (+)-catechin require elucidation. Further analyses of the remaining liver tissue could be conducted to identify levels of cholesterol and TG in the liver using tissue homogenate, and if changes in the lipids are seen, the remaining sections could be stained to measure PCSK9 expression. Since PCSK9 induces internalisation/degradation of the LDLR to prevent LDL uptake (Lagace 2014), alterations in PCSK9 expression may be responsible for, and correlate with, changes in liver lipid levels. Additionally, picosirius red staining of the remaining sections could also be used to stain for collagen content, enabling analysis of the degree of fibrosis present in the liver tissue (this was initially attempted but further optimisation of the staining protocol is required), and further assess the severity of hepatic morphological alterations. Beyond hepatic steatosis, HFD feeding has also been associated with liver oxidative stress, loss of omega-3 PUFAs and mitochondrial dysfunction (Anstee and Goldin 2006; Zhukova et al. 2014). Therefore, liver oxidative stress profile could also be investigated, for example via determination of MDA concentration (e.g., using reverse-phase high-performance liquid chromatography) and the activities of antioxidant enzymes, such as superoxide dismutase and catalase (Chassot et al. 2018). This would provide valuable insights to how (+)-catechin reverses HFD-induced hepatic injury and possible dysfunction without reversing hepatocyte lipid

accumulation, especially as (+)-catechin has previously demonstrated potent anti-oxidative activity *in vitro* in various studies conducted in the host laboratory.

### 6.3.4 Changes in other organs

Beyond the liver weights, changes were also seen in the weights of the thymus between the groups; the chow and HFD groups all had increased thymus weights compared to the baseline group. The fact that the younger mice had reduced thymic weights (i.e., those fed HFD for 12 weeks) compared to those continued on the experimental protocol for 20 weeks, suggests age-related changes in the thymus rather than those relating to dietary intervention. Thymic changes are clinically important, since the thymus (specifically the cortex) is the site of T cell differentiation and maturation, and hence is essential for the normal function of the immune system (Elmore 2007). Further analyses are hence required to identify any differences in thymic architecture and lipid content between the groups. HFD feeding has been shown to increase thymic weight and lipid content, and induce detrimental changes in the anatomy (Gulvady et al. 2013), as well as encourage apoptosis of the thymocytes (Li et al. 2020) and developing T cell populations (Yang et al. 2009). Therefore, sections of the thymus could be taken and stained with haematoxylin and eosin and ORO, as done for the liver samples, to analyse cellularity parameters and lipid content. Immunofluorescence staining could also be applied to the thymus sections to stain for the presence of different subsets of T cells etc., to correlate changes in thymic architecture with function. This would be important as a reduction in thymic cellularity tends to correlate with compromised mature T cell output and disrupted T cell maturation (Yang et al. 2009). Additionally, although the mean heart weight of the chow - group was significantly greater than that of the HFD group, there were no significant differences in cardiac hypertrophy index between the two or any of the other groups. This suggests that chow intervention with or without (+)-catechin does not affect cardiac hypertrophy, although beneficial changes in the aortic root atherosclerotic plaques was seen (discussed later).

### 6.3.5 Changes in immune profile

Due to school closures resulting from the pandemic, flow cytometry analysis of the bone marrow and peripheral blood cell populations could not be completed for all mice that were part of this regression study. Therefore, reduced *n* numbers are available for the chow groups (in comparison to the baseline group), whilst no HFD mouse samples could be analysed. Although according to our collaborators, *n*=6 per group is sufficient to identify changes, interpretation of these results is limited due to the lack of data for the HFD group for both bone marrow and peripheral blood cell population analyses. This is as immunophenotyping of the bone marrow and peripheral blood samples are required to be conducted within 24 and 4 hours of extraction respectively (and cannot be stored), to maintain a minimum of 80% viable cells as required for successful flow cytometry analyses. In the bone marrow, no significant changes in the proportion of HSCs were seen between all groups. However, the chow + group had significantly increased proportion of MPP in the bone marrow compared to the baseline group, although the proportion of HPCs was reduced in both chow groups, possibly due to reduced proliferation. Both chow groups had significantly reduced proportion of HPC I in the bone marrow compared to the baseline group. Moreover, both chow groups had significantly reduced HPC II compared to the baseline group. Despite this reduction in the proportion of HPCs in the chow + group compared to the baseline group, the proportion of CMPs was increased (trend), which translated to an increase in the percentage of MEPs (significant). In the lineage<sup>+</sup> cell populations, only the chow + group had increased proportion of T cells (trend) compared to the baseline group (although further analyses are required to identify which subsets of T cells are increased).

Conversely, no significant differences were found between the chow - and chow + groups themselves in any of the classes of cells in the bone marrow, although in general, more significant changes were seen in the chow + group (than the chow - group) compared to the baseline group. However, data interpretation is limited by the much lower *n* numbers of the chow groups compared to that of the baseline group, as well as the lack of data for the HFD group. A summary of changes is illustrated in Figure 6.24.

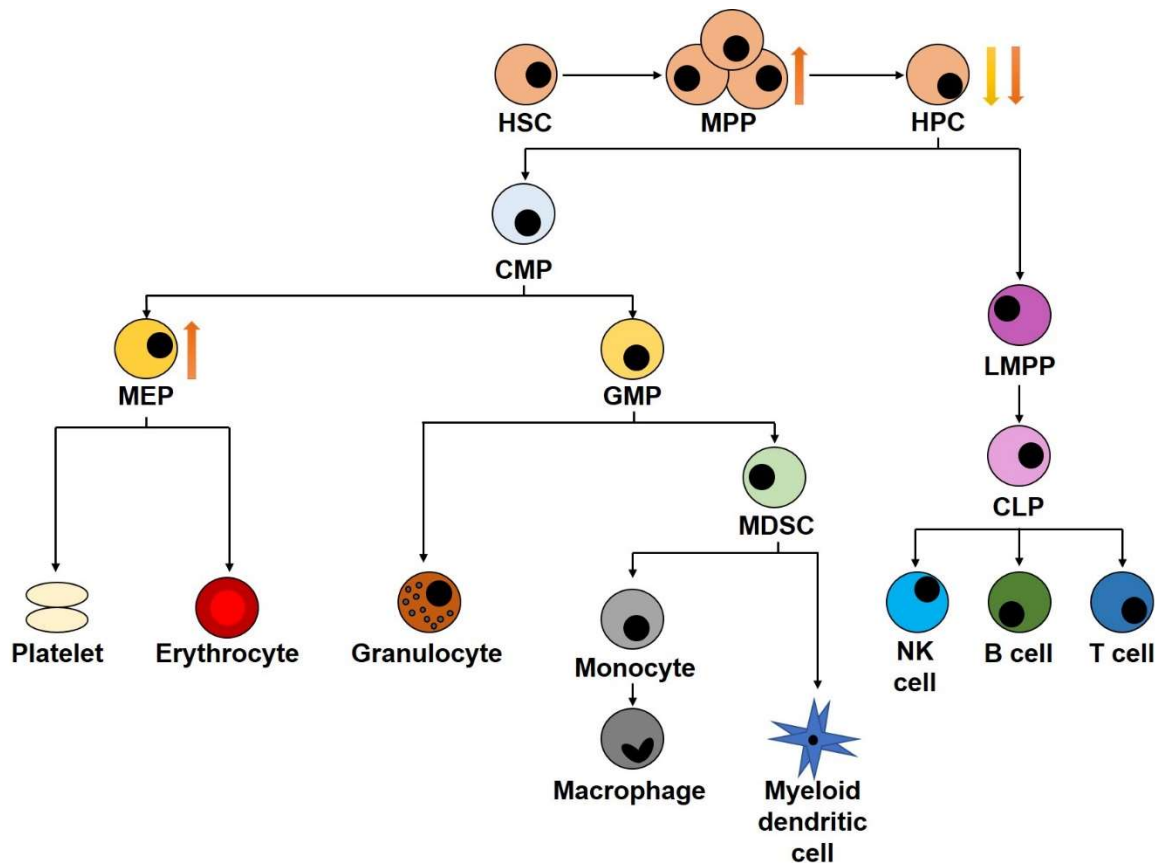


**Figure 6.24 Summary of changes in the bone marrow cell populations.**

Significant changes in the bone marrow are indicated by the arrows adjacent to the cell type. Orange arrows indicate changes in the chow + group whereas the yellow arrow indicates changes in the chow - group compared to the baseline group. Abbreviations: HSC, haematopoietic stem cell; MPP, multipotent progenitor; HPC, haematopoietic progenitor cell; CMP, common myeloid progenitor; MEP, megakaryocyte-erythroid progenitor; GMP, granulocyte-macrophage progenitor; MDSC, myeloid derived suppressor cell; LMPP, lymphoid-primed multipotent progenitor; CLP, common lymphoid progenitor; NK, natural killer.

In the peripheral blood, the chow - group had increased number of total WBCs compared to the baseline group (trend), whereas the chow + group had similar WBC numbers compared to the baseline group. This suggests that chow intervention may stimulate the egress of leukocytes from atherosclerotic plaques, resulting in their increased abundance in the peripheral blood, although no significant differences in any of the lymphoid or myeloid cell populations were identified compared to the baseline group. Greater *n* numbers may hence be required to detect more subtle changes. On the other hand, despite the chow + group having similar numbers of total WBCs to the baseline group, changes in lymphoid and myeloid cell populations were seen. The chow + group had significantly reduced number of NK cells compared to the baseline group, consistent with previous results obtained from the progression

study whereby a trend of reduction in these cells was seen (Chapter 5). Monocyte dynamics are intrinsically implicated in the regression of atherosclerotic plaques, including decreased recruitment of circulating monocytes, efflux of macrophages from the lesion or dampened cell proliferation within the lesion (Burke and Huff 2018). In the previous progression study, the abundance of Ly6C<sup>high</sup> monocytes in the peripheral blood was increased in mice receiving (+)-catechin hydrate supplemented HFD (Chapter 5). In this study, the chow + group had significantly increased number of circulating monocytes compared to the chow - group, which was attributed to an increase in Ly6C<sup>middle</sup> monocytes compared to both the baseline (significant) and chow - (trend) groups.

Both Ly6C<sup>middle</sup> and Ly6C<sup>high</sup> monocytes are considered inflammatory monocytes (Tacke et al. 2007); (+)-catechin hydrate supplemented chow may hence promote the efflux of pro-inflammatory monocytes from both developing and regressing atherosclerotic plaques, resulting in their increased presence in the peripheral blood. Indeed, a reduction in plaque macrophage content was observed in comparison to the baseline group, along with decreased presence of M1 macrophages in the plaque compared to the HFD group. However, although a trend of increase in T cells in the bone marrow was seen in the chow + group compared to the baseline group, this did not translate to the peripheral blood, suggesting the involvement of other sites and factors affecting the pool of circulating immune cells. Hence immunophenotyping of other relevant organs, such as the spleen and thymus, could also be conducted using flow cytometry analysis to gain a more detailed and global view of inflammatory profile. However, comparisons with the HFD group could not be made (along with the presence of limited *n* numbers for the chow groups), and so only limited insights are provided. A summary of changes seen in both the bone marrow and peripheral blood are illustrated in Figure 6.25.

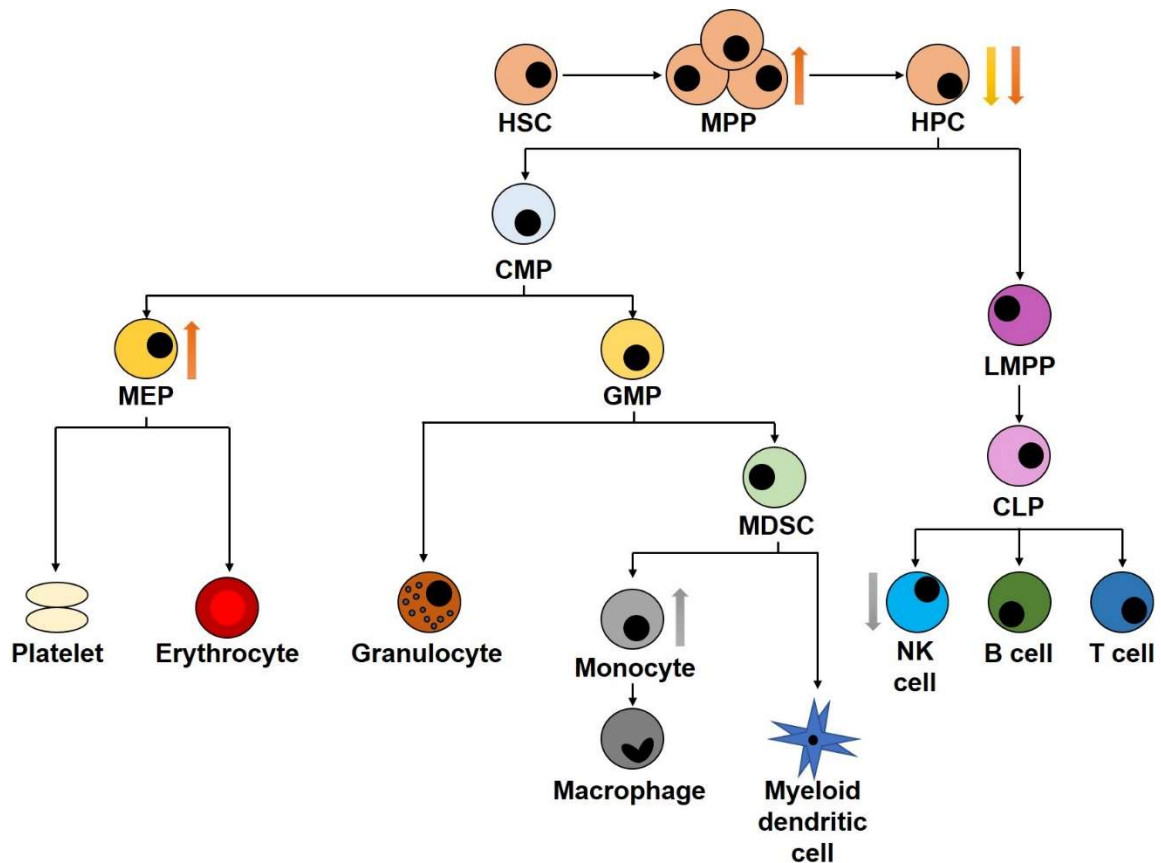


**Figure 6.25 Summary of changes in the bone marrow and peripheral blood cell populations.**

Significant changes in the bone marrow and peripheral blood are indicated by the arrows adjacent to the cell type. Orange arrows indicate bone marrow cell population changes in the chow + group whereas the yellow arrow indicates changes in the chow - group compared to the baseline group. Grey arrows indicate changes in peripheral blood cell populations for the chow + group compared to the baseline group. Abbreviations: HSC, haematopoietic stem cell; MPP, multipotent progenitor; HPC, haematopoietic progenitor cell; CMP, common myeloid progenitor; MEP, megakaryocyte-erythroid progenitor; GMP, granulocyte-macrophage progenitor; MDSC, myeloid derived suppressor cell; LMPP, lymphoid-primed multipotent progenitor; CLP, common lymphoid progenitor; NK, natural killer.

Preliminary analysis of the levels of key cytokines in the plasma found no significant differences between the chow - and chow + groups. However, marked reductions in the levels of IL-6 and CXCL1 by 83.61% and 54.38% respectively were seen based upon  $n=5$  per group. Although an increased number of intermediate inflammatory monocytes (Ly6C<sup>middle</sup> monocytes) were identified in the peripheral blood, no significant changes in the levels of various associated pro-inflammatory cytokines were seen in the plasma. However, more  $n$  numbers per group are required due to the variation of the data, although the substantial cost of the cytokine arrays is a major limiting factor. Other methods that involve a lower cost could be used, such as ELISAs, to verify changes in the levels of certain cytokines in the plasma seen with the array.

Nevertheless, these preliminary data suggest that chow combined with (+)-catechin might reverse HFD-induced systemic inflammation to a greater extent than chow intervention alone.

### 6.3.6 Effects on atherosclerotic plaque regression

Intervention with NCD completely halted atherosclerosis progression, whilst worsened plaque burden and disease severity was observed in the HFD group compared to the baseline group. Additionally, the HFD group demonstrated signs of outward vessel remodelling, as shown by the significant increased lumen area compared to the baseline group, and vessel area compared to all other groups. Despite this, the HFD group had significantly greater plaque content, occlusion and plaque size compared to all other groups, suggesting greater plaque burden and disease severity despite lower lipid content in the plaques compared to the baseline (trend) and chow + (significant) groups. Although the chow + group had significantly greater plaque lipid content compared to the HFD group, this did not translate to enhanced plaque burden or plaque inflammation.

Statistically significant differences in parameters associated with plaque burden or lipid content were not found between the chow + and baseline groups. This suggests that regression of plaque burden and lipid content was not stimulated after 8 weeks of intervention. This is in accordance with results of another study using *Ldlr*<sup>-/-</sup> mice fed atherogenic diet for 8 weeks followed by a regular diet for 8 weeks supplemented with red wine, which found no effects on the regression of fatty streaks (Chassot et al. 2018). Although plaque regression may not have been stimulated, plaque progression was certainly halted by chow intervention (with or without (+)-catechin hydrate). Analysis of plaques within the brachiocephalic artery could also be conducted to identify possible differential effects of intervention on the regression of plaques in a different vascular bed.

Although plaque burden and lipid content were not significantly attenuated by chow intervention compared to the baseline group, changes were seen in plaque inflammation and stability. The HFD group had significantly increased presence of

these iNOS<sup>+</sup> M1 macrophages compared to the baseline group, although similar percentages of MOMA-2<sup>+</sup> macrophages and CD3<sup>+</sup> T cells were seen between the two groups. This suggests enhanced M1 macrophage polarisation and associated inflammation occurs in the plaque as the disease progresses. Indeed, M1 macrophages predominate in disease progression whilst M2 macrophages predominate in disease regression (Peled and Fisher 2014). Both chow groups had reduced MOMA-2<sup>+</sup> macrophages compared to the baseline group, and decreased CD3<sup>+</sup> T cells compared to both the baseline and HFD groups, suggesting dampened plaque inflammation. This suggests that intervention with chow alone induces similar anti-inflammatory effects on the atherosclerotic plaque to reverse plaque inflammation compared to chow combined with (+)-catechin. Further immunohistochemical analyses are required to identify which subset(s) of T cells are affected, especially given the disparate roles and activities between different T cell types in atherosclerosis. Only the chow + group had reduced presence of pro-inflammatory M1-activated macrophages in the plaque compared to the HFD group (trend); this is consistent with results of the progression study (Chapter 5), whereby mice receiving (+)-catechin hydrate supplemented HFD had significantly reduced macrophage, and specifically, M1 macrophage, accumulation in developing plaques. Therefore, it would also be of interest to see if the proportion of M2 macrophages is also greater in regressing plaques following (+)-catechin intervention. However, *in vitro* studies conducted in the host laboratory found a lack of effect of (+)-catechin on macrophage polarisation, and so the reduced plaque M1 macrophages may be attributed to its effects on the clearance of pro-inflammatory monocytes/macrophages from developed lesions to regress and resolve plaque inflammation.

Only the chow + group had significantly increased percentage of  $\alpha$ SMA<sup>+</sup> VSMCs in the plaques compared to either the baseline or the HFD groups. When the chow groups were compared in isolation using an unpaired t-test, the chow + group also had significantly greater presence of plaque VSMCs compared to the chow - group. Furthermore, only the chow + group had increased plaque stability compared to the baseline and HFD groups. These observations correlate with those of the progression study (Chapter 5), whereby mice receiving (+)-catechin hydrate supplemented HFD had significantly increased VSMC and collagen content in the aortic root plaques and attenuated plaque progression. Taken together, this suggests that (+)-catechin

consistently enhances plaque stability in both progression and regression protocols, and could potentially be combined with a plaque regression-stimulating agent used to delay the onset of atherosclerotic complications and protecting against plaque rupture. However, plaque collagen content was significantly increased to a similar extent in both chow groups compared to both the baseline and the HFD groups. This suggests maintenance of a stable fibrous cap phenotype induced by chow intervention that is slightly improved by intervention with chow combined with (+)-catechin. Therefore, (+)-catechin intervention may inhibit the loss of  $\alpha$ SMA expression which occurs during the transformation of VSMCs into foam cells (Pidkovka et al. 2007; Gomez and Owens 2012). However, further studies are necessary to ascertain whether (+)-catechin inhibits VSMC foam cell formation, and how VSMC activity and phenotypic switching is affected. Furthermore, lineage-tracing studies could be employed to determine the origin of  $\alpha$ SMA<sup>+</sup> cells during atherosclerosis regression and how (+)-catechin intervention promotes the maintenance of these cells. As a result, only the chow + group had an increased plaque stability index compared to the baseline (significant) and HFD (trend) groups. Although there were no significant differences in percentage plaque necrosis between all groups, comparison of the total necrotic area values themselves (not standardised to total plaque area) found that this was significantly increased in the HFD group compared to all other groups. This was done due to significant differences in plaque size and demonstrates that growth of the necrotic core coincides with plaque progression.

### 6.3.7 Future directions

Intervention with NCD for 8 weeks following 12 weeks of HFD feeding did not induce the regression of plaque burden and lipid content as expected, although disease progression was entirely halted. This suggests a possible need for further optimisation of the feeding protocol, perhaps by extending the intervention duration from 8 weeks to 10. Furthermore, exploration of the ability of chow combined with (+)-catechin to induce atherosclerosis regression in *Apoe*<sup>-/-</sup> mice could be conducted, since these mice develop lesions spontaneously on a NCD without the need for dietary manipulation. *Apoe*<sup>-/-</sup> mice fed HFD also develop less severe metabolic dysfunction in comparison to *Ldlr*<sup>-/-</sup> mice (Getz and Reardon 2016), and so the effect of (+)-catechin

to induce atherosclerosis regression could be investigated in both cases to study its pleiotropic effects beyond its metabolic activities. This could also be done by combining (+)-catechin with HFD instead of chow, to determine whether regression continues with intervention in the context of HFD feeding. Aside from this, it would also be interesting to combine chow combined with (+)-catechin intervention with other agents, such as statins, to determine whether plaque regression can be stimulated and plaque stability further enhanced, given the ability of (+)-catechin to consistently promote fibrous cap maintenance as part of both prevention and therapeutic strategies. Indeed, other nutraceutical agents have demonstrated potential in lowering cardiovascular risk further as a co-therapy with statins. For example, daily intake of 4 g of purified EPA ethyl ester has been shown to reduce the occurrence of cardiovascular events by 32% (Bhatt et al. 2019) and unstable plaque burden without affecting TG levels (Budoff et al. 2020) in patients on statin therapy. Therefore, nutraceuticals represent promising alternative preventative and therapeutic avenues that can be exploited as part of combinational therapies with current pharmacological agents for atherosclerotic CVD. Further studies investigating the actions and underlying mechanisms of individual nutraceutical agents in isolation are still required. The data obtained as part of this project support the promise of (+)-catechin in the prevention of atherosclerosis development and progression via its inhibitory effects on multiple key processes implicated in early atherogenesis associated with endothelial and VSMC dysfunction. However, further investigations are needed to elucidate the underlying mechanisms responsible for its actions in the context of atherosclerosis regression and examples of these are included in Figure 6.26.

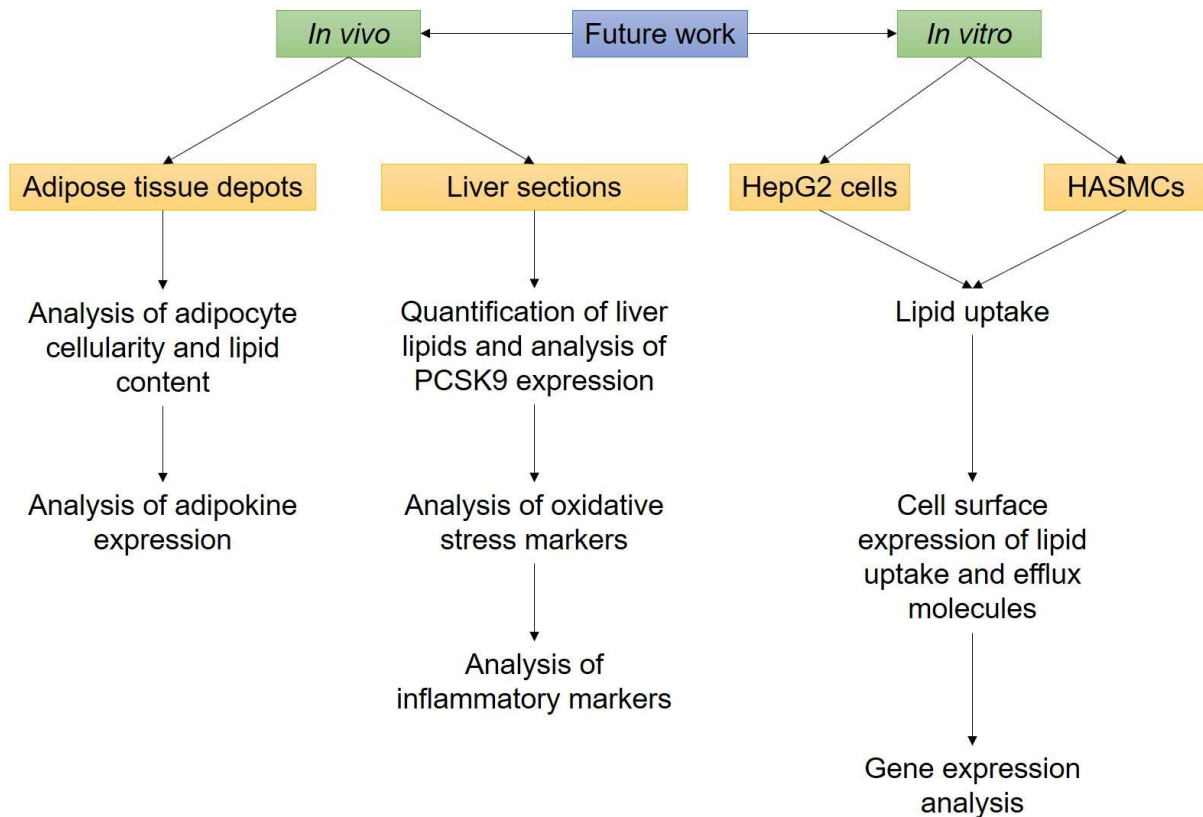


**Figure 6.26 Further investigations into the effects of (+)-catechin on atherosclerosis regression.** Abbreviations: PCSK9, proprotein convertase subtilisin/kexin 9; HASMC, human aortic smooth muscle cell.

### 6.3.8 Conclusion

In conclusion, intervention with (+)-catechin hydrate combined with chow modulates various atherosclerosis associated risk factors, for example by reversing HFD-induced adiposity and hepatic injury, at a greater extent than intervention with chow alone. Additionally, chow combined with (+)-catechin enhanced the maintenance of  $\alpha$ SMA<sup>+</sup> VSMCs better than chow intervention alone. Further investigations are required to determine how (+)-catechin consistently enhances plaque stability in *Ldlr*<sup>-/-</sup> mice and modulates the activity and phenotype of VSMCs. Whilst (+)-catechin is capable of attenuating atherosclerosis development and progression, results of this chapter suggest (+)-catechin is less efficacious at stimulating atherosclerosis regression in the *Ldlr*<sup>-/-</sup> model, since less significant changes were detected between the chow groups themselves. Overall, comparable results were obtained from both chow groups,

## Chapter 6: Effect of (+)-catechin on atherosclerosis regression

suggesting that (+)-catechin demonstrates more promise as a preventative agent rather than a therapeutic one for atherosclerosis.

## 7 General Discussion

### 7.1 Introduction

Globally, CVD remains a substantial health and economic burden in current society that is no longer restricted to developed nations, due to widespread increasing prevalence of risk factors such as obesity and diabetes. Atherosclerosis is the key underlying cause of CVD, a chronic, low-grade inflammatory disorder of the vasculature that develops over decades, leading to the erosion or rupture of fibrous plaques within the arterial wall (Frostedgard 2013; Libby 2021). The end consequence of plaque rupture most commonly manifests as MI and cerebrovascular accident, with others including coronary heart disease and peripheral vascular disease (Virani et al. 2021). Although the widespread application of statins (the mainstay therapeutic intervention), which inhibit endogenous cholesterol synthesis and have additional anti-inflammatory and pleiotropic effects, has positively impacted CVD mortality rates, various issues and limitations are associated with their use. These include adverse side effects, such as myalgias, hepatic abnormalities and rhabdomyolysis (rare but severe) (Calderon et al. 2010), which may contribute to patient non-compliance and consequently uncontrolled plasma cholesterol levels. Importantly, clinical trials have identified that cardiovascular risk persists post therapy (Campbell et al. 2007; Libby et al. 2011; Sampson et al. 2012), derived from, for example, residual IL-1 $\beta$ -driven inflammation that drives MACE independently of hypercholesterolaemia (Libby 2017). Particularly, since the efficacy of anti-IL-1 $\beta$  monoclonal antibody, Canakinumab, in attenuating cardiovascular risk in previous MI patients with elevated CRP levels (the key marker of chronic IL-1/6 inflammation) was identified (Ridker et al. 2017), clinical trials investigating anti-inflammatory agents (for example, use of broad spectrum anti-inflammatory agents such as colchicine) for the prevention of atherosclerosis-associated complications have increased (Nidorf et al. 2013; Tardif et al. 2019; Nidorf et al. 2020). Natural products have also gained attention for the prevention of atherosclerosis, particularly due to their various anti-inflammatory and anti-oxidative effects and potential to be combined with current pharmacological therapies (Moss and Ramji 2016b; Moss et al. 2018). Nutraceuticals, such as catechins and omega-3 PUFAs, have gained increasing recognition as promising alternative preventative/therapeutic avenues for atherosclerosis (Moss and Ramji 2016b; Moss

et al. 2018). Advantages include the generally good safety profiles at high doses, lower cost, and greater availability in comparison to pharmaceutical agents. A key example being EPA, which has demonstrated the ability to reduce the occurrence of cardiovascular events (Bhatt et al. 2019) and unstable, rupture-prone plaque burden without affecting TG levels (Budoff et al. 2020) in patients already receiving statins in the REDUCE-IT trial. Similar to EPA, catechins also possess potent anti-oxidative and anti-inflammatory activities that could be exploited for the prevention and treatment of atherosclerosis (Moss and Ramji 2016b; Moss et al. 2018). This is supported by results of a large prospective study identifying a strong inverse correlation between (+)-catechin and (-)-epicatechin intake with risk of coronary heart disease (Arts et al. 2001b). Despite this, there have been a lack of studies (both in animal models and in humans) investigating the actions and underlying mechanisms of (+)-catechin itself in the context of atherosclerosis. Therefore, although there has been an abundance of evidence supporting the cardioprotective effects of foods rich in flavanols (Rees et al. 2018), effects of individual flavanols in the context of atherosclerosis remain elusive. As such, atherosclerosis research conducted in the host laboratory has been focused on uncovering the actions and mechanisms of individual natural products. Previous studies conducted in the host laboratory found (+)-catechin to demonstrate various anti-atherogenic activities in human monocytes and macrophages, and in WT mice fed HFD for 3 weeks, daily gavage of (+)-catechin hydrate modulated several atherosclerosis-associated risk factors (Moss 2018). Furthermore, in *ApoE*<sup>-/-</sup> mice, (+)-catechin supplementation attenuated atherosclerotic plaque burden and modulated the expression of numerous genes (Auclair et al. 2009). Therefore, although (+)-catechin demonstrates promise in attenuating atherosclerosis *in vitro* and *in vivo*, further studies are required to characterise its effects and underlying mechanisms of action. This project was hence focused on delineating the *in vitro* effects of (+)-catechin further and determine its preventative and therapeutic potential in the *Ldlr*<sup>-/-</sup> mouse model of atherosclerosis. A summary of the key aims, objectives and the associated experimental approach is illustrated in Figure 7.1.

## Chapter 7: General Discussion

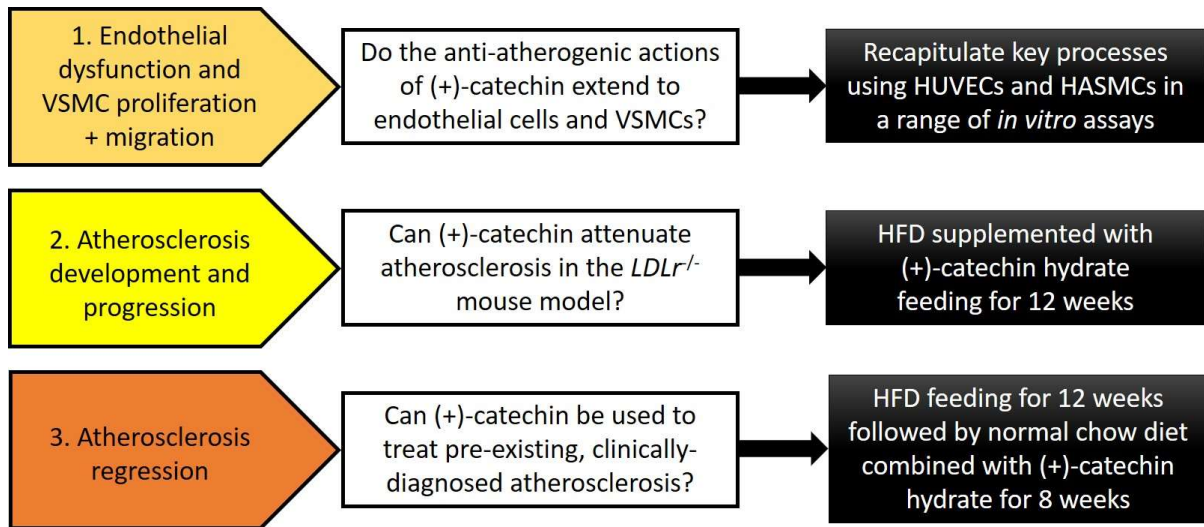


**Figure 7.1 Summary of key aims and objectives with outlines of experimental approach.**

Abbreviations: VSMC; vascular smooth muscle cell; HUVEC, human umbilical vein endothelial cells; HASMC, human aortic smooth muscle cell; *Ldlr*, low-density lipoprotein receptor; HFD, high-fat diet.

## 7.2 Summary of key findings

### 7.2.1 *In vitro*

The first aim of this project was to determine whether the anti-atherogenic effects of (+)-catechin demonstrated in monocytes and macrophages also extend to ECs and VSMCs, to attenuate parameters associated with endothelial and VSMC dysfunction respectively. As (+)-catechin previously demonstrated anti-inflammatory and anti-atherogenic effects in human monocytes and macrophages (Moss 2018), it was hypothesised that these effects would also apply to other key cell types implicated in atherosclerosis. This was especially important since oxLDL is a potent and key instigator of endothelial dysfunction (the key initiating step of atherogenesis), and one of the ways in which oxLDL acts, is via TNF- $\alpha$ . Furthermore, VSMCs have been increasingly recognised as a key source of plaque cells, with much greater plasticity and heterogeneity than previously thought (Basatemur et al. 2019), and hence able to contribute to pathogenesis via various mechanisms. Therefore, it was important to extend *in vitro* studies beyond monocytes and macrophages, to further characterise the anti-atherogenic actions of (+)-catechin (Chapter 3). Key results obtained previously in the host laboratory were also confirmed using primary HMDMs, to verify that previous observations associated with human monocytes/macrophages were not specific to the cell line. Concurring with previously obtained data, (+)-catechin-treated

HMDMs indeed demonstrated reduced proliferation (Figure 3.6C), ROS production (Figure 3.8A) and MMP activity (Figure 3.14B). Furthermore, the ability of (+)-catechin to attenuate monocytic migration (Figure 3.16A) and ROS production (Figure 3.16B) was confirmed in this study, with comparable effects to its isomers, (-)-catechin and (-)-epicatechin.

A range of *in vitro* assays were utilised to recapitulate parameters associated with endothelial and VSMC dysfunction (with focus on VSMC proliferation and migration). This was done using HUVECs (stimulated with oxLDL or TNF- $\alpha$  to induce their activation) and HASMCs respectively (Chapter 3). Key findings include the attenuation of ROS production in both unstimulated ECs (Figure 3.8B) and VSMCs (Figure 3.8C and D), as well as in TNF- $\alpha$ -stimulated ECs after pre-treatment (Figure 3.9B). Moreover, (+)-catechin attenuated PDGF-induced migration (invasion) of VSMCs (Figure 3.13B) without affecting basal proliferation (Figure 3.13C). Given the promising results seen in macrophages and ECs so far, further experiments were conducted to determine the effect of (+)-catechin on mitochondrial function in these cell types (Chapter 4). Since shifts in cellular metabolism can indicate pathophysiological changes, the maintenance of mitochondrial function is hence important for cellular homeostasis. Increasing evidence supports the involvement of mitochondrial dysfunction in driving atherosclerosis progression (Yu et al. 2013; Yu and Bennett 2014; Wang et al. 2017; Yu et al. 2017; Peng et al. 2019). Hence, assays enabling investigation of mitochondrial membrane potential, ROS production and respiration etc. were utilised. Preliminary data suggest that in both unstimulated macrophages and ECs, (+)-catechin treatment resulted in enhanced spare respiratory capacity (Figures 4.7F and 4.13F). Moreover, in macrophages, non-mitochondrial respiration was increased (Figure 4.7H) and mitochondrial ROS production was decreased (Figure 4.11A). In ECs, basal respiration was reduced (Figure 4.13B). In pro-inflammatory M1 macrophages, (+)-catechin decreased basal and ATP-linked respiration (Figures 4.9B and D), and in activated ECs, (+)-catechin attenuated oxLDL-stimulated mitochondrial membrane depolarisation (Figure 4.12B) and increased non-mitochondrial respiration (Figure 4.14F). Taken together, (+)-catechin attenuates various key processes implicated in early atherogenesis via anti-inflammatory and anti-oxidative effects (e.g., attenuation of monocytic migration, macrophage proliferation and ROS production by multiple sources), and demonstrates protective

effects on mitochondrial function. However, limitations of the bioenergetics data (as discussed in Chapter 4) mean that interpretation of these results is limited, and further repeats and experiments are required to verify these observations. A summary of the key *in vitro* effects of (+)-catechin are illustrated in Figure 7.2.

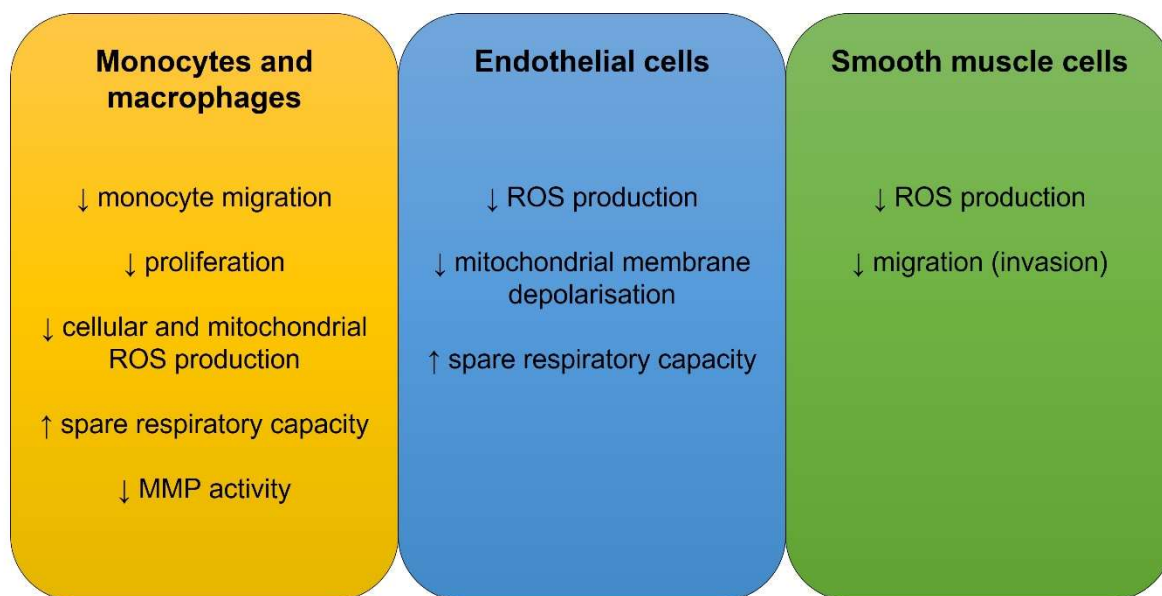


**Figure 7.2 Summary of key findings *in vitro*.**

Abbreviations: ROS, reactive oxygen species; MMP, matrix metalloproteinase.

### 7.2.2 *In vivo*

Given the anti-atherogenic effects of (+)-catechin in all key cell types implicated in atherosclerosis (i.e., monocytes and macrophages, ECs and VSMCs), along with its ability to modulate several risk factors associated with atherosclerosis in HFD-fed WT mice in previous research conducted in the host laboratory, the hypothesis that (+)-catechin can attenuate atherosclerosis development and progression *in vivo* was solidified. This was reinforced by results from a transcriptomic study using *ApoE*<sup>-/-</sup> mice, which found (+)-catechin supplementation (at a low nutritional level of 0.02% in the diet for 6 weeks) to attenuate atherosclerotic plaque burden without affecting plasma (or liver) lipid profile, antioxidant capacity and inflammatory status (Auclair et al. 2009). Whilst this approach provided valuable insights to the potential mechanisms underlying the actions of (+)-catechin *in vivo*, analysis of resulting plaques was highly restricted. Although this was the only published study to use (+)-catechin in a mouse

model of atherosclerosis, analysis of plaque immune cells (such as presence of macrophages and T cells) was lacking, and even plaque burden analysis was only based upon lesion size e.g., no quantification of lipid content etc. Hence, correlation of the gene expression changes in the aorta with plaque burden and inflammation etc. was limited. For example, although it was hypothesised that a reduction in *LPL* and *scavenger receptor class A, member 5 (SCARA5)* gene expression could potentially dampen the formation and uptake of LDL by macrophages and subsequent foam cell formation (Auclair et al. 2009), the presence of macrophage foam cells within atherosclerotic plaques was not investigated. Furthermore, the ability of (+)-catechin to attenuate atherosclerosis in the less aggressive *Ldlr*<sup>-/-</sup> model, which is more akin to diet-induced atherosclerosis in humans, was yet to be investigated. Therefore, an important aim of this project was to determine whether (+)-catechin supplementation could attenuate plaque formation and development and encourage plaque stabilisation in the *Ldlr*<sup>-/-</sup> model of atherosclerosis (Chapter 5). *Ldlr*<sup>-/-</sup> mice that had received (+)-catechin (in the form of (+)-catechin hydrate at a dose of 200 mg/kg/day) supplemented HFD for 12 weeks demonstrated attenuated plaque development within the aortic root. This was shown by the reduction in plaque burden (Figure 5.19C-E) and inflammation (associated with macrophages) (Figure 5.20B) without affecting lipid content (Figure 5.19B). This was accompanied by a reduction in haematopoiesis, whereby the proportion of HPSCs (Figures 5.9C and Figure 5.10E) and T cells (Figure 5.11E) were reduced in the bone marrow. However, the presence of Ly6C<sup>high</sup> monocytes in the peripheral blood was enhanced (Figure 5.14G). Despite this, there were no significant changes in the levels of measured cytokines in the plasma, apart from a small but significant reduction in IL-5 levels (Figure 5.17F). Furthermore, plaque stability was enhanced (Figure 5.21F), owing to the increased presence of SMCs (Figure 5.21D) and collagen content (Figure 5.21C) combined with decreased macrophage presence (Figure 5.20B), suggesting inhibition of progression towards an unstable phenotype. A summary of the key changes seen *in vitro* and *in vivo* in the context of atherosclerosis development and progression are illustrated in Figure 7.3.

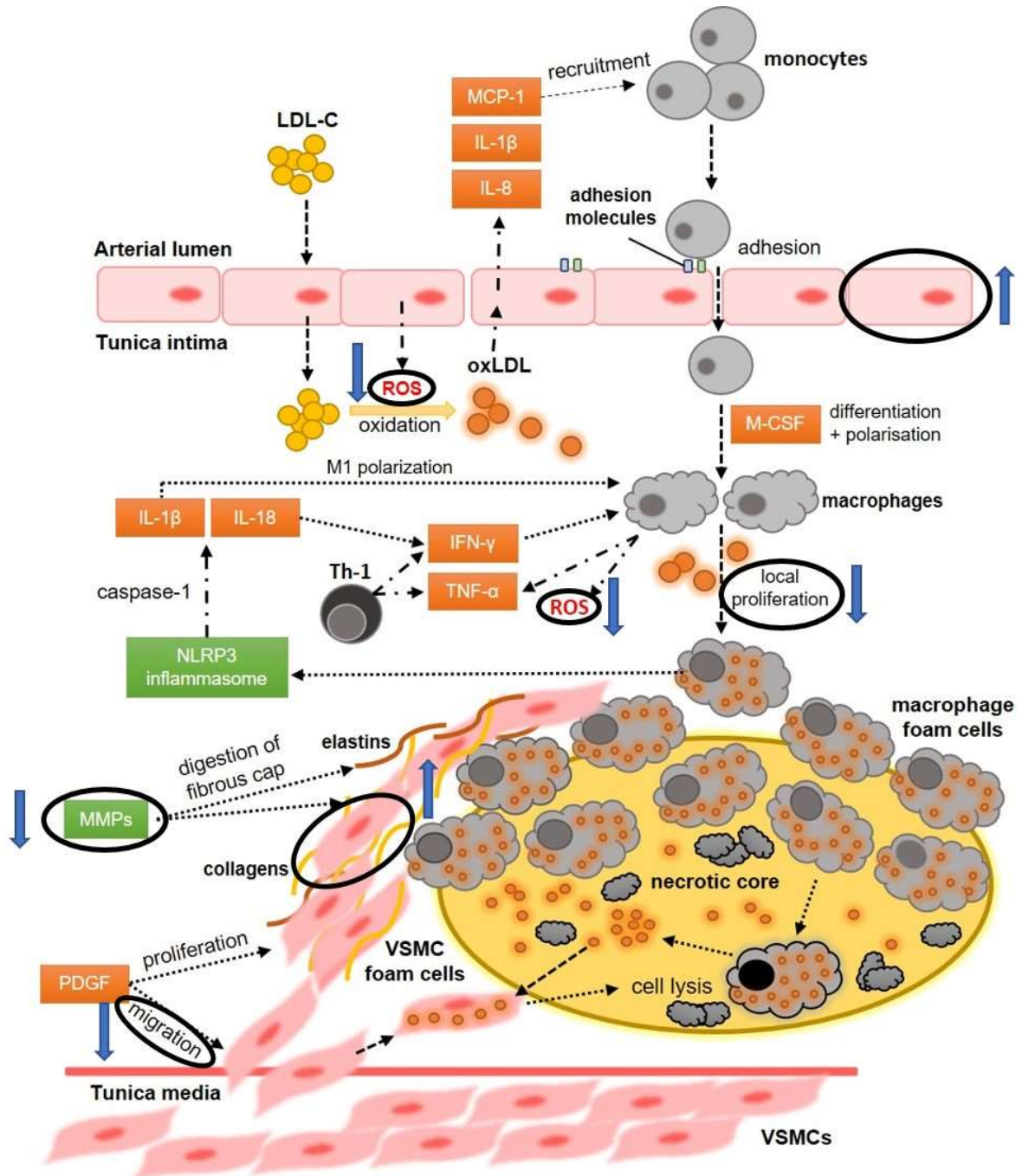


**Figure 7.3 Summary of key findings *in vivo* relating to atherosclerosis development and progression.**

Modified from Chan and Ramji (2020). Processes significantly modulated by (+)-catechin are highlighted with a black circle and changes indicated by arrows. Abbreviations: LDL, low-density lipoprotein; SR-B1, scavenger receptor-B1; MCP-1, monocyte chemotactic protein-1; IL-1 $\beta$ , interleukin-1 $\beta$ ; IL-8, interleukin-8; ROS, reactive oxygen species; oxLDL, oxidised LDL; M-CSF, macrophage colony-stimulating factor; GM-CSF, granulocyte-macrophage colony-stimulating factor; SR, scavenger receptor; IL-18, interleukin-18; IFN- $\gamma$ , interferon- $\gamma$ ; TNF- $\alpha$ , tumor necrosis factor- $\alpha$ ; IL-2, interleukin-2; T<sub>H1</sub>, T-helper 1 cell; NLRP3, nucleotide oligomerisation domain (NOD) leucine-rich repeat (LRR) and pyrin domain (PYD) containing protein 3; MMPs, matrix metalloproteinases; PDGF; platelet-derived growth factor; VSMC, vascular smooth muscle cell.

## Chapter 7: General Discussion

Since atherosclerosis development and progression was attenuated by (+)-catechin supplementation in HFD-fed *Ldlr*<sup>-/-</sup> mice, it was hypothesised that intervention with (+)-catechin could also induce the regression of established atherosclerotic plaques. However, to date, there have been no published studies investigating the ability of catechins (or (+)-catechin itself), to induce atherosclerosis regression *in vivo*, with few studies investigating natural agents in this regard. Therefore, the last study conducted as part of this project investigated the therapeutic potential of (+)-catechin, by determining the effect of (+)-catechin combined with chow intervention on established atherosclerosis and associated risk factors (Chapter 6). In *Ldlr*<sup>-/-</sup> mice fed HFD for 12 weeks to induce established atherosclerosis, intervention with chow combined with (+)-catechin for 8 weeks reversed HFD-induced adiposity associated with white adipose tissue deposits and hepatic injury to a greater extent than chow intervention alone. This was despite the fact that HFD-induced hyperlipidaemia was reversed to similar extent after intervention with chow alone or in combination with (+)-catechin. Although there were no differences in plaque inflammation between the two chow groups, plaque stability was enhanced to a greater extent by (+)-catechin combined with chow intervention compared to chow intervention alone. A summary of the effects of (+)-catechin on atherosclerosis regression in the *Ldlr*<sup>-/-</sup> mouse model are illustrated in Figure 7.4. Therefore, results obtained thus far demonstrate that (+)-catechin appears to elicit more beneficial effects on developing atherosclerotic plaques than those in recession, since lesion regression was not achieved.

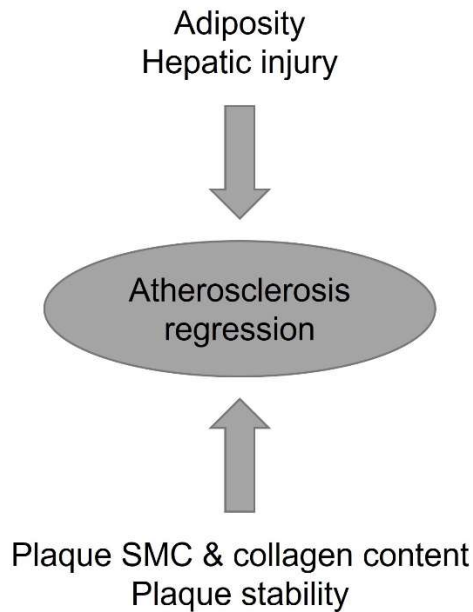


**Figure 7.4 Summary of key findings *in vivo* relating to atherosclerosis regression.**

Intervention with catechin combined with chow (rather than chow alone) reverses HFD-induced adiposity and hepatic injury. Plaque stability was also enhanced, derived from increased presence of smooth muscle cells (SMCs) and collagen.

In summary, and to answer the three original key questions proposed, the anti-atherogenic actions of (+)-catechin do indeed extend to other key cell types of the disease, i.e., ECs and VSMCs. However, (+)-catechin may have more potent atheroprotective effects (associated with its antioxidative and anti-inflammatory actions) on monocytes/macrophages in comparison to the other two investigated cell types based upon results presented in Chapters 3 and 4 (see Figure 7.2). This is as, more significant changes are induced in monocytes/macrophages compared to HUVECs and HASMCs. Furthermore, mice that had received (+)-catechin supplemented HFD for 12 weeks demonstrated reduced atherosclerosis (as shown by decreased plaque content and occlusion), which was associated with a marked reduction in plaque macrophage content (Chapter 5). This was also accompanied by enhanced plaque stability parameters i.e., plaque SMC and collagen content (to a lesser extent). However, additional studies in ECs and VSMCs are required to fully substantiate this conclusion since studies conducted thus far in the host laboratory have largely focused on monocytes/macrophages, and further optimisation of assays using ECs (and other cell types) is still required. In the context of atherosclerosis regression, there were much fewer beneficial changes observed, both in the plaques

and in other associated parameters, when data from the two chow intervention groups were directly compared (Chapter 6). Therefore, although (+)-catechin is able to attenuate atherosclerosis development and progression and promote plaque stability, (+)-catechin does not appear to be able to stimulate the regression of established atherosclerotic plaques in *Ldlr*<sup>-/-</sup> mice, suggesting more promise in disease prevention rather than treatment.

### 7.3 Potential mechanisms of action

#### 7.3.1 Atherosclerosis development and progression

In normal physiological homeostasis, the endothelium does not recruit circulating immune cells and is impermeable to these along with lipoproteins in the plasma (Libby 2021). Various risk factors can stimulate endothelial dysfunction, whereby changes associated with activated ECs facilitate the infiltration of circulating leukocytes (and lipoprotein molecules). During inflammation, the recruitment and adhesion of circulating monocytes (and other leukocytes) are critical processes that facilitate their infiltration into the arterial sub-endothelial layer, where they drive atherogenesis and lesion formation. The adherence of leukocytes to the activated endothelium is facilitated by an array of adhesion molecules, such as E-selectin and VCAM-1 together with other selectins and integrins (Ramji and Davies 2015).

Combining findings of previous studies conducted in the host laboratory, (+)-catechin attenuated MCP-1-stimulated monocyte migration, along with the proliferation and ROS production of both monocytes and macrophages (which was confirmed in primary macrophages). This was combined with protective effects on mitochondrial function in both PMA-differentiated and M1 polarised macrophages. Furthermore, (+)-catechin also demonstrated protective effects on oxLDL-induced mitochondrial dysfunction in ECs, suggesting attenuation of parameters associated with endothelial dysfunction and maintenance of EC and macrophage homeostasis. Therefore, results suggest that (+)-catechin targets multiple key processes implicated in early atherosclerosis development associated with its anti-inflammatory and anti-oxidative actions on monocytes, macrophages, and ECs.

## Chapter 7: General Discussion

In another study, *Apoe*<sup>-/-</sup> mice that had received (+)-catechin supplementation for 6 weeks had down-regulated expression of adhesion molecules involved in mediating the adherence of leukocytes to the endothelium, *CD34* and *PSGL-1* (Auclair et al. 2009). Furthermore, (+)-catechin treated human macrophages also had reduced expression of genes encoding adhesion molecules implicated in cell recruitment and migration; *laminin subunit alpha-1 (LAMA1)*, *E-selectin* and *L-selectin* (Moss 2018). However, the effect of (+)-catechin treatment on the expression of these molecules involved in immune cell recruitment and chemotaxis in oxLDL or TNF- $\alpha$ -stimulated ECs still requires elucidation. These effects may be responsible for the attenuation of plaque development *in vivo*, as shown by the reduction in plaque content within the vessel, plaque occlusion and plaque size (results of Chapter 5). Moreover, these changes were associated with a marked reduction in the presence of macrophages within the plaque, and in particular, reduced abundance of proinflammatory M1 macrophages. This may also be attributed to the anti-proliferative effects of (+)-catechin in both monocytes and macrophages, attenuating their local proliferation within the lesion. Therefore, (+)-catechin may attenuate atherogenesis by dampening the recruitment of monocytes, their infiltration through the activated endothelium, and the proliferation of intimal monocytes and macrophages, resulting in their reduced presence and retention within the arterial wall.

Indeed, analysis of gene expression changes in the descending aorta found (-)-epicatechin (an isomer of (+)-catechin) supplementation to modulate 77 genes induced by a high-cholesterol diet, involved in cell chemotaxis and accumulation of myeloid cells (Morrison et al. 2014). This was associated with a reduction in the presence of neutrophils within lesions, and attenuated activation of NF- $\kappa$ B, a master regulator of inflammation. Both these studies report attenuation of atherosclerosis development by these catechins without affecting lipid profile (Auclair et al. 2009; Morrison et al. 2014). Therefore, evidence supports the conclusion that (+)-catechin mediates its anti-atherogenic effects via its anti-inflammatory and anti-oxidative properties, rather than restorative effects on dyslipidaemia and lipid metabolism. In previous studies conducted in the host laboratory, no significant effects were seen in macrophage apoptosis, cholesterol efflux and uptake (Moss 2018). Furthermore, lipid accumulation was not affected in murine macrophages, nor was their polarisation into the M1 phenotype (Moss 2018). Therefore, rather than affecting macrophage

polarisation or lipid metabolism, (+)-catechin may transduce its anti-inflammatory effects by attenuating monocyte recruitment to the site of dysfunction and protection against endothelial dysfunction, resulting in reduced *trans*-endothelial diapedesis and infiltration of these cells into the arterial wall. Reduced monocyte accumulation in developing plaques, hence the reduced presence of differentiated macrophages and a reduction in their local proliferation may thereby contribute to attenuate plaque development and inflammation.

Indeed, *in vivo*, this study found that (+)-catechin supplementation positively modified the composition of plaques within the aortic root. The plaques were smaller in size, resulting in reduced plaque content and occlusion within the vessel, and had reduced presence of macrophages, despite no effect on plaque lipid content or the levels of LDL within the plasma. Given that (+)-catechin consistently demonstrated anti-oxidative effects in all investigated cell types (after short-term treatment of 3 hours) as shown by the potent reductions in ROS production (Chapter 3), along with protective effects on mitochondrial ROS and function (Chapter 4), it is likely that its observed anti-inflammatory and anti-atherogenic effects are mediated via signalling pathways that involve ROS. Importantly, NF- $\kappa$ B, for example, may be activated when its inhibitor is degraded by ROS (Moris et al. 2017). It has been suggested that catechins may also inhibit NF- $\kappa$ B activation via regulation of upstream protein kinases, such as JNK1/2, p38, and phosphatidylinositol 3-kinase (PI3K/Akt) (Fan et al. 2017). Therefore, perhaps (+)-catechin mediates its anti-atherogenic effects via its anti-ROS and oxidative stress-preventing capabilities to inhibit pro-inflammatory signalling pathways. Indeed, it has been proposed that various other flavonoids transduce their anti-inflammatory effects via modulation of this transcription factor (Choy et al. 2019). Notably, *ApoE*<sup>-/-</sup> mice fed high-cholesterol diet supplemented with epicatechin, dampened NF- $\kappa$ B activation resulting in reduced presence of systemic pro-inflammatory markers (Morrison et al. 2014). Similar to (-)-epicatechin, (+)-catechin may transduce its anti-inflammatory effects via modulation of NF- $\kappa$ B signalling, which may be mediated by its protective effects against elevations in ROS and potentially ROS-induced oxidative stress. This transcription factor, a master regulator of inflammation, has long been implicated in atherosclerosis and other inflammatory pathologies, due to its ability to regulate various processes, including cell migration, adhesion and invasion, T cell differentiation and cell proliferation and survival (Kumar

et al. 2004; Liu et al. 2017). Both NF- $\kappa$ B and AP-1 are redox-sensitive transcription factors implicated in the response to oxidative stress (Braicu et al. 2013). Normal redox signalling is necessary for the maintenance of cardiovascular homeostasis, and various transcription factors are under the regulation of redox signalling. Sources of ROS within the cardiovascular system are various (summarised in Figure 7.5), and normal redox signalling is paramount for the maintenance of homeostasis.

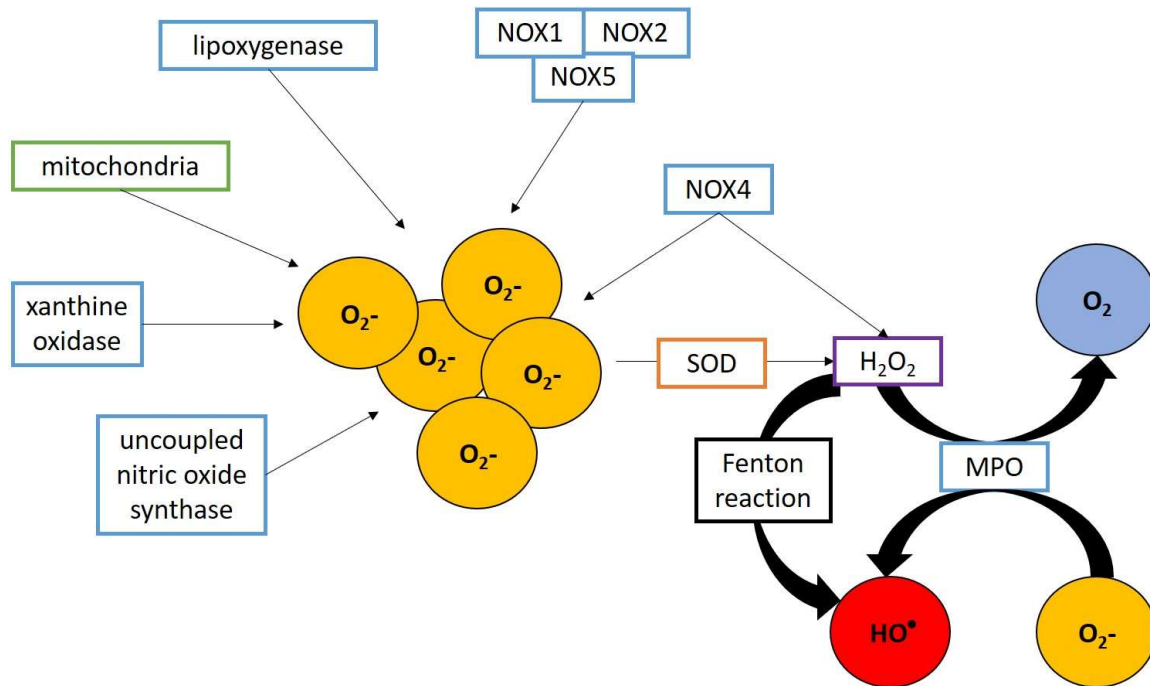


**Figure 7.5 Sources of reactive oxygen species in the vascular wall.**

Abbreviations: NOX, nicotinamide adenine dinucleotide phosphate (NADPH) oxidase; SOD, superoxide dismutase; MPO, myeloperoxidase.

As previously mentioned, sustained elevations in ROS can contribute to endothelial dysfunction and encourage EC senescence and activation of pro-inflammatory signalling, leading to atherogenesis. Oxidative stress can dampen NO production and activity via LDL-independent mechanisms; for example,  $O_2^-$ , superoxide, can inactivate NO and eliminate tetrahydrobiopterin (a cofactor imperative for NO generation) (Chen et al. 2010; Moris et al. 2017). Therefore, elevations in ROS can mediate endothelial dysfunction and vascular abnormalities via the disruption of NO signalling, resulting in NOS uncoupling and further ROS generation. Moreover, NOX, a major source of ROS in the vascular wall, is also activated by TNF- $\alpha$ . NOX has been shown to be involved in the regulation of TNF- $\alpha$ -induced NF- $\kappa$ B activation and

upregulation of proinflammatory mediators, IL-1 $\beta$  and VCAM-1, in human cardiomyocytes (Moe et al. 2014). Indeed, in atherosclerosis-prone regions, endothelial NF- $\kappa$ B is primed for enhanced activation in response to systemic pro-atherogenic stimuli (Hajra et al. 2000).

It has also been proposed that catechin may improve hypertension by forming a stable radical with ROS-derived NOX, thus preventing the assembly of NADPH oxidase (NOX) subunits (Yousefian et al. 2019). Furthermore, excessive ROS production occurs during mitochondrial dysfunction and induces irreversible damage to mitochondria, leading to dysfunction and compromised respiratory output. Mitochondrial oxidative stress can also lead to further ROS production, resulting in mtDNA damage and mitochondrial dysfunction (Mikhed et al. 2015), and has been shown to promote atherosclerosis progression via the formation of neutrophil extracellular traps (Wang et al. 2017). Therefore, (+)-catechin may attenuate parameters of endothelial dysfunction via protection against oxidative stress-induced EC activation and subsequent NF- $\kappa$ B-mediated inflammation by attenuating ROS production from multiple sources.

However, despite being able to reduce intracellular ROS production in multiple cell types *in vitro* (and even mitochondrial ROS in macrophages), plasma oxidative stress parameters (plasma ROS/RNS and MDA concentrations) were not found to be attenuated *in vivo* (Chapter 5). These results coincided with those of the previous pilot study conducted in the host laboratory using WT mice (Moss 2018). A lack of effect on LDL oxidation and plasma antioxidant status have also been reported in humans following intake of catechins in the form of tea in both smokers (Princen et al. 1998; de Maat et al. 2000) and non-smokers (van het Hof et al. 1997; van het Hof et al. 1999). This is despite studies in humans whereby administration of green tea (as a beverage or extract) increased plasma antioxidant activity/capacity and reduced plasma MDA concentrations (Freese et al. 1999; Sung et al. 2000; Young et al. 2002). This is possibly attributed to the type of catechins and the use of them in combination, as well as their dose and duration and study population used. Further exploration of the effects of (+)-catechin itself on oxidative stress parameters are required, for example by using dihydroethidium, a superoxide indicator, to evaluate the presence of ROS within the atherosclerotic lesion itself.

Conversely, it is important to note that based upon previously presented data and other published studies, unfavourable changes to plasma parameters does not necessarily translate to detrimental effects on the atherosclerotic plaque. For example, as mentioned previously, multiple studies have reported attenuation of atherosclerosis despite a lack of effect on plasma lipid profile or antioxidant capacity, and in Chapters 5 and 6, elevations in circulating levels of pro-inflammatory Ly6C<sup>middle/high</sup> monocytes in the peripheral blood was not accompanied by enhanced disease severity, suggesting involvement of ROS-independent anti-inflammatory effects associated with leukocyte emigration. Indeed, use of antioxidants such as ascorbic acid (vitamin C) failed to confer the anti-atherogenic effects and cardiovascular risk attenuation as expected in multiple clinical trials (Moss and Ramji 2016b). For example, combined supplementation of vitamin C and E had no effect on atherosclerosis progression in women (Salonen et al. 2000). Moreover, high vitamin E intake was not associated with any cardioprotective effects (Knekt et al. 2004), and failed to reduce the occurrence of cardiovascular mortality (Stephens et al. 1996). This emphasises the importance of other mechanisms independent of ROS attenuation in driving atherosclerosis; for example, those that impact on inflammation by dampening the presence of lesional M1 macrophages and CD3<sup>+</sup> T cells and enhancing T<sub>regs</sub> etc. Therefore, further mechanistic studies are required to ascertain the exact methods by which (+)-catechin induces its beneficial effects, including those that are independent of ROS-lowering, on plaque development *in vivo*. Results of RNA-seq analyses of thoracic aorta samples (which was sent to Novogene at the end of this project) from the progression study will hopefully provide verification on hypothesised mechanisms of actions, and link *in vitro* observations with *in vivo* effects.

### 7.3.2 Plaque progression and stability

In cultured VSMCs (HASMCs), (+)-catechin treatment attenuated cellular ROS production and PDGF-stimulated cell migration (invasion), without affecting basal proliferation over a prolonged period (Chapter 3). Furthermore, macrophage MMP activity was attenuated based on results from previous studies in THP-1 and primary macrophages. *In vivo*, (+)-catechin hydrate supplementation with HFD or NCD as part of progression and regression protocols respectively, consistently enhanced plaque

stability by increasing the presence of  $\alpha$ SMA-expressing VSMCs and collagen content within the aortic root plaques (Chapters 5 and 6). Hence, both (+)-catechin supplementation and intervention consistently improved the stability of developing and established atherosclerotic plaques respectively.

Injury or inflammatory stimulation causes VSMCs to lose their expression of contractile proteins, such as  $\alpha$ SMA, acquiring a synthetic phenotype. This phenotype is characterised by enhanced ECM production, migration and proliferation (Rensen et al. 2007; Alexander and Owens 2012). Whilst the migration and proliferation of VSMCs was previously considered a pro-atherogenic process occurring at the later stages of the disease (McLaren et al. 2011; Michael et al. 2012b), VSMC proliferation may be beneficial throughout atherosclerosis (Bennett et al. 2017). Due to their heterogeneity and plasticity, the roles of VSMCs in atherosclerosis can be both pro- and anti-atherogenic. For example, VSMC synthesis of ECM components facilitate the formation of a plaque-stabilising fibrous cap, whereas VSMC-derived macrophage-like cells contribute to the presence of lipid-laden foam cells (Bennett et al. 2017; Basatemur et al. 2019). Furthermore, conditional activation of PDGF receptor- $\beta$  signalling in VSMCs has been shown to induce inflammation in both the tunica media and adventitia layers of the aorta, accelerating plaque formation in both *ApoE*<sup>-/-</sup> and *Ldlr*<sup>-/-</sup> mice (He et al. 2015). VSMCs are hence a critical component of stable fibrous caps which is necessary for the maintenance of plaque stability. However, VSMC apoptosis and senescence, along with increasing presence of VSMC-derived macrophage-like cells promotes plaque inflammation and progression. (+)-Catechin may inhibit atherosclerosis progression but allow the proliferation of VSMCs and their ability to lay down collagen, and attenuate ROS-induced oxidative stress and subsequent inflammation/dysfunction. However, given the complex roles of VSMCs on atherosclerosis progression, the effects may go beyond these, hence further investigations are required.

Therefore, (+)-catechin might dampen PDGFR signalling-induced inflammation (as shown by the reduction in PDGF-stimulated invasion of VSMCs), whilst enabling the normal proliferation and maintenance of VSMCs (as shown by the lack of effect on proliferation but ROS production was reduced). Furthermore, (+)-catechin might attenuate atherosclerotic plaque progression by maintaining the presence and

proliferation of VSMCs and their collagen synthesis capabilities and preserving fibrous cap components by inhibiting the activity of proteases produced by macrophages and other resident plaque cells. In the context of atherosclerosis regression, (+)-catechin intervention may enhance plaque stability by promoting the efflux and clearance of pro-inflammatory leukocytes (e.g., M1 macrophages). As a result, this may attenuate macrophage-associated inflammation and MMP production, thus preserving SMC viability and proliferative capacity. However, further studies investigating the effect of (+)-catechin on VSMCs in atherosclerosis are required to identify the affected processes and mechanisms responsible for these observations. Given the increasing appreciation of the diverse roles that these cells play throughout atherosclerosis, there will no doubt be increasing studies in the future focused on elucidating how VSMCs and VSMC-derived cells affect the inflammation and phenotype of developing plaques.

### 7.3.3 Atherosclerosis regression

Beyond preventative measures and approaches, therapeutic avenues capable of stimulating the regression of established atherosclerosis are also of clinical importance. Previous studies conducted in the host laboratory have focused on recapitulating key cellular processes that occur in atherosclerosis development and progression, such as macrophage dysfunction and foam cell formation, monocytic recruitment, adhesion and migration etc. Therefore, determination of how (+)-catechin may induce regression of plaque inflammation and the reversal of other associated risk factors is still required. Gene expression analyses (e.g., via RNA-seq or basic RT-qPCR on expression of genes involved in atherosclerosis using RNA extracted from the stored samples of thoracic aorta, liver and adipose tissue depots where changes were seen) would be a good place to start. Possible mechanisms responsible for lesion regression include reduced apoB particles in the arterial wall, efflux of lipids and lesional foam cells from the arterial wall, and the influx of healthy phagocytes mediating the clearance of necrotic debris and other pro-atherogenic components from the plaque.

In male *Ldlr*<sup>-/-</sup> mice fed HFD for 12 weeks to induce atherosclerosis and the formation of established plaques, intervention with chow supplemented with (+)-catechin hydrate

reversed adiposity attributed to white adipose tissue depots, halted hepatic injury and plaque inflammation to a greater extent than chow intervention alone. This was despite similar restorative effects on plasma lipid profile in comparison to chow intervention alone. Importantly, when the chow groups were compared in isolation, the chow + group had significantly lower body weight and inguinal adipose tissue, along with increased ratio of brown to white adipose tissue, presence of plaque  $\alpha$ SMA<sup>+</sup> cells, and mean liver cellular area and hepatocyte size (without affecting hepatic steatosis assessed via ORO staining) compared to the chow - group. Therefore, (+)-catechin may induce positive effects independently of steatosis and hypercholesterolaemia to halt HFD-induced hepatic injury and dysfunction. The egress of inflammatory immune cells from the plaque (i.e., monocytes, macrophages and T cells) may hence mediate disease regression, which was induced with chow intervention but achieved at a greater extent when the chow was combined with (+)-catechin. Intracellular lipid uptake by SMCs impairs their ability to assemble ECM components (Frontini et al. 2009), and hence increased formation of SMC foam cells may contribute to reduced plaque stability. In a regression environment, unlike macrophages which may egress from the plaque, SMCs may remain, becoming more differentiated and contribute to enhanced plaque stability (Allahverdian et al. 2018). Therefore, (+)-catechin may have beneficial effects on the phenotype of VSMCs to promote its plaque-stabilising capabilities, although its effect on VSMC foam cell formation is yet to be investigated and is being pursued in subsequent studies in the host laboratory.

### **7.4 Strengths and limitations**

#### 7.4.1 Use of mouse models

The complex aetiology and heterogeneity of atherosclerosis, along with limited availability of, and difficulty in obtaining, human samples, has meant much reliance on animal models to gain mechanistic insights and understanding of the underlying pathophysiology. Mice are a particularly popular animal model system of choice in atherosclerosis research due to many advantages. These include the ability to control environmental conditions and dietary intake; low cost; short generation time and ease of breeding; possibility of genetic manipulation; and relatively short time frame required to induce advanced disease (Getz and Reardon 2012; Emini Veseli et al. 2017; Lee

et al. 2017). This means that evaluation of disease progression and regression can be conducted in a relatively short period of time, and the low-cost implications allow higher  $n$  numbers and greater statistical power, in comparison to other models involving larger animals. However, lipid metabolism in mice differs to that of humans, for example due to a lack of cholesterol ester transfer protein (CETP), with differences in inflammation and lesion distribution (Getz and Reardon 2012; Emini Veseli et al. 2017; Lee et al. 2017). For example, one of the key differences is in atherosclerotic lesion distribution between humans and mice; in the former, this occurs in peripheral and coronary arteries and in the latter, in the aortic root and brachiocephalic artery. The parameters influencing atherogenesis may also differ between humans and mice, however, the critical features of atherosclerotic processes are homologous. Nevertheless, translation of any findings from such models to humans should be done with caution.

WT mice are naturally resistant to atherosclerosis, since cholesterol transport is mediated via HDL particles, and so alteration of normal cholesterol homeostasis via genetic manipulation is necessary (Getz and Reardon 2012; Emini Veseli et al. 2017). As such, both *ApoE*<sup>-/-</sup> and *Ldlr*<sup>-/-</sup> mice have been extensively utilised in atherosclerosis research, although other mouse models also exist. Of the two, the *ApoE*<sup>-/-</sup> model is considered the more aggressive model since atherosclerosis develops spontaneously without the need for dietary manipulation (although disease development can be accelerated with a Western-type i.e., atherogenic diet) (Getz and Reardon 2012; Emini Veseli et al. 2017). This results in enhanced levels of VLDL and chylomicron fractions (Getz and Reardon 2012; Emini Veseli et al. 2017; Oppi et al. 2019). However, apoE also influences other processes including inflammation, RCT from macrophages and oxidation, along with SMC proliferation and migration, all of which affect atherosclerosis (Greenow et al. 2005; Getz and Reardon 2012; Emini Veseli et al. 2017).

On the other hand, *Ldlr*<sup>-/-</sup> mice possess a plasma lipid profile more akin to that of humans, such as LDL-based hypercholesterolaemia, and LDLR deficiency has no impact on inflammation (Getz and Reardon 2012; Emini Veseli et al. 2017; Oppi et al. 2019). As such, this model demonstrates several characteristic similarities to human familial hypercholesterolaemia. *Ldlr*<sup>-/-</sup> mice require feeding with a Western-type diet,

such as HFD, to induce atherosclerosis, and plaque development is less rapid in comparison to *ApoE*<sup>-/-</sup> mice (Getz and Reardon 2012; Emini Veseli et al. 2017; Oppi et al. 2019). Therefore, *Ldlr*<sup>-/-</sup> mice have been the model of choice in the host laboratory and thus used in this study. The composition of HFD (21% (w/w) pork lard and 0.15% (w/w) cholesterol) employed in this study is based upon the use of lard as the sole source of fat. Whilst this is necessary for driving atherosclerosis development in these mice, the HFD may be considered an 'extreme' diet, due to questionable similarity to components of the actual 'Westernised' diet consumed by humans. However, the high fat concentration is necessary as the feeding duration is relatively short, and hence use of HFD is a convenient and practical method of inducing the formation of established lesions. This is particularly valuable, given that atherosclerosis development in humans occurs over decades. Therefore, the balance of dietary manipulation with feeding duration and dose of supplementation also require consideration.

The selection of HFD type used as well as duration of feeding period was based upon previous optimisation studies conducted in, and experience of, the host laboratory and their collaborators. Established atherosclerotic lesions were indeed induced after 12 weeks of HFD feeding in 8-week-old *Ldlr*<sup>-/-</sup> mice, as shown by the presence of characteristic atherosclerotic lesions and hypercholesterolaemia attributed to LDL. Therefore, this set up has been verified to produce consistent and quantifiable intermediate atherosclerotic lesions and hence was utilised in this study. Subsequent detailed plaque morphometric and histological analyses were carried out using image analysis conducted in a blinded manner where possible, providing greater confidence in the results and minimising unconscious bias. Moving forward, it is of utmost importance that all analyses as such are conducted in a blinded fashion to ensure consistency and reliability of results. As part of this study, optimisation of image analysis methods was also conducted, establishing a more systematic and consistent method that can be utilised by all researchers within the host laboratory in future. This will no doubt help mitigate some of the subjectivity that comes with analyses such as these and reduce variation of results obtained from different studies using the same mouse model, diet composition and feeding duration.

### 7.4.2 The dose and administration of (+)-catechin

The concentration of pure (+)-catechin used for all *in vitro* experiments in this project, 1.5 µg/ml, was based upon previous optimisation experiments conducted in the host laboratory using a range of assays. Results of these identified the lowest effective concentration of (+)-catechin, which was thus proceeded with in all subsequent experiments. However, the same was not done for *in vivo* studies, due to the ethical implications associated with animal work. Hence, the dose used for all *in vivo* studies as part of this project, 200 mg/kg/day, was based upon the previous short-term study conducted in the host laboratory (Moss 2018), which was in accordance with a previously published study of similar duration conducted in rats (Potenza et al. 2007). However, calculation of the amount of (+)-catechin hydrate required to achieve this dose involved estimation of the average maximum consumption of HFD per day (which was based upon results of a previous experiment monitoring daily consumption conducted in the host laboratory). Therefore, the actual dose consumed by individual mice may vary slightly, based upon the exact amount of diet consumed (or indeed, the volume of water drank), which may vary slightly between the mice. The amount of diet consumed could not be accurately measured due to the presence of multiple mice per cage within conventional cages. However, consumption of HFD (with or without (+)-catechin hydrate) was measured for all cages for the duration of all studies and was generally comparable between the different groups. Therefore, determining level of (+)-catechin and its metabolites in the plasma, tissues and urine/faecal samples of the mice would be an important future avenue.

As the (+)-catechin hydrate solution was administered by mixing in with the HFD as homogeneously as possible, the exact dose consumed by individual mice cannot be quantified accurately. Although this issue could be mitigated by administering the exact dose of (+)-catechin hydrate via daily gavage, this was impractical for the number of mice per group utilised in the studies (n=15-20), and the long study duration of 12 weeks. Oral gavage is usually only employed for studies of relatively short durations, such as a few weeks. This is since prolonged repeated gavage increases the risk of complications (Germann and Ockert 1994; Murphy et al. 2001) such as enhanced stress, oesophageal trauma, aspiration pneumonia and gastric rupture,

introducing complicating factors that could affect inflammation and hence study results (Kinder et al. 2014).

An average of 126 mg of catechins is present per 100 mL of green tea according to the EFSA and 35 mg of free (+)-catechin is present in 120 mL of red wine (Bell et al. 2000), with the average range of flavonoid intake measured in several populations being 11-121 mg/day (Erdman Jr et al. 2007). In humans, studies involving the intake of purified forms of catechins have ranged from 100 mg (Dower et al. 2015) to 1 g (Suzuki-Sugihara et al. 2016), and in animals, doses of up to 0.5% (Lee et al. 2009) and 1% (w/w) in the diet (Klaus et al. 2005) have been used. The 200 mg/kg dose of (+)-catechin hydrate used in this project would equate to approximately 0.08-0.1% (w/w) in the diet and an intake of approximately 400-500 mg/day in humans, based on 0.02% being the equivalent of 100 mg/day (Auclair et al. 2009). Although exceeding the average range of flavonoid consumption in humans, the 200 mg/kg dose is well within the range used in previously published studies, and the safe range for human consumption. However, only 0.2-5.0% of ingested doses have been identified in circulating plasma after consumption of tea catechins (Lee et al. 1995; Nakagawa et al. 1997; Miyazawa 2000; Lee et al. 2002). Hence, gas chromatography-mass spectrometry of the trimethylsilylated derivatives should be carried out to confirm the absorption and assimilation (and bioavailability) of (+)-catechin and its metabolite, 3'-O-methylcatechin, in plasma samples (as well as in urine and other tissue samples) (Donovan et al. 1999; Ebeler et al. 2002).

### 7.4.3 Use of *in vitro* assays

A limitation of the experimental approach in this study may be the use of commercially available assays to investigate the actions of (+)-catechin. Although the *in vitro* assays may be deemed oversimplifications of *in vivo* processes, it is difficult to accurately model the pathogenesis of atherosclerosis due to its inherent complexity and multifaceted nature. Furthermore, there are still unknowns in our understanding of the disease, such as the exact roles that certain cytokines and subtypes of various immune cells play in driving disease progression. Nevertheless, the assays provide a way of studying select cellular processes in isolation, and thus a quantifiable way of

investigating the effects of different agents, and characterisation of their actions. Therefore, this provides insights to possible underlying mechanisms that may be responsible for effects seen *in vivo*, guiding subsequent studies, and enabling direct comparisons of different agents. This was the first study that employed a combination of *in vitro* assays with *in vivo* studies using an established mouse model of atherosclerosis to investigate the actions and potential mechanisms of (+)-catechin. The use of both *in vitro* and *in vivo* studies, offer greater insights to individual actions and potential underlying mechanisms of actions usually lacking in nutraceutical research. To date, this is the first study that investigates the actions of (+)-catechin in such detail, from cellular processes involving multiple key cell types implicated in the disease, to atherosclerotic plaque development, progression and even, regression, (along with analyses of associated risk factors). Therefore, future *in vivo* studies of atherosclerosis should incorporate detailed plaque morphometric and histological analyses that go beyond calculation of plaque size and lipid content. This is important since plaque cellularity and composition are also key parameters that provide insights to atherosclerosis disease severity. For example, subsets of macrophages and T cells present within lesions should be explored in further detail, and this could be combined with co-cultures to explore interactions between different leukocytes and how these shape the inflammatory phenotype of the plaque.

### 7.5 Further work and future perspectives

Whilst it was intended to carry out comparative analyses on (+)-catechin and its metabolite, 3'-O-methylcatechin, in a range of *in vitro* assays, it was not possible to obtain this metabolite from any UK-based suppliers or distributors at the time of requirement. However, in future, it would be important to investigate the effects of 3'-O-methylcatechin *in vitro*, given that metabolites of (+)-catechin, rather than (+)-catechin itself, have been found to inhibit the adhesion of monocytes to IL-1 $\beta$ -stimulated human aortic ECs (HAOECs) and ROS production in these cells (Koga and Meydani 2001). Therefore, metabolic conversion of (+)-catechin may affect its biological activity, and its metabolites may be, in part at least, responsible for the observed effects, although catechins can also be present in a free (unconjugated), "active" form in human plasma (Miyazawa 2000). Hence determination of the concentrations of (+)-catechin and its metabolites in plasma, urine and tissues would

be an important future avenue. In a human study, flavonoid consumption in the form of red wine resulted in an increase of (+)-catechin, 3'-O-methylcatechin and all conjugates to 81-91 nmol/l in the plasma, with over a quarter of the metabolites existing in methylated forms, and less than 2% of (+)-catechin and 3'-O-methylcatechin being unconjugated (Donovan et al. 1999). Therefore, investigation of the metabolites of (+)-catechin and other nutraceutical agents should also be included in subsequent studies. Indeed, other nutraceutical agents under investigation in the host laboratory, such as dihomono- $\gamma$ -linolenic acid and punicalagin, have also incorporated their metabolites in *in vitro* studies, such as prostaglandin-E1 and epigallocatechin gallate and urolithins respectively.

Although various beneficial effects of (+)-catechin were seen *in vitro*, these still require correlation to changes in gene expression at both the mRNA and protein level. Furthermore, *in vitro* and *in vivo* observations still need to be connected via verification of the exact mechanisms responsible for the beneficial actions of (+)-catechin. Results of RNA-seq analyses of the thoracic aorta should provide valuable insights to the underlying mechanisms of (+)-catechin, and verification of previously mentioned hypotheses regarding the potential mechanisms in play. The difficulty in uncovering these stems from the presence of multiple actions and mechanisms involved, since natural products typically exert a range of effects in comparison with pharmacological agents which have established and specific targets. To gain mechanistic insights to how (+)-catechin attenuates atherosclerosis development and progression, results of RNA-seq analyses of the thoracic aorta will hopefully bridge the gap between *in vitro* observations and *in vivo* effects. This will also guide the generation of future mechanistic hypotheses in relation to the actions of (+)-catechin, allowing a more guided approach in future experiments.

ScRNA-seq approaches could also be employed to determine how (+)-catechin alters the transcriptome, for example of ECs and VSMCs, at the cellular level. This could provide valuable insights to how (+)-catechin protects against endothelial dysfunction and encourages fibrous cap maintenance. This approach could be combined with investigation of the effect of (+)-catechin on VSMC senescence, apoptosis and parameters associated with foam cell formation to explore the effect of (+)-catechin on VSMC dysfunction further. Potential experimental strategies include the use of cell-

based assays such as annexin-V labelling to measure apoptosis, detection of senescence markers, such as senescence-associated- $\beta$  galactosidase by immunocytochemical staining (Matthews et al. 2006), and ORO staining (Xu et al. 2010) to quantify intracellular lipid uptake. Given the integral roles of VSMCs in contributing to plaque burden, inflammation and stability, future studies should incorporate strategies to determine how catechins affect populations of VSMCs and VSMC-derived cells. This is important given the key roles of VSMCs and their synthesis of ECM proteins, such as collagens and elastins, in promoting plaque stability and protection against rupture. Plaque rupture is a critical event involved in the onset of clinical complications in humans but is extremely rare in both the *Apoe*<sup>-/-</sup> and *Ldlr*<sup>-/-</sup> models (and most other mouse models of atherosclerosis). Hence, *in vivo* studies of plaque rupture have been limited, given that the lack of animal models available that accurately mimic plaque destabilisation that occurs in humans. In both the *Ldlr*<sup>-/-</sup> and *Apoe*<sup>-/-</sup> models, plaque rupture is a sporadic, unpredictable event which may only occur after a prolonged duration in select vascular beds, such as the brachiocephalic artery (Emini Veseli et al. 2017). Hence, it is not possible to study plaque rupture in these mice. Given the consistent effects of (+)-catechin on promoting fibrous cap formation and maintenance, its ability to protect against plaque rupture could be investigated using the *Apoe*<sup>-/-</sup>*Fbn1*<sup>C1039+/-</sup> model (*Apoe*<sup>-/-</sup> mice crossed with mice possessing a mutation in the *fibrillin 1* gene). These mice demonstrate accelerated plaque development and spontaneous rupture with complications (Emini Veseli et al. 2017). Beyond this, progression onto human clinical trials to investigate the ability of (+)-catechin to attenuate primary MACE could be explored as an add-on to statin therapy, after optimisation of the lowest effective dose and duration in humans. Combinatory strategies with other promising nutraceutical agents, such as EPA, could also be explored. A summary of other possible future directions is illustrated in Figure 7.6.

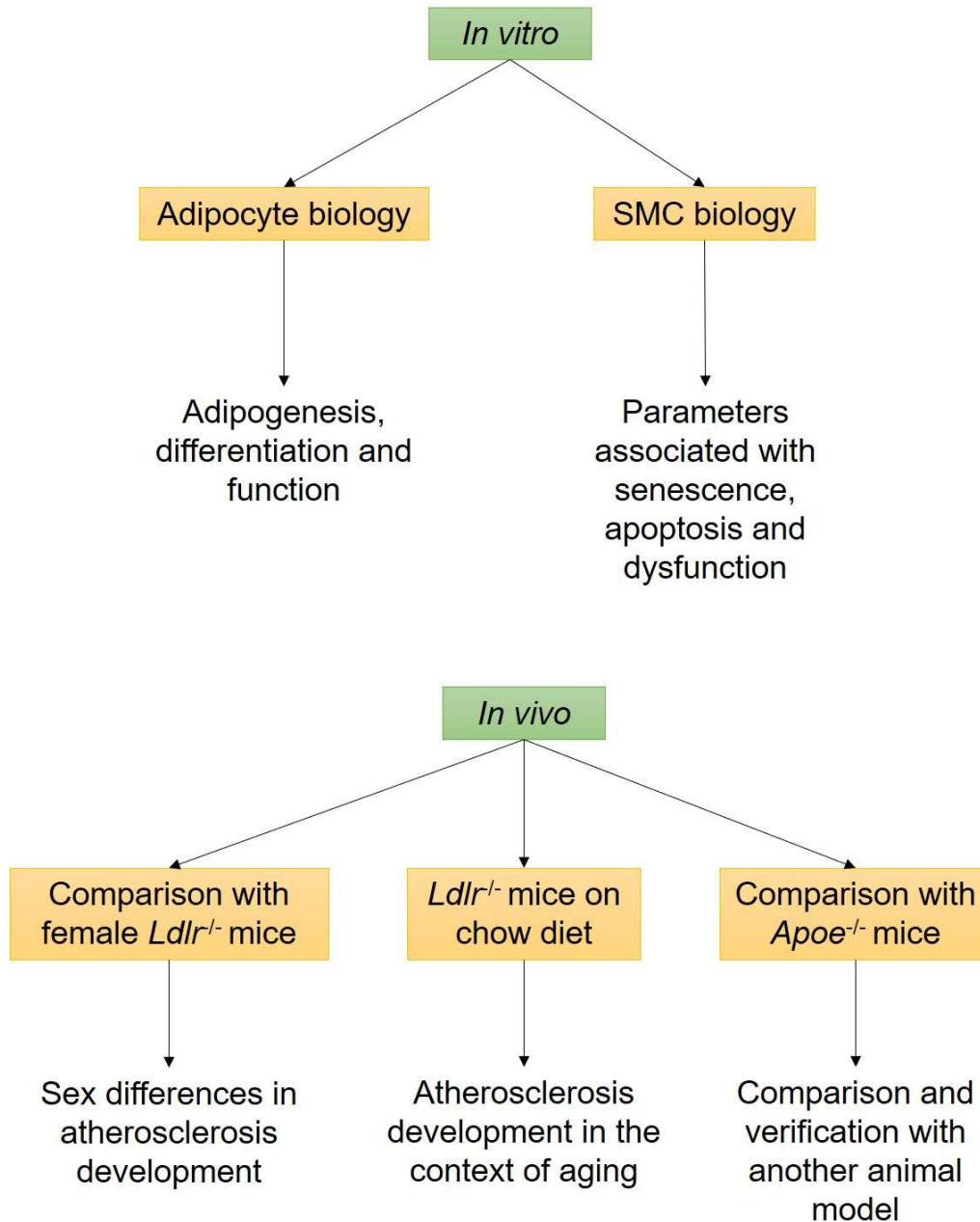


**Figure 7.6 Summary of possible future directions.**

Abbreviations: SMC, smooth muscle cell; *Ldlr*, low-density lipoprotein; *Apoe*, apolipoprotein E.

## 7.6 Conclusion

In conclusion, (+)-catechin attenuates multiple key processes implicated in early atherosclerosis associated with monocytes/macrophages, along with endothelial and VSMC dysfunction *in vitro*. (+)-catechin supplementation attenuated atherosclerosis development and progression associated with reduced plaque burden and macrophage-driven inflammation *in vivo*. Furthermore, in the context of

## Chapter 7: General Discussion

atherosclerosis regression, intervention with (+)-catechin combined with chow reversed HFD-induced adiposity and hepatic injury to a greater extent than chow intervention alone. However, overall, there were less differences within the atherosclerotic lesions between the chow intervention groups. Importantly, in both progression and regression studies, mice that had received (+)-catechin demonstrated consistently enhanced plaque stability. These findings warrant further investigations to characterise the effect of (+)-catechin on VSMCs in the context of phenotypic switching, foam cell formation and senescence, etc. Overall, (+)-catechin demonstrates substantial potential in inhibiting atherogenesis and delaying disease progression by attenuating multiple key processes that occur early on, even enhancing plaque stability. Therefore, (+)-catechin possesses promising anti-atherogenic properties that could be exploited for the prevention of atherosclerosis and encourage plaque stability to protect against rupture. Data obtained as part of project provides evidence supporting the progression of (+)-catechin to clinical trials for the prevention of primary atherosclerotic MACE, due to its various athero-protective effects. Although the underlying mechanisms of actions responsible for these beneficial effects still require verification, (+)-catechin is a promising nutraceutical candidate that could be applied to combinatory preventative strategies for atherosclerosis.

## References

- Abbate, A. et al. 2015. Comparative safety of interleukin-1 blockade with anakinra in patients with ST-segment elevation acute myocardial infarction (from the VCU-ART and VCU-ART2 pilot studies). *American Journal of Cardiology* 115(3), pp. 288-292.
- Abbate, A. et al. 2010. Interleukin-1 blockade with anakinra to prevent adverse cardiac remodeling after acute myocardial infarction (Virginia Commonwealth University Anakinra Remodeling Trial [VCU-ART] Pilot study). *American Journal of Cardiology* 105(10), pp. 1371-1377.
- Abbate, A. et al. 2020. Interleukin-1 blockade inhibits the acute inflammatory response in patients with ST-segment-elevation myocardial infarction. *Journal of the American Heart Association* 9(5), p. e014941.
- Abd El-Aziz, T. A., Mohamed, R. H., Pasha, H. F. and Abdel-Aziz, H. R. 2011. Catechin protects against oxidative stress and inflammatory-mediated cardiotoxicity in adriamycin-treated rats. *Clinical and Experimental Medicine* 12, pp. 233-240.
- Abe, J. et al. 1998. Tyrosin phosphorylation of platelet-derived growth factor  $\beta$  receptors in coronary artery lesions: implications for vascular remodelling after directional coronary atherectomy and unstable angina pectoris. *Heart* 79, pp. 400-406.
- Adler, B. J., Green, D. E., Pagnotti, G. M., Chan, M. E. and Rubin, C. T. 2014. High fat diet rapidly suppresses B lymphopoiesis by disrupting the supportive capacity of the bone marrow niche. *PLoS ONE* 9(3), p. e90639.
- Aikawa, M. et al. 1998. Lipid lowering by diet reduces matrix metalloproteinase activity and increases collagen content of rabbit atheroma: a potential mechanism of lesion stabilization. *Circulation* 97, pp. 2433-2444.
- Ait-Oufella, H., Sage, A., Mallat, Z. and Tedgui, A. 2014. Adaptive (T and B Cells) immunity and control by dendritic cells in atherosclerosis. *Circulation Research* 114(10), pp. 1640-1660.
- Ait-Oufella, H., Taleb, S., Mallat, Z. and Tedgui, A. 2011. Recent advances on the role of cytokines in atherosclerosis. *Arteriosclerosis, Thrombosis, and Vascular Biology* 31(5), pp. 969-979.
- Akhlaghi, M. and Kohanmoo, A. 2018. Mechanisms of anti-obesity effects of catechins: a review. *International Journal of Nutrition Sciences* 3(3), pp. 127-132.
- Alahmadi, W. A. 2019. *The role of the ERK1:STAT1 serine 727 phosphorylation axis on key atherosclerosis-associated cellular processes and the anti-atherogenic actions of Hydroxytyrosol*. Cardiff University.
- Alexander, M. and Owens, G. 2012. Epigenetic control of smooth muscle cell differentiation and phenotypic switching in vascular development and disease. *Annual Review of Physiology* 74, pp. 13-40.

## References

- Alexander, M. R., Moehle, C. W., Johnson, J. L., Yang, Z., Lee, J., Jackson, C. and Owens, G. 2012. Genetic inactivation of IL-1 signaling enhances atherosclerotic plaque instability and reduces outward vessel remodeling in advanced atherosclerosis in mice. *Journal of Clinical Investigation* 122(1), pp. 70-79.
- Allahverdian, S., Chaabane, C., Boukais, K., Francis, G. and Bochaton-Piallat, M.-L. 2018. Smooth muscle cell fate and plasticity in atherosclerosis. *Cardiovascular Research* 114(4), pp. 540-550.
- Amberger, A. et al. 1997. Co-expression of ICAM-1, VCAM-1, ELAM-1 and Hsp60 in human arterial and venous endothelial cells in response to cytokines and oxidized low-density lipoproteins. *Cell Stress Chaperones* 2, pp. 94-103.
- An, G., Miwa, T., Song, W., Lawson, J., Rader, D., Zhang, Y. and Song, W. 2009. CD59 but not DAF deficiency accelerates atherosclerosis in female ApoE knockout mice. *Molecular Immunology* 46, pp. 1702-1709.
- Andres-Manzano, M. J., Andres, V. and Dorado, B. 2015. Oil red O and hematoxylin and eosin staining for quantification of atherosclerosis burden in mouse aorta and aortic root. *Methods in Molecular Biology* 1339, pp. 85-99.
- Anstee, Q. and Goldin, R. 2006. Mouse models in non-alcoholic fatty liver disease and steatohepatitis research. *International Journal of Experimental Pathology* 87(1), pp. 1-16.
- Antonopoulos, A., Margaritis, M., Lee, R., Channon, K. and Antoniades, C. 2012. Statins as anti-inflammatory agents in atherogenesis: molecular mechanisms and lessons from the recent clinical trials. *Current Pharmaceutical Design* 18(11), pp. 1519-1530.
- Arakawa, M. et al. 2010. Inhibition of monocyte adhesion to endothelial cells and attenuation of atherosclerotic lesion by a glucagon-like peptide-1 receptor agonist, exendin-4. *Diabetes* 59(4), pp. 1030-1037.
- Arts, I. C. W., Hollman, P. C., Feskens, E. J. M., Bueno de Mesquita, H. B. and Kromhout, D. 2001a. Catechin intake might explain the inverse relation between tea consumption and ischemic heart disease: the Zutphen Elderly Study. *The American Journal of Clinical Nutrition* 74, pp. 227-232.
- Arts, I. C. W., Jacobs Jr, D. R., Harnack, L. J., Gross, M. and Folsom, A. R. 2001b. Dietary catechins in relation to coronary heart disease death among postmenopausal women. *Epidemiology* 12, pp. 668-675.
- Arts, I. C. W., van de Putte, B. and Hollman, P. C. H. 2000. Catechin contents of foods commonly consumed in the Netherlands. 1. Fruits, vegetables, staple foods, and processed foods. *Journal of Agricultural and Food Chemistry* 48, pp. 1746-1751.

## References

- Asmis, R. and Begley, J. 2002. Oxidized LDL promotes peroxide-mediated mitochondrial dysfunction and cell death in human macrophages. *Circulation Research* 92(1), pp. e20-e29.
- Auclair, S. et al. 2009. Catechin reduces atherosclerotic lesion development in apo E-deficient mice: a transcriptomic study. *Atherosclerosis* 204, pp. e21-e27.
- Auffray, C. et al. 2007. Monitoring of blood vessels and tissues by a population of monocytes with patrolling behavior. *Science* 317, pp. 666-670.
- Ayala, A., Munoz, M. F. and Arguelles, S. 2014. Lipid peroxidation: production, metabolism, and signaling mechanisms of malondialdehyde and 4-hydroxy-2-nonenal. *Oxidative Medicine and Cellular Longevity* 2014, p. 360438.
- Back, M., Yurgadul Jr, A., Tabas, I., Oorni, K. and Kovanen, P. T. 2019. Inflammation and its resolution in atherosclerosis: mediators and therapeutic opportunities. *Nature Reviews Cardiology* 16, pp. 389-406.
- Bae, Y., Lee, J., Choi, S., Kim, S., Almazan, F., Witztum, J. and Miller, Y. 2009. Macrophages generate reactive oxygen species in response to minimally oxidized low-density lipoprotein: toll-like receptor 4- and spleen tyrosine kinase-dependent activation of NADPH oxidase 2. *Circulation Research* 104, pp. 210-218.
- Baigent, C. et al. 2005. Efficacy and safety of cholesterol-lowering treatment: prospective meta-analysis of data from 90,056 participants in 14 randomised trials of statins. *Lancet* 366, pp. 1267-1278.
- Ballantyne, C. M., Banach, M., Mancini, G. B. J., Lepor, N., JC, H., Zhao, X. and Leiter, L. 2018. Efficacy and safety of bempedoic acid added to ezetimibe in statin-intolerant patients with hypercholesterolemia: a randomized, placebo-controlled study. *Atherosclerosis* 277, pp. 195-203. doi: 10.1016/j.atherosclerosis.2018.06.002.
- Ballantyne, C. M. et al. 2020. Bempedoic acid plus ezetimibe fixed-dose combination in patients with hypercholesterolemia and high CVD risk treated with maximally tolerated statin therapy. *European Journal of Preventive Cardiology* 27(6), pp. 593-603.
- Ballinger, S., Van Houten, B., Jin, G.-F., Conklin, C. and Godley, B. 1999. Hydrogen peroxide causes significant mitochondrial DNA damage in human RPE cells. *Experimental Eye Research* 68, pp. 765-772.
- Bao, M.-H. et al. 2016. Impact of high fat diet on long non-coding RNAs and messenger RNAs expression in the aortas of ApoE(-/-) mice. *Scientific Reports* 6, p. 34161.
- Baron, C. et al. 2018. Single-cell transcriptomics reveal the dynamic of haematopoietic stem cell production in the aorta. *Nature Communications* 9, p. 2517.

## References

- Basatemur, G. L., Jorgensen, H. F., Clarke, M. C. H., Bennett, M. R. and Mallat, Z. 2019. Vascular smooth muscle cells in atherosclerosis. *Nature Reviews Cardiology* 16(12), pp. 727-744.
- Bassuk, S. R., N and Ridker, P. M. 2004. High-sensitivity C-reactive protein: clinical importance. *Current Problems in Cardiology* 29, pp. 439-443.
- Bedoui, J., Oak, M.-H., Anglard, P. and Schini-Kerth, V. 2005. Catechins prevent vascular smooth muscle cell invasion by inhibiting MT1-MMP activity and MMP-2 expression. *Cardiovascular Research* 67(2), pp. 317-325.
- Bell, J. R. C., Donovan, J. L., Wong, R., Waterhouse, A. L., German, J. B., Walzem, R. L. and Kasim-Karakas, S. E. 2000. (+)-Catechin in human plasma after ingestion of a single serving of reconstituted red wine. *The American Journal of Clinical Nutrition* 71, pp. 103-108.
- Bennett, M., Sinha, S. and Owens, G. 2017. Vascular smooth muscle cells in atherosclerosis. *Circulation Research* 118(4), pp. 692-702.
- Bentzon, J., Weile, C., Sondergaard, C., Hindkjaer, J., Kassem, M. and Falk, E. 2006. Smooth muscle cells in atherosclerosis originate from the local vessel wall and not circulating progenitor cells in ApoE knockout mice. *Arteriosclerosis, Thrombosis, and Vascular Biology* 26(12), pp. 2696-2702.
- Berda-Haddad, Y. et al. 2011. Sterile inflammation of endothelial cell-derived apoptotic bodies is mediated by interleukin-1 $\alpha$ . *Proceedings of the National Academy of Sciences of the United States of America* 108(51), pp. 20684-20689.
- Bergheanu, S. C., Bodde, M. C. and Jukema, J. W. 2017. Pathophysiology and treatment of atherosclerosis: current view and future perspective on lipoprotein modification treatment. *Netherlands Heart Journal* 25(4), pp. 231-242.
- Bernatoniene, J. and Kopustinskiene, D. 2018. The role of catechins in cellular responses to oxidative stress. *Molecules* 23, p. 965.
- Bhardwaj, P., Khanna, D. and Balakumar, P. 2013. Catechin averts experimental diabetes mellitus-induced vascular endothelial structural and functional abnormalities. *Cardiovascular Toxicology* 14, pp. 41-51.
- Bhaskar, V. et al. 2011. Monoclonal antibodies targeting IL-1 beta reduce biomarkers of atherosclerosis in vitro and inhibit atherosclerotic plaque formation in Apolipoprotein E-deficient mice. *Atherosclerosis* 216(2), pp. 313-320.
- Bhatt, D. L. et al. 2019. Cardiovascular risk reduction with icosapent ethyl for hypertriglyceridemia. *New England Journal of Medicine* 380(1), pp. 11-22.
- Bick, A. et al. 2020. Genetic interleukin 6 signaling deficiency attenuates cardiovascular risk in clonal hematopoiesis. *Circulation* 141, pp. 124-131.

## References

- Bidar, A. et al. 2012. In vivo imaging of lipid storage and regression in diet-induced obesity during nutrition manipulation. *American Journal of Physiology-Endocrinology and Metabolism* 303, pp. E1287-E1295.
- Bohula, E. A. et al. 2018. Inflammatory and cholesterol risk in the FOURIER trial. *Circulation* 138(2), pp. 131-140.
- Boozer, C., Schoenbach, G. and Atkinson, R. 1995. Dietary fat and adiposity - a dose-response relationship in adult male rats fed isocalorically. *The American Journal of Physiology-Endocrinology and Metabolism* 268, pp. E546-E550.
- Boring, L., Gosling, J., Cleary, M. and Charo, I. F. 1998. Decreased lesion formation in CCR2<sup>-/-</sup> mice reveals a role for chemokines in the initiation of atherosclerosis. *Nature* 394, pp. 894-897.
- Bose, M., Lambert, J., Ju, J., Reuhl, K., Shapses, S. and Yang, C. 2008. The major green tea polyphenol, (-)-epigallocatechin-3-gallate, inhibits obesity, metabolic syndrome, and fatty liver disease in high-fat-fed mice. *Journal of Nutrition* 138, pp. 1677-1683.
- Bostrom, P. et al. 2012. A PGC1- $\alpha$ -dependent myokine that drives brown-fat-like development of white fat and thermogenesis. *Nature* 481, pp. 463-468.
- Bourgeois, F., Alexiu, A. and Lemonnier, D. 1983. Dietary-induced obesity: effect of dietary fats on adipose tissue cellularity in mice. *British Journal of Nutrition* 49, pp. 17-26.
- Braicu, C., Ladomery, M. R., Chedea, V. S., Irimie, A. and Berindan-Neagoe, I. 2013. The relationship between the structure and biological actions of green tea catechins. *Food Chemistry* 141, pp. 3282-3289.
- Brew, K., Dinakarandian, D. and Nagase, H. U. 2000. Tissue inhibitors of metalloproteinases: evolution, structure and function. *Biochimica et Biophysica Acta* 1477, pp. 267-283.
- Buckley, M. L. and Ramji, D. P. 2015. The influence of dysfunctional signaling and lipid homeostasis in mediating the inflammatory responses during atherosclerosis. *Biochimica et Biophysica Acta* 1853, pp. 1498-1515.
- Budoff, M. J. et al. 2020. Effect of icosapent ethyl on progression of coronary atherosclerosis in patients with elevated triglycerides on statin therapy: final results of the EVAPORATE trial. *European Heart Journal* 41(40), pp. 3925-3932.
- Buettner, R., Scholmerich, J. and Bollheimer, L. 2007. High-fat diets: modeling the metabolic disorders of human obesity in rodents. *Obesity* 15, pp. 798-808.
- Burke, A. and Huff, M. 2018. Regression of atherosclerosis: lessons learned from genetically modified mouse models. *Current Opinion in Lipidology* 29, pp. 87-94.

## References

- Calderon, R. M., Cubeddu, L. X., Goldberg, R. B. and Schiff, E. 2010. Statins in the treatment of dyslipidemia in the presence of elevated liver aminotransferase levels: a therapeutic dilemma. *Mayo Clinic Proceedings* 85(4), pp. 349-356.
- Calligaris, S. et al. 2013. Mice long-term high-fat diet feeding recapitulates human cardiovascular alterations: an animal model to study the early phases of diabetic cardiomyopathy. *PLoS ONE* 8(4), p. e60931.
- Campbell, C., Rivera, J. and Blumenthal, R. 2007. Residual risk in statin-treated patients: future therapeutic options. *Current Cardiology Reports* 9(6), pp. 499-505.
- Canault, M., Peiretti, F., Mueller, C. and et, a. I. 2004. Exclusive expression of transmembrane TNF-alpha in mice reduces the inflammatory response in early lipid lesions of aortic sinus. *Atherosclerosis* 172, pp. 211-218.
- Cannon, C. P. et al. 2015. Ezetimibe added to statin therapy after acute coronary syndromes. *New England Journal of Medicine* 372(25), pp. 2387-2397.
- Carlin, L. et al. 2013. Nr4a1-dependent Ly6C(low) monocytes monitor endothelial cells and orchestrate their disposal. *Cell* 153, pp. 362-375.
- Carrasco-Pozo, C., Cires, M. and Gotteland, M. 2019. Quercetin and epigallocatechin gallate in the prevention and treatment of obesity: from molecular to clinical sciences. *Journal of Medicinal Food* 22(8), pp. 753-770.
- Castell, J. V., Gomez-Lechon, M. J., David, M. and et, a. I. 1990. Acute-phase response of human hepatocytes: regulating of acute-phase protein synthesis by interleukin-6. *Hepatology* 12, pp. 1179-1186.
- Chan, K., Siegel, M. and Lenardo, J. 2000. Signaling by the TNF receptor superfamily and T cell homeostasis. *Immunity* 13, pp. 419-422.
- Chan, Y.-H. and Ramji, D. P. 2020. A perspective on targeting inflammation and cytokine actions in atherosclerosis. *Future Medicinal Chemistry* 12(7), pp. 613-626.
- Chassot, L., Scolaro, B., Roschel, G., Cogliati, B., Cavalcanti, M., Abdalla, D. and Castro, I. 2018. Comparison between red wine and isolated trans-resveratrol on the prevention and regression of atherosclerosis in LDLr<sup>(-/-)</sup> mice. *Journal of Nutritional Biochemistry* 61, pp. 48-55.
- Chatree, S. et al. 2020. Epigallocatechin gallate decreases plasma triglyceride, blood pressure, and serum kisspeptin in obese human subjects. *Experimental Biology and Medicine* 246(2), pp. 163-176.
- Chen, C., Jiang, W., Via, D., Luo, S., Li, T., Lee, Y. and Henry, P. 2000. Oxidized low-density lipoproteins inhibit endothelial cell proliferation by suppressing basic fibroblast growth factor expression. *Circulation* 101(2), pp. 171-177.

## References

- Chen, C. and Khismatulin, D. 2015. Oxidized low-density lipoprotein contributes to atherogenesis via co-activation of macrophages and mast cells. *PLoS ONE* 10(3), p. e0123088.
- Chen, L., Yang, X., Jiao, H. and Zhao, B. 2003. Tea catechins protect against lead-induced ROS formation, mitochondrial dysfunction, and calcium dysregulation in PC12 cells. *Chemical Research in Toxicology* 16, pp. 1155-1161.
- Chen, S. et al. 2020. Sex-specific effects of the NLRP3 inflammasome on atherogenesis in LDL receptor-deficient mice. *JACC: Basic to Translational Science* 5(6), pp. 582-598.
- Chen, X., Andresen, B., Hill, M., Zhang, J., Booth, F. and Zhang, C. 2010. Role of reactive oxygen species in tumor necrosis factor-alpha induced endothelial dysfunction. *Current Hypertension Reviews* 4(4), pp. 245-255.
- Cheng, H., Zheng, Z. and Cheng, T. 2019. New paradigms on hematopoietic stem cell differentiation. *Protein & Cell* 11, pp. 34-44.
- Chien, C.-T. et al. 2004. Ascorbate supplement reduces oxidative stress in dyslipidemic patients undergoing apheresis. *Arteriosclerosis, Thrombosis, and Vascular Biology* 24(6), pp. 1111-1117.
- Chien, C.-T. et al. 2014. Glucagon-like peptide-1 receptor agonist activation ameliorates venous thrombosis-induced arteriovenous fistula failure in chronic kidney disease. *Thrombosis and Haemostasis* 112(5), pp. 1051-1064.
- Chinetti-Gbaguidi, G., Colin, S. and Staels, B. 2015. Macrophage subsets in atherosclerosis. *Nature Reviews Cardiology* 12(1), pp. 10-17.
- Chistiakov, D., Orekhov, A. and Bobryshev, Y. 2016. Immune-inflammatory responses in atherosclerosis: Role of an adaptive immunity mainly driven by T and B cells. *Immunobiology* 221, pp. 1014-1033.
- Chistiakov, D., Shkurat, T., Melnichenko, A., Grechko, A. and Orekhov, A. 2018. The role of mitochondrial dysfunction in cardiovascular disease: a brief review. *Annals of Medicine* 50, pp. 121-127.
- Chiva-Blanch, G. et al. 2011. Differential effects of polyphenols and alcohol of red wine on the expression of adhesion molecules and inflammatory cytokines related to atherosclerosis: a randomized clinical trial. *The American Journal of Clinical Nutrition* 95(2), pp. 326-334.
- Choi, H. K., Hernan, M. A., Seeger, J. D., Robins, J. and Wolfe, F. 2002. Methotrexate and mortality in patients with rheumatoid arthritis: a prospective study. *Lancet* 359(9313), pp. 1173-1177.
- Chowdhury, S., Sangle, G., Xie, X., Stelmack, G., Halayko, A. and Shen, G. 2009. Effects of extensively oxidized low-density lipoprotein on mitochondrial function and

## References

reactive oxygen species in porcine aortic endothelial cells. *American Journal of Physiology-Endocrinology and Metabolism* 298, pp. E89-E98.

Choy, K., Murugan, D., Leong, X.-F., Abas, R., Alias, A. and Mustafa, M. 2019. Flavonoids as natural anti-inflammatory agents targeting nuclear factor-kappa B (NFκB) signaling in cardiovascular disease: a mini review. *Frontiers in Pharmacology* 10, p. 1295.

Clarke, M., Talib, S., Figg, N. and Bennett, M. 2010. Vascular smooth muscle cell apoptosis induces interleukin-1-directed inflammation. *Circulation Research* 106(2), pp. 363-372.

Collins, R., Velji, R., Guevara, N., Hicks, M. and Beaudet, A. 2000. P-Selectin or intercellular adhesion molecule (ICAM)-1 deficiency substantially protects against atherosclerosis in apolipoprotein E-deficient mice. *Journal of Experimental Medicine* 191(1), pp. 189-194.

Colonnello, J. S. et al. 2003. Transient exposure to elastase induces mouse aortic wall smooth muscle cell production of MCP-1 and RANTES during development of experimental aortic aneurysm. *Journal of Vascular Surgery* 38, pp. 138-146.

Cong, L. et al. 2020. Catechin relieves hypoxia/reoxygenation-induced myocardial cell apoptosis via down-regulating lncRNA MIAT. *Journal of Cell and Molecular Medicine* 14, pp. 2356-2368.

Coppe, J.-P., Desprez, P.-Y., Krtolica, A. and Campisi, J. 2010. The senescence-associated secretory phenotype: the dark side of tumor suppression. *Annual Review of Pathology* 5, pp. 99-118.

Corda, S., Laplace, C., Vicaut, E. and Duranteau, J. 2000. Rapid reactive oxygen species production by mitochondria in endothelial cells exposed to tumor necrosis factor-α is mediated by ceramide. *American Journal of Respiratory Cell and Molecular Biology* 24(6), pp. 762-768.

Crea, F. and Libby, P. 2017. Acute coronary syndromes. *Circulation* 138, pp. 1155-1166.

Cremonini, E. et al. 2020. (-)-Epicatechin and the comorbidities of obesity. *Archives of Biochemistry and Biophysics* 690, p. 108505.

Crysanndt, M. et al. 2011. Hypercholesterolemia and its association with enhanced stem cell mobilization and harvest after high-dose cyclophosphamide+G-CS. *Bone Marrow Transplant* 46(11), pp. 1426-1429.

Curat, C., Miranville, A., Sengenès, C., Diehl, M., Tonus, C., Busse, R. and Bouloumie, A. 2004. From blood monocytes to adipose tissue-resident macrophages induction of diapedesis by human mature adipocytes. *Diabetes* 53, pp. 1285-1292.

Dandapat, A., Hu, C., Sun, L. and Mehta, J. 2007. Small concentrations of oxLDL induce capillary tube formation from endothelial cells via LOX-1-dependent redox-

## References

sensitive pathway. *Arteriosclerosis, Thrombosis, and Vascular Biology* 27(11), pp. 2435-2442.

Davignon, J. and Ganz, P. 2004. Role of endothelial dysfunction in atherosclerosis. *Circulation* 109, pp. III-27-III-32.

Dawson, T. C., Kuziel, W. A., Osahar, T. A. and Maeda, N. 1999. Absence of CC chemokine receptor-2 reduces atherosclerosis in apolipoprotein E-deficient mice. *Atherosclerosis* 143, pp. 205-211.

De Donatis, A. et al. 2008. Proliferation versus migration in platelet-derived growth factor signaling: the key role of endocytosis. *Journal of Biological Chemistry* 283(29), pp. 19948-19956.

de Maat, M., Pijl, H., Kluft, C. and Princen, H. 2000. Consumption of black and green tea had no effect on inflammation, haemostasis and endothelial markers in smoking healthy individuals. *European Journal of Clinical Nutrition* 54(10), pp. 757-763.

dela Paz, N., Simionidis, S., Leo, C., Rose, D. and Collins, T. 2007. Regulation of NF-kappaB-dependent gene expression by the POU domain transcription factor Oct-1. *Journal of Biological Chemistry* 282(11), pp. 8424-8434.

Demeule, M., Brossard, M., Page, M., Gingras, D. and Beliveau, R. 2000. Matrix metalloproteinase inhibition by green tea catechins. *Biochimica et Biophysica Acta* 1478(1), pp. 51-60.

Demeule, M. et al. 2002. Green tea catechins as novel antitumor and antiangiogenic compounds. *Current Medicinal Chemistry - Anti-Cancer Agents* 2, pp. 441-463.

Deshmane, S. L., Kremlev, S., Amini, S. and Sawaya, B. E. 2009. Monocyte chemoattractant protein-1 (MCP-1): an overview. *Journal of Interferon & Cytokine Research* 29, pp. 313-326.

Devlin, C. M., Kuriakose, G., Hirsch, E. and Tabas, I. 2002. Genetic alterations of IL-1 receptor antagonist in mice affect plasma cholesterol level and foam cell lesion size. *Proceedings of the National Academy of Sciences of the United States of America* 99(9), pp. 6280-6285.

Docherty, C., Carswell, A., Friel, E. and Mercer, J. 2018. Impaired mitochondrial respiration in human carotid plaque atherosclerosis: A potential role for Pink1 in vascular smooth muscle cell energetics. *Atherosclerosis* 268, pp. 1-11.

Donovan, J. L., Bell, J. R., Kasim-Karakas, S., German, J. B., Walzem, R. L., Hansen, R. J. and Waterhouse, A. L. 1999. Catechin is present as metabolites in human plasma after consumption of red wine. *The Journal of Nutrition* 129, pp. 1662-1668.

Douglas, G. et al. 2018. Roles for endothelial cell and macrophage Gch1 and tetrahydrobiopterin in atherosclerosis progression. *Cardiovascular Research* 114, pp. 1385-1399.

## References

- Dower, J. I., Geleijnse, J. M., Gijbbers, L., Schalkwijk, C., Kromhout, D. and Hollman, P. C. 2015. Supplementation of the pure flavonoids epicatechin and quercetin affects some biomarkers of endothelial dysfunction and inflammation in (pre)hypertensive adults: a randomized double-blind, placebo-controlled, crossover trial. *Journal of Nutrition* 145(7), pp. 1459-1463.
- Dranka, B., Hill, B. and Darley-Usmar, V. 2010. Mitochondrial reserve capacity in endothelial cells: the impact of nitric oxide and reactive oxygen species. *Free Radical Biology & Medicine* 48, pp. 905-914.
- Drechsler, M., Megens, R., van Zandvoort, M., Weber, C. and Soehnlein, O. 2010. Hyperlipidemia-triggered neutrophilia promotes early atherosclerosis. *Circulation* 122, pp. 1837-1845.
- Du, Y. et al. 2021. Epigallocatechin-3-gallate dampens non-alcoholic fatty liver by modulating liver function, lipid profile and macrophage polarisation. *Nutrients* 13(2), p. 599.
- Duewell, P. et al. 2010. NLRP3 inflammasomes are required for atherogenesis and activated by cholesterol crystals. *Nature* 464, pp. 1357-1361.
- Ebeler, S. et al. 2002. Dietary catechin delays tumor onset in a transgenic mouse model. *The American Journal of Clinical Nutrition* 76(4), pp. 865-872.
- Echeverria, F. et al. 2019. High-fat diet induces mouse liver steatosis with a concomitant decline in energy metabolism: attenuation by eicosapentaenoic acid (EPA) or hydroxytyrosol (HT) supplementation and the additive effects upon EPA and HT co-administration. *Food & Function* 10(9), pp. 6170-6183.
- Eichenberger, P., Colombani, P. and Mettler, S. 2009. Effects of 3-week consumption of green tea extracts on whole-body metabolism during cycling exercise endurance-trained men. *International Journal for Vitamin and Nutrition Research* 79(1), pp. 24-33.
- Elhage, R., Maret, A., Pieraggi, M. T., Thiers, J., Arnal, J. and Bayard, F. 1998. Differential effects of interleukin-1 receptor antagonist and tumor necrosis factor binding protein on fatty-streak formation in apolipoprotein E-deficient mice. *Circulation* 97(3), pp. 242-244.
- Ellulu, M., Patimah, I., Khaza'ai, H., Rahmat, A. and Abed, Y. 2017. Obesity and inflammation: the linking mechanism and the complications. *Archives of Medical Science* 13(4), pp. 851-863.
- Elmore, S. 2007. Enhanced histopathology of the thymus. *Toxicologic Pathology* 34(5), pp. 656-665.
- Emini Veseli, B., Perrotta, P., De Meyer, G., Roth, L., Van der Donckt, C., Martinet, W. and De Meyer, G. 2017. Animal models of atherosclerosis. *European Journal of Pharmacology* 816, pp. 3-13.

## References

- Eng, Q. Y., Thanikachalam, P. V. and Ramamurthy, S. 2018. Molecular understanding of Epigallocatechin gallate (EGCG) in cardiovascular and metabolic diseases. *Journal of Ethnopharmacology* 210, pp. 296-310.
- Engelbertsen, D. et al. 2012. Increased inflammation in atherosclerotic lesions of diabetic *Akita-LDLr<sup>-/-</sup>* mice compared to nondiabetic *LDLr<sup>-/-</sup>* mice. *Journal of Diabetes Research* 2012, p. 176162.
- Erdman Jr, J. et al. 2007. Flavonoids and heart health: proceedings of the ILSI North America Flavonoids Workshop, May 31-June 1, 2005, Washington, DC. *Journal of Nutrition* 137(3 Suppl. 1), pp. 718S-737S.
- Esterbauer, H., Eckl, P. and Ortner, A. 1990. Possible mutagens derived from lipids and lipid precursors. *Mutation Research* 238(3), pp. 223-233.
- Fan, F., Sang, L. and Jiang, M. 2017. Catechins and their therapeutic benefits to inflammatory bowel disease. *Molecules* 22, p. 484.
- Fang, Y., Wu, D. and Birukov, K. G. 2019. Mechanosensing and mechanoregulation of endothelial cell functions. *Comprehensive Physiology* 9(2), pp. 873-904.
- Faridi, Z., Njike, V., Dutta, S., Ali, A. and Katz, D. 2008. Acute dark chocolate and cocoa ingestion and endothelial function: a randomized controlled crossover trial. *The American Journal of Clinical Nutrition* 88(1), pp. 58-63.
- Fatkhullina, A., Peshkova, L. and Koltsova, E. 2017. The role of cytokines in the development of atherosclerosis. *Biochemistry (Moscow)* 81(11), pp. 1358-1370.
- Feldman, D., Mogelesky, T., Liptak, B. and Gerrity, R. 1991. Leukocytosis in rabbits with diet-induced atherosclerosis. *Arteriosclerosis, Thrombosis, and Vascular Biology* 11, pp. 985-994.
- Feng, Y. et al. 2012. Hematopoietic stem/progenitor cell proliferation and differentiation is differentially regulated by high-density and low-density lipoproteins in mice. *PLoS ONE* 7(11), p. e47286.
- Feoktistova, M., Geserick, P. and Leverkus, M. 2016. Crystal violet assay for determining viability of cultured cells. *Cold Spring Harbor Protocols* 2016(4), p. pdb.prot087379. doi: 10.1101/pdb.prot087379
- Fernandez-Ruiz, I. 2019. Neutrophil-driven SMC death destabilizes atherosclerotic plaques. *Nature Reviews Cardiology* 16, p. 455.
- Ferreira, L., de Sousa Filho, C., Marinovic, M., Rodrigues, A. and Otton, R. 2020. Green tea polyphenols positively impact hepatic metabolism of adiponectin-knockout lean mice. *Journal of Functional Foods* 64, p. 103679.
- Finger, E., Puri, K., Alon, R., Lawrence, M., von Andrian, U. and Springer, T. 1996. Adhesion through L-selectin requires a threshold hydrodynamic shear. *Nature* 379(6562), pp. 266-269.

## References

- Fisher, N. D. L., Hughes, M., Gerhard-Herman, M. and Hollenberg, N. K. 2003. Flavanol-rich cocoa induces nitric-oxide-dependent vasodilation in healthy humans. *Journal of Hypertension* 21(12), pp. 2281-2286.
- Flammer, A. J. et al. 2011. Cardiovascular effects of flavanol-rich chocolate in patients with heart failure. *European Heart Journal* 33(17), pp. 2172-2180.
- Flores, M. E. J. 2019. Cocoa flavanols: natural agents with attenuating effects on metabolic syndrome risk factors. *Nutrients* 11(4), p. 751.
- Fontana, L., Eagon, J., Trujillo, M., Scherer, P. and Klein, S. 2007. Visceral fat adipokine secretion is associated with systemic inflammation in obese humans. *Diabetes* 56, pp. 1010-1013.
- Forstermann, U. and Sessa, W. 2012. Nitric oxide synthases: regulation and function. *European Heart Journal* 33(7), pp. 829-837.
- Franck, G. et al. 2019. Haemodynamic stress-induced breaches of the arterial intima trigger inflammation and drive atherogenesis. *European Heart Journal* 40(11), pp. 928-937.
- Frank, J., George, T. W., Lodge, J. K., Rodriguez-Mateos, A., Spencer, J. P. E., Minihane, A. M. and Rimbach, G. 2008. Daily consumption of an aqueous green tea extract supplement does not impair liver function or alter cardiovascular disease risk biomarkers in healthy men. *Journal of Nutrition* 139(1), pp. 58-62.
- Freese, R., Basu, S., Hietanen, E., Nair, J., Nakachi, K., Bartsch, H. and Mutanen, M. 1999. Green tea extract decreases plasma malondialdehyde concentration but does not affect other indicators of oxidative stress, nitric oxide production, or hemostatic factors during a high-linoleic acid diet in healthy females. *European Journal of Nutrition* 38(3), pp. 149-157.
- Frontini, A. and Cinti, S. 2010. Distribution and development of brown adipocytes in the murine and human adipose organ. *Cell Metabolism* 11(4), pp. 253-256.
- Frontini, M., O'Neil, C., Sawyez, C., Chan, B., Huff, M. and Pickering, J. 2009. Lipid incorporation inhibits Src-dependent assembly of fibronectin and type I collagen by vascular smooth muscle cells. *Circulation Research* 104, pp. 832-841.
- Frostegard, J. 2013. Immunity, atherosclerosis and cardiovascular disease. *BMC Medicine* 11, p. 117. doi: 10.1186/1741-7015-11-117
- Galis, Z. S., Asanuma, K., Godin, D. and Meng, X. 1998. N-acetyl-cysteine decreases the matrix-degrading capacity of macrophage-derived foam cells: new target for antioxidant therapy? *Circulation* 97, pp. 2445-2453.
- Galis, Z. S. and Khatri, J. J. 2002. Matrix metalloproteinases in vascular remodeling and atherogenesis: the good, the bad, and the ugly. *Circulation Research* 90(3), pp. 251-262.

## References

- Galis, Z. S. et al. 1994a. Cytokine-stimulated human vascular smooth muscle cells synthesize a complement of enzymes required for extracellular matrix digestion. *Circulation Research* 75, pp. 181-189.
- Galis, Z. S., Sukhova, G. K., Kranzhofer, R., Clark, S. and Libby, P. 1995a. Macrophage foam cells from experimental atheroma constitutively produce matrix-degrading proteinases. *Proceedings of the National Academy of Sciences of the United States of America* 92, pp. 402-406.
- Galis, Z. S., Sukhova, G. K., Lark, M. W. and Libby, P. 1994b. Increased expression of matrix metalloproteinases and matrix degrading activity in vulnerable regions of human atherosclerotic plaques. *Journal of Clinical Investigation* 94, pp. 2493-2503.
- Galis, Z. S., Sukhova, G. K. and Libby, P. 1995b. Microscopic localization of active proteases by in situ zymography: detection of matrix metalloproteinase activity in vascular tissue. *The FASEB Journal* 9(10), pp. 974-980.
- Gallagher, H. 2016. *Anti-atherogenic actions of dihomo-gamma-linolenic acid in macrophages*. Cardiff University.
- Gawel, S., Wardas, M., Niedworok, E. and Wardas, P. 2004. Malondialdehyde (MDA) as a lipid peroxidation marker. *Wiadomości Lekarskie* 57(9-10), pp. 453-455.
- Gebuhrer, V., Murphy, J. F., Bordet, J. C., P, R. M. and L, M. J. 1995. Oxidized low-density lipoprotein induces the expression of P-selectin (GMP140/PADGEM/CD62) on human endothelial cells. *Biochemical Journal* 306, pp. 293-298.
- Geissmann, F., Jung, S. and Littman, D. 2003. Blood monocytes consist of two principal subsets with distinct migratory properties. *Immunity* 19, pp. 71-82.
- Gendron, M.-E. et al. 2010. Late chronic catechin antioxidant treatment is deleterious to the endothelial function in aging mice with established atherosclerosis. *American Journal of Physiology-Heart and Circulatory Physiology* 298, pp. H2062-H2070.
- Germann, P. and Ockert, D. 1994. Granulomatous inflammation of the oropharyngeal cavity as a possible cause for unexpected high mortality in a Fischer 344 rat carcinogenicity study. *Laboratory Animal Science* 44(4), pp. 338-343.
- Gerszten, R. E., Garcia-Zepeda, E. A., Lim, Y. C. and et, a. I. 1999. MCP-1 and IL-8 trigger firm adhesion of monocytes to vascular endothelium under flow conditions. *Nature* 398, pp. 718-723.
- Getz, G. and Reardon, C. 2016. Do the Apoe<sup>-/-</sup> and Ldlr<sup>-/-</sup> mice yield the same insight on atherogenesis? *Arteriosclerosis, Thrombosis, and Vascular Biology* 36(9), pp. 1734-1741.
- Getz, G. S. and Reardon, C. A. 2005. Diet and murine atherosclerosis. *Arteriosclerosis, Thrombosis, and Vascular Biology* 26, pp. 242-249.

## References

- Getz, G. S. and Reardon, C. A. 2012. Animal models of atherosclerosis. *Arteriosclerosis, Thrombosis, and Vascular Biology* 32(5), pp. 1104-1115.
- Ghibaudi, L., Cook, J., Farley, C., van Heek, M. and Hwa, J. 2002. Fat intake affects adiposity, comorbidity factors, and energy metabolism of Sprague-Dawley rats. *Obesity Research* 10, pp. 956-963.
- Gijbels, M., van der Cammen, M., van der Laan, L., Emeis, J., Havekes, L., Hofker, M. and Kraal, G. 1999. Progression and regression of atherosclerosis in APOE3-Leiden transgenic mice: an immunohistochemical study. *Atherosclerosis* 143(1), pp. 15-25.
- Gimbrone Jr, M. A. and Garcia-Cardena, G. 2016. Endothelial cell dysfunction and the pathobiology of atherosclerosis. *Circulation Research* 118(4), pp. 620-636.
- Gomes, A., Carvalho, T., Serpa, J., Torre, C. and Dias, S. 2010. Hypercholesterolemia promotes bone marrow cell mobilization by perturbing the SDF-1:CXCR4 axis. *Blood* 115, pp. 3886-3894.
- Gomez, D. and Owens, G. 2012. Smooth muscle cell phenotypic switching in atherosclerosis. *Cardiovascular Research* 95(2), pp. 156-164.
- Gordon, D. et al. 1989. High-density lipoprotein cholesterol and cardiovascular disease. four prospective American studies. *Circulation* 79, pp. 8-15.
- Gottlieb, E., Armour, S., Harris, M. and Thompson, C. 2003. Mitochondrial membrane potential regulates matrix configuration and cytochrome c release during apoptosis. *Cell Death & Differentiation* 10, pp. 709-717.
- Grant, L. et al. 2008. Stat4-dependent, T-bet-independent regulation of IL-10 in NK cells. *Genes & Immunity* 9(4), pp. 316-327.
- Grebe, A., Hoss, F. and Latz, E. 2018. NLRP3 inflammasome and the IL-1 pathway in atherosclerosis. *Circulation Research* 122, pp. 1722-1740.
- Greenow, K., Oearce, N. and Ramji, D. 2005. The key role of apolipoprotein E in atherosclerosis. *Journal of Molecular Medicine* 83(5), pp. 329-342.
- Grootaert, M. O. J. and Bennett, M. R. 2021. Vascular smooth muscle cells in atherosclerosis: time for a re-assessment. *European Society of Cardiology* 0, pp. 1-14.
- Grzesik, M., Naparło, K., Bartosz, G. and Sadowska-Bartoszyńska, I. 2018. Antioxidant properties of catechins: comparison with other antioxidants. *Food Chemistry* 241, pp. 480-492.
- Gu, L., Okada, Y., Clinton, S. K., Gerard, C., Sukhova, G. K., Libby, P. and Rollins, B. J. 1998. Absence of monocyte chemoattractant protein-1 reduces atherosclerosis in low density lipoprotein receptor-deficient mice. *Molecular Cell* 2, pp. 275-281.

## References

- Gulvady, A., Ciolino, H., Cabrera, R. and Jolly, C. 2013. Resveratrol inhibits the deleterious effects of diet-induced obesity on thymic function. *The Journal of Nutritional Biochemistry* 24(9), pp. 1625-1633.
- Guo, Y. et al. 2018. Synthetic high-density lipoprotein-mediated targeted delivery of liver X receptors agonist promotes atherosclerosis regression. *EBioMedicine* 28, pp. 225-233.
- Hadjiphilippou, S. and Ray, K. K. 2017. PCSK9 inhibition and atherosclerotic cardiovascular disease prevention: does reality match the hype? *Heart* 103(21), pp. 1670-1679.
- Hafiane, A. and Genest, J. 2013. HDL, atherosclerosis, and emerging therapies. *Cholesterol* 2013, p. 891403.
- Hajra, L., Evans, A., Chen, M., Hyduk, S., Collins, T. and Cybulsky, M. I. 2000. The NF-kappa B signal transduction pathway in aortic endothelial cells is primed for activation in regions predisposed to atherosclerotic lesion formation. *Proceedings of the National Academy of Sciences of the United States of America* 97(16), pp. 9052-9057.
- Halberg, N., Wernstedt-Asterholm, I. and Scherer, P. 2008. The adipocyte as an endocrine cell. *Endocrinology & Metabolism Clinics of North America* 37, pp. 753-768.
- Hamers, A. et al. 2012. Bone marrow-specific deficiency of nuclear receptor Nur77 enhances atherosclerosis. *Circulation Research* 110, pp. 428-438.
- Hanemaaijer, R., Koolwijk, P., le Clercq, L., de Vree, W. J. and van Hinsbergh, V. W. 1993. Regulation of matrix metalloproteinase expression in human vein and microvascular endothelial cells: effects of tumor necrosis factor  $\alpha$ , interleukin 1 and phorbol ester. *Biochemical Journal* 296, pp. 803-809.
- Hanna, R. et al. 2012. NR4A1 (Nur77) deletion polarizes macrophages toward an inflammatory phenotype and increases atherosclerosis. *Circulation Research* 110, pp. 416-427.
- Hansson, G. K., Libby, P. and Tabas, I. 2015. Inflammation and plaque vulnerability. *Journal of Internal Medicine* 278(5), pp. 483-493.
- Hashimoto, D. et al. 2013. Tissue-resident macrophages self-maintain locally throughout adult life with minimal contribution from circulating monocytes. *Immunity* 38, pp. 792-804.
- Haslinger-Loffler, B. 2008. Multiple effects of HMG-CoA reductase inhibitors (statins) besides their lipid-lowering function. *Kidney International* 74(5), pp. 553-555.
- Hayek, T. et al. 1997. Reduced progression of atherosclerosis in apolipoprotein E-deficient mice following consumption of red wine, or its polyphenols quercetin or catechin, is associated with reduced susceptibility of LDL to oxidation and aggregation. *Arteriosclerosis, Thrombosis, and Vascular Biology* 17, pp. 2744-2752.

## References

- He, C., Medley, S., Hu, T., Hinsdale, M., Lupu, F., Virmani, R. and Olson, L. 2015. PDGFR $\beta$  signalling regulates local inflammation and synergizes with hypercholesterolaemia to promote atherosclerosis. *Nature Communications* 6, p. 7770.
- He, M.-Q. et al. 2020. High-fat diet-induced adipose tissue expansion occurs prior to insulin resistance in C57BL/6J mice. *Chronic Diseases and Translational Medicine* 6(3), pp. 198-207.
- Heinloth, A., Heermeier, K., Raff, U., Wanner, C. and Galle, J. 2000. Stimulation of NADPH oxidase by oxidized low-density lipoprotein induces proliferation of human vascular endothelial cells. *American Society of Nephrology* 11(10), pp. 1819-1825.
- Heiss, C. et al. 2015. Impact of cocoa flavanol intake on age-dependent vascular stiffness in healthy men: a randomized, controlled, double-masked trial. *Age (Dordr)* 37(3), p. 9794.
- Heo, S. H. et al. 2011. Plaque rupture is a determinant of vascular events in carotid artery atherosclerotic disease: involvement of matrix metalloproteinases 2 and 9. *Journal of Clinical Neurology* 7(2), pp. 69-76.
- Hilgendorf, I. et al. 2014. Ly-6Chigh monocytes depend on Nr4a1 to balance both inflammatory and reparative phases in the infarcted myocardium. *Circulation Research* 114, pp. 1611-1622.
- Hill, B., Benavides, G., Lancaster, J., Ballinger, S., Dell'italia, L., Zhang, J. and Darley-Usmar, V. 2012. Integration of cellular bioenergetics with mitochondrial quality control and autophagy. *Journal of Biological Chemistry* 393, pp. 1485-1512.
- Hort, M. et al. 2014. Diphenyl diselenide protects endothelial cells against oxidized low density lipoprotein-induced injury: Involvement of mitochondrial function. *Biochimie* 105, pp. 172-181.
- Horton, J. D., Goldstein, J. I. and Brown, M. S. 2002. SREBPs: activators of the complete program of cholesterol and fatty acid synthesis in the liver. *Journal of Clinical Investigation* 109(9), pp. 1125-1131.
- Hotamisligil, G. 2006. Inflammation and metabolic disorders. *Nature* 444, pp. 860-867.
- Hsu, S.-P., Wu, M.-S., Yang, C.-C., Huang, K.-C., Liou, S.-Y., Hsu, S.-M. and Chien, C.-T. 2007. Chronic green tea extract supplementation reduces hemodialysis-enhanced production of hydrogen peroxide and hypochlorous acid, atherosclerotic factors, and proinflammatory cytokines. *The American Journal of Clinical Nutrition* 86(5), pp. 1539-1547.
- Huang, K.-C., Yang, C.-C., Lee, K. T. and Chien, C.-T. 2003. Reduced hemodialysis-induced oxidative stress in end-stage renal disease patients by electrolyzed reduced water. *Kidney International* 64, pp. 704-714.

## References

- Huang, L. et al. 2019. SR-B1 drives endothelial cell LDL transcytosis via DOCK4 to promote atherosclerosis. *Nature* 569(7757), pp. 565-569.
- Huang, S.-C. et al. 2014. Cell-intrinsic lysosomal lipolysis is essential for alternative activation of macrophages. *Nature Immunology* 15, pp. 846-855.
- Hyogo, H., Chayama, K. and Yamagishi, S. 2014. Nonalcoholic fatty liver disease and cardiovascular disease. *Current Pharmaceutical Design* 20(14), pp. 2403-2411.
- Ihm, S.-H., Lee, J.-O., Kim, S.-J., Seung, K.-B., Schini-Kerth, V., Chang, K. and Oak, M.-H. 2009. Catechin prevents endothelial dysfunction in the prediabetic stage of OLETF rats by reducing vascular NADPH oxidase activity and expression. *Atherosclerosis* 206, pp. 47-53.
- Ikeda, Y., Kawakami, K., Sato, I., Tajima, S., Ito, K. and Nose, T. 1984. Effect of cyanidanol (KB-53) on the activity of mouse natural killer cells. *Journal of Pharmacobiodynamics* 7(1), pp. 21-23.
- Inami, S. et al. 2007. Tea catechin consumption reduces circulating oxidized low-density lipoprotein. *International Heart Journal* 48(6), pp. 725-732.
- Ishibashi, S., Brown, M., Goldstein, J., Gerard, R., Hammer, R. and Herz, J. 1993. Hypercholesterolemia in low density lipoprotein receptor knockout mice and its reversal by adenovirus-mediated gene delivery. *Journal of Clinical Investigation* 92(2), pp. 883-893.
- Islam, M. 2012. Cardiovascular effects of green tea catechins: progress and promise. *Recent Patents on Cardiovascular Drug Discovery* 7(2), pp. 88-99.
- Isoda, K. et al. 2004. Lack of interleukin-1 receptor antagonist modulates plaque composition in apolipoprotein E-deficient mice. *Arteriosclerosis, Thrombosis, and Vascular Biology* 24(6), pp. 1068-1073.
- Ito, F., Sono, Y. and Ito, T. 2019. Measurement and clinical significance of lipid peroxidation as a biomarker of oxidative stress: oxidative stress in diabetes, atherosclerosis, and chronic inflammation. *Antioxidants (Basel)* 8(3), p. 72.
- Jablonski, K., Amici, S., Webb, L., Ruiz-Rosado, J., Popovich, P., Partida-Sanchez, S. and Guerau-de-Arellano, M. 2015. Novel markers to delineate murine M1 and M2 macrophages. *PLoS ONE* 10(12), p. e0145342.
- Jacobsen, K. et al. 2017. Diverse cellular architecture of atherosclerotic plaque derives from clonal expansion of a few medial SMCs. *JCI Insight* 2(19), p. e95890.
- Jaiswal, S. et al. 2014. Age-related clonal hematopoiesis associated with adverse outcomes. *New England Journal of Medicine* 371, pp. 2488-2498.
- Jaiswal, S. et al. 2017. Clonal hematopoiesis and risk of atherosclerotic cardiovascular disease. *New England Journal of Medicine* 377, pp. 111-121.

## References

- Jenkins, S. J. et al. 2011. Local macrophage proliferation, rather than recruitment from the blood, is a signature of TH2 inflammation. *Science* 332, pp. 1284-1288.
- Jia, L., Betters, J. and Yu, L. 2011. Niemann-pick C1-like 1 (NPC1L1) protein in intestinal and hepatic cholesterol transport. *Annual Review of Physiology* 73, pp. 239-259.
- Jiang, Y., Ding, S., Li, F., Zhang, C., Sun-Waterhouse, D. and Chen, Y. 2019. Effects of (+)-catechin on the differentiation and lipid metabolism of 3T3-L1 adipocytes. *Journal of Functional Foods* 62, p. 103558.
- Johnson, J. L., Jackson, C. L., Angelini, G. D. and George, S. J. 1998. Activation of matrix-degrading metalloproteinases by mast cell proteases in atherosclerotic plaques. *Arteriosclerosis, Thrombosis, and Vascular Biology* 18, pp. 1707-1715.
- Jongstra-Bilen, J., Haidari, M., Zhu, S.-N., Chen, M., Guha, D. and Cybulsky, M. I. 2006. Low-grade chronic inflammation in regions of the normal mouse arterial intima predisposed to atherosclerosis. *Journal of Experimental Medicine* 203(9), pp. 2073-2083.
- Jou, P.-C., Ho, B.-Y., Hsu, Y.-W. and Pan, T.-M. 2010. The effect of monascus secondary polyketide metabolites, monascin and ankaflavin, on adipogenesis and lipolysis activity in 3T3-L1. *Journal of Agricultural and Food Chemistry* 58(24), pp. 12703-12709.
- Jovinge, S., Ares, M. P. S., Kallin, B. and Nilsson, J. 1996. Human monocytes/macrophages release TNF-(alpha) in response to ox-LDL. *Arteriosclerosis, Thrombosis, and Vascular Biology* 16, pp. 1573-1579.
- Kajimura, S., Spiegelman, B. and Seale, P. 2015. Brown and beige fat: physiological roles beyond heat generation. *Cell Metabolism* 22(4), pp. 546-559.
- Kalluri, A. et al. 2019. Single-cell analysis of the normal mouse aorta reveals functionally distinct endothelial cell populations. *Circulation* 140(2), pp. 147-163.
- Kalra, H., Drummen, G. and Mathivanan, S. 2016. Focus on extracellular vesicles: introducing the next small big thing. *International Journal of Molecular Science* 17, p. 170.
- Karastergiou, K. and Mohamed-Ali, V. 2010. The autocrine and paracrine roles of adipokines. *Molecular and Cellular Endocrinology* 318, pp. 69-78.
- Kelly, B. and O'Neill, L. A. 2015. Metabolic reprogramming in macrophages and dendritic cells in innate immunity. *Cell Research* 25, pp. 771-784.
- Khallou-Laschet, J., Varthaman, A., Fornasa, G. and et, a. I. 2010. Macrophage plasticity in experimental atherosclerosis. *PLoS ONE* 5, p. e8852.
- Khera, A. et al. 2011. Cholesterol efflux capacity, high-density lipoprotein function, and atherosclerosis. *The New England Journal of Medicine* 364, pp. 127-135.

## References

- Kim-Park, W., Allam, E., Palasuk, J., Kowolik, M., Park, K. and Windsor, L. 2015. Green tea catechin inhibits the activity and neutrophil release of Matrix Metalloproteinase-9. *Journal of Traditional and Complementary Medicine* 6(4), pp. 343-346.
- Kim, S.-H. et al. 2006. Epigallocatechin-3-gallate protects toluene diisocyanate-induced airway inflammation in a murine model of asthma. *FEBS Letters* 580(7), pp. 1883-1890.
- Kinder, J., Then, J., Hansel, P., Molinero, L. and Bruns, H. 2014. Long-term repeated daily use of intragastric gavage hinders induction of oral tolerance to ovalbumin in mice. *Comparative Medicine* 64(5), pp. 369-376.
- Klaus, S., Pultz, S., Thone-Reineke, C. and Wolfram, S. 2005. Epigallocatechin gallate attenuates diet-induced obesity in mice by decreasing energy absorption and increasing fat oxidation. *International Journal of Obesity* 29, pp. 615-623.
- Knekt, P. et al. 2004. Antioxidant vitamins and coronary heart disease risk: a pooled analysis of 9 cohorts. *The American Journal of Clinical Nutrition* 80(6), pp. 1508-1520.
- Knutsson, A., Bjorkbacka, H., Duner, P., Engstrom, G., Binder, C., Nilsson, A. and Nilsson, J. 2019. Associations of interleukin-5 with plaque development and cardiovascular events. *JACC: Basic to Translational Science* 4(8), pp. 891-902.
- Ko, K., Fujiwara, K., Krishnan, S. and Abe, J. 2017. *En face* preparation of mouse blood vessels. *Journal of Visualized Experiments* (123), p. 55460. doi: 10.3791/55460
- Koelwyn, G., Corr, E., Erbay, E. and Moore, K. 2019. Regulation of macrophage immunometabolism in atherosclerosis. *Nature Immunology* 19(6), pp. 526-537.
- Koenen, R. R. and Weber, C. 2010. Therapeutic targeting of chemokine interactions in atherosclerosis. *Nature Reviews Drug Discovery* 141, pp. 141-153.
- Koga, T. and Meydani, M. 2001. Effect of plasma metabolites of (+)-catechin and quercetin on monocyte adhesion to human aortic endothelial cells. *The American Journal of Clinical Nutrition* 73, pp. 941-948.
- Kozaki, K. et al. 2002. Blockade of platelet-derived growth factor or its receptors transiently delays but does not prevent fibrous cap formation in ApoE null mice. *The American Journal of Pathology* 161(4), pp. 1395-1407.
- Krzysztozek, J., Wierzejska, E. and Zielińska, A. 2015. Obesity. An analysis of epidemiological and prognostic research. *Archives of Medical Science* 11, pp. 24-33.
- Kuchan, M. and Frangos, J. 1994. Role of calcium and calmodulin in flow-induced nitric oxide production in endothelial cells. *The American Journal of Physiology* 266, pp. C628-C636.

## References

- Kumar, A., Takada, Y., Boriek, A. and Aggarwal, B. 2004. Nuclear factor- $\kappa$ B: its role in health and disease. *Journal of Molecular Medicine* 82, pp. 434-448.
- Kumar, P., Nagarajan, A. and Uchil, P. D. 2018. Analysis of cell viability by the lactate dehydrogenase assay. *Cold Spring Harbor Protocols* 2018(6), doi: 10.1101/pdb.prot095497
- Kuo, C.-L., Chen, T.-S., Liou, S.-Y. and Hsieh, C.-C. 2014. Immunomodulatory effects of EGCG fraction of green tea extract in innate and adaptive immunity via T regulatory cells in murine model. *Immunopharmacology and Immunotoxicology* 36(5), pp. 364-370.
- Kuzuya, M., Nakamura, K., Sasaki, T., Cheng, X. W., Itohara, S. and Iguchi, A. 2006. Effect of MMP-2 deficiency on atherosclerotic lesion formation in ApoE-deficient mice. *Arteriosclerosis, Thrombosis, and Vascular Biology* 26(5), pp. 1120-1125.
- Lagace, T. 2014. PCSK9 and LDLR degradation regulatory mechanisms in circulation and in cells. *Current Opinion in Lipidology* 25(5), pp. 387-393.
- Latz, E., Xiao, T. S. and Stutz, A. 2013. Activation and regulation of the inflammasomes. *Nature Reviews Immunology* 13, pp. 397-411.
- Laufs, U. et al. 2019. Efficacy and safety of bempedoic acid in patients with hypercholesterolemia and statin intolerance. *Journal of the American Heart Association* 8(7), p. e011662.
- Lawrence, M., Kansas, G., Kunkel, E. and Ley, K. 1997. Threshold levels of fluid shear promote leukocyte adhesion through selectins (CD62L,P,E). *Journal of Cell Biology* 136(3), pp. 717-727.
- Laxton, R. C. et al. 2009. A role of matrix metalloproteinase-8 in atherosclerosis. *Circulation Research* 105(9), pp. 921-929.
- Le, N. 2014. Lipoprotein-associated oxidative stress: A new twist to the postprandial hypothesis. *International Journal of Molecular Sciences* 16, pp. 401-419.
- Lee, M.-J. et al. 2002. Pharmacokinetics of tea catechins after ingestion of green tea and (-)-epigallocatechin-3-gallate by humans: formation of different metabolites and individual variability. *Cancer Epidemiology, Biomarkers & Prevention* 11(10 Pt. 1), pp. 1025-1032.
- Lee, M.-S., Kim, C.-T. and Kim, Y. 2009. Green tea (-)-epigallocatechin-3-gallate reduces body weight with regulation of multiple genes expression in adipose tissue of diet-induced obese mice. *Annals of Nutrition and Metabolism* 54(2), pp. 151-157.
- Lee, M. et al. 1995. Analysis of plasma and urinary tea polyphenols in human subjects. *Cancer Epidemiology, Biomarkers & Prevention* 4(4), pp. 393-399.
- Lee, Y. et al. 2017. Animal models of atherosclerosis. *Biomedical Reports* 6(3), pp. 259-266.

## References

- Leitinger, N. and Schulman, I. G. 2013. Phenotypic polarization of macrophages in atherosclerosis. *Arteriosclerosis, Thrombosis, and Vascular Biology* 33(6), pp. 1120-1126.
- Ley, K., Laudanna, C., Cybulsky, M. I. and Nourshargh, S. 2007. Getting to the site of inflammation: the leukocyte adhesion cascade updated. *Nature Reviews Immunology* 7, pp. 678-689.
- Li, A. and Glass, C. 2002. The macrophage foam cell as a target for therapeutic intervention. *Nature Medicine* 8, pp. 1235-1242.
- Li, D., Liu, L., Chen, H., Sawamura, T. and Mehta, J. L. 2003. LOX-1 an oxidized LDL endothelial receptor, induces CD40/CD40L signaling in human coronary artery endothelial cells. *Arteriosclerosis, Thrombosis, and Vascular Biology* 23, pp. 816-821.
- Li, D. and Mehta, J. L. 2000. Antisense to LOX-1 inhibits oxidized LDL-mediated upregulation of monocyte chemoattractant protein-1 and monocyte adhesion to human coronary artery endothelial cells. *Circulation* 101, pp. 2889-2895.
- Li, F. et al. 2018. EGCG reduces obesity and white adipose tissue gain partly through AMPK activation in mice. *Frontiers in Pharmacology* 9, p. 1366.
- Li, H., Wetchapinant, C., Zhang, L. and Wu, K. 2020. High-fat diet from weaning until early adulthood impairs T cell development in the thymus. *Lipids* 55(1), pp. 35-44.
- Li, W. et al. 2021. The inhibitory effect of (-)-Epicatechin gallate on the proliferation and migration of vascular smooth muscle cells weakens and stabilizes atherosclerosis. *European Journal of Pharmacology* 891, p. 173761.
- Li, Z., Fang, P., Mai, J., Choi, E., Wang, H. and Yang, X.-F. 2013. Targeting mitochondrial reactive oxygen species as novel therapy for inflammatory diseases and cancers. *Journal of Hematology & Oncology* 6, p. 19.
- Libby, P. 2013. Mechanisms of acute coronary syndromes and their implications for therapy. *The New England Journal of Medicine* 368(21), pp. 2004-2013.
- Libby, P. 2017. Interleukin-1 beta as a target for atherosclerosis therapy: The biological basis of CANTOS and beyond. *Journal of the American College of Cardiology* 70(18), pp. 2278-2289.
- Libby, P. 2019. Once more unto the breach: endothelial permeability and atherogenesis. *European Heart Journal* 40, pp. 938-940.
- Libby, P. 2021. The changing landscape of atherosclerosis. *Nature* 592, pp. 524-533.
- Libby, P. et al. 2019a. Atherosclerosis. *Nature Reviews Disease Primers* 5(56), pp. 1-18.

## References

- Libby, P., Lichtman, A. H. and Hansson, G. K. 2013. Immune effector mechanisms implicated in atherosclerosis: from mice to humans. *Immunity* 38, pp. 1092-1104.
- Libby, P., Pasterkamp, G., Crea, F. and Jang, I. K. 2019b. Reassessing the mechanisms of acute coronary syndromes. *Circulation Research* 124, pp. 150-160.
- Libby, P., Ridker, P. M. and Hansson, G. K. 2009. Inflammation in atherosclerosis: from pathophysiology to practice. *Journal of the American College of Cardiology* 54(23), pp. 2129-2138.
- Libby, P., Ridker, P. M. and Hansson, G. K. 2011. Progress and challenges in translating the biology of atherosclerosis. *Nature*. 473(7347), pp. 317-325. doi: 10.1038/nature10146
- Libby, P., Warner, S. J. and Friedman, G. B. 1988. Interleukin 1: a mitogen for human vascular smooth muscle cells that induces the release of growth-inhibitory prostanoids. *Journal of Clinical Investigation* 81, pp. 487-498.
- Lichtman, A. H., Binder, C. J., Tsimikas, S. and Witztum, J. 2013. Adaptive immunity in atherogenesis: new insights and therapeutic approaches. *Journal of Clinical Investigation* 123(1), pp. 27-36.
- Lisinski, T. J. and Furie, M. B. 2002. Interleukin-10 inhibits proinflammatory activation of endothelium in response to *Borrelia burgdorferi* or lipopolysaccharide but not interleukin-1 beta or tumor necrosis factor alpha. *Journal of Leukocyte Biology* 72, pp. 503-511.
- Liu, H., Dong, W., Lin, Z., Lu, J., Wan, H., Zhou, Z. and Liu, Z. 2013. CCN4 regulates vascular smooth muscle cell migration and proliferation. *Molecules and Cells* 36(2), pp. 112-118.
- Liu, L. et al. 2016. Proinflammatory signal suppresses proliferation and shifts macrophage metabolism from Myc-dependent to HIF1 $\alpha$ -dependent. *Proceedings of the National Academy of Sciences of the United States of America* 113(6), pp. 1564-1569.
- Liu, T., Zhang, L., Joo, D. and Sun, S.-C. 2017. NF- $\kappa$ B signaling in inflammation. *Signal Transduction and Targeted Therapy* 2, p. 17023.
- Liu, X. et al. 2019. *Gpihbp1* deficiency accelerates atherosclerosis and plaque instability in diabetic *Ldlr*<sup>-/-</sup> mice. *Atherosclerosis* 282, pp. 100-109.
- Lodoen, M. and Lanier, L. 2006. Natural killer cells as an initial defense against pathogens. *Current Opinion in Immunology* 18(4), pp. 391-398.
- Lonardo, A., Nascimbeni, F., Mantovani, A. and Targher, G. 2018. Hypertension, diabetes, atherosclerosis and NASH: cause or consequence? *Journal of Hepatology* 68(2), pp. 335-352.

## References

- Lushchak, V. 2014. Free radicals, reactive oxygen species, oxidative stress and its classification. *Chemico-Biological Interactions* 224, pp. 164-175.
- Lusis, A. J. 2000. Atherosclerosis. *Nature* 407(6801), pp. 233-241.
- Mach, F., Schonbeck, U., Sukhova, G. K., Bourcier, T., Bonnefoy, J. Y., Pober, J. S. and Libby, P. 1997. Functional CD40 ligand is expressed on human vascular endothelial cells, smooth muscle cells, and macrophages: implications for CD40-CD40 ligand signaling in atherosclerosis. *Proceedings of the National Academy of Sciences of the United States of America* 94(5), pp. 1931-1936.
- Mackesy, D. Z. and Goalstone, M. L. 2014. ERK5: novel mediator of insulin and TNF-stimulated VCAM-1 expression in vascular cells. *J Diabetes* 6, pp. 595-602.
- Madamanchi, N. and Runge, M. 2007. Mitochondrial dysfunction in atherosclerosis. *Circulation Research* 100, pp. 460-473.
- Madjid, M., Awan, I., Willerson, J. and Casscells, S. 2004. Leukocyte count and coronary heart disease: implications for risk assessment. *Journal of the American College of Cardiology* 44, pp. 1945-1956.
- Maejima, Y., Adachi, S., Ito, H., Hirao, K. and Isobe, M. 2008. Induction of premature senescence in cardiomyocytes by doxorubicin as a novel mechanism of myocardial damage. *Aging Cell* 7, pp. 125-136.
- Mahley, R. W. 2016. Apolipoprotein E: from cardiovascular disease to neurodegenerative disorders. *Molecules in Medicine* 94, pp. 739-746.
- Mallat, Z., Taleb, S., Ait-Oufella, H. and Tedgui, A. 2009. The role of adaptive T cell immunity in atherosclerosis. *Journal of Lipid Research* 50, pp. S364-S339.
- Man, J., Beckman, J. and Jaffe, I. 2020. Sex as a biological variable in atherosclerosis. *Circulation Research* 126, pp. 1297-1319.
- Mangels, D. R. and Mohler (III), E. R. 2017. Catechins as potential mediators of cardiovascular health. *Arteriosclerosis, Thrombosis, and Vascular Biology* 37, pp. 757-763.
- Mantovani, A., Garlanda, C. and Locati, M. 2009. Macrophage diversity and polarization in atherosclerosis: a question of balance. *Arteriosclerosis, Thrombosis, and Vascular Biology* 29, pp. 1419-1423.
- Marek, I. et al. 2017. Sex differences in the development of vascular and renal lesions in mice with a simultaneous deficiency of Apoe and the integrin chain Itga8. *Biology of Sex Differences* 8, p. 19. doi: <https://doi.org/10.1186/s13293-017-0141-y>
- Martinez, G. J., Celermajer, D. S. and Patel, S. 2018. The NLRP3 inflammasome and the emerging role of colchicine to inhibit atherosclerosis-associated inflammation. *Atherosclerosis* 269, pp. 262-271.

## References

- Mastroiacovo, D. et al. 2015. Cocoa flavanol consumption improves cognitive function, blood pressure control, and metabolic profile in elderly subjects: the Cocoa, Cognition, and Aging (CoCoA) Study—a randomized controlled trial. *The American Journal of Clinical Nutrition* 101(3), pp. 538-548.
- Matsumoto, T. et al. 2016. Overexpression of cytotoxic T-lymphocyte-associated antigen-4 prevents atherosclerosis in mice. *Arteriosclerosis, Thrombosis, and Vascular Biology* 36, pp. 1141-1151.
- Matsuyama, T., Tanaka, Y., Kamimaki, I., Nagao, T. and Tokimitsu, I. 2008. Catechin safely improved higher levels of fatness, blood pressure, and cholesterol in children. *Obesity (Silver Spring)* 16(6), pp. 1338-1348.
- Matthews, C. et al. 2006. Vascular smooth muscle cells undergo telomere-based senescence in human atherosclerosis: effects of telomerase and oxidative stress. *Circulation Research* 99, pp. 156-164.
- McLaren, J. E., Michael, D. R., Ashlin, T. G. and Ramji, D. P. 2011. Cytokines, macrophage lipid metabolism and foam cells: Implications for cardiovascular disease therapy. *Progress in Lipid Research* 50, pp. 331-347.
- Mehta, J. L. et al. 2007. Deletion of LOX-1 reduces atherogenesis in LDLR knockout mice fed high cholesterol diet. *Circulation Research* 100(11), pp. 1634-1642.
- Meo, S., Reed, T., Venditti, P. and Victor, V. 2016. Role of ROS and RNS sources in physiological and pathological conditions. *Oxidative Medicine and Cellular Longevity* 2016, p. 1245049.
- Micha, R., Imamura, F., Wyler Von Ballmoos, M., Solomon, D., Hernan, M. A., Ridker, P. M. and Mozaffarian, D. 2011. Systematic review and meta-analysis of methotrexate use and risk of cardiovascular disease. *American Journal of Cardiology* 108(9), pp. 1362-1370.
- Michael, D. R., Ashlin, T. G., Buckley, M. L. and Ramji, D. P. 2012a. Liver X receptors, atherosclerosis and inflammation. *Current Atherosclerosis Reports* 14, pp. 284-293.
- Michael, D. R., Ashlin, T. G., Buckley, M. L. and Ramji, D. P. 2012b. Macrophages, lipid metabolism and gene expression in atherogenesis: a therapeutic target of the future? *Journal of Clinical Lipidology* 7(1), pp. 37-48.
- Michael, D. R., Ashlin, T. G., Davies, C. S., Gallagher, H., Stoneman, T. W., Buckley, M. L. and Ramji, D. P. 2013. Differential regulation of macropinocytosis in macrophages by cytokines: Implications for foam cell formation and atherosclerosis. *Cytokine* 64(1), pp. 357-361.
- Michel, T. et al. 2012. Mouse lung and spleen natural killer cells have phenotypic and functional differences, in part influenced by macrophages. *PLoS ONE* 7(12), p. e51230.

## References

- Mikhed, Y., Daiber, A. and Steven, S. 2015. Mitochondrial oxidative stress, mitochondrial DNA damage and their role in age-related vascular dysfunction. *International Journal of Molecular Sciences* 16, pp. 15918-15953.
- Mistry, Y., Poolman, T., Williams, B. and Herbert, K. 2013. A role for mitochondrial oxidants in stress induced premature senescence of human vascular smooth muscle cells. *Redox Biology* 1, pp. 411-417.
- Mitchell, P. and Moyle, J. 1965. Evidence discriminating between the chemical and the chemiosmotic mechanisms of electron transport phosphorylation. *Nature* 208, pp. 1205-1206.
- Miura, Y. et al. 2001. Tea catechins prevent the development of atherosclerosis in apoprotein E-deficient mice. *Journal of Nutrition* 131(1), pp. 27-32.
- Miyazaki, R. et al. 2012. Minor effects of green tea catechin supplementation on cardiovascular risk markers in active older people: A randomized controlled trial. *Geriatrics & Gerontology International* 13(3), pp. 622-629.
- Miyazawa, T. 2000. Absorption, metabolism and antioxidative effects of tea catechin in humans. *Biofactors* 13, pp. 55-59.
- Miyoshi, N., Pervin, M., Suzuki, T., Unno, K., Isemura, M. and Nakamura, Y. 2015. Green tea catechins for well-being and therapy: prospects and opportunities. *Botanics: Targets and Therapy* 5, pp. 85-96.
- Moe, K., Khairunnisa, K., Yin, N., Chin-Dusting, J., Wong, P. and Wong, M. 2014. Tumor necrosis factor- $\alpha$ -induced nuclear factor-kappaB activation in human cardiomyocytes is mediated by NADPH oxidase. *Journal of Physiology and Biochemistry* 70(3), pp. 769-779.
- Moens, U., Kostenko, S. and Sveinbjörnsson, B. 2013. The role of mitogen-activated protein kinase-activated protein kinases (MAPKAPKs) in inflammation. *Genes (Basel)* 4(2), pp. 101-133.
- Molinaro, R. et al. 2021. Targeted delivery of Protein Arginine Deiminase-4 inhibitors to limit arterial intimal NETosis and preserve endothelial integrity. *Cardiovascular Research*, doi: 10.1093/cvr/cvab074
- Moore, K. J., Sheedy, F. J. and Fisher, E. A. 2013. Macrophages in atherosclerosis: a dynamic balance. *Nature Reviews Immunology* 13, pp. 709-721.
- Moris, D. et al. 2017. The role of reactive oxygen species in myocardial redox signaling and regulation. *Annals of Translational Medicine* 5(16), p. 324.
- Morrison, M. et al. 2014. Epicatechin attenuates atherosclerosis and exerts anti-inflammatory effects on diet-induced human-CRP and NF $\kappa$ B in vivo. *Atherosclerosis* 233(1), pp. 149-156.

## References

- Morton, A. C., Arnold, N. D., Gunn, J., Varcoe, R., Francis, S., Dower, S. and Crossman, D. 2005. Interleukin-1 receptor antagonist alters the response to vessel wall injury in a porcine coronary artery model. *Cardiovascular Research* 68(3), pp. 493-501.
- Morton, A. C. et al. 2015. The effect of interleukin-1 receptor antagonist therapy on markers of inflammation in non-ST elevation acute coronary syndromes: the MRC-ILA Heart study. *European Heart Journal* 36(6), pp. 377-384.
- Moss, J. W. E. 2018. *Anti-inflammatory actions of nutraceuticals*. Cardiff University.
- Moss, J. W. E. and Ramji, D. P. 2016a. Cytokines: Roles in atherosclerosis disease progression and potential therapeutic targets. *Future Medicinal Chemistry* 8(11), pp. 1317-1330.
- Moss, J. W. E. and Ramji, D. P. 2016b. Nutraceutical therapies for atherosclerosis. *Nature Reviews Cardiology* 13(9), pp. 513-532.
- Moss, J. W. E., Williams, J. O. and Ramji, D. P. 2018. Nutraceuticals as therapeutic agents for atherosclerosis. *Biochimica et Biophysica Acta - Molecular Basis of Disease* 1864(5 Pt A), pp. 1562-1572.
- Murphy, A. et al. 2011. ApoE regulates hematopoietic stem cell proliferation, monocytosis, and monocyte accumulation in atherosclerotic lesions in mice. *Journal of Clinical Investigation* 121, pp. 4138-4149.
- Murphy, A. and Tall, A. 2016. Disordered haematopoiesis and athero-thrombosis. *European Heart Journal* 37(14), pp. 1113-1121.
- Murphy, S., Smith, P., Shaivitz, A., Rossberg, M. and Hurn, P. 2001. The effect of brief halothane anesthesia during daily gavage on complications and body weight in rats. *Contemporary Topics in Laboratory Animal Science* 40(2), pp. 9-12.
- Nahapetyan, H. et al. 2019. Altered mitochondrial quality control in Atg7-deficient VSMCs promotes enhanced apoptosis and is linked to unstable atherosclerotic plaque phenotype. *Cell Death & Disease* 10, p. 119.
- Nakagawa, K., Okuda, S. and Miyazawa, T. 1997. Dose-dependent incorporation of tea catechins, (-)-epigallocatechin-3-gallate and (-)-epigallocatechin, into human plasma. *Bioscience, Biotechnology, and Biochemistry* 61, pp. 1981-1985.
- Nicklin, M. J., Hughes, D. E., Barton, J. L., Ure, J. and Duff, G. 2000. Arterial inflammation in mice lacking the interleukin 1 receptor antagonist gene. *Journal of Experimental Medicine* 191(2), pp. 303-312.
- Nidorf, S. M., Eikelboom, J. W., Budgeon, C. A. and Thompson, P. 2013. Low-dose colchicine for secondary prevention of cardiovascular disease. *Journal of the American College of Cardiology* 61(4), pp. 404-410.

## References

- Nidorf, S. M., Eikelboom, J. W. and Thompson, P. L. 2014. Targeting cholesterol crystal-induced inflammation for the secondary prevention of cardiovascular disease. *Journal of Cardiovascular Pharmacology and Therapeutics* 19(1), pp. 45-52.
- Nidorf, S. M. et al. 2020. Colchicine in patients with chronic coronary disease. *New England Journal of Medicine* 383(19), pp. 1838-1847.
- Niemeyer, E. D. and Brodbelt, J. S. 2008. Isomeric differentiation of green tea catechins using gas-phase hydrogen/deuterium exchange reactions. *Journal of the American Society for Mass Spectrometry* 18(10), pp. 1749-1759.
- Nirengi, S. et al. 2016. Daily ingestion of catechin-rich beverage increases brown adipose tissue density and decreases extramyocellular lipids in healthy young women. *SpringerPlus* 5(1), p. 1363.
- Noll, C., Lameth, J., Paul, J.-L. and Janel, N. 2013. Effect of catechin/epicatechin dietary intake on endothelial dysfunction biomarkers and proinflammatory cytokines in aorta of hyperhomocysteinemic mice. *European Journal of Nutrition* 52, pp. 1243-1250.
- Norata, G., Marchesi, P., Passamonti, S., Pirillo, A., Violi, F. and Catapano, A. 2007. Anti-inflammatory and anti-atherogenic effects of catechin, caffeic acid and trans-resveratrol in apolipoprotein E deficient mice. *Atherosclerosis* 191, pp. 265-271.
- Nunnari, J. and Suomalainen, A. 2012. Mitochondria: in sickness and in health. *Cell* 148(6), pp. 1145-1159.
- Nus, M. and Mallat, Z. 2016. Immune-mediated mechanisms of atherosclerosis and implications for the clinic. *Expert Review of Clinical Immunology* 12(11), pp. 1217-1237.
- O'Morain, V. 2019. *The beneficial effects of the Lab4 probiotic consortium in atherosclerosis*. Cardiff University.
- O'Neill, L., Kishton, R. and Rathmell, J. 2016. A guide to immunometabolism for immunologists. *Nature Reviews Immunology* 16, pp. 553-565.
- Ohta, H., Wada, H., Niwa, T. and et, a. I. 2005. Disruption of tumor necrosis factor- $\alpha$  gene diminishes the development of atherosclerosis in apoE-deficient mice. *Atherosclerosis* 180, pp. 11-17.
- Ohyama, K., Furuta, C., Nogusa, Y., Nomura, K., Miwa, T. and Suzuki, K. 2011. Catechin-rich grape seed extract supplementation attenuates diet-induced obesity in C57BL/6J mice. *Annals of Nutrition and Metabolism* 58, pp. 250-258.
- Olejarz, W., Lacheta, D. and Kubiak-Tomaszewska, G. 2020. Matrix metalloproteinases as biomarkers of atherosclerotic plaque instability. *International Journal of Molecular Medicine* 21(11), p. 3946.

## References

- Olivares, R., Ducimetière, P. and Claude, J. 1993. Monocyte count: a risk factor for coronary heart disease? *American Journal of Epidemiology* 137(1), pp. 49-53.
- Ono, K. 2012. Current concept of reverse cholesterol transport and novel strategy for atheroprotection. *Journal of Cardiology* 60(5), pp. 339-343.
- Oppi, S., Luscher, T. and Stein, S. 2019. Mouse models for understanding human atherosclerosis-Which is my line? *Frontiers in Cardiovascular Medicine* 6, p. 46.
- Otsuka, E. et al. 2016. Natural progression of atherosclerosis from pathologic intimal thickening to late fibroatheroma in human coronary arteries: a pathology study. *Atherosclerosis* 241(2), pp. 772-782.
- Oyama, J.-I. et al. 2010. Green tea catechins improve human forearm endothelial dysfunction and have antiatherosclerotic effects in smokers. *Circulation Journal* 74(3), pp. 578-588.
- Palmer, R. M., Ashton, D. S. and Moncada, S. 1988. Vascular endothelial cells synthesize nitric oxide from L-arginine. *Nature* 333, pp. 664-666.
- Pan, Z. et al. 2018. Against NF- $\kappa$ B/thymic stromal lymphopoietin signaling pathway, catechin alleviates the inflammation in allergic rhinitis. *International Immunopharmacology* 61, pp. 241-248.
- Paone, S., Baxter, A., Hulett, M. and Poon, I. 2018. Endothelial cell apoptosis and the role of endothelial cell-derived extracellular vesicles in the progression of atherosclerosis. *Cellular and Molecular Life Sciences* 76, pp. 1093-1106.
- Patel, M. N. et al. 2017. Inflammasome priming in sterile inflammatory disease. *Trends in Molecular Medicine* 23(2), pp. 165-180.
- Peled, M. and Fisher, E. 2014. Dynamic aspects of macrophage polarization during atherosclerosis progression and regression. *Frontiers in Immunology* 5, p. 579.
- Peled, M., Nishi, H., Weinstock, A., Barrett, T., Zhou, F., Quezada, A. and Fisher, E. 2017. A wild-type mouse-based model for the regression of inflammation in atherosclerosis. *PLoS ONE* 12(3), p. e0173975.
- Peng, N. et al. 2014. An activator of mtor inhibits oxLDL-induced autophagy and apoptosis in vascular endothelial cells and restricts atherosclerosis in apolipoprotein e(-)/(-) mice. *Scientific Reports* 4, p. 5519.
- Peng, W. et al. 2019. Mitochondrial dysfunction in atherosclerosis. *DNA and Cell Biology* 38(7), pp. 597-606.
- Perrotta, P. et al. 2020. Partial inhibition of glycolysis reduces atherogenesis independent of intraplaque neovascularization in mice. *Arteriosclerosis, Thrombosis, and Vascular Biology* 40(5), pp. 1168-1181.

## References

- Pettersson, U., Walden, T., Carlsson, P.-O., Jansson, L. and Phillipson, M. 2012. Female mice are protected against high-fat diet induced metabolic syndrome and increase the regulatory T cell population in adipose tissue. *PLoS ONE* 7(9), p. e46057.
- Phan, B., Dayspring, T. and Toth, P. 2012. Ezetimibe therapy: mechanism of action and clinical update. *Vascular Health and Risk Management* 8, pp. 415-427.
- Phillips, M. C. 2014. Molecular mechanism of cellular cholesterol efflux. *Journal of Biological Chemistry* 289(35), pp. 24020-24029.
- Pidkovka, N. et al. 2007. Oxidized phospholipids induce phenotypic switching of vascular smooth muscle cells in vivo and in vitro. *Circulation Research* 101(8), pp. 792-801.
- Pinkosky, S. L. et al. 2013. AMP-activated protein kinase and ATP-citrate lyase are two distinct molecular targets for ETC-1002, a novel small molecule regulator of lipid and carbohydrate metabolism. *Journal of Lipid Research* 54(1), pp. 134-151.
- Pinkosky, S. L. et al. 2016. Liver-specific ATP-citrate lyase inhibition by bempedoic acid decreases LDL-C and attenuates atherosclerosis. *Nature Communications* 7, p. 13457. doi: 10.1038/ncomms13457
- Pober, J. S. and Cotran, R. S. 1990. Cytokines and endothelial cell biology. *Physiological Reviews* 70, pp. 427-451.
- Pober, J. S. and Sessa, W. C. 2007. Evolving functions of endothelial cells in inflammation. *Nature Reviews Immunology* 7(10), pp. 803-815.
- Potenza, M. A. et al. 2007. EGCG, a green tea polyphenol, improves endothelial function and insulin sensitivity, reduces blood pressure, and protects against myocardial I/R injury in SHR. *American Journal of Physiology-Endocrinology and Metabolism* 292(5), pp. E1378-E1387.
- Prasanth, M. L., Sivamaruthi, B. S., Chaiyasut, C. and Tencomnao, T. 2019. A review of the role of green tea (*Camellia sinensis*) in antiphotaging, stress resistance, neuroprotection, and autophagy. *Nutrients* 11(2), p. 474.
- Preiss-Landl, K., Zimmermann, R., Hammerle, G. and Zechner, R. 2002. Lipoprotein lipase: the regulation of tissue specific expression and its role in lipid and energy metabolism. *Current Opinion in Lipidology* 13, pp. 471-481.
- Prieto, M. A. V. et al. 2015. Catechin and quercetin attenuate adipose inflammation in fructose-fed rats and 3T3-L1 adipocytes. *Molecular Nutrition & Food Research* 59(4), pp. 622-633.
- Princen, H. et al. 1998. No effect of consumption of green and black tea on plasma lipid and antioxidant levels and on LDL oxidation in smokers. *Arteriosclerosis, Thrombosis, and Vascular Biology* 18(5), pp. 833-841.

## References

- Puri, R. et al. 2013. C-reactive protein, but not low-density lipoprotein cholesterol levels, associate with coronary atheroma regression and cardiovascular events after maximally intensive statin therapy. *Circulation* 128(22), pp. 2395-2403.
- Quintero, M., Colombo, S., Godfrey, A. and Moncada, S. 2006. Mitochondria as signaling organelles in the vascular endothelium. *Proceedings of the National Academy of Sciences of the United States of America* 103, pp. 5379-5384.
- R Core Team. 2017. R: A language and environment for statistical computing. Vienna, Austria.
- Rafiei, H., Omidian, K. and Bandy, B. 2019. Dietary polyphenols protect against oleic acid-induced steatosis in an in vitro model of NAFLD by modulating lipid metabolism and improving mitochondrial function. *Nutrients* 11, p. 541.
- Rajasingh, J. et al. 2006. IL-10-induced TNF- $\alpha$  mRNA destabilization is mediated via IL-10 suppression of p38 MAP kinase activation and inhibition of HuR expression. *The FASEB Journal* 20, pp. 2112-2114.
- Ramalho, L., da Jornada, M., Antunes, L. and Hidalgo, M. 2017. Metabolic disturbances due to a high-fat diet in a non-insulin resistant animal model. *Nutrition & Diabetes* 7, p. e245.
- Ramji, D. P. and Davies, T. S. 2015. Cytokines in atherosclerosis: Key players in all stages of disease and promising therapeutic targets. *Cytokine Growth Factor Reviews* 26, pp. 673-685.
- Rassaf, T. et al. 2016. Vasculoprotective effects of dietary cocoa flavanols in patients on hemodialysis: a double-blind, randomized, placebo-controlled trial. *Clinical Journal of the American Society of Nephrology* 11(1), pp. 108-118.
- Rastogi, S., Rizwani, W., Joshi, B., Kunigal, S. and Chellappan, S. 2011. TNF- $\alpha$  response of vascular endothelial and vascular smooth muscle cells involve differential utilization of ASK1 kinase and p73. *Cell Death & Differentiation* 19, pp. 274-283.
- Ray, K. K. et al. 2020. Two phase 3 trials of inclisiran in patients with elevated LDL cholesterol. *New England Journal of Medicine* 382(16), pp. 1507-1519.
- Rayner, K. J. et al. 2011. Antagonism of miR-33 in mice promotes reverse cholesterol transport and regression of atherosclerosis. *Journal of Clinical Investigation* 121(7), pp. 2921-2931.
- Rees, A., Dodd, G. and Spencer, J. 2018. The effects of flavonoids on cardiovascular health: a review of human intervention trials and implications for cerebrovascular function. *Nutrients* 10(12), p. 1852.
- Reinhold, J., Uryga, A., Murphy, M. and Bennett, M. 2017. Mitochondrial function in human atherosclerotic plaques and effects of atherogenic lipids on vascular smooth muscle cells. *The Lancet* 389, p. S82.

## References

- Rekhter, M. et al. 2000. Hypercholesterolemia causes mechanical weakening of rabbit atheroma: local collagen loss as a prerequisite of plaque rupture. *Circulation Research* 86, pp. 101-108.
- Rensen, S., Doevendans, P. and van Eys, G. 2007. Regulation and characteristics of vascular smooth muscle cell phenotypic diversity. *Netherlands Heart Journal* 15, pp. 100-108.
- Richardson, A. and Schadt, E. 2014. The role of macromolecular damage in aging and age-related disease. *Journal of Gerontology* 69, pp. S28-S32.
- Ridker, P. 2017. How common is residual inflammatory risk? *Circulation Research* 120, pp. 617-619.
- Ridker, P. M. et al. 2005. C-reactive protein levels and outcomes after statin therapy. *New England Journal of Medicine* 352(1), pp. 20-28.
- Ridker, P. M. et al. 2019. Low-dose methotrexate for the prevention of atherosclerotic events. *New England Journal of Medicine* 380(8), pp. 752-762.
- Ridker, P. M. et al. 2017. Antiinflammatory therapy with canakinumab for atherosclerotic disease. *New England Journal of Medicine* 377(12), pp. 1119-1131.
- Ridker, P. M. et al. 2018. Modulation of the interleukin-6 signaling pathway and incidence rates of atherosclerotic events and all-cause mortality: analyses from the Canakinumab Anti-Inflammatory Thrombosis Outcomes Study (CANTOS). *European Heart Journal* 39(38), pp. 3499-3507.
- Rippe, C. et al. 2017. Hypertension reduces soluble guanylyl cyclase expression in the mouse aorta via the Notch signaling pathway. *Scientific Reports* 7, p. 1334.
- Ritchey, J. G. and Waterhouse, A. L. 1999. A standard red wine: monomeric phenolic analysis of commercial cabernet sauvignon wines. *American Journal of Enology and Viticulture* 50, pp. 91-100.
- Robbins, C. S. et al. 2013. Local proliferation dominates lesional macrophage accumulation in atherosclerosis. *Nature Medicine* 19(9), pp. 1166-1172.
- Romero-Prado, M. M., Curiel-Beltran, J., Miramontes-Espino, M. V., Cardona-Munoz, E. G., Rios-Arellano, A. and Balam-Salazar, L.-B. 2015. Dietary flavonoids added to pharmacological antihypertensive therapy are effective in improving blood pressure. *Basic and Clinical Pharmacology and Toxicology* 117(1), pp. 57-64.
- Ross, R. 1999. Atherosclerosis: an inflammatory disease. *New England Journal of Medicine* 340, pp. 115-126.
- Rostami, A. et al. 2015. High-cocoa polyphenol-rich chocolate improves blood pressure in patients with diabetes and hypertension. *ARYA Atherosclerosis* 11(1), pp. 21-29.

## References

- Rothwell, N. and Stock, M. 1984. The development of obesity in animals - the role of dietary factors. *The Journal of Clinical Endocrinology & Metabolism* 13, pp. 437-449.
- Ruan, Z.-H., Xu, Z.-X., Zhou, X.-Y., Zhang, X. and Shang, L. 2019. Implications of necroptosis for cardiovascular diseases. *Current Medical Science* 39(4), pp. 513-522.
- Ryoo, S., Bhunia, A., Chang, F., Shoukas, A., Berkowitz, D. and Romer, L. 2011. OxLDL-dependent activation of arginase II is dependent on the LOX-1 receptor and downstream RhoA signaling. *Atherosclerosis* 214(2), pp. 279-287.
- Sage, A., Tsiantoulas, D., Binder, C. and Mallat, Z. 2019. The role of B cells in atherosclerosis. *Nature Reviews Cardiology* 16, pp. 180-196.
- Salonen, J. et al. 2000. Antioxidant Supplementation in Atherosclerosis Prevention (ASAP) study: a randomized trial of the effect of vitamins E and C on 3-year progression of carotid atherosclerosis. *Journal of Internal Medicine* 248(5), pp. 377-386.
- Sampson, U., Fazio, S. and Linton, M. 2012. Residual cardiovascular risk despite optimal LDL cholesterol reduction with statins: the evidence, etiology, and therapeutic challenges. *Current Atherosclerosis Reports* 14(1), pp. 1-10.
- Sanda, G., Belur, A., Teague, H. and Nehta, N. 2017. Emerging associations between neutrophils, atherosclerosis, and psoriasis. *Current Atherosclerosis Reports* 19, p. 53.
- Sandoo, A., van Zanten, J. J. C. S. V., Metsios, G. S., Carroll, D. and Kitas, G. D. 2010. The endothelium and its role in regulating vascular tone. *The Open Cardiovascular Medicine Journal* 4, pp. 302-312.
- Sang, S., Lambert, J., Ho, C.-T. and Yang, C. 2011. The chemistry and biotransformation of tea constituents. *Pharmacological Research* 64(2), pp. 87-99.
- Sangle, G., Chowdhury, S., Xie, X., Stelmack, G., Halayko, A. and Shen, G. 2010. Impairment of mitochondrial respiratory chain activity in aortic endothelial cells induced by glycated low-density lipoprotein. *Free Radical Biology & Medicine* 48(6), pp. 781-790.
- Sano, H. et al. 2001. Functional blockade of platelet-derived growth factor receptor-beta but not of receptor-alpha prevents vascular smooth muscle cell accumulation in fibrous cap lesions in apolipoprotein E-deficient mice. *Circulation* 103(24), pp. 2955-2960.
- Sansbury, B., Jones, S., Riggs, D., Darley-Usmar, V. and Hill, B. 2011. Bioenergetic function in cardiovascular cells: the importance of the reserve capacity and its biological regulation. *Chemico-Biological Interactions* 191, pp. 288-295.
- Sansone, R. et al. 2015. Cocoa flavanol intake improves endothelial function and Framingham Risk Score in healthy men and women: a randomised, controlled, double-masked trial: the Flaviola Health Study. *British Journal of Nutrition* 114(8), pp. 1246-1255.

## References

- Santos, L., Stolfo, A., Calloni, C. and Salvador, M. 2016. Catechin and epicatechin reduce mitochondrial dysfunction and oxidative stress induced by amiodarone in human lung fibroblasts. *Journal of Arrhythmia* 33(3), pp. 220-225.
- Sawamura, T. et al. 1997. An endothelial receptor for oxidized low-density lipoprotein. *Nature* 386, pp. 73-77.
- Schafer, S. and Zerneck, A. 2020. CD8<sup>+</sup> T cells in atherosclerosis. *Cells* 10(1), p. 37.
- Scheffler, I. 2001. Mitochondria make a come back. *Advanced Drug Delivery Reviews* 49, pp. 3-26.
- Scherer, D. J., Nelson, A. J., Psaltis, P. J. and Nicholls, S. J. 2017. Targeting low-density lipoprotein cholesterol with PCSK9 inhibition. *International Medicine Journal* 47(8), pp. 856-865.
- Schmidt-Arras, D. and Rose-John, S. 2016. IL-6 pathway in the liver: from physiopathology to therapy. *Journal of Hepatology* 64(6), pp. 1403-1415.
- Schrauwen, P. and Westerterp, K. 2000. The role of high-fat diets and physical activity in the regulation of body weight. *British Journal of Nutrition* 84, pp. 417-427.
- Schulze-Osthoff, K., Bakker, A., Vanhaesebroeck, B., Beyart, R., Jacob, W. and Fiers, W. 1992. Cytotoxic activity of tumor necrosis factor is mediated by early damage of mitochondrial functions Evidence for the involvement of mitochondrial radical generation. *Journal of Biological Chemistry* 267(8), pp. 5317-5323.
- Schwartz, S., de Blois, D. and O'Brien, E. 1995. The Intima. *Circulation Research* 77(3), pp. 445-465.
- Schwartz, S., Virmani, R. and Rosenfeld, M. E. 2000. The good smooth muscle cells in atherosclerosis. *Current Atherosclerosis Reports* 2, pp. 422-429.
- Sehested, T. S. G. et al. 2019. Cost-effectiveness of Canakinumab for prevention of recurrent cardiovascular events. *JAMA Cardiology* 4(2), pp. 128-135.
- Seibold, S., Schürle, D., Heinloth, A., Wolf, G., Wagner, M. and Galle, J. 2004. Oxidized LDL induces proliferation and hypertrophy in human umbilical vein endothelial cells via regulation of p27Kip1 expression: role of RhoA. *American Society of Nephrology* 15(12), pp. 3026-3034.
- Shah, P. et al. 1995. Human monocyte-derived macrophages induce collagen breakdown in fibrous caps of atherosclerotic plaques: potential role of matrix-degrading metalloproteinases and implications for plaque rupture. *Circulation* 92, pp. 1565-1569.
- Sheng, D. et al. 2019. BabaoDan attenuates high-fat diet-induced non-alcoholic fatty liver disease via activation of AMPK signaling. *Cell & Bioscience* 9, p. 77.

## References

- Shimada, K. et al. 2012. Oxidized mitochondrial DNA activates the NLRP3 inflammasome during apoptosis. *Immunity* 36, pp. 401-414.
- Shirai, T., Hilhorst, M., Harrison, D. G., Goronzy, J. and Weyand, C. 2015. Macrophages in vascular inflammation - From atherosclerosis to vasculitis. *Autoimmunity* 48(3), pp. 139-151.
- Siasos, G. et al. 2018. Mitochondria and cardiovascular disease-from pathophysiology to treatment. *Annals of Translational Medicine* 6, p. 256.
- Silva, C. et al. 2019. Selective pro-apoptotic and antimigratory effects of polyphenol complex catechin:lysine 1:2 in breast, pancreatic and colorectal cancer cell lines. *European Journal of Pharmacology* 859, p. 172533.
- Silveira, A. et al. 2015. Plasma IL-5 concentration and subclinical carotid atherosclerosis. *Atherosclerosis* 239(1), pp. 125-130.
- Sitia, S. et al. 2010. From endothelial dysfunction to atherosclerosis. *Autoimmunity Reviews* 9(12), pp. 830-834.
- Smart, N., Marshall, B., Daley, M., Boulos, E., Windus, J., Baker, N. and Kwok, N. 2011. Low-fat diets for acquired hypercholesterolaemia. *The Cochrane Database of Systematic Reviews* 2011(2), p. CD007957.
- Soehnlein, O. et al. 2013. Distinct functions of chemokine receptor axes in the atherogenic mobilization and recruitment of classical monocytes. *EMBO Molecular Medicine* 5, pp. 471-481.
- Solanki, S., Dube, P. R., Birnbaumer, L. and Vazquez, G. 2016. Reduced necrosis and content of apoptotic M1 macrophages in advanced atherosclerotic plaques of mice with macrophage-specific loss of Trpc3. *Scientific Reports* 7, p. 42526.
- Spann, N. J. et al. 2012. Regulated accumulation of desmosterol integrates macrophage lipid metabolism and inflammatory responses. *Cell* 151(1), pp. 138-152.
- Sparwel, J. et al. 2009. Differential effects of red and white wines on inhibition of the platelet-derived growth factor receptor: impact of the mash fermentation. *Cardiovascular Research* 81, pp. 758-770.
- Stanford, K. et al. 2013. Brown adipose tissue regulates glucose homeostasis and insulin sensitivity. *Journal of Clinical Investigation* 123(1), pp. 215-223.
- Stephens, N., Parsons, A., Schofield, P., Kelly, F., Cheeseman, K. and Mitchinson, M. 1996. Randomised controlled trial of vitamin E in patients with coronary disease: Cambridge Heart Antioxidant Study (CHAOS). *Lancet* 347(9004), pp. 781-786.
- Stewart, C. R. et al. 2010. CD36 ligands promote sterile inflammation through assembly of a Toll-like receptor 4 and 6 heterodimer. *Nature Immunology* 11(2), pp. 155-161.

## References

- Stienstra, R., Netea-Maier, R., Riksen, N., Joosten, L. and Netea, M. 2017. Specific and complex reprogramming of cellular metabolism in myeloid cells during innate immune responses. *Cell Metabolism* 26(1), pp. 142-156.
- Stoekenbroek, R. M., Kallend, D., Wijngaard, P. L. and Kastelein, J. J. 2018. Inclisiran for the treatment of cardiovascular disease: the ORION clinical development program. *Future Cardiology* 14(6), pp. 433-442.
- Sugimoto, K. et al. 2009. LOX-1-MT1-MMP axis is crucial for RhoA and Rac1 activation induced by oxidized low-density lipoprotein in endothelial cells. *Cardiovascular Research* 84(1), pp. 127-136.
- Sun, C., Wu, M. and Yuan, S. 2011. Nonmuscle myosin light-chain kinase deficiency attenuates atherosclerosis in apolipoprotein e-deficient mice via reduced endothelial barrier dysfunction and monocyte migration. *Circulation* 124, pp. 48-57.
- Sunderkötter, C., Nikolic, T., Dillon, M., Van Rooijen, N., Stehling, M., Drevets, D. and Leenen, P. 2004. Subpopulations of mouse blood monocytes differ in maturation stage and inflammatory response. *Journal of Immunology* 172, pp. 4410-4417.
- Sung, H., Nah, J., Chun, S., Park, H., Yang, S. and Min, W. 2000. In vivo antioxidant effect of green tea. *European Journal of Clinical Nutrition* 54, pp. 527-529.
- Suzuki-Sugihara, N. et al. 2016. Green tea catechins prevent low-density lipoprotein oxidation via their accumulation in low-density lipoprotein particles in humans. *Nutrition Research* 36(1), pp. 16-23.
- Suzuki, T. et al. 2013. Green tea extract containing a highly absorbent catechin prevents diet-induced lipid metabolism disorder. *Scientific Reports* 3, p. 2749.
- Swanson, K., Deng, M. and Ting, J. P.-Y. 2019. The NLRP3 inflammasome: molecular activation and regulation to therapeutics. *Nature Reviews Immunology* 19, pp. 477-489.
- Swirski, F., Libby, P., Aikawa, E., Alcaide, P., Luscinskas, F., Weissleder, R. and Pittet, M. 2007. Ly-6Chi monocytes dominate hypercholesterolemia-associated monocytosis and give rise to macrophages in atheromata. *Journal of Clinical Investigation* 117, pp. 195-205.
- Swirski, F., Pittet, M., Kircher, M., Aikawa, E., Jaffer, F., Libby, P. and Weissleder, R. 2006. Monocyte accumulation in mouse atherogenesis is progressive and proportional to extent of disease. *Proceedings of the National Academy of Sciences of the United States of America* 103, pp. 10340-10345.
- Szpak, D., Izem, L., Verbovetskiy, D., Soloviev, D., Yakubenki, V. and Pluskota, E. 2018.  $\alpha$ M $\beta$ 2 is antiatherogenic in female but not male mice. *The Journal of Immunology* 200(7), pp. 2426-2438.

## References

- Tabassum, H., Parvez, S., Rehman, H., Banerjee, B. and Raisuddin, S. 2007. Catechin as an antioxidant in liver mitochondrial toxicity: Inhibition of tamoxifen-induced protein oxidation and lipid peroxidation. *Journal of Biochemical and Molecular Toxicology* 21(3), pp. 110-117.
- Tacke, F. et al. 2007. Monocyte subsets differentially employ CCR2, CCR5, and CX3CR1 to accumulate within atherosclerotic plaques. *Journal of Clinical Investigation* 117, pp. 185-194.
- Takahashi, M., Ikemoto, S. and Ezaki, O. 1999. Effect of the fat/carbohydrate ratio in the diet on obesity and oral glucose tolerance in C57BL/6J mice. *Journal of Nutritional Science and Vitaminology* 45, pp. 583-593.
- Takano, F., Tanaka, T., Aoi, J., Yahagi, N. and Fushiya, S. 2004. Protective effect of (+)-catechin against 5-fluorouracil-induced myelosuppression in mice. *Toxicology* 201(1-3), pp. 133-142.
- Tall, A. R. and Yven-Charvet, L. 2015. Cholesterol, inflammation and innate immunity. *Nature Reviews Immunology* 15(2), pp. 104-116.
- Tanizawa, S., Ueda, M., van der Loos, C., van der Wal, A. and Becker, A. 1996. Expression of platelet-derived growth factor B chain and beta receptor in human coronary arteries after percutaneous transluminal coronary angioplasty: an immunohistochemical study. *Heart* 75, pp. 549-556.
- Tardif, J.-C. et al. 2019. Efficacy and safety of low-dose colchicine after myocardial infarction. *New England Journal of Medicine* 381(26), pp. 2497-2505.
- Tedgui, A. and Mallat, Z. 2006. Cytokines in atherosclerosis: pathogenic and regulatory pathways. *Physiological Reviews* 86(2), pp. 515-581.
- Tinahones, F. J., Rubio, M. A., Garrido-Sanchez, L., Ruiz, C., Gordillo, E., Cabrerizo, L. and Cardona, F. 2008. Green tea reduces LDL oxidability and improves vascular function. *Journal of the American College of Nutrition* 27(2), pp. 209-213.
- Tomkin, G. H. and Owens, D. 2012. The chylomicron: relationship to atherosclerosis. *International Journal of Vascular Medicine* 2012, p. 784536.
- Tousoulis, D., Oikonomou, E., Economou, E. K., Crea, F. and Kaski, J. 2016. Inflammatory cytokines in atherosclerosis: current therapeutic approaches. *European Heart Journal* 37(22), pp. 1723-1732.
- Trautwein, E., Du, Y., Meynen, E., Yan, X., Wen, Y., Wang, H. and Molhuizen, O. 2009. Purified black tea theaflavins and theaflavins/catechin supplements did not affect serum lipids in healthy individuals with mildly to moderately elevated cholesterol concentrations. *European Journal of Nutrition* 49, pp. 27-35.
- Tresserra-Rimbau, A. et al. 2014. Inverse association between habitual polyphenol intake and incidence of cardiovascular events in the PREDIMED study. *Nutrition, Metabolism and Cardiovascular Diseases* 24, pp. 639-647.

## References

- Trifunovic, A. et al. 2004. Premature ageing in mice expressing defective mitochondrial DNA polymerase. *Nature* 429(6990), pp. 417-423.
- Trigatti, B., Rigotti, A. and Braun, A. 2000a. Cellular and physiological roles of SR-B1, a lipoprotein receptor which mediates selective lipid uptake. *Biochimica et Biophysica Acta* 1529(1-3), pp. 276-286.
- Trigatti, B. L., Rigotti, A. and Krieger, M. 2000b. The role of the high-density lipoprotein receptor SR-B1 in cholesterol metabolism. *Current Opinion in Lipidology* 11(2), pp. 123-131.
- Tschopp, J. and Schroder, K. 2010. NLRP3 inflammasome activation: the convergence of multiple signalling pathways on ROS production? *Nature Reviews Immunology* 10(3), pp. 210-215.
- Tsuchiya, K. et al. 2019. Macrophage mannose receptor CD206 predicts prognosis in community-acquired pneumonia. *Scientific Reports* 9, p. 18750.
- Tsujita, K. et al. 2015. Impact of dual lipid-lowering strategy with ezetimibe and atorvastatin on coronary plaque regression in patients with percutaneous coronary intervention. *Journal of the American College of Cardiology* 66(5), pp. 495-507.
- Upadhyaya, S., Mooteri, S., Peckham, N. and Pai, R. 2004. Atherogenic effect of interleukin-2 and antiatherogenic effect of interleukin-2 antibody in apo-E-deficient mice. *Angiology* 55, pp. 289-294.
- van den Berg, S. M. et al. 2016. Diet-induced obesity in mice diminishes hematopoietic stem and progenitor cells in the bone marrow. *The FASEB Journal* 30(5), pp. 1779-1788.
- Van den Bossche, J. et al. 2016. Mitochondrial dysfunction prevents repolarization of inflammatory macrophages. *Cell Reports* 17, pp. 684-696.
- Van den Bossche, J., O'Neill, L. and Menon, D. 2017. Macrophage immunometabolism: where are we (going)? *Trends in Immunology* 38, pp. 395-406.
- van der Valk, F. et al. 2017. Increased haematopoietic activity in patients with atherosclerosis. *European Heart Journal* 38, pp. 425-432.
- Van Dyken, S. and Locksley, R. 2013. Interleukin-4- and interleukin-13-mediated alternatively activated macrophages: roles in homeostasis and disease. *Annual Review of Immunology* 31, pp. 317-343.
- van het Hof, K., de Boer, H., Wiseman, S., Lien, N., Weststrate, J. and Tijburg, L. 1997. Consumption of green or black tea does not increase resistance of low-density lipoprotein to oxidation in humans. *The American Journal of Clinical Nutrition* 66(5), pp. 1125-1132.

## References

- van het Hof, K., Wiseman, S., Yang, C. and Tijburg, L. 1999. Plasma and lipoprotein levels of tea catechins following repeated tea consumption. *Proceedings of the Society for Experimental Biology and Medicine* 220(4), pp. 203-209.
- Vanderlaan, P. A., Reardon, C. A. and Getz, G. S. 2003. Site specificity of atherosclerosis. *Arteriosclerosis, Thrombosis, and Vascular Biology* 24(1), pp. 12-22.
- Vanhie, J., Ngu, M. and De Lisio, M. 2020. Recent advances in understanding the role of high fat diets and their components on hematopoiesis and the hematopoietic stem cell niche. *Current Opinion in Food Science* 34, pp. 30-37.
- Velazquez, K. et al. 2019. Prolonged high-fat-diet feeding promotes non-alcoholic fatty liver disease and alters gut microbiota in mice. *World Journal of Hepatology* 11(8), pp. 619-637.
- Virani, S. S. et al. 2021. Heart Disease and Stroke Statistics - 2021 Update. *Circulation* 143(8), pp. e254-e743.
- Visse, R. and Nagase, H. 2003. Matrix metalloproteinases and tissue inhibitors of metalloproteinases. *Circulation Research* 92(8), pp. 827-839.
- Vyssokikh, M. et al. 2020. Mild depolarization of the inner mitochondrial membrane is a crucial components of an anti-aging program. *Proceedings of the National Academy of Sciences of the United States of America* 117(12), pp. 6491-6501.
- Wang-Polagruto, J. F. et al. 2006. Chronic consumption of flavanol-rich cocoa improves endothelial function and decreases vascular cell adhesion molecule in hypercholesterolemic postmenopausal women. *Journal of Cardiovascular Pharmacology* 47, pp. S177-S186.
- Wang, J., Toan, S. and Zhou, H. 2020. New insights into the role of mitochondria in cardiac microvascular ischemia/reperfusion injury. *Angiogenesis* 23, pp. 299-314.
- Wang, Q. et al. 2018. Green tea polyphenol epigallocatechin-3-gallate increases atherosclerotic plaque stability in apolipoprotein E-deficient mice fed a high-fat diet. *Kardiologia Polska (Polish Heart Journal)* 76(8), pp. 1263-1270.
- Wang, T. et al. 2011. Docosahexaenoic acid attenuates VCAM-1 expression and NF- $\kappa$ B activation in TNF- $\alpha$ -treated human aortic endothelial cells. *The Journal of Nutritional Biochemistry* 22(2), pp. 187-194.
- Wang, Y., Wang, G., Rabinovitch, P. and Tabas, I. 2014. Macrophage mitochondrial oxidative stress promotes atherosclerosis and nf-kb-mediated inflammation in macropahges. *Circulation Research* 114, pp. 421-433.
- Wang, Y., Wang, W., Wang, N., Tall, A. and Tabas, I. 2017. Mitochondrial oxidative stress promotes atherosclerosis and neutrophil extracellular traps in aged mice. *Arteriosclerosis, Thrombosis, and Vascular Biology* 37(8), pp. e99-e107.

## References

- Warwick, Z. and Sciffman, S. 1992. Role of dietary fat in calorie intake and weight gain. *Neuroscience & Behavioural Reviews* 16, pp. 585-596.
- Weber, C. and Noels, H. 2011. Atherosclerosis: current pathogenesis and therapeutic options. *Nature Medicine* 17, pp. 1410-1422.
- Westlake, S. L., Colebatch, A. N., Baird, J. and et, a. I. 2010. The effect of methotrexate on cardiovascular disease in patients with rheumatoid arthritis: a systematic literature review. *Rheumatology* 49(2), pp. 295-307.
- Winkels, H. and Ley, K. 2018. Natural killer cells at ease-Atherosclerosis is not affected by genetic depletion or hyperactivation of natural killer cells. *Circulation Research* 122(1), pp. 6-7.
- Witztum, J. and Lichtman, A. 2014. The influence of innate and adaptive immune responses on atherosclerosis. *Annual Review of Pathology: Mechanisms of Disease* 9, pp. 73-102.
- Wojcik-Cichy, K., Koslinska-Berkan, E. and Piekarska, A. 2018. The influence of NAFLD on the risk of atherosclerosis and cardiovascular diseases. *Journal of Clinical and Experimental Hepatology* 4(1), pp. 1-6.
- Wolfram, S., Raederstroff, D., Wang, Y., Teixeira, S., Elste, V. and Weber, P. 2005. TEAVIGO™ (epigallocatechin gallate) supplementation prevents obesity in rodents by reducing adipose tissue mass. *Annals of Nutrition and Metabolism* 49, pp. 54-63.
- Wolfs, I. M. J., Donners, M. M. P. C. and de Winther, M. P. J. 2011. Differentiation factors and cytokines in the atherosclerotic plaque micro-environment as a trigger for macrophage polarisation. *Journal of Thrombosis and Haemostasis* 106(5), pp. 763-771.
- Wongmekiat, O., Peerapanyasut, W. and Kobroob, A. 2018. Catechin supplementation prevents kidney damage in rats repeatedly exposed to cadmium through mitochondrial protection. *Naunyn-Schmiedeberg's Archives of Pharmacology* 391, pp. 385-394.
- Wraith, K. S., Magwenzi, S., Aburima, A., Wen, Y., Leake, D. S. and Naseem, K. M. 2013. Oxidised low-density lipoproteins induce rapid platelet activation and shape change through tyrosine kinase and Tho kinase-signaling pathways. *Blood* 122, pp. 580-589.
- Wu, H. et al. 2010. CD11c expression in adipose tissue and blood and its role in diet-induced obesity. *Arteriosclerosis, Thrombosis, and Vascular Biology* 30, pp. 186-192.
- Xanthoulea, S., Thelen, M., Pottgens, C. and et, a. I. 2011. Absence of p55 TNF receptor reduces atherosclerosis, but has no major effect on angiotensin II induced aneurysms in LDL receptor deficient mice. *PLoS* 4(7), p. e1113.

## References

- Xiao, N. et al. 2009. Tumor necrosis factor- $\alpha$  deficiency retards early fatty-streak lesion by influencing the expression of inflammatory factors in apoE-null mice. *Molecular Genetics and Metabolism* 96(4), pp. 239-244.
- Xiao, Y. et al. 2020. High-fat diet selectively decreases bone marrow lin<sup>-</sup>/CD117<sup>+</sup> cell population in aging mice through increased ROS production. *Journal of Tissue Engineering and Regenerative Medicine* 14(6), pp. 884-892.
- Xie, X., Chowdhury, S., Sangle, G. and Shen, G. 2010. Impact of diabetes-associated lipoproteins on oxygen consumption and mitochondrial enzymes in porcine aortic endothelial cells. *Acta Biochimica Polonica* 57(4), pp. 393-398.
- Xu, R., Yokoyama, W. H., Irving, D., Rein, D., Walzem, R. L. and German, J. B. 1998. Effect of dietary catechin and vitamin E on aortic fatty streak accumulation in hypercholesterolemic hamsters. *Atherosclerosis* 137(1), pp. 29-36.
- Xu, S. et al. 2010. Evaluation of foam cell formation in cultured macrophages: an improved method with Oil Red O staining and Dil-oxLDL uptake.
- Xu, X. et al. 1999. Oxidized low-density lipoprotein regulates matrix metalloproteinase-9 and its tissue inhibitor in human monocyte-derived macrophages. *Circulation* 99, pp. 993-998.
- Yakes, F. and Van Houten, B. 1997. Mitochondrial DNA damage is more extensive and persists longer than nuclear DNA damage in human cells following oxidative stress. *Proceedings of the National Academy of Sciences of the United States of America* 94(2), pp. 514-519.
- Yan, J., Zhao, Y. and Zhao, B. 2013. Green tea catechins prevent obesity through modulation of peroxisome proliferator-activated receptors. *Science China Life Sciences* 56(9), pp. 804-810.
- Yang, H., Youm, Y.-H., Vandanmagsar, B., Rood, J., Kumar, K., Butler, A. and Dixit, V. 2009. Obesity accelerates thymic aging. *Blood* 114(18), pp. 3803-3812.
- Yang, Q. et al. 2018. PRKAA1/AMPK $\alpha$ 1-driven glycolysis in endothelial cells exposed to disturbed flow protects against atherosclerosis. *Nature Communications* 9, p. 4667.
- Yona, S. et al. 2013. Fate mapping reveals origins and dynamics of monocytes and tissue macrophages under homeostasis. *Immunity* 38, pp. 79-91.
- Yoneshiro, T. et al. 2017. Tea catechin and caffeine activate brown adipose tissue and increase cold-induced thermogenic capacity in humans. *The American Journal of Clinical Nutrition* 105(4), pp. 873-881.
- Yoshida, H. and Kisugi, R. 2010. Mechanisms of LDL oxidation. *Clinica Chimica Acta* 411, pp. 1875-1882.

## References

- Young, J. et al. 2002. Green tea extract only affects markers of oxidative status postprandially: lasting antioxidant effect of flavonoid-free diet. *British Journal of Nutrition* 87(4), pp. 343-355.
- Yousefian, M., Shakour, N., Hosseinzadeh, H., Hayes, A., Hadizadeh, F. and Karimi, G. 2019. The natural phenolic compounds as modulators of NADPH oxidases in hypertension. *Phytomedicine* 55, pp. 200-213.
- Yu, E. and Bennett, M. 2014. Mitochondrial DNA damage and atherosclerosis. *Trends in Endocrinology & Metabolism* 25, pp. 481-487.
- Yu, E. et al. 2013. Mitochondrial DNA damage can promote atherosclerosis independently of reactive oxygen species through effects on smooth muscle cells and monocytes and correlates with higher-risk plaques in humans. *Circulation* 128, pp. 702-712.
- Yu, E. P. K. et al. 2017. Mitochondrial respiration is reduced in atherosclerosis, promoting necrotic core formation and reducing relative fibrous cap thickness. *Arteriosclerosis, Thrombosis, and Vascular Biology* 37(12), pp. 2322-2332.
- Yu, H. et al. 2011a. Bone marrow-derived smooth muscle-like cells are infrequent in advanced primary atherosclerotic plaques but promote atherosclerosis. *Arteriosclerosis, Thrombosis, and Vascular Biology* 31(6), pp. 1291-1299.
- Yu, S., Wong, S., Lau, C., Huang, Y. and Yu, C. 2011b. Oxidized LDL at low concentration promotes in-vitro angiogenesis and activates nitric oxide synthase through PI3K/Akt/eNOS pathway in human coronary artery endothelial cells. *Biochemical and Biophysical Research Communications* 407(1), pp. 44-48.
- Yu, S., Zhang, L., Liu, C., Yang, J., Zhang, J. and Huang, L. 2019. PACS2 is required for ox-LDL-induced endothelial cell apoptosis by regulating mitochondria-associated ER membrane formation and mitochondrial Ca<sup>2+</sup> elevation. *Experimental Cell Research* 379(2), pp. 191-202.
- Yvan-Charvet, L. et al. 2010a. Cholesterol efflux potential and antiinflammatory properties of high-density lipoprotein after treatment with niacin or anacetrapib. *Arteriosclerosis, Thrombosis, and Vascular Biology* 30(7), pp. 1430-1438.
- Yvan-Charvet, L. et al. 2010b. ATP-binding cassette transporters and HDL suppress hematopoietic stem cell proliferation. *Science* 328(5986), pp. 1689-1693.
- Zernecke, A. and Weber, C. 2014. Chemokines in atherosclerosis: proceedings resumed. *Arteriosclerosis, Thrombosis, and Vascular Biology* 34, pp. 742-750.
- Zhang, C. et al. 2017a. oxLDL induces endothelial cell proliferation via Rho/ROCK/Akt/p27kip1 signaling: opposite effects of oxLDL and cholesterol loading. *American Journal of Physiology-Cell Physiology* 313(3), pp. C340-C351.
- Zhang, D. et al. 2019a. Metabolic regulation of gene expression by histone lactylation. *Nature* 574, pp. 575-580.

## References

- Zhang, H. et al. 2009. Role of TNF- $\alpha$  in vascular dysfunction. *Clinical Science* 116, pp. 219-230.
- Zhang, T. et al. 2017b. (+)-Catechin prevents methylglyoxal-induced mitochondrial dysfunction and apoptosis in EA.hy926 cells. *Archives of Physiology and Biochemistry* 123(2), pp. 121-127.
- Zhang, X., Li, X., Fang, H., Guo, F., Li, F., Chen, A. and Huang, S. 2019b. Flavonoids as inducers of white adipose tissue browning and thermogenesis: signalling pathways and molecular triggers. *Nutrition & Metabolism* 16, p. 47.
- Zhang, Y., Gao, S., Xia, J. and Liu, F. 2018. Hematopoietic hierarchy - an updated roadmap. *Trends in Cell Biology* 28(12), pp. 976-986.
- Zhang, Y., Wang, X., Vales, C., Lee, F., Lee, H., Lusis, A. and Edwards, P. 2006. FXR deficiency causes reduced atherosclerosis in *Ldlr*<sup>-/-</sup> mice. *Arteriosclerosis, Thrombosis, and Vascular Biology* 26, pp. 2316-2321.
- Zhao, R.-Z., Jiang, S., Zhang, L. and Yu, Z.-B. 2019. Mitochondrial electron transport chain, ROS generation and uncoupling (Review). *International Journal of Molecular Medicine* 44(1), pp. 3-15.
- Zhao, W. et al. 2015. Macrophage-specific overexpression of interleukin-5 attenuates atherosclerosis in LDL receptor-deficient mice. *Gene Therapy* 22, pp. 645-652.
- Zheng, J. and Lu, C. 2020. Oxidized LDL causes endothelial apoptosis by inhibiting mitochondrial fusion and mitochondria autophagy. *Frontiers in Cell and Development Biology* 8, p. 600950. doi: <https://doi.org/10.3389/fcell.2020.600950>
- Zhou, H., Shi, C., Hu, S., Zhu, H., Ren, J. and Chen, Y. 2018. B1 is associated with microvascular protection in cardiac ischemia reperfusion injury via repressing Syk-Nox2-Drp1-mitochondrial fission pathways. *Angiogenesis* 21, pp. 599-615.
- Zhou, Z. et al. 2011. Lipoprotein-derived lysophosphatidic acid promotes atherosclerosis by releasing CXCL1 from the endothelium. *Cell Metabolism* 13, pp. 592-600.
- Zhukova, N., Novgorodtseva, T. and Denisenko, Y. 2014. Effect of the prolonged high-fat diet on the fatty acid metabolism in rat blood and liver. *Lipids in Health and Disease* 13, p. 49. doi: <https://doi.org/10.1186/1476-511X-13-49>
- Zimmer, S. et al. 2016. Cyclodextrin promotes atherosclerosis regression via macrophage reprogramming. *Science Translational Medicine* 8(333), p. 333ra350.
- Zmijewski, J., Moellering, D., Le Goffe, C., Landar, A., Ramachandran, A. and Darley-Usmar, V. 2005. Oxidized LDL induces mitochondrially associated reactive oxygen/nitrogen species formation in endothelial cells. *American Journal of Physiology-Heart and Circulatory Physiology* 289(2), pp. H852-H861.

## References